Cranfield University

PhD Thesis

Evangelos Tsoudis

Technoeconomic Environmental and Risk Analysis of Marine Gas Turbine Power Plants

School of Engineering

July 2008

Cranfield University

School of Engineering

PhD Thesis

Evangelos Tsoudis

Technoeconomic Environmental and Risk Analysis of Marine Gas Turbine Power Plants

Supervisor:

Professor Pericles Pilidis

July 2008

ABSTRACT

A novel generic Technoeconomic, Environmental and Risk Analysis (*TERA*) computational method was developed for marine power plants that are composed of existing or at preliminary design stage marine gas turbines. The method is composed of several numerical models in order to realistically approach the life cycle operation of a marine gas turbine power plant-according to the operational profile of the platform marine vessel type-coupled to an integrated full electric propulsion system and stochastically estimate the power plant's life cycle net present cost. The development of the *TERA* method led to the creation of an integrated computational marine vessel operation environment which was given the name "*Poseidon*".

The performance and exhaust emissions (nitric oxide, carbon monoxide, carbon dioxide and unburned hydrocarbon) of five 25 Megawatt marine gas turbines of the same technology level and design-point overhaul interval were simulated and modelled in "*Poseidon*". The exhaust emissions of the modelled gas turbines were calibrated for two combustor technologies: conventional and dry-low emissions for both distillate fuel and natural gas used as fuel. The marine gas turbines are: existing simple cycle, novel twin-mode intercooled cycle, fictional intercooled cycle, fictional recuperated cycle and partly based on an existing design, intercooled/recuperated cycle. Three marine vessel types that require the same power plant output power and configuration but they utilise different operational profiles were also realistically modelled. The marine vessels are: Destroyer, RoPax fast ferry and LNG carrier. It was assumed that the Destroyer's and RoPax fast ferry's power plants use distillates fuel and the LNG carrier's power plant uses compressed natural gas as fuel.

Three case studies defined by each of the marine vessels were performed in order to investigate the economic feasibility of the advanced cycle gas turbine power plants in comparison with the power plant composed by existing gas turbines, in a possible future scenario were all four modelled exhaust emission quantities are accurately measured and taxed. The investment on dry-low emissions combustor technology was also investigated as part of each case study. Both technical and economic input datasets are realistic. Due to time restrains the LNG carrier case study features only the intercooled/recuperated gas turbine power plant. Obtained results are presented and discussed separately for each case study.

Acknowledgements

My supervisor Professor Pericles Pilidis for his guidance, support and patience during all the stages of this PhD study.

Dr. David Mba for his support before and during this PhD study.

Dr. Stephen Ogaji, Dr. Vasilios Pachidis and Dr. Panagiotis Laskaridis for sharing their knowledge with the author literally at any time.

Mr. Bhavik Mody for being a good friend and colleague.

Mr. Daniele Pascovici and Mr. Fernando Colmenares for their friendship and corporation.

My parents Emilia and Aris, and my grandmother Martha for their support and encouragement.

List of Contents

Thesis Main Body

Thesis Appendices

List of Figures

List of Tables

Nomenclature

Technical & Environmental Related

Latin	
A_{BT}	Transverse area of the bulbous bulb
A_E / A_O	Propeller Blade area ratio
A_F	Frontal projected area
A_{GP}	Gas path area at the entry of the turbine
A_L	Lateral projected area
A_T	Immersed area of the transom stern at zero speed
B	Breadth at water line
c	Coefficient that accounts for specific shape of afterbody or propeller's chord (2.5.2.4)
c_{stern}	Coefficient that defines the form of the afterbody
C_1	Hull form coefficient
C_2	Coefficient that accounts for the effect of the bulbous bulb on the wave resistance
C_3	Coefficient that accounts for the influence of a transom stern on the wave resistance
C_A	Correlation allowance coefficient
C_{AA}	Hull roughness coefficient
C_B	Block coefficient
C_{BTO}	Coefficient of position of thruster
ΔC_D	Difference in drag coefficient of the propeller's profile section
C_M	Midship coefficient
C_p	Prismatic coefficient
C_F	Water plane coefficient
C_{WP}	Frictional resistance coefficient
CD_i	Non-dimensional drag in head wind
CD_t	Non-dimensional drag in beam wind
CD_{iAF}	Longitudinal drag with respect to A_F
CS	Turbine relative rotational speed
d_{BTO}	Diameter of the thruster tunnel
D	Propeller diameter
D_H	Hub diameter
D_T	Tip diameter
EF	Gas turbine exhaust temperature
FF	Fuel flow
f_w	Sea-wave frequency
Fn	Froude number
g	Gravitational acceleration
GF	Gas flow
h	Altitude of concern

h_0	Reference altitude
h_b	Gas turbine blade height
h_B	Height of the centroid of the area A_{BT} above the base line
h_w	Significant height of the wave
HTR	Hub to tip ratio
i_E	Half angle of entrance of the load waterline
J	Advance ratio
k	Effective form factor of both hull and appendices
k_1	Form factor of bare hull
$1+k_2$	Effective form factor of appendages
k_h	Hull surface roughness
k_p	Propeller's blade surface roughness
K_Q	Propeller torque coefficient
$K_{Q\text{-}cor}$	Corrected propeller torque coefficient
K_s	Shroud parameter
K_T	Propeller thrust coefficient
$K_{T\text{-}cor}$	Corrected propeller thrust coefficient
L	Length at water line
L_R	Length of the run
lcb	Longitudinal centre of buoyancy
LMP	Larson-Miller parameter
n_{BTO}	Number of bow thrusters
M	Molar Mass of air (28.9644 g/mol) or Mach Number (4.4.3.1)
M_p	Molar mass of the exhaust output quantity
MF	Gas Turbine intake mass flow
N	Design point turbine's rotational speed or number of propeller blades (2.5.2.4)
N_{eng}	Number of prime movers
N_{od}	Off-design turbine's shaft rotational speed
N_{prop}	Number of Propellers
N_S	Propeller shaft rotational speed
P/D	Propeller pitch to diameter ratio
P	Propeller pitch or input ambient pressure (2.2.2)
P_{amb}	Ambient air pressure
P_0	Reference ambient pressure
P_{aux}	Auxiliary power
P_B	Break power
P_E	Effective power
P_D	Delivered power
P_{PT}	Power turbine rating
P_T	Thrust power or Pressure of gas flow (4.4.3.1)
PR	Total compression pressure ratio
q_b	Total blade life consumption
q_p	Quantity of the product of the output prime mover parameter
r_B	Effective submergence of the bulbous bulb

r_{mb}	Mid-shaft to mid-blade distance
R	Universal gas constant (8.31432 J/molK)
R_{AA}	Wind additional resistance on marine vessel
R_{bt}	Bow thruster additional resistance on hull
Rn	Reynolds number
R_{SW}	Sea-wave additional resistance on marine vessel's total resistance
R_T	Total resistance of hull
R_v	Hull viscous resistance
R_w	Hull wave resistance
S_α	Superfluous journey distance
S_{qc}	Gas dynamic constant
S_H	Wetted surface of bare hull
S_j	Total journey distance
S_{tot}	Total wetted surface (hull and appendages)
t	Thrust deduction factor or actual time of day (2.7.2.2)
t/c	Propeller thickness to chord length ratio
t_α	Sum of the superfluous time intervals
t_d	Time from midnight to sunrise
t_f	Blade's time to failure
t_j	Sum of total schedule time intervals
t_p	Time from sunrise to time that temperature peaks
t_T	Journey schedule time
$t_{T+\alpha}$	Journey total time
t_φ	Unit of time rate to quantity conversion factor
T	Mean draft or Marine vessel required thrust (2.5.2.3 & 2.5.2.4)
T_a	Aft draft
T_{amb}	Ambient air temperature
T_{amp}	Amplitude of daily temperature variation
T_b	Gas turbine blade temperature
T_{exh}	Exhaust gas temperature
T_f	For draft
T_g	Gas turbine gas temperature
T_{IET}	Intercooler inlet temperature
T_{IOT}	Intercooler outlet temperature
T_m	Mean daily temperature
T_{min}	Minimum day temperature
T_{max}	Maximum day temperature
T_{sea}	Sea water temperature
T_p	Propeller thrust
T_T	Gas flow temperature
$TBLADE$	Compressor turbine blade temperature
TET	Turbine entry temperature
V	Hull speed
V_A	Speed of advance

V_{ε}	Apparent wind speed
$V_{fluegas}$	Volume of 1,000,000 m^3 of flue gas
V_{mole}	Volume occupied by one mole of gas at standard conditions (24.45 L)
V_T	True wind speed
w	Wake fraction
y	Rate of the product of the output prime mover parameter
Z	Propeller number of blades
∇	Marine vessel volume displacement
Δ	Marine vessel weight displacement

Greek	
β	Angle between vessel's head direction and true wind
δ	Cross force parameter
γ	Ratio of specific heats at the turbine section
ε	Blade cooling effectiveness (2.4.2) or apparent wind angle (2.5.2.7)
η^b	Shaft bearing efficiency
η_H	Hull efficiency
η^{OWE}	Propeller open water efficiency
η^R	Relative rotational efficiency
η^s	Sterntube seal efficiency
η^t	Transmission efficiency
η^{th}	Thermal efficiency
ν	Kinematic viscosity
σ^{cfd}	Blade's design point centrifugal stress
σ^{cfo}	Blade's off-design centrifugal stress
ρ^{air}	Density of air
ρ^b	Density of gas turbine blade material
ρ^{sea}	Density of sea water
ϕ	Flow coefficient
ψ	Velocity coefficient at the entry of the turbine

Subscripts	
p	Prime mover output quantity (Fuel flow or emission quantity)

Economic & Risk Related

Latin	
A	One dimensional array that the cost component values are recorded in
C	Value of the cost component of the distribution
C_{amb}	Maintenance administrative, logistics and required energy costs
C_{CO}	Annual CO emissions cost
C_{CO2}	Annual CO_2 emissions cost
C_F	Annual cost of fuel
C_{INS}	Annual insurance cost on the actual prime mover purchase cost
C_{INT}	Annual interest cost on the actual prime mover purchase cost
$C_{lab/eng}$	Maintenance labour cost for every scheduled journey
C_{Maint}	Maintenance cost
$C_{mat/engb/hr}$	Cost of maintenance materials for each prime mover per hour of scheduled journey
C_{NOx}	Annual NO_x emissions cost
C_p	Cost of emission quantity per unit mass
C_{UHC}	Annual UHC emissions cost
DOC	Direct operating cost
EP_{DP}	Design point prime mover power output (kW)
$ESPPF$	Spare parts cost factor
$F_{amb/lab}$	Overhead labour factor
$F_{amb/mat}$	Materials distribution factor
Hem	Number of hours between engine overhaul
$I_{1,2...}$	Value of the variable at every interval number
I_{jd}	Journey distribution risk factor
$IPMC$	Initial prime mover purchase cost
IR	Interest rate for the overall operational life of the vessel
J	Position number of the value of the cost component at every risk scenario
K_{tech}	Gas turbine combustor technology factor
MHR_{mengbl}	Engine maintenance hours per operational hour
N_{asj}	Annual number of scheduled journeys
N_{prob}	Probability of the value of the cost component at every interval
N_{sum}	Cumulative probability at every interval
NPC	Net present cost
P_p	Cost of the prime mover's output quantity per unit mass
PD_0	Estimated percentage difference of cost from the reference prime mover
PD_1	Estimated percentage difference cost due to different technology components
PD_{AVLB}	Prime mover availability percentage per annum
PMC	Actual prime mover purchase cost (or capital cost)
PMC_0	Cost of the prime mover derived from the percentage difference from the cost of the reference prime mover
PMC_1	Estimated cost of the prime mover due to different technology components

$q_{annual\text{-}p(b)}$	Prime mover output quantity
R_{leng}	Maintenance labour rate per hour
SD	Standard deviation value
t_{annual}	Annual operational time
$t_{annual\text{-}WP1}$	Operational time of the prime mover under weather profile 1
$t_{annual\text{-}WP2}$	Operational time of the prime mover under weather profile 2
t_{down}	Downtime of the prime mover subtracted from t_{annual}
t_{op}	Operational time per scheduled journey

Greek	
ν	Value of variable
χ	Pseudo-random number

Subscripts	
ave	Average
max	Maximum
min	Minimum
n	Number of interval
p	Prime mover output quantity (i.e. Fuel)

1 Introduction

1.1 Background

This research was initialised as part of the Advanced Marine Electric Propulsion Systems project (*AMEPS*), which was an academic partnership (sponsored by the EPSRC) between three universities (Cranfield University, Strathclyde University and University of Manchester) with the aim to profoundly investigate the integrated full electric propulsion (*IFEP*) technology at a before specification stage in order to provide technology support, technical and economic risk mitigation. The main objective to achieve the previously mentioned aim, was defined as, the adoption of a systems engineering approach, in order to develop a fully integrated electro-mechanical simulation environment and apply advanced electrical system protection, control schemes and systems integration methods**.** The main tasks of each of the three partners are defined below according to the area of their expertise:

- Strathclyde University was responsible for the development of the electric power systems and network models.
- The University of Manchester was responsible for the development of the machine and drive models.
- Cranfield University was responsible for the development of the gas turbine models and investigation on the economic feasibility of the selected gas turbine cycles as part of an *IFEP* system.

The responsibilities of Cranfield University in the *AMEPS* project required the initiation of two research projects. The main task of the first research project was the development and creation of the gas turbine models (simulation and modelling required off-design and transient performance) in order to be integrated with the simulated electrical power systems, and the main task of the second research project which was undertaken by the author was to develop a Technoeconomic, Environmental and Risk Analysis (*TERA*) method and apply it on the selected marine gas turbine cycles.

1.2 Integrated Full Electric Propulsion System (IFEP)

The concept of using electric propulsion in marine vessels dates back to the 1900s, but it was not until the 1980s that developments in power electronic device construction allowed their application for power conversion and control, and even more recently developments in switching device implementation allowed the technological progression of marine electrical power systems [1]. Figure 1.1 presents a typical gas turbine mechanical propulsion system of a naval vessel that can be either a COGOG (combined gas turbine or gas turbine) or a COGAG (combined gas turbine and gas turbine) using a reduction gear-box (*GB*) to connect each set of gas turbine prime movers (low-power for cruise and/or high-power for boost) to each of the propellers and uses a separate set of diesel generators (*DG)* and electrical system for the service load requirements of the marine vessel.

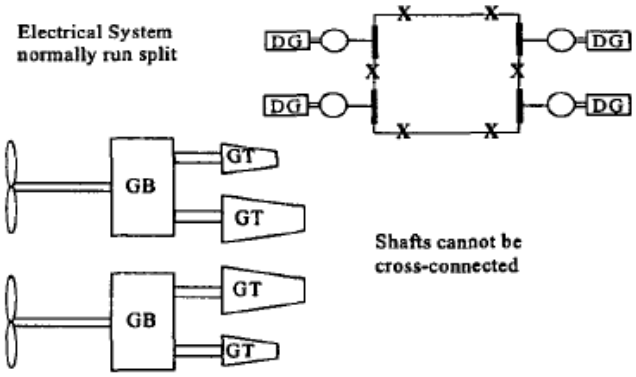

Figure 1.1: Gas turbine mechanical propulsion system [1]

Figure 1.2 presents an *IFEP* configuration proposed for the same naval vessel [1], where no reduction gearboxes or clutches are necessary. As it can be seen the number of diesel generators has decreased to half as also the number of gas turbines. The *IFEP* system provides the capability of utilising only one prime mover during cruising (rotating both propellers) which can also provide the required service load by the auxiliary electrical systems of the vessel. The diesel secondary prime movers are operated at very low cruise speeds or in port manoeuvring and during docking/undocking (where any installed thrusters can be also operated by the secondary prime movers), cases that the gas turbine main prime mover would stall. It needs to be stated that the secondary prime movers can also be gas turbines.

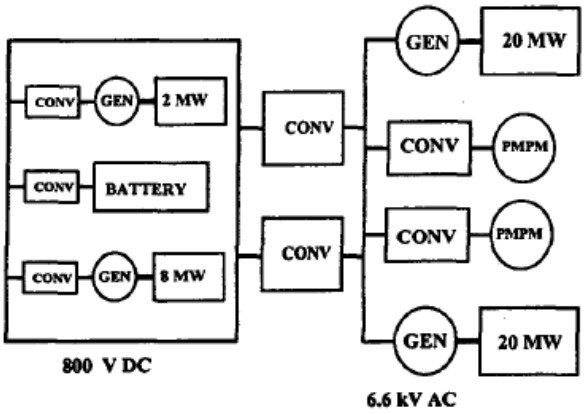

Figure 1.2: Representative sample of an integrated full electric propulsion system [1]

The integration of the propulsion and auxiliary systems except that reduces the number of prime movers and auxiliary engines; it increases the loading of the operating prime mover at cruising conditions. An *IFEP* system does not require the installation of controllable pitch propeller (*CPP*) due to the fact that electric motors have maximum torque from zero rotational speed. The combination of gas turbine prime movers and an *IFEP* system provides flexibility on the positioning of the prime movers, generators and propeller electric drives especially on volume sensitive ships carrying low density cargo (i.e. ferries, cruise ships). The prime mover(s) can be installed on the upper decks or top decks (depending primarily on the prime mover weight/marine vessel displacement ratio) of a marine vessel, the generator(s) can be located near the stern of the vessel (permitting a greater utilisation of the below the superstructure volume between for and aft perpendiculars) and the propeller electric drives can be installed externally on pods that if they are azimuthing a dynamic positioning system can be installed and the need for rudders can be dismissed.

1.3 Marine Gas Turbine Market Share

The following tables (1.1 and 1.2) present a forecasting analysis on the marine gas turbine market share from 2004 to 2013 [2]. According to the analysis the leading marine gas turbine supplier in the high-power sector is General Electric with the LM2500/LM2500+ having the highest demand and second is Rolls-Royce [2]. The following tables include the General Electric allied companies on the LM2500/LM2500+. It needs to be mentioned that all marine gas turbines available in

the market incorporate a simple thermodynamic cycle. As from 2004 the only available advanced dry cycle marine gas turbine in the maritime market is the intercooled/recuperated Rolls-Royce WR21 which belongs to the high power sector.

MARINE GAS TURBINES BY POWER OUTPUT: 2004-2013		
Power Output	**# of Machines**	**Market Share**
Up to 3,000 SHP	27	3.5%
3,000 SHP up to 10,000 SHP	205	27.0%
10,000 SHP up to 20,000 SHP	41	5.4%
20,000 SHP & Larger	487	64.1%
TOTAL	**760**	**100.0%**

Table 1.1: Gas turbine market share by power output [2]

MARINE GAS TURBINES BY MANUFACTURER: 2004-2013		
Manufacturer	**# of Machines**	**Market Share**
General Electric Company (USA)	251	33.0%
Rolls-Royce	216	28.4%
Vericor Power Systems	96	12.6%
UTC Pratt & Whitney Power Systems	55	7.2%
Mitsubishi Heavy Industries	29	3.8%
All Others	113	15.0%
TOTAL	**760**	**100.0%**

Table 1.2: Gas turbine market share by manufacturer [2]

1.4 Research Main Objectives, Definitions and Assumptions

1.4.1 Research main objectives

The main objectives of this research are:

- To initialise the development of a novel generic Technoeconomic, Environmental and Risk Analysis (*TERA*) computational method that can be used to investigate the economic feasibility of marine power plants composed of gas turbines that their status can range from preliminary design to production.

- The use of the developed method to perform a series of case studies each defined by a simulated marine vessel type in order to investigate the

economic feasibility of four advanced cycle marine power plants-assumed at preliminary design stage-compared with a marine power plant that is composed of a broadly used and in production simple cycle marine gas turbine type, in a futuristic emissions tax scenario, featuring two different existing combustor technologies: conventional and dry-low emissions. All simulated marine vessels are assumed that incorporate integrated full electric propulsion (*IFEP*) system.

1.4.2 Research main definitions

All gas turbines that are simulated in this research have a design-point power output of 25 Megawatt and adopt the same technology level in accordance to the current industry capabilities. The same is assumed for the combustors that are simulated in this research. The simulated marine gas turbines are:

- Simple cycle
- Twin mode intercooled cycle
- Intercooled cycle
- Recuperated cycle
- Intercooled/recuperated cycle

The simple cycle gas turbine is the reference cycle in this research and is simulated as a combined version of the performance characteristics of the two offered marine versions of the General Electric LM2500. The intercooled and the recuperated gas turbines are fictional designs, the intercooled/recuperated is partly based on basic characteristics of the newly introduced Rolls-Royce WR21, and the twin mode intercooled cycle is a novel gas turbine propulsion system proposed in Cranfield University and its configuration is primarily based on an initial preliminary performance investigation.

All simulated marine vessels share the same power plant configuration and output power rating (50MW twin main prime mover), ambient conditions, weather profiles, hull fouling levels, number of scheduled journey for every installed type of power plant, scheduled journey duration and the maximum allowable *TET* is common for all gas turbine prime movers, irrelevantly of the type of marine vessel. The marine vessels are:

- Destroyer
- RoPax fast ferry
- LNG Carrier (Q-max class)

The phase “futuristic emissions tax scenario” is used to describe a tax emissions policy were exhaust emission quantities can be constantly monitored, recorded and are charged according to their cumulative emitted mass. The emission quantities that are taken into consideration in this research are: nitric oxide, carbon monoxide, carbon dioxide and unburned hydrocarbons. Sulphur oxide and soot are not considered.

1.4.3 Research main assumptions

The phrase “power plant” indicates both of the main prime movers of the marine vessel’s propulsion system assuming that they operate only in the open-sea. Port manoeuvring and docking/undocking procedures are not considered in this research thus any secondary prime movers needed in a typical *IFEP* system are neither simulated nor included.

The operational profile of the simulated marine vessels is assumed to be the same throughout their operational life. In the case that a marine vessel has a variable operational profile (i.e. naval marine vessel which can use one prime mover for cruising and both prime movers for sprinting) the role of the prime movers is not exchanged at any fashion, thus remains the same during the operational life of the vessel.

The effects of gas turbine components performance degradation is not considered in this research.

The effects of intake and exhaust ducting on the performance of the simulated marine gas turbine prime movers are assumed included within their produced results.

1.5 Thesis Structure

At this point it needs to be stated that any literature background is included within the chapters of this thesis according to the requirements of each task that compose the

substantialness of this research. The author has structured the thesis by separating the fundamental components of this research between "*Technical and Environmental*" and "*Economic* and *Risk*". The main body of the thesis is composed by eight chapters and a brief description of each one is provided below.

Chapter 2 describes the methods and tools used to create the numerical models that constitute the integrated computational marine vessel operation environment scheme that forms the technical and environmental part of the *TERA* method. The scheme was given the name "*Poseidon*" from the ancient Greek god of sea.

Chapter 3 describes the methods and tools used to create the economic and risk numerical model that forms the economic and risk analysis part of the *TERA* method.

Chapter 4 presents the design-point and off-design performance, the procedure of exhaust emissions indexes calibration with presentation of the off-design exhaust emission rates and the procedure of setting the design point hot section rotor blade life to failure with presentation of the off-design hot section rotor blade temperature, for each of the five 25MW simulated marine gas turbines that were modelled in "*Poseidon*".

Chapter 5 presents the dataset supplied to "*Poseidon*" and defines the specification of each of the three case studies of this research.

Chapter 6 presents the economic and risk dataset supplied to the life cycle costs model including the scenarios that compose each of the case studies.

Chapter 7 presents the "*Poseidon*" results for each of the case studies that are supplied as the technical and environmental dataset to the life cycle costs model. Additional dataset that is used on the life cycle costs model is essentially presented in this chapter. The three case studies results are presented and discussed.

Chapter 8 presents the conclusions of this research and the author's recommendations for further work.

1.6 References

1. Hodge, C, G., *"Modern Applications of Power Electronics to Marine Propulsion Systems"*, Proceedings of the 14th International Symposium on Power Semiconductor Devices and ICs, pp 9-16, June 2002.

2. "*Analysis 4-The Gas Turbine Marine Power Market: 2004-2013*", Performed by: Forecast International, 22 Commerce Road, Newtown, CT 06470, September 2004.

2 Implementation of the Technical & Environmental Part of *TERA* Method

2.1 Introduction

This chapter describes the methods and the tools that were used to develop and create the numerical models that constitute the integrated computational marine vessel operation environment "*Poseidon*" that forms the technical and environmental part of the Technoeconomic Environmental and Risk Analysis (*TERA*) method. *"Poseidon"* is implemented in M-code (MATLAB) and is composed of seven models:

- Gas turbine performance
- Gas turbine emissions
- Hot section rotor blade creep life
- Marine vessel power prediction
- Power plant operation management
- Journey management

Each model is described by introducing its task in "*Poseidon*" and where necessary the preliminary development procedure is stated. Modelling methodology is then analyzed, where the model's mathematical expressions, functions and capabilities are presented, as also (where necessary, separately) conditions and limitations. The model's inputs and outputs are described and any previous work used for the creation and implementation of the models is overviewed. Finally any standards (i.e. ISA) taken as reference for the creation or operation of the model are also mentioned.

2.2 Gas Turbine Performance Model

2.2.1 Introduction

The task of the gas turbine performance model is to be able to deliver the performance parameters of the under investigation gas turbine thermodynamic cycles at a range of off-design conditions, that a marine gas turbine installed on a vessel may be required to operate.

For the gas turbine off-design performance simulation the *"Turbomatch"* scheme was used (see section 2.2.5), and the first step was to construct the input files of each

of the investigated gas turbines and obtain their design point performance (appendix A.1). After establishing the design point performance (section 4.3) for each of the engines the second step was to obtain the required for the project's case studies off-design performance of each of the gas turbines. In the beginning of the project it was decided that the variables that would determine the gas turbine off-design conditions would be the turbine entry temperature (*TET*), ambient temperature (T_{amb}) and ambient pressure (P_{amb}).

Although all three variables were included in the model, as it is mentioned in chapter 4, only the first two were used as variables in the three case studies of the project as ambient pressure was assumed constant.

2.2.2 Modelling methodology

The method that was chosen to model the off-design operational parameters of each of the gas turbines under investigation was, after obtaining their off-design performance parameters with *"Turbomatch"* then tabulate them separately in two dimensional look-up tables in a M-file (MATLAB program files), in order to create a single three dimensional table for each parameter (figure 2.1) and apply linear interpolation between the reference points in order to obtain the rate of the required output engine parameter. The interpolation overall is three dimensional and is implemented by the use of an appropriate MATLAB function. The relationship between the output engine parameter and the variables that define the off-design state of the gas turbine is expressed in equation 2-1.

$$p_i = f(T_{amb}, P_{amb}, TET) \qquad \text{Equation 2-1}$$

Where: p_i is the output engine parameter and symbol *f* means "some function of".

At this point two declarations need to be made. First *"Turbomatch"* recognises altitude instead of ambient pressure and second it adjusts ambient temperature in altitude according to the International Standard Atmosphere (ISA). Therefore in the *"Turbomatch"* off-design input file (supplement sample in appendix A.1, table A.1), ambient temperature was calibrated to ISA sea level standards (section 2.2.6), in every altitude increasing off-design simulation step, and an interface formula as expressed in equation 2-2 [1] was added later in the M-file to convert ambient pressure to altitude.

$$h = \frac{\ln \frac{P}{P_0} RT_0}{-gM} + h_0 \qquad \text{Equation 2-2}$$

Where: h is the altitude of concern, h_0 is the reference altitude, P is the input ambient pressure, P_0 is reference ambient pressure, R is the air's universal gas constant and g is the gravitational acceleration, M is the molar mass of air.

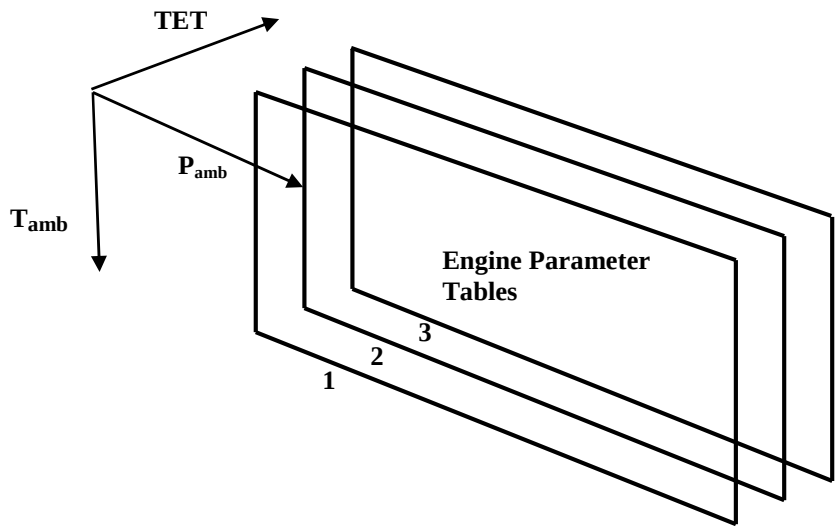

Figure 2.1: 3-D tabulation principle of output engine parameters

The principle idea behind the interpolation method chosen is when ambient conditions are defined, to iterate turbine entry temperature in very small increments from the lowest value obtained to the matching value that corresponds to the required power by the marine vessel thus the rest of the output parameters. Each of the two dimensional interpolation tables represents a 25 K increment in turbine entry temperature, table rows represent 200 meter increment in altitude, and each table column represents 10 ^{o}C increments in ambient temperature as is shown in tables 2.1 and 2.2). The modelling procedure was followed for each gas turbine separately that is investigated in the project's case studies (see chapter 4).

2.2.3 Gas turbine off-design operational range

The standards that were set and implemented (any exceptions are mentioned in chapter 4, section 4.3) for the engine operational range that the model should cover are: ambient temperature from -30 to +40 ^{o}C, ambient pressure from approximately 96.63 kN/m^2 to 103.76 kN/m^2 (which is translated in an altitude range approximately from -200 to +400 meters) and turbine entry temperature from a point that power turbine shaft power is low enough to provide the ability to investigate any of the thermodynamic cycles of interest installed on vessels with low service speed requirements (hence low power requirements) in their mission profiles (e.g. destroyer), to much beyond the specified design point in order to provide the vessel with the ability to maintain its service speed in increased hydrodynamic and aerodynamic resistance conditions.

Table 2.1: Two dimensional sample table representing gas turbine power output (MW) for 1500 K TET in different ambient conditions

T_{amb} (^{o}C)/Alt (m)	-200	0	200	400
-30	29.12	28.446	27.781	27.102
-20	28.226	27.565	26.918	26.284
-10	27.399	26.756	26.127	25.511
0	26.354	25.738	25.232	24.638
10	25.228	24.634	24.046	23.488
20	24.034	23.472	22.925	22.383
30	22.957	22.42	21.896	21.379
40	21.988	21.472	20.967	20.475

Table 2.2: Two dimensional sample table representing gas turbine power output (MW) for 1525 K TET in different ambient conditions

T_{amb} (^{o}C)/Alt (m)	-200	0	200	400
-30	31.155	30.428	29.712	29.011
-20	30.174	29.468	28.776	28.101
-10	29.255	28.569	27.898	27.241
0	28.134	27.475	26.83	26.198
10	26.929	26.3	25.682	25.076
20	25.968	25.359	24.765	24.179
30	24.778	24.199	23.63	23.076
40	23.725	23.171	22.631	22.093

2.2.4 Model inputs and outputs

The input parameters for the model were identified to be the engine power (*EP*) required by the vessel to maintain its required speed, ambient temperature T_{amb} and ambient pressure P_{amb}, and the output parameters are (at every time interval): fuel

flow (*FF*), mass flow (*MF*), turbine entry temperature (*TET*), compressor overall pressure ratio (PR), compressor overall outlet temperature (*COT*) and high pressure compressor relative rotational speed (*CS*) (or just compressor relative rotational speed in the case of 2-shaft engines).

2.2.5 "Turbomatch" scheme overview

The *"Turbomatch"* scheme [2] is a FOTRAN programmed software, that has been developed at Cranfield University by the School of Engineering, Department of Power and Propulsion, to enable calculations of design-point and off-design performance of existing and concept gas turbine thermodynamic cycles.

The scheme uses all necessary pre-programmed routines which are named "bricks" and with the use of interface "codewords" provides the ability to simulate the operational state of the engine's different components, and as a result the engine's output power or thrust, fuel consumption, mass flow etc. The scheme assumes that the fuel used for the simulations is kerosene with low calorific value of 43.165 MJ/kg.

It also provides detailed information of the performance of every component, and also of the gas properties at every engine's station. The results are presented not only in ".txt" files but also in a special made ".xls" file which provides great flexibility if the engine's (or components) performance parameters are to be tabulated and interpolated. The scheme is used in the majority of projects at Cranfield University that require gas turbine performance calculations, either for aero, marine or stationary gas turbines.

2.2.6 International Standard Atmosphere (ISA)

The International Standard Atmosphere is defined at sea level altitude:

- Ambient temperature T_{amb} at 15 ^{o}C (288.15 K)
- Ambient pressure P_{amb} at 101.325 kN/m^2
- Air's density at ρ_{air} at 1225 g/m^3
- Universal gas constant R at 8.31432 J/molK
- Air's molar mass M at 28.9644 g/mol
- The lapse rate up to 11 km of altitude is -6.5 ^{o}C/km

2.3 Gas Turbine Exhaust Emissions Model

2.3.1 Introduction

The task of the gas turbine exhaust emissions model is to deliver the quantities of exhaust emissions at the range of off-design conditions that are described in section 2.3.1. For the off-design exhaust emission quantities calculation, the *"APPEM"* (Analysis and Prediction of Pollutant Emissions) scheme was used (see section 2.3.4).

2.3.2 Modelling methodology

The required by the *"APPEM"* scheme engine performance parameters (mass flow, compressor overall pressure, compressor outlet temperature and fuel flow) were obtained from the "Turbomatch" gas turbine off-design performance results, and the method that was used to model the exhaust emissions quantities is identical with the method described in section 2.2.3 for the gas turbine off-design performance, as the quantities of exhaust emissions of a certain gas turbine are specific at specified off-design conditions assuming no components degradation. The model is integrated in the same M-file with the gas turbine performance model.

2.3.3 Model inputs and outputs

The model requires the same input parameters as the gas turbine performance model and the output emission quantities that are presented are the output rate (at every time interval) of nitric oxide (NO_x), carbon monoxide (CO), carbon dioxide (CO_2) and unburned hydrocarbons (UHC).

2.3.4 "APPEM" scheme overview

The *"APPEM"* (Analysis and Prediction of Pollutant Emissions) scheme is a FORTRAN programmed software has been developed in Cranfield University by the School of Engineering, Department of Power and Propulsion, for combustor performance and exhaust emissions calculation (NO_x, CO, CO_2, UHC). The exhaust emissions are quantified by the use of efficiency correlations and semi-empirical model published by A.H. Lefebvre [3]. The scheme simulates a single annular combustor (SAC), and incorporates a technology factor in order to provide the ability to calibrate the quantities of exhaust emissions to standards that apply to different technology combustors. It has been used in numerous projects in Cranfield University that require combustor performance simulation or exhaust emission analysis, in aero, marine or stationary gas turbines.

2.4 Hot Section Rotor Blade Creep Life Model

2.4.1 Introduction

The task of the gas turbine hot section rotor blade creep life model is to predict the rotor's blade life consumption of the hot section (high pressure turbine or just turbine in the case of 2-shaft gas turbines), at the range of off-design conditions that are described in section 2.2.3. The model is able to quantify the blade's creep life consumption in every change of the off-design conditions during a scheduled journey that the gas turbine is requested to operate. The model is integrated with the gas turbine performance model, and obtains the required input parameters from it.

2.4.2 Modelling methodology

The method that was used is to calculate the blade's creep life fraction t_f at a specific gas turbine off-design condition is based on the Larson-Miller criterion [4], which is defined in equation 2-3. The Larson-Miller diagram was implemented in an M-file and is interpolated linearly.

$$t_f = 10^{\frac{LMP}{T_b} - 20} \qquad \text{Equation 2-3}$$

Where: t_f is the blade's time to failure, LMP is the Larson-Miller parameter and T_b is the blade temperature.

The blade is assumed that it experiences only centrifugal stress (no bending stress from gas momentum and pressure on the air foil), it has a rectangular shape and one blade represents the creep life of all the blades of the turbine stage. The centrifugal stress σ_{cfd} on the blade at turbine design point is defined as [4]:

$$\sigma_{cfd} = \rho_b \times K_s \times h_b \times \left(\frac{2\pi N}{60} \right)^2 \times r_{mb} \qquad \text{Equation 2-4}$$

Where: ρ_b is the blade's material density, K_s is the shroud parameter, h_b is the height of blade, N is the design point turbine's shaft rotational speed and r_{mb} is the distance from mid-shaft to mid-blade.

To calculate the centrifugal stress σ_{cfo} on the blade any turbine off-design point, equation 2-5 is used [4].

$$\sigma_{cfo} = \sigma_{cfd} \left(\frac{N_{od}}{N} \right)^2 \qquad \text{Equation 2-5}$$

Where: N_{od} is the off-design turbine's shaft rotational speed.

To calculate the temperature of an air cooled blade, equation 2-6 [4] was implemented assuming that overall blade cooling effectiveness remains constant at all gas turbine off-design conditions, the gas temperature is the same as the turbine entry temperature and the compressor derived blade cooling air temperature is the same as the compressor outlet temperature.

$$T_b = T_g - \varepsilon \times (T_g - T_c) \qquad \text{Equation 2-6}$$

Where: T_g is the gas temperature, T_c is the blade cooling air temperature and ε is the blade cooling effectiveness.

2.4.3 Model inputs and outputs

The direct inputs that the model requires by the user before any scheduled mission are the blade's design parameters: the shroud parameter K_s, the height of blade h_b, the design point rotational speed of the turbine's shaft N, the distance from mid-shaft to mid-blade r_{mb} and the blade's material density ρ_b. The variable parameters that define the blade's life fraction t_f (blade cooling air temperature T_c, turbine shaft off-design rotational speed N_{od} and gas temperature T_g) are obtained from the gas turbine performance model (section 2.2.4). The output parameters are (at every time interval): the blade's time to failure t_f, and the turbine blade temperature T_b.

2.5 Marine Vessel Power Prediction Model

2.5.1 Introduction

The task of the marine vessel power prediction model is to simulate the hydrodynamic and aerodynamic resistance of a marine vessel and calculate the brake power that needs to be applied by the vessel's power plant in order the vessel to maintain a certain speed, under various weather conditions. The effect of shallow water in the hydrodynamic resistance of the hull as also propeller cavitation phenomenon and propeller were not taken into consideration. The model is composed by the following modules:

- Hull resistance prediction
- Propulsion factors prediction
- Propeller open water characteristics
- Hull fouling resistance
- Sea-wave resistance
- Wind resistance

2.5.2 Modelling Methodology

2.5.2.1 Hull resistance module

A statistical method [5] was used to simulate the hull resistance of a marine vessel under trial conditions, in preliminary design stage. The method which is based in statistical and semi-statistical correlations is widely utilized in the Marine Engineering field and is included within several marine vessel power prediction software packages available in the market. The method can be applied to displacement and semi-displacement hulls. All equations are referred to the adopted method unless otherwise is stated within the content of this section. To calculate the form factor of bare hull k_1 equation 2-7 is proposed.

$$1+k_1 = 0.93 + 0.4871c(B/L)^{1.0681}(T/L)^{0.4611} (L/L_R)^{0.1216}(L^3/\nabla)^{0.3649}(1-C_p)^{-0.6042} \quad \text{Equation 2-7}$$

Where: L is the length at water line, B is the breadth at water line, T is the mean draft at water line, ∇ is the volume displacement as can approximately estimated in equation 2-8 [6], C_p is the hull's prismatic coefficient, the coefficient c that accounts for the specific shape of the afterbody is given by equation 2-9.

$$\nabla = C_B LBT \quad \text{Equation 2-8}$$

Where: C_B is the hull's block coefficient.

$$c = 1 + 0.011c_{stern} \quad \text{Equation 2-9}$$

Where: c_{stern} is the coefficient that defines the form of the afterbody and recommended values are presented in table 2.3.

Table 2.3: Relationship between the c_{sterm} value and afterbody form

c_{stern}	Afterbody form
-25	Pram with gondola
-10	V-shaped sections
0	Normal section shape
10	U-shaped sections

L_R is the length of the run, which if unknown can be estimated from equation 2-10.

$$L_R = (1 - C_p + 0.06C_p lcb/(4C_p - 1))L \quad \text{Equation 2-10}$$

Where: *lcb* is the longitudinal centre of buoyancy forward (+) of, abaft (-) midship as a percentage of L.

The wetted surface S_H of the bare hull can be estimated from the statistically derived equation 2-11.

$$S_H = L(2T + B)C_M^{0.5}(0.4530 + 0.4425C_B - 0.2862C_M - 0.003467B/T + 0.3696C_{WP} + 2.38A_{BT}/C_B \quad \text{Equation 2-11}$$

Where: A_{BT} is the transverse area of the bulb where the still water intersects the bulb's stem, C_{WP} is the hull's water plane coefficient and C_M is the hull's midship section coefficient.

It needs to be indicated that all form coefficients are based on the length of the waterline L. The resistance of the appendages is also presented in the form of an effective form factor k, including the effect of the appendages, as defined in equation 2-12.

$$1 + k = 1 + k_1 + [1 + k_2 - (1 + k_1)]\frac{S_{app}}{S_{tot}} \quad \text{Equation 2-12}$$

Where: $(1+k_2)$ is the effective form factor of appendages, S_{app} is the total wetted surface of appendages, S_{tot} is the total wetted surface of bare hull and appendages. Table 2.4 presents the effective form factor values k_2 for different appendages.

Table 2.4 Effective form factor values for different appendages (in brackets is the implemented value)

Type of Appendage	**Value of $1+k_2$**
Rudder of single screw vessel	1.3 to 1.5 (1.4)
Spade-type rudders of twin screw vessel	2.8
Skeg-type rudders of twin screw vessel	1.5 to 2.0 (1.75)
Shaft Brackets	3.0
Bossings	2.0
Bilge keels	1.4
Stabiliser fins	2.8
Shafts	2.0
Sonar dome	2.7

The effective form factor is used to calculate the viscous resistance of the hull as defined in equation 2-13.

$$R_v = \tfrac{1}{2}\rho_s V^2 C_F (1 + k) S_{tot} \quad \text{Equation 2-13}$$

Where: ρ_s is the density of sea water (table F.1, appendix F shows ρ_s variation with sea water temperature T_{sea} [7]), V is the speed of the vessel and C_F is the

frictional resistance according to the ITTC-1957 (International Towing Tank Conference) friction line [7] as defined in equation 2-14.

$$C_F = \frac{0.075}{(\log_{10} Rn - 2)^2} \qquad \text{Equation 2-14}$$

Where: *Rn* is the Reynolds number which is define in equation 2-15.

$$Rn = \frac{VL}{\nu} \qquad \text{Equation 2-15}$$

Where: ν is the kinematic viscosity of sea water (table F.1, appendix F shows ν variation with sea water temperature [7]).

The effective form factor when more than one appendage is to be accounted is expressed in equation 2-16.

$$(1+k_2)_{effective} = \frac{\sum S_i (1+k_2)_i}{\sum S_i} \qquad \text{Equation 2-16}$$

Where: S_i and $(1+k_2)$ are the wetted area and appendage factor of each appendage that is included, respectively.

To calculate the wave resistance of the hull the equation 2-17 is proposed.

$$R_w = \Delta C_1 C_2 C_3 e^{m_1 Fn^d + m_2 \cos(\lambda Fn^{-2})} \qquad \text{Equation 2-17}$$

Where: Δ is the hull's weight displacement as defined in equation 2-17, C_1, C_2, C_3, m_1, m_2, λ and d (suggested value is -0.9) are coefficients that depend on the hull form, *Fn* is the froude number and is defined in equation 2-18 [7].

$$\Delta = \rho_s g \nabla \qquad \text{Equation 2-17}$$

$$Fn = \frac{V}{\sqrt{gL}} \qquad \text{Equation 2-18}$$

If $Fn \leq 0.4$ the following coefficients are suggested:

$$C_1 = 2223105 C_4^{3.7861} (T/B)^{1.0796} (90 - i_E)^{-1.3757} \qquad \text{Equation 2-19}$$

Where: C_4 is defined in equations 2-20 to 2-22 and i_E which is the half angle of entrance of the load waterline is defined in equation 2-23.

If $B/L \leq 0.11$ then $C_4 = 0.2296(B/L)^{0.3333}$ Equation 2-20

If $0.11 < B/L \leq 0.25$ then $C_4 = B/L$ Equation 2-21

If $B/L > 0.25$ then $C_4 = 0.5 - 0.0625 L/B$ Equation 2-22

$$i_E = 125.67B/L - 162.25C_p^2 + 234.32C_p^2 + \\ + 0.1551(lcb + \frac{6.8T_a - T_f}{T})^3$$ Equation 2-23

Where: T_a is the molded draft at the aft perpendicular and T_f is the molded draft at the for perpendicular. The coefficient m_1 is defined in equation 2-24.

$$m_1 = 0.01404L/T - 1.7525\nabla^{1/3}/L - 4.7932B/L - C_5$$ Equation 2-24

Where: C_5 is defined in equations 2-25 and 2-26.

If $C_p \leq 0.8$ then $C_5 = 8.0798C_p - 13.8673C_p^2 + \\ + 6.9844C_p^3$ Equation 2-25

If $C_p > 0.8$ then $C_5 = 1.7301 - 0.7067C_p$ Equation 2-26

The coefficient m_2 is defined in equation 2-27.

$$m_2 = C_6 0.4e^{-.0.034Fn^{-3.29}}$$ Equation 2-27

Where: C_6 is defined in equations 2-28 to 2-30.

If $L^3/\nabla \leq 512$ then $C_6 = -1.69385$ Equation 2-28

If $512 < L^3/\nabla \leq 1727$ then $C_6 = 1.69385 + \frac{(L/\nabla^{1/3} - 8.0)}{2.36}$ Equation 2-29

If $L^3/\nabla > 1727$ then $C_6 = 0.0$ Equation 2-30

The coefficient λ is defined in equations 2-31 and 2-32.

If L/B ≤ 12 then $\lambda = 1.446C_p - 0.03L/B$ Equation 2-31

If L/B > 12 then $\lambda = 1.446C_p - 0.36$ Equation 2-32

According to a published technical report [8], the coefficient λ can be used to determine if the parameters of the hull under consideration are within the limits of the proposed method and should never exceed values above the line as it is presented in figure 2.2.

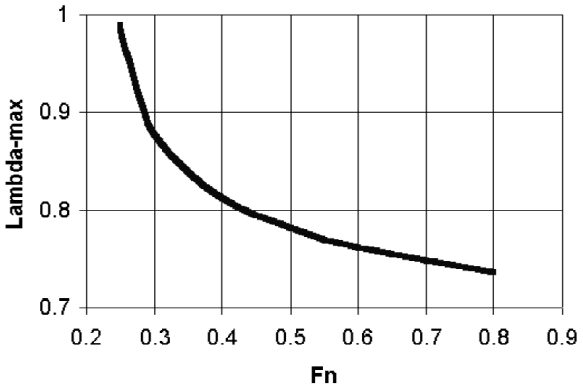

Figure 2.2: λ should always correspond to values below the line for a specified froude number

Coefficient C_2 corresponds to the effect of the bulbous bulb on the wave resistance created by the hull. If a vessel is designed without a bulb $C_2 = 1$. C_2 can be calculated using equation 2-33.

$$C_2 = e^{-1.89\frac{A_{BT} r_B}{BT(r_B + i)}} \qquad \text{Equation 2-33}$$

Where: r_B is the effective submergence of the bulb defined 2-34.

$$r_B = 0.56 A_{BT}^{0.5} \qquad \text{Equation 2-34}$$

Where: i expresses the effective submergence of the bulb as defined in 2-35.

$$i = T_f - h_B - 0.4464 r_B \qquad \text{Equation 2-35}$$

Where: h_B is the height of the centroid of the area A_{BT} above the base line.

The coefficient C_3 expresses the influence of a transom stern on the wave resistance and is defined in equation 2-36.

$$C_3 = 1 - 0.8 A_T / (BTC_M) \qquad \text{Equation 2-36}$$

Where: A_T is the immersed area of the transom stern at zero speed.

For the high speed range (Fn>0.55*)* the following coefficients is suggested to calculate C_1 and m_1.

$$C_1 = 6919.3 C_M^{-1.3346} (\nabla / L^3)^{2.0098} (L/B - 2)^{1.4069} \qquad \text{Equation 2-37}$$

$$m_1 = -7.2035 (B/L)^{0.3269} (T/B)^{0.6054} \qquad \text{Equation 2-38}$$

For the intermediate speed ($0.4 < Fn \leq 0.55$) an interpolation formula is suggested:

$$Rw = [Rw(Fn = 0.4) + (10Fn - 4)\{(Fn = 0.55) - \\ - Rw(Fn = 0.4)\}/1.5] \qquad \text{Equation 2-39}$$

The method suggests a correlation allowance coefficient C_A, which corrects the results to ideal trial conditions (still air resistance and hull roughness) as it is expressed in equations 2-40 and 2-41.

$$\text{If} \quad T_f/L \geq 0.04 \quad \text{then} \quad C_A = 0.006(L + 100)^{-0.16} - 0.00205 \qquad \text{Equation 2-40}$$

$$\text{If} \quad T_f/L < 0.04 \quad \text{then} \quad C_A = 0.006(L + 100)^{-0.16} - 0.00205 + \\ + 0.003(L/7.5)^{0.5} C_B^4 C_2 (0.04 - T_f/L) \qquad \text{Equation 2-41}$$

If the vessel's hull has bow thruster(s) installed the additional effect on the hull's resistance is calculated from the suggested equation 2-42 [9].

$$R_{bt} = \rho_s \pi d_{BTO}{}^2 C_{BTO} \qquad \text{Equation 2-42}$$

Where: d_{BTO} is the diameter of the tunnel, and C_{BTO} ranges from 0.003 to 0.012 with lowest value to be applied when bow thruster is installed in the bulbous bow.

The total resistance of the hull can be calculated with equation 2-43.

$$R_T = \tfrac{1}{2} \rho_s V^2 S_{tot} [C_F (1+k) + C_A] + Rw + n_{BTO} R_{bt} \qquad \text{Equation 2-43}$$

Where: n_{BTO} is the number of bow thrusters.

2.5.2.2 Prediction of propulsion factors module

The following method [5] is used for the estimation of the effective wake fraction, the thrust deduction factor and the relative-rotational efficiency of the propulsion system installed on a marine vessel. The method covers single-propeller arrangement with a conventional stern, single propeller with an open stern and twin-propeller. All equations are referred to the method. For a single-screw vessel with a conventional stern arrangement equation 2-44 is suggested to calculate the hull's wake fraction.

$$w = c_9 c_{20} C_V \frac{L}{T_a} (0.050776 + 0.93405 c_{11} \frac{C_F (1+k) + C_A}{(1 - C_{P1})}) + \\ + 0.27915 c_{20} \sqrt{\frac{B}{L(1 - C_{P1})}} + c_{19} c_{20} \qquad \text{Equation 2-44}$$

Where: the coefficients c_9, c_{20}, c_{11}, c_{19} and C_{P1} are defined below.

The coefficient c_9 depends on the coefficient c_8 which can be calculated by using equations 2-45 and 2-46.

$$\text{If} \quad B/T_A \le 5 \quad \text{then} \quad c_8 = BS/(LDT_A) \qquad \text{Equation 2-45}$$

$$\text{If} \quad B/T_A > 5 \quad \text{then} \quad c_8 = S(7B/T_a - 25)/(LD(B/T_a - 3)) \qquad \text{Equation 2-46}$$

Where: D is the diameter of the propeller.

Equations 2-47 and 2-48 define the calculation of c_9 coefficient.

$$\text{If} \quad c_8 \le 28 \quad \text{then} \quad c_9 = c_8 \qquad \text{Equation 2-47}$$

$$\text{If} \quad c_8 > 28 \quad \text{then} \quad c_9 = 32 - 16/(c_8 - 24) \qquad \text{Equation 2-48}$$

Coefficient c_{11} is defined in equations 2-49 and 2-50.

If $T_a/D \leq 2$ then $c_{11} = T_a/D$ Equation 2-49

If $T_a/D > 2$ then $c_{11} = 0.083333(T_a/D)^3 + 1.33333$ Equation 2-50

Coefficient c_{19} is defined in equations 2-51 and 2-52.

If $C_P \leq 0.7$ then $c_{19} = 0.12997/(0.95 - C_B) - 0.11056/(0.95 - C_P)$ Equation 2-51

If $C_P > 0.7$ then $c_{19} = 0.18567/(1.3571 - C_M) - 0.71276 + 0.38648C_P$ Equation 2-52

Coefficient c_{20} is defined in equations 2-53.

$$c_{20} = 1 + 0.015c_{stern}$$ Equation 2-53

The coefficient C_{P1} can be found by using equation 2-54:

$$C_{P1} = 1.45C_P - 0.315 - 0.0225lcb$$ Equation 2-54

The following equation expresses the thrust deduction factor t of single-screw vessels with conventional stern.

$$t = 0.25014(B/L)^{0.28956}(\sqrt{BT/D})^{0.2624} / (1 - C_P + 0.0225lcb)^{0.01762} + 0.0015c_{stern}$$ Equation 2-55

The relative-rotational efficiency can be found by using the following formula:

$$\eta_R = 0.9922 - 0.05908A_E/A_o + 0.07424(C_P - 0.0225lcb)$$ Equation 2-56

Where: A_E/A_O is the propeller's blade area ratio.

For single-propeller vessels with open sterns the following equations can be used though because of the small number of models that have been tested; it can be possible to produce approximate results for the wake fraction, the thrust deduction factor and the relative rotational efficiency as presented in equations 2-57, 2-58 and 2-59 respectively.

$$w = 0.3C_B + 10[C_F(1+k) + C_A]C_B - 0.1$$ Equation 2-57

$$t = 0.10$$ Equation 2-58

$$\eta_R = 0.98$$ Equation 2-59

For twin-propeller vessels equations 2-60, 2-61 and 2-62 are suggested to calculate the wake fraction, the thrust deduction factor and relative rotational efficiency.

$$w = 0.3095C_B + 10[C_F(1+k) + C_A]C_B - 0.23D/\sqrt{BT}$$ Equation 2-60

$$t = 0.325C_B - 0.1885D/\sqrt{BT} \quad \text{Equation 2-61}$$

$$\eta_R = 0.9737 + 0.111(C_P - 0.0225lcb) - \\ - 0.06325(P/D) \quad \text{Equation 2-62}$$

Where: *P/D* is propeller's pitch to diameter ratio.

2.5.2.3 Interaction between hull and propeller module

The interaction between the hull and propeller can be calculated by the following universally adopted method [10]. All equations are referred to the method. The hull without a propeller installed has a total resistance R_T at a speed V and is defined as the effective power P_E in equation 2-63.

$$P_E = R_T V \quad \text{Equation 2-63}$$

The open water test of a propeller without a hull in front of it will produce a thrust T at a speed V_A, with an open water propeller efficiency η_{OWE} and this can be expressed as the thrust power P_T in equation 2-64.

$$P_T = TV_A \quad \text{Equation 2-64}$$

Where: V_A is the speed of advance as defined in equation 2-65 and thrust T is defined in equation 2-66.

$$V_A = V(1-w) \quad \text{Equation 2-65}$$

$$T = R_T/(1-t) \quad \text{Equation 2-66}$$

The effective power P_E is correlated to thrust power P_T according to equation 2-67.

$$P_E = \frac{(1-w)/(1-t)}{P_T} \quad \text{Equation 2-67}$$

The hull efficiency η_H is defined according to equation 2-68.

$$\eta_H = (1-w)/(1-t) = P_E/P_T \quad \text{Equation 2-68}$$

The power delivered to the propeller P_D is defined in equation 2-69.

$$P_D = P_E/(\eta_H \eta_{OWE} \eta_R) \quad \text{Equation 2-69}$$

The shaft power P_S is defined in equation 2-70.

$$P_S = P_D/\eta_s \eta_b \quad \text{Equation 2-70}$$

Where: η_s is the sterntube seal efficiency and η_b the shaft bearing efficiency.

The shaft power P_S is related to the required brake power P_B from the vessel's power plant by the transmission efficiency η_t of the reduction gear or electrical

alternator and motor (assuming constant in off-design conditions) as defined in equation 2-71.

$$P_B = P_s / \eta_t \qquad \text{Equation 2-71}$$

The relationship between effective power P_E and the break power P_B required by the power plant is defined in equation 2-72.

$$P_B = P_E /(\eta_H \eta_{OWE} \eta_R \eta_s \eta_b \eta_t) \qquad \text{Equation 2-72}$$

2.5.2.4 Propeller open water characteristics module

The propeller module contains a proposed method [11] that contains the open water characteristics of the Wageningen B-series propellers. The effects of propeller cavitation and partial submergence have not been taken into account. The module produces the open water efficiency η_{OWE} of fixed pitch (*FPP*) Wageningen B-series propellers at off-design conditions. All equations are referred to the adopted method unless otherwise is stated within the content of this section. The method allows only first quadrant operation of the propeller (positive thrust and speed of advance), and for Reynolds number other than $2x10^6$ results need to be corrected (see equations 2-77 and 2-78).

The propeller's thrust and torque coefficients, K_T and K_Q respectively are expressed in polynomials (appendix F.2, table F.2) as functions of the advance ratio *J*, the propeller pitch to diameter ratio *P/D,* the propeller blade area ratio A_E/A_O, the blade number *Z*, the effect of Reynolds number and the thickness to chord length ratio t/c of the propeller's blades, as expressed in equations 2-73 and 2-74.

$$K_T = f_1(J, P/D, A_E/A_O, Z, Rn, t/c) \qquad \text{Equation 2-73}$$

$$K_Q = f_2(J, P/D, A_E/A_O, Z, Rn, t/c) \qquad \text{Equation 2-74}$$

To calculate the thrust and torque coefficients of the propeller the following relationships are proposed as expressed in equations 2-75 and 2-76.

$$K_T = \sum_{s.t.u.v} [C_{T\,s,t,u,v} (J)^s (P/D)^t (A_E/A_O)^u (Z)^v] \qquad \text{Equation 2-75}$$

$$K_Q = \sum_{s.t.u.v} [C_{Q\,s,t,u,v} (J)^s (P/D)^t (A_E/A_O)^u (Z)^v] \qquad \text{Equation 2-76}$$

For Reynolds number other than $2x10^6$ the thrust and torque coefficients are corrected according to the following proposed method [9].

$$K_{T-cor} = K_T + \Delta C_D 0.3 \frac{P c_{0.75} Z}{D^2} \quad \text{Equation 2-77}$$

$$K_{Q-cor} = K_Q - \Delta C_D 0.25 \frac{P c_{0.75} Z}{D^2} \quad \text{Equation 2-78}$$

Where: ΔC_D is the difference in drag coefficient of the propeller's profile section as defined in equation 2-79 [9], P is the propeller's pitch and $c_{0.75}$ is the propeller's blades chord length at 75% radius as defined in 2-80 [9].

$$\Delta C_D = (2 + 4((t/c)_{0.75})[0.003605 - (1.89 + \\ + 1.62 \log(c_{0.75} / k_p))^{-2.5}] \quad \text{Equation 2-79}$$

$$c_{0.75} = 2.073(A_E / A_O) D / Z \quad \text{Equation 2-80}$$

Where: $(t/c)_{0.75}$ is the thickness to chord length ratio at 75% of propeller's blade ratio as defined in equation 2-81 and k_p is the propeller's blade surface roughness (recommended value for new propellers is $3x10^{-5}$ m).

$$(t/c)_{0.75} = (0.0185 - 0.00125Z) D / c_{0.75} \quad \text{Equation 2-81}$$

To obtain the Reynolds number for the Wageningen B-series propellers at a specific operating condition equation 2-82 is suggested, and the number is calculated at 75% of the propeller radius.

$$Rn = \frac{c_{0.75} \sqrt{V_A^2 + (\pi N_S D)^2}}{\nu} \quad \text{Equation 2-82}$$

Where: N_S is the propeller's shaft rotational speed.

In order to be able to obtain the open water efficiency at any required off-design conditions a method [12] was applied, that uses the advance ratio as an iteration variable in the M-file. The advance ratio is programmed to iterate from 0 to 2 in increments of 0.0001 and by using equation 2-83 and 2-84 the propeller's shaft rotational speed N and the thrust produced by the propeller T_P, can be found.

$$N_S = \frac{V_A}{JD} \quad \text{Equation 2-83}$$

$$T_P = K_{T-cor} \rho_s D^4 {N_S}^2 \quad \text{Equation 2-84}$$

The iteration is programmed to stop when the thrust produced by the propeller matches the thrust required by the vessel to maintain its specified service speed, as defined in equation 2-85.

$$T_P = \frac{T}{N_{prop}}$$ Equation 2-85

Where: N_{prop} is the number of propellers installed on the vessel.

To obtain the propeller's open water efficiency equation 2-86 is applied, and the relationship between $K_{Q,}$ K_T, J and η_{OWE} can be seen in figure 2.3.

$$\eta_{OWE} = \frac{JK_{T-cor}}{2\pi K_{Q-cor}}$$ Equation 2-86

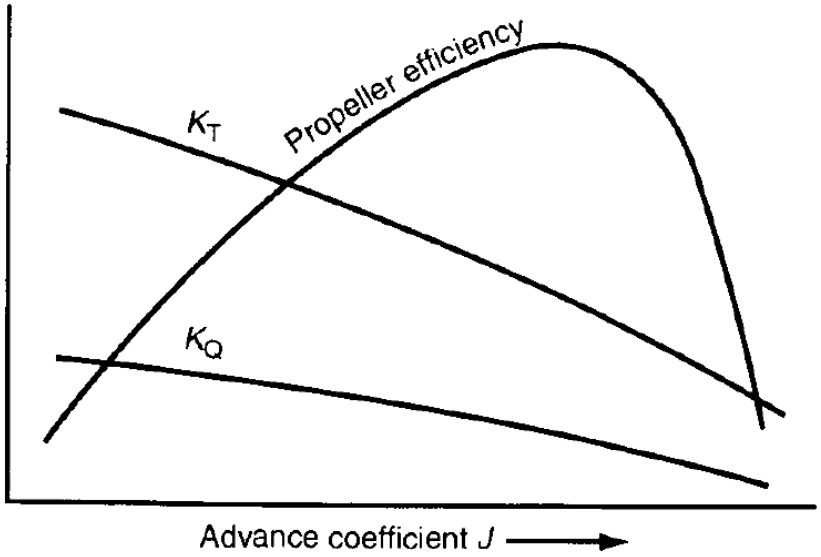

Figure 2.3: Typical propeller diagram that shows the relationship between $K_{Q,}$ K_T, J and η_{OWE}

The method can be used when the following propeller design parameters satisfy the conditions specified as:

- The number of propeller blades N can be between 2 and 7.
- The propeller's pitch to diameter ratio P/D can be between 0.5 and 1.4.
- The propeller's blade area ratio A_E/A_O can be between 0.3 and 1.05.
- Maximum marine vessel speed can be between 30 to 35 knots.

2.5.2.5 Hull fouling resistance module

A simplified method was adopted to calculate the increment of the vessel's resistance due to hull fouling or more practically hull roughness. The method was proposed by the ITTC [13], and the recommended guideline is to be used for hull roughness from 150 μm and higher. The method was tested by simulating a Destroyer, a RoPax ferry and a LNG carrier with a hull roughness value as low as 120 μm. The results (Appendix B.2 figures B.16, B.17 and B.18 respectively) showed that

the average difference in hull resistance increment (assuming the same increase in roughness for the bottom and the sides of the hull) when hull roughness increases from 120 μm to 150 μm is approximately 2% and when hull roughness increases from 150 μm to 180 μm is approximately 2.2%. The reason for testing the vessels with a hull roughness value lower than the recommended one is that average hull roughness for modern vessels has decreased and lies in the order of 90~125 μm [14]. The method is defined in a simple formula as presented in equation 2-87 and is incorporated in the vessel's total hull resistance (equation 2-43) as shown in equation 2-88.

$$C_{AA} = \frac{(0.105\sqrt[3]{k_h} - 0.005579)}{\sqrt[3]{L}} \qquad \text{Equation 2-87}$$

$$R_T = \tfrac{1}{2}\rho_s V^2 S_{tot}[C_F(1+k) + (C_A + C_{AA})] + Rw + nR_{bt} \qquad \text{Equation 2-88}$$

Where: k_h is the mean amplitude of the hull roughness.

2.5.2.6 Sea-wave resistance module

A simplified method [15] was introduced in the marine vessel power prediction model to predict the effect of sea-waves on the vessel's total resistance in open water, at a certain speed. Any effects on the vessel's resistance by motion responses (surging, swaying, heaving, pitching, rolling, yawing) due to sea-waves are not included at this stage in the current marine vessel power prediction model, and their direction when generated is assumed constant in a head direction towards the vessel's bow. The method is defined in equation 2-89, and the effect of sea waves in the total resistance (from equation 2-88) of the vessel is defined in equation 2-90.

$$R_{SW} = \tfrac{1}{2}\rho_s g\left[\sqrt[3]{\nabla\rho_s}\right]2\pi f_W h_W^2\left[\sqrt{\frac{\sqrt[3]{\nabla\rho_s}}{g}}\right][1+k] \qquad \text{Equation 2-89}$$

$$R_T = \tfrac{1}{2}\rho_s V^2 S_{tot}[C_F(1+k) + (C_A + C_{AA})] + Rw + n_{BTO}R_{bt} + R_{SW} \qquad \text{Equation 2-90}$$

Where: f_W is the sea-wave frequency and h_W is the significant height of the wave.

The module is supplied with data that provides the sea-wave frequency f_W and the significant height of the wave h_W according to sea-state number [16]. The data is presented in table 2.5.

Table 2.5: Sea-state number and corresponding significant wave height and sea-wave frequency [16]

Sea State Number	**Significant wave height, h_w (m)**	Sea-wave frequency, fW (Hz)
0-1	0.05	0.0
2	0.3	0.158
3	0.88	0.133
4	1.88	0.114
5	3.25	0.103
6	5.0	0.080
7	9.0	0.067
8	13.0	0.061

The adopted method does not intended at its current development stage of the model to accurately simulate the effects of sea-state on the hydrodynamic resistance of any simulated marine vessel as this would require a significant amount of time and effort beyond the scope of this research. By the use of the current method results of realistic magnitude can be obtained and the effects of different sea-state numbers on the hydrodynamic resistance of any simulated marine vessel can clearly be observed.

2.5.2.7 Wind resistance module

The task of the wind resistance module is to calculate the effect of the wind on the total resistance of the vessel in open water, at a certain speed. The method [17] that was implemented in *"Poseidon"* can be applied to a wide range of vessel types and provides the ability to take in account wind with direction other than head towards the vessel's bow, though the latter was not used in the case studies of the project. At the current development stage wind direction is assumed constant during the whole duration of a scheduled journey. The method is defined in equations 2-91 and 2-92 and the wind is assumed that affects the total resistance of the vessel from 10 meter above the water line.

$$R_{AA} = \tfrac{1}{2}\rho_{air} V_{\varepsilon}^2 A_L CD_l \frac{\cos\varepsilon}{1-\frac{\delta}{2}(1-\frac{CD_l}{CD_t})\sin^2\varepsilon} \qquad \text{Equation 2-91}$$

$$CD_l = \frac{A_L / A_F}{CD_{iAF}} \qquad \text{Equation 2-92}$$

Where: ρ_{air} is density of the air, V_{ε} is the apparent wind speed, A_L is the lateral projected area of the vessel, A_F is the frontal projected area of the vessel, CD_i is the non-dimensional drag in head wind, CD_t is the non-dimensional drag in

beam wind, ε is the apparent wind angle (0^o in head wind), δ is the cross-force parameter and CD_{iAF} is the longitudinal drag with respect to A_F.

The values for CD_t, CD_{iAF} and δ for different vessel types are given in figure 2.4 [17] and were not implemented in the code but they have to be inserted manually.

	CD_t	CD_{IAF}	δ
Car carrier	0.95	0.55	0.80
Cargo ship, container on deck, bridge aft	0.85	0.65/0.55	0.40
Containership, loaded	0.90	0.55	0.40
Destroyer	0.85	0.60	0.65
Diving support vessel	0.90	0.60	0.55
Drilling vessel	1.00	0.70–1.00	0.10
Ferry	0.90	0.45	0.80
Fishing vessel	0.95	0.70	0.40
LNG tanker	0.70	0.60	0.50
Offshore supply vessel	0.90	0.55	0.55
Passenger liner	0.90	0.40	0.80
Research vessel	0.85	0.55	0.60
Speed boat	0.90	0.55	0.60
Tanker, loaded	0.70	0.90	0.40
Tanker, in ballast	0.70	0.75	0.40
Tender	0.85	0.55	0.65

Figure 2.4: Values for CD_t, CD_{iAF} and δ for different vessel types [17]

To calculate the apparent wind speed V_ε and angle simple trigonometry was applied and was implemented in the model as described in figure 2.5 and defined in equations 2-93 and 2-94.

$$V_\varepsilon = \sqrt{(V_T \cos(\frac{\pi}{2} - \beta)^2 + (V_T \sin(\frac{\pi}{2} - \beta) + V)^2} \qquad \text{Equation 2-93}$$

$$\varepsilon = \arctan(\frac{V_T \sin(\pi/2 - \beta) + V}{V_T \cos(\pi/2 - \beta)}) \qquad \text{Equation 2-94}$$

Where: V_T is the true wind speed, V is the vessel's speed, β is the angle between the vessel's head direction and the true wind.

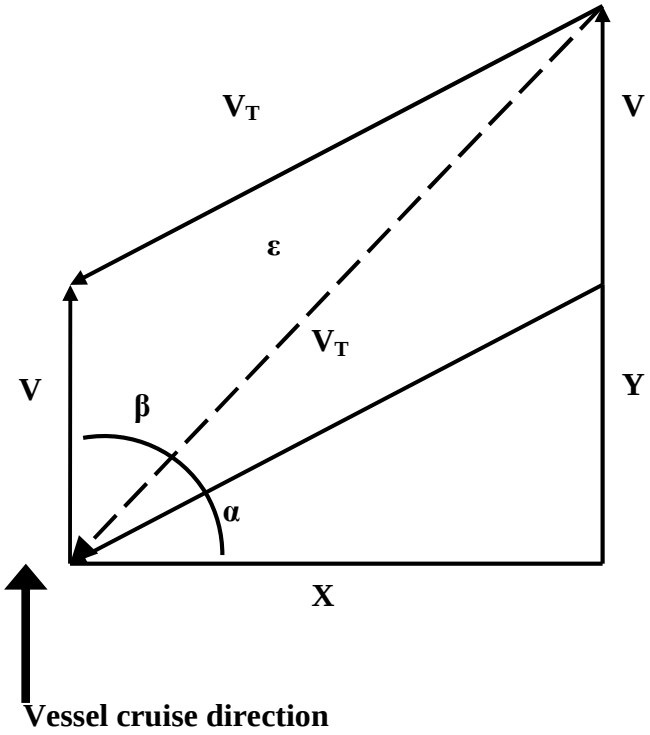

Figure 2.5: Vector components created by the travelling vessel and wind

The total resistance (from equation 2-90) of the vessel is affected by the effect of wind as defined in equation 2-95.

$$R_T = \tfrac{1}{2}\rho_s V^2 S_{tot}[C_F(1+k)+(C_A+C_{AA})]+Rw+ \\ +n_{BTO}R_{bt}+R_{SW}+R_{AA} \qquad \text{Equation 2-95}$$

The module is supplied with data that provides the true wind speed according to sea-state number [16]. The data is presented in table 2.6.

Table 2.6: Sea-state number and corresponding true wind speed [16]

Sea State Number	True wind speed, V_{wind} (m/s)
0-1	3.0
2	7.0
3	13.0
4	18.0
5	24.0
6	36.0
7	50.0
8	60.0

2.5.3 Model inputs and outputs

The model inputs are shown with and asterisk (*) in tables A.1 and A.2 in appendix A, in an exact manner as in the input file of the model. The sea-water density ρ_{sea} and sea-state number W_{sea} are handled by the journey management model (section 3.7.1.2). The outputs of the model are (at every time interval): the shaft rotational speed N_S, the vessel's speed V, the effective power P_E delivered by each propeller, the delivered power P_D to each propeller and the brake power P_B required by the vessel's power plant.

2.5.4 Ideal marine vessel trial conditions

The ideal marine vessel trial conditions are defined as [9]:

- No wind, current, waves or swell
- Deep water at 15 ^{o}C (ρ_s=1025 g/m^3).
- Clean hull and propeller with a surface in accordance with modern standards

2.6 Power Plant Operation Management Model

2.6.1 Introduction

The task of the power plant operation management model is to integrate the gas turbine models with the marine vessel power prediction model. It distributes the required brake power P_B by the marine vessel to the prime movers (if more than one) of the vessel's power plant, in accordance with its service speed V and weather conditions, handles the required service load P_{aux} from the vessel's power plant, defines the maximum turbine entry temperature (TET) that the prime movers are allowed to operate at, where extra power output is needed (i.e. adverse weather conditions, higher service speed, increased hull fouling) and in cases that increased resistance conditions are high enough to prohibit the vessel to obtain its specified service speed, it tests the maximum power output of the power plant at the specified ambient conditions and estimate the maximum speed that the vessel can travel up to.

It is composed of two modules:

- Power distribution module
- Power availability module

2.6.2 Modelling methodology

2.6.2.1 Power distribution module

In the case that the marine vessel's power plant is constituted by more than one prime mover the distribution of brake power P_B and service load P_{aux} required by the vessel under specified service conditions can be arranged according to the principal of IFEP system, to operate the lowest possible number of the installed prime movers N_{eng} where operational conditions allow. There are no limitations in the number of prime movers that the module can handle. When more than a single prime mover operates the required brake power is assumed that is distributed evenly as also the required service load as expressed in equation 2-96. The service load is assumed constant during the whole duration of the journey.

$$EP = \frac{P_B + P_{aux}}{N_{eng}} \qquad \text{Equation 2-96}$$

In the case that a vessel has a variable service speed profile (i.e. destroyer with 2 prime movers installed) and travels at a low speed requiring, at favourable weather conditions, only one prime mover to operate, if weather conditions become adverse then the module can accept the number of sea-state at which the second prime mover (boost) needs to be engaged and assume the vessel's sea-worthiness.

2.6.2.2 Power availability module

The power availability module uses the gas turbine performance module at every time interval, after the marine vessel power prediction model has calculated the required brake power P_B, to determine the maximum engine power EP available at the specified ambient conditions that the marine gas turbine under investigation can produce, and according to the arranged power distribution, ambient and weather conditions and hull fouling state, estimate the ability of the power to maintain the vessel's scheduled speed.

The maximum turbine entry temperature (TET) can be defined that the prime movers are allowed to operate up to. If the maximum available output power produced by the power plants is lower than the demand by the sum of the hydrodynamic and aerodynamic resistance of the vessel then the module calculates the maximum possible speed that the vessel can obtain. This is accomplished by iterating using the marine vessel power prediction model from zero speed (which can require a significant amount of power to maintain under adverse weather conditions) up to the

point where the vessel's speed matches approximately the maximum output power by the power plant.

The condition "approximately" is used in the previous phrase because the speed iteration step is programmed at 0.1 knots as a smaller iteration step would require a significant additional amount of computational time and in marine vessel trial reports, speed accuracy up to first decimal place is considered satisfactory [18].

2.6.2.3 Model inputs and outputs

The model inputs are: the maximum turbine entry temperature (*TET*) that the prime movers are allowed to operate up to, the service load (or auxiliary power) P_{aux} of the marine vessel, the number of prime movers of the vessel's power plant and the sea-state number that the boost prime mover is needed to be engaged, if the vessel has a variable operational profile.

2.7 Journey Management Model

2.7.1 Introduction

The journey management model which is integrated with the power plant operation model is composed of three modules:

- Journey schedule
- Ambient conditions management
- Engine parameters quantification

The journey schedule module handles the journey scheduled distance, the amount of the journey scheduled time, the time intervals that ambient conditions change and calculates the journey time prolongation in case the vessel is required to operate in increased resistance conditions (i.e. adverse weather conditions) in which the power plant's maximum power rating is below the power required by the vessel to maintain its scheduled service speed. The model provides two modes of operation, one mode for vessels with a constant service speed profile (i.e. ferries) and one mode for vessels with a variable service speed profile (i.e. naval vessels).

The ambient conditions management module handles the ambient temperature (air and sea) and sea-state profile at the specified time intervals during journey.

The engine parameters quantification module quantifies the essential gas turbine parameter products for the determination its life cycle direct operating costs (DOC)

which are, the hot section's blade creep life consumption, fuel consumption and the total emission quantities (NO_x, CO, CO_2 and UHC) produced by each of the prime movers (if more than one) after a scheduled journey. The model is integrated with the journey management model.

2.7.2 Modelling methodology

2.7.2.1 Journey schedule module

When a vessel with constant service speed profile is simulated the total journey distance S_j is determined by simply multiplying the journey schedule time t_T with the vessel's service speed V as expressed in equation 2-97.

$$S_j = Vt_T \qquad \text{Equation 2-97}$$

The principle idea remains the same when a vessel with variable service speed profile is simulated with the difference that the service speed needs to be specified at every time interval of the journey and the average service speed determines the journey distance as expressed in equation 2-98.

$$S_j = \left(\frac{\sum_n V_n}{\sum n}\right) t_T \qquad \text{Equation 2-98}$$

Where: n is the time interval number.

The time interval in which the ambient conditions change during a scheduled journey at the current stage of *"Poseidon"*, is fixed at 1 hour, and is implemented in the code in the form of iterations that the model needs to make in order to obtain the total scheduled journey distance.

The journey time prolongation is estimated, by recording the vessel's speed and the total distance that has covered at the end of every time interval. If the vessel is not able to obtain the required distance, at the scheduled journey time, then the program continues to iterate until the total distance in the last iteration equals or surpasses the scheduled one, as the time interval is fixed at 1 hour. If at the last iteration the distance is more that the scheduled one, the total journey time t_{T+a} is found between n_{max} and $n_{(max-1)}$ and is calculated as defined in equation 2-99 which subtracts the time that the vessel requires to cover the superfluous distance, and adjusts it to the time that

is required to cover the scheduled distance under journey average speed lower than its schedule one.

$$t_{T+a} = (t_j + t_a - 1) + [(t_j + t_a - \frac{S_a - S_j}{V_{LI}}) - (t_j + t_a - 1)] \qquad \text{Equation 2-99}$$

Where: t_j is the sum of total scheduled time intervals, t_a is the sum of total superfluous time intervals, S_a is the superfluous journey distance and V_{LI} is the vessel's speed at the last iteration

2.7.2.2 Ambient conditions module

The profile of ambient temperature T_{amb} of air during a full day cycle (i.e. 24 hours) is simulated by a proposed method [19] that recommends three cosine functions, each one representing a day period. The first period is defined from midnight to sunrise (t_d) (equation 2-100), the second period from t_d to the time of day that temperature peaks (t_p) (equation 2-101) and the third from t_p to midnight (equation 2-102).

$$T_{amb}(t) = T_m - T_{amp} \cos[\pi(t_d - t)/(24 + t_d - t_p)] \qquad \text{Equation 2-100}$$

$$T_{amb}(t) = T_m - T_{amp} \cos[\pi(t_p - t)/(t_p - t_d)] \qquad \text{Equation 2-101}$$

$$T_{amb}(t) = T_m - T_{amp} \cos[\pi(24 + t_d - t)/(24 + t_d - t_p)] \qquad \text{Equation 2-102}$$

Where: t is the actual time of the day, T_m is the mean daily temperature (equation 2-103) and T_{amp} is the amplitude of daily temperature variation (equation 2-104).

$$T_m = \frac{(T_{\min} + T_{\max})}{2} \qquad \text{Equation 2-103}$$

$$T_{amp} = \frac{(T_{\max} - T_{\min})}{2} \qquad \text{Equation 2-104}$$

The change in the actual day temperature is defined by the time interval step change.

The sea water temperature T_{sea} and sea-state W_{sea} profile can be defined manually by entering the correspondent value of the each one of the two variables for every time interval of the journey. T_{sea} can vary from 0 to 30 ^{o}C and W_{sea} from 0 to 8.

2.7.2.3 Engine parameters quantification module

To calculate the cumulative creep life consumption of the hot section rotor blade after a journey at t_j or (t_j+t_a), the linear damage summation law or Miner's law [4] was implemented as expressed in equations 2-105 and 2-106 respectively.

$$\underset{\max=1}{q_b} = \sum_n (1/t_f)_n \qquad \text{Equation 2-105}$$

$$\underset{\max=1}{q_b} = \sum_n (1/t_f)_n - [(1/t_f)_{\max(n)}(n - (t_j + t_a - \frac{S_j - S_a}{V_{LI}})] \qquad \text{Equation 2-106}$$

Where: q_b is the total blade life consumption ($q_{b,max}$=1) after a journey.

To calculate the products of the output parameters q_p of each of the prime movers of the simulated vessel after a journey at t_j or (t_j+t_a), equations 2-107 and 2-108 are recommended respectively.

$$q_p = \sum_n (y_n t_\phi) \qquad \text{Equation 2-107}$$

$$q_p = \sum_n (y_n t_\phi) - [y_{\max(n)}(t_j + t_a - \frac{S_a - S_j}{V_{LI}})t_\phi] \qquad \text{Equation 2-108}$$

Where: q_p is the quantity of the product of the output prime mover parameter after a journey, the subscript p identifies the quantity other than blade life consumption, y is the rate of the product of the output prime mover parameter and t_φ is the unit of time rate to quantity conversion factor.

2.7.3 Model inputs and outputs

The model input parameters are: the schedule time of journey t_T, the schedule distance S_j of journey, the service speed of the vessel at every time interval V_n in the case that the type of the simulated marine vessel has a variable service speed profile, the time of the day t_{start} that journey starts, the sunrise time of day t_d, the time of day that temperature peaks t_p, the minimum and maximum day temperature T_{min} and T_{max} respectively, the sea water temperature T_{sea} and the sea-state number W_{sea} at every time interval. The model output parameters are: the total journey time t_{T+a} and the quantity of the products of each of the operational prime mover(s) output parameters after a schedule journey, which are the mass fuel consumption q_{FF}, the hot section rotor's blade creep life consumption q_b, the mass quantity of nitric oxide (NO_x), carbon monoxide (CO), carbon dioxide (CO_2) and unburned hydrocarbons (UHC) exhaust emissions, q_{NOx}, q_{CO}, q_{CO2} and q_{UHC} respectively.

2.8 References

1. *"U.S Standard Atmosphere"*, U.S. Government Printing Office, Washington, D.C, 1976. Available at http://ntrs.nasa.gov/archive/nasa/casi.ntrs.nasa.gov

2. *"The Turbomatch Scheme for Aero/Industrial Gas Turbine Engine Design Point/ Off Design Performance Calculation"*, Cranfield University, October 1999.

3. Lefebvre, A.H., "*Fuel Effects on Gas Turbine Combustion"*, Performed by: School of Mechanical Engineering, Purdue University, West Lafayette IN 47907, Controlled by: Aero Propulsion Laboratory, Air Force Wright Aeronautical Laboratories, Wright Paterson Air Force Base, Ohio 45433, Status: Unlimited distribution, January 1983.

4. Torres, G.O., *"Gas Turbine Hot Section Life Usage Considerations"*, MSc Thesis, Cranfield University, Academic Year 1986-1987.

5. Holtrop, J., *"A Statistical Re-analysis of Resistance and Propulsion"*, International Shipbuilding Progress, Vol. 31, Part 363, pp 272-276, July 1984.

6. *"The Specialist Committee on Powering Performance Prediction"*, Proceedings of the 24th International Towing Tank Conference (ITTC), UK, 2005.

7. *"Principles of Naval Architecture, Resistance, Propulsion and Vibration"*, Society of Naval Architects and Marine Engineers, ISBN No. 0-939772-01-5, Vol. 2, pp 58-59.

8. *"Applicability Range of Holtrop-1984 Method"*, A HydroComp Technical Report, 2003.

9. Holtrop, J., and Mennen, G.G.J., *"An Approximate Power Prediction Method"*, International Shipbuilding Progress, Vol. 29, Part 335 pp 166-170, July 1982.

10. *"Ship Design and Construction"*, Society of Naval Architects and Marine Engineers, ISBN No. 0-939772-41-4, Vol. 1, Chapter 11, pp 28-31.

11. Oosterveld, M.W.C, and Oossanen, P. van, *"Further Computer Analysed Data of the Wageningen B-screw Series"*, International Ship Building Progress, Vol. 22, Part 251, pp 251-262, July 1975.

12. Hugel, M.A., *"An Evaluation of Propulsors for Several Navy Ships"*, MSc Thesis, Massachusetts Institute of Technology, Academic Year 1992-1993.

13. *"The Specialist Committee on Powering Performance Prediction"*, Proceedings of the 15th International Towing Tank Conference (ITTC), The Netherlands, 1978.

14. Townsin, R.L., Byrne, D., Svensen, T.E. and Milne, A., *"Fuel Economy due to Improvements in Ship Hull Roughness 1976-1986"*, International Shipbuilding Progress, Vol. 33, Part 383, pp 127-130, July 1986.

15. *www.tudelft.nl (*The source of the reference has been withdrawn from the world wide web)

16. "*Principles of Naval Architecture, Motion in Waves and Controllability*", Society of Naval Architects and Marine Engineers, ISBN No. 0-939772-02-3, Vol. 3, pp 28.

17. Schneekluth, H. and Bertram, V., **"***Ship Design for Efficiency and Economy, Second Edition"*, Butterworth and Heinemann, ISBN No. 0-7506 4132-9, Chapter 6, pp 201-202, 1998.

18. www.kyma.no/sitefiles/site59/files/files/KSP_Trial_Report.pdf

19. Huld, A.T., Marcel, Š., Dunlop, D.E. and Micale, F., *"Estimating Average Daytime and Daily Temperature profiles within Europe"*, Environmental Modelling and Software 21, pp 1650-1661, 2006.

3 Implementation of the Economic & Risk Part of *TERA* Method

3.1 Introduction

This chapter describes the methods and the tools that were used to develop and create the numerical model that forms the economic and risk part of the Technoeconomic Environmental and Risk Analysis (*TERA*) method. The model is described by introducing its task, its composition and any definitions that apply in this chapter. Modelling methodology is then analyzed, where the model's mathematical expressions, functions and capabilities are presented. The model inputs and outputs are finally described.

3.2 Life Cycle Costs Model

3.2.1 Introduction

The task of the life cycle costs model is to calculate the net present cost (*NPC*) of the direct operating cost (*DOC*) of the candidate marine vessel's power plant throughout its operational life cycle. The life cycle costs model is composed of the following modules:

- Life cycle
- Capital related costs
- Maintenance cost
- Taxed emissions and fuel cost
- Net present cost (*NPC*)
- Random numbers generator
- Normal distribution

It needs to be mentioned that wherever the word "concept" is mentioned in the next section (3.2.2), it describes a function without the incorporation of the risk element and the function is defined with it later in the chapter.

3.2.2 Modelling methodology

3.2.2.1 Life cycle

The life cycle module defines the operational life time of the vessel and the time interval that the vessel's hull average roughness amplitude is restored to its design value. The assumptions are that the vessel has an operational life time of thirty years and hull fouling increases in five annual steps but remains constant between them. For each prime mover that composes the marine vessel's power plant the prime mover's quantified output parameters (section 2.7.3) are produced by using "*Poseidon*" for two data sets of five scheduled journeys (i.e. the format can be seen in Appendix D.5, tables D.1 to D.5 for first data set and tables D.6 to D.10 for second data set).

Each set contains the output parameters that are obtained under a certain weather profile that the vessel is operated under, and each of the schedule journeys of the data set represents a certain value of hull roughness due to fouling which increases annually from year one to year five in annual steps. After every five year hull fouling cycle until year thirty, the marine vessel is assumed that has been dry-docked and starts a new hull fouling cycle where its average hull roughness amplitude is restored back to its design value. The concept of calculating the annual operational time t_{annual} of each prime mover is defined by its operational time per scheduled journey t_{op} and the annual number of scheduled journeys N_{asj} as described in equation 3-1.

$$t_{annual} = t_{op} N_{asj} \qquad \text{Equation 3-1}$$

3.2.2.2 Maintenance cost

The maintenance cost module is constructed by utilising a proposed method [1] that is primarily applied on aircraft turboprop-turbofan engines. The decision to adopt the mentioned method is based on the assumption that the marine gas turbines investigated in this project are aero-derivative and the fact that the design principles between aero-derivative gas turbines incorporating a power turbine and aircraft turboprop aircraft engines are very similar. All equations are referred to the adopted method unless otherwise is stated within the content of this section.

The engine maintenance hours per operational hour MHR_{mengbl} is defined in equation 3-2. When the method is applied to turbofan engines the equation presented below is modified to accommodate thrust, but as it is of no usage in this research consequently is not presented.

$$MHR_{mengbl} = (0.4956 + 0.0532\{\frac{(1.341EP_{DP})}{1000}\})(\frac{1100}{Hem}) + 0.1 \qquad \text{Equation 3-2}$$

Where: EP_{DP} is the design point prime mover power output (kW) and *Hem* is the number of hours between engine overhaul.

The concept of calculating the number of hours between engine overhaul is defined in equation 3-3, suggested by the author.

$$Hem = \frac{t_{op}}{q_b} \qquad \text{Equation 3-3}$$

The maintenance labour cost for every scheduled journey $C_{lab/eng}$ is defined in equation 3-4.

$$C_{lab/eng/sj} = 1.03(1.3)(MHR_{mengbl})(R_{leng})(t_{op}) \qquad \text{Equation 3-4}$$

Where: R_{leng} is the maintenance labour rate per hour.

The factor that depends on the number of hours between engine overhaul K_{Hem} is defined in equation 3-5.

$$K_{Hem} = 0.021(\frac{Hem}{100}) + 0.164 \qquad \text{Equation 3-5}$$

The cost of maintenance materials for each prime mover per hour of scheduled journey $C_{mat/\text{engb/hr}}$ is defined in equation 3-6.

$$C_{mat/eng/hr} = [(5.43 \times 10^{-5} PMC)(ESPPF) - 0.47](\frac{1}{K_{Hem}}) \qquad \text{Equation 3-6}$$

Where: *PMC* is the actual prime mover purchase cost (or capital cost) as defined in section 3.2.2.4 and *ESPPF* is the spare parts cost factor (i.e. if the cost of a spare part is the same to its proportion on the cost of a new prime mover then *ESPPF* = 1).

The cost of maintenance materials for each prime mover for every scheduled journey is defined in equation 3-7.

$$C_{mat/eng/sj} = 1.339(C_{mat/eng/hr})(t_{op}) \qquad \text{Equation 3-7}$$

The cost of the maintenance administrative, logistics and required energy (i.e. generators operation) costs for every scheduled journey C_{amb} can be estimated by using equation 3-8.

$$C_{amb} = 1.03[(F_{amb/lab})(MHR_{mengbl})(R_{leng}) + \\ + (F_{amb/mat})(C_{mat/eng/hr})](t_{op})$$ Equation 3-8

Where: $F_{amb/lab}$ and $F_{amb/mat}$ are overhead labour and materials distribution factors respectively. The range of $F_{amb/lab}$ and $F_{amb/mat}$ for a certain type of prime movers installed in a fleet of vessels that are utilised for commercial purposes is 1.0-1.4 and 0.3-0.7 respectively.

The annual maintenance cost is defined in equation 3-9.

$$C_{Ma\,int} = [(C_{lab/eng/sj} + C_{mat/eng/sj} + C_{amb})/(t_{op})](t_{annual})$$ Equation 3-9

3.2.2.3 Taxed emissions and fuel cost

The taxed emissions and fuel cost module calculates the cost of the exhaust emissions produced and the fuel consumed by each of the operating prime movers (if more than one) per annum. The module contains a gas turbine combustor technology factor K_{tech} that can be adjusted to approximately simulate exhaust emissions quantities produced by different combustor technologies (i.e. conventional, dry low-emissions etc.) or by different fuels (i.e. distillate diesel, natural gas etc.), without the necessity of producing and tabulating exhaust emission results (as described in chapter 2, section 2.3) more than once according to the supposed case study's requirements, for each simulated marine gas turbine. The concept of calculating the annual cost of exhaust emissions and fuel consumed quantities for each prime mover is defined in equation 3-10 [2].

$$C_p = K_{tech} q_p P_p N_{asj}$$ Equation 3-10

Where: C_p is the annual cost of the quantity and P_p is the cost of the quantity per unit mass. The subscript p represents the identity of the quantity (chapter 2, section 2.7.3). When the equation is used for fuel quantity, K_{tech} is not applied.

3.2.2.4 Capital related costs

The capital related costs module adopts a method [2], which has been modified in accordance with requirements of the project, to calculate the costs that are assumed are related to the initial purchase cost of the prime mover and need to be taken into account before investing on a particular prime mover. All equations are referred to the adopted method unless otherwise is stated within the content of this section. The module is structured to accept a reference initial prime mover purchase cost *IPMC*,

and in the case that prime movers of different *IPMC* (i.e. different thermodynamic cycle, output power etc.) are compared then the estimated percentage difference PD_0 in the initial purchase cost can be entered, as also the estimated percentage difference PD_1 due to a different technology component (i.e. conventional or dry low-emissions combustor). The concept of calculating the actual purchase cost (or capital cost) of the prime mover *PMC* is defined in equations 3-11, 3-12 proposed by the author and 3-13 [2].

$$PMC_0 = IPMC + [(IPMC)(PD_0)] \quad \text{Equation 3-11}$$

$$PMC_1 = PMC_0 + [(PMC_0)(PD_1)] \quad \text{Equation 3-12}$$

$$PMC = PMC_1(1 + \frac{t_{down}}{Hem + t_{down}}) \quad \text{Equation 3-13}$$

Where: PMC_0 is the cost of the prime mover derived from the percentage difference from the cost of the reference prime mover, PMC_1 is the estimated cost of the prime mover due to different technology components, PD_0 is the estimated percentage difference of cost from the reference prime mover, PD_1 is the estimated percentage difference cost due to different technology components and t_{down} is the downtime of the prime mover subtracted from t_{annual}.

The prime mover downtime t_{down} is calculated from the concept of the assumed prime mover availability as defined in equation 3-14 proposed by the author.

$$t_{down} = \frac{t_{annual}(100 - PD_{AVLB})}{100} \quad \text{Equation 3-14}$$

Where: PD_{AVLB} is the prime mover availability percentage per annum.

The annual interest cost C_{INT} on the actual prime mover purchase cost is defined in equation 3-15.

$$C_{INT} = (IR)(PMC) \quad \text{Equation 3-15}$$

Where: *IR* is the interest rate for the overall operational life of the vessel.

The annual insurance cost C_{INS} on the actual prime mover purchase cost is defined in equation 3-16.

$$C_{INS} = (ISR)(PMC) \quad \text{Equation 3-16}$$

Where: *ISR* is the insurance rate.

3.2.2.5 Net present cost (*NPC*)

The direct operating cost *DOC* for each prime mover per annum is defined in equation 3-17 [2].

$$DOC = (1.05C_F + C_{NOx} + C_{CO} + C_{CO2} + \\ + C_{UHC} + C_{INT} + C_{INS} + C_{Ma\,int}) \quad \text{Equation 3-17}$$

Where: C_F is the annual cost of fuel and is multiplied by a factor of 1.05 to reflect logistics and handling costs, C_{NOx} is the annual NO_x emissions cost, C_{CO} is the annual CO emissions cost, C_{CO2} is the annual CO_2 emissions cost and C_{UHC} is the annual UHC emissions cost.

The net present cost for each prime mover throughout its operational life cycle is defined in equation 3-18 [2].

$$NPC = PMC + \sum_{i=1}^{30} \frac{(DOC)_i}{(1+IR)^i} \quad \text{Equation 3-18}$$

Where: i is the number of years in service.

3.2.2.6 Random numbers generator

The modelling of the random numbers generator module is derived from an existing method [2] in which the generation of normal random variables is obtained by the use of discrete uniformly distributed pseudo-random numbers that arrange the output value of the variable with a standard deviation between maximum and minimum value that is arranged by eleven intervals. All equations are referred to the adopted method unless otherwise is stated within the content of this section. The standard deviation intervals are defined in equation 3-19.

$$
\left.
\begin{aligned}
SD &= \frac{(v_{\max} - v_{\min})}{6} \\
I_1 &= v_{\min} \\
I_2 &= v_{\min} + SD \\
I_3 &= v_{\min} + 2(SD) \\
I_4 &= v_{\min} + 2.5(SD) \\
I_5 &= v_{\min} + 3(SD) \\
I_6 &= v_{\min} + 3.5(SD) \\
I_7 &= v_{\min} + 4(SD) \\
I_8 &= v_{\min} + 4.5(SD) \\
I_9 &= v_{\min} + 5(SD) \\
I_{10} &= v_{\min} + 5.5(SD) \\
I_{11} &= v_{\min} + 6(SD)
\end{aligned}
\right\}
$$

Equation 3-19

Where: SD is the standard deviation value, v_{max} is the maximum value of the variable, v_{min} is the minimum value of the variable and $I_{1,\ 2,\ldots,11}$ is the value of the variable at every interval number.

The generation of the pseudo-random numbers is accomplished by the use of an appropriate MATLAB function that generates uniformly distributed pseudo-random numbers between zero and one. The output value of the variable I is calculated at the last iteration of a series of fifty thousand pseudo-random number generation attempts as it is described in table 3.1, in which x is the pseudo-random number's value.

Table 3.1: The relationship between the range of the values of pseudo-random number x and number of interval I.

x	≤0.005	≤0.015	≤0.085	≤0.155	≤0.325	≤0.495	≤0.665	≤0.835	≤0.905	≤0.985	<1.0
I	I_1	I_2	I_3	I_4	I_5	I_6	I_7	I_8	I_9	I_{10}	I_{11}

The module is incorporated within the life costs model code as expressed in equation 3-20, and when the cost of the prime mover's output quantity per unit mass P_p is stochastically estimated then the minimum and maximum cost $P_{p\text{-}min}$ and $P_{p\text{-}max}$ respectively, of the quantity per unit mass needs to be entered (see also equation 3-10)

$$I = "name"(v_{\min}, v_{\max}) \qquad \text{Equation 3-20}$$

Where: "*name*" is the call name of the function.

Weather probability

The random numbers generator module is used to introduce at this preliminary stage of the *TERA* for marine gas turbines the element of forecasting the annual journey weather conditions. The method was proposed by the author. As it is described in section 3.2.2.1 the life cycle costs model uses results from two data sets that each one represents a certain weather profile, so the random numbers generator module is used to estimate the amount of total journeys thus the annual operational time of each of the prime movers per annum under each of the two weather profiles. This is calculated by using equation 3-20 where v_{min} and v_{max} are given values of zero and one respectively as expressed in equation 3-21.

$$I_{jd} = "name"(0,1) \qquad \text{Equation 3-21}$$

Where: I_{jd} is the journey distribution risk factor.

Then the annual operational time of the prime mover under each of the two weather profiles and the same hull roughness amplitude if they are named $t_{annual\text{-}WP1}$ and $t_{annual\text{-}WP2}$ respectively is expressed in equations 3-22 and 3-23.

$$t_{annual-WP1} = t_{op}(1 - I_{jd})N_{asj} \qquad \text{Equation 3-22}$$

$$t_{annual-WP2} = t_{op}(I_{jd})N_{asj} \qquad \text{Equation 3-23}$$

The total average operational time of each of the prime movers per journey is then defined in equation 3-24, which is used in equation 3-1 to substitute t_{op}, in order to obtain the annual operational time of the prime mover t_{annual}.

$$t_{op-ave} = \frac{t_{annual-WP1} + t_{annual-WP2}}{N_{asj}} \qquad \text{Equation 3-24}$$

Prime mover output parameters quantification per annum

The calculation of the prime mover's output quantities $q_{annual\text{-}p}$ per annum as also the hours between engine overhaul *Hem* are calculated first by deriving the annual amount of the quantity produced under each weather profile with the same hull roughness amplitude as defined in equations 3-25 and 3-26 proposed by the author.

$$q_{annual-p(b)1} = (q_{p(b)1})(t_{annual-WP1}) \qquad \text{Equation 3-25}$$

$$q_{annual-p(b)2} = (q_{p(b)2})(t_{annual-WP2}) \qquad \text{Equation 3-26}$$

Where: $q_{annual\text{-}p(b)1}$ and $q_{annual\text{-}p(b)2}$ apply for both the prime movers annual output quantities (subscript *p* can be fuel consumption *(FF), NOx, CO, CO_2, UHC*) and hot section rotor blade's life consumption.

The total annual prime mover output quantities $q_{annual\text{-}p}$ and the hours between engine overhaul *Hem* are defined in equations 3-27 and 3-28 respectively proposed by the author.

$$q_{annual-p} = q_{annual-p1} + q_{annual-p2} \quad \text{Equation 3-27}$$

$$Hem = \frac{(t_{op-ave})N_{asj}}{q_{annual-b1} + q_{annual-b2}} \quad \text{Equation 3-28}$$

Then equation 3-10 is implemented in the M-code as defined in equation 3-29.

$$C_p = K_{tech} q_{annual-p}[P_p = "name"(P_{p-\min}, P_{p-\max})]N_{asj} \quad \text{Equation 3-29}$$

Where: $P_{p\text{-}min}$ and $P_{p\text{-}max}$ is the minimum and maximum estimated cost of the prime mover's output quantity per unit mass (fuel is entered per unit volume and is converted in unit mass, as defined in chapter 6, equation 6-1).

Downtime probability

Equation 3-14 that defines the downtime per annum of each of the prime movers is re-expressed with the incorporation of the random numbers generator module in equation 3-30 proposed by the author.

$$t_{down} = \frac{t_{annual}\{100 - [PD_{AVLB} = "name"(PD_{AVLB-\min}, PD_{AVLB-\max})]\}}{100} \quad \text{Equation 3-30}$$

Where: $PD_{AVLB\text{-}min}$ and $PD_{AVLB\text{-}max}$ are the minimum and maximum percentage availability of the prime mover per annum respectively.

Prime mover actual purchase cost probability

If the prime mover actual purchase cost is unknown comparing to the cost of a reference prime mover the random numbers generator module is incorporated by re-expressing equations 3-11 and 3-12 proposed by the author.

$$PMC_0 = IPMC + \{(IPMC)[PD_0 = "name"(PD_{0-\min}, PD_{0-\max})]\} \quad \text{Equation 3-31}$$

$$PMC_1 = PMC_0 + \{(PMC_0)[PD_1 = "name"(PD_{1-\min}, PD_{1-\max})]\} \quad \text{Equation 3-32}$$

Where: $PD_{0\text{-}min}$ and $PD_{0\text{-}max}$ are the estimated minimum and maximum percentage difference of cost from the reference prime mover respectively, $PD_{1\text{-}min}$ and $PD_{1\text{-}max}$ are the estimated minimum and maximum percentage difference of cost due different technology components respectively.

Interest rate probability

The interest rate *IR* (equation 3-15) is assumed steady for the thirty years of the operational life of the marine vessel and randomly changes at every risk scenario as it is explained in section 3.2.2.7. The annual interest cost C_{INT} is re-expressed in equation 3-33 [2].

$$C_{INT} = [IR = "name"(IR_{\min}, IR_{\max})](PMC) \qquad \text{Equation 3-33}$$

Where: IR_{min} and IR_{max} are the minimum and maximum interest rate for the overall operational life of the vessel respectively.

3.2.2.7 Normal Distribution

The normal distribution module is derived from a proposed method [2] and its use has been extended not only to calculate the probable values of the *NPC* of the power plant but also the probable values of cost of NO_x, *CO*, CO_2 and *UHC* emissions, maintenance cost and fuel cost. The module records the value of each of the prime mover life cycle cost components including the *NPC* at every iteration-which represents a risk scenario- in single dimensional arrays, where the standard deviation of each of the components is obtained, by subtracting the minimum recorded value of the cost component from the maximum one and dividing the outcome value with the number of intervals which are eleven. The value of the cost component at every interval (iteration begins from interval one) of the distribution is calculated by counting the number of values (probability) N_{prob} of the cost component that satisfy the following condition as expressed in equation 3-34 [2].

$$\left.\begin{array}{l} IF \ldots A(J) \geq A_{\min} + (I_n - 1)(NDSD) \\ \& \\ IF \ldots A(J) < A_{\min} + I_n(NDSD) \end{array}\right\} \qquad \text{Equation 3-34}$$

Where: *A* is the one dimensional array that the cost component values are recorded in, *J* is the position number of the value of the cost component at every risk scenario, A_{min} is the first value (J=1) of the cost component in the array, I_n is

the number of the interval of the distribution and *NDSD* is the standard deviation of the distribution.

The value of the cost component of the distribution *C*, the probability of the value of the cost component N_{prob} and the cumulative probability N_{sum} at every interval are defined in equation 3-35, 3-36 and 3-37 respectively [2].

$$C = A_{\min} + (I_n - 1)(NDSD) + (NDSD/2) \quad \text{Equation 3-35}$$

$$N_{prob} = Value\ of\ J \quad \text{Equation 3-36}$$

$$N_{sum} = \sum_{n=1}^{11} J_n \quad \text{Equation 3-37}$$

3.2.3 Economic and risk analysis of power plant

The modelling methodology (sections 3.2.2.1-6) applies for the economic and risk analysis of a single prime mover. To perform an economic and risk analysis for the power plant then the output quantified parameters are entered for each of the prime movers separately, and the program uses the same number of risk scenarios for every prime mover of the power plant. The values of each of the cost components of all prime movers are added together at every value of *J* in an array (as described in 3.2.2.7) so the array still has the same number of values as the number of risk scenarios but every value responds to all prime movers of the power plant. Then the normal distribution module operates as described in section 3.2.2.7.

3.2.4 Model inputs and outputs

3.2.4.1 Economic and risk related input parameters

The economic and risk input parameters that the model requires in order to operate are: the reference initial prime mover purchase cost *IPMC*, the maintenance labour rate R_{leng} , the insurance rate *ISR*, the estimated minimum and maximum percentage difference of cost from the reference prime mover $PD_{0\text{-}min}$ and $PD_{0\text{-}max}$ respectively, the estimated minimum and maximum percentage difference of cost due different technology components $PD_{1\text{-}min}$ and $PD_{1\text{-}max}$ respectively, the estimated minimum and maximum fuel cost per unit volume $P_{FF\text{-}min}$ and $P_{FF\text{-}max}$ respectively, the minimum and maximum interest rate IR_{min} and IR_{max} respectively, the minimum and maximum NO_x emission tax cost per unit mass $P_{NOx\text{-}min}$ and $P_{NOx\text{-}max}$ respectively, the minimum and maximum *CO* emission tax cost per unit mass $P_{CO\text{-}min}$ and $P_{CO\text{-}max}$ respectively, the

minimum and maximum CO_2 emission tax cost per unit mass $P_{CO2\text{-}min}$ and $P_{CO2\text{-}max}$ respectively, the minimum and maximum UHC emission tax cost per unit mass $P_{UHC\text{-}min}$ and $P_{UHC\text{-}max}$ respectively, the spare parts cost factor $ESPPF$ and the number of risk scenarios.

3.2.4.2 Technical related input parameters

The technical input parameters that the model requires in order to operate are: the prime mover's design point output power EP_{DP} (kW), the estimated minimum and maximum annual percentage availability $PD_{AVLB\text{-}min}$ and $PD_{AVLB\text{-}max}$ respectively, the prime mover quantified output parameters for every scheduled journey of the two sets of journeys each under a certain weather profile (every set is composed of 5 journeys with increasing hull roughness amplitude due to fouling) which are the mass fuel consumption q_{FF}, the hot section rotor's blade creep life consumption q_b, the mass quantity of nitric oxide (NO_x), carbon monoxide (CO), carbon dioxide (CO_2) and unburned hydrocarbons (UHC) exhaust emissions, q_{NOx}, q_{CO}, q_{CO2} and q_{UHC} respectively, the prime mover operational time t_{op} in every journey and the annual number of scheduled journeys N_{asj}.

3.2.4.3 Overall output parameters

The model's output parameters which apply for the life cycle of the power plant are the probability normal distribution and the cumulative probability normal distribution of: the net present cost (NPC), the maintenance cost and the cost of each of the taxed emissions (NO_x, CO, CO_2, UHC) separately.

3.3 References

1. Roskam, J., *"Airplane Design Part VIII; Airplane Cost Estimation: Design, Development, Manufacturing and Operating"*, Roskam Aviation and Engineering Corporation, ISBN No: 1-8848-8555-1, pp 85-102, 1990.
2. Pascovici, D., Colmenares, F., *"A Technoeconomic and Risk Model"*, VITAL Project, Cranfield University, 2006.

4 *TERA* Case Studies Dataset: The Simulated Marine Gas Turbines

4.1 Introduction

This chapter starts with a general overview of the gas turbine thermodynamic cycles that are incorporated in the simulated marine gas turbines in the case studies of this project. The chapter continues with definitions and assumption regarding the derivation of the off-design performance of the engines which are associated with the off-design variables range (turbine entry and ambient temperature as ambient pressure is used as a constant) and with the common cycle design and component performance parameters that the marine gas turbines were simulated at design-point. Then the design-point and off-design performance of the simulated gas turbines is separately presented, including any background information regarding reference existing gas turbines and technical description associated with their operation.

The hot section rotor blade creep life dataset is then presented following the gas turbine performance where essential definitions are mentioned regarding any assumptions made for the calculation of the hot section rotor dimensions and design-point turbine rotational speed (for each of the simulated gas turbines) required by the hot section rotor blade creep life model, in order to obtain the required design-point blade life time to failure. The blade material data, the gas-path sizing methodology adopted and the results of the hot section rotor dimensions and design-point turbine rotational speed are consequently presented.

The gas turbine exhaust emissions dataset is presented, starting with an overview on the generation mechanism principles of the emission quantities considered in this project (NO_x, *CO*, *UHC* and CO_2). The calculation procedure and the results of the design-point emissions index calibration are described and presented respectively, for both conventional and dry-low emissions combustors and for both distillate and natural gas assumed as combustion fuels. Finally the off-design exhaust emission quantity rates are presented.

4.2 General Overview of the Gas Turbine Cycles

4.2.1 Simple cycle

The simple cycle (figures 4.1 & 4.2) is the fundamental gas turbine cycle where the working fluid is compressed in the compressor(s), mixed with fuel and heated in the combustor and then is expanded by the turbine(s), where the power produced is used to power the compressor(s) and the remaining is used as an output.

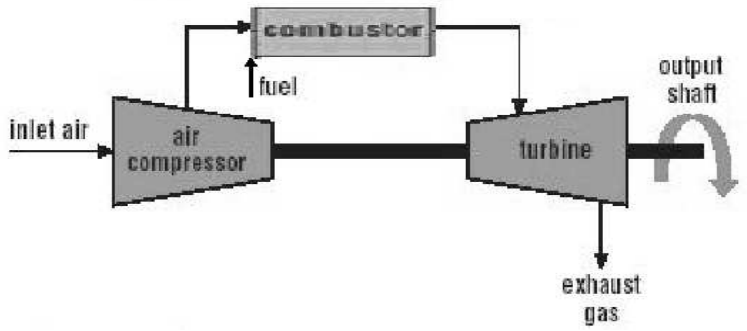

Figure 4.1: Simple cycle gas turbine in a single shaft configuration [1]

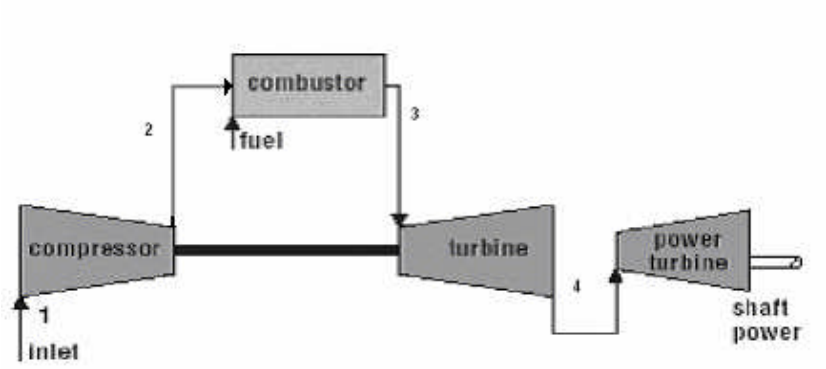

Figure 4.2: Simple cycle gas turbine in a two shaft configuration [1]

The basic shaft configuration is the single shaft (figure 4.1) where the output power shaft is structurally coupled on the turbine of the gas generator. This arrangement is almost exclusively used for power generation applications as the gas generator rotates at a constant rotational speed, irrelevantly of the power output requirement. The installation of a free power turbine (figure 4.2) enchases the part load thermal efficiency of the cycle as the gas generator shaft is independent of the aerodynamically coupled power turbine which for power generation needs to rotate at a constant speed. When the gas turbine is required to operate at part load the rotational speed of the compressor of the gas generator reduces and this results in higher working fluid mass flow, pressure ratio and temperature which reduces the required power by the compressor unlike with a single shaft configuration where at part load

the constant rotational speed of the compressor of the gas generator does not reduce its power requirements as significantly and thermal efficiency drops more rapidly [2]. Also the power turbine provides the advantage of having high torque at low rotational speeds [3], which makes the starting of the engine easier as the low and high pressure turbomachinery can reach their autonomous operational points without taking in consideration the high inertia of the rotating machinery of the coupled electrical generator of the marine vessel's propulsion system.

At high total compression pressure ratios the compression can be split between two compressors, a low pressure *LPC* and a high pressure compressor *HPC*. The advantages are that the high pressure compressor can rotate at higher rotational speeds and this provides the advantage that it can be designed with larger gas path area, where in a single compressor especially at the last stages of the compression there would be a loss in efficiency due to aerodynamic restrains that are created from the small height of the annulus area of the gas path. The low and high pressure compressor configuration can result in a shorter length gas turbine. At part load conditions the pressure ratio across the low pressure turbine *LPT* falls more rapidly than across the high pressure turbine *HPT*, and if the *LPT* is chocked then the *HPT* does not experience any change in its non dimensional flow or pressure ratio [4]. In general at part load the high pressure shaft does not experience fluctuations in rotational speed as high as the low pressure shaft. Overall there are not significant differences in thermal efficiency at design-point or off-design between the single and the two shaft arrangement of the gas generator.

At a specified turbine entry temperature (*TET*) the optimum total compression pressure ratio (*PR*) for optimum thermal efficiency η_{th} is higher than that for specific power [4], though specific power thus the dimensions of the gas turbine is not a major restrain factor on the marine vessels that take part in the case studies of this project. The optimum thermal efficiency of the cycle is obtained at the point where the temperature difference between the compressor outlet temperature and the combustor outlet temperature divided by the exhaust gas temperature reaches a minimum value, which is simply translated as the minimum wasted amount of heat input. The optimum specific power is obtained when the difference between the compressor outlet temperature and the combustor outlet temperature subtracted by the exhaust gas

temperature reaches a maximum value, which can be adjusted primarily by reducing the power requirements of the compressor.

4.2.2 Intercooled cycle

The intercooled cycle (figure 4.3) incorporates an intercooler (more than one can be considered) at a point during the compression process. The intercooler reduces the work that needs to be utilized by the high pressure compressor turbine in order to further compress the working fluid and for the same pressure ratio without any intercooling the working fluid requires less volume to be compressed.

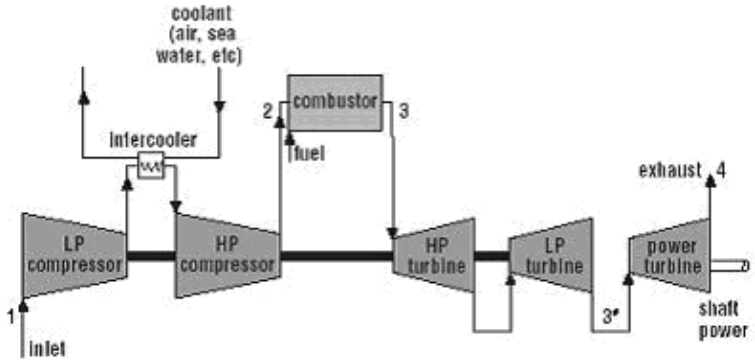

Figure 4.3: Intercooled cycle in a three shaft configuration [1]

An advantage of an intercooled gas turbine comparing with a simple cycle that has the same power output, pressure ratio, turbine entry temperature and component efficiencies is that there is an increase in the specific power, but at a cost of thermal efficiency as more heat input is needed (more fuel of the same low calorific value) to compensate for the extracted work [5]. Research has shown that for optimum thermal efficiency, the low pressure compressor pressure ratio should be in the range 2.0-4.5 for high total pressure ratio cycles ($30 \leq PR \leq 60$) and 1.4-3.0 for low total pressure ratio cycles. [5]

In order to increase the efficiency of the intercooled cycle high pressure ratios are needed, and in fact the maximum pressure ratio for optimum thermal efficiency of an intercooled gas turbine is higher than that of a simple cycle gas turbine of identical specification [3], and at the same turbine entry temperature slightly higher thermal efficiencies can be obtained.

4.2.3 Recuperated cycle

The recuperated cycle (figure 4.4) incorporates a heat-exchanger (recuperator type) which utilises the temperature of the exhaust gases of the gas turbine in order to add heat in the compressed working fluid before entering the combustor. This means that the less heat input needs to be added to the working fluid for the gas turbine to produce the same output power comparing with a simple cycle having the same power output, turbine entry temperature and component efficiencies. The optimum thermal efficiency of the cycle is obtained at lower total compression pressure ratios than that of a simple cycle and the reason for that is that low expansion ratios produce high temperature exhaust gases.

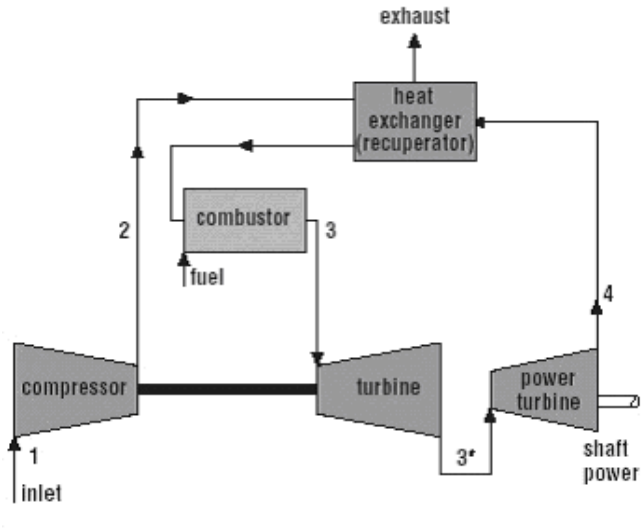

Figure 4.4: Recuperated cycle in a two shaft configuration [1]

The part load thermal efficiency of the recuperated cycle at fuel flow control only is lower than of that of the simple cycle at an equivalent design-point thermal efficiency, and it can be increased by increasing the total compression pressure ratio further than for optimum design-point thermal efficiency (the design-point specific power will increase) [6].

By increasing turbine entry temperature the optimum total compression pressure ratio increases [7] because of the fact that there is an optimum point between the compression outlet temperature and the heat recovery of the working fluid. By increasing the recuperator effectiveness at constant turbine entry temperature the optimum total compression pressure ratio decreases because the amount of heat recovery of the working fluid compensates for the lower thermal efficiency of the cycle it was simple [7]. If specific power (which is lower than that of a simple cycle

gas turbine) is of more interest then the optimum total compression pressure ratio is slightly reduced comparing with the simple cycle because of the recuperator pressure losses and recuperator effectiveness does not affect it [7]. The recuperator effectiveness depends as every heat-exchanger's (i.e. regenerator, intercooler) mainly on the heat transfer coefficient of the construction material, the heat capacities of the heat exchanging fluids per unit volume, and the volume of the recuperator.

The incorporation of variable area nozzles *VAN* in the first stage of the free power turbine of a recuperated gas turbine is proved to be beneficial because by varying the area between the low pressure turbine and the power turbine the pressure drop ratio between them can be changed so to keep the core gas generator turbine(s) near their design-point efficiency, and produce high gas path temperatures, which increase further the thermal efficiency of the cycle at part load conditions [8].

4.2.4 Intercooled/Recuperated cycle

The intercooled/recuperated cycle (figure 4.5) incorporates both an intercooler and a recuperator, and the cycle inherits some of the characteristics of both the intercooled and the recuperated cycle but with higher design-point and off-design thermal efficiency than both of them and the simple cycle assuming that all cycles incorporate the same technology level and are optimized for optimum thermal efficiency [8].

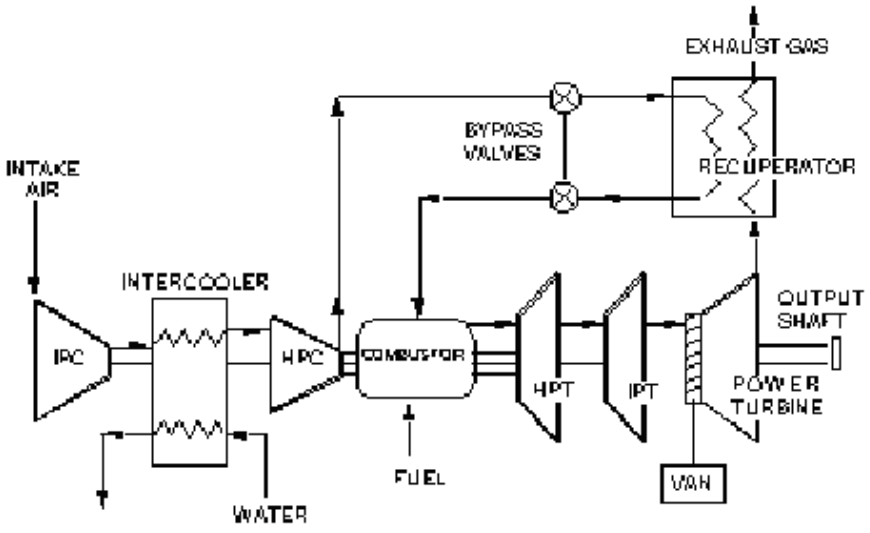

Figure 4.5: Intercooled/Recuperated cycle in a three shaft configuration with variable area nozzles before the power turbine [9]

The cycle requires lower total compression pressure ratio than that of the simple and intercooled cycles for maximum thermal efficiency, but higher than the recuperated cycle. For optimum efficiency the total compression pressure ratio is split between the low and high pressure compressor at approximately 40% and 60% respectively [10]. For optimum specific power (which is lower than that of the intercooled cycle but higher than the simple cycle) the split becomes equal for both *LP* and *HP* compressors [7].

4.3 Design-Point and Off-design Performance of Marine Gas Turbines

4.3.1 Off-design performance definitions

The off-design performance of the simulated gas turbines is presented as function of the air ambient temperature T_{amb} and the turbine entry temperature *TET*. The ambient pressure P_{amb} although it is included in the simulated gas turbine models (chapter 2, section 2.2) was not used as a variable in the case studies of the project because this would require a significant amount of time, beyond the time constrains that defined the completion this research. The use of P_{amb} as off-design variable is ready to be used in future projects that may require it. The off-design performance results of the simulated gas turbines that are presented in this chapter were produced by using the gas turbine performance model (chapter 2, section 2.2) integrated with the hot section blade creep life model (chapter 2, section 2.4).

The range of the ambient temperature T_{amb} that the off-design performance of the gas turbines where simulated is from -30 to +40 ^{o}C and the range of the turbine entry temperature *TET* is from 1100 K to 1550 K, which satisfies the lowest power settings at the specified ambient temperatures T_{amb} that the gas turbines as prime movers are required to operate at in the case studies of this project. Most of the gas turbines were simulated with *TET* lower than 1100 K but in some cases the results obtained were not considered reliable, and because of the fact that power settings that required *TET* lower than 1100 K proved to be unnecessary in the operational profile of the marine vessels in the case studies of this project (see chapter 7), for most of the simulated gas turbines the lowest value of the already mentioned *TET* range was decided to be

presented. The exception is the twin mode intercooled gas turbine (*TMI*) and further details are given in section 4.3.4.4.

The off-design parameters that are presented later in this chapter are the essential for the technoeconomic and risk analysis (engine power *EP*, fuel flow *FF*, high pressure turbine or (just turbine in the case of single shaft gas generator) blade temperature T_b (or *TBLADE* in the figures), high pressure compressor (or just compressor relative rotational speed) *CS* of the simulated gas turbines and to obtain a basic understanding of the behaviour of the engines at off-design conditions (mass flow *MF*, total compression pressure ratio *PR*), but in future projects if it is needed, more gas turbine off-design performance parameters can be investigated, by simply adding more performance parameter tables in the gas turbine model (chapter 2, section 2.2). *TBLADE* is derived by assuming a cooling effectiveness ε of 0.6 which remains constant at all off-design conditions. The rotational speed of the aerodynamically coupled power turbine of all simulated gas turbines is assumed constant at off-design conditions according to the power law index appropriate for electricity generation available in "*Turbomatch*".

4.3.2 Common cycle design and component performance parameters

Because of the fact that there is limited information published by gas turbine manufacturers on the detailed technical specification of their products, it was necessary to make a number of assumptions about the cycle design and component performance parameters of the simulated gas turbines of this project, based on published academic literature and the limited information published by the gas turbine manufacturers. It needs to be mentioned that these assumptions are made in order to reflect some of the capabilities of the technology level of cycle design and component performance parameters of gas turbines at design stage at the time that this research was in development stage. The common cycle design-point parameter (appendix A.1,"*Turbomatch*" input files) on all marine gas turbines that are investigated in this project is the turbine entry temperature (*TET*), which is set at 1509.5 K [11] [12] [13]. The common component performance parameters at design-point are (appendix A.1,"*Turbomatch*" input files) the low and high pressure compressor isentropic efficiency at 90% [2], except for the twin mode intercooled gas turbine (*TMI*) which is set at 89% because of assumed dimensional and geometrical restrictions (i.e. frontal

area, blade tip to casing distance etc.) of the 5MW core gas turbine [8], the air-cooled turbine isentropic efficiency at 87% [2], the non-cooled turbine isentropic efficiency at 89% [8], the combustion efficiency and pressure loss at 99.8% and 3.5% respectively [8], assuming low combustor loading and intensity as combustor volume is not a major design restrain for a marine gas turbine. The extracted cooling flow for the air cooled turbines is assumed at 10% [8].

The intercooler on all gas turbines that incorporate one is assumed on-engine, liquid-gas type and common performance parameters at design-point are the pressure losses which are set at 1% [11]. The intercooler output temperature of the intercooled (*INT*) and intercooled/recuperated (*ICR*) gas turbines is a common component performance parameter, though the twin mode intercooled gas turbine (*TMI*) is simulated with a different value as it is explained in sections 4.3.4.1 and 4.3.4.4. The effectiveness was not used as a performance parameter in the intercooler as although "*Turbomatch*" accepts the intercooler effectiveness as input it requires the intercooler output temperature in order to operate which remains steady at off-design conditions. The intercooler inlet cooling water temperature (sea water temperature) is assumed to be at 15 ^{o}C at all conditions.

The recuperator (it has a different implementation than the intercooler in "*Turbomatch*") common performance parameters at design-point are the effectiveness which is set at 73% which a proposed value of the recuperator effectiveness of the Rolls-Royce WR21 intercooled/recuperated marine gas turbine [12] [14], cold and hot section pressure loss at 10% [12] and mass flow leakage at 2% [8].

4.3.3 Simple cycle gas turbine performance

4.3.3.1 Design-point performance

The simple cycle (*SC*) gas turbine is a two shaft engine (figure 4.2) and resembles an approximate proposed simulation of the General Electric LM2500 marine gas turbine. The word "*approximate"* is used because "GE energy" and "GE aviation" both offer a marine version of the LM2500 [15] [16] [17] but with small differences in the limited published specification so it was decided to simulate the engine by combining the published manufacturers and academic information together with the common design cycle and component performance parameters adopted all the

simulated marine gas turbines. Table 4.1 shows a comparison between the published design point parameters of the LM2500 [15] [16] [17] [18] and the simulated simple cycle gas turbine, at ISA conditions in zero altitude. Detailed information on the design-point performance of the simulated 25MW simple cycle gas turbine can be read in its "*Turbomatch*" input file in appendix A.1.

Table 4.1: Design-point performance parameters of simulated SC gas turbine and GE LM2500

Performance parameter	Simulated 25MW simple cycle gas turbine	General Electric LM2500
Power turbine rating, P_{PT}	25.0 MW	25.05 MW
Inlet mass flow, *MF*	70.86 kg/s	68.96 kg/s
Exhaust mass flow, *EF*	72.40 kg/s	70.54 kg/s
Exhaust gas temperature, T_{exh}	814.26 K	836.26 K
Fuel flow, *FF*	1.545 kg/s	1.581 kg/s
Total compression pressure ratio, *PR*	18:1	18:1
Thermal efficiency, η_{th}	0.375	0.37

4.3.3.2 Off-design performance

The effects of ambient temperature T_{amb} (in degrees Celsius) and turbine entry temperature (*TET*) on the engine power (*EP*) and fuel flow (*FF*), total compressor pressure ratio (*PR*) and intake mass flow (*MF*), compressor turbine blade temperature (*TBLADE*) and compressor relative rotational speed (*CS*) relative to design-point are presented in figures 4.6, 4.7 and 4.8 respectively.

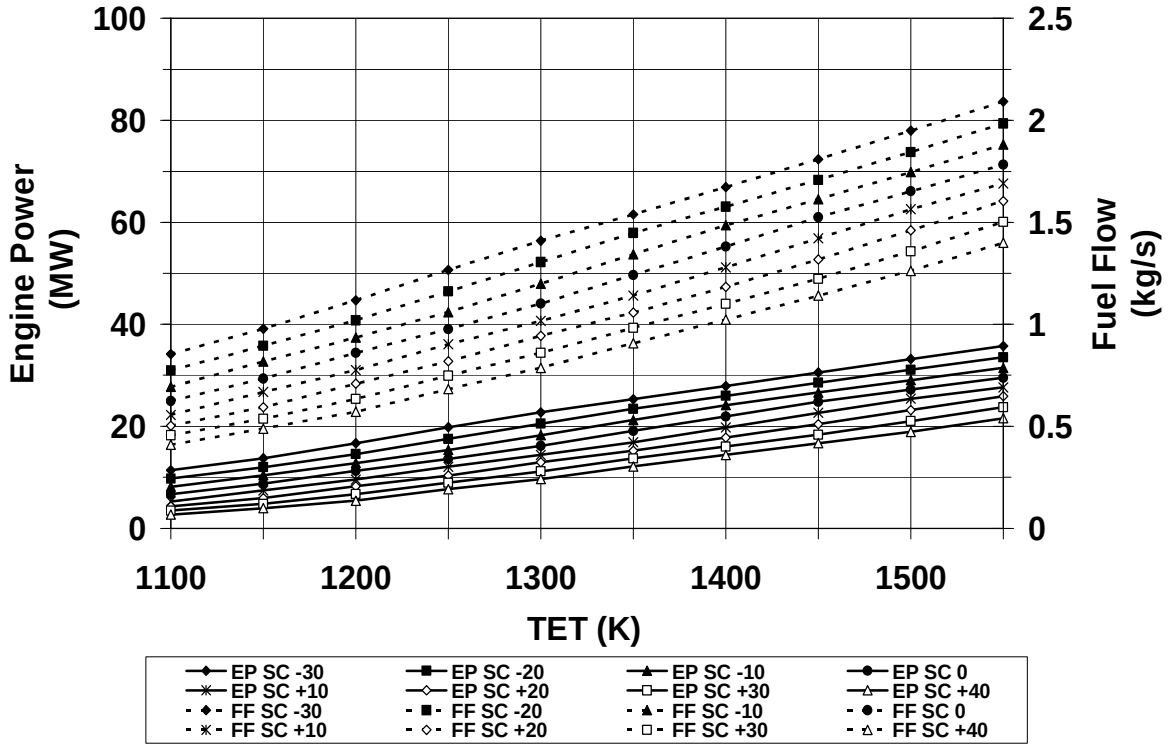

Figure 4.6: Simple Cycle (SC) – The effect of Ambient (T_{amb}, ^{o}C) & Turbine Entry Temperature (TET) on Engine Power (EP) & Fuel Flow (FF)

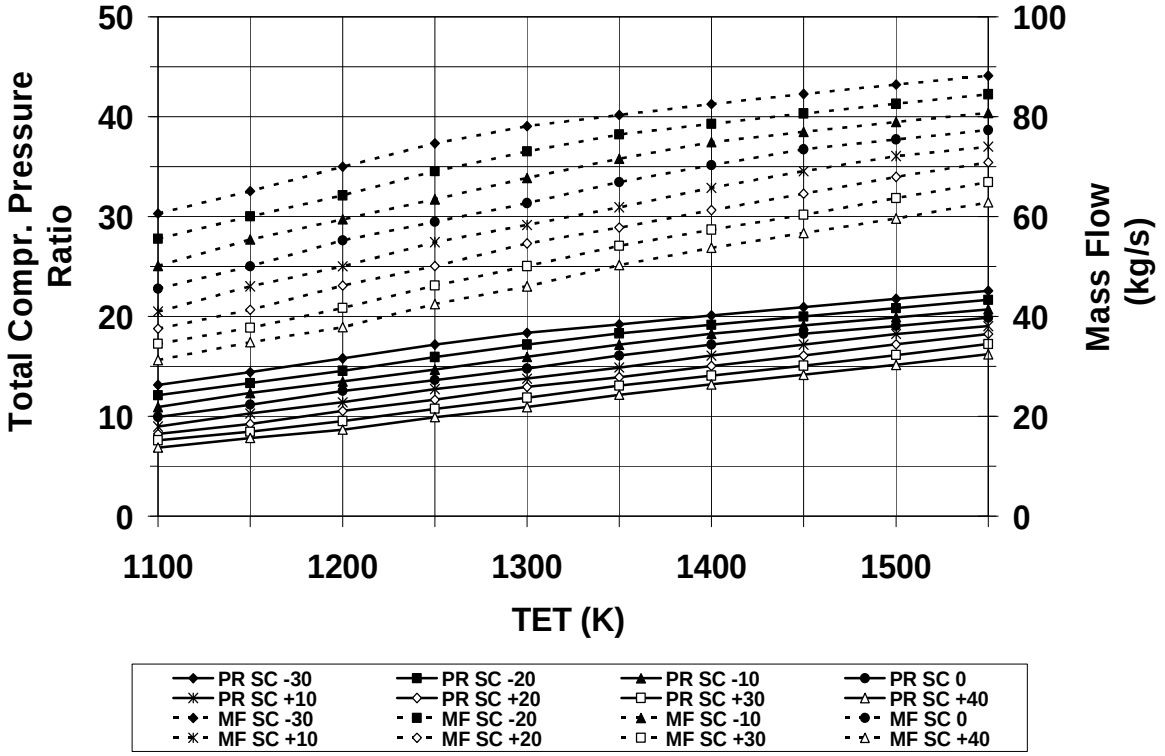

Figure 4.7: Simple Cycle (SC) – The effect of Ambient (T_{amb}, ^{o}C) & Turbine Entry Temperature (TET) on Total Compression Pressure Ratio (PR) and Mass Flow (MF)

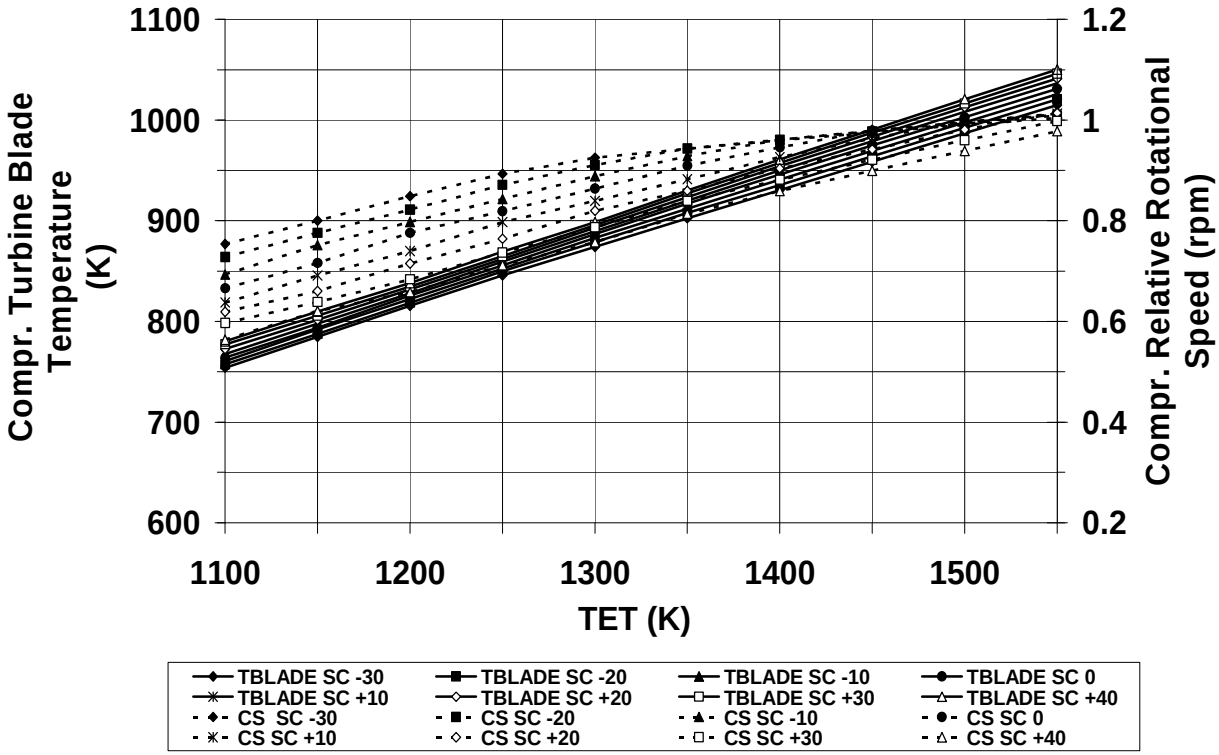

Figure 4.8: Simple Cycle (SC) – The effect of Ambient (T_{amb}, ^{o}C) & Turbine Entry Temperature (TET) on Compressor Turbine Blade Temperature (TBLADE) & Compressor Relative Rotational Speed (CS) to Design-Point

4.3.4 Twin mode intercooled cycle gas turbine performance

4.3.4.1 Twin mode intercooled cycle gas turbine concept overview

The gas turbine is a proposal for a novel and compact marine propulsion system [11]. A high amount of space savings has been predicted from the installation of the engine on a naval marine vessel as a prime mover as it deletes the necessity of installing low power gas turbines for cruising and high power gas turbines for sprinting (boost), which require separate intake and exhaust ducts, and results in large volumes of overall ducting [11]. It has also been predicted that high thermal efficiencies in both cruise and boost modes can be attained. The engine as it can be seen in figure 4.9 is composed of a low power core three-shaft gas turbine which is installed in one of the lower decks of the vessel and a fourth shaft which is installed on the weather deck of the vessel and features a low pressure compressor, an intercooler and a low pressure turbine. The installation of the fourth shaft on the weather deck of the marine vessel further reduces the ducting volume comparing with an installation arrangement that would require the fourth shaft to be installed at the lower deck of the vessel.

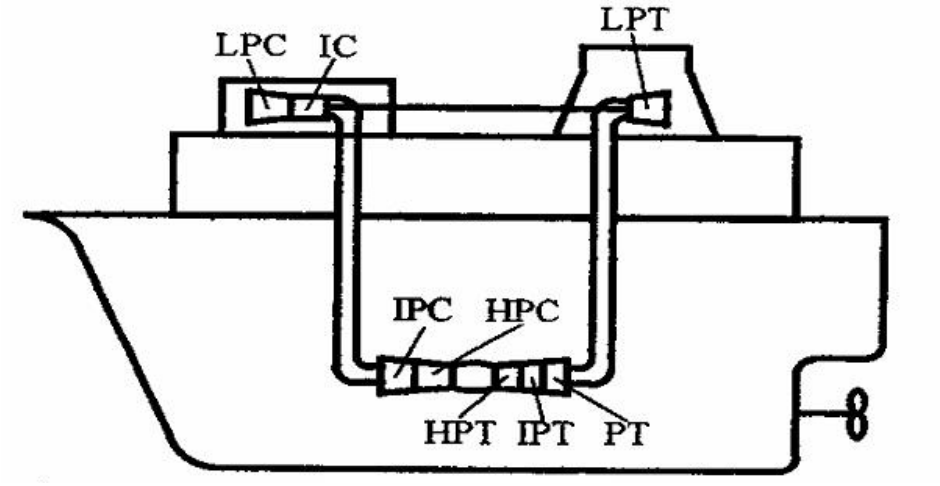

Figure 4.9: General representation of the twin mode cycle gas turbine components arrangement [11]

When the engine operates in the cruise mode (low power) the intake air flow is by-passed from the weather deck compressor and intercooler with the operation of an air-tight valve and the same happens at the exhaust side where another air-tight valve by-passes the exhaust gases straight to the environment instead of the weather deck turbine as it is shown in figure 4.10. When the engine is required to operate at the boost mode (high power) then the weather deck shaft is in operation and the intake air

is first compressed from the weather deck low pressure compressor, heat extracted by the intercooler and after the heat extraction the same ducting is used for the air flow to be further compressed by the core engine. At the exhaust side the gases are not wasted straight to the environment but they are further expanded by the weather deck low pressure turbine.

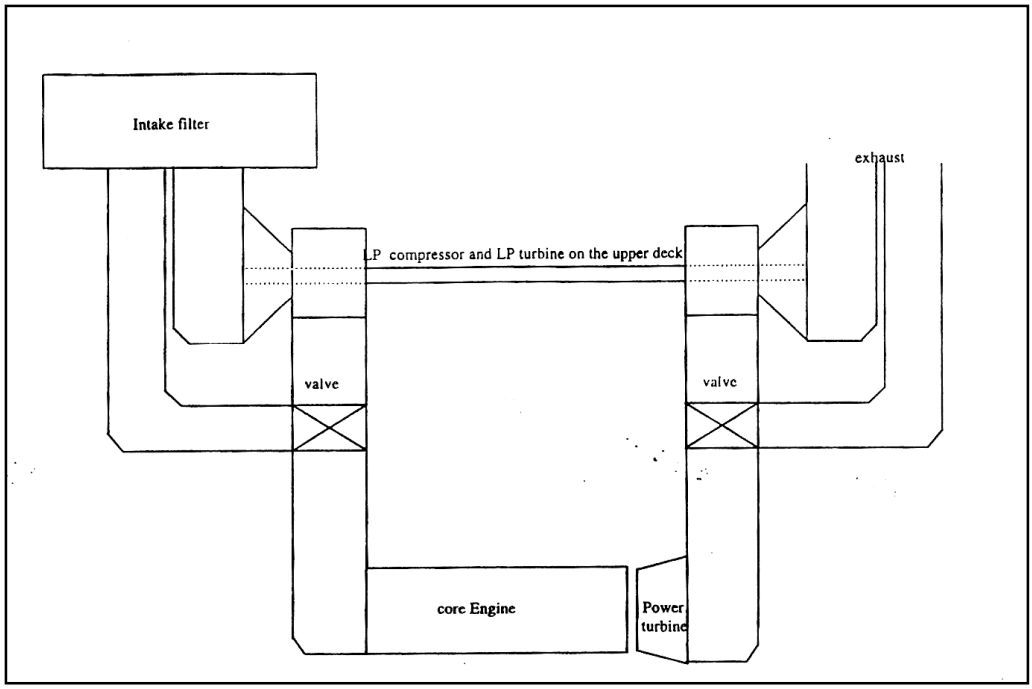

Figure 4.10: General representation of the ducting arrangement of the twin mode cycle gas turbine [11]

The common use of the low and high pressure turbomachinery of the core engine require for optimum efficiencies at design-point and off-design conditions that the engine non dimensional parameters to be very similar at both modes at design-point conditions as it can be seen in figure 4.14 in section 4.3.4.4, which also explains the use of the same ducting, from the exit of intake air flow from the intercooler until before the weather deck turbine [11]. In order the weather deck low pressure turbine to be able to provide the weather deck low pressure compressor with the required power to compress the intake air flow, the pressure drop available for expansion before the power turbine is not fully utilized by it, and a small percentage is available for expansion by the weather deck low pressure turbine [11].

The initial design-point and off-design performance investigation of the twin mode intercooled cycle gas turbine was performed with the design point power rating of the low power mode set at 5MW and the high power mode set at 24MW, and the design-

point thermal efficiency of the two modes of the engine, were 0.3565 and 0.4203 for the low and high power mode respectively. The total compression pressure ratio of the engine in the high power mode is very high (*PR*>85) comparing with gas turbines in production, and this can be a major restrain factor in the structural integrity of the engine.

In this technoeconomic investigation the original configuration of the engine was adopted, with the difference that the high power mode power rating was increased to 25MW, and the turbomachinery's component isentropic efficiencies were increased giving higher design-point thermal efficiency at both modes.

4.3.4.2 Design-point performance of the 5MW gas turbine mode

The core gas turbine (*TMI* low power mode) of the twin mode intercooled cycle is a 5MW simple cycle three-shaft design (figure 4.10) as it was described in section 4.3.4.1 [11]. The design point performance of the core gas turbine at ISA conditions at zero altitude is shown in table 4.2. Detailed information on the specification and design-point performance of the low power mode of the engine can be read in its "*Turbomatch*" input file in appendix A.1.

Table 4.2: Design-point performance parameters of the low power mode of the simulated TMI gas turbine

Performance parameter	**Simulated 5MW simple cycle gas turbine**
Power turbine rating, P_{PT}	5.0 MW
Inlet mass flow, *MF*	14.90 kg/s
Exhaust mass flow, *EF*	15.20 kg/s
Exhaust gas temperature, T_{exh}	776.30 K
Fuel flow, *FF*	0.3031 kg/s
Total compression pressure ratio, *PR*	22.4:1
Thermal efficiency, η_{th}	0.383

4.3.4.3 Off-design performance of the 5MW gas turbine mode

The effects of ambient temperature T_{amb} (in degrees Celsius) and turbine entry temperature (*TET*) on the engine power (*EP*) and fuel flow (*FF*), total compressor pressure ratio (*PR*) and intake mass flow (*MF*), compressor turbine blade temperature (*TBLADE*) and compressor relative rotational speed (*CS*) relative to design-point are presented in figures 4.11, 4.12 and 4.13 respectively.

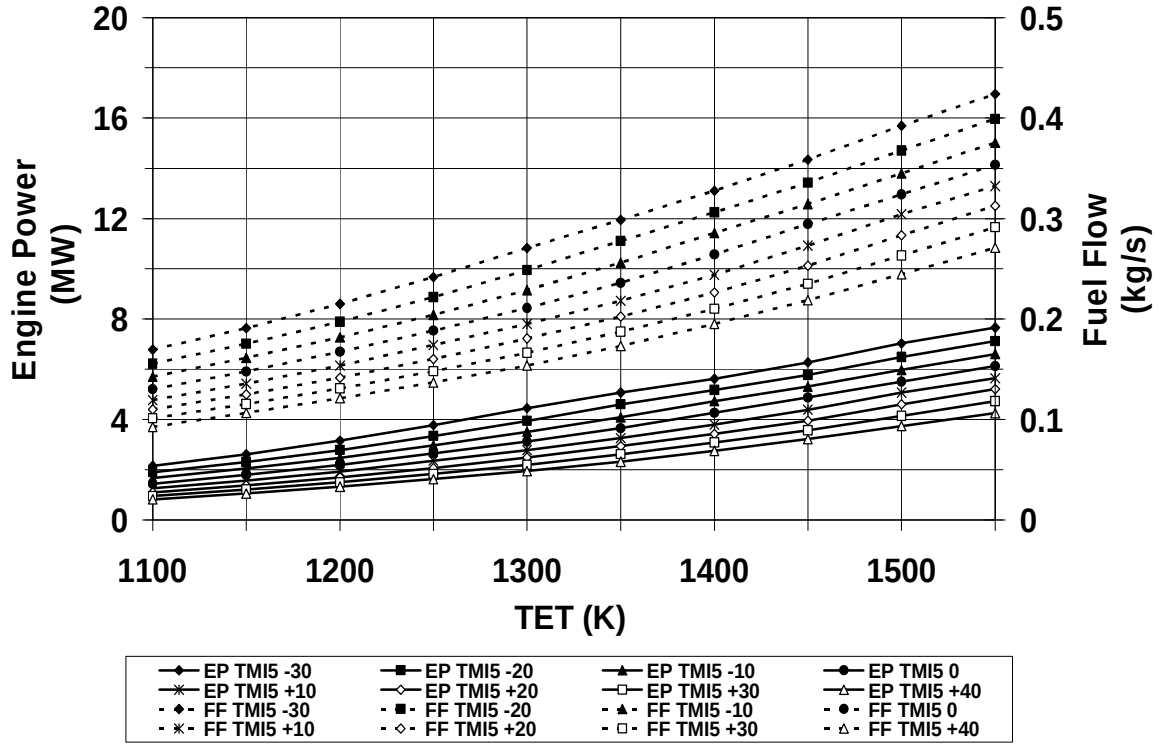

Figure 4.11: Twin Mode Intercooled Cycle (TMI) (Low Power) – The effect of Ambient (T_{amb}, ^{o}C) & Turbine Entry Temperature (TET) on Engine Power (EP) & Fuel Flow (FF)

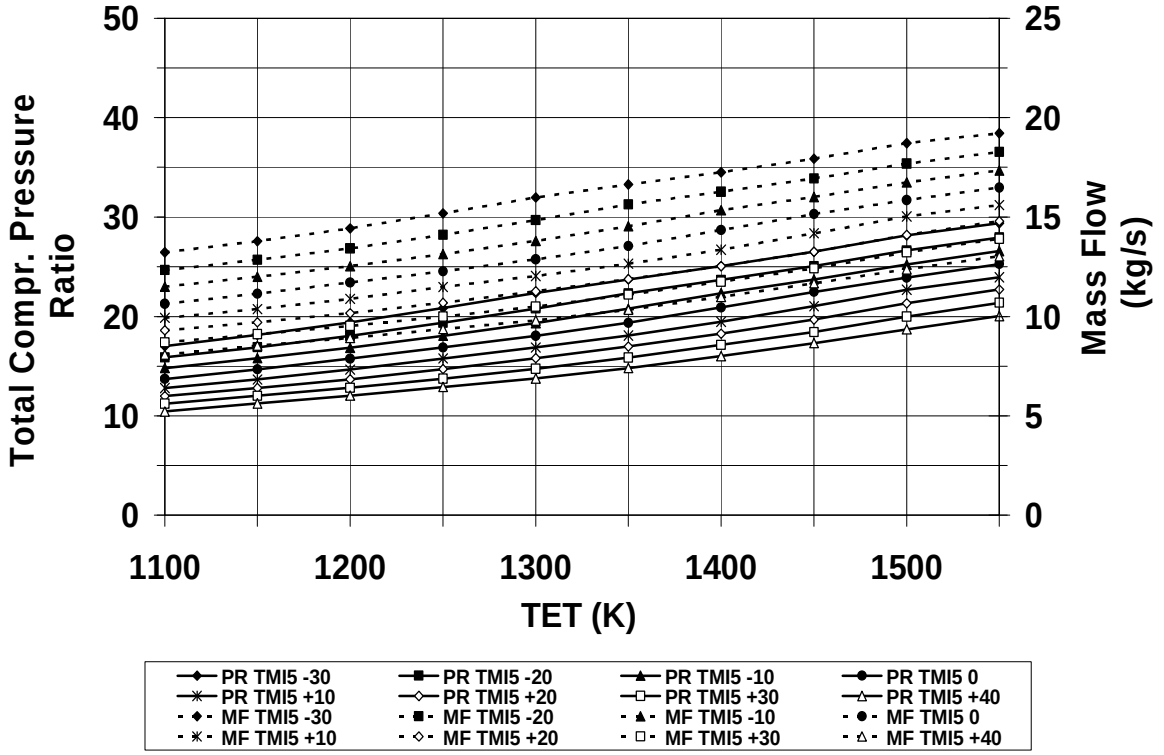

Figure 4.12: Twin Mode Intercooled Cycle (TMI) (Low Power) – The effect of Ambient (T_{amb}, ^{o}C) & Turbine Entry Temperature (TET) on Total Compression Pressure Ratio (PR) and Mass Flow (MF)

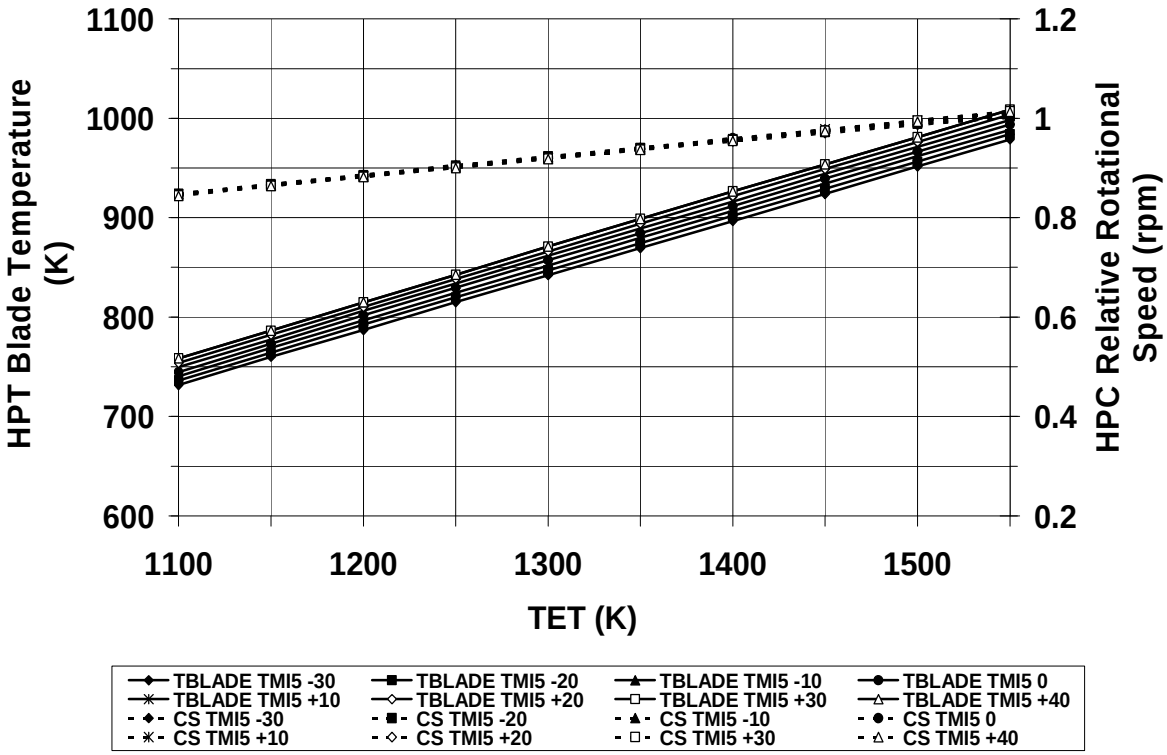

Figure 4.13: Twin Mode Intercooled Cycle (TMI) (Low Power) – The effect of Ambient (T_{amb}, ^{o}C) & Turbine Entry Temperature (TET) on HP Turbine Blade Temperature (TBLADE) & HP Compressor Relative Rotational Speed (CS) to Design-Point

4.3.4.4 Design-point performance of the 25MW gas turbine mode

The high power mode of the *TMI* gas turbine was upgraded from the 24MW initially proposed design-point power turbine rating [11] to 25MW in order to make the engine directly comparable with the other four gas turbines that take part in this project. The design-point performance of the high power mode of the gas turbine is shown in table 4.3. Detailed information on the specification and design-point performance of the high power mode of the engine can be read below its "*Turbomatch*" input file in appendix A.1.

Table 4.3: Design-point performance parameters of the high power mode of the simulated TMI gas turbine

Performance parameter	Simulated 5MW simple cycle gas turbine
Power turbine rating, P_{PT}	25.0 MW
Inlet mass flow, *MF*	61.71 kg/s
Exhaust mass flow, *EF*	62.95 kg/s
Exhaust gas temperature, T_{exh}	561.50 K
Fuel flow, *FF*	1.2409 kg/s
Total compression pressure ratio, *PR*	92.51:1
Intercooler outlet temperature, T_{IOT}	298.0 K
Thermal efficiency, η_{th}	0.467

The design-point non dimensional mass flow of the gas turbine operating in the high power as it was explained in section 4.3.4.1 is almost identical with the 5MW core gas turbine from the intercooler outlet to the entry of the power turbine. The slight difference as it can be seen in figure 4.14 occurs because of the almost 10 K higher temperature at the entry of the low pressure compressor when the gas turbine operates at the high power mode, due to the cooling capabilities of the intercooler. It was decided to do this intentionally as the initial off-design simulation [11] of the 5MW core gas turbine was made with a reference ambient temperature of 298 K and the author changed it to ISA (288.15 K) in order to provide a more realistic view of the operational differences of the two operating modes in off-design conditions, assuming that the core engine's component maps would be optimised for operation in the low power mode. Detailed information on the specification and design-point performance of the high power mode of the engine can be read in its "*Turbomatch*" input file in appendix A.1.

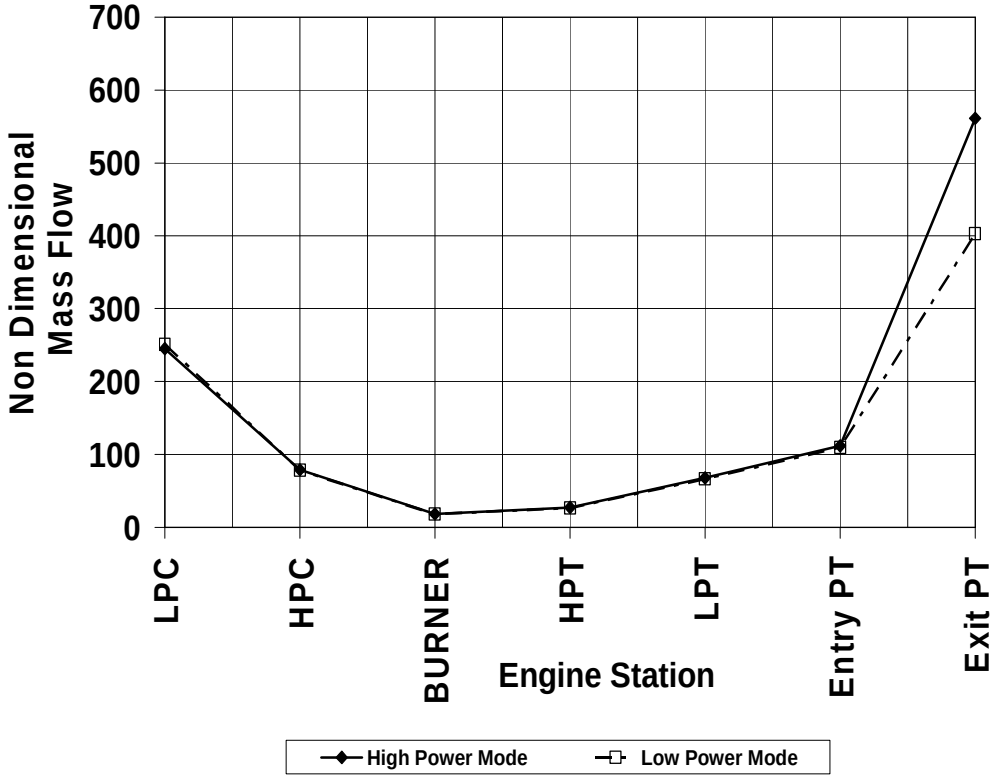

Figure 4.14: Non dimensional flow comparison between high and low power mode at design-point

4.3.4.5 Intercooler design-point effectiveness

As it was mentioned before in this chapter "*Turbomatch*" although it accepts the intercooler effectiveness as an input, in order to operate it requires the intercooler outlet temperature in the input gas turbine simulation file, which remains steady at off-design simulations, and the input intercooler effectiveness does not apply. In order to evaluate the design-point intercooler output temperature and as a consequence overall design point performance of the engine the following calculations are presented in equation 4-1 in order to provide the assumed effectiveness of the intercooler at design-point $\varepsilon_{INT\text{-}DP}$ [11] (see reference equation 2-6):

$$\varepsilon_{INT-DP} = \frac{T_{IET} - T_{IOT}}{T_{IET} - T_{sea}} = \frac{457.98K - 298K}{457.98K - 288.15K} = 0.9411 \qquad \text{Equation 4-1}$$

Where: T_{IET} is the intercooler inlet temperature.

4.3.4.6 Off-design performance of the 25MW gas turbine mode

The off-design performance of the gas turbine in the intercooled 25MW mode was obtained for an ambient temperature range from -10 to +40 ^{o}C and for turbine temperature range from 1150 to 1550 K. At turbine entry temperatures below 1300 K with ambient temperatures below -10 ^{o}C "*Turbomatch*" could not converge as also at turbine entry temperatures below 1150 K and at the complete range of ambient temperature. Nevertheless, as it can be observed in the off-design performance figures 4.11 and 4.15 the engine will never be needed to operate below *TET* 1150 K in high power mode at ambient temperatures down to -10 ^{o}C, as this power bandwidth can be covered by the low power mode having better thermal efficiency as far as the engine can be allowed to operate at an off-design *TET* higher than approximately 1525 K.

The effects of ambient temperature T_{amb} (in degrees Celsius) and turbine entry temperature (*TET*) on the engine power (*EP*) and fuel flow (*FF*), total compressor pressure ratio (*PR*) and intake mass flow (*MF*), compressor turbine blade temperature (*TBLADE*) and compressor relative rotational speed (*CS*) relative to design-point are presented in figures 4.15, 4.16 and 4.17 respectively.

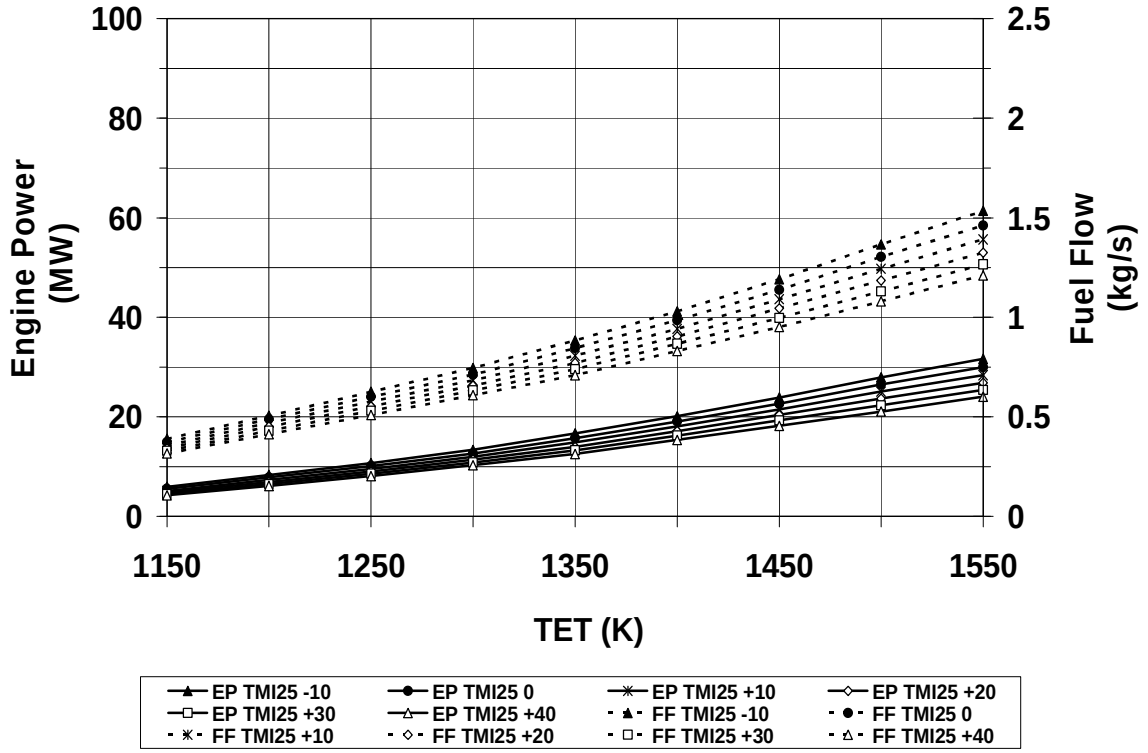

Figure 4.15: Twin Mode Intercooled Cycle (TMI) (High Power) – The effect of Ambient (T_{amb}, ^{o}C) & Turbine Entry Temperature (TET) on Engine Power (EP) & Fuel Flow (FF)

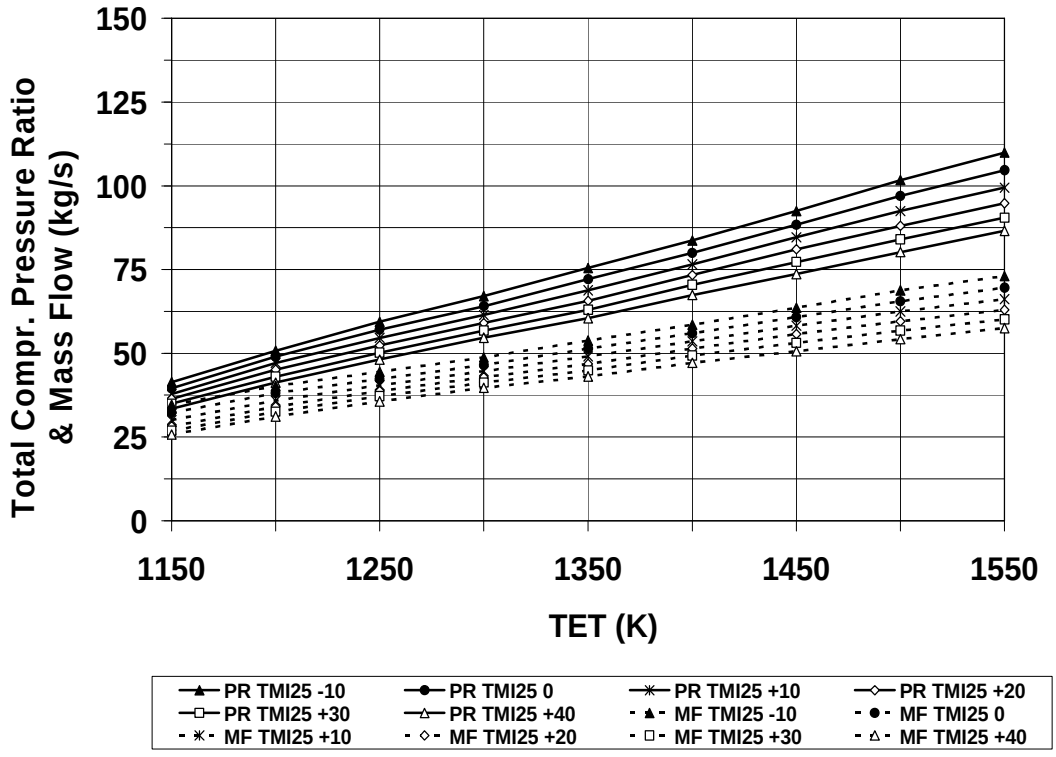

Figure 4.16: Twin Mode Intercooled Cycle (TMI) (High Power) – The effect of Ambient (T_{amb}, ^{o}C) & Turbine Entry Temperature (TET) on Total Compression Pressure Ratio (PR) and Mass Flow (MF)

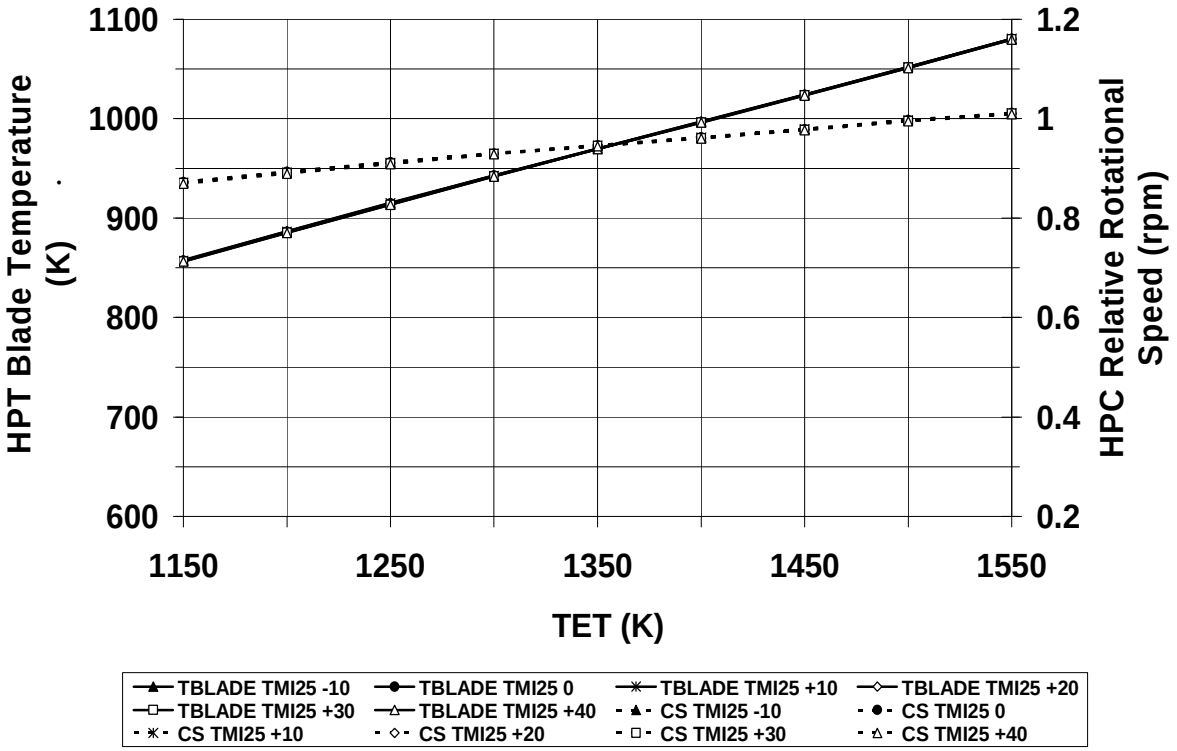

Figure 4.17: Twin Mode Intercooled Cycle (TMI) (High Power) – The effect of Ambient (T_{amb}, ^{o}C) & Turbine Entry Temperature (TET) on HP Turbine Blade Temperature (TBLADE) & HP Compressor Relative Rotational Speed (CS) to Design-Point

4.3.5 Intercooled gas turbine performance

4.3.5.1 Design-point performance

The intercooled gas turbine (*INT*) is a three shaft (figure 4.3) concept design that incorporates the on-engine intercooler between the low and high pressure compressors. The total compression pressure ratio at design-point is 25:1, and the optimum thermal efficiency of the gas turbine at the already mentioned total pressure ratio is obtained by setting the low pressure compressor at pressure ratio of 10.8 % of the total [5]. The reason for choosing the previously specified total compression pressure ratio is although better thermal efficiencies can be obtained at higher total pressure ratios at the specified design-point turbine entry temperatures [5] as it is already shown in the case of the twin mode intercooled *TMI* gas turbine it is of interest of the author to investigate the economic feasibility of an intercooled gas turbine with relatively low total compression pressure ratio as a marine prime mover. The design-point performance of the intercooled gas turbine is shown in table 4.4. Detailed information on the specification and design-point performance of the intercooled gas turbine can be read in its "*Turbomatch*" input file in appendix A.1.

Table 4.4: Design-point performance parameters of the simulated intercooled gas turbine

Performance parameter	Simulated 25MW intercooled gas turbine
Power turbine rating, P_{PT}	25.0 MW
Inlet mass flow, *MF*	59.99 kg/s
Exhaust mass flow, *EF*	61.41 kg/s
Exhaust gas temperature, T_{exh}	754.75 K
Fuel flow, *FF*	1.4217 kg/s
Total compression pressure ratio, *PR*	25:1
Intercooler outlet temperature, T_{IOT}	310.0 K
Thermal efficiency, η_{th}	0.408

4.3.5.2 Intercooler design-point effectiveness

The intercooled gas turbine in contrast with the twin mode intercooled gas turbine is assumed that operates constantly with the intercooler engaged at all off-design conditions and the complication of matching the operational points of the two modes in the compressor and turbine maps does not exist. This allows the intercooler to operate at lower design-point effectiveness, which can affect the prime mover cost *PMC* of the gas turbine and also its life cycle cost. In order to evaluate the design-point intercooler output temperature and as a consequence overall design point performance of the engine the following calculations are presented in equation 4-2 in order to provide the assumed effectiveness of the intercooler at design-point $\varepsilon_{INT\text{-}DP}$ (see reference equation 2-6):

$$\varepsilon_{INT-DP} = \frac{T_{IET} - T_{IOT}}{T_{IET} - T_{sea}} = \frac{392.95K - 310K}{392.95K - 288.15K} = 0.7915 \qquad \text{Equation 4-2}$$

4.3.5.3 Off-design performance

The effects of ambient temperature T_{amb} (in degrees Celsius) and turbine entry temperature (*TET*) on the engine power (*EP*) and fuel flow (*FF*), total compressor pressure ratio (*PR*) and intake mass flow (*MF*), compressor turbine blade temperature (*TBLADE*) and compressor relative rotational speed (*CS*) relative to design-point are presented in figures 4.18, 4.19 and 4.20 respectively.

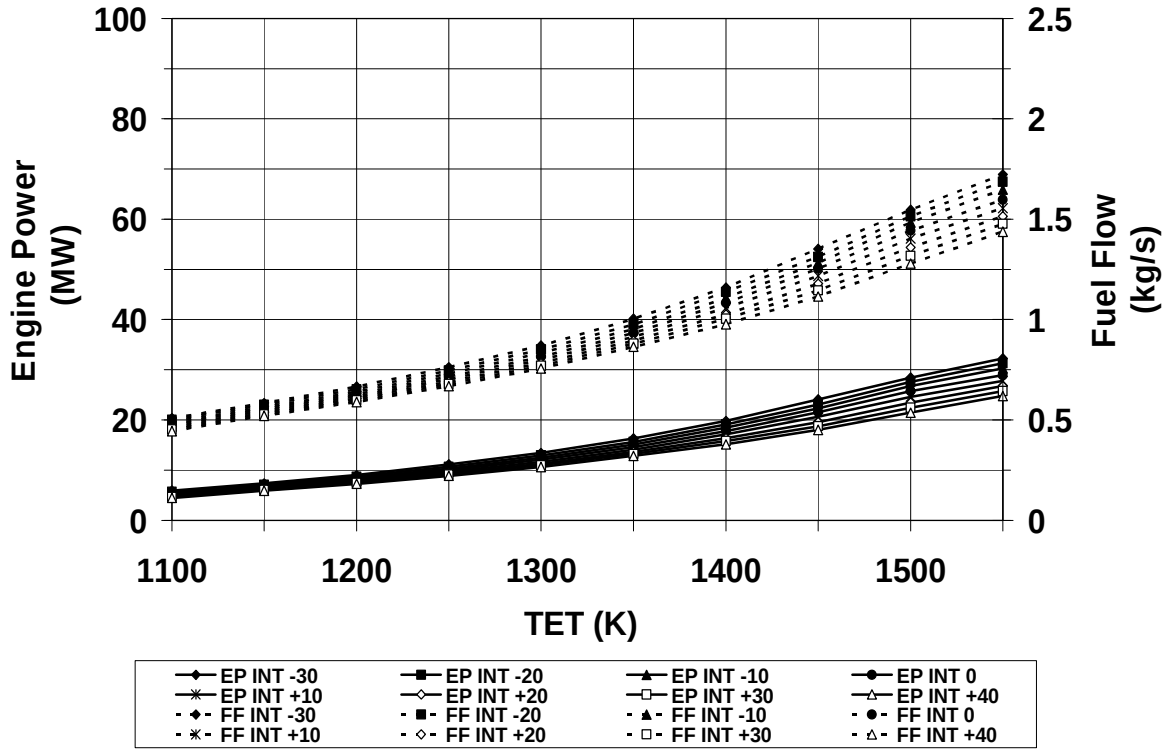

Figure 4.18: Intercooled Cycle (INT) – The effect of Ambient (T_{amb}, ^{o}C) & Turbine Entry Temperature (TET) on Engine Power (EP) & Fuel Flow (FF)

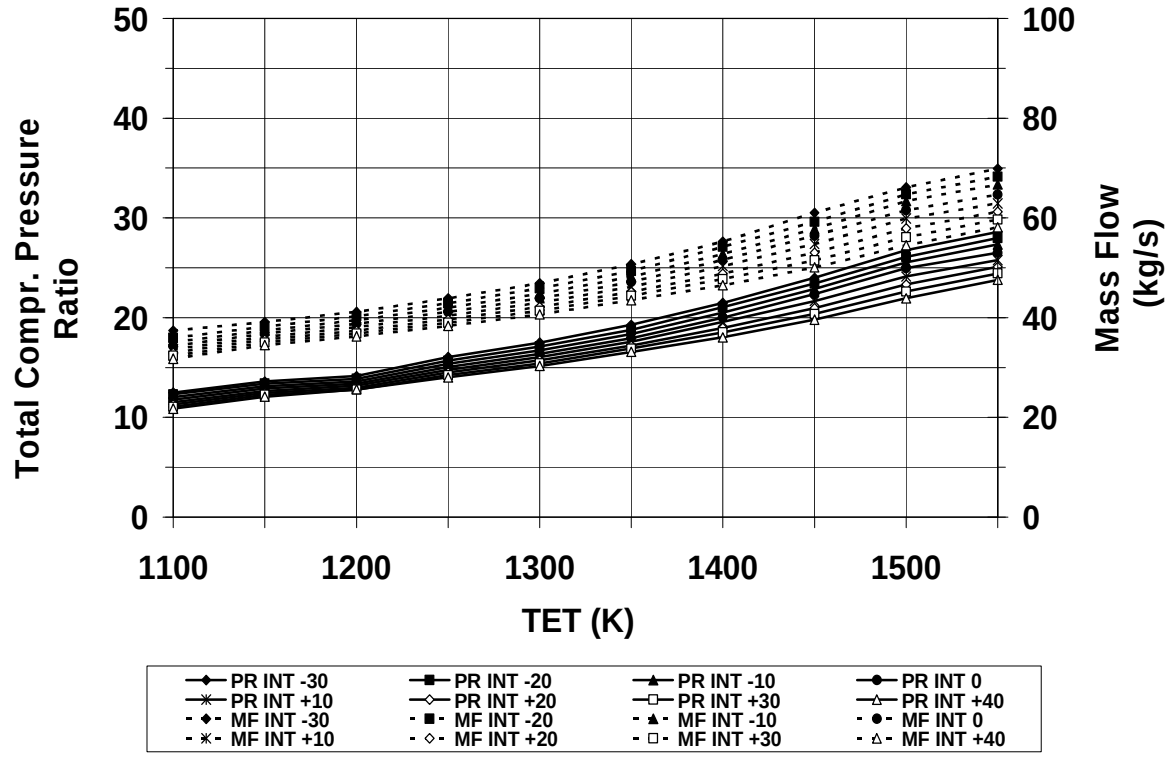

Figure 4.19: Intercooled Cycle (INT) – The effect of Ambient (T_{amb}, ^{o}C) & Turbine Entry Temperature (TET) on Total Compression Pressure Ratio (PR) and Mass Flow (MF)

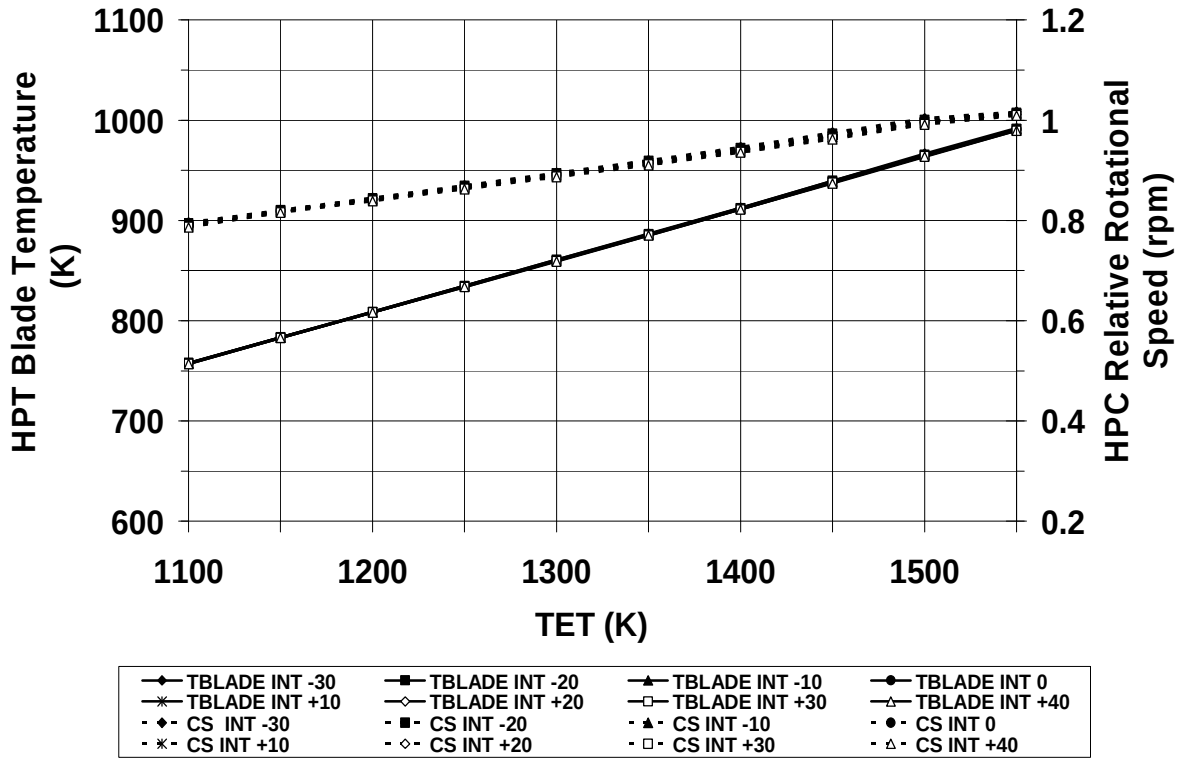

Figure 4.20: Intercooled Cycle (INT) – The effect of Ambient (T_{amb}, ^{o}C) & Turbine Entry Temperature (TET) on HP Turbine Blade Temperature (TBLADE) & HP Compressor Relative Rotational Speed (CS) to Design-Point

4.3.6 Recuperated gas turbine performance

4.3.6.1 Design-point performance

The recuperated gas turbine (*REQ*) is a two shaft concept design (figure 4.4) and its performance simulation does not incorporate the use of variable area nozzles. The engine is a concept design that incorporates a recuperator in order to elevate the temperature of the compressed mass flow (by transferring the heat from the exhaust mass flow) before entering the engine's burner (section 4.2.3). The engine was optimized for optimum efficiency according to the recuperator specification and the specified design-point turbine entry temperature, and it was obtained at 13:1 total compressor pressure ratio. The design-point performance of the recuperated gas turbine is shown in table 4.5. Detailed information on the specification and design-point performance of the recuperated gas turbine can be read in its "*Turbomatch*" input file in appendix A.1.

Table 4.5: Design-point performance parameters of the simulated recuperated gas turbine

Performance parameter	Simulated 25MW recuperated gas turbine
Power turbine rating, P_{PT}	25.0 MW
Inlet mass flow, *MF*	76.25 kg/s
Exhaust mass flow, *EF*	77.68 kg/s
Exhaust gas temperature, T_{exh}	879.61 K
Fuel flow, *FF*	1.4260 kg/s
Total compression pressure ratio, *PR*	13:1
Thermal efficiency, η_{th}	0.407

4.3.6.2 Off-design performance

The effects of ambient temperature T_{amb} (in degrees Celsius) and turbine entry temperature (*TET*) on the engine power (*EP*) and fuel flow (*FF*), total compressor pressure ratio (*PR*) and intake mass flow (*MF*), compressor turbine blade temperature (*TBLADE*) and compressor relative rotational speed (*CS*) relative to design-point are presented in figure 4.21, 4.22 and 4.23 respectively.

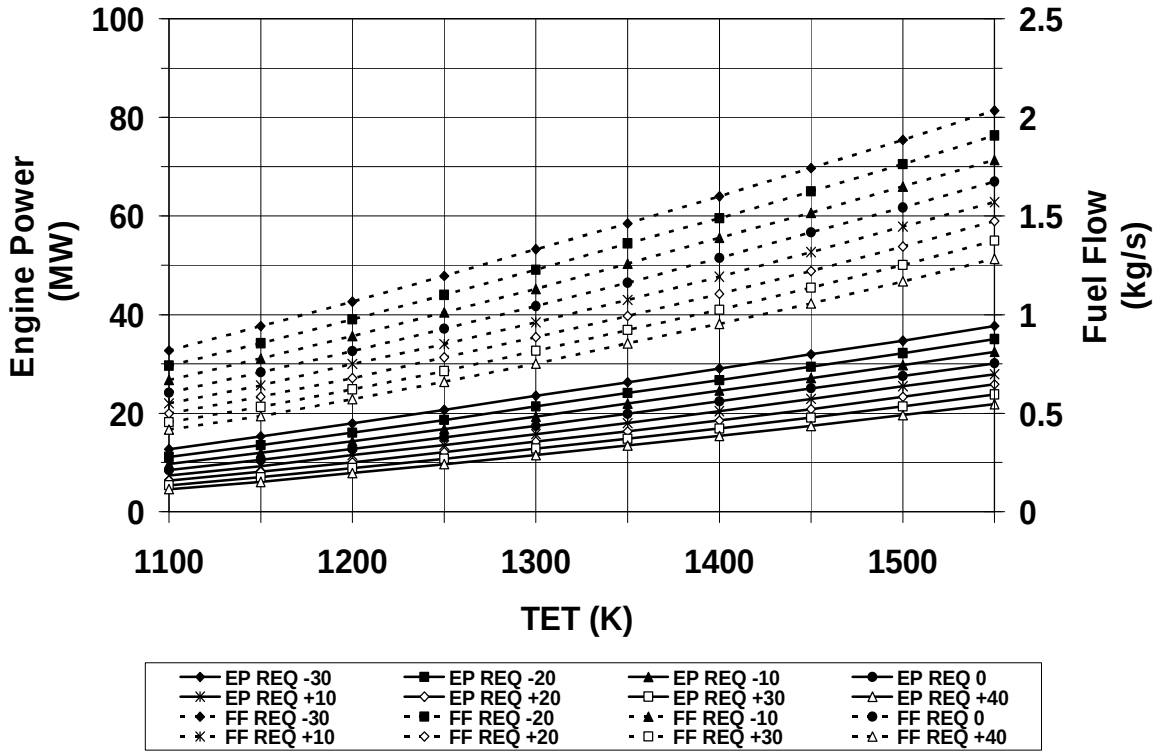

Figure 4.21: Recuperated Cycle (REQ) – The effect of Ambient (T_{amb}, ^{o}C) & Turbine Entry Temperature (TET) on Engine Power (EP) & Fuel Flow (FF)

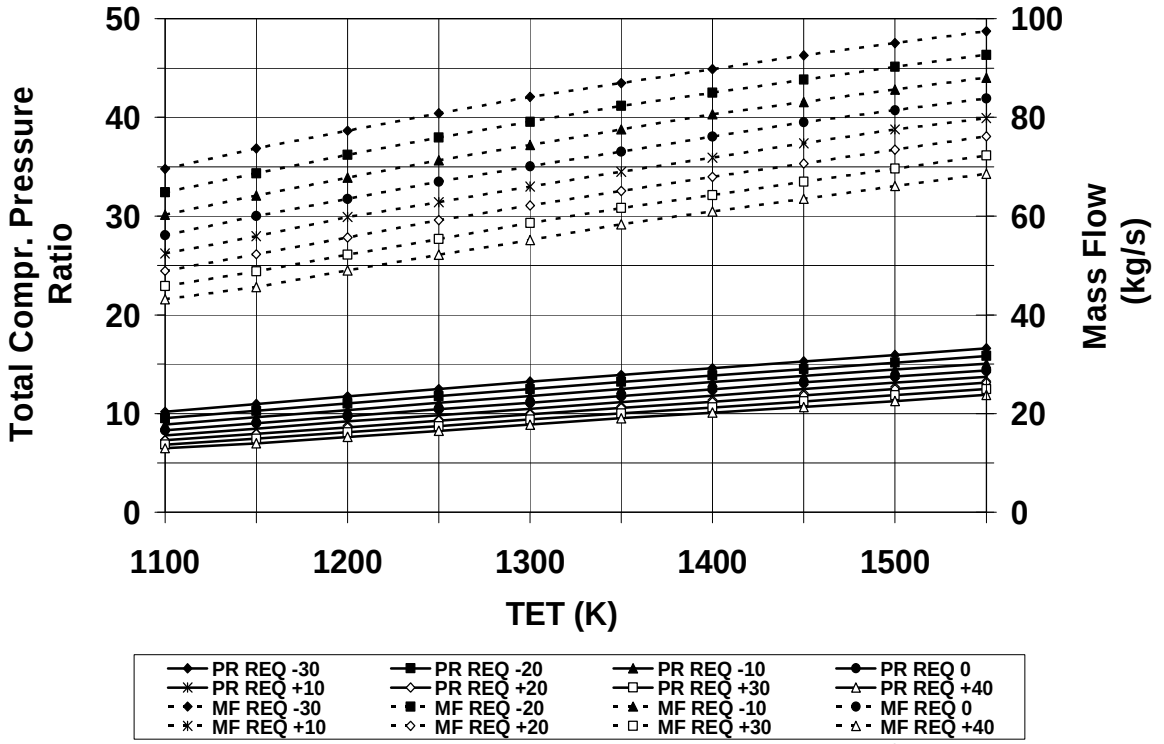

Figure 4.22: Recuperated Cycle (REQ) – The effect of Ambient (T_{amb}, ^{o}C) & Turbine Entry Temperature (TET) on Total Compression Pressure Ratio (PR) and Mass Flow (MF)

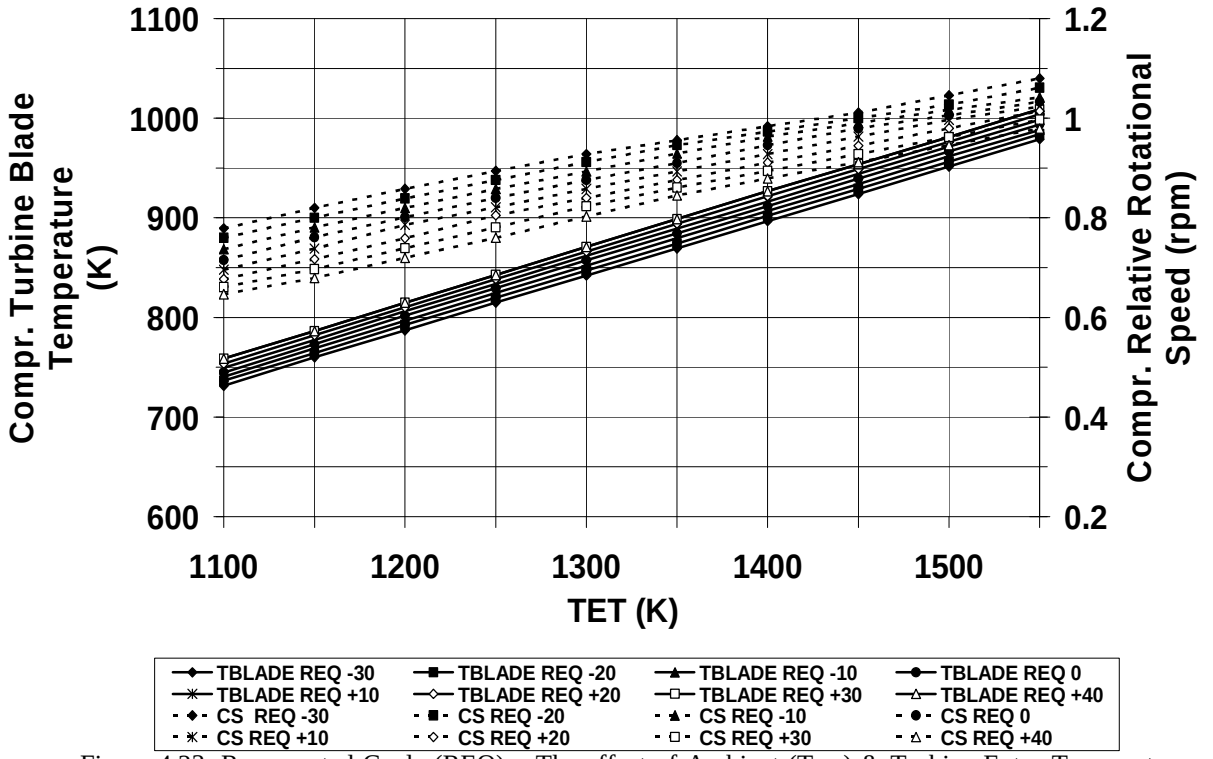

Figure 4.23: Recuperated Cycle (REQ) – The effect of Ambient (T_{amb}) & Turbine Entry Temperature (TET) on HP Turbine Blade Temperature (TBLADE) & HP Compressor Relative Rotational Speed (CS) to Design-Point

4.3.7 Intercooled/Recuperated gas turbine performance

4.3.7.1 Design-point performance

The intercooled/recuperated gas turbine (*ICR*) is a three shaft design (figure 4.5) and its configuration as also its output power rating is modelled having as reference the existing Rolls-Royce WR21 intercooled/recuperated marine gas turbine [14] [19] [20], as also the total compression pressure ratio and the pressure ratios of the low and high pressure compressors. The simulated engine does not incorporate variable area nozzles. The design-point performance of the intercooled/recuperated gas turbine is shown in table 4.6. Detailed information on the specification and design-point performance of the intercooled/recuperated gas turbine can be read in its "*Turbomatch*" input file in appendix A.1.

Table 4.6: Design-point performance parameters of the simulated intercooled/recuperated gas turbine

Performance parameter	**Simulated 25MW intercooled/recuperated gas turbine**
Power turbine rating, P_{PT}	25.0 MW
Inlet mass flow, *MF*	66.80 kg/s
Exhaust mass flow, *EF*	68.13 kg/s
Exhaust gas temperature, T_{exh}	642.53 K
Fuel flow, *FF*	1.3330 kg/s
Total compression pressure ratio, *PR*	14.7:1
Thermal efficiency, η_{th}	0.4349

4.3.7.2 Intercooler design-point effectiveness

The intercooler design-point effectiveness of the intercooled/recuperated gas turbine is presented in equation 4-3.

$$\varepsilon_{INT-DP} = \frac{T_{IET} - T_{IOT}}{T_{IET} - T_{sea}} = \frac{406.24K - 310K}{406.24K - 288.15K} = 0.8149 \qquad \text{Equation 4-3}$$

4.3.7.3 Off-design performance

The effects of ambient temperature T_{amb} (in degrees Celsius) and turbine entry temperature (*TET*) on the engine power (*EP*) and fuel flow (*FF*), total compressor pressure ratio (*PR*) and intake mass flow (*MF*), compressor turbine blade temperature (*TBLADE*) and compressor relative rotational speed (*CS*) relative to design-point are presented in figure 4.24, 4.25 and 4.26 respectively.

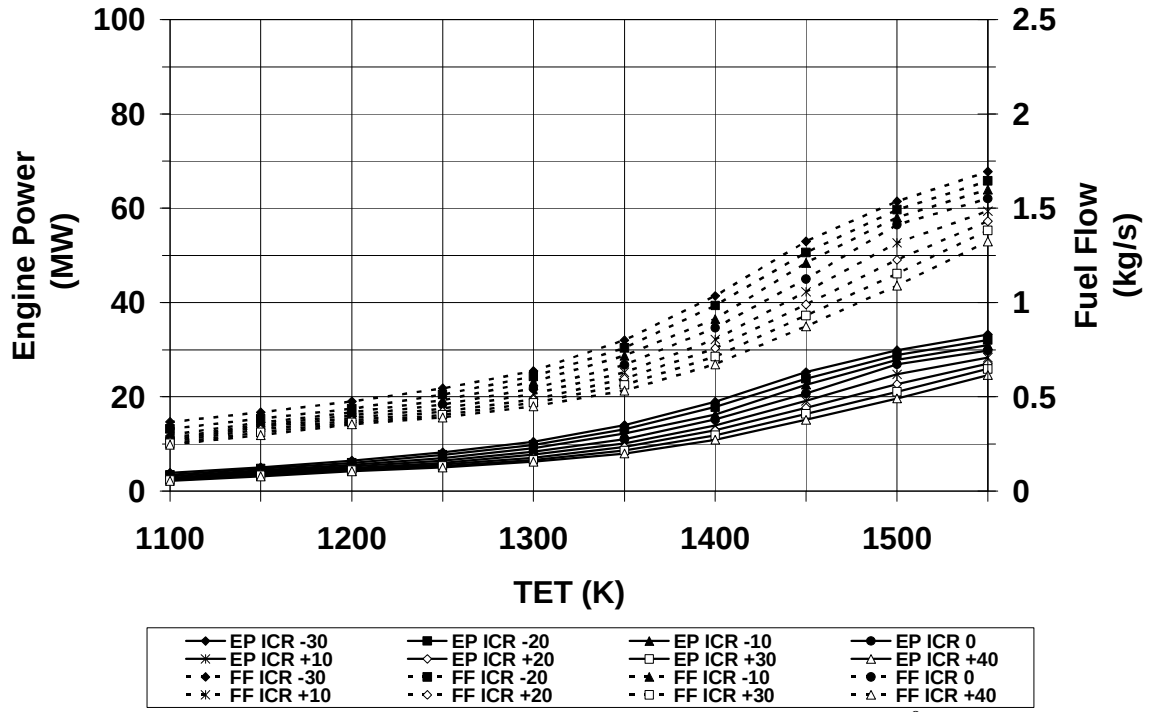

Figure 4.24: Intercooled/Recuperated Cycle (ICR) – The effect of Ambient (T_{amb}, ^{o}C) & Turbine Entry Temperature (TET) on Engine Power (EP) & Fuel Flow (FF)

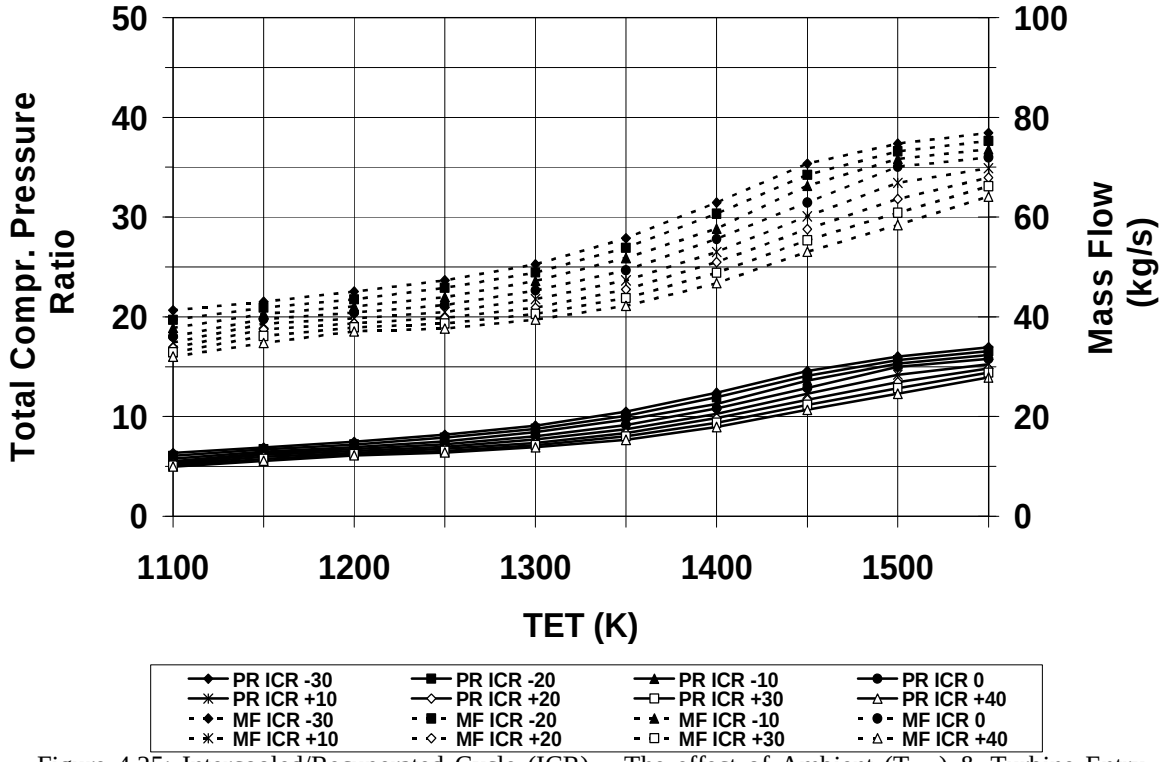

Figure 4.25: Intercooled/Recuperated Cycle (ICR) – The effect of Ambient (T_{amb}) & Turbine Entry Temperature (TET) on Total Compression Ratio (PR) and Mass Flow (MF)

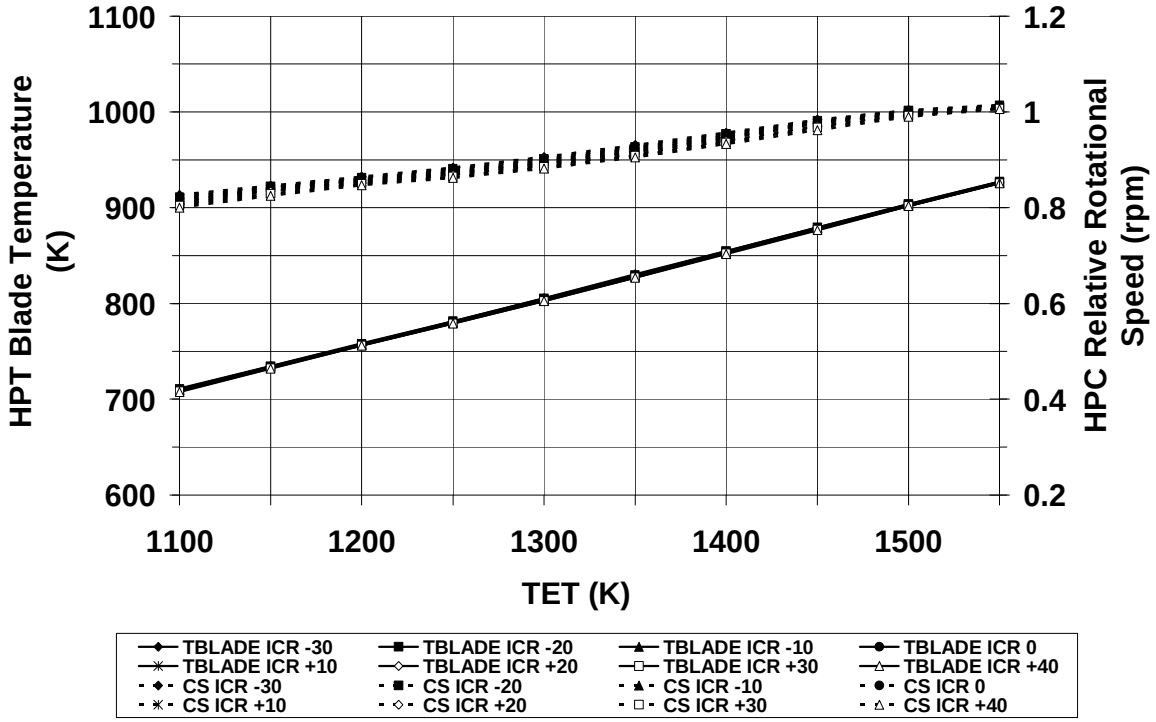

Figure 4.26: Intercooled/Recuperated Cycle (ICR) – The effect of Ambient (T_{amb}) & Turbine Entry Temperature (TET) on HP Turbine Blade Temperature (TBLADE) & HP Compressor Relative Rotational Speed (CS) to Design-Point

4.4 Hot Section Rotor Blade Creep Life Dataset

4.4.1 Definitions

A primitive hot section gas path sizing was performed for each of the simulated gas turbines in order to obtain the hot section rotor blade height and distance from mid-shaft to mid-blade, and as a consequence the design-point rotational speed of the high pressure turbine shaft *N* (or just turbine shaft in the case of single shaft gas generator) at the specified design point blade time to failure t_f (hot section design-point overhaul interval) which is set at **30,000 hours**. The calculations were performed without taking into account the amount of cooling mass flow that is mixed with the main gas flow exiting the combustor, as the off-design results are not affected by this assumption because what determines the off-design centrifugal stress σ_{cfo} is the ratio between the off-design N_{od} and design-point *N* shaft rotational speed (relative rotational shaft speed) which is expressed in equation 2-5. Of greater importance is the calculation of the design-point turbine rotational speed which in combination with the design-point turbine entry temperature *TET*, design-point cooling flow

temperature T_c, constant assumed blade cooling effectiveness ε and blade material properties, design and dimensions determine the Larson-Miller parameter *LMP*, thus the specified design-point blade time to failure t_f. No coatings are assumed that are applied on the surface of the hot section turbine blade.

4.4.2 Hot section rotor blade material data

4.4.2.1 Material general description

The material that the hot section turbine blade is assumed that is made of, was chosen to be the polycrystalline GTD-111 Nickel based superalloy which has been developed by General Electric in the mid-70's and is used as a stage one blade construction material in a wide range of industrial and aeroderivative gas turbines [21]. The material possesses a 20 ^{o}C creep rupture advantage over the also widely used stage one turbine blade material IN738 which substitutes [21] [13] [20], and its composition suggests that it is a derivative of IN738 and the also widely used aero-gas turbine alloy René 80 [13].

4.4.2.2 Material Larson-Miller data

The Larson-Miller diagram [13] of the polycrystalline GTD-111 nickel based super alloy is presented in figure 4.27. The diagram contains data from a study [13] and published data, of which the latter was implemented in the gas turbine hot section rotor blade creep life model. The implementation method of the diagram in the model is described in chapter 2, section 2.4.2.

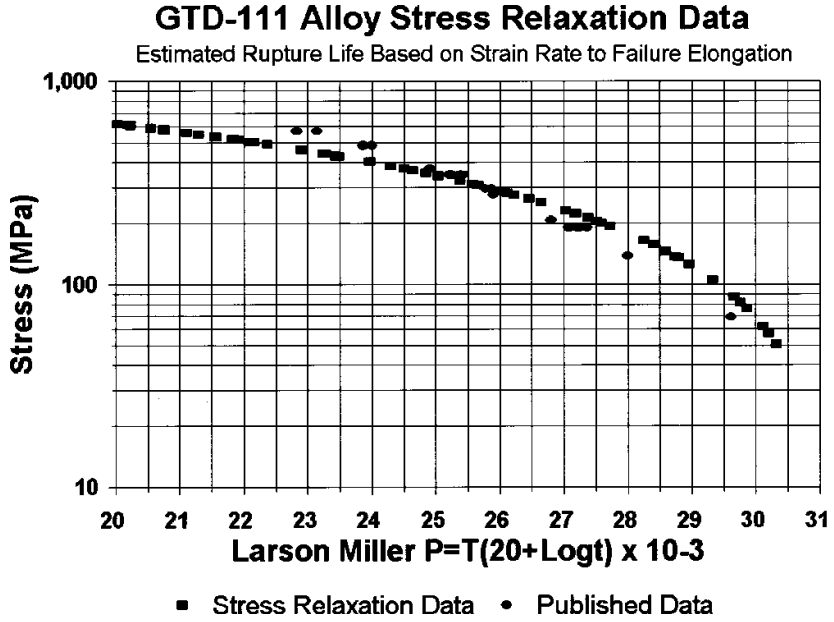

Figure 4.27: Larson-Miller diagram of the polycrystalline GTD-111 hot section turbine blade material [13]

4.4.2.3 Material density

The density of the polycrystalline GTD-111 at room temperature as aged or any other conditions was not found in any published or academic literature and a approximate value was assumed to be used as blade material density which is ρ_b=8500 kg/m^3. The estimation was based first on the density of IN738, which was found to be 8110 kg/m^3 at 1033 K [22], and second on the reduction of the density of the Nickel based superalloy stage one aero-gas turbine blade material CMSX-4 which was found to be approximately 4% at temperatures between 298 K and 1050 K [23].

4.4.3 Hot section gas path sizing and shaft rotational speed

4.4.3.1 Gas path sizing methodology

The gas path sizing procedure was performed in order to obtain a very approximate value of the hot section turbine blade height h_b and the distance from mid-shaft to mid-blade r_{mb}. The method that is described in this section is based on small part of a complete study on the gas-flow-path sizing and aero-engine weight [24] and uses a combination of gas-dynamic and geometric formulas as they are presented later in this section. In order to obtain the hot section turbine blade height h_b and the distance from mid-shaft to mid-blade r_{mb}, the initial step is to calculate the velocity coefficient ψ at the entry of the turbine which is defined in the gas-dynamic equation 4-4 [24].

$$\psi = \sqrt{\frac{1}{(1+[(\frac{\gamma-1}{2})]M^2)(1-\frac{\gamma-1}{\gamma+1})}} \qquad \text{Equation 4-4}$$

Where: γ is the ratio of specific heats which at the hot section is assumed 1.33 and M is the mach number of the gas flow at the entry of the turbine which is assumed at all cases at 0.3.

The next step is the estimation of flow coefficient φ which is defined in the gas-dynamic equation 4-5 [24].

$$\varphi = \psi(\frac{\gamma+1}{2})^{1/(\gamma-1)}(1-\frac{\gamma-1}{\gamma+1}\psi^2)^{1/(\gamma-1)} \qquad \text{Equation 4-5}$$

The gas path area A_{GP} at the entry of the turbine can then be calculated as defined in the gas-dynamic equation 4-6 [24].

$$A_{GP} = \frac{(GF)\sqrt{T_T}}{S_{gc} P_T \varphi} \qquad \text{Equation 4-6}$$

Where: GF is the gas mass flow, T_T is the temperature of the gas flow, P_T the pressure of the gas flow at the entry of the turbine and S_{gc} is a gas dynamic constant which is defined in equation 4-7 [24].

$$S_{gc} = (\frac{\gamma}{R})\sqrt{[\frac{2}{(\gamma+1)}]^{\frac{(\gamma+1)}{(\gamma-1)}}} \qquad \text{Equation 4-7}$$

Where: R is the gas is the universal gas constant (8.31432 J/molK).

Then the tip diameter D_T is calculated as it is defined in equation 4-8 [24].

$$D_T = \sqrt{\frac{4A_{GP}}{\pi[1-(HTR)^2]}} \qquad \text{Equation 4-8}$$

Where: HTR is the hub-to-tip ratio, which at the entry of the hot section turbine is assumed 0.82 for all simulated marine gas turbines.

The hub diameter D_H is calculated by using equation 4-9 and the blade height h_b is defined in equation 4-10 [24].

$$D_H = D_T(HTR) \qquad \text{Equation 4-9}$$

$$h_b = \frac{D_T - D_H}{2} \qquad \text{Equation 4-10}$$

Finally the mid-shaft to mid-blade distance r_{mb} is calculated by using equation 4-11 [24].

$$r_{mb} = \frac{h_b + D_H}{2} \qquad \text{Equation 4-11}$$

4.4.3.2 Calculation of hot section blade height and distance from mid-shaft to mid-blade

The calculation of the hot section blade height and distance from mid-shaft to mid-blade was performed for each of the simulated marine gas turbine by implementing the method described in the previous section on an excel spreadsheet. The gas mass flow properties required by equation 4-6 at the engine station that represents the entry of the hot section turbine were obtained from the detailed design-point performance results below the "*Turbomatch*" input file in appendix A.1. The supplemented input

data for the calculation of the hot section blade dimensions required by the method described in the previous section is presented in table 4.7, where in the case of the *TMI* cycle gas turbine the calculation is performed by using the 5MW low-power *HPT* thermodynamic state as there is a little difference in the simulation of design-point results in the non-dimensional flow and speed of the *HPC* between the low and high power mode, but it needs to be mentioned that during operation at design-point there is a difference in the *HPC* outlet temperature of +9 K between the high-power and the low-power mode (see also section 4.3.4.4).

Table 4.7: Supplement input data for the calculation of the hot section blade height and distance from mid-shaft to mid-blade for each of the simulated marine gas turbines

Parameter/Engine	**Simple cycle**	**TMI cycle (both modes)**	**Intercooled cycle**	**Recuperated cycle**	**Intercccoled/ Recuperated cycle**
Pressure at turbine entry (N/m^2)	168721.6	218831.8	233089.9	112412.2	123674
Gas mass flow *GF* (kg/s)	65.41	13.6	55.41	70.051	61.453

The calculated results, with the use of the method described in the previous section, of the hot section turbine blade height h_b and distance from mid-shaft to mid-blade r_{mb} are presented in table 4.8 and were used as input data for the calculation of the design point turbine rotational speed *N*. The results describe from a very general point of view the dimensional differences between the hot section rotor blades of the simulated gas turbines due to their adopted thermodynamic cycles and power output.

Table 4.8: Results presentation of the calculated blade height and distance from mid-shaft to mid-blade for each of the simulated marine gas turbines

Parameter/Engine	**Simple cycle**	**TMI cycle (both modes)**	**Intercooled cycle**	**Recuperated cycle**	**Intercooled/ Recuperated cycle**
Blade height, h_b (cm)	10.94	4.38	8.57	13.88	12.39
Distance from mid-shaft to mid-blade, r_{mb} (cm)	55.35	22.16	43.34	70.17	62.66

4.4.3.3 Calculation of design-point turbine rotational speed

The calculation of the hot section shaft rotational speed was performed in order to adjust the design-point blade time to failure t_f at 30,000 hours, as the thermodynamic state and the essential dimensional properties of the hot section rotor blade are already

calculated. For the calculation of the design-point turbine rotational speed N the rotor blade creep life model (chapter 2, section 2.4) was used independent from "*Poseidon*", and an iteration routine was added to the model which performed turbine rotational speed steps of 0.01 rpm from to low to high values, until the Larson-Miller criterion (equation 2-3) calculated the nearest design-point blade time to failure t_f value to 30,000 hours. The supplement input data that were used are presented in table 4.8 and table 4.9. The shroud parameter K_s was given a universal value of 1.2.

Table 4.9: Supplement input data for the calculation of the turbine rotational speed of each of the simulated marine gas turbines

Parameter/Engine	**Simple cycle**	**TMI cycle (both modes)**	**Intercooled cycle**	**Recuperated cycle**	**Intercccoled/ Recuperated cycle**
Cooling flow temperature, T_c (K)	687.06	746.00	609.38	626.53	505.65

The calculated results of the design-point turbine rotational speed N for each of the simulated marine gas turbines that were obtained with the method described earlier in this section and define the design-point blade time to failure t_f at 30,000 hours are presented in table 4.10.

Table 4.10: The design-point turbine rotational speed of each of the simulated marine gas turbines

Parameter/Engine	**Simple cycle**	**TMI cycle (both modes)**	**Intercooled cycle**	**Recuperated cycle**	**Intercccoled/ Recuperated cycle**
Turbine design point rotational speed, N (rpm)	7279.3	16706.0	10000.0	6068.2	7524.2

Note: The +9 K difference in the *HPC* outlet temperature between the high-power and the low-power mode of the *TMI* cycle gas turbine causes the design-point blade time to failure t_f to drop to approximately **23,000 hours**, a phenomenon that will have a negative effect in the maintenance cost of the *TMI* power plant.

4.5 Gas Turbine Emissions Dataset

4.5.1 Emissions background overview

4.5.1.1 Nitric oxide (NO_x) emissions

The nitric oxide (NO_x) compounds are toxic and environmentally hazardous because when they are emitted in the atmosphere they initiate chemical reactions that form nitric acid which is part of the components of acid rain and they take part in the creation of low level or tropospheric ozone. Nitric oxide is produced by three different mechanisms:

- "Thermal" NO_x
- **"**Fuel*"* NO_x
- "Prompt" NO_x

"Thermal" NO_x

"Thermal" NO_x which utilises the Zeldovich mechanism is produced at high temperatures in the flame post flame gases (>1850 K) during combustion and it is proportional to the residence time and is affected by pressure [25]. The production of "Thermal" NO_x reaches its highest values at the lean-fuel side of the stoichiometric mixture ratio, because of the potential of fuel and nitrogen to react with the available oxygen, and it is highly affected by fluctuations in the mass flow temperature entering the combustor, as increasing the mass flow temperature the levels of "Thermal" NO_x also increase. The effects of fuel type (i.e. liquid and gaseous fuels) on the production of "Thermal" NO_x are significant especially at lower regions of flame temperature (<1900 K) where gaseous fuels have the advantage of producing lower levels of "Thermal" NO_x than liquid fuels though at higher regions of flame temperature (>1900 K) gaseous fuels start to approach the "Thermal" NO_x production levels of liquid fuels [26].

"Fuel" NO_x

In the case that fuel contains organically bounded nitrogen then at the combustion process it will form an amount of the so-called "Fuel" NO_x. The percentage of the nitrogen that will create nitric oxide compounds depends on the characteristics of the combustion process [27]. Distillate fuels contain a small amount of organically bounded nitrogen which averages at 0.06%. Gaseous fuels (i.e. natural gas) can

contain more than 4% of organically bounded nitrogen, but it is removed in a high percentage before it is commercially available.

"Prompt" *NOx*

The "Prompt" *NOx* is mainly formed in low temperature fuel-rich flames a phenomenon that is not compatible with the kinetically overall process and its levels cannot be predicted at any degree of precision, but it becomes an important NO_x emissions factor in combustor that incorporates lean premixed combustion [27].

4.5.1.2 Carbon monoxide (*CO*) emissions

Carbon monoxide emissions are toxic and they can theoretically be created first if the primary zone of the combustor operates at fuel-rich conditions where the oxygen levels do not allow the formation of carbon dioxide (CO_2) and second if the mixture ratio in the primary zone is stoichiometric or slightly fuel-lean, where these conditions advance the dissociation of carbon dioxide (CO_2) [27]. Practically carbon monoxide is formed at low flame temperatures where there is incomplete combustion and some of the reasons that cause it, are[27]:

- Inadequate burning rates in the primary zone due to very low fuel/air ratio and residence time.
- Not complete mixing of fuel with air where mixture can be very lean to support combustion or very rich which create high concentrations of carbon monoxide.
- Rapid cool-down of the post-flame products caused from the liner wall cooling air. That is the reason annular combustors inherently produce lower carbon monoxide levels than tubular.

4.5.1.3 Unburned hydrocarbons (*UHC*) emissions

Unburned hydrocarbons emissions are toxic and are believed to be created primarily by poor atomisation, inadequate burning rates in the primary zone and the rapid cool-down of the post flame products caused from the liner wall cooling air [27]. Generally unburned hydrocarbons are produced (as carbon monoxide) at low flame temperatures where both emission compounds are produced in high amounts and significantly decrease with increasing flame temperatures and pressures thus engine power, which is also a characteristic of carbon monoxide emissions.

4.5.1.4 Carbon dioxide (CO_2) emissions

Carbon dioxide is primarily responsible for the phenomenon of global warming and its emitted quantities are governed by the quality and quantity of the fuel. Methods of decreasing the carbon dioxide emissions are:

- The use of high low-calorific value fuels.
- Adoption of advanced thermodynamic cycles and technologies which promote part and full load thermal efficiency.

4.5.2 Design-point emissions index calibration

4.5.2.1 Dry-low emissions combustor (*DLE*)

The design-point exhaust emission indexes (*EI*) (grams of exhaust emission quantity per kilogram fuel, g/kg, as required by "*APPEM*") of NO_x, *CO* and *UHC* of all simulated gas turbine combustors needed to be calibrated to the same levels before obtaining and tabulating their off-design rates into the gas turbine exhaust emissions model (chapter 2, section 2.3). The design-point exhaust emissions rates were mostly (see *UHC* emission index) modelled from published information on already in production and measured dry-low emissions combustors (*DLE*) [16] [28]. The units that the information on the exhaust emission output quantities is usually published are parts per million on a volume dry basis (ppmv) corrected to a certain percentage of excess oxygen (3%, 7%, 15% etc.) with the majority of publications (as discovered by the author) presenting the emission quantities output rates corrected to 15% oxygen at standard conditions (20 ^{o}C, 1 atm). The conversion from parts per million on volume dry basis (ppmv) assuming standard conditions to *EI* (g/kg) can be accomplished by the proposed equation 4-12. The conversion is independent of the percentage of excess oxygen the exhaust emission quantity samples are corrected to.

$$EI_p(g/kg) = \frac{1}{FF}\frac{[(ppmv)(GF/\rho_{air})(M_p)]}{[(V_{mole}/1000)(V_{fluegas})]} \qquad \text{Equation 4-12}$$

Where: Subscript *p* can be NO_x, *CO* and *UHC*, ρ_{air} is assumed 1.225 kg/m^3, M_p is the molar mass of the exhaust emission output quantity, V_{mole} is the volume occupied by one mole of gas at standard conditions (24.45 L) and $V_{fluegas}$ equals with 1,000,000 m^3 of flue gas.

It needs to be stated at that point that because the twin-mode intercooled cycle (*TMI*) operates at two different total compression pressure ratios-although combustor inlet temperature is almost the same which means that there are two standards of exhaust emission quantity rates depending on the operational power mode, it had to be decided whether the emission indexes should be calibrated by taking the low or high power mode as point of reference (section 4.3.4). Because of the fact that there is not a production *DLE* combustor that operates at such high compression pressure ratios as the high power mode of the *TMI* cycle gas turbine which would be of considerable high volume and mechanical integrity thus of higher technological level of the *DLE* combustors currently in the market, the emission indexes were calibrated by taking as point of reference the low power mode. In the case that any investigation requires the emission indexes of the high power mode to be at the same level as production *DLE* combustors results can be easily obtained by "*APPEM*" and can be modelled in the gas turbine emissions model (chapter 2, section 2.3) with no additional procedure steps.

NO_x emissions index (EI_{NOx})

The NO_x design-point exhaust emissions quantity output level for all simulated gas turbines (except for the *TMI* cycle gas turbine) using distillate fuel as it is assumed in the case studies of the RoPax ferry and the Destroyer (chapter 5, section 5.5.1) was calibrated at 100 ppmv dry corrected to 15% O_2 [16]. In the case study (chapter 5, section 5.5.2) of the intercooled/recuperated gas turbine which is used as a prime mover in the LNG carrier and it is assumed that uses natural gas as fuel the NO_x design-point emissions quantity output level was calibrated at 25 ppmv dry corrected to 15% O_2 [16]. The molar mass M_{NOx} of NO_x was assumed to be the same as of nitric dioxide (NO_2) at 46 g/mole. The design-point NO_x emissions index EI_{NOx} for the two different fuels, distillate and natural gas respectively, is presented in table 4.11, together with the design-point NO_x emissions index EI_{NOx} of the high power mode of the *TMI* cycle gas turbine.

Table 4.11: NO_x design-point emissions index for distillate and natural gas

Parameter/Fuel	Distillate		Natural Gas
	All gas turbines	TMI high power mode	ICR only in LNG carrier
NO_x emissions index, EI_{NOx} (g/kg)	7.20	13.36	2.62

CO emissions index (EI_{CO})

The procedure of calibrating the *CO* design-point exhaust emissions output quantity level is identical with procedure that was described in the previous section for the NO_x. The *CO* exhaust emissions output quantity level for distillate fuel and natural gas was calibrated at 20 ppmv and 7 ppmv dry corrected to 15% O_2, respectively [16]. The molar mass M_{CO} of *CO* is 28 g/mole. The design-point *CO* emissions index EI_{CO} for the two different fuels, distillate and natural gas respectively, is presented in table 4.12, together with the design-point *CO* emissions index EI_{CO} of the high power mode of the *TMI* cycle gas turbine.

Table 4.12: CO design-point emissions index for distillate and natural gas

Parameter/Fuel	Distillate		Natural Gas
	All gas turbines	TMI high power mode	ICR only in LNG carrier
CO emissions index, EI_{CO} (g/kg)	1.35	0.22	0.443

UHC emissions index (EI_{UHC})

The calibration of *UHC* exhaust emissions quantity output rate for distillate fuel was accomplished with an "approximation" method as no specific values (ppmv, dry corrected to 15% O_2) were found in the open literature for gas turbines that approximately have similar cycle design parameters (turbine entry temperature, total compression pressure ratio etc.) so the ICAO aero-gas turbine database [28] was studied and it was found that there is not a certain ratio between EI_{UHC} and EI_{CO} although they are created at similar conditions (sections 4.5.1.2 and 4.5.1.3). The liberation was taken to calibrate the *UHC* emissions index EI_{UHC} directly at a ratio $EI_{CO}/\ EI_{UHC}$ of approximately 5.5 resulting in an EI_{UHC} of 0.245 g/kg which if it is assumed that the molar mass M_{UHC} of *UHC* exhaust emissions for distillate fuel is the same as of propylene (C_3H_6) at 42 g/mole [29] then by using equation 4-12 the *UHC*

design-point exhaust emissions quantity output level is calculated to be approximately 4 ppmv dry corrected to 15% O_2.

The calibration of *UHC* exhaust emissions quantity output level for natural gas fuel was obtained by taking as point of reference published information [16] and was set at 2.75 ppmv dry corrected to 15% O_2. The molar mass M_{UHC} of *UHC* for natural gas was assumed to be the same as of methane (CH_4) at 16 g/mole. The design-point *UHC* emissions index EI_{UHC} for natural gas, is presented in table 4.13 including also the EI_{UHC} for distillate fuel, together with the design-point *UHC* emissions index EI_{UHC} of the high power mode of the *TMI* cycle gas turbine.

Table 4.13: UHC design-point emissions index for distillate and natural gas

Parameter/Fuel	**Distillate**		**Natural Gas**
	All gas turbines	TMI high power mode	ICR only in LNG carrier
UHC emissions index, EI_{UHC} (g/kg)	0.245	0.006	0.069

***CO_2 emissions index* (EI_{CO2})**

The CO_2 emissions index did not need to be calibrated as it solely depends on the low-calorific value (*LCV*) of the fuel. The assumption concerning the low-calorific value of distillate (assumed at 43.165 MJ/kg) and natural gas (depends between 38-50 MJ/kg) fuel respectively is that both have a similar *LCV* [30]. The CO_2 emissions index EI_{CO2} (which is directly obtained from "*APPEM*") is rated at 3137g/kg.

4.5.2.2 Conventional combustor (*SAC*)

Distillate fuel

The calibration of the emission indexes *EI* of NO_x, *CO* and *UHC* for distillate fuel, in order to reflect the exhaust emission output quantities of a conventional single annular combustor, was accomplished by taking as point of reference published information on uncontrolled NO_x exhaust emissions output quantity levels (ppmv dry corrected at 15% O_2) [16] [31] and adjusting at the same incremental proportion the *CO* and *UHC* exhaust emissions output quantity levels. The NO_x exhaust emission output quantity level was increased by a factor of 3.1 (310 ppmv dry corrected to 15% O_2) which was applied also to *CO* and *UHC* (62 ppmv and approximately 12.4 ppmv,

respectively). The increased values of the exhaust emission quantities were implemented at the life cycle costs model (chapter 3, section 3.2.2.6, equation 3-29) by setting the combustor technology factor K_{tech} at 3.1, as the combustor adopted technology is assumed to have a linear effect on the exhaust emissions output products (chapter 2, section 2.3). The design-point NO_x, *CO* and *UHC* emissions indexes EI_{NOx}, EI_{CO}, EI_{UHC} for distillate fuel, are presented in table 4.14, together with the design-point emissions indexes of the high power mode of the *TMI* cycle gas turbine.

Table 4.14: Emission indexes of conventional combustor for distillate fuel

Parameter/Fuel	**Distillate**	
	All gas turbines	TMI high power mode
NO_x emissions index, EI_{NOx} (g/kg)	22.32	41.16
CO emissions index, EI_{CO} (g/kg)	4.19	0.682
UHC emissions index, EI_{UHC} (g/kg)	0.76	0.018

Natural gas fuel

The calibration of the emission indexes *EI* of NO_x, *CO* and *UHC* for natural gas fuel was obtained by following the same procedure as described in the previous sub-section. The uncontrolled NO_x exhaust emissions output quantity levels (ppmv dry corrected at 15% O_2) were calibrated at 208 ppmv [16] [31] by setting the combustor technology factor K_{tech} at 2.08. The uncontrolled *CO* and *UHC* exhaust emissions output quantity levels were set at approximately 37.8 ppmv and 7.5 ppmv respectively by setting the combustor technology factor K_{tech} at 1.89 for both exhaust emission quantities [28]. The design-point NO_x, *CO* and *UHC* emissions indexes EI_{NOx}, EI_{CO}, EI_{UHC} for distillate fuel, are presented in table 4.15.

Table 4.15: Emission indexes of conventional combustor for natural gas fuel

Parameter/Fuel	**Natural gas**
	ICR only in LNG carrier
NO_x emissions index, EI_{NOx} (g/kg)	14.98
CO emissions index, EI_{CO} (g/kg)	2.55
UHC emissions index, EI_{UHC} (g/kg)	0.463

4.5.3 Off-design exhaust emissions quantity rates

The off-design exhaust emissions quantity rates for each simulated gas turbine including the two power modes of the *TMI* gas turbine cycle which were obtained with the use of the gas turbine performance and gas turbine emissions models are presented in appendix B.1 in the following format:

- The effect of ambient (T_{amb}) & turbine entry temperature (*TET*) on carbon dioxide (CO_2) and unburned hydrocarbons (*UHC*) exhaust emissions rates.
- The effect of ambient (T_{amb}) & turbine entry temperature (*TET*) on nitric oxide (*NOx*) and carbon monoxide (*CO*) exhaust emissions rates.

4.6 References

1. http://www.cospp.com/articles/

2. Polyzakis, A.L., *"Technoeconomic Evaluation of Trigeneration Plant: Gas Turbine Performance, Absorption Cooling and District Heating"*, PhD Thesis, Cranfield University, Academic Years 2002-2006.

3. Boyce, M.P, "*Gas Turbine Engineering Handbook, Third Edition*", *Gulf Professional Publishing, ISBN No.* 0-88414-732-6, Chapter 2, pp 67-75, 2006.

4. Pilidis, P., Palmer, J.R., "*Gas Turbine Theory and Performance*", MSc Thermal Power Lecture Notes, Cranfield University, October 2006.

5. Cunha Alves da, M.A., Franca Mendes Carneiro de, H.F., Barbosa, J.R., Travieso, L.E., Pilidis, P., "*An Insight on Intercooling and Reheat Gas Turbine Cycles*", Proceedings of the Institution of Mechanical Engineers, Vol. 215, Part A, pp 163-171, 2001.

6. Kim, T.S., Hwang, S.H., "*Part Load Performance Analysis of Recuperated Gas Turbines Considering Engine Configuration and Operation Strategy*", Journal of Energy, Vol. 31, Issues 2-3, pp 260-277, February-March 2006.

7. Walsh, P.P., Fletcher, P., "*Gas Turbine Performance, Second Edition*", Blackwell Science Ltd., ISBN No. 0-632-06434-X, Chapter 6, pp 299-301.

8. Walsh, P.P., Fletcher, P., "*Gas Turbine Performance, Second Edition*", Blackwell Science Ltd., ISBN No. 0-632-06434-X, Chapter 5, pp159-166, pp 191-195, pp 243-245.

9. http://library.thinkquest.org/C007007/energy/conventional/Gas_turbine.htm

10. Marx, M., "*Investigation and Optimisation of Intercooling in an Intercooled Recuperative Aero Engine*", MSc Thesis, Cranfield University, Academic Year 2006-2007.

11. Kazatzis, P., *"A Novel and Compact Marine Propulsion System"*, MSc Thesis, Cranfield University, Academic Year 1996-1997.

12. www.benwiens.com/enenrgy2.html

13. Daleo, J.A., Wilson J.R., *"GTD-111 Alloy Material Study"*, Journal of Engineering for Gas Turbines and Power, Vol. 120, pp 374-382, April 1998.

14. "*WR 21 Propulsion Module, Fact Sheet*", Rolls-Royce plc, Ref: MP/37/00, 2000.

15. "*LM 2500 Marine Gas Turbine*", GE Marine, Ref: AE-28203F, August 2006.

16. Badeer, G.H., "*GE Aeroderivative Gas Turbines-Design and Operating Features*", GE Power Systems, Ref: GER-3695E, October 2000.

17. "*LM 2500 Gas Turbine*", GE Aero Energy*.
*http://gepower.com/prod_serv/products/aero_turbines/en/downloads/lm2500.pdf

18. Andreini, A., Facchini, B., "*Gas Turbine Design and Off-design Performance Analysis with Emissions Evaluation*", Journal of Engineering for Gas Turbines and Power, Vol. 126, pp 83-91, January 2004

19. Parker, M.L., MacLeod, P.K., Coulson, M., "*Advances in a Gas Turbine System for Ship Propulsion*", RTO AVT Symposium on "Gas Turbine Engine Combustion, Emissions and Alternative Fuels", Lisbon, Portugal, 12-16 October 1998.

20. Shepard, S.B., Bowen, T.L., Chiprich, J.M., "*Design and Development of the WR-21 Intercooled Recuperated (ICR) Marine Gas Turbine*", Journal of Engineering for Gas Turbines and Power, Vol. 117, pp 557-562.

21. Schilke, B., "*Advanced Gas Turbine Materials and Coatings*", GE Energy, Ref: GER-3569G, August 2004.

22. Thakur, A., "*Microstructular Responses of a Nickel-Base IN-738 Superalloy to a Variety of Pre-Weld Heat-Treatments*", MSc Thesis, The University of Manitoba, Academic Year 1996-1997.

23. Mills, K.C., Youssef, Y.M., Li, Z., Su, Y., "*Calculation of Thermophysical Properties of Ni-based Superalloys*", ISIJ International, Vol. 46, No. 5, pp 623-632, 2006.

24. Shanghi, V., Kishore Kumar, S., Sundararajan, V., "*Preliminary Estimation of Engine Gas-Flow-Path Size and Weight*", Journal of Propulsion and Power, Vol. 14, No. 2, pp 208-214, March-April 1998.

25. Razdan, M.K., Chin, J.S., "*Marine Gas Turbine Engine Emissions: Current State of the Art and Future Needs*", 30th AIAA/ASME/SAE/ASEE Joint Propulsion Conference, Indianapolis, IN, June 27-29, 1994.

26. Lefebvre, A.H., "*Gas Turbine Combustion, Second Edition*", Taylor and Francis, ISBN No. 1-560-32673-5, Chapter 9, pp 324-333.

27. Lefebvre, A.H., "*Fuel Effects on Gas Turbine Combustion"*, Performed by: School of Mechanical Engineering, Purdue University, West Lafayette IN 47907, Controlled by: Aero Propulsion Laboratory, Air Force Wright Aeronautical Laboratories, Wright Paterson Air Force Base, Ohio 45433, Status: Unlimited distribution, January 1983.

28. "*ICAO Engine Emissions Databank*", Issue 15, 16 July 2007.

29. Dake, A.R., "*Modelling and Control of Cold Start Hydrocarbons Emissions*", MSc Thesis, Indian Institute of Technology, Bombay, Academic Year 2004-2005.

30. Walsh, P.P., Fletcher, P., "*Gas Turbine Performance, Second Edition*", Blackwell Science Ltd., ISBN No. 0-632-06434-X, Chapter 13, pp 587-592.

31. "*Alternative Control Techniques Document-NOx Emissions from Stationary Gas Turbines*", U.S Environmental Protection Agency, Office of Air and Radiation, Office of Air Quality Planning and Standards, Ref: EPA-453/R-93-007, Chapter 2, pp. 4-10, January 1993.

5 *TERA* Case Studies Dataset: "*Poseidon*" Scheme and Scenarios

5.1 Introduction

This chapter starts with the description and specification of the existing and in pre-production stage marine vessels that were used as reference for their simulated equivalent expressions implemented on the marine vessel power prediction model, based on published and academic literature. Consequently, the simulated marine vessels are described and their specification and performance is presented, including essential definitions on common procedures, parameters and assumptions made during pre-modelling and modelling stage. Information is also given on the modelling procedure and any evaluation tools used. The chapter continues with definitions and background information on the supplementing dataset that was implemented on each of the models that compose the "*Poseidon*" scheme; and delimit the structure of the three case studies that fulfil the technical and environmental part of *TERA* of this project. There more, the journey scenarios dataset are defined for each of the marine vessels and as a consequence each case study.

5.2 Marine Vessel Power Prediction Model Dataset

5.2.1 Reference marine vessels description and specification

5.2.1.1 Reference RoPax fast ferry

The marine vessel that was chosen to be used as reference for the simulation of the RoPax fast ferry is a typical example of a 3rd generation fast monohull roll-on/roll-off passenger ferry that exceeds an overall length of 180 m and has a service/or maximum speed of 29 knots [1] [2] [3].All these vessels typically have a diesel engine four stroke medium speed power plant (2-4 prime movers) coupled with a twin propeller arrangement via mechanical transmission (reduction shaft speed gear box and engaging/disengaging clutch) and for the auxiliary service load they incorporate 1~4 four stroke high speed diesel generators. Their hull design is of normal shape and universally incorporates a bulbous bow and a transom stern that reduce the hydrodynamic resistance of the vessel [4]. The number of thrusters installed on the

hull can vary from one to two positioned for and zero to two positioned aft, with the reference vessel having two positioned for and one positioned aft. For good stability the reference vessel incorporates a pair of anti-vortex stabilizer fins positioned mid-ship. Information on the propeller design parameters of the reference RoPax fast ferry in not published in the public domain, but research on marine vessels of similar size, form and propeller arrangement showed that propeller diameter can vary from 4.5 to 5.5m [3] [5] [6] [7] depending on limitations from the draft and the breadth of the marine vessel and other factors which are beyond the scope of the current research. The published information on the technical specification of the reference RoPax fast ferry is shown in table 5.1 [1] [8] [9].

Table 5.1: Reference RoPax fast ferry published design parameters

Parameter	
Length overall, Loa (m)	194.30
Length between perpendiculars, Lpp (m)	176.0
Length at water line, L	188.54
Breadth, B (m)	25.0
Design draft, T (m)	6.40
Displacement, Δ (tons)	16997.3
Wetted surface area, S_H (m^2)	5116
Service speed at 85-90% MCR (knots)	28.5
Prime movers	4 x geared medium speed 4-stroke diesels
Installed prime mover power (MW)	42.24
Auxiliary generators	3
Installed auxiliary power (MW)	4.38
Propulsion devices	2 x controllable pitch propellers (CPP)
Thrusters	2 for, 1 aft

5.2.1.2 Reference Destroyer

The marine vessel that was chosen to be used as reference for the simulation of the Destroyer is a last generation naval vessel (Type 45 Destroyer) that incorporates an integrated full electric propulsion system (*IFEP*) (figure 5.1, see also chapter 1, section 1.2). The vessel's prime movers are two de-rated WR-21 21MW intercooled/recuperated gas turbines, together with two 4-stroke high speed diesel generators, rated at approximately 2MW each, for port manoeuvring and very low cruising speeds [10]. The vessel was designed for a boost speed of 28 knots but at sea trials it was able to obtain a speed of approximately 30.5 knots [11]. Each of the prime movers is attached to an alternator and there are two 20MW electric propulsion motors installed within the lower decks, each coupled via a conventionally installed shaft (from engine room to propulsion devices) to a fixed pitch propeller (*FPP*). The

hull design is of V-shape and incorporates both a bulbous bow (with the sonar installed inside it) and a transom stern, but it was not found in published literature the position and the number of thrusters installed on the hull, though these type of vessels normally incorporate at least one thrusters positioned for and one positioned aft. No information on the public domain was found on reference propeller design parameters. The limited published information on the technical specification of the reference Destroyer naval vessel is shown in table 5.2 [11] [12] [13].

Table 5.2: Reference Destroyer published design parameters

Parameter	
Length overall, Loa (m)	152.4
Length between perpendiculars, Lpp (m)	Not published
Length at water line, L	Not published
Breadth, B (m)	18.0
Design draft, T (m)	5.1
Displacement, Δ (tons)	7350.0 (full load)
Wetted surface area, S_H (m^2)	Not published
Service speed (Cruise)/ (Boost), V_s (knots)	18/28+ (max. 30.5 at sea trials)
Prime movers	2 x Intercooled/recuperated alternator gas turbines & 2 x 4-stroke high speed diesels
Installed prime mover power (MW)	Approximately 54MW
Auxiliary generators	Prime movers
Installed auxiliary power (MW)	Not published
Propulsion devices	2 x Fixed pitch propellers (FPP)
Thrusters	Not published

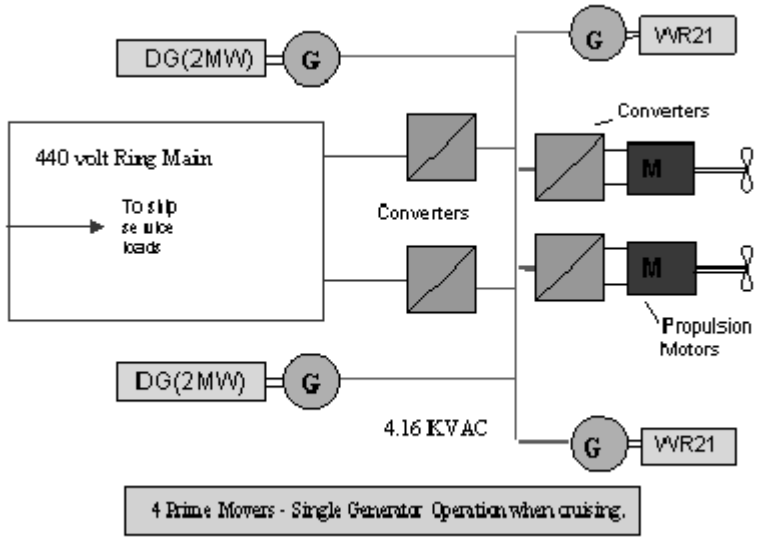

Figure 5.1: General representation of the IFEP system of the reference Destroyer [10]

5.2.1.3 Reference liquefied natural gas (LNG) carrier (Q-max)

The simulation model of the LNG carrier is based on published information that defines the design specifications of the Q-max class, which is a new generation on LNG carriers with volumetric capacity of liquefied natural gas from 260,000 m^3 and more. Until the completion of the research on available information on LNG carriers there was not a Q-max class marine vessel in service, but it is confirmed that at least one has floated out of dry-dock and it is being outfitted and 14 Q-max class marine vessels have been signed for construction [14]. This class of marine vessels depending on the unit configuration will either use compressed boil-off gas (which can vary from 0.1% to 0.2% daily of the total LNG cargo quantity) as fuel for the power plant or they can incorporate a reliquefaction system for the boil-off gas and use liquid fuel (i.e. heavy fuel oil, distillate fuel etc. depending on the prime mover type) for a dual-fuel power plant [15]. The Q-max class of marine vessels can either incorporate a single or twin propeller arrangement [15], attached to a mechanical or electrical propulsion system.

The hull of these vessels incorporates a bulbous bow and the stern is of a single or twin gondola type unless podded propulsion is preferred where a transom stern design can be adopted. Thrusters may be installed for and aft on the vessel's hull for easier docking manoeuvring [16]. The design draught of this class of vessels is limited to 12m because of limitation in port facilities [15] and as a guideline if a twin propeller propulsion system is chosen a preliminary estimation on the propeller diameter can be obtained by calculating as equal to 76% of the design draft [15], as due to the low density of the LNG cargo the ballast draft is close to the design draft. By adopting the above guideline the diameter of each of the propeller of the Q-max marine vessel is estimated at 9.12m. The limited published information on the technical specification of the reference Q-max class LNG carrier is shown in table 5.3 [15], and is a product of research concerning preliminary estimation of the powering requirements of this class of marine vessels.

Table 5.3: Reference Q-max class published guide design parameters

Parameter	
Length overall, Loa (m)	345.0
Length between perpendiculars, Lpp (m)	332.0
Length at water line, L	Not published
Breadth (m)	54.0
Design draft, T (m)	12.0
Displacement, Δ (tons)	Not published
Wetted surface area, S_H (m^2)	Not published
Service speed at 90% MCR	20.0
Prime movers	2 x 2-stroke slow speed diesels
Installed prime mover power (MW)	41.60
Auxiliary generators	Not Published
Installed auxiliary power (MW)	Not published
Propulsion devices	2 x FPP Propellers
Thrusters	Not published

5.2.2 Simulated marine vessels description and specification

5.2.2.1 Definitions

All simulated marine vessels incorporate a 50MW at design-point power plant which is composed by two marine gas turbines and they utilise a twin propeller arrangement. The main form coefficients and elements of the hull shape of the simulated marine vessels were obtained from published literature [4] (appendix F.5, figure F.2) that provides information on the variation of the above mentioned coefficients and elements according to the type of the marine vessel. Information or general guidelines on the design parameters of a bulbous bow and the transom stern (cross sectional area of the bulb on the vertical plane A_{BT}, height of the centroid of the area A_{BT} above the base line h_B and the immersed area of the transom stern at zero speed A_T) was not found in the public domain and an extensive trial and error procedure was adopted after estimating the bulbous bow required design parameters from published drawings and figures, as the effect of the bulbous bow on the hydrodynamic resistance and propulsive efficiency of the vessel can result in a reduction of 10-15% and 4-5% respectively, resulting in an up to 20% reduction in the required power delivered to the propeller P_D in calm sea [4]. The same procedure was applied for the estimation of the lateral and frontal projected areas of the vessels, A_L and A_F respectively, as the effect of the aerodynamic resistance of the marine vessel on its total resistance R_T can be an additional 2-4% in no wind conditions [17]. The estimation of the appendages areas (bilge keels, rudder(s), shaft brackets, bossing etc) and thrusters position and diameter was also obtained by implementing the above

mentioned procedure, as shaft brackets and bossing can increase the hydrodynamic resistance of the marine vessel by 5-12%, though bilge keels and rudders can contribute to a small increase of 1-2% [18]. Bow thrusters if carefully positioned do not affect the hydrodynamic resistance of the marine vessel, but transverse thrusters positioned in the afterbody can increase resistance by 1-6% [18].

The RoPax fast ferry and the LNG carrier are both assumed that they utilise azimuthing pod-drives to deliver any required power P_D to the propellers. Podded propulsion reduces the hydrodynamic resistance of a marine vessel comparing with conventional shaft drive arraignment as/and it neglects the need for shaft brackets, rudders, stern thrusters and bossings [19]. On the other hand they reduce propulsive efficiency but the improvement in hydrodynamic resistance is more influential than the loss in propulsive efficiency [19]. Currently the maximum power output that a single pod-drive, available in the market, can transmit is 28MW [20]. Because "*Poseidon*" at its current stage cannot formally facilitate marine vessels equipped with pod-drives, in order to approximate the total appendages area of the RoPax ferry and the LNG carrier were kept to a minimum, and the propellers open water efficiency η_{OWE} of both previously mentioned marine vessels was kept to an estimated 1-2% lower than optimum. The optimum open water efficiency of the propellers thus the pitch to diameter ratio P/D and the blade area ratio A_E/A_O was obtained with the aid of the academically developed propeller optimisation program (*POP*) [21] which is available in the public domain and simulates the Wageningen B-series propellers.

The mean initial hull roughness amplitude k_h applied to all simulated marine vessels is assumed to be 120μm and the transmission efficiency η_t of the electrical propulsion system is assumed to be 95% including alternator efficiency [10]. The design-point and off-design performance of the simulated marine vessels were obtained with the use of the marine vessel power prediction model (chapter 2, section 2.5) independent from the "*Poseidon*" scheme.

5.2.2.2 Simulated RoPax fast ferry

The simulated RoPax fast ferry differs from the published technical specification of the reference Ropax fast ferry, in the length at water line L, breadth B and design draft T which were increased accordingly in order the 50MW power plant to operate at

approximately 85% maximum continuous rating (*MCR*) (trial conditions, clean hull) at a service speed V_s of 29 knots including the service load P_{aux} required, resulting in a design-point overall power requirement of 42.23MW. The marine vessel is assumed that sails averagely at every journey at design draft condition because the typical operational profile of a RoPax ferry is to unload in-bound and load out-bound passengers and vehicles at every terminal or intermediate scheduled ports. The marine vessel and propeller design parameters are shown in appendix A.2, tables A.2 and A.3 respectively. The off-design performance of the marine vessel and propellers including the effects of hull fouling (see section 5.2.3) in trial conditions can be found in appendix B.5, figure B.14.

5.2.2.3 Simulated Destroyer

The length at water line of the simulated Destroyer was estimated from published figures of similar marine vessels as detailed information was not available at the time of modelling to public domain. The vessel's propeller diameter was estimated by also using published figures, and tested by using the propeller optimisation program (*POP*). The propeller design-point open water efficiency η_{OWE} was adjusted at 28 knots (trial conditions) and the overall power requirement including the service load P_{aux} was calculated to be 27.11MW. Setting the boost speed at 30.5 knots the overall power requirement was increased to 41.34MW (approximately 83% MCR). The cruise speed of the Destroyer was adjusted at 19 knots with an overall power requirement of 8.12 MW (trial conditions, clean hull). The marine vessel is assumed that operates constantly at design draft carrying the same amount of personnel and weaponry. The marine vessel and propeller design parameters are shown in appendix A.2, tables A.2 and A.3 respectively. The off-design performance of the marine vessel and propellers including the effects of hull fouling (see section 5.2.3) in trial conditions can be found in appendix B.5, figure B.13.

5.2.2.4 Simulated Liquefied Natural Gas (LNG) carrier (Q-max)

The length at water line of the simulated LNG carrier was estimated from published figures of similar marine vessels as detailed information was not available at the time of modelling to public domain. The overall total power requirement including service load P_{aux} at 20 knots (trial conditions, clean hull) of the LNG carrier is 44.25MW (88% MCR). The LNG carrier was simulated only in laden (design draft) condition due to constrains in available time for the completion of the current research, and for

reference purposes a general guideline on the variation of the required brake power P_B of an LNG carrier from a ballast to a laden condition is an increase of approximately 4% [22]. The fuel supplied to the prime movers is assumed to be compressed natural gas (needs to be higher than the total compression ratio of the gas turbine prime mover) obtained from boil-off quantities. The marine vessel and propeller design parameters are shown in appendix A.2, tables A.2 and A.3 respectively. The off-design performance of the marine vessel and propellers including the effects of hull fouling (see section 5.2.3) in trial conditions can be found in appendix B.5, figure B.15.

5.2.3 Hull fouling resistance dataset

5.2.3.1 Background

The hull of all the simulated marine vessels is assumed that is coated with a hydrid TBT self polishing anti-fouling system, which a balanced mixture of SPC (Self Polishing Copolymer) and CDP (Controlled Depletion Polymer) [23]. The average annual increase in hull roughness amplitude due to fouling when a hydrid TBT self polishing antifouling system is used is 30μm. For SPC and CDP anti-fouling systems the average annual increase in hull roughness amplitude due to fouling is 20μm and 40μm respectively, and the cost of an anti-fouling system is proportional to its performance [23]. The most technologically advanced anti-fouling systems are the "foul release" with an average annual increase in hull roughness amplitude due to fouling of 5μm [23].

5.2.3.2 Hull fouling progression

The initial (F1) average hull roughness amplitude that corresponds to all simulated marine vessels is 120μm [23], assumed for both the bottom and sides of the hull (chapter 2, section 2.5.2.5). Table 5.4 presents the average annual increase in hull roughness amplitude due to fouling that is used for all the case studies in this project.

Table 5.4: Average annual increase in hull roughness amplitude used in all three case studies

Year	Average hull roughness amplitude, k_h (μm)
F1	120
F2	150
F3	180
F4	210
F5	240

The evaluation of the effects of hull fouling increase on the resistance of the each of the simulated marine vessels is presented in appendix B.5, figures B.34, B.35, B.36.

5.3 Power Plant Operation Management Model Dataset

5.3.1 Power distribution module dataset

5.3.1.1 Service load (or auxiliary power)

The service load P_{aux} required by the auxiliary systems of each of the simulated marine vessels is assumed constant during the duration of all the case study scheduled journeys (chapter 2, section 2.6.2.1). Each of the simulated marine vessels has a different required service load which depends on the type of the vessel, size, season of year, time of day and mission profile, and for the estimation of the required service load for each of the simulated marine vessels an effort was made to average the values that are used in the case studies of this project based on academic and published literature [1][22][24]. The average service load P_{aux} assumed for each simulated marine vessels in all case study journey scenarios are presented in table 5.5. The service load for the LNG carrier is assumed that includes the power required for the natural gas fuel compressor (generally around 6% of the prime mover output power) [25].

Table 5.5: Assumed service load required by each of the simulated marine vessels

Marine vessel	Service load, P_{aux} (MW)
RoPax Ferry	3.5 [1]
Destroyer	2.5 [24]
LNG carrier	3 [22]

5.3.1.2 RoPax fast ferry and LNG carrier power plant operation

Both the RoPax fast ferry and the LNG carrier have a similar operational profile, and are assumed that they both travel in open sea and ideal ambient conditions constantly at service speed where both prime movers are in operation. At adverse weather conditions and/or increased hull fouling both the marine vessels are programmed to travel at the maximum possible speed that can be obtained (with both

prime movers in operation) in combination with the maximum capabilities of the power plant under these conditions.

5.3.1.3 Destroyer power plant operation

The Destroyer has a variable operational profile and generally naval vessels of this type spend 75% of their operational life at cruise speeds and 25% at boost speeds [26]. The plural as expressed in the word “speeds” briefly describes a typical marine engineering difficulty which is the commonality of naval vessel to operate with profiles different than those they are designed to [24]. In the case study regarding the Destroyer one operational profile is adopted due to restrains in the available time to complete the current research: At ideal weather conditions the naval marine vessel uses a single prime mover at cruise mode (19 knots) and both prime movers at boost mode (30.5 knots). At adverse weather conditions and cruise mode the naval marine vessel uses a single prime mover up to sea-state W_{sea} seven where is programmed to travel up to cruise speed if possible and at sea state eight the second prime mover engages and the marine vessel is allowed to travel up to cruise speed if possible. At adverse weather conditions and boost mode both prime movers are constantly in operation. In the case that scheduled journey time is prolonged due to adverse weather conditions or high hull roughness amplitude due to fouling the Destroyer is programmed to travel at cruise speed for the remaining of the journey. It is assumed that the prime movers do not exchange operational roles, which means during the operational life of the marine vessel, the same prime mover is used for cruising and as a consequence the same prime mover engages at sprinting (boost). The chosen hull fouling progression profile does not require any modification or further additions in the power plant operation profile (exception is described below in the case of the *TMI* power plant).

Twin mode intercooled cycle gas turbine power plant

When the Destroyer is equipped with the *TMI* gas turbine power plant, both prime movers are in constant operation in cruise and boost speeds. At ideal weather conditions the low-power mode is used for cruising and the high-power mode is used for boost. When cruising at adverse weather conditions the low power mode is engaged up to sea state seven where the vessel is allowed to travel up to cruise speed, and at sea state eight the high power mode engages where the vessel is allowed to

travel again up to cruise speed. At adverse weather conditions and boost speed the high power mode is constantly in operation. In the case that hull fouling phenomenon prevents the naval vessel to obtain the required cruise speed (independently of sea condition) the high power mode engages in order to obtain it.

5.3.2 Power availability module dataset

The maximum turbine temperature (*TET*) that all gas turbine prime movers are allowed to operate up to in all scheduled journeys of the case studies of this project is set to 1530 K, as no components degradation of the prime movers is assumed in the case studies of this project, which can cause the turbine entry temperature to be elevated (if allowed) at values much beyond the design-point in order the marine vessel to obtain any required under certain performance conditions.

5.4 Journey Management Model Dataset

5.4.1 Journey schedule

The journey schedule time t_T is set to 24 hours for all the simulated marine vessels and all schedule journeys, at ideal conditions and clean hull (k_h=120μm), and was chosen as first it can be a realistic journey schedule time for all three marine vessels types in real case scenarios (though a marine vessel can change numerous schedule routes during its operational life which in most cases would be impossible to predict unless a risk or even stochastic approach can be undertaken) and second simulation time was kept at reasonable amounts. In addition no port manoeuvring and entering/exiting port procedure is included in the case studies of this project and what is of more significance than the journey schedule time, at this stage, is the annual operational time of the marine vessel thus the annual operational time t_{annual} of each prime mover. The journey distance S_j which directly depends on the vessel's speed profile is presented in table 5.6.

Table 5.6: Scheduled journey distance of each of the simulated marine vessels

Marine vessel	Scheduled journey distance, $\boldsymbol{S_j}$ (Nautical miles)
RoPax Ferry	696
Destroyer	525
LNG carrier	480

5.4.2 Ambient conditions

5.4.2.1 Air ambient temperature profile

The air ambient temperature T_{amb} profile that is applied to all scheduled journeys of the case studies, was obtained by using the data presented in table 5.7 and appendix F.3, figure F.1 and table F.3 [27]. The derived air ambient temperature profile is presented in figure 5.2. The journey start time t_{start} is applied to all scheduled journeys.

Table 5.7: Air ambient conditions input data

Parameter	
Minimum day temperature, T_{min} (^oC)	10
Maximum day temperature, T_{max} (^oC)	25
Sunrise time of day t_d (hh:mm)	06:00
Peak day temperature, t_p (hh:mm)	14:00
Journey start time, t_{start} (hh:mm)	07:00

5.4.2.2 Sea ambient temperature profile

The sea ambient temperature T_{sea} is assumed to be constant during the duration of all the scheduled journeys at 15 ^oC which is the same as the assumed intercooler cooling water temperature used by the correspondent gas turbine prime movers (chapter 4, section 4.3.2).

5.4.2.3 Sea-state profiles

As it was described in chapter 3, section 3.2.2.1, the required by the life cycle costs model is two sea-state W_{sea} profiles. The first profile that was adopted assumes trial conditions (or no weather conditions) (sea state 0-1) at all schedule journeys of the case studies. The second weather profile contains a variable sea-state profile where all sea-state numbers are included from 0 to 8. In the case that there is a journey time prolongation (t_{T+a}) all remaining time intervals assume trial conditions. The variable weather profile is presented in figure 5.2.

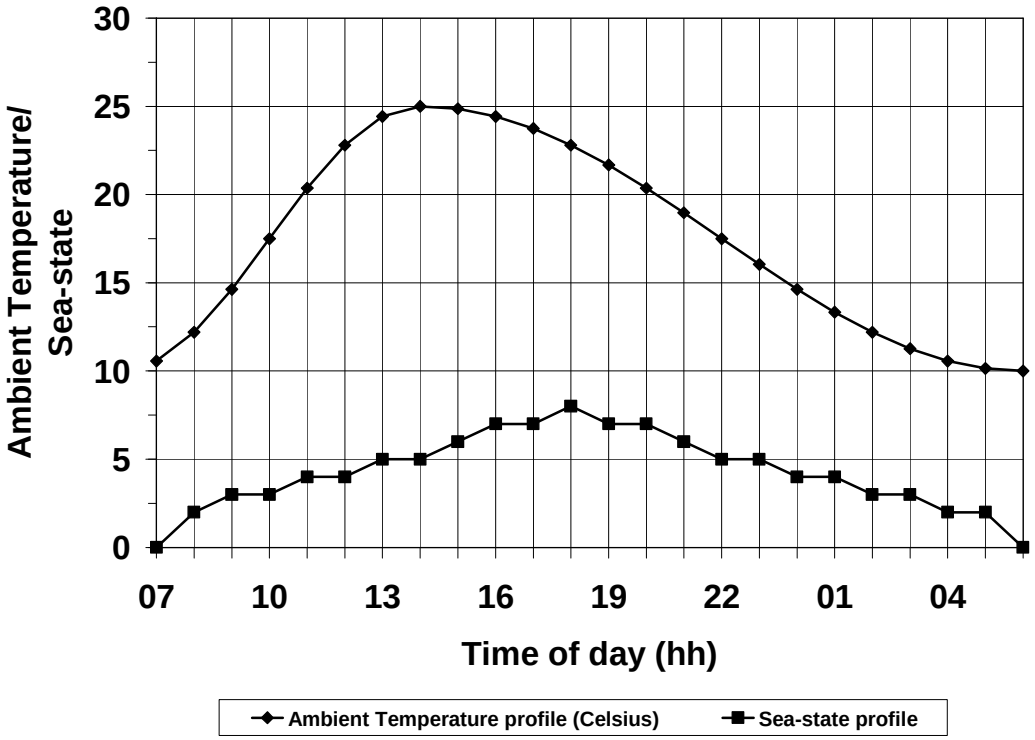

Figure 5.2: Ambient temperature and sea-state profile against time of day

5.5 Journey Scenarios Dataset

5.5.1 RoPax fast ferry and Destroyer case studies

The number journey scenarios dataset of the RoPax fast ferry and the Destroyer is identical and each marine vessel represents a case study. All five marine gas turbine prime movers are investigated individually under the same conditions, which were described in the previous sections of this chapter, as power plants of both marine vessels. The dataset is composed of five gas turbine power plants, single value of service load required, five hull fouling progression profiles, two sea-state profiles and single air ambient temperature profile. The schedule journey scenarios simulation sequence which applies to both vessels is presented in appendix F.4, table F.4

5.5.2 LNG carrier case studies

The implementation procedure of the case study of the LNG carrier is identical to case studies of the RoPax fast ferry and Destroyer with the difference that only one gas turbine power plant is investigated, due to constrains in time availability. The prime mover type of the LNG power plant that is investigated in the homonymous

case study is the intercooled/recuperated cycle gas turbine. The schedule journey scenarios simulation sequence which applies only for the LNG carrier is presented in appendix F.4, table F.5.

5.6 References

1. www.ship-technology.com/projects/superfast/
2. www.ship-technology.com/projects/knossos/
3. www.ship-technology.com/projects/bluestar/
4. *"Principles of Naval Architecture, Resistance, Propulsion and Vibration"*, Society of Naval Architects and Marine Engineers, ISBN No. 0-939773-01-5, Vol. 2, pp 70-71, pp 79-86.
5. www.ship-technology.com/projects/rotter/
6. www.ship-technology.com/projects/sea_france/
7. www.ship-technology.com/projects/nilsholgersson/
8. *"Ship Design and Construction"*, Society of Naval Architects and Marine Engineers, ISBN No. 0-939773-41-4, Vol. 2, Chapter 38, pp 24.
9. Grigoropoulos, G.J., Harries, S., Damala, D.P., Birk, L., Heimann, J., "*Seakeeping Assessment for High-Speed Monohulls-A Comparative Study*", IMDC-2003, Athens, May 2003.
10. Colin, R., "*The WR-21 Intercooled Recuperated Gas Turbine Engine-Integration into Future Ships*", Proceedings of the International Gas Turbine Congress, Tokyo, November 2003.
11. www.baesystems.com/ProductsServices/bae_product_type45.html
12. www.royalnavy.mod.uk/server/show/nav.2227
13. www.naval-technology.com/projects/horizon/
14. www.gulfbase.com/site/interface/newsarchivedetails.aspx?n=46257
15. "*Propulsion Trends in LNG Carriers*", MAN Diesel A/S, Copenhagen, 2007.
16. Kosomaa, J., "*The DF-Electric LNG Carrier Concept*", Wärtlilä The Ship Power Supplier, January 2002.
17. Rawson, K.J., Tupper E.C., "*Basic Ship Theory, Fifth Edition*", Butterworth and Heinemann, ISBN No. 0-7506-5398-1, Chapter 10, pp 378, 2001.
18. Bertram, V., "*Practical Ship Hydrodynamics, First Edition*", Butterworth and Heinemann, ISBN No. 0-7506 5712-X, Chapter 3, pp 81, 2001.
19. Mewis, F., "*The Efficiency of Pod Propulsion*", 22nd HADMAR International Conference, Varna, October 2001.
20. http://library.abb.com/global/scot/scot293.nsf/veritydisplay/64fffbc0d09506a9c125727b003f6b7d/$File/Azipod%20and%20CRP%20Azipod%20Brochure.pdf

21. "*POP Propeller Optimisation Program*", COMPASS Project, Department of Naval Architecture and Marine Engineering, University of Michigan, 1997.

22. Hansen, J.F., Lysedo, R., "*Electric Propulsion for LNG Carriers*", LNG Journal, pp 11-12, September/October 2004.

23. "*Hull Roughness Penalty Calculator*", International Paint Ltd., Akzo Nobel, 2004.

24. Hodge, C.G., Mattick, D.J., "*The Electric Warship III*", Transactions of the Institute of Marine Engineers, Vol. 110, Part 2, pp 119-134, 1997.

25. Laurilehto, M.,, "*Propulsion systems for future LNG carriers*", Wärtlilä The Ship Power Supplier, February 2002.

26. "*Fundamentals of Gas Turbine Operation in the Marine Environment"*, Short Course Lecture Notes, Cranfield University, November 2004.

27. www.gaisma.com/en/location/athens.htm

6 *TERA* Case Studies Dataset: Economic and Risk Model

6.1 Introduction

This chapter describes the dataset that was implemented on the life cycle costs model for the completion of the three case studies of this research, according to the model inputs defined in chapter 3, sections 3.2.4.1 and 3.2.4.2. All model inputs are defined providing the implementation methodologies, assumptions made and input variables range, except the prime mover quantified output parameters q_p for every scheduled journey of the two sets of journeys each under the two already defined weather (or sea-state) profiles (chapter 5, section 5.4.2.3) which are presented in chapter 7, as part of the case studies technical related results. The economic and risk part of the *TERA* method is composed of three scenarios based on the PMC_0 of the simulated marine gas turbines (except the simple cycle) where every scenario is performed assuming two different cases: conventional or *DLE* combustor. The reference scenario which represents the simple cycle marine gas turbine is also performed assuming the two already defined combustor cases. The rest of the input variables are used having the same values or range of values on all risk scenarios (which are **10,000** iterations in this research).

6.2 Capital Costs Dataset

6.2.1 Initial prime mover cost

Generally, published gas turbine purchase costs include electrical generator (alternator), single fuel capability, air intake stack, basic filter, exhaust stack, auxiliary systems (i.e. gear box), starter and controls and conventional combustion system, and they can considerably fluctuate according to the design needs of the marine vessel and the fleet's volume(i.e. number of prime movers, auxiliary systems, air intake and exhaust stack volume etc.), currency fluctuations and market competitive conditions [1]. Installation and shipment costs can be estimated at around 10% of the published gas turbine purchase costs [2]. The initial prime mover cost *IPMC* was estimated from published cost figures of the reference **simple cycle gas turbine** (chapter 4 section

4.3.3.1) including installation costs [1][3], assuming that it is the contract purchase cost per gas turbine for the two prime mover power plant of the three simulated marine vessels. The initial prime mover cost *IPMC* that was implemented on the life cycle costs model is $430 per kW, and for 25MW that is the design-point power output rating EP_{DP} (kW,x100) of the simple cycle gas turbine equals to a total of $10,750,000. The purchase cost was converted from U.S dollars (USD) to Great Britain pounds (GBP) at an exchange rate of 0.49 (11/12/07) which results to an initial prime mover cost *IPMC* of **£5,267,500**. The *IPMC* is used as actual prime mover cost *PMC* in scenarios where the simple cycle gas turbine composes the power plant of the RoPax fast ferry or the Destroyer.

6.2.2 Advanced cycle prime mover cost range

Research on marine gas turbine purchase costs showed that the purchase cost of the **25MW *ICR*** cycle gas turbine available in the market, is approximately **£10,000,000** [4] which is an approximately 89.84% difference over the assumed initial prime mover cost *IPMC* not including installation and shipment costs. The marine gas turbine market does not offer any prime movers that incorporate a just intercooled or a just recuperated cycle and the assumption that was made is that the minimum purchase cost of a just intercooled or just recuperated engine is higher than of a simple cycle gas turbine with the same design-point power output but does not surpass the purchase cost of an intercooled/recuperated gas turbine. The *TMI* cycle gas turbine is a novel proposal and taking in consideration its design principals and technical specification (chapter 4, section 4.3.4) is assumed that its minimum purchase cost is higher than of a simple cycle gas turbine of the same design power output and that there are possibilities that it can also surpass the purchase cost of an *ICR* gas turbine. Three different prime mover cost risk scenarios are investigated on the possible PMC_0 for each of the simulated marine gas turbines. The first two apply on all the simulated marine gas turbines and the third is applied only on the simulated *TMI* gas turbine due to the assumption mentioned before in this section on its possible maximum purchase cost. The estimated minimum and maximum percentage difference of cost from the reference prime mover, $PD_{0\text{-}min}$ and $PD_{0\text{-}max}$ respectively is presented in table 6.1. In the case study of the LNG carrier PMC_0 assumes that the essential equipment for the compression of natural gas before is delivered to the fuel injection system of the prime mover is included within the $PD_{0\text{-}min}$ and $PD_{0\text{-}max}$ range.

Table 6.1: The three different scenarios each representing a PD_0 range

Scenario Number	$PD_{0\text{-}min}$ (%)	$PD_{0\text{-}max}$ (%)
Scenario 1	20	65
Scenario 2	65	110
Scenario 3 (TMI only)	110	155

6.2.3 *DLE* combustor cost range

The installation of a *DLE* combustor instead of a conventional one, can increase the purchase cost of an aeroderivative gas turbine from 5% to 30% according to its technological level, cycle design characteristics, power output, nature of operational conditions, company policies, contract arrangements etc. [1][2][5]. The estimated minimum and maximum percentage difference of cost due to different technology components (installation of a *DLE* combustor instead of a conventional) $PD_{1\text{-}min}$ and $PD_{1\text{-}max}$ respectively, that is applied to all simulated marine gas turbines is presented in table 6.2. Two cases are performed for each prime mover cost scenario: one assuming a conventional combustor and one assuming a *DLE* combustor. The actual prime mover cost *PMC* is calculated at every risk scenario which is directly connected to the position number of the value of the cost component *J* (chapter 3, section 3.2.2.7), and depends also on the calculated prime mover downtime t_{down} (equation 3-14 and 3-30).

Table 6.2: The estimated minimum and maximum percentage difference of cost due different technology components PD_1

Scenario Number	$PD_{1\text{-}min}$ (%)	$PD_{1\text{-}max}$ (%)
Scenario 1, 2, 3	10	30

6.2.4 Insurance cost

Typical insurance schemes can cover partial or total system failure (or total loss in the case of an on-board accident due to external factors), compensation of lost income and compensation of lost deposits [2]. The cost of insurance of a prime mover depends on the nature of the operational conditions, type of installation platform, user statistical data, reliability and availability data and system design [2]. The insurance cost can typically range from 0.25% to 2% of the purchase cost of the prime mover [2]. The annual cost of insurance C_{INS} that is implemented on the life cycle costs

model is assumed to be 1%, and applies to all simulated marine gas turbines in all three case studies.

6.2.5 Interest rate

The interest rate describes the depreciation of the value of money during the operational life of each of the marine power plants, and as a consequence it is the factor that determines net present cost *NPC* (chapter 3, section 3.2.2.5). As it was described in chapter 3, section 3.2.2.6 the interest rate is assumed steady for 30 years and changes randomly at every risk scenario. The average interest rate for 30 years of operational can fluctuate at every risk scenario as presented in table 6.3 [6].

Table 6.3: Minimum and maximum interest rate fluctuation at every risk scenario

Interest rate fluctuation	
IRmin (%)	***IR***max (%)
2	7

6.3 Maintenance Cost Dataset

6.3.1 Maintenance labour rate

The maintenance labour rate per man hour R_{leng} is assumed that includes routine, major overhaul and unscheduled maintenance. The value of R_{leng} that was implemented on the life cycle costs model is £23 per hour based on information on maintenance cost of electricity generation technologies, including gas turbines [7], though maintenance labour rate can fluctuate depending on several factor such as: gas turbine and marine vessel company salary rates, companies' registered location, maintenance site, special requirements (i.e. time limitations) etc.

6.3.2 Spare parts factor

The recommended value of the spare parts factor *ESPPF* which apply for aero-gas turbines (turbojet, turbofan and turboprop) is 1.5 [8], but because the number of gas turbines used in the aviation sector is vastly higher than in the marine sector which means that spare parts sales for aero-gas turbines are superior than for marine aeroderivative gas turbines, the value of the spare parts factor *ESPPF* is assumed to be 2.

6.3.3 Power plant availability

All simulated marine gas turbines is assumed that they are reliable engines according to any manufacture's specifications and appropriate diagnostic techniques, recommended maintenance time intervals and procedures are applied on them. Further more, availability depends on the power plant's number of prime movers [9], which means that in the case of the three marine vessels that are used in the current project, adding the above assumptions, if one prime is not available then the marine vessel can sail on one prime mover. In the case of the Destroyer its operational profile can be fulfilled at least 75% as it needs only one prime mover to cruise, taking into account that if the importance of the mission is high the vessel may sail with only one operational main prime mover (25 MW gas turbine) relying also on the manoeuvring prime movers (1-2 MW engines) (assuming a gas turbine *IFEP* propulsion system, as it is described in chapter 1, section 1.2 and chapter 5, section 5.2.1.2). In the case of the RoPax fast ferry and LNG carrier, if only one main prime mover is operational then cruise speed will not be possible to be obtained and safety laws may prohibit the unberth of the vessel unless the prime mover has become unavailable during journey. Another factor that needs to be taken in account is that inherently naval vessels have lower annual operational time than ferries and LNG carriers. Availability of certain in production marine gas turbine types [10] has reached values of 99.6% and in combination with the assumed scenarios described above the estimated values of the minimum and maximum annual percentage availability $PD_{AVLB\text{-}min}$ and $PD_{AVLB\text{-}max}$ of the simulated gas turbines regardless of their cycle, but according to vessel type are presented in table 6.4.

Table 6.4: The estimated annual percentage availability PD_{AVLB} and PD_{AVLB} of the simulated gas turbines

Vessel Type	**$PD_{AVLB\text{-}min}$ (%)**	**$PD_{AVLB\text{-}max}$ (%)**
Destroyer	98	100
RoPax fast ferry	97	100
LNG carrier	97	100

6.4 Fuel and Emissions Cost Dataset

6.4.1 Fuel cost

6.4.1.1 Distillate fuel cost

The distillate fuel that is assumed that the power plants of the RoPax fast ferry and the Destroyer use is ultra low-sulphur (sulphur S<0.0015% by weight) No. 2 fuel oil (marine classification: bunker A). The maximum fluctuation in the price of low sulphur No. 2 fuel oil (data on ultra low sulphur No. 2 fuel oil was available from January to September 2007, but its price was almost identical to low sulphur No. 2 fuel oil) from December 2004 to August 2007 was from approximately 145 U.S. cents/gallon to approximately 255 U.S. cents/gallon respectively (not taxed fuel) as presented in figure 6.1 [11].

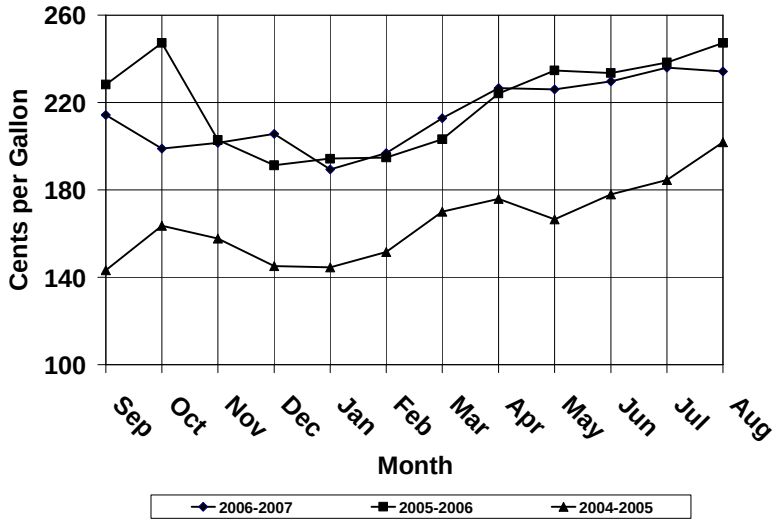

Figure 6.1: Low sulphur No.2 fuel oil not taxed price variation from September 2004 to August 2007[11]

Assuming that the price of the fuel will never drop below the minimum obtained price, but can increase beyond the maximum obtained price including interest rate but excluding inflation at a prime mover operational life of 30 years, the minimum and maximum fuel cost per unit volume, that was implemented in the life costs model, is from 145 to 340 U.S cents/gallon respectively and was converted to GBP/kg by using equation 6-1 which is implemented in the life cycle costs model.

$$P_{FF-GBP/kg} = \frac{P_{FF-vol}(EX_{(C1-C2)})}{100U_V\rho_{fuel}} \qquad \text{Equation 6-1}$$

Where: ρ_{fuel} is the density of fuel in kg/lt (assumed 0.85 kg/lt at ambient temperature T_{amb} case studies range), $EX_{(C1\text{-}C2)}$ is the exchange rate of the converting currency to the converted currency (USD->GBP = 0.49 as defined in section 6.2.1), U_V is the converting volume unit (3.785 from gallons to litres) and $P_{FF\text{-}vol}$ is the fuel cost per gallon.

The minimum and maximum fuel cost per unit mass (GBP/kg) $P_{FF\text{-}min}$ and $P_{FF\text{-}max}$ that was implemented in the life costs model is presented in table 6.5.

Table 6.5: The minimum and maximum distillate fuel cost per unit mass

Fuel Type	$P_{FF\text{-}min}$ (GBP/kg)	$P_{FF\text{-}max}$ (GBP/kg)
Ultra low sulphur No.2 fuel oil	0.188	0.518

6.4.1.2 Natural gas fuel cost

Natural gas is assumed that is used as fuel only by the power plant of the LNG carrier and the concept is that, naturally and forced boil-off cargo natural gas is charged at not taxed natural gas rates. According to the above concept, cargo natural gas is bought and utilised even when the vessel sails unloaded, towards the natural gas loading facility. The maximum fluctuation in the price of natural gas from December 2004 to August 2007 was from approximately 18.5 U.S. cents/m^3 to approximately 44 U.S. cents/m^3 respectively (not taxed fuel) as is presented in figure 6.2 [12].

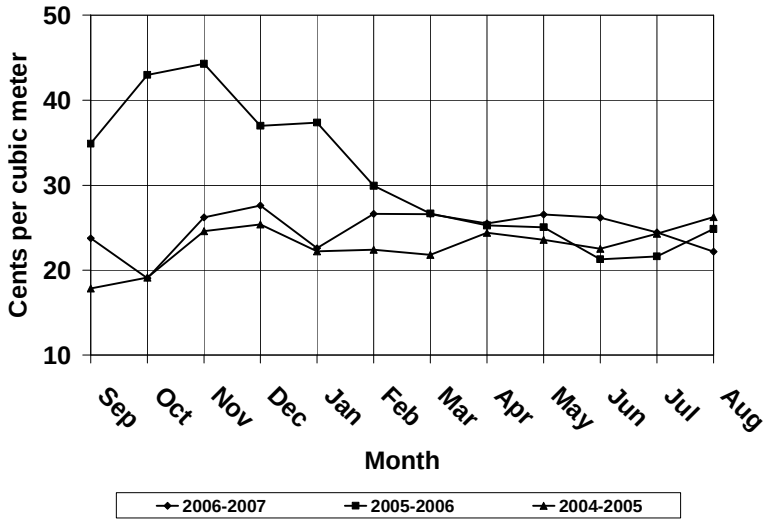

Figure 6.2: Natural gas not taxed price variation from September 2004 to August 2007[12]

Assuming that the price of natural gas can drop below the minimum obtained price according to the 2006-2007 price slop (figure 6.2) and can increase beyond the maximum obtained price, including interest rate but excluding inflation at a prime mover operational life of 30 years, the minimum and maximum fuel cost per unit volume, that was implemented in the life costs model, is from 15 to 60 U.S cents/m^3 respectively and was converted to GBP/kg by using equation 6-1 which is implemented in the life cycle costs model. The natural gas density ρ_{fuel} is assumed $72x10^{-5}$ kg/lt at the case studies ambient temperature range. The minimum and maximum fuel cost per unit mass (GBP/kg) $P_{FF\text{-}min}$ and $P_{FF\text{-}max}$ that was implemented in the life costs model is presented in table 6.6.

Table 6.6: The minimum and maximum natural gas cost per unit mass

Fuel Type	$P_{FF\text{-}min}$ (GBP/kg)	$P_{FF\text{-}max}$ (GBP/kg)
Natural Gas	0.102	0.408

6.4.2 Exhaust Emissions cost

As it was mentioned before a possible future concept of emissions taxation is adopted in this research (chapter 1, section 1.4.2) which is not newly conceived as the Massachusetts Department of Public Utilities proposed in 1990 a taxation scheme that exhaust emission quantities are taxed per produced unit mass, though it needs to be mentioned that it does not apply as an international policy, as it is assumed in this research. The suggested values of the cost of the exhaust emission quantities are presented in table 6.7 [9].

Table 6.7: Cost of exhaust emissions proposed by the Massachusetts Department of Public Utilities proposed in 1990

Exhaust emission quantity	Cost (U.S. cent/kg)
NO_x	393.7
CO	52.7
CO_2	1.4
UHC	13.3

The values presented in table 6.7 were adjusted by taking as point of reference the cost per unit mass of nitric oxide (NO_x) exhaust emissions emitted by marine vessels according to present Norwegian marine emissions policy [13], and apply the proportion difference between the two nitric oxide values to the rest exhaust emissions quantities (CO, CO_2, UHC). Nitric oxide exhaust emissions emitted by

international marine vessels that sail in Norwegian waters on domestic routes are charged at approximately 300 U.S. cents/kg. The offsetting of emission values before the introduction of the risk element from table 6.7 is presented in table 6.8 and values are converted to GBP/kg at the indicated exchange rate in this chapter.

Table 6.8: Assumed cost of exhaust emissions before the introduction of risk element

Exhaust emission quantity	**Cost (U.S. cent/kg)**	**Cost (GBP/kg)**
NO_x	300.0	1.47
CO	40.15	0.20
CO_2	1.07	0.0052
UHC	10.11	0.049

The minimum and maximum estimated cost (GBP of the prime mover's output exhaust emission quantities per kg, $P_{p\text{-}min}$ and $P_{p\text{-}max}$ (where p can be NO_x, CO, CO_2 and UHC) are presented in table 6.9.

Table 6.9: Assumed cost of exhaust emissions with the introduction of risk element

Exhaust emission quantity ***p***	$\mathbf{P_{p\text{-}min}}$ **(GBP/kg)**	$\mathbf{P_{p\text{-}max}}$ **(GBP/kg)**
NO_x	0.75	2.25
CO	0.15	0.45
CO_2	0.005	0.015
UHC	0.03	0.09

6.5 References

1. "*Gas Turbine World Handbook*", Pequot Publishing Inc., Vol. 25, 2006

2. Polyzakis, A.L., "*Technoeconomic Evaluation of Trigeneration Plant: Gas Turbine Performance, Absorption Cooling and District Heating"*, PhD Thesis, Cranfield University, Academic Years 2002-2006.

3. www.nyethermodynamics.com/trader/kwprice.htm

4. http://ir.rolls-royce.com/rr/investors/finresults/results/interim2003/interims2003.pdf

5. Wei, A., "*Technologies for Next Generation Turbine Systems*", Turbine Power Systems Conference and Condition Monitoring Workshop, Galveston, February 2002.

6. http://openscotland.gov.uk/Publications/2006/06/27171110/9

7. Badr, M., Benjamin, R., "*Comparative Cost of California Central Station Electricity Generation Technologies*", California Energy Commission, Final Staff Report, June 2003.

8. Roskam, J., *"Airplane Design Part VIII; Airplane Cost Estimation: Design, Development, Manufacturing and Operating"*, Roskam Aviation and Engineering Corporation, ISBN No: 1-8848-8555-1, pp 20, pp 85, 1990.

9. "*Fundamentals of Gas Turbine Operation in the Marine Environment"*, Short Course Lecture Notes, Cranfield University, November 2004.

10. http://www.geae.com/engines/marine/lm2500.html , Accessed in 2006.

11. "*U.S. No. 2 Distillate Fuel Prices by Sales Type*", Energy Information Administration, Release date 30th November 2007, Available at: http://tonto.eia.doe.gov/dnav/pet/pet_pri_dist_dcu_nus_m.htm

12. "*U.S. Natural Gas Prices*", Energy Information Administration, Release date: 30th November 2007, Available at: http://tonto.eia.doe.gov/dnav/ng/ng_pri_sum_dcu_nus_m.htm

13. "*Introduction of a Norwegian Tax on NOx Emissions from International Shipping Operating Between Two Norwegian Ports*", The chamber of Shipping, No. 10, March 2007.

7 *TERA* Case Studies: Results & Discussion

7.1 Introduction

This chapter begins with the presentation of the case study results separately for each marine vessel in the same format. The quantified output parameters q_p are presented first, as they compose the technical related input parameters of the life cycle costs model, followed by the selected number of scheduled journeys and the annual utilisation of the prime movers of each of the investigated power plants. As all the life cycle costs input data is defined and derived, the power plant economic and risk analysis results are presented. The presentation of the results for each of the marine vessels separately is followed by a discussion on the gas turbine off-design operation in accordance with the ambient and weather conditions simulated in the case studies of this research. The power plant economic feasibility is then discussed, where for every marine vessel separately all advanced cycle gas turbine power plants are compared with the reference power plant (in the case of the LNG carrier the investigated power plant is only one, but is discussed in accordance to the results produced by each of the two scenarios) . The discussion on the power plant economic feasibility is also extended to the comparison of the advanced cycle gas turbine power plants. Finally, a brief discussion is made on validity of the simulation of the marine vessel sea-keeping performance.

7.2 Case Studies Results: Technical & Economic

7.2.1 Destroyer

7.2.1.1 Quantified output parameters

The prime mover quantified output parameters q_p for every scheduled journey of the Destroyer, produced by using "*Poseidon*", of the two sets of journeys under each of the two already defined weather (or sea-state) profiles which are part of the technical related input data of the life cycle costs model (chapter 3, section 3.2.4.2 and chapter 6, section 6.1) are presented in two sets of tables in appendix C.5 (tables C.1 to C.10), with each table representing a hull roughness amplitude due to fouling (F1-

F5, chapter 5, section 5.2.3.2). Each of the table sets represents the weather profile (ideal or adverse) and the results are presented separately for the cruise and the boost prime mover, except for the *TMI* cycle power plant where both prime movers operate constantly (chapter 5, section 5.3.1.3). Analytical graphical presentation of the cycle performance (turbine entry temperature and fuel flow), engine power-ship (marine vessel) speed relationship, exhaust emissions rate and hot section rotor blade time to failure of each of the five prime movers at every time interval during every of the fifty in total scheduled journeys are presented for each simulated gas turbine in appendices C.1, C.2, C.3 and C.4 respectively. The boost prime mover (except for the *TMI* cycle power plant) is programmed to engage at the following times of the day (as it is expressed on the representing figures) where sea-state number can be maximum seven: **10, 13, 16, 20, 23 and 02**. At time of day **18** sea-state is programmed at number eight and the boost prime mover engages although the marine vessel is programmed to travel at cruise speed (see chapter 5, section 5.3.1.3).

7.2.1.2 Annual Utilisation

The annual number of scheduled journeys N_{asj} of the Destroyer which is a major factor that contributes to the life cycle costs of a marine vessel's power plant is estimated according to the average annual number of hours that a naval vessel of this type typically spends in the open sea, during its operational life. Annual utilisation can vary but under a general purpose operating profile a value of 4800 hours (55% annually) is considered representing [1], though values between 25% lower and 5-10% higher can be considered realistic. The life cycle costs model was supplemented assuming an annual number of scheduled journeys $\boldsymbol{N_{asj}}$ of **210** and the annual operational time of the prime movers (cruise and boost, except *TMI*)) can fluctuate due to the weather probability module (chapter 3, section 3.2.2.6) according to the calculated values presented in table 7.1. The values were calculated from the "*Poseidon*" results presented in the appendix C.5, by considering the minimum and maximum operational time per journey t_{op} (see tables C.1 and C.10).

Table 7.1: Minimum and maximum annual operational time per prime mover type

Engine **Cruise** ---------- **Boost**	**Minimum operational time t_{annual} (hours)**	**Maximum operational time t_{annual} (hours)**
SC	5040	5111.4 (0%)
	1260	1470
TMI x2	5040	5086 (-0.5%)
INT	5040	5098.8 (-0.24%)
	1260	1470
REQ	5040	5113.5 (0.041%)
	1260	1470
ICR	5040	5103 (-0.016%)
	1260	1470

7.2.1.3 Power plant economic and risk analysis

The results that describe the economic performance of each of the power plants installed on the Destroyer according to the case scenarios investigated during this research were obtained as it was described in chapter 3, with the use of the life cycle costs model and the input dataset was implemented to it as described in chapter 6 and in this chapter in sections 7.2.1.1 and 7.2.1.2. The graphical expression of the probability and cumulative probability distribution of the net present cost [*NPC* in GBP (£) million] of each of the power plants incorporating either the conventional or the *DLE* combustors described in chapter 4, section 4.5 and chapter 6, section 6.2.3, are presented in two sets of figures: the first set (figures 7.1 and 7.2) expresses the first scenario and the second set (figures 7.3. and 7.4) expresses the second and third scenario (the three economic scenarios are described in chapter 6, section 6.2.2). It is reminded that the reference gas turbine power plant is the simple cycle. The graphical expression of the rest of the probability and cumulative probability distributions of the overall output parameters (chapter 3, section 3.2.4.3) are presented in appendix C.6, figures C.47-C.66.

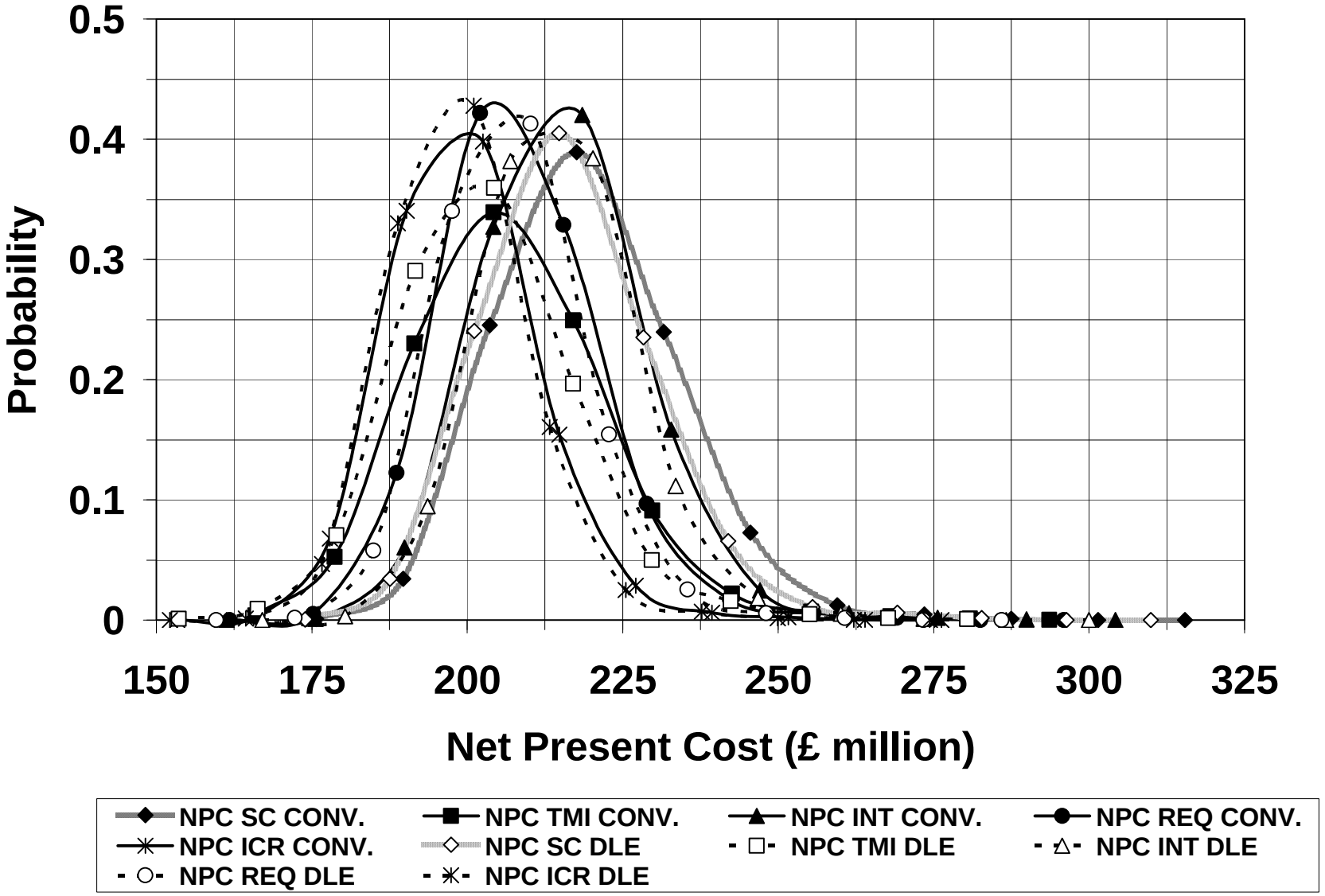

Figure 7.1: Destroyer – Probability distribution of the NPC of each power plant (Scenario 1)

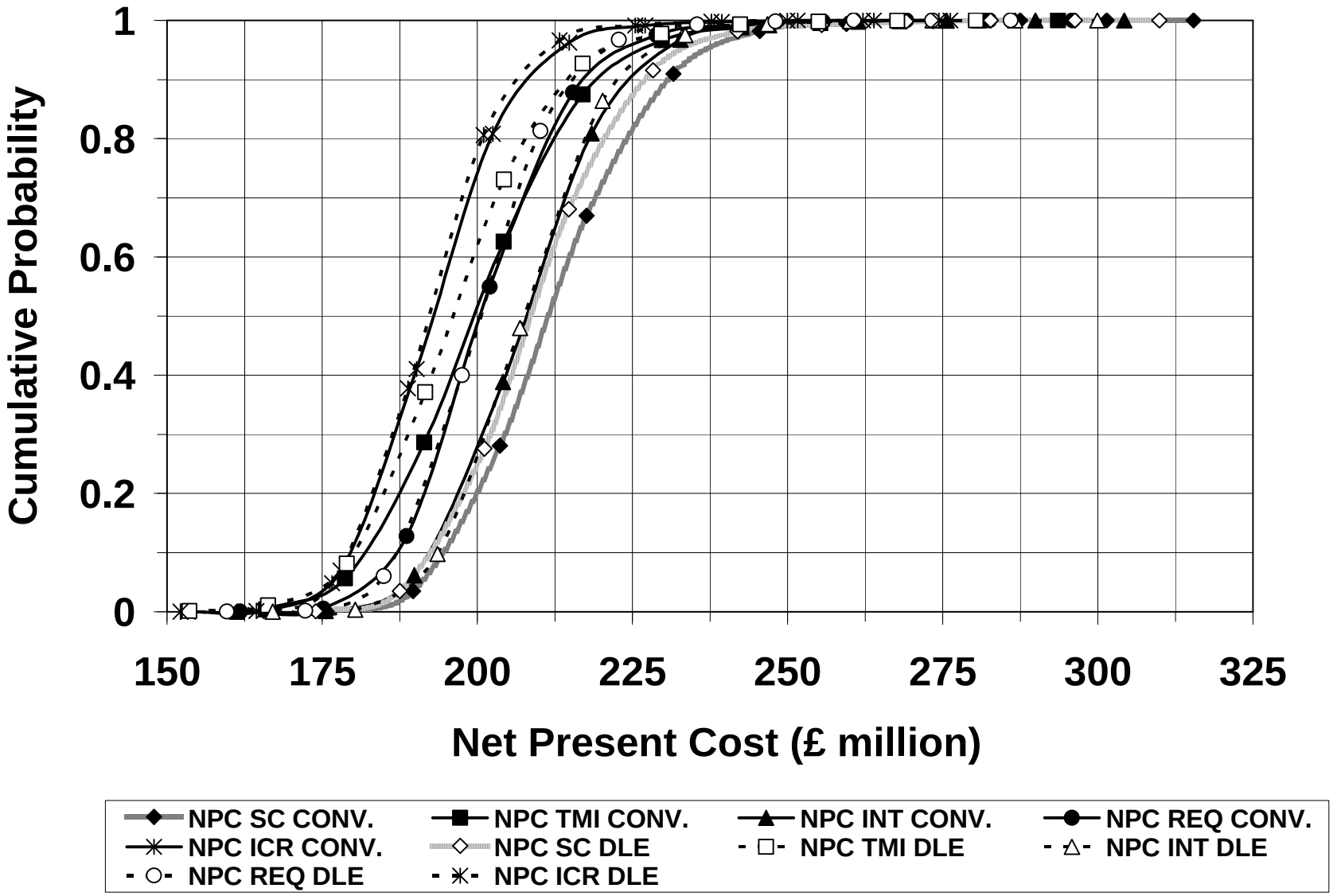

Figure 7.2: Destroyer – Cumulative probability distribution of the NPC of each power plant (Scenario 1)

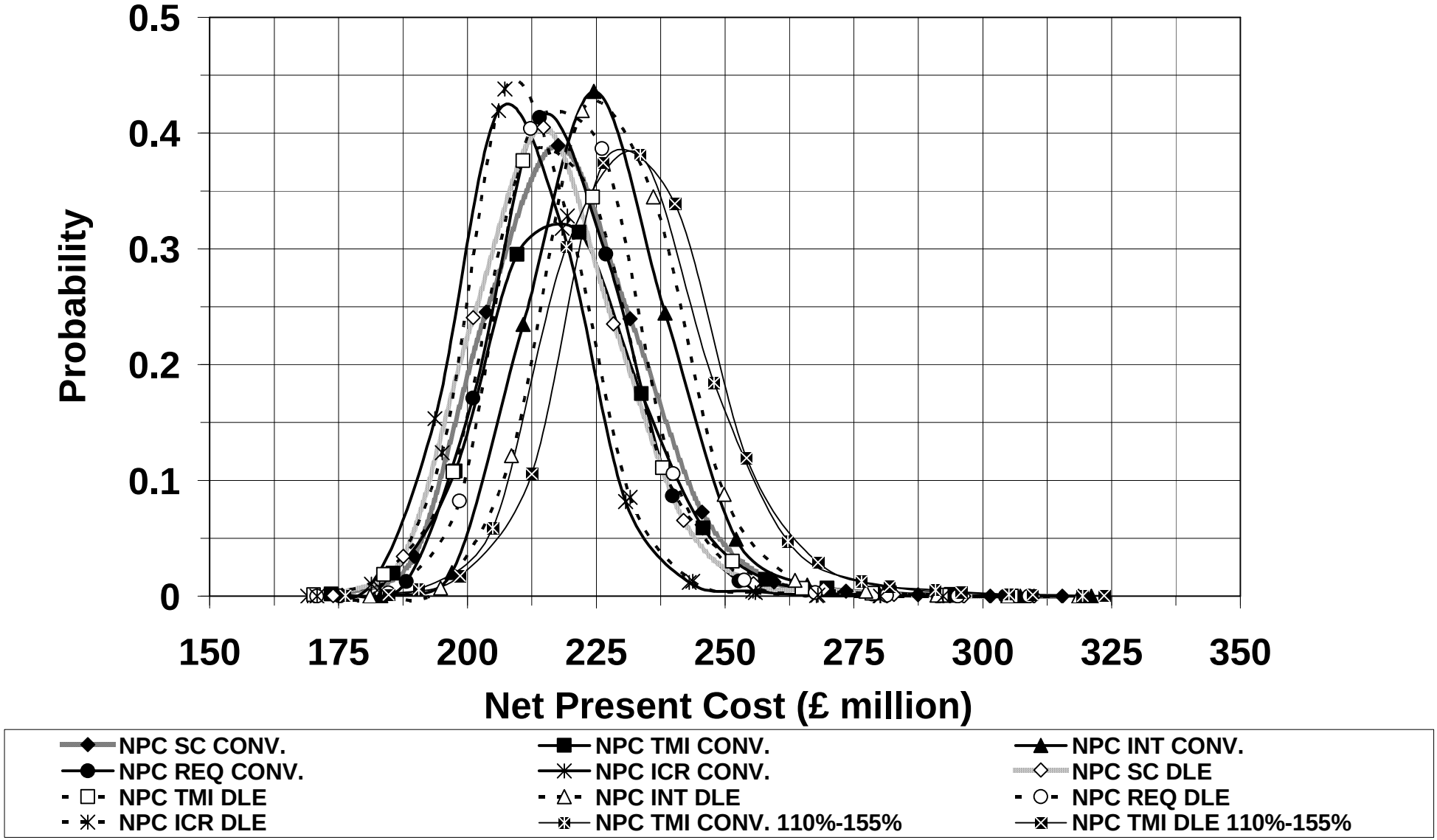

Figure 7.3: Destroyer – Probability distribution of the NPC of each power plant (Scenarios 2 and 3)

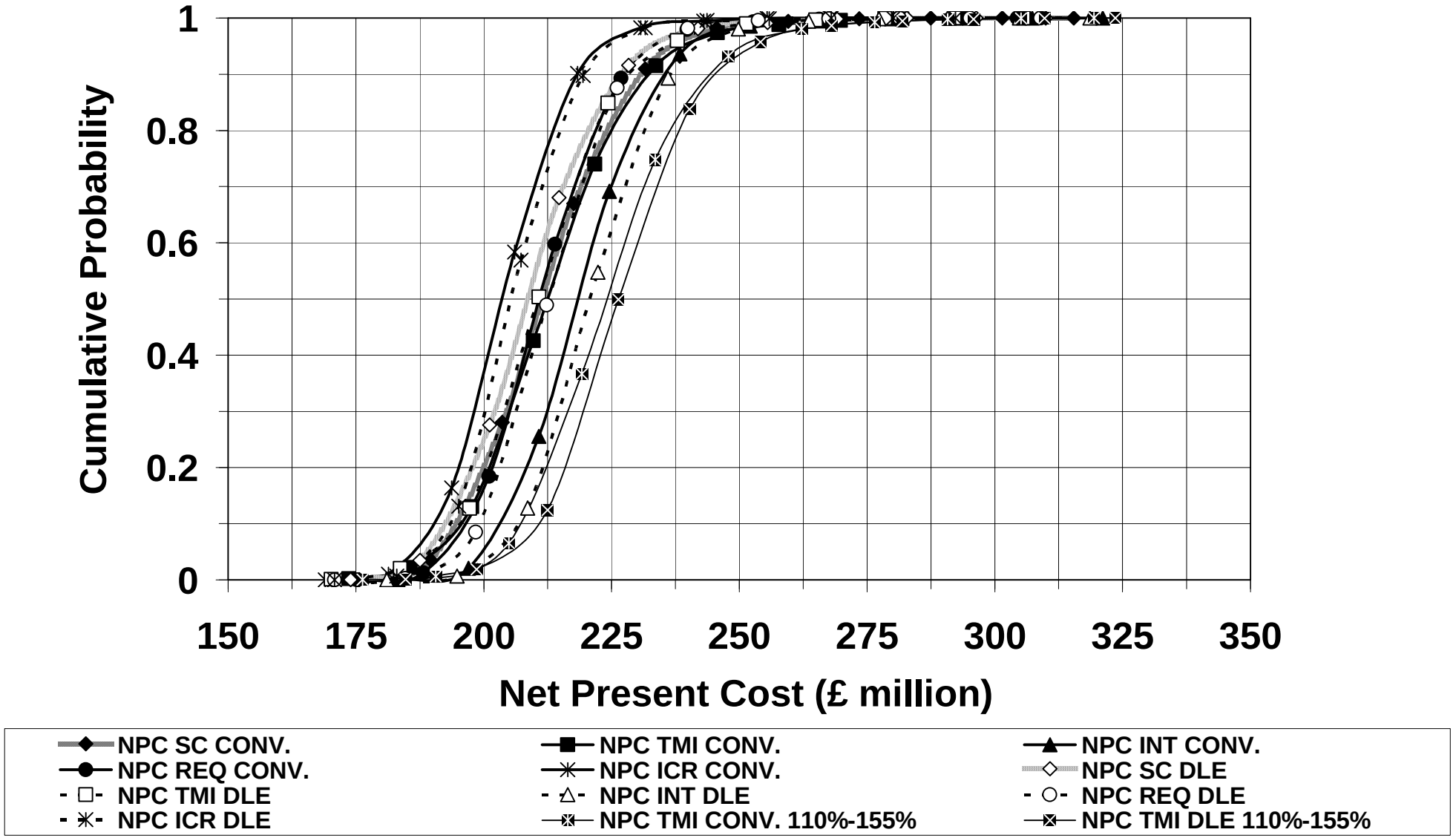

Figure 7.4: Destroyer – Cumulative probability distribution of the NPC of each power plant (Scenarios 2 and 3)

Tables 7.2 to 7.10 present the minimum-maximum and standard deviation percentage difference of the overall output parameters of each of the power plants according to the three different scenarios comparing with reference simple cycle gas turbine power plant. The minimum-maximum values in the above mentioned tables (including the tables presented in section 7.2.2.3 regarding the RoPax fast ferry) represent a probability of zero, but the definition of the standard deviation, and the already specified nature of the chosen distribution adding the fact that for each of the overall output parameters (life cycle cost components including *NPC*) the peak probabilities do not fluctuate significantly (Destroyer only: exception is the *TMI* power plant that both prime movers operate constantly and for that reason including the fixed number of risk scenarios it shows *NPC* and life cycle maintenance cost probability distribution with higher variability), an adequate understanding can be obtained on the variability of the distributions of the overall output parameters, thus the range of the probable *NPC* of each of the simulated power plants. In appendix C.7, tables C.11 to C.19 present the actual minimum-maximum and standard deviation of each of the overall output parameters of the power plants in millions GBP (£).

Table 7.2: Destroyer - Minimum-maximum and standard deviation percentage difference of NPC of all power plants from reference cycle (Scenario 1)

Engine (20%-65%) Conventional & DLE Combustor	**Minimum NPC (% from SC)**		**Maximum NPC (% from SC)**		**Standard Deviation (% from SC)**	
SC-Reference Cycle	0	0	0	0	0	0
TMI	-5.45	-11.85	-6.95	-9.47	-8.66	-6.77
INT	-8.65	-4.01	-3.41	-3.19	2.29	-2.14
REQ	-8.06	-8.26	-6.14	-7.70	-4.01	-7.00
ICR	-12.74	-12.57	-12.41	-11.43	-12.10	-10.01

Table 7.3: Destroyer - Minimum-maximum and standard deviation percentage difference of NPC of all power plants from reference cycle (Scenarios 2 and 3)

Engine (65%-110%) Conventional & DLE Combustor	**Minimum NPC (% from SC)**		**Maximum NPC (% from SC)**		**Standard Deviation (% from SC)**	
SC-Reference Cycle	0	0	0	0	0	0
TMI	-0.65	-2.21	-7.20	-1.36	-13.89	-0.29
TMI (110%-155%)	0.24	6.40	1.30	4.36	2.43	2.21
INT	4.51	4.25	1.71	2.78	-1.36	1.25
REQ	0.06	-1.92	-3.60	-0.25	-7.59	1.69
ICR	-3.50	-1.38	-7.38	-5.78	-11.67	-10.60

Table 7.4: Destroyer - Minimum-maximum and standard deviation percentage difference of maintenance cost of all power plants from reference cycle (Scenario 1)

Engine (20%-65%) Conventional & DLE Combustor	Minimum Maint. Cost (% from SC)		Maximum Maint. Cost (% from SC)		Standard Deviation (% from SC)	
SC-Reference Cycle	0	0	0	0	0	0
TMI	98.25	71.21	113.47	104.32	122.54	122.22
INT	-1.75	10.65	37.61	42.93	61.97	60.00
REQ	-15.10	-22.99	15.88	9.69	35.21	27.78
ICR	12.04	1.31	29.11	34.16	39.44	52.22

Table 7.5: Destroyer - Minimum-maximum and standard deviation percentage difference of maintenance cost of all power plants from reference cycle (Scenarios 2 and 3)

Engine (65%-110%) Conventional & DLE Combustor	Minimum Maint. Cost (% from SC)		Maximum Maint. Cost (% from SC)		Standard Deviation (% from SC)	
SC-Reference Cycle	0	0	0	0	0	0
TMI	169.15	160.93	140.42	174.21	150.70	182.22
TMI (110%-155%)	200.22	229.72	225.90	236.39	243.66	242.22
INT	55.14	51.40	75.30	87.43	88.73	107.78
REQ	24.07	7.48	40.10	57.13	50.70	84.44
ICR	62.36	57.20	75.14	72.77	84.51	82.22

Table 7.6: Destroyer - Minimum-maximum and standard deviation percentage difference of fuel cost of all power plants from reference cycle (All scenarios)

Engine	Minimum Fuel Cost (% from SC)	Maximum Fuel Cost (% from SC)	Standard Deviation (% from SC)
SC-Reference Cycle	0	0	0
TMI	-21.04	-19.63	-18.27
INT	-13.51	-7.62	-1.90
REQ	-14.16	-10.29	-6.49
ICR	-20.15	-17.35	-14.63

Table 7.7: Destroyer - Minimum-maximum and standard deviation percentage difference of cost of taxed NOx exhaust emissions of all power plants from reference cycle

Engine Conventional & DLE Combustor	Minimum NOx Cost (% from SC)		Maximum NOx Cost (% from SC)		Standard Deviation (% from SC)	
SC-Reference Cycle	0	0	0	0	0	0
TMI	58.25	46.15	57.85	57.91	55.79	68.97
INT	-5.88	-6.64	-2.56	-0.98	0.00	6.90
REQ	-12.23	-11.19	-9.36	-8.16	-7.37	-3.45
ICR	-2.54	-4.20	-3.03	-1.79	-3.16	0.00

Table 7.8: Destroyer - Minimum-maximum and standard deviation percentage difference of cost of taxed CO exhaust emissions of all power plants from reference cycle

Engine Conventional & DLE Combustor	Minimum CO Cost (% from SC)		Maximum CO Cost (% from SC)		Standard Deviation (% from SC)	
SC-Reference Cycle	0	0	0	0	0	0
TMI	-65.85	-65.79	-64.97	-65.54	-62.67	-65.85
INT	-14.36	-10.96	-11.21	-12.08	-8.00	-14.36
REQ	9.21	10.09	8.09	9.70	8.00	9.21
ICR	-13.41	-9.65	-12.04	-12.28	-10.67	-13.41

Table 7.9: Destroyer - Minimum-maximum and standard deviation percentage difference of cost of taxed CO2 exhaust emissions of all power plants from reference cycle

Engine	Minimum CO2 Cost (% from SC)	Maximum CO2 Cost (% from SC)	Standard Deviation (% from SC)
SC-Reference Cycle	0	0	0
TMI	-19.59	-19.35	-19.61
INT	-8.14	-7.64	-6.86
REQ	-11.65	-10.56	-9.80
ICR	-15.26	-16.29	-16.67

Table 7.10: Destroyer - Minimum-maximum and standard deviation percentage difference of cost of taxed UHC exhaust emissions of all power plants from reference cycle

Engine Conventional & DLE Combustor	Minimum UHC Cost (% from SC)		Maximum UHC Cost (% from SC)		Standard Deviation (% from SC)	
SC-Reference Cycle	0	0	0	0	0	0
TMI	-88.46	-89.41	-88.70	-89.46	-89.47	-88.89
INT	-19.23	-23.53	-19.13	-18.92	-19.30	-16.67
REQ	9.62	5.88	11.30	10.81	14.04	11.11
ICR	-28.85	-29.41	-30.43	-29.73	-29.82	-33.33

7.2.2 RoPax fast ferry

7.2.2.1 Quantified output parameters

The prime mover quantified output parameters q_p for every scheduled journey of the RoPax fast ferry, produced by using "*Poseidon*", of the two sets of journeys under each of the two already defined weather (or sea-state) profiles which are part of the technical related input data of the life cycle costs model (chapter 3, section 3.2.4.2 and chapter 6, section 6.1) are presented in two sets of tables in appendix D.5 (tables D.1 to D.10), with each table representing a hull roughness amplitude due to fouling (F1-F5, chapter 5, section 5.2.3.2). Each of the table sets represents the weather profile (ideal or adverse) and as it was mentioned in chapter 5, section 5.3.1.2 both prime movers are constantly in operation. Analytical graphical presentation of the cycle performance (turbine entry temperature and fuel flow), engine power-ship (marine vessel) speed relationship, exhaust emissions rate and hot section rotor blade time to failure of each of the five prime movers at every time interval during every of the ten in total scheduled journeys are presented for each simulated gas turbine in appendices D.1, D.2, D.3 and D.4 respectively

7.2.2.2 Annual Utilisation

The annual number of scheduled journeys N_{asj} of the RoPax fast ferry is estimated assuming that the marine vessel is in constant annual operation assuming a five hours berth at every scheduled journey, due to schedule arrangements, refuelling, passengers and vehicles loading unloading etc. The life cycle costs model was supplemented assuming an annual number of scheduled journeys $\boldsymbol{N_{asj}}$ of **280** assuming non-operational time due to scheduled factors such as annual maintenance of the marine vessel, and non-scheduled factors such as no-sail decisions or permissions due to highly adverse weather conditions. The minimum-maximum annual operational time t_{annual} of the prime movers that are presented in table 7.11 were calculated from the "*Poseidon*" results presented in appendix D.5 by considering the minimum and maximum operational time per journey t_{op} (see tables D.1 and D.10).

Table 7.11: Minimum and maximum annual operational time per prime mover type

Engine	**Minimum operational time t_{annual} (hours)**	**Maximum operational time t_{annual} (hours)**
SC	6720	7291.2 (0%)
TMI	6720	7151.2 (-1.92%)
INT	6720	7145.6 (-2.0%)
REQ	6720	7291.2 (0%)
ICR	6720	7159.6 (-1.8%)

7.2.2.3 Power plant economic and risk analysis

The results that describe the economic performance of each of the power plants installed on the RoPax fast ferry according to the case scenarios investigated during this research were obtained as it was described in chapter 4, with the use of the life cycle costs model and the input dataset was implemented to it as described in chapter 6 and in this chapter in sections 7.2.2.1 and 7.2.2.2. The graphical expression of the probability and cumulative probability distribution of the net present cost [*NPC* in GBP (£) million] of each of the power plants incorporating either the conventional or the *DLE* combustors described in chapter 4, section 4.5 and chapter 6, section 6.2.3, are presented in two sets of figures: the first set (figures 7.5 and 7.6) expresses the first scenario and the second set (figures 7.7. and 7.8) expresses the second and third scenario (the three economic scenarios are described in chapter 6, section 6.2.2). The graphical expression of the rest of the probability and cumulative probability distributions of the overall output parameters (chapter 3, section 3.2.4.3) are presented in appendix D.6, figures D.47-D.66.

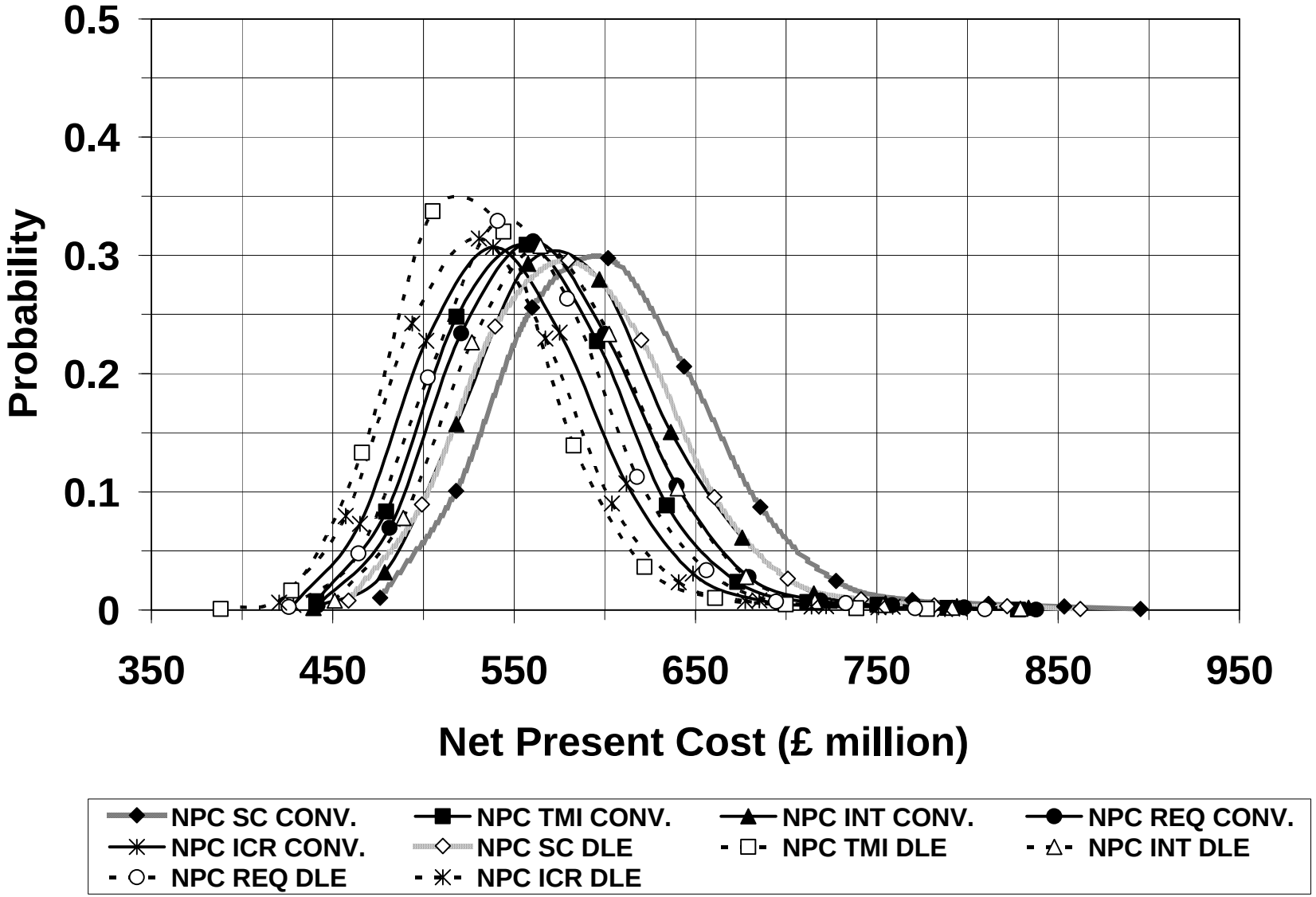

Figure 7.5: RoPax fast ferry – Probability distribution of the NPC of each power plant (Scenario 1)

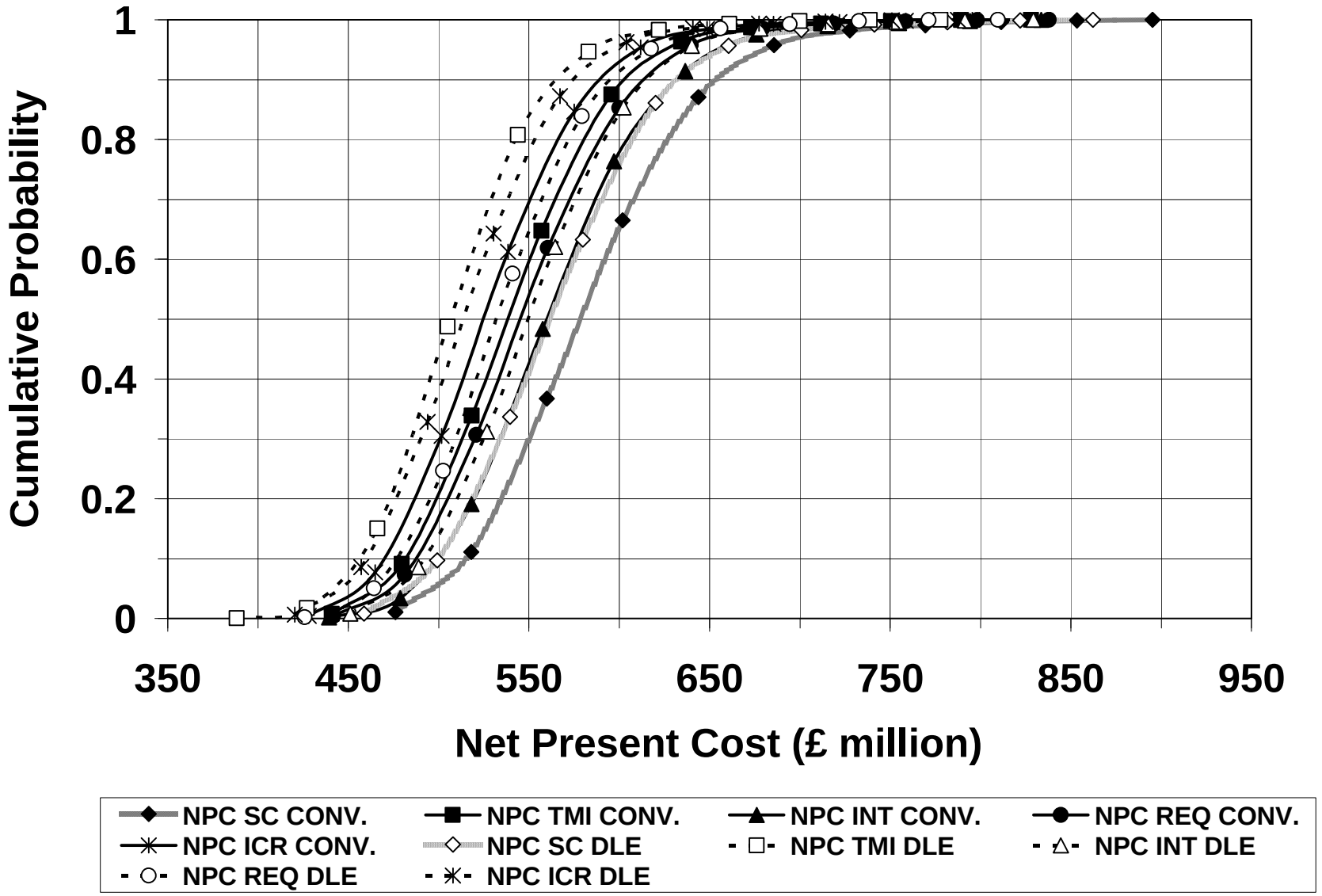

Figure 7.6: RoPax fast ferry – Cumulative probability distribution of the NPC of each power plant (Scenario 1)

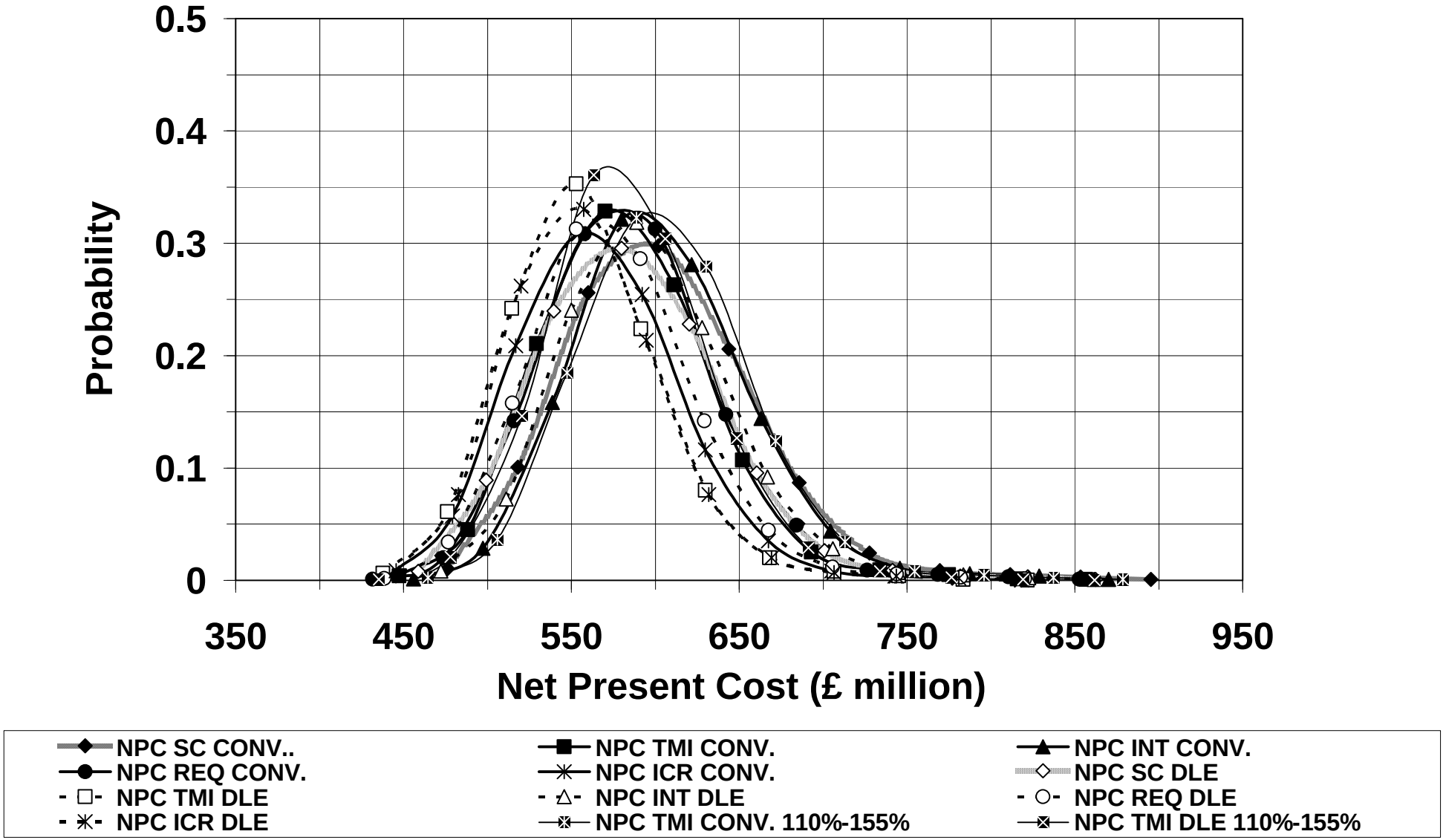

Figure 7.7: RoPax fast ferry – Probability distribution of the NPC of each power plant (Scenarios 2 and 3)

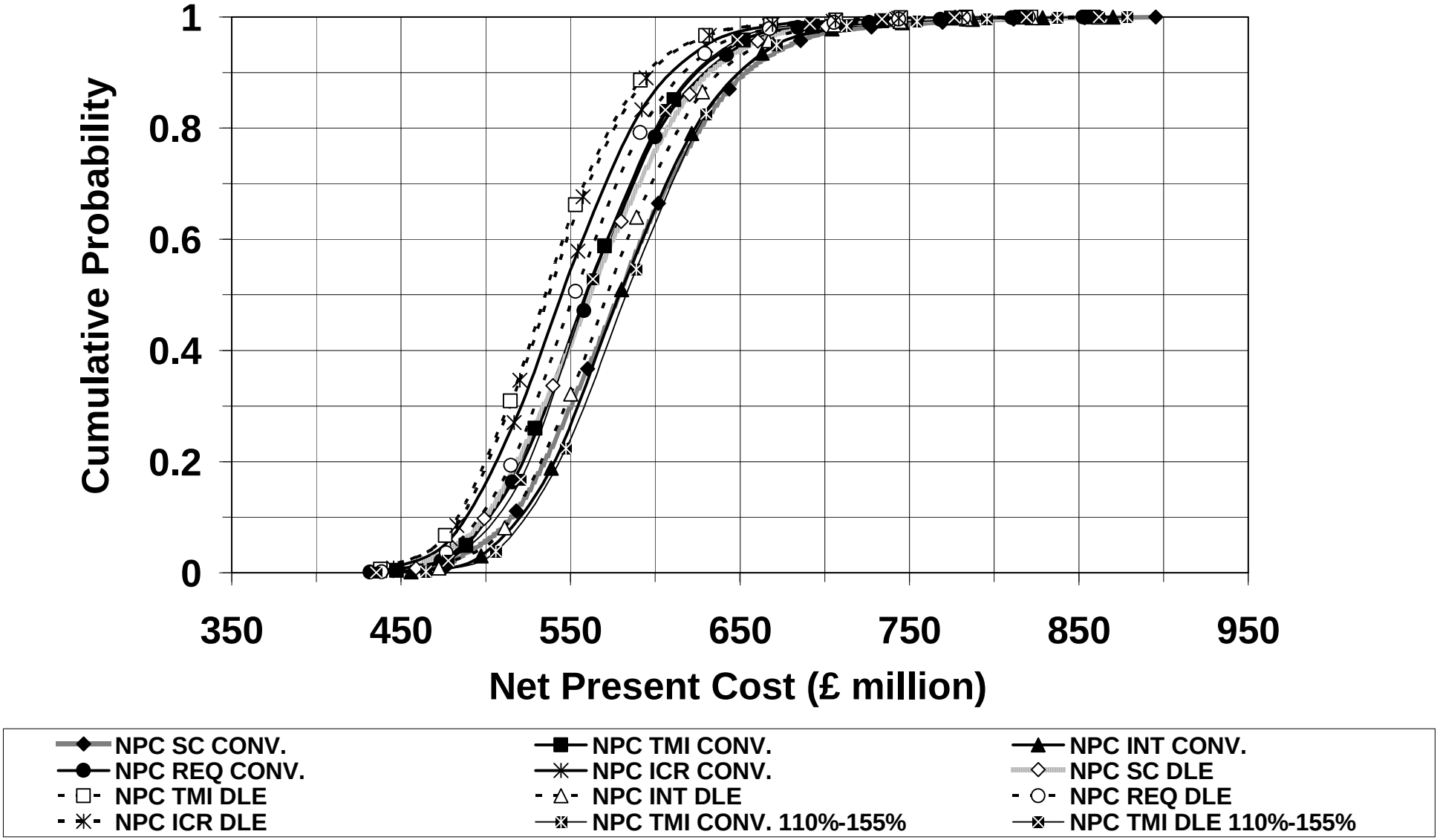

Figure 7.8: RoPax fast ferry – Cumulative probability distribution of the NPC of each power plant (Scenarios 2 and 3)

Tables 7.12 to 7.20 present the minimum-maximum and standard deviation percentage difference of the overall output parameters of each of the power plants according to the three different scenarios comparing with reference simple cycle gas turbine power plant.. In appendix D.7, tables D.11 to D.19 present the actual minimum-maximum and standard deviation of each of the overall output parameters of the power plants in millions GBP (£).

Table 7.12: RoPax ferry - Minimum-maximum and standard deviation percentage deference of NPC of all power plants from reference cycle (Scenario 1)

Engine (20%-65%) Conventional & DLE Combustor	**Minimum NPC (% from SC)**		**Maximum NPC (% from SC)**		**Standard Deviation (% from SC)**	
SC-Reference Cycle	0	0	0	0	0	0
TMI	-7.38	-15.93	-7.54	-9.66	-7.71	-3.13
INT	-7.82	-1.46	-6.87	-3.81	-5.96	-5.95
REQ	-7.31	-7.29	-6.40	-6.14	-5.53	-4.53
ICR	-9.95	-8.344	-11.18	-8.69	-12.19	-8.71

Table 7.13: RoPax ferry - Minimum-maximum and standard deviation percentage difference of NPC of all power plants from reference cycle (Scenarios 2 and 3)

Engine (65%-110%) Conventional & DLE Combustor	**Minimum NPC (% from SC)**		**Maximum NPC (% from SC)**		**Standard Deviation (% from SC)**	
SC-Reference Cycle	0	0	0	0	0	0
TMI	-6.22	-0.23	-4.28	-4.70	-2.39	-4.30
TMI (110%-155%)	-2.48	-5.63	-1.86	0.07	-1.86	6.07
INT	-4.39	3.21	-2.85	-0.18	-1.19	-3.18
REQ	-9.80	-4.40	-4.67	-4.91	0.38	-5.07
ICR	-7.16	-2.69	-8.68	-5.17	-10.16	-7.31

Table 7.14: RoPax ferry - Minimum-maximum and standard deviation percentage difference of maintenance cost of all power plants from reference cycle (Scenario 1)

Engine (20%-65%) Conventional & DLE Combustor	**Minimum Maint. Cost (% from SC)**		**Maximum Maint. Cost (% from SC)**		**Standard Deviation (% from SC)**	
SC-Reference Cycle	0	0	0	0	0	0
TMI	58.59	14.27	81.63	96.23	96.75	141.12
INT	6.32	10.38	35.26	43.95	54.88	69.53
REQ	-8.09	-17.33	19.43	21.41	38.21	42.60
ICR	40.02	21.41	40.84	41.48	41.46	50.89

Table 7.15: RoPax ferry - Minimum-maximum and standard deviation percentage difference of maintenance cost of all power plants from reference cycle (Scenarios 2 and 3)

Engine (65%-110%) Conventional & DLE Combustor	**Minimum Maint. Cost (% from SC)**		**Maximum Maint. Cost (% from SC)**		**Standard Deviation (% from SC)**	
SC-Reference Cycle	0	0	0	0	0	0
TMI	102.88	88.51	138.03	130.63	161.79	152.07
TMI (110%-155%)	128.27	102.13	193.05	179.49	236.99	220.71
INT	65.41	45.97	81.36	94.07	91.87	119.53
REQ	2.99	18.07	48.83	42.23	79.67	54.14
ICR	68.07	52.27	88.14	77.91	102.03	90.53

Table 7.16: RoPax ferry - Minimum-maximum and standard deviation percentage difference of fuel cost of all power plants from reference cycle (All scenarios)

Engine	Minimum Fuel Cost (% from SC)	Maximum Fuel Cost (% from SC)	Standard Deviation (% from SC)
SC-Reference Cycle	0	0	0
TMI	-18.52	-19.70	-20.86
INT	-9.24	-8.42	-7.77
REQ	-9.24	-8.68	-8.18
ICR	-15.24	-14.54	-13.88

Table 7.17: RoPax ferry - Minimum-maximum and standard deviation percentage difference of cost of taxed NOx exhaust emissions of all power plants from reference cycle

Engine Conventional & DLE Combustor	Minimum NOx Cost (% from SC)		Maximum NOx Cost (% from SC)		Standard Deviation (% from SC)	
SC-Reference Cycle	0	0	0	0	0	0
TMI	65.63	70.03	70.13	71.63	73.75	73.27
INT	-7.82	-5.10	-7.57	-5.01	-7.50	-4.95
REQ	-10.98	-13.63	-9.05	-10.12	-7.19	-5.94
ICR	-9.37	-10.30	-9.42	-8.29	-9.38	-5.94

Table 7.18: RoPax ferry - Minimum-maximum and standard deviation percentage difference of cost of taxed CO exhaust emissions of all power plants from reference cycle

Engine Conventional & DLE Combustor	Minimum CO Cost (% from SC)		Maximum CO Cost (% from SC)		Standard Deviation (% from SC)	
SC-Reference Cycle	0	0	0	0	0	0
TMI	-62.48	-63.54	-63.60	-63.61	-64.41	-63.16
INT	-11.13	-9.39	-11.07	-10.43	-11.02	-10.53
REQ	-7.45	-7.18	-2.90	-4.58	0.00	-2.63
ICR	-12.57	-10.22	-13.52	-13.23	-14.41	-15.79

Table 7.19: RoPax ferry - Minimum-maximum and standard deviation percentage difference of cost of taxed CO2 exhaust emissions of all power plants from reference cycle

Engine	Minimum CO2 Cost (% from SC)	Maximum CO2 Cost (% from SC)	Standard Deviation (% from SC)
SC-Reference Cycle	0	0	0
TMI	-18.70	-20.64	-22.22
INT	-8.95	-10.38	-11.11
REQ	-9.60	-8.98	-8.17
ICR	-11.70	-15.76	-18.95

Table 7.20: RoPax ferry - Minimum-maximum and standard deviation percentage difference of cost of taxed UHC exhaust emissions of all power plants from reference cycle

Engine Conventional & DLE Combustor	Minimum UHC Cost (% from SC)		Maximum UHC Cost (% from SC)		Standard Deviation (% from SC)	
SC-Reference Cycle	0	0	0	0	0	0
TMI	-94.09	-94.29	-94.11	-94.19	-93.48	-94.00
INT	-18.18	-7.14	-11.58	-12.90	-6.52	-13.33
REQ	-4.55	0.00	-5.26	-9.68	-2.17	-6.67
ICR	-13.64	-14.29	-15.79	-16.13	-17.39	-13.33

7.2.3 LNG carrier

7.2.3.1 Quantified output parameters

The prime mover quantified output parameters q_p for every scheduled journey of the LNG carrier, produced by using "*Poseidon*", of the two sets of journeys under each of the two already defined weather (or sea-state) profiles which are part of the technical related input data of the life cycle costs model (chapter 3, section 3.2.4.2 and chapter 6, section 6.1) are presented in two tables in appendix E.5 (tables E.1 and E.2), with each table representing a hull roughness amplitude due to fouling (F1-F5, chapter 5, section 5.2.3.2). Each of the table sets represents the weather profile (ideal or adverse) and as it was mentioned in chapter 5, section 5.3.1.2 both prime movers are constantly in operation. Analytical graphical presentation of the cycle performance (turbine entry temperature and fuel flow), engine power-ship (marine vessel) speed relationship, exhaust emissions rates and hot section rotor blade time to failure of the intercooled/recuperated gas turbine (*ICR*) at every time interval during every of the ten in total scheduled journeys are presented for each simulated gas turbine in appendices E.1, E.2, E.3 and E.4 respectively

7.2.3.2 Annual Utilisation

The annual number of scheduled journeys N_{asj} of the LNG carrier is estimated assuming that the marine vessel is in constant annual operation. Modern LNG carriers are designed to spend minimum possible time at the charge/discharge natural gas docking stations, and their operational profile is very similar to ferries, as their journeys are scheduled and in principle they operate on a constant route. The cargo charge/ discharge time, in this study, is assumed to be 12 hours [2], and the life cycle costs model was supplemented assuming an annual number of scheduled journeys $\boldsymbol{N_{asj}}$ of **200**. The required power from the cargo charging/discharging pumps can be as high as approximately 38% of the total installed power plant power [3], and when an IFEP system is installed on a LNG carrier that incorporates a twin main prime mover arrangement the required by the pumps power is provided by one of the vessel's prime movers, a procedure that adds considerable amount of operational time thus operating cost on the vessel's power plant, and because as it has been previously mentioned this study is concentrated on the technoeconomic, environmental and risk analysis of the power plants of the marine vessels in the open-sea, the power plant

operation for charging/discharging cargo from the marine vessel is not taken into consideration. An important difference in the operation of a LNG carrier comparing with a ferry is that under highly adverse weather conditions the LNG carrier will be required to sail, in order to satisfy schedule and contract arrangements. The minimum-maximum annual operational time t_{annual} of the prime movers that are presented in table 7.21 were calculated from the "*Poseidon*" results presented in appendix E.5 by considering the minimum and maximum operational time per journey t_{op} (see tables E.1, hull fouling F1-F5 and E.2, hull fouling F5).

Table 7.21: Minimum and maximum annual operational time per prime mover type

Engine	**Minimum operational time t_{annual} (hours)**	**Maximum operational time t_{annual} (hours)**
ICR	4800	5816

7.2.3.3 Power plant economic and risk analysis

The results that describe the economic performance of each of the intercooled/recuperated gas turbine power plant installed on the LNG carrier according to the case scenarios investigated during this research were obtained as it was described in chapter 3, with the use of the life cycle costs model and the input dataset was implemented to it as described in chapter 6 and in this chapter in sections 7.2.3.1 and 7.2.3.2. The graphical expression of the probability and cumulative probability distribution of the net present cost of scenarios 1 and 2 [*NPC* in GBP (£) million] of the intercooled/recuperated gas turbine power plant incorporating either the conventional or the *DLE* combustor described in chapter 4, section 4.5 and chapter 6, section 6.2.3, is presented in figures 7.9 and 7.10 respectively. The economic scenarios 1 and 2 are described in chapter 6, section 6.2.2). The graphical expression of the rest of the probability and cumulative probability distributions of the overall output parameters (chapter 3, section 3.2.4.3) are presented in appendix E.6, figures E.11-E.22.

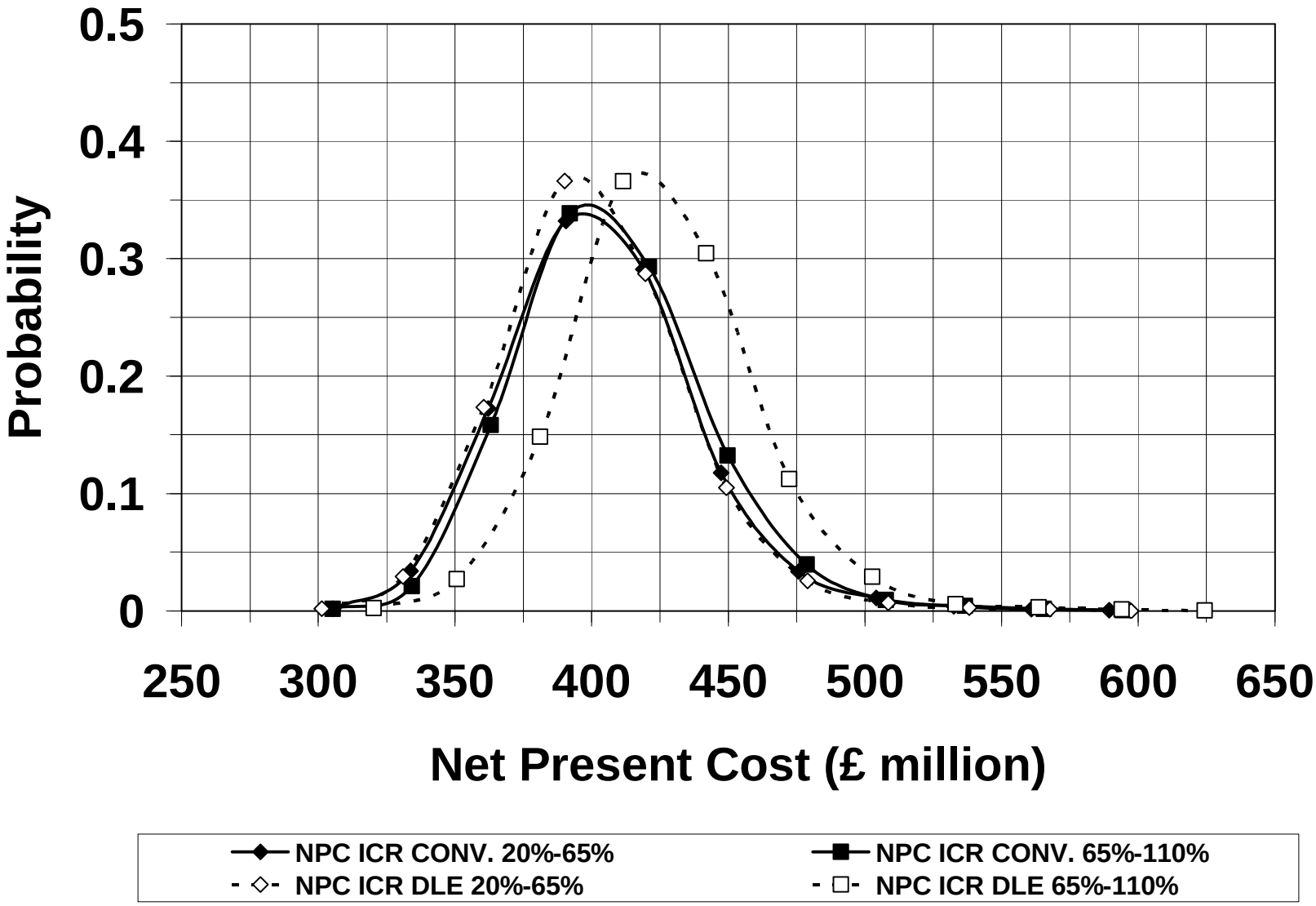

Figure 7.9: LNG carrier – Probability distribution of the NPC of the ICR power plant (Scenarios 1and 2)

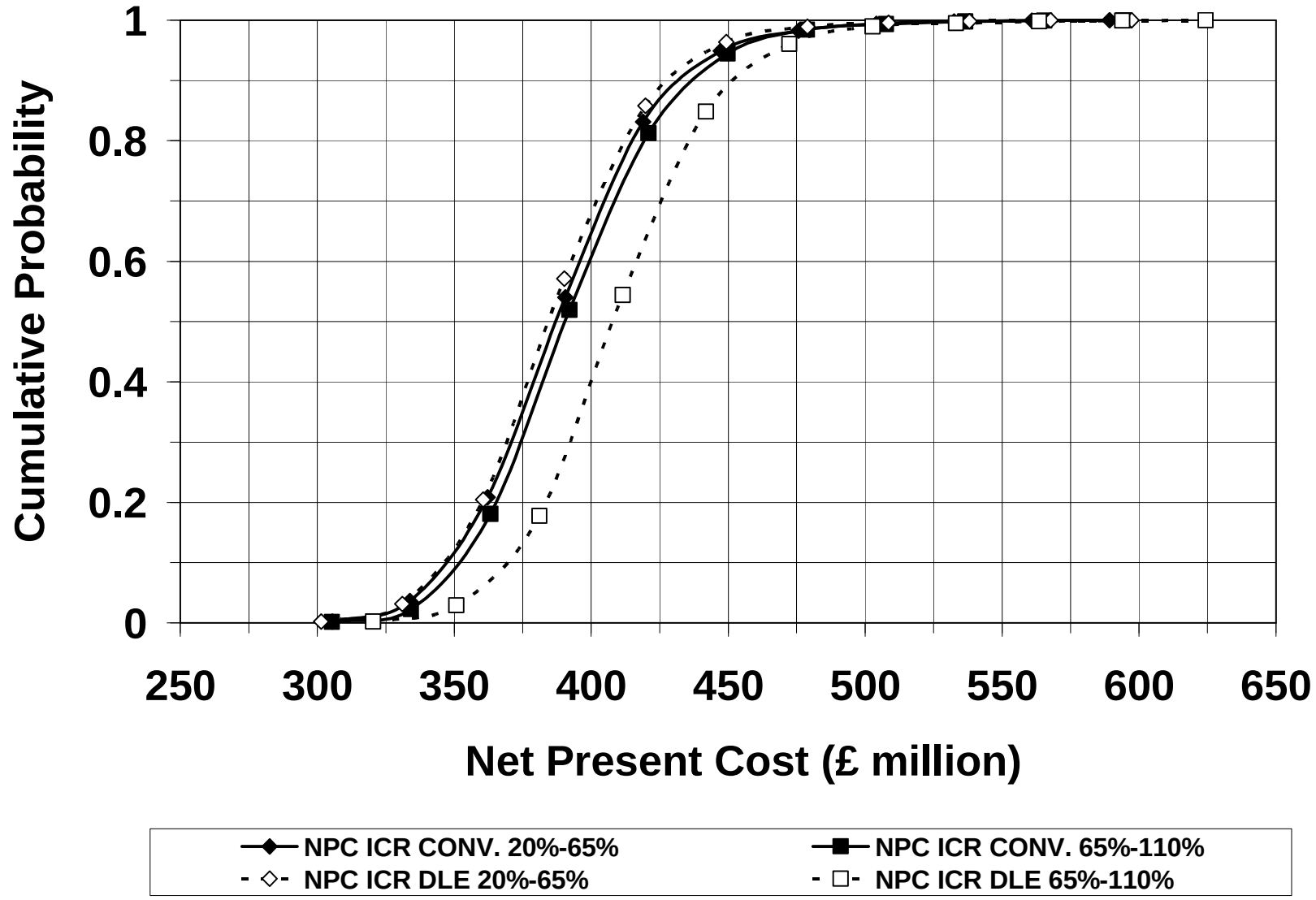

Figure 7.10: LNG carrier-Cumulative probability distribution of the NPC of the ICR power plant (Scenarios 1 and 2)

7.3 Gas Turbine Off-design Operation

7.3.1 General overview

7.3.1.1 Ideal weather conditions

The principal task of the simulated marine gas turbine power plants is to provide the required by the marine vessel power to maintain a scheduled speed. Assuming that the vessel travels at ideal weather conditions and a constant speed profile (RoPax fast ferry: appendix D.2, figure D.11 and LNG carrier: appendix E.2, figure E.3) the factors that affect the thermodynamic performance (RoPax fast ferry: appendix D.1, figures D.1 to D.5 and LNG carrier: appendix E.1, figure E.1) of the gas turbine prime movers is only the air ambient temperature, as the sea temperature remains constant during all scheduled journeys as also air ambient pressure. As at every journey time interval air ambient temperature increases (chapter 5, section 5.4.2.3) the prime mover is required to maintain the same power output which means that the density of air decreases, the entropy of air increases, total compression work increases, total compression pressure ratio decreases as also intake mass flow and more fuel needs to be added, which results in higher turbine entry temperature and a drop in the thermal efficiency.

The effects of the increasing air ambient temperature on the gas turbine NO_x exhaust emissions rates is that the increase in the turbine entry temperature (increased combustor flame temperature) and fuel flow rate have a more significant effect on the NO_x production than the decreased total compression pressure ratio which results in an increase in the gas turbine NO_x exhaust emission rates (RoPax fast ferry: appendix C.3, figures C.27 to C.31 and LNG carrier: appendix E.3, figure E.7). The *CO* (presented in the same figures with NO_x) and *UHC* (RoPax fast ferry: appendix C.3, figures C.17 to C.21 and LNG carrier: appendix E.3, figure E.5) exhaust emission rates are dictated by the increase in the turbine entry temperature and although fuel flow increases the emission rates of *CO* and *UHC* decrease. The production of CO_2 solely depends on fuel flow rate and is directly proportional to it (presented in the same figures with *UHC*).

The effects of increasing air ambient temperature on the gas turbine hot section rotor blade time to failure is that the compressor outlet temperature and relative rotational speed increases as also the turbine entry temperature which results in a decrease in the blade's time to failure (RoPax fast ferry: appendix C.4, figures C.37 to C.41 and LNG carrier: appendix E.4, figure E.9), and consequently an increase in gas turbine maintenance cost.

When the air ambient temperature decreases at constant output power the effects on gas turbine performance and as a consequence exhaust emission rates and hot section rotor blade time to failure are exactly the opposite.

7.3.1.2 Adverse weather conditions

The response of the performance parameters of a marine gas turbine in increasing sea-state numbers (appendices: C.1, D.1, E.1, figures: C.6 to C.10, D.6 to D.10 and E.2 for the Destroyer, RoPax fast ferry and LNG carrier respectively) is identical in principal to the increasing power requirements difference of the Destroyer between cruise and boost speed (appendix C.2, figure C.11) and the increasing power requirement due to hull fouling. Assuming that air ambient temperature between time intervals is constant, when the required prime mover output power increases, all gas turbine performance parameters, that form the basis of this technoeconomic study, increase. This means that NO_x and CO_2 exhaust emissions rate increase and *CO* and *UHC* emissions rate decrease, as also the hot section rotor blade life to failure. The effects of a decreasing required output power on gas turbine performance and as a consequence exhaust emission rates and hot section rotor blade time to failure are exactly the opposite.

When the hydrodynamic resistance of the marine vessel at a certain speed is greater than the maximum available output power produced by the installed power plant, due to increased sea-state numbers and/or hull fouling progression, then the operating turbine entry temperature of the engaged prime mover(s) peaks at the maximum input value of 1530 K which stops to be a variable performance factor and the maximum prime mover power output depends on the variation of the air ambient temperature with time of day. As air ambient temperature decreases maximum power output increases, due to increased intake mass flow rate, total compression ratio and as a

result increased fuel flow rate. The NO_x exhaust emissions rates (appendices: C.3, D.3, E.3, figures: C.32 to C.36, D.32 to D.36 and E.8 for the Destroyer, RoPax fast ferry and LNG carrier respectively) show to increase due to the higher values of the performance parameters, and a similar phenomenon is observed with *CO* exhaust emission rates (presented in the same figures with NO_x), where the dominant factor appears to be the increased fuel flow rate rather than the *CO* exhaust emissions index. On the other hand *UHC* exhaust emissions index seems to be a more significant factor than fuel flow rate in the production of *UHC* exhaust emission quantities (at least at the specified *TET* and T_{amb} range) and as a consequence *UHC* exhaust emission rates decrease (appendices: C.3, D.3, E.3, figures: C.22 to C.26, D.22 to D.26 and E.6 for the Destroyer, RoPax fast ferry and LNG carrier respectively).

Under the conditions defined earlier in this sub-section the hot section rotor blade time to failure decreases (appendices: C.4, D.4, E.4, figures: C.42 to C.46, D.42 to D.46 and E.10 for the Destroyer, RoPax fast ferry and LNG carrier respectively) as both compressor outlet temperature and relative rotational speed increase.

When the air ambient temperature increases, at maximum allowable turbine entry temperature, the effects on gas turbine performance and as a consequence exhaust emission rates and hot section rotor blade time to failure are exactly the opposite.

7.3.1.3 Effects of intercooling

As it was stated in chapter 4, section 4.3.2 the intercooler output temperature T_{IOT} of the simulated high-power mode *TMI, INT* and *ICR* marine gas turbines remains constant at off-design conditions. This means that the *HP* shaft (all three designs are 3-shaft, chapter 4, sections 4.3.4, 4.3.5 and 4.3.7 for the high-power *TMI, INT* and *ICR* respectively) is isolated from changes in the air ambient temperature and the only performance handling variable that define its off-design state is the turbine entry temperature (chapter 2, section 2.2.2), thus the required output power. This can be observed in figures 4.17, 4.20 and 4.26 (chapter 4, high-power *TMI, INT* and *ICR* respectively) where *TBLADE* remains practically unchanged with air ambient temperature variation. It needs to be added that the exhaust gas temperature delivered to the recuperator of the *ICR* gas turbine is primarily affected by the expansion ratio of the *LP* turbine as the *LP* compressor is exposed to the variation of the ambient

conditions, a phenomenon that causes *TBLADE* to vary inconsiderably with changes in the air ambient temperature but still much less than in the case of the *SC*, low-power mode *TMI* and *REQ* (chapter 4, figures 4.8, 4.13 and 4.23 respectively). The relative rotational speed *CS* of the *HP* shaft which is presented in the same figures with *TBLADE*, in the case of the 3-shaft engines, varies according the gas turbine performance principles described in chapter 4, section 4.2.1.

It can be observed that the variation of intake mass flow *MF* (chapter 4, figures 4.16, 4.19 and 4.25 for high-power *TMI*, *INT* and *ICR* respectively), total compression pressure ratio *PR* (presented in the same figures with intake mass flow *MF*), fuel flow *FF* (chapter 4, figures 4.15, 4.18 and 4.24 for high-power *TMI*, *INT* and *ICR* respectively), and as a consequence engine power (power turbine output) *EP* (presented in the same figures with fuel flow *FF*), with air ambient temperature from design-point of the marine gas turbines incorporating an intercooler, is significantly lower in amplitude comparing with the *SC* (chapter 4, figures 4.6 for *FF* and *EP*, 4.7 for *MF* and *PR*) and *REQ* (chapter 4, figures 4.21 for *FF* and *EP*, 4.22 for *MF* and *PR*) cycles and the reason for that is the fact that only the *LP* compressor of the intercooler featuring cycles is affected by the changes in ambient conditions. For that reason in the information contained within tables C.6 to C.10 and D.6 to D.10 (appendices C.5 and C.6 for the Destroyer and RoPAx ferry respectively) the scheduled journey prolongation due to adverse weather conditions in combination with increased hull roughness amplitude due to fouling is kept in lower values when the power plant platform marine vessel incorporates intercooled gas turbine prime movers. The *ICR* power plant because of the installed recuperator, as it was mentioned earlier in this section, shows to be more affected by the changes in the air ambient temperature than the *TMI* (high-power mode) and *INT* power plants.

The effects of intercooling in exhaust emissions rates (appendix B.1, figures B.1 to B.12) due to different air ambient temperatures are similar to the effects on the performance parameters described earlier in this section. The exception in the emission rates is the NO_x where does not show to follow the above observation, as in the *INT* and *TMI* (high-power mode) gas turbines when the *TET* increases after 1350-1400 K nitric oxide exhaust emission rates become more affected by air ambient

temperature. On the other hand the *ICR* gas turbine does not show the above described sensitivity.

The effects of intercooling in the hot section rotor blade time to failure is that it is observed that at part load conditions (i.e. Destroyer cruise mode) in the *TMI* (high-power mode), *INT* and *ICR* gas turbine prime movers turbine entry temperature is kept higher at the same output power requirement comparing with the *SC* and *REQ* (even lower) prime movers which means that hot section blade life is reduced in contrast with the *SC* and *REQ* gas turbines although cooling air temperature in some cases (i.e. *INT* and *ICR*) is lower due to intercooling. At the maximum allowed turbine entry temperature (1530 K) and decreasing air ambient temperature the advantage of the non-intercooled gas turbines starts to fade as the compressor outlet temperature increases more significantly than in the gas turbines that accommodate an intercooler. The marine gas turbine that shows the highest turbine entry temperature at part load conditions is the *ICR* followed by the (in a higher to lower order) *INT*, *SC* and *REQ*, something that can be seen in the case studies results of both the Destroyer and the RoPax fast ferry (appendices C.1 and D.1, figures C.5 and C.10, and D.5 and D.10 respectively). The *TMI* gas turbine prime mover has a different operational profile (when installed on the Destroyer) and for that reason is not directly compared with the other four marine gas turbines on the above mentioned phenomenon.

7.4 Case Studies Discussion: Power Plant Economic Feasibility

7.4.1 Destroyer

7.4.1.1 Intercooled/recuperated cycle gas turbine power plant

According to the results of the three economic scenarios, the power plant that is estimated to be the most economically feasible option in powering the Destroyer is the *ICR*, equipped either with conventional or *DLE* combustors. The installation of *DLE* combustors on the power plant's (all) prime movers is a marginally more economical solution in the case of scenario 1, but in scenario 2 the increased probable PMC_0 (chapter 3, sections 3.2.2.4 and 3.2.2.6) leads to a higher PMC_1 as the *DLE* combustors cost more than in scenario 1 (*PMC* also increase), which means that the

overall probable maintenance costs also increase (chapter 3, equation 3-6), and in this case (scenario 2) makes the installation of conventional combustors a marginally more economically proposal. As it was stated in chapter 6, sections 6.2.2 and 6.2.3 all prime movers depending on the scenario number have the same $PD_{0\text{-}min}$ -$PD_{0\text{-}max}$ and $PD_{1\text{-}min}$-$PD_{1\text{-}max}$ range, and the main factor that differentiates the C_{maint} of each of the prime movers (assuming the investigation concerns a single marine vessel type and have the same operational profile i.e. cruise or boost) is the number of hours between engine overhaul *Hem* (journey time prolongation in the case of the Destroyer is not a major factor) which according to chapter 3, sections 3.2.2.3 and 3.2.2.4 it affects *PMC* and as a consequence C_{maint} (*Hem* inherently affects C_{maint}). The turbine entry temperature is the main parameter in determining the hot section rotor blade time to failure (thus *Hem*) and as it can be seen in the relative figures in appendices C.1 and C.4 (ideal weather conditions, all hull fouling levels) the *ICR* prime movers (both cruise and boost prime movers operate at part-load, but in a different level) operate at the highest *TET* comparing with the *SC*, *INT* and *REQ* (the *TMI* power plant is described in the next section) producing the second lowest *Hem* (both cruise and boost prime movers, second to *TMI* power plant). At adverse weather conditions (see relative figures in appendices C.1 and C.4) and referring to sections 7.3.1.2 and 7.3.1.3, the *Hem* of both the cruise and boost *ICR* prime movers increase comparing the *SC* and the *INT* power plant (similar q_b values especially between the boost prime movers). In both scenarios the *ICR* power plant is probably more expensive to maintain than the reference power plant (which in general as the lowest maintenance cost as also the *REQ* power plant either with conventional or *DLE* combustors). Comparing the maintenance cost of the *ICR* and *INT* power plants in both scenarios, the *ICR* equipped with conventional combustors is benefited by the smaller variability of the maintenance cost distributions although its minimum maintenance cost is higher than the *INT* power plant equipped with the same combustor technology. When the two power plants are compared (both scenarios), equipped with *DLE* combustors the *INT* power plant shows a probability of higher $C_{maint.}$ At this point a comment needs to be made: due to the fact that the normal distributions are defined, in general, by eleven intervals, their shape may not be presented perfectly according to their ideal shape, and this limitation can be considerably compensated by knowing the number of risk scenarios, the minimum-maximum of the distributions and their variability (standard deviation).

In terms of probable fuel cost (which is the most influential cost component in the *NPC* of all power plants in this *TERA* research) the *ICR* power plant not only benefits from its second highest design-point thermal efficiency (η_{th}=0.4349) but also from its highest part-load thermal efficiency (approximately 80% of design-point at air ambient temperature of 10.6 ^{o}C at 8.12MW which is the lowest required brake power by the Destroyer at cruise mode) and operational profile. The *ICR* power plant produces the second lowest probable fuel cost behind the *TMI* power plant. The highest probable fuel cost is produced as expected by the *SC* power plant.

The probable cost of CO_2 exhaust emissions is dictated by the thermal efficiency characteristics of the power plant, and the two reasons that is differentiated from the probable fuel cost in terms of minimum-maximum cost and distribution variability is the emission tax rate and the range of it (chapter 6, sections 6.4.1 and 6.4.2). The probable NO_x exhaust emissions cost of the *ICR* and *INT* power plants is marginally lower in minimum-maximum cost range and variability either equipped with conventional or *DLE* combustors comparing with the *SC* power plant (table 7.7, appendix C.7, table C.16 and appendix C.6, figures C.53, C.54, C.55 and C.56), and it needs to be mentioned that the only factor that differentiates the probable NO_x exhaust emissions cost (in a proportional manner) thus minimum-maximum cost and distribution variability produced by either using conventional or *DLE* combustors is the combustor technology factor K_{tech} (applies to probable *CO* and *UHC* exhaust emissions cost). The *CO* and *UHC* exhaust emission quantities (especially *UHC*) are considered as secondary influential factors in the estimation of the probable *NPC* of the power plants as generally the quantities produced by the power plants are lower than that of NO_x as also their cost per produced unit mass (chapter 6, section 6.4.2). By changing the cost of emission quantities per unit mass the effect of each of the exhaust emission quantity can change. The high turbine entry temperatures sustained by the *ICR* prime movers at part-load (and the very good part-load thermal efficiencies) produce smaller quantities of *CO* and *UHC* exhaust emissions comparing with the *SC* and *REQ* power plants. Comparing the probable *CO* exhaust emissions cost of the *ICR* and *INT* power plants the produced results are very similar either when the power plants are equipped with *DLE* or conventional combustors. It is interesting the fact that the *ICR* and *INT* prime movers either as cruise or boost prime movers (the cruise prime movers in general, naturally produce larger *CO* and *UHC*

exhaust emission quantities, first because of their extensive operation at part load and second because of the their higher operational time per scheduled journey) produce similar *CO* exhaust emission quantities. On the other hand the *ICR* power plant produce lower probable *UHC* exhaust emissions cost comparing with the *INT* power plant as at both weather conditions and prime mover operational modes the *ICR* prime movers produce lower *UHC* exhaust emissions quantities.

7.4.1.2 Twin-mode intercooled cycle gas turbine power plant

According to the results of scenario 1 the *TMI* power plant equipped with *DLE* combustors is clearly the option that produces the second lowest probable *NPC* with a minimum value very close to the minimum probable *NPC* cost of the *ICR* power plant equipped also with controlled exhaust emissions combustors, but with a larger standard deviation that results in a higher maximum probable *NPC*, thus a higher probability that the *TMI* power plant may produce a higher *NPC* value. The installation of conventional combustors increase the probable *NPC* and the *TMI* power plant produces an economic feasibility similar to the *REQ* power plant equipped with conventional combustors with a higher minimum probable *NPC* but with smaller variability. Either with controlled or uncontrolled combustion the system remains a more economical option than the reference power plant equipped with either conventional or *DLE* combustors. According to the results of scenario 2 the *TMI* power plant equipped with conventional combustors is a more economical option than the reference power plant equipped also with technologically the same combustion system as it produces a marginally smaller minimum *NPC* and the distribution has a smaller variability. When the two power plants are compared equipped with *DLE* combustors (the reference power plant equipped with *DLE* combustors is clearly a more economically feasible option than equipped with conventional combustors) the *TMI* power plant remains a marginally more economical system. According to the results of scenario 3 the *TMI* power plant is considered as the least economically feasible option in comparison with all power plants and in addition the conventional combustion system produces a lower probable *NPC* than the *DLE*.

As it was mentioned in the previous section the *TMI* power plant produces the lowest probable fuel cost. The prime movers of the power plant when they operate at

the low-power mode their minimum thermal efficiency at 10.6 ^{o}C (ideal weather conditions and clean hull, required brake power 8.112MW divided by two) is 96% of the low-power mode design-point, which is the highest thermal efficiency at cruise mode comparing with all power plants. At ideal weather conditions the high-power mode does not engage in order the Destroyer to maintain its cruise speed, and at an air ambient temperature of 10.6 ^{o}C the high-power mode (boost speed, ideal weather conditions clean hull) has a minimum thermal efficiency η_{th} of approximately 0.45 which is also the highest thermal efficiency at sprinting. At adverse weather conditions (appendix C.1, figure C.23) (clean hull) the high-power mode of the *TMI* power plant according to the Destroyer power plant operation (chapter 5, section 5.3.1.3) is required to engage at, at least 6 time intervals (raising to 7 time intervals at hull fouling level F5) forcing the prime movers to operate at power as low as 5.5MW each. As the high-power mode engages at so low required brake power the thermal efficiency of the power plant reduces. The thermal efficiency of each of the *TMI* prime movers at an air ambient temperature of 10.6 ^{o}C (clean hull, 5.5 MW required power) is approximately 71.8% of the high-power mode design-point (a further example of the part-load thermal efficiency of the high power mode which directly compares it with the other four simulated marine gas turbines is: at 8.12MW and air ambient temperature 10.6 ^{o}C the thermal efficiency η_{th} is approximately 79% of the high-power mode design-point). A proposal on optimizing thermal efficiency during the scheduled journeys under adverse weather conditions would be the prohibition of the engagement of the high-power mode for the maintenance of cruise speed in order the Destroyer to cruise only on low-power mode (high-power mode may engage in high sea-state numbers), something that can also prolong journey time, but further investigation is needed in order to obtain the economical feasibility of the proposal (**note: recommendation for further work**), as restraints in available time for the completion of the current research did not allow its additional implementation.

The operational profile of the *TMI* power plant inherently produces the highest probable maintenance cost C_{maint} comparing with the other four power plants as its standard operation requires high average turbine entry temperatures, and when the prime movers of the power plant operate in the high-power mode the design-point blade time to failure t_f drops to approximately 23,000 hours (chapter 4, section 4.4.3.3), affecting equally the blade time to failure at off-design conditions. Off-

standard operation of the power plant is when the high-power mode engages at adverse weather conditions in order the Destroyer to sustain cruise speed and at the corresponding time intervals the hot section rotor blade time to failure increases due to the reduction of the turbine entry temperature (appendix C.4, figure C.43), although the above described operation is not adequate to reduce probable maintenance cost to the levels of the other four power plants. In scenario 1, the *TMI* power plant equipped with conventional combustors produces a minimum probable C_{maint} of 98.25 % higher than that of the reference power plant and the normal distribution extends to a maximum probable C_{maint} of 113.47% having a 122.54% higher variability. The installation of *DLE* combustors has the effect of raising the variability of distribution 26% more, at a similar minimum probable maintenance cost. At scenarios 2 and 3 maintenance costs increase even further as due to the phenomena described in the previous section.

The probable cost of CO_2 exhaust emissions is as stated before directly connected with the thermal efficiency characteristics of the power plant and for that reason the *TMI* power plant produces the lowest probable CO_2 exhaust emissions cost. The probable cost of NO_x exhaust emissions is the highest comparing with the other four power plants equipped with conventional or *DLE* combustors respectively. When the power plant operates at the low-power mode the produced NO_x exhaust emission rates per prime mover are significantly lower comparing with each of the cruise prime movers of the other four power plants, but because of the fact that both *TMI* prime movers are in constant operation the resulting total NO_x exhaust emission rates of the *TMI* power plant operating at the low-power mode are higher comparing with all the other power plants. When the *TMI* power plant is requested to operate at the high-power mode the EI_{NOx} increases at approximately 85.5% and as it was mentioned before according to the power plant operation management at adverse weather conditions the high-power mode is requested to operate more than the standard 25%. The above mentioned factors are primarily connected with the high probable cost of the NO_x exhaust emissions. On the other hand the probable cost of *CO* and *UHC* exhaust emissions respectively (equipped with conventional or *DLE* combustors) is the lowest comparing with the other four power plants (comparisons at the same combustor technology level). This can be explained from the facts that when the *TMI* power plant operates at the low-power mode the minimum *TET* is much closer to

design-point comparing with the single-mode prime mover power plants as also thermal efficiency and when the *TMI* power plant is requested to operate at the high-power mode (taking into account the previously described operational profile) the EI_{CO} and EI_{UHC} decrease approximately 83.7% and 97.55% respectively.

7.4.1.3 Recuperated cycle gas turbine power plant

According to the results of scenario 1, the minimum probable *NPC* of the *REQ* power plant equipped either with conventional or *DLE* combustors (marginally lower probable *NPC* comparing with the conventional combustion system) is a more economically feasible option than the reference power plant irrelevantly of the installed combustor technology. Also the *REQ* power plant is clearly a more economically feasible solution comparing also with the *INT* power plant regardless of the installed combustor technology. According to the results of scenario 2 the power plant regardless of combustion technology still performs better than the *INT* power plant, but comparing with the reference power plant, its economic performance is very similar. When the two power plants are equipped with conventional combustors produce an almost identical minimum probable *NPC* but the *REQ* power plant shows a smaller variability. When the two power plants are equipped with *DLE* combustors, both perform critically better than when equipped with conventional combustors, and the *REQ* power plant shows a marginally lower overall probable *NPC* but with an also marginally larger variability.

Regarding probable fuel cost, the *REQ* power plant cannot compete the *TMI* and *ICR* plant mainly because of the lower design point thermal efficiency of the *REQ* marine gas turbine (η_{th}=0.407), but it produces a lower probable fuel cost comparing with the *SC* and *INT* power plant. The *SC* marine gas turbine has the lowest design-point thermal efficiency (η_{th}=0.375) and the *INT* marine gas turbine has a design-point efficiency η_{th} of 0.408 which is almost identical to the *REQ* engine. Comparison of the part-load thermal efficiency of the three prime movers with their design-point at a brake power of 8.12MW and air ambient temperature of 10.6 ^{o}C (Destroyer: cruise speed, ideal weather conditions, clean hull) shows:

- Simple cycle: approximately 71.4% of design-point
- Intercooled cycle: approximately 73.4% of design-point
- Recuperated cycle: approximately 78.9% of design-point

As the operation of the Destroyer incorporating an IFEP system requires extensive single-prime operation (except *TMI* power plant) at part-load the *REQ* power plant has a lower overall fuel consumption. It needs to be added that the boost prime mover (and the cruise at boost speed) operates also at part-load under ideal weather conditions (increased hull fouling level increases the required brake power but *TET* never increases beyond design-point at ideal weather conditions) although the difference in part-load efficiency is smaller as at boost speed the required brake power is significantly higher. At full-load and beyond both *INT* and *REQ* show an almost identical thermal efficiency (at the range of ambient temperatures of the equivalent profile).

The *REQ* power plant produces the lowest probable maintenance cost comparing with the advanced cycle power plants at all three scenarios. In scenario 1 it produces significantly lower minimum probable maintenance cost comparing with the reference power plant, where the *REQ* power plant equipped with *DLE* combustors has a lower minimum probable maintenance cost comparing with reference power plant equipped with conventional combustors. The overall probability of lower probable maintenance cost declines significantly due to the fact that both maintenance cost distributions (conventional and *DLE* combustors) of the *REQ* power plant show a higher variability, and as a consequence a higher maximum probable maintenance cost. The *TET* range that the *REQ* prime movers operate during the scheduled journeys of the Destroyer is the greatest comparing with all other gas turbine prime movers. At part load-conditions the operational turbine entry temperatures of the *REQ* prime movers are the lowest in comparison with the other gas turbine prime movers a phenomenon that significantly increases *Hem*, at every time interval (in comparison with the other power plants), thus decrease C_{maint}. The low turbine temperature can be explained by the fact that low specific power values are maintained at the above described conditions, as mass flow decreases at lower rates (as also overall compression pressure ratio) comparing with the other simulated gas turbines. At design-point *TET* and beyond the *REQ* marine gas turbine shows to be affected by the fluctuation of the air ambient temperature more than the other four marine gas turbines (more also than the *SC* marine gas turbine, see also section 7.3.1.3).

The probable cost of CO_2 exhaust emissions as it has been mentioned before depends on the thermal efficiency characteristics of the prime mover of the power plant and no further comments are about to be made. The *REQ* power plant produces the lowest probable NO_x emissions cost equipped with either optional combustion systems. This can be explained by the low turbine entry temperatures at part-load conditions and also the good part-load thermal efficiency characteristics. The low turbine entry temperatures at part-load operation have the opposite effect on the probable *CO* and *UHC* exhaust emissions cost. The *REQ* power plant produces the highest probable *CO* and *UHC* exhaust emissions cost comparing with the other advanced cycle power plants, and it is the only power plant that produces *CO* and *UHC* exhaust emissions cost distributions that have a positive percentage difference in minimum-maximum cost and variability in comparison with the reference power plant.

7.4.1.4 Intercooled cycle gas turbine power plant

According to the results of scenario 1 the *INT* power plant is a more economically feasible option than the reference power plant equipped either with conventional or *DLE* combustors. The installation of *DLE* combustors on the prime movers of the *INT* power plant increases the minimum probable *NPC* but the distribution is characterised by a lower variability which decreases almost equally the maximum probable *NPC*, resulting in an almost equal *NPC* in terms of risk assessment. In scenario 1 the *INT* power plant (equipped with either of the two combustion systems) can be considered as the least economically feasible option comparing with the other three advanced cycle power plants. According to the results of scenario 2 the *INT* power plant equipped with conventional combustors produces a lower probable *NPC* in comparison with *INT* power plant equipped with *DLE* combustors. Both options though, are considered as the least economically feasible in scenario 2, producing a lower probable *NPC* than the *TMI* power plant investigated in scenario 3.

The *INT* marine gas turbine when it operates at part-load it experiences a high drop of mass flow (and overall compression pressure ratio) a phenomenon that causes the turbine entry temperature to sustain high minimum values (lower than the *ICR* but higher that then *SC* and the *REQ* gas turbines). The *INT* power plant shows in both scenarios equipped either with conventional or *DLE* combustors a higher probable

maintenance cost comparing with the reference power plant (*SC* power plant: maintenance cost with conventional combustors is lower than with *DLE*).

As it was described in the previous section (7.4.1.3) regarding the design-point and part-load thermal efficiency of the *SC*, *INT* and *REQ* gas turbine prime movers , the *INT* power plant is clearly a more economical option in terms of probable fuel cost comparing with the *SC* power plant, but it is the least economical option in comparison with the other advanced cycle power plants, and this is reflected also in the probable CO_2 exhaust emission cost.

The probable NO_x exhaust emissions cost is marginally lower comparing with the reference power plant and comparing the variability of the distributions of the two power plants equipped with conventional combustors the variability of the distributions is equal. When they are equipped with *DLE* combustors the distribution of the *INT* shows a marginally larger variability. It needs to be mentioned that due to the higher sustained turbine entry temperatures at part-load of the *INT* gas turbine the expectation would be that the probable NO_x exhaust emissions cost would be higher comparing with the reference power plant, but the decisive factor is the higher design-point thermal efficiency of the *INT* gas turbine and its better part-load performance. The probable *CO* and *UHC* exhaust emission costs are lower in comparison with the probable costs produced by the *SC* power plant, primarily because of the higher sustained turbine entry temperatures at part-load and secondarily because of, as described above, its better thermal efficiency characteristics.

7.4.2 RoPax fast ferry

7.4.2.1 Definitions

The operational profile of the RoPax fast ferry is much simpler than the Destroyer's. Both of the power plant's prime movers are always engaged and share equal load, having a minimum operational power rating of approximately 85% MCR, which resembles the operation of the power plants installed on the Destroyer, at boost speed (minimum 83% MCR). This means that gas turbine part-load performance is of less importance comparing with the operational profile of the Destroyer, and design-point thermal efficiency has a more important role not only in the probable fuel cost of each of the power plants but also in the probable cost of the exhaust emissions. The

variation on the performance differences between the simulated marine gas turbines that were identified in the previous main section (7.4.1) are apply also in the operation of the RoPax fast ferry but in a smaller magnitude (i.e. part-load thermal efficiency, turbine entry temperature levels at part-load operation etc.) as the prime movers of the under investigation power plants operate much closer to the design-point turbine entry temperature.

7.4.2.2 Twin-mode intercooled cycle gas turbine power plant

According to the results of scenario 1, the power plant that is estimated to be the most economically feasible option in powering the RoPax fast ferry is the *TMI* power plant equipped with *DLE* combustors. The results derived from scenario 1 also show, that the option of investing on *DLE* combustion results in a lower probable *NPC* of all power plants in comparison with investing on their equivalents equipped with conventional combustors. The *TMI* power plant due to its high output rates of NO_x exhaust emissions (chapter 4, section 4.5.2.1) shows that the *DLE* combustors investment is financially the most beneficial in comparison with the other four power plants. It needs to be stated that the reference power plant, even if it is incorporated with controlled exhaust emissions combustors, produces the highest probable *NPC* in scenario 1. According to the results of scenario 2, the *TMI* power plant equipped with *DLE* combustors is also the most economically feasible option in powering the RoPax fast ferry and produces a marginally lower probable *NPC* in comparison with the *ICR* power plant equipped also with *DLE* combustors. In general the results of scenario 2 show also that the installation of a *DLE* combustion system on the prime movers of each of the power plants produce a lower probable *NPC* in comparison with the equivalents equipped with conventional combustors. Results from scenario 3 show that the *TMI* power plant equipped with *DLE* combustors is a more economical option in comparison with its equivalent equipped with conventional combustors. The *TMI* power plant equipped with *DLE* combustors produces a lower probable *NPC* in comparison with the reference power plant equipped with conventional combustors, and produces a similar probable *NPC* with the reference plant equipped also with *DLE* combustors, with the main difference of having, a lower minimum probable *NPC* with a distribution of higher variability resulting in an almost equal maximum probable *NPC*. The *TMI* power plant equipped with conventional combustors (scenario 3) produces together with the *INT* and the reference power plant (scenario 2)

respectively the higher probable *NPC*, with the reference power plant producing the higher risk of the three, but not of considerable magnitude in difference.

The *TMI* power plant produces in general the highest maintenance costs with distributions of high variability. In terms of probable fuel and CO_2 exhaust emissions cost the *TMI* power plant produces the lowest probable values and the reason is the highest design-point efficiency of the *TMI* gas turbine operating in the high power mode. The probable cost of NO_x is the highest among all the other power plants as it was explained in section 7.4.1.2, and the probable cost of *CO* and *UHC* respectively are the lowest (see section 7.4.1.2).

7.4.2.3 Intercooled/recuperated cycle gas turbine power plant

The results from scenario 1 and 2 show that the *ICR* power plant equipped with *DLE* combustors produces the second lowest probable *NPC* and when is equipped with conventional combustors it produces the third lowest probable *NPC* respectively. In all scenarios and combustor configurations the power plant is regarded as a more economical option in comparison with the reference power plant equipped either with conventional or *DLE* combustors.

The probable maintenance cost of the *ICR* power plant (conventional and *DLE*) in both scenarios, is as expected (section 7.4.1.1) higher than the reference power plant's in both combustors configuration. The power plant in general requires higher probable maintenance costs in comparison with the *REQ* power plant, but in comparison with the *INT* power plant in scenario 1, when both power plants are equipped with conventional combustors the probable maintenance cost is regarded as similar (appendix D, figure D.50) and the same can be expressed when the two power plants are equipped with *DLE* combustors. In scenario 2, both power plants produce a similar minimum probable maintenance cost but the distribution of the *ICR* power plant shows a higher variability and a higher maximum probable maintenance cost. When the two power plants are equipped with *DLE* combustors the minimum probable maintenance cost is still similar among them but the distribution of the *INT* power plant shows a higher variability and a higher maximum probable maintenance cost.

The probable fuel and CO_2 exhaust emissions costs of the *ICR* power plant, respectively, are as expected, the second lowest behind the *TMI* power plant. The probable cost of NO_x produced by the *TMI* power plant is lower comparing with the reference power plant (comparison is between combustors of the same technology) and the differences observed in the case of the destroyer apply also in the case of the RoPax fast ferry taking into account, that fuel flow rate and intercooling (see section 7.3.1.3) has more important role in the probable NO_x, CO and *UHC* exhaust emissions cost (see section 7.4.2.1). The *ICR* power plant also produces a lower probable NO_x emissions cost in comparison with the *INT* power plant (comparison is between combustors of the same technology) but in comparison with the *REQ* power plant their probable NO_x exhaust emissions cost is regarded as practically equal. The probable *CO* and *UHC* exhaust emissions cost is lower comparing with the reference power plant, and also lower in comparison with the *REQ* and *INT* power plants.

7.4.2.4 Recuperated cycle gas turbine power plant

According to the results of scenario 1, the *REQ* power plant equipped with conventional combustors produces a lower probable *NPC* in comparison with the reference and the *INT* power plant, both equipped with *DLE* combustors. Equipped with *DLE* combustors is a more economically feasible option in comparison with the *TMI* power plant equipped with conventional combustors because its distribution produces a lower variability. Scenario 2 results show that the *REQ* power plant equipped with *DLE* combustors is still a more economically feasible option than the reference power plant equipped with the same combustors. The *REQ* power plant equipped with *DLE* combustors is considered, in both scenarios, as financially more suitable option in comparison with both the reference and the *INT* power plant both equipped with conventional combustors.

The probable maintenance cost of the *REQ* power plant is as in the case study of the Destroyer the lowest in comparison with the other three advanced cycle power plants in both scenarios. In comparison with the reference power plant, according to scenario 1 results, although the minimum probable maintenance cost of the *REQ* power plant is lower, its variability is considerably higher, due to the fact that the reference power plant has a fixed PMC_1. This applies to combustors of the same

technology. In scenario 2 results the *REQ* produces a higher probable maintenance cost, than the *SC* power plant, of equivalent combustion technology.

The probable fuel and CO_2 exhaust emissions costs of the *REQ* power plant are lower in comparison with the reference power plant, and they practically equal with the *INT* power plant. At ideal weather conditions and minimum required brake power at 85% MCR the *REQ* gas turbines have a better part-load performance in comparison with the *INT* gas turbines, a phenomenon that is observed in all five hull fouling levels, and this difference is compensated at adverse weather conditions, beyond the design-point *TET* where the *INT* gas turbines perform better (higher thermal efficiency). It needs to be added that in general, scheduled journey time is prolonged more when the RoPax fast ferry is equipped with the *REQ* power plant, which means that the additional operational time, increases the quantified output parameters q_p.

The probable NO_x exhaust emissions cost produced by the *REQ* power plant is lower in comparison with the reference and *INT* power plants (comparison is between combustors of the same technology). The reason is that the *REQ* power plant operates at part-load with lower turbine entry temperatures (and higher part-load thermal efficiency), than both power plants (see section 7.4.1.3). The probable cost of *CO* and *UHC* exhaust emissions of the *REQ* power plant, is lower in comparison with the reference power plant but higher than the *INT* power plant (comparison is between combustors of the same technology). This can be partly explained from the facts that although the *SC* gas turbines operate at higher turbine entry temperatures at part-load (still lower than the *INT* gas turbines) their thermal efficiency characteristics are considerably lower, in comparison with the *REQ* gas turbine. On the other hand the higher part-load turbine entry temperatures of the *INT* gas turbines seem to be the most important factor in its lower probable cost of *CO* and *UHC* exhaust emissions.

7.4.2.5 Intercooled cycle gas turbine power plant

According to the results derived from scenario 1, the *INT* power plant produces the highest probable *NPC* in comparison with the three advanced cycle power plants. When it is equipped with conventional combustors it can be regarded as a marginally more economically feasible option in comparison with the reference power plant equipped with *DLE* combustors. The results derived from scenario 2, the *INT* power

plant equipped with *DLE* combustors produce a higher probable *NPC* than the equivalent reference power plant, though it can still be regarded as a more feasible investment than the reference power plant equipped with conventional combustors. The above observation applies also to the *INT* power plant equipped with conventional combustors although the cost range difference is more marginal but still of lower overall risk.

The probable maintenance cost of the *INT* power plant is significantly higher than the reference power plant, but the probable cost of all four exhaust emission quantities is lower, and what can be observed is that although the same phenomena are observed in the case of the *ICR* power plant, design-point and part-load thermal efficiency have a significant impact on the economic feasibility of the power plant (at the same design-point emission indexes).

7.4.3 LNG carrier

7.4.3.1 Definitions

The operational profile of the LNG carrier's power plant in the open sea is identical to the RoPax fast ferry with the difference that the maximum continuous rating (MCR) is in this case, approximately, 88%. Because of the fact that the investigation takes into account the power plant operating in the open-sea (see section 7.2.3.2) the net present costs (as also the cost components that compose it) produced in the two scenarios, with the power plant equipped either with conventional or *DLE* combustors, are lower (*NPC* distribution parameters) in minimum, maximum and also variability, in comparison with an investigation that adds in the power plant life cycle costs, the operation of the prime mover(s) during cargo loading/unloading, but restrains in available time for the completion of this *TERA* research did not allow the implementation of the above remark.

7.4.3.2 Intercooled/recuperated cycle gas turbine power plant

The results derived from scenario 1 show that the power plant equipped with *DLE* combustors, produces a lower minimum probable *NPC* in comparison with the power plant equipped with conventional combustors, but its distribution is characterised by a higher variability, which results in a higher maximum probable *NPC* and as an investment can be considered of higher risk. Results derived from scenario shows that

the installation of *DLE* combustors increases the probable *NPC* considerably, and although the investment does not produce major additional risks, the minimum-maximum values of the normal distribution are higher. Comparing scenarios 1 and 2, it is observed that both combustor option of scenario 2, cannot be regarded as more economical feasible in comparison with the option of installing conventional combustors on the power plant in accordance with the probable capital costs range of scenario 1. The use of different fuel (natural gas instead of distillate) shows that the installation of *DLE* combustors can have a negative effect on the probable *NPC* of the power plant, due to the fact that the selected price range of the *DLE* combustors in combination with the increased maintenance cost, do not compensate the reduction in exhaust emission quantities, although an exhaust emissions taxation of higher rates per unit exhaust emission mass, can result in transforming the *DLE* combustor option as more economically feasible. The same can be suggested in the case that $PD_{1\text{-}min}$ and $PD_{1\text{-}max}$ had a smaller range (both above comments apply also for the option of using distillate fuel).

7.5 Marine Vessel Sea-keeping Performance

An important hull form design parameter that affects the sea-keeping performance of a marine vessel is the block coefficient C_B, where when it is increased, the additional resistance created by sea-waves on the cruising marine vessel, increases [4]. The effects of C_B on the additional resistance created by the waves in adverse weather conditions can be observed in the cases of the LNG carrier and RoPax fast ferry. An example is that when the Ropax fast ferry (C_B = 0.55) equipped with the *ICR* power plant, sails in adverse weather conditions at sea-state number 8 (clean hull) the vessel's speed (appendix D.2, figure D.16) drops approximately 58.5%, and at the same conditions the LNG carrier's speed (C_B = 0.75) potentially drops more than 100% (appendix E.2, figure E.4). The word "potentially" is used in order to describe that the LNG carrier under the above described conditions could have a negative speed value. The difference in the maximum continuous rating between the two marine vessels at trial conditions is approximately 3% higher for the LNG carrier, which means that it has less power margin at adverse weather conditions, something that partly composes the overall difference between the LNG carrier and the RoPax fast ferry in their previously described speed drop, also taking in account the larger

frontal area of the LNG carrier, which increases the overall resistance of the marine vessel. The purpose of the sea-wave resistance module in the current developing stage of "*Poseidon*" is not to accurately simulate the effects of waves on the resistance of a marine, but to describe them as close as possible in combination with the research time restrains. The above described phenomenon does not affect the performance simulation of the prime movers as at the above described weather conditions the power plant's gas turbines would operate at their maximum allowed turbine entry temperature as the marine vessel is forced to reduce its speed, which means that the total journey time is affected (less time to complete scheduled journey). From a technoeconomic point of view, comparisons between different cycle technology power plants (or different components technology) are still valid as all of them would experience the same effects, assuming that they operate at the maximum allowable turbine entry temperature.

7.6 References

1. Hodge, C.G., Mattick, D.J., "*The Electric Warship III*", Transactions of the Institute of Marine Engineers, Vol. 110, Part 2, pp 119-134, 1997.

2. www.ship-technology.com/projects/inigo%5Ftapias/

3. Hansen, J.F., Lysedo, R., "*Electric Propulsion for LNG Carriers*", LNG Journal, pp 11-12, September/October 2004.

4. Schneekluth, H. and Bertram, V., **"***Ship Design for Efficiency and Economy, Second Edition"*, Butterworth and Heinemann, ISBN No. 0-7506 4133-9, Chapter 3, pp 100, 1998.

8 Conclusions & Recommendations

8.1 Conclusions

A novel generic Technoeconomic, Environmental, Economic and Risk Analysis (*TERA*) method was developed for the investigation of the life cycle economic feasibility of existing and novel marine gas turbine power plants operating as part of an integrated full electric propulsion system (*IFEP*), based on the initial proposal regarding the Advanced Marine Electric Propulsion Systems (*AMEPS*) project.

Chapter 1 described the research background, provided information to the reader on principles of marine integrated full electrical propulsion (*IFEP*), a brief forecast on the marine gas turbine market share and specified a) the research objectives followed by main definitions that were intended to be useful to the reader in order to obtain a spherical view of the tasks of this research and b) main assumptions created at the beginning and during its progress.

Chapter 2 described the methods and tools used to create the numerical models that constitute the integrated computational marine vessel operation environment scheme "*Poseidon*" that forms the technical and environmental part of the *TERA* method. The validity of the methods used to construct the scheme is supported by their extensive use in their relative fields. The exception is the method used in the wave-resistance module which was a compromise between the available time to complete the current research and the complexity characterised the modelling of the effects of sea-waves on the power requirements of a marine vessel. The scheme does not take into account the effects of shallow water in the hydrodynamic resistance of the marine vessel as also cavitation and partial submergence of the propeller(s). The scheme was created to be able to simulate without modifications different fundamental power plant operational strategies according to the type of the marine vessel. The main outputs of "*Poseidon*" per scheduled journey are: Prime mover fuel consumption, hot section rotor blade life consumption, exhaust emissions mass quantities (NO_x, CO, CO_2 and *UHC* separately), operational time.

Chapter 3 described the methods and tools used to create the economic and risk numerical model that forms the economic and risk analysis part of the *TERA* method. The validity of the methods used to construct the model is supported by the facts that, first, although the version of the method used to predict the maintenance cost of the simulated marine gas turbines corresponds to turboprops engines, their design similarities is fundamental and second, the method has been successfully used in a number of projects in Cranfied University. The operational life time of the gas turbine prime movers was set at 30 years. The model included a technology factor to provide the ability to adjust the exhaust emissions quantities in accordance with the technology level of the installed combustor. Due to restrains in available time, the model can only accommodate two different weather profiles.

Chapter 4 presented the design-point and off-design performance, the procedure of exhaust emissions indexes calibration with presentation of the off-design exhaust emission rates and the procedure of setting the design point hot section rotor blade life to failure with presentation of the off-design hot section rotor blade temperature, for each of the five 25MW simulated marine gas turbines that were modelled in "*Poseidon*". The effects of gas turbine component degradation were not included in this research. The simulated marine gas turbines all featuring a power turbine were:

- Simple cycle (2-shaft)
- Twin mode intercooled (3-shaft simple cycle at low-power mode and 4-shaft intercooled cycle at high power mode)
- Intercooled cycle (3-shaft)
- Recuperated cycle (2-shaft)
- Intercooled/recuperated cycle (3-shaft)

The simple cycle gas turbine was the reference cycle in this research and was simulated as combined version of the performance characteristics of the two offered marine versions of the General Electric LM2500. The intercooled and the recuperated gas turbines are fictional designs, the intercooled/recuperated was partly based on basic characteristics of the Rolls-Royce WR21, and the twin mode intercooled cycle is a novel proposal that its configuration is primarily based on its initial preliminary performance investigation. The simulations were performed assuming distillate fuel. The technology level of the gas turbine components and the main cycle design

parameter (*TET*) are identical for all simulated gas turbines, within the boundaries of the capabilities of the gas turbine industry at the time of the gas turbine models preparation. The above condition was applied in the calibration of the emissions indexes (EI_{NOx}, EI_{CO} and EI_{UHC}), of the conventional and *DLE* combustor of each of the simulated gas turbines, which were set according to design-point values of existing designs (the exhaust emissions indexes of the *ICR* gas turbine were also calibrated for natural gas fuel, assuming a LCV equal with distillate fuel). Consequently it was discovered that the twin mode intrecooled cycle gas turbine- because of its high overall compression ratios of the high power mode will need a *DLE* combustor of higher technology in order to obtain a design-point NO_x emissions index equal with the other four single-mode gas turbines when operating in the high power mode. The design point hot section rotor blade life to failure of the twin mode intercooled gas turbine was calibrated taking as reference again the core gas turbine and when the gas turbine switches to high power mode the intercooler outlet temperature increases by approximately 9 K (ISA conditions) the hot section rotor blade life to failure drops by approximately 23%.

Chapter 5 presented the dataset supplied to "*Poseidon*" including the three case studies of this research. Each of the case studies was defined by a different type of marine vessel. The marine vessels were:

- Destroyer
- RoPax fast ferry
- LNG Carrier (Q-max)

All three marine vessels shared the same power plant configuration and output power rating (50MW twin main prime mover), ambient conditions, weather profiles, hull fouling levels, number of scheduled journey for every installed type of power plant, scheduled journey duration and the maximum allowable *TET* was common for all gas turbine prime movers, irrelevantly of the type of marine vessel. The operational profile of each of the vessels as also the service load (which remained constant during every journey) was adjusted in accordance with the type of the vessel and the flexibility that an *IFEP* system can provide. The Destroyer and the RoPax fast ferry acted as platforms for all five marine gas turbine power plants and every set (2 weather profiles times 5 hull fouling levels, a hull fouling level represented a year and

after 5 years of operation the hull was considered as cleaned) scheduled journeys was performed two times, one with the power plant equipped with conventional combustors and one equipped with *DLE* combustors. Due to time constrains, the LNG carrier acted as a platform on the intercooled/recuperated gas turbine power plant only (natural gas fuel), but both combustor types were simulated. All dataset was based in the maximum degree possible on realistic background information, but an extensive trial and error procedure was undertaken to calibrate the design-point required brake power by each of the three marine vessels according to design and hull form parameters that describe their type, due to lack of published information.

Chapter 6 presented the economic and risk dataset supplied to the life cycle costs model including the scenarios that completed each of the case studies, assuming a futuristic maritime policy that NO_x, CO, CO_2 and UHC emissions are taxed per unit mass in the open-sea. The scenarios were directly connected with the estimated minimum and maximum percentage difference of cost from the reference prime mover (reference scenario), $PD_{0\text{-}min}$ and $PD_{0\text{-}max}$ of the advanced cycle gas turbine prime movers in comparison with the reference one. It was assumed that the probable purchase cost of either the *INT* or the *REQ* gas turbines cannot be higher than the *ICR's* as an indicated purchase cost for a Rolls-Royce WR-21 falls within the PD_0 range of scenario 2. The scenarios correspond to an economic and risk analysis as if the advanced cycle gas turbine prime movers are in pre-design stage. The scenarios were:

1. $PD_{0\text{-}min}$ and $PD_{0\text{-}max}$ at 20% and 65% respectively
2. $PD_{0\text{-}min}$ and $PD_{0\text{-}max}$ at 65% and 110% respectively
3. $PD_{0\text{-}min}$ and $PD_{0\text{-}max}$ at 110% and 155% respectively (only *TMI* prime mover)

Each scenario included two cases: one assuming conventional combustion and one assuming *DLE* combustion. In the case of *DLE* combustion the estimated minimum and maximum percentage difference of cost due to different technology components was assumed as:

1. $PD_{1\text{-}min}$ and $PD_{1\text{-}max}$ at 10% and 30% respectively

Additionally the economic variables that adopted the risk element were: interest rate, power plant availability, fuel cost and exhaust emissions cost. The economic variables that did not adopt the risk element were: insurance cost, maintenance labour rate and

spare parts factor. All dataset was based in the maximum degree possible on realistic background information.

Chapter 7 presented the "*Poseidon*" results for each of the case studies that were supplied as the technical and environmental dataset to the life cycle costs model. The number of annual journeys of each of the three marine vessels was also defined which completed the dataset of the life cycle costs model. The economic and risk analysis results were presented and discussed. A general overview was discussed on the gas turbine off-design operation including the effects of intercooling. The following conclusions are products of the obtained normal distributions of the net present cost of each of the power plants equipped with conventional or *DLE* combustors regarding each of the three marine vessels.

Destroyer: According to **scenario 1** all advanced cycle gas turbine power plants showed to be more economical options in comparison with the reference power plant, with the intercooled power plant to be the least favourable option. The first three choices to power the Destroyer are:

1. Intercooled/recuperated power plant with *DLE* combustors
2. Intercooled/recuperated power plant with conventional combustors
3. Twin mode intercooled power plant with *DLE* combustors

According to **scenario 2** the only power plant that can be regarded as a more economical option than the reference power plant is the intercooled/recuperated. The first three choices to power the Destroyer are:

1. Intercooled/recuperated power plant with conventional combustors
2. Intercooled/recuperated power plant with *DLE* combustors
3. Reference power plant with *DLE* combustors

RoPax fast ferry: According to **scenario 1**, again, all advanced cycle gas turbine power plants showed to be more economical options in comparison with the reference power plant, with the intercooled power plant to be the least favourable option. The first three choices to power the RoPax fast ferry are:

1. Twin mode intercooled power plant with *DLE* combustors
2. Intercooled/recuperated power plant with *DLE* combustors
3. Intercooled/recuperated power plant with conventional combustors

According to **scenario 2** the gas turbine power plants that are considered as noticeably more economical options than the reference power plant are:

1. Twin mode intercooled power plant with *DLE* combustors
2. Intercooled/recuperated power plant with *DLE* combustors
3. Intercooled/recuperated power plant with conventional combustors
4. Recuperated power plant with *DLE* combustors

Both Destroyer and RoPax fast ferry: **Scenario 3** results showed that the twin mode intercooled power plant cannot be considered as a more economically profitable option to the reference power plant, installed either on the Destroyer and the RoPax fast ferry.

LNG carrier: The case study showed that according to the economic scenarios of this research, the choice of *DLE* combustors on the intercooled/recuperated power plant using natural gas as fuel to power the LNG carrier in the open-sea has an environmental value, and cannot be considered as a choice of higher economic feasibility.

8.2 Recommendations

8.2.1 Project case studies

The following recommendations were created during the preparation and at the end of completion of the three case studies, assuming no modifications in the models of the *TERA* method (see section 8.2.2):

- The simulation and modelling of a marine version of a 25MW air bottoming cycle (*ABC*) gas turbine system is recommended. An attempt was made to implement the above recommendation but it was not completed due to time restrains.
- Further investigation can be undertaken, in connection with the intercooled marine gas turbine. The adoption of higher possible compression pressure ratios (at the same component performance parameters and turbine entry temperature) which can result in higher design-point thermal efficiency may be considered.
- Further investigation can be undertaken in connection with the recuperated marine gas turbine. The gas turbine can be optimised for operation at part-load performance.

- The twin mode intercooled cycle can be simulated and modelled optimised in the high-power mode using distillate fuel. The recommendation concerns the design-point hot section rotor blade to failure, and the exhaust emission indexes when the gas turbine is equipped with a *DLE* combustor.
- The incorporation of at least two air ambient temperature profiles in the case studies is advisable. One to describe average winter temperatures and one to describe average summer temperatures.
- The LNG carrier case study should include all five power plants (may include the air bottoming cycle), the ballast and laden draft should be taken into account as also the use of the main prime mover(s) of the power plant during cargo loading/unloading. Marine gas turbine dual fuel capability can also be considered as also the adjustment of the low calorific value of natural gas used as fuel, to higher than the distillate fuel.
- Both the Destroyer and RoPax fast ferry case studies can be modified, to include the use of natural gas as fuel instead of distillate fuel.
- The operational profile of the Destroyer can be enriched with additional cruise and/or boost speeds.
- A case study that is defined by a cruise marine vessel can be investigated.

8.2.2 *TERA* method

The development of the models of the current *TERA* method is currently in its initial stages and limitations that have been identified during the research, but could not be eliminated due to constrains in available time, are expressed as recommendations for further work including suggested references:

- The effects of gas turbine component performance degradation can be included in the gas turbine performance and exhaust emissions models.
- The effects of bending stress from gas momentum and pressure on the air foil can be modelled in the hot section rotor blade creep life model. The modelling of the effects of low-cycle fatigue on the hot section rotor is also recommended [1].
- "*Poseidon*" can be enriched with the capability of simulating multi-hull marine vessels (i.e. catamarans, small waterplane area twin hull vessels etc) [2]. Planning marine vessels can also be considered either mono-hull or multi-

hull. This will require propulsors more suitable for high speeds than the Wageningen B-series propellers, and initially two suggestions can be considered: Gawn-Burill series propellers [3] and waterjets [4] [5]. The capability of simulating more than two propulsors may also be considered [4], as also propeller cavitation effects and partial submergence (i.e. heavy sea) [5]. In the case that marine vessel port manoeuvring is decided to be included in any case studies in the future the propeller model will require the selected propulsor(s) to operate in all four-quadrants, as also the modelling of secondary low-power prime movers may be required, including the effects of shallow-water in the hydrodynamic resistance of a marine vessel.

- The applicability range of the current sea-wave resistance method should be further examined. The sea-wave resistance module can be enriched with a method that considers marine vessel motion responses to regular waves, and be able to have the opposite effects of a head direction towards the vessel's bow [6].
- The life cycle costs model can be modified to accommodate more than two weather profiles in order to provide a more realistic approach to the simulation of weather phenomena though every case study will require a greater amount of computational time. Insurance cost, maintenance labour rate and spare parts factor can be easily modified to incorporate the risk element. The capital cost of non-existing or novel gas turbine prime movers can be modified to be calculated according to suitable cost functions for the gas turbine components [7].
- "*Poseidon*" and the life cycle costs model if integrated can save a considerable amount of time for the completion of a case study. More time can be saved if results are represented on tables and graphs derived directly from MATLAB.

8.2.2.1 Recommended references

1. Suria, V.O., "A Flexible Lifing Model for Gas Turbines: Creep and Low Cycle Fatigue Approach", MSc Thesis, Cranfield University, Academic Year 2005-2006.

2. Zouridakis, F., "A Preliminary Design Tool for Resistance and Power Prediction of Catamaran Vessels", MSc Thesis, Massachusetts Institute of Technology, Academic Year 2004-2005.

3. Carlton, J., **"***Marine Propellers and Propulsion*", Butterworth and Heinemann, ISBN No. 0-75068150-0, Chapter 6, pp 108-109, 2007.

4. Holtrop, J., “Extrapolation of Propulsion Tests for Ships with Appendages and Complex Propulsors”, Marine Technology, Vol. 38, No. 3, pp 145-157, July 2001.

5. Hugel, M.A., *“An Evaluation of Propulsors for Several Navy Ships”*, MSc Thesis, Massachusetts Institute of Technology, Academic Year 1992-1993.

6. “*Principles of Naval Architecture, Motion in Waves and Controllability*”, Society of Naval Architects and Marine Engineers, ISBN No. 0-939773-02-3, Vol. 3, pp 41-83.

7. Massardo A.F., Scialò, M., D., *“Thermoeconomic Analysis of Gas Turbine Based Cycles”*, Journal of Engineering for Gas Turbines and Power, Vol. 122, pp 664-671, October 2000.

APPENDICES

APPENDIX A

Contains:

Appendix A.1

```
TURBOMATCH SCHEME - Windows NT version (October 1999)

 LIMITS:100 Codewords, 800 Brick Data Items, 50 Station Vector
 15 BD Items printable by any call of:-
 OUTPUT, OUTPBD, OUTPSV, PLOTIT, PLOTBD or PLOTSV

  Input "Program" follows

 !25MW SIMPLE CYCLE 2-SHAFT MARINE GAS TURBINE


 OD SI KE CT FP
  -1
  -1
 INTAKE  S1-2         D1-4          R100
 COMPRE  S2-3       D5-10          R101    V5  V6
 PREMAS  S3,13,4   D11-14
 BURNER  S4-5        D15-17         R102
 DUCTER  S5-6        D18-21
 MIXEES  S6,13,7
 TURBIN  S7-8        D22-29,101              V23
 TURBIN  S8-9        D30-38                  V30 V31
 DUCTER  S9-10       D39-42
 NOZCON  S10-11,1 D43             R107
 PERFOR  S1,0,0    D30,44-46,107,100,102,0,0,0,0,0,0
 CODEND

 DATA ITEMS
 !INTAKE
 1 0.0         !INTAKE ALTITUDE
 2 0.0         !ISA DEVIATION
 3 0.0         !MACH NO
 4 0.9951     !PRESSURE RECOVERY
 !COMPRESSOR
 5 0.85        !SURGE MARGIN (DEFAULT=0.85)
 6 0.999       !SPOOL SPEED (DEFAULT=1.0)
 7 18.0        !PRESSURE RATIO
 8 0.90        !ISENTROPIC EFFICIENCY
 9 0.0         !ERROR SELECTION
 10 2.0        !COMPRESSOR MAP NUMBER
 !TURBINE COOLING
 11 0.1        !BLEED AIR
 12 0.0        !FLOW LOSS
 13 1.0        !PRESSURE RECOVERY
 14 0.00       !PRESSURE LOSS
 !BURNER
 15 0.065      !PRESSURE LOSS
 16 0.998     !COMBUSTION EFFICIENCY
 17 -1.0       !FUEL FLOW
 !DUCTER
 18 0.0        !NO INTERCOOLING
 19 0.02       !PRESSURE LOSS
 20 0.0        !EFFICIENCY
 21 0.0        !LIMITING VALUE OF FUEL FLOW
 !COMPRESSOR TURBINE
 22 0.0        !AUXILIARY POWER REQUIRED
 23 0.81       !NON-DIMENSIONAL MASSFLOW (DEFAULT=0.8)
 24 0.6        !NON-DIMENSIONAL SPEED (DEFAULT=0.6)
 25 0.87       !ISENTROPIC EFFICIENCY
 26 -1.0       !RELATIVE ROTATIONAL
 27 1.0        !COMPRESSOR NUMBER
 28 4.0        !TURBINE MAP NUMBER
 29 -1.0       !POWER LAW INDEX
 !POWER TURBINE
 30 25000000.00 ! AUXILIARY POWER REQUIRED
 31 0.89           !NON-DIMENSIONAL MASSFLOW (DEFAULT=0.8)
 32 0.68           !NON-DIMENSIONAL SPEED (DEFAULT=0.6)
 33 0.89           !ISENTROPIC EFFICIENCY
 34 1.0            !RELATIVE ROTATIONAL
 35 0.0            !COMPRESSOR NUMBER
 36 5.0            !TURBINE MAP NUMBER
 37 1000.0        !POWER LOW INDEX
 38 -1.0           !COMPRESSOR WORK
```

Appendix A.1

```
!DUCTER
39 0.0       !NO INTERCOOLING
40 0.026     !PRESSURE LOSS
41 0.0       !EFFICIENCY
42 0.0       !LIMITING VALUE OF FUEL FLOW
!CONVERGENT NOZZLE
43 -1.0      !AIR FIXED
!PERFOR
44 1.0       !PROPELLER EFFICIENCY
45 0.0       !SCALING INDEX
46 0.0       !REQUIRED THRUST
-1
1 2 70.86      !INLET MASS FLOW
5 6 1509.5     !COMBUSTION OUTLET TEMPERATURE
-1
                                Time Now 01:51:50

************************************************


            The Units for this Run are as follows:-

 Temperature = K   Pressure = Atmospheres   Length = metres

 Area = sq metres  Mass Flow = kg/sec       Velocity = metres/sec

 Force = Newtons   s.f.c.(Thrust) =  mg/N sec   s.f.c.(Power) = mug/J

 Sp. Thrust =    N/kg/sec     Power =   Watts
1

     ***** DESIGN POINT ENGINE CALCULATIONS *****



***** AMBIENT AND INLET PARAMETERS *****
Alt. =      0.0      I.S.A. Dev. =    0.000       Mach No. =  0.00
Etar = 0.9951        Momentum Drag =      0.00

***** COMPRESSOR  1 PARAMETERS *****
PRSF =  0.27824E+02    ETASF =  0.10477E+01    WASF =  0.24022E+00
Z = 0.85000            PR =  18.000            ETA = 0.90000
PCN =   0.9990         CN = 0.99900            COMWK =  0.29126E+08

***** COMBUSTION CHAMBER PARAMETERS *****
ETASF =  0.99800E+00
ETA = 0.99800          DLP = 1.2538            WFB =   1.5449

***** TURBINE  1 PARAMETERS *****
CNSF =  0.78134E+02    ETASF =  0.10226E+01    TFSF =  0.24794E+01
DHSF =  0.15941E+05
TF =  416.674          ETA = 0.87000           CN =  2.060
AUXWK =  0.00000E+00

***** TURBINE  2 PARAMETERS *****
CNSF =  0.78582E-02    ETASF =  0.10097E+01    TFSF =  0.44658E+00
DHSF =  0.27915E+05
TF =  242.033          ETA = 0.89000           CN =  2.360
AUXWK =  0.25000E+08

Additional Free Turbine Parameters:-
Speed = 100.0%         Power =  0.25000E+08

***** CONVERGENT NOZZLE  1 PARAMETERS *****
NCOSF =  0.10000E+01
Area =  1.6188         Exit Velocity =  102.57  Gross Thrust =   7213.98
Nozzle Coeff. =  0.97136E+00



Scale Factor on above Mass Flows, Areas, Thrusts & Powers =     1.0000
```

Appendix A.1

Station	F.A.R.	Mass Flow	Pstatic	Ptotal	Tstatic	Ttotal	Vel	Area
1	0.00000	70.860	1.00000	1.00000	288.15	288.15	0.0	******
2	0.00000	70.860	******	0.99510	******	288.15	******	******
3	0.00000	70.860	******	17.91181	******	687.06	******	******
4	0.00000	63.774	******	17.91181	******	687.06	******	******
5	0.02422	65.319	******	16.65799	******	1509.50	******	******
6	0.02422	65.319	******	16.32483	******	1509.50	******	******
7	0.02180	72.405	******	16.32483	******	1435.74	******	******
8	0.02180	72.405	******	4.44838	******	1108.71	******	******
9	0.02180	72.405	******	1.04735	******	814.26	******	******
10	0.02180	72.405	******	1.02011	******	814.26	******	******
11	0.02180	72.405	1.00000	1.02011	809.64	814.26	102.6	1.6188
12	0.00000	0.000	******	0.00000	******	0.00	******	******
13	0.00000	7.086	******	17.91181	******	687.06	******	******

Shaft Power = 25000000.00
Net Thrust = 7213.98
Equiv. Power = 25465136.00
Fuel Flow = 1.5449
S.F.C. = 61.7963
E.S.F.C. = 60.6675
Sp. Sh. Power = 352808.38
Sp. Eq. Power = 359372.50
Sh. Th. Effy. = 0.3752
Time Now 01:51:50

Appendix A.1

```
TURBOMATCH SCHEME - Windows NT version (October 1999)

 LIMITS:100 Codewords, 800 Brick Data Items, 50 Station Vector
 15 BD Items printable by any call of:-
 OUTPUT, OUTPBD, OUTPSV, PLOTIT, PLOTBD or PLOTSV

  Input "Program" follows

 !5MW SIMPLE CYCLE 3-SHAFT MARINE GAS TURBINE AND CORE FOR THE 25MW NOVEL INTERCOOOLED
CYCLE


 OD SI KE CT FP
  -1
  -1
 INTAKE S1-2            D1-4          R100
 COMPRE S2-3          D5-11         R101    V5 V6
 DUCTER S3-4          D12-15        R102
 COMPRE S4-5          D16-22        R103   V16 V17
 PREMAS S5,6,16       D23-26
 PREMAS S16,17,18     D27-30
 BURNER S6-7          D31-33        R104
 MIXEES S17,7,8
 TURBIN S8-9          D34-41,103            V35
 DUCTER S9-10         D42-45
 MIXEES S10,18,11
 TURBIN S11-12        D46-53,101            V47
 TURBIN S12-13        D54-61                V54 V55
 DUCTER S13-14        D62-65
 NOZCON S14-15,1      D66           R105
 PERFOR S1,0,0        D54,67-69,105,100,104,0,0,0,0,0,0
 CODEND



 DATA ITEMS
 !INTAKE
 1 0.0          !INTAKE ALTITUDE
 2 0.0          !ISA DEVIATION
 3 0.0          !MACH NO
 4 0.9951       !PRESSURE RECOVERY
 !LP COMPRESSOR
 5 0.85         !SURGE MARGIN (DEFAULT=0.85)
 6 1.0          !SPOOL SPEED (DEFAULT=1.0)
 7 4.0          !PRESSURE RATIO
 8 0.89         !ISENTROPIC EFFICIENCY
 9 0.0          !ERROR SELECTION
 10 4.0         !COMPRESSOR MAP NUMBER
 11 0.0         !ANGLE
 !DUCTER
 12 0.0         !NO INTERCOOLING
 13 0.0         !PRESSURE LOSS
 14 0.0         !EFFICIENCY
 15 0.0         !LIMITING VALUE OF FUEL FLOW
 !HP COMPRESSOR
 16 0.85        !SURGE MARGIN (DEFAULT=0.85)
 17 1.0         !SPOOL SPEED (DEFAULT=1.0)
 18 5.6         !PRESSURE RATIO
 19 0.89        !ISENTROPIC EFFICIENCY
 20 1.0         !ERROR SELECTION
 21 4.0         !COMPRESSOR MAP NUMBER
 22 0.0         !ANGLE
 !TURBINE COOLING 1
 23 0.90        !BLEED AIR
 24 0.0         !FLOW LOSS
 25 1.0         !PRESSURE RECOVERY
 26 0.0         !PRESSURE LOSS
 !TURBINE COOLING 2
 27 0.70        !BLEED AIR
 28 0.0         !FLOW LOSS
 29 1.0         !PRESSURE RECOVERY
 30 0.0         !PRESSURE LOSS
 !BURNER
```

```
31 0.065     !PRESSURE LOSS
32 0.998     !COMBUSTION EFFICIENCY
33 -1.0      !FUEL FLOW
!HP TURBINE
34 0.0       !AUXILIARY POWER REQUIRED
35 0.8       !NON-DIMENSIONAL MASSFLOW (DEFAULT=0.8)
36 0.6       !NON-DIMENSIONAL SPEED (DEFAULT=0.6)
37 0.87      !ISENTROPIC EFFICIENCY
38 -1.0      !COMPRESSOR TURBINE
39 2.0       !COMPRESSOR NUMBER
40 1.0       !TURBINE MAP NUMBER
41 -1.0      !POWER LAW INDEX
!DUCTER
42 0.0       !NO INTERCOOLING
43 0.015     !PRESSURE LOSS
44 0.0       !EFFICIENCY
45 0.0       !LIMITING VALUE OF FUEL FLOW
!IP TURBINE
46 0.0       !AUXILIARY POWER REQUIRED
47 0.8       !NON-DIMENSIONAL MASSFLOW (DEFAULT=0.8)
48 0.6       !NON-DIMENSIONAL SPEED (DEFAULT=0.6)
49 0.87      !ISENTROPIC EFFICIENCY
50 -1.0      !COMPRESSOR TURBINE
51 1.0       !COMPRESSOR NUMBER
52 3.0       !TURBINE MAP NUMBER
53 -1.0      !POWER LAW INDEX
!POWER TURBINE
54 5000000.00  !AUXILIARY POWER REQUIRED
55 -1.0          !NON-DIMENSIONAL MASS FLOW (DEFAULT=0.8)
56 0.599         !NON-DIMENSIONAL SPEED (DEFAULT=0.6)
57 0.89          !ISENTROPIC EFFICIENCY
58 1.0           !RELATIVE ROTATIONAL
59 0.0           !COMPRESSOR NUMBER
60 5.0           !TURBINE MAP NUMBER
61 1000.0        !POWER LAW INDEX
!DUCTER
62 0.0      !NO INTERCOOLING
63 0.02     !PRESSURE LOSS
64 0.0      !EFFICIENCY
65 0.0      !LIMITING VALUE OF FUEL FLOW
!CONVERGENT NOZZLE
66 -1.0     !AIR FIXED
!PERFORMANCE
67 1.00     !PROPELLER EFFICIENCY
68 0.0      !SCALING INDEX
69 0.0      !REQUIRED THRUST
-1
1 2  14.9     !INLET MASS FLOW
7 6  1509.5   !COMBUSTION OUTLET TEMPERATURE
-1
                                Time Now 01:57:01

************************************************


            The Units for this Run are as follows:-

 Temperature = K   Pressure = Atmospheres   Length = metres

 Area = sq metres  Mass Flow = kg/sec       Velocity = metres/sec

 Force = Newtons   s.f.c.(Thrust) =  mg/N sec   s.f.c.(Power) = mug/J

 Sp. Thrust =    N/kg/sec     Power =   Watts
1

     ***** DESIGN POINT ENGINE CALCULATIONS *****



***** AMBIENT AND INLET PARAMETERS *****
Alt. =      0.0      I.S.A. Dev. =    0.000       Mach No. =  0.00
Etar = 0.9951        Momentum Drag =      0.00

***** COMPRESSOR  1 PARAMETERS *****
```

PRSF = 0.29412E+01 ETASF = 0.10723E+01 WASF = 0.84099E-01
Z = 0.85000 PR = 4.000 ETA = 0.89000
PCN = 1.0000 CN = 1.00000 COMWK = 0.23542E+07

***** COMPRESSOR 2 PARAMETERS *****
PRSF = 0.45098E+01 ETASF = 0.10723E+01 WASF = 0.26116E-01
Z = 0.85000 PR = 5.600 ETA = 0.89000
PCN = 1.0000 CN = 1.00000 COMWK = 0.47176E+07

***** COMBUSTION CHAMBER PARAMETERS *****
ETASF = 0.99800E+00
ETA = 0.99800 DLP = 1.4489 WFB = 0.3031

***** TURBINE 1 PARAMETERS *****
CNSF = 0.10698E+03 ETASF = 0.10132E+01 TFSF = 0.14847E+02
DHSF = 0.61712E+04
TF = 401.640 ETA = 0.87000 CN = 2.800
AUXWK = 0.00000E+00

***** TURBINE 2 PARAMETERS *****
CNSF = 0.94820E+02 ETASF = 0.97041E+00 TFSF = 0.63315E+01
DHSF = 0.38586E+04
TF = 430.924 ETA = 0.87000 CN = 2.750
AUXWK = 0.00000E+00

***** TURBINE 3 PARAMETERS *****
CNSF = 0.71568E-02 ETASF = 0.10608E+01 TFSF = 0.19579E+01
DHSF = 0.54556E+05
TF = 219.627 ETA = 0.89000 CN = 2.198
AUXWK = 0.50000E+07

Additional Free Turbine Parameters:-
Speed = 100.0% Power = 0.50000E+07

***** CONVERGENT NOZZLE 1 PARAMETERS *****
NCOSF = 0.10000E+01
Area = 0.3415 Exit Velocity = 97.37 Gross Thrust = 1437.83
Nozzle Coeff. = 0.97134E+00

Scale Factor on above Mass Flows, Areas, Thrusts & Powers = 1.0000

Station	F.A.R.	Mass Flow	Pstatic	Ptotal	Tstatic	Ttotal	Vel	Area
1	0.00000	14.900	1.00000	1.00000	288.15	288.15	0.0	******
2	0.00000	14.900	******	0.99510	******	288.15	******	******
3	0.00000	14.900	******	3.98040	******	444.61	******	******
4	0.00000	14.900	******	3.98040	******	444.61	******	******
5	0.00000	14.900	******	22.29025	******	746.00	******	******
6	0.00000	13.410	******	22.29025	******	746.00	******	******
7	0.02260	13.713	******	20.84139	******	1509.50	******	******
8	0.02097	14.756	******	20.84139	******	1459.78	******	******
9	0.02097	14.756	******	7.81936	******	1201.37	******	******
10	0.02097	14.756	******	7.70207	******	1201.37	******	******
11	0.02034	15.203	******	7.70207	******	1188.88	******	******
12	0.02034	15.203	******	4.41293	******	1060.19	******	******
13	0.02034	15.203	******	1.04000	******	776.30	******	******
14	0.02034	15.203	******	1.01920	******	776.30	******	******
15	0.02034	15.203	1.00000	1.01920	772.09	776.30	97.4	0.3415
16	0.00000	1.490	******	22.29025	******	746.00	******	******
17	0.00000	1.043	******	22.29025	******	746.00	******	******
18	0.00000	0.447	******	22.29025	******	746.00	******	******

Shaft Power = 5000000.00
Net Thrust = 1437.83
Equiv. Power = 5092707.00
Fuel Flow = 0.3031
S.F.C. = 60.6133
E.S.F.C. = 59.5099
Sp. Sh. Power = 335570.47
Sp. Eq. Power = 341792.41

```
Sh. Th. Effy. =   0.3826
        Time Now 01:57:01
TURBOMATCH SCHEME - Windows NT version (October 1999)

LIMITS:100 Codewords, 800 Brick Data Items, 50 Station Vector
15 BD Items printable by any call of:-
OUTPUT, OUTPBD, OUTPSV, PLOTIT, PLOTBD or PLOTSV

 Input "Program" follows

!25MW 4-SHAFT NOVEL INTERCOOLED MARINE GAS TURBINE SIMULATION (5MW CORE ENGINE)


OD SI KE CT FP
 -1
 -1
INTAKE  S1-2          D1-4           R300
COMPRE  S2-3        D5-11          R301   V5 V6
DUCTER  S3-4        D12-15          R306
COMPRE  S4-5        D16-22         R302   V16 V17
DUCTER  S5-6        D23-26
COMPRE  S6-7        D27-33         R303   V27 V28
PREMAS  S7,8,20     D34-37
PREMAS  S20,21,22 D38-41
BURNER  S8-9         D42-44         R305
MIXEES  S21,9,10
TURBIN  S10-11       D45-52,303            V46
DUCTER  S11-12      D53-56
MIXEES  S12,22,13
TURBIN  S13-14       D57-64,302            V58
TURBIN  S14-15       D65-72                V65 V66
TURBIN  S15-16       D73-80,301            V74
DUCTER  S16-17     D81-84
NOZCON  S17-18,1 D85              R304
PERFOR  S1,0,0     D65,86-88,304,300,305,0,0,0,0,0,306
CODEND

DATA ITEMS
!INTAKE
1 0.0         !INTAKE ALTITUDE
2 0.0         !ISA DEVIATION
3 0.0         !MACH NUMBER
4 0.9951     !PRESSURE RECOVERY
!LP COMPRESSOR
5 0.8696      !SURGE MARGIN (DEFAULT=0.85)
6 0.997       !SPOOL SPEED (DEFAULT=1.0)
7 4.41        !PRESSURE RATIO
8 0.89        !ISENTROPIC EFFICIENCY
9 0.0         !ERROR SELECTION
10 2.0        !COMPRESSOR MAP NUMBER
11 0.0        !ANGLE
!INTERCOOLER
12 2.0         !2: INTERCOOLER
13 0.01       !PRESSURE LOSS
14 0.95       !EFFECTIVENESS
15 0.0        !LIMITING VALUE OF FUEL FLOW
!IP COMPRESSOR
16 0.86       !SURGE MARGIN (DEFAULT=0.85)
17 0.999      !SPOOL SPEED (DEFAULT=1.0)
18 3.83       !PRESSURE RATIO
19 0.89       !ISENTROPIC EFFICIENCY
20 0.0        !ERROR SELECTION
21 4.0        !COMPRESSOR MAP NUMBER
22 0.0        !ANGLE
!DUCTER
23 0.0       !NO INTERCOOLING
24 0.0       !PRESSURE LOSS
25 0.0       !EFFICIENCY
26 0.0       !LIMITING VALUE OF FUEL FLOW
!HP COMPRESSOR
27 0.859     !SURGE MARGIN (DEFAULT=0.85)
28 1.0       !SPOOL SPEED (DEFAULT=1.0)
29 5.477     !PRESSURE RATIO
30 0.89      !ISENTROPIC EFFICIENCY
31 0.0       !ERROR SELECTION
```

```
32 4.0        !COMPRESSOR MAP NUMBER
33 0.0        !ANGLE
!TURBINE COOLING 1
34 0.90       !BLEED AIR
35 0.0        !FLOW LOSS
36 1.0        !PRESSURE RECOVERY
37 0.0        !PRESSURE LOSS
!TURBINE COOLING 2
38 0.70       !BLEED AIR
39 0.0        !FLOW LOSS
40 1.0        !PRESSURE RECOVERY
41 0.0        !PRESSURE LOSS
!BURNER
42 0.065      !PRESSURE LOSS
43 0.998      !EFFICIENCY
44  -1.0      !FUEL FLOW
!HP TURBINE
45 0.0        !AUXILIARY POWER REQUIRED
46 0.889      !NON-DIMENSIONAL MASSFLOW (DEFAULT=0.8)
47 0.664      !NON-DIMENSIONAL SPEED (DEFAULT=0.6)
48 0.87       !ISENTROPIC EFFICIENCY
49 -1.0       !COMPRESSOR TURBINE
50 3.0        !COMPRESSOR NUMBER
51 5.0        !TURBINE MAP NUMBER
52 -1.0       !POWER LAW INDEX
!DUCTER
53 0.0        !NO INTERCOOLING
54 0.0        !PRESSURE LOSS
55 0.0        !COMBUSTION EFFICIENCY
56 0.0        !LIMITING VALUE OF FUEL FLOW
! IP TURBINE
57 0.0        !AUXILIARY POWER REQUIRED
58 0.73       !NON-DIMENSIONAL MASS FLOW (DEFAULT=0.8)
59 0.43       !NON-DIMENSIONAL SPEED (DEFAULT=0.6)
60 0.87       !ISENTROPIC EFFICIENCY
61 -1.0       !COMPRESSOR TURBINE
62 2.0        !COMPRESSOR NUMBER
63 5.0        !TURBINE MAP NUMBER
64 -1.0       !POWER LAW INDEX
!POWER TURBINE
65 25000000.00 !AUXILIARY POWER REQUIRED
66 0.703          !NON-DIMENSIONAL MASS FLOW (DEFAULT=0.8)
67 0.64           !NON-DIMENSIONAL SPEED (DEFAULT=0.6)
68 0.89           !ISENTROPIC EFFICIENCY
69 1.0            !RELATIVE ROTATIONAL
70 0.0            !COMPRESSOR NUMBER
71 5.0            !TURBINE MAP NUMBER
72 1000.0         !POWER LAW INDEX
!LP TURBINE
73 0.0        !AUXILIARY POWER REQUIRED
74 0.652      !NON-DIMENSIONAL MASS FLOW (DEFAULT=0.8)
75 0.678      !NON-DIMENSIONAL SPEED (DEFAULT=0.6)
76 0.89       !ISENTROPIC EFFICIENCY
77 -1.0       !RELATIVE ROTATIONAL SPEED
78 1.0        !COMPRESSOR NUMBER
79 5.0        !TURBINE MAP NUMBER
80 1000.0  !POWER LAW INDEX
!DUCTER
81 0.0        !NO INTERCOOLING
82 0.015      !PRESSURE LOSS
83 0.0        !COMBUSTION EFFIECINCY
84 0.0        !LIMITING VALUE OF FUEL FLOW
!CONVERGENT NOZZLE
85 -1.0       !AIR FIXED
!PERFORMANCE
86 1.0        !PROPELLER EFFICIENCY
87 0.0        !SCALING INDEX
88 0.0        !REQUIRED THRUST
-1
1 2  61.71     !INLET MASS FLOW
4 6  298.0     !INTERCOOLER OUTLET TEMPERATURE
9 6  1509.5    !COMBUSTION OUTLET TEMPERATURE
-1
```

Time Now 01:52:45

Appendix A.1

```
*********************************************

          The Units for this Run are as follows:-

 Temperature = K   Pressure = Atmospheres   Length = metres

 Area = sq metres  Mass Flow = kg/sec       Velocity = metres/sec

 Force = Newtons   s.f.c.(Thrust) =  mg/N sec   s.f.c.(Power) = mug/J

 Sp. Thrust =    N/kg/sec     Power =   Watts
1

    ***** DESIGN POINT ENGINE CALCULATIONS *****


***** AMBIENT AND INLET PARAMETERS *****
Alt. =      0.0      I.S.A. Dev. =    0.000       Mach No. =  0.00
Etar = 0.9951        Momentum Drag =      0.00

***** COMPRESSOR  1 PARAMETERS *****
PRSF =  0.54737E+01    ETASF =  0.10356E+01    WASF =  0.21087E+00
Z = 0.86960           PR =   4.410           ETA = 0.89000
PCN =   0.9970        CN = 0.99700           COMWK =  0.10592E+08

***** DUCT/AFTER BURNING 1 PARAMETERS *****
ETA =  0.9000         DLP = 0.0439           WFB =   0.0000

DUCTER IS USED AS AN INTERCOOLER!
****INTERCOOLER****HEAT REMOVED:11200.55      KWATTS

***** COMPRESSOR  2 PARAMETERS *****
PRSF =  0.27468E+01    ETASF =  0.10720E+01    WASF =  0.81456E-01
Z = 0.86000           PR =   3.830           ETA = 0.89000
PCN =   0.9990        CN = 0.99900           COMWK =  0.97020E+07

***** COMPRESSOR  3 PARAMETERS *****
PRSF =  0.43432E+01    ETASF =  0.10723E+01    WASF =  0.26197E-01
Z = 0.85900           PR =   5.477           ETA = 0.89000
PCN =   1.0000        CN = 1.00000           COMWK =  0.19599E+08

***** COMBUSTION CHAMBER PARAMETERS *****
ETASF =  0.99800E+00
ETA = 0.99800         DLP = 5.9237           WFB =   1.2409

***** TURBINE  1 PARAMETERS *****
CNSF =  0.88962E+02    ETASF =  0.98735E+00    TFSF =  0.88239E+01
DHSF =  0.19709E+05
TF =  241.784         ETA = 0.87000          CN =  2.328
AUXWK =  0.00000E+00

***** TURBINE  2 PARAMETERS *****
CNSF =  0.64192E+02    ETASF =  0.10704E+01    TFSF =  0.29685E+01
DHSF =  0.27171E+05
TF =  202.201         ETA = 0.87000          CN =  1.860
AUXWK =  0.00000E+00

***** TURBINE  3 PARAMETERS *****
CNSF =  0.74251E-02    ETASF =  0.12017E+01    TFSF =  0.17455E+01
DHSF =  0.11358E+06
TF =  195.479         ETA = 0.89000          CN =  2.280
AUXWK =  0.25000E+08

Additional Free Turbine Parameters:-
Speed = 100.0%        Power =  0.25000E+08

***** TURBINE  4 PARAMETERS *****
CNSF =  0.63231E+02    ETASF =  0.13539E+01    TFSF =  0.32157E+00
DHSF =  0.12299E+06
TF =  182.783         ETA = 0.89000          CN =  2.356
AUXWK =  0.00000E+00

***** CONVERGENT NOZZLE  1 PARAMETERS *****
NCOSF =  0.10000E+01
```

Appendix A.1

Area = 1.2616 Exit Velocity = 78.94 Gross Thrust = 4827.10
Nozzle Coeff. = 0.97133E+00

Scale Factor on above Mass Flows, Areas, Thrusts & Powers = 1.0000

Station	F.A.R.	Mass Flow	Pstatic	Ptotal	Tstatic	Ttotal	Vel	Area
1	0.00000	61.710	1.00000	1.00000	288.15	288.15	0.0	******
2	0.00000	61.710	******	0.99510	******	288.15	******	******
3	0.00000	61.710	******	4.38839	******	457.98	******	******
4	0.00000	61.710	******	4.34451	******	298.00	******	******
5	0.00000	61.710	******	16.63947	******	453.53	******	******
6	0.00000	61.710	******	16.63947	******	453.53	******	******
7	0.00000	61.710	******	91.13438	******	755.28	******	******
8	0.00000	55.539	******	91.13438	******	755.28	******	******
9	0.02234	56.780	******	85.21065	******	1509.50	******	******
10	0.02073	61.100	******	85.21065	******	1460.32	******	******
11	0.02073	61.100	******	31.86317	******	1200.93	******	******
12	0.02073	61.100	******	31.86317	******	1200.93	******	******
13	0.02011	62.951	******	31.86317	******	1188.69	******	******
14	0.02011	62.951	******	18.30564	******	1060.56	******	******
15	0.02011	62.951	******	2.96345	******	715.99	******	******
16	0.02011	62.951	******	1.03388	******	561.50	******	******
17	0.02011	62.951	******	1.01837	******	561.50	******	******
18	0.02011	62.951	1.00000	1.01837	558.58	561.50	78.9	1.2616
19	0.00000	0.000	******	0.00000	******	0.00	******	******
20	0.00000	6.171	******	91.13438	******	755.28	******	******
21	0.00000	4.320	******	91.13438	******	755.28	******	******
22	0.00000	1.851	******	91.13438	******	755.28	******	******

Shaft Power = 25000000.00
Net Thrust = 4827.10
Equiv. Power = 25311236.00
Fuel Flow = 1.2409
S.F.C. = 49.6346
E.S.F.C. = 49.0243
Sp. Sh. Power = 405120.75
Sp. Eq. Power = 410164.28
Sh. Th. Effy. = 0.4672
Time Now 01:52:45

Appendix A.1

```
TURBOMATCH SCHEME - Windows NT version (October 1999)

 LIMITS:100 Codewords, 800 Brick Data Items, 50 Station Vector
 15 BD Items printable by any call of:-
 OUTPUT, OUTPBD, OUTPSV, PLOTIT, PLOTBD or PLOTSV

  Input "Program" follows

 !25MW INTERCOOLED 3-SHAFT MARINE GAS TURBINE SIMULATION



 OD SI KE CT FP
  -1
  -1
 INTAKE  S1-2          D1-4          R300
 COMPRE  S2-3        D5-11         R301   V5 V6
 DUCTER  S3-4         D12-15        R305
 COMPRE  S4-5        D16-22        R302   V16 V17
 PREMAS  S5,6,15    D23-26
 PREMAS  S15,16,17 D27-30
 BURNER  S6-7         D31-33        R303
 MIXEES  S7,16,8
 TURBIN  S8-9          D34-41,302,42        V35
 MIXEES  S9,17,10
 TURBIN  S10-11       D43-50,301,51        V44
 TURBIN  S11-12       D52-60               V52 V53
 DUCTER  S12-13     D61-64
 NOZCON  S13-14,1   D65             R304
 PERFOR  S1,0,0      D52,66-68,304,300,303,0,0,305,0,0,0,0,0
 CODEND

 DATA ITEMS
 1 0.0         !INTAKE ALTITUDE
 2 0.0         !ISA DEVIATION
 3 0.0         !MACH NUMBER
 4 0.9951     !PRESSURE RECOVERY
 !LP COMPRESSOR
 5 -1.0        !SURGE MARGIN (DEFAULT=0.85)
 6 -1.0        !SPOOL SPEED (DEFAULT=1.0)
 7 2.7         !PRESSURE RATIO
 8 0.90        !ISENTROPIC EFFICIENCY
 9 0.0         !ERROR SELECTION
 10 4.0        !COMPRESSOR MAP NUMBER
 11 0.0        !ANGLE
 !INTERCOOLER
 12 2.0           !2:INTERCOOLER
 13 0.03         !PRESSURE LOSS
 14 0.90         !INTERCOOLER EFFECTIVENESS
 15 100000.00 !LIMITING VALUE OF FUEL FLOW
 !HP COMPRESSOR
 16 -1.0       !SURGE MARGIN (DEFAULT=0.85)
 17 -1.0       !SPOOL SPEED (DEFAULT=1.0)
 18 9.26       !PRESSURE RATIO
 19 0.90       !ISENTROPIC EFFICIENCY
 20 0.0        !ERROR SELECTOR
 21 4.0        !COMPRESSOR MAP NUMBER
 22 0.0        !ANGLE
 !TURBINE COOLING 1
 23 0.90       !BLEED AIR
 24 0.0        !FLOW LOSS
 25 1.0        !PRESSURE RECOVERY
 26 0.0        !PRESSURE LOSS
 !TURBINE COOLING 2
 27 0.70       !BLEED AIR
 28 0.0        !FLOW LOSS
 29 1.0        !PRESSURE RECOVERY
 30 0.0        !PRESSURE LOSS
 !BURNER
 31 0.065      !PRESSURE LOSS
 32 0.998      !EFFICIENCY
 33 -1.0       !FUEL FLOW
```

Appendix A.1

```
!HP TURBINE
34 0.0        !AUXILIARY POWER REQUIRED
35 0.8        !NON-DIMENSIONAL MASSFLOW (DEFAULT=0.8)
36 0.6        !NON-DIMENSIONAL SPEED (DEFAULT=0.6)
37 0.87       !EFFICIENCY
38 -1.0       !COMPRESSOR TURBINE
39 2.0        !COMPRESSOR NUMBER
40 3.0        !TURBINE MAP NUMBER
41 -1.0       !POWER LAW INDEX
42 0.0        !ANGLE
!IP TURBINE
43 0.0        !AUXILIARY POWER REQUIRED
44 0.8        !NON-DIMENSIONAL MASS FLOW (DEFAULT=0.8)
45 0.6        !NON-DIMENSIONAL SPEED (DEFAULT=0.6)
46 0.87       !ISENTROPIC EFFICIENCY
47 -1.0       !COMPRESSOR TURBINE
48 1.0        !COMPRESSOR NUMBER
49 3.0        !TURBINE MAP NUMBER
50 -1.0       !POWER LAW INDEX
51 0.0        !ANGLE
!POWER TURBINE
52 25000000.00 !POWER REQUIRED
53 -1.0            !NON-DIMENSIONAL MASS FLOW (DEFAULT=0.8)
54 -1.0            !NON-DIMENSIONAL SPEED (DEFAULT=0.6)
55 0.89            !ISENTROPIC EFFICIENCY
56 1.0             !RELATIVE ROTATIONAL
57 0.0             !COMPRESSOR NUMBER
58 5.0             !TURBINE MAP NUMBER
59 1000.0          !POWER LAW INDEX
60 0.0             !COMPRESSOR WORK
!DUCTER
61 0.0        !NO INTERCOOLING
62 0.005      !PRESSURE LOSS
63 0.0        !EFFICIENCY
64 0.0        !LIMITING VALUE OF FUEL FLOW
!CONVERGENT NOZZLE
65 -1.0       !AIR FIXED
!PERFORMANCE
66 1.00       !PROPELLER EFFICIENCY
67 0.0        !SCALING INDEX
68 0.0        !REQUIRED THRUST
-1
1 2  59.99     !INLET MASS FLOW
4 6  310.00    !INTERCOOLER OUTLET TEMPERATURE
7 6  1509.5    !COMBUSTION OUTLET TEMPERATURE
-1
                                    Time Now 01:50:44

************************************************

              The Units for this Run are as follows:-

 Temperature = K   Pressure = Atmospheres   Length = metres

 Area = sq metres  Mass Flow = kg/sec       Velocity = metres/sec

 Force = Newtons   s.f.c.(Thrust) =  mg/N sec   s.f.c.(Power) = mug/J

 Sp. Thrust =    N/kg/sec     Power =   Watts
1

     ***** DESIGN POINT ENGINE CALCULATIONS *****



***** AMBIENT AND INLET PARAMETERS *****
Alt. =      0.0      I.S.A. Dev. =    0.000       Mach No. =  0.00
Etar = 0.9951        Momentum Drag =      0.00

***** COMPRESSOR  1 PARAMETERS *****
PRSF =  0.16667E+01     ETASF =  0.10843E+01     WASF =  0.33860E+00
Z = 0.85000            PR =   2.700            ETA = 0.90000
PCN =   1.0000          CN = 1.00000            COMWK =  0.63307E+07

***** DUCT/AFTER BURNING 1 PARAMETERS *****
```

ETA = 0.9000 DLP = 0.0806 WFB = 0.0000

DUCTER IS USED AS AN INTERCOOLER!
****INTERCOOLER****HEAT REMOVED: 5630.35 KWATTS

***** COMPRESSOR 2 PARAMETERS *****
PRSF = 0.80980E+01 ETASF = 0.10843E+01 WASF = 0.13410E+00
Z = 0.85000 PR = 9.260 ETA = 0.90000
PCN = 1.0000 CN = 1.00000 COMWK = 0.18393E+08

***** COMBUSTION CHAMBER PARAMETERS *****
ETASF = 0.99800E+00
ETA = 0.99800 DLP = 1.5687 WFB = 1.4217

***** TURBINE 1 PARAMETERS *****
CNSF = 0.10479E+03 ETASF = 0.97041E+00 TFSF = 0.42805E+01
DHSF = 0.62945E+04
TF = 430.924 ETA = 0.87000 CN = 2.750
AUXWK = 0.00000E+00

***** TURBINE 2 PARAMETERS *****
CNSF = 0.94792E+02 ETASF = 0.97041E+00 TFSF = 0.17817E+01
DHSF = 0.25703E+04
TF = 430.924 ETA = 0.87000 CN = 2.750
AUXWK = 0.00000E+00

***** TURBINE 3 PARAMETERS *****
CNSF = 0.73073E-02 ETASF = 0.10609E+01 TFSF = 0.65583E+00
DHSF = 0.64828E+05
TF = 219.627 ETA = 0.89000 CN = 2.200
AUXWK = 0.25000E+08

Additional Free Turbine Parameters:-
Speed = 100.0% Power = 0.25000E+08

***** CONVERGENT NOZZLE 1 PARAMETERS *****
NCOSF = 0.10000E+01
Area = 1.3121 Exit Velocity = 99.48 Gross Thrust = 5934.12
Nozzle Coeff. = 0.97137E+00

Scale Factor on above Mass Flows, Areas, Thrusts & Powers = 1.0000

Station	F.A.R.	Mass Flow	Pstatic	Ptotal	Tstatic	Ttotal	Vel	Area
1	0.00000	59.990	1.00000	1.00000	288.15	288.15	0.0	******
2	0.00000	59.990	******	0.99510	******	288.15	******	******
3	0.00000	59.990	******	2.68677	******	392.95	******	******
4	0.00000	59.990	******	2.60617	******	310.00	******	******
5	0.00000	59.990	******	24.13312	******	609.38	******	******
6	0.00000	53.991	******	24.13312	******	609.38	******	******
7	0.02633	55.413	******	22.56447	******	1509.50	******	******
8	0.02443	59.612	******	22.56447	******	1452.10	******	******
9	0.02443	59.612	******	8.75251	******	1204.12	******	******
10	0.02370	61.412	******	8.75251	******	1188.16	******	******
11	0.02370	61.412	******	6.09097	******	1103.22	******	******
12	0.02370	61.412	******	1.02577	******	754.75	******	******
13	0.02370	61.412	******	1.02064	******	754.75	******	******
14	0.02370	61.412	1.00000	1.02064	750.35	754.75	99.5	1.3121
15	0.00000	5.999	******	24.13312	******	609.38	******	******
16	0.00000	4.199	******	24.13312	******	609.38	******	******
17	0.00000	1.800	******	24.13312	******	609.38	******	******

Shaft Power = 25000000.00
Net Thrust = 5934.12
Equiv. Power = 25382614.00
Fuel Flow = 1.4217
S.F.C. = 56.8692
E.S.F.C. = 56.0120
Sp. Sh. Power = 416736.09
Sp. Eq. Power = 423114.06

Appendix A.1

```
Sh. Th. Effy. =   0.4078
        Time Now 01:50:44

 TURBOMATCH SCHEME - Windows NT version (October 1999)

LIMITS:100 Codewords, 800 Brick Data Items, 50 Station Vector
15 BD Items printable by any call of:-
OUTPUT, OUTPBD, OUTPSV, PLOTIT, PLOTBD or PLOTSV

 Input "Program" follows

!25MW RECUPERATED 2-SHAFT MARINE GAS TURBINE


OD SI KE CT FP
 -1
 -1
INTAKE  S1-2         D1-4          R100
COMPRE  S2-3        D5-10         R101    V5  V6
PREMAS  S3,20,4    D11-14
HETCOL  S4-5        D15-18
BURNER  S5-6        D19-21        R102
MIXEES  S6,20,7
TURBIN  S7-8         D22-29,101           V23
TURBIN  S8-9         D30-38               V30 V31
HETHOT  S4,9,13     D39-42
DUCTER  S9-10       D43-46
NOZCON  S10-11,1    D47           R107
PERFOR  S1,0,0      D30,48-50,107,100,102,0,0,0,0,0,0
CODEND



DATA ITEMS
!INTAKE
1 0.0         !INTAKE ALTITUDE
2 0.0         !ISA DEVIATION
3 0.0         !MACH NO
4 0.9951     !PRESSURE RECOVERY
!COMPRESSOR
5 0.4511     !SURGE MARGIN (DEFAULT=0.85)
6 0.998      !SPOOL SPEED (DEFAULT=1.0)
7 13.0       !PRESSURE RATIO
8 0.90       !ISENTROPIC EFFICIENCY
9 0.0        !ERROR SELECTION
10 1.0       !COMPRESSOR MAP NUMBER
!TURBINE COOLING
11 0.10      !BLEED AIR
12 0.0       !FLOW LOSS
13 1.0       !PRESSURE RECOVERY
14 0.0       !PRESSURE LOSS
!COLD SIDE HEAT EXCHANGER
15 0.1        !COLD SIDE PRESSURE LOSS
16 0.73       !EFFECTIVENESS
17 1.0        !TYPE:RECUPERATOR
18 0.02       !MASS FLOW LEAKAGE
!BURNER
19 0.065     !PRESSURE LOSS
20 0.998     !COMBUSTION EFFICIENCY
21 -1.0      !FUEL FLOW
!COMPRESSOR TURBINE
22 0.0       !AUXILIARY POWER REQUIRED
23 0.682     !NON-DIMENSIONAL MASSFLOW (DEFAULT=0.8)
24 0.49      !NON-DIMENSIONAL SPEED (DEFAULT=0.6)
25 0.87      !ISENTROPIC EFFICIENCY
26 -1.0      !RELATIVE ROTATIONAL
27 1.0       !COMPRESSOR NUMBER
28 4.0       !TURBINE MAP NUMBER
29 -1.0      !POWER LAW INDEX
!POWER TURBINE
30 25000000.00 !AUXILIARY POWER REQUIRED
31 0.89          !NON-DIMENSIONAL MASSFLOW (DEFAULT=0.8)
32 0.62          !NON-DIMENSIONAL SPEED (DEFAULT=0.6)
33 0.89          !ISENTROPIC EFFICIENCY
34 1.0           !RELATIVE ROTATIONAL
```

```
35 0.0             !COMPRESSOR NUMBER
36 5.0             !MAP NUMBER
37 1000.0          !POWER LAW INDEX
38 -1.0            !COMPRESSOR WORK
!HOT SIDE HEAT EXCHANGER
39 0.1         !HOT SIDE PRESSURE LOSS
40 0.73        !EFFECTIVENESS
41 1.0         !TYPE:RECUPERATOR
42 0.02        !MASS FLOW LEAKAGE
!DUCTER
43 0.0          !NO INTERCOOLING
44 0.02         !PRESSURE LOSS
45 0.0          !EFFICIENCY
46 0.0          !LIMITING VALUE OF FUEL FLOW
!CONVERGENT NOZZLE
47 -1.0        !AIR FIXED
!PERFOR
48 1.0         !PROPELLER EFFICIENCY
49 0.0         !SCALING INDEX
50 0.0         !REQUIRED THRUST
-1
1 2 76.25      !INLET MASS FLOW
6 6 1509.5     !COMBUSTION OUTLET TEMPERATURE
-1
                                Time Now 01:51:08

************************************************


            The Units for this Run are as follows:-

 Temperature = K   Pressure = Atmospheres   Length = metres

 Area = sq metres  Mass Flow = kg/sec       Velocity = metres/sec

 Force = Newtons   s.f.c.(Thrust) =  mg/N sec   s.f.c.(Power) = mug/J

 Sp. Thrust =    N/kg/sec     Power =   Watts
1

     ***** DESIGN POINT ENGINE CALCULATIONS *****



***** AMBIENT AND INLET PARAMETERS *****
Alt. =      0.0      I.S.A. Dev. =    0.000       Mach No. =  0.00
Etar = 0.9951        Momentum Drag =      0.00

***** COMPRESSOR  1 PARAMETERS *****
PRSF =  0.55605E+02     ETASF =  0.11567E+01     WASF =  0.12196E+00
Z = 0.45110             PR =  13.000             ETA = 0.90000
PCN =   0.9980          CN = 0.99800             COMWK =  0.26429E+08


HETYP =  1.0 HEUA =       85.178


HETYP =  1.0 HEUA =       88.082


HETYP =  1.0 HEUA =       87.985


***** HEAT EXCHANGER COLD SIDE PARAMETERS *****

ETAD =  0.73000E+00
ETA = 0.73000           DLP = 1.2936


***** COMBUSTION CHAMBER PARAMETERS *****
ETASF =  0.99800E+00
```

Appendix A.1

ETA = 0.99800 DLP = 0.7568 WFB = 1.4260

***** TURBINE 1 PARAMETERS *****
CNSF = 0.67219E+02 ETASF = 0.10264E+01 TFSF = 0.14302E+01
DHSF = 0.19060E+05
TF = 386.881 ETA = 0.87000 CN = 1.774
AUXWK = 0.00000E+00

***** TURBINE 2 PARAMETERS *****
CNSF = 0.76049E-02 ETASF = 0.10111E+01 TFSF = 0.34027E+00
DHSF = 0.24434E+05
TF = 242.033 ETA = 0.89000 CN = 2.240
AUXWK = 0.25000E+08

Additional Free Turbine Parameters:-
Speed = 100.0% Power = 0.25000E+08

HETYP = 1.0 HEUA = 87.985

***** HEAT EXCHANGER HOT SIDE PARAMETERS *****

ETAD = 0.73000E+00 HEUA = 87.985 ETASF = 0.00000E+00
ETA = 0.7300 DLP = 0.1041 TOTHOT = 723.7771

***** CONVERGENT NOZZLE 1 PARAMETERS *****
NCOSF = 0.10000E+01
Area = 1.9423 Exit Velocity = 99.15 Gross Thrust = 7481.22
Nozzle Coeff. = 0.97136E+00

Scale Factor on above Mass Flows, Areas, Thrusts & Powers = 1.0000

Station	F.A.R.	Mass Flow	Pstatic	Ptotal	Tstatic	Ttotal	Vel	Area
1	0.00000	76.250	1.00000	1.00000	288.15	288.15	0.0	******
2	0.00000	76.250	******	0.99510	******	288.15	******	******
3	0.00000	76.250	******	12.93631	******	626.53	******	******
4	0.00000	68.625	******	12.93631	******	626.53	******	******
5	0.00000	68.625	******	11.64268	******	811.18	******	******
6	0.02078	70.051	******	10.88590	******	1509.50	******	******
7	0.01870	77.676	******	10.88590	******	1430.03	******	******
8	0.01870	77.676	******	3.70548	******	1152.65	******	******
9	0.01870	77.676	******	1.04081	******	879.61	******	******
10	0.01870	77.676	******	1.02000	******	879.61	******	******
11	0.01870	77.676	1.00000	1.02000	875.33	879.61	99.2	1.9423
12	0.00000	0.000	******	0.00000	******	0.00	******	******
13	0.01870	77.676	******	0.93673	******	723.78	******	******
14	0.00000	0.000	******	0.00000	******	0.00	******	******
15	0.00000	0.000	******	0.00000	******	0.00	******	******
16	0.00000	0.000	******	0.00000	******	0.00	******	******
17	0.00000	0.000	******	0.00000	******	0.00	******	******
18	0.00000	0.000	******	0.00000	******	0.00	******	******
19	0.00000	0.000	******	0.00000	******	0.00	******	******
20	0.00000	7.625	******	12.93631	******	626.53	******	******

Shaft Power = 25000000.00
Net Thrust = 7481.22
Equiv. Power = 25482366.00
Fuel Flow = 1.4260
S.F.C. = 57.0380
E.S.F.C. = 55.9583
Sp. Sh. Power = 327868.84
Sp. Eq. Power = 334194.97
Sh. Th. Effy. = 0.4066
Time Now 01:51:08

Appendix A.1

```
TURBOMATCH SCHEME - Windows NT version (October 1999)

 LIMITS:100 Codewords, 800 Brick Data Items, 50 Station Vector
 15 BD Items printable by any call of:-
 OUTPUT, OUTPBD, OUTPSV, PLOTIT, PLOTBD or PLOTSV

  Input "Program" follows

  !25MW INTERCOOLED/RECUPERATED 3-SHAFT MARINE GAS TURBINE
  OD SI KE CT FP
  -1
  -1
  INTAKE  S1-2          D1-4          R300
  COMPRE  S2-3        D5-11          R301   V5  V6
  DUCTER  S3-4        D12-15          R305
  NOZCON  S4,5,1      D16             R307
  COMPRE  S5-6        D17-23          R302   V17 V18
  PREMAS  S6,7,20     D24-27
  PREMAS  S20,21,22 D28-31
  HETCOL  S7-8          D32-35
  DUCTER  S8-9          D36-39
  BURNER  S9-10         D40-42        R303
  MIXEES  S10,21,11
  TURBIN  S11-12        D43-50,302,51       V44
  MIXEES  S12,22,13
  DUCTER  S13-14      D52-55
  TURBIN  S14-15        D56-63,301,64       V57
  DUCTER  S15-16      D65-68
  TURBIN  S16-17         D69-77               V69 V70
  HETHOT  S7,17,23     D78-81
  DUCTER  S17-18       D82-85       R306
  NOZCON  S18-19,1     D86          R304
  PERFOR  S1,0,0       D69,87-89,304,300,303,307,0,305,0,0,0
  CODEND



  DATA ITEMS
  1 0.0         !INTAKE ALTITUDE
  2 0.0         !ISA DEVIATION
  3 0.0         !MACH NUMBER
  4 0.9951     !PRESSURE RECOVERY
  !LP COMPRESSOR
  5 -1.0        !SURGE MARGIN (DEFAULT=0.85)
  6 -1.0        !SPOOL SPEED (DEFAULT=1.0)
  7 3.01        !PRESSURE RATIO
  8 0.90        !ISENTROPIC EFFICIENCY
  9 0.0         !ERROR SELECTION
  10 4.0        !COMPRESSOR MAP NUMBER
  11 0.0        !ANGLE
  !INTERCOOLER
  12 2.0           !2:INTERCOOLER
  13 0.03         !PRESSURE LOSS
  14 0.90         !INTERCOOLER EFFECTIVENESS
  15 100000.00 !LIMITING VALUE OF FUEL FLOW
  !CONVERGENT NOZZLE (Experimental. No effect on the performance of the cycle.)
  16 -1.0          !AIR FIXED
  !HP COMPRESSOR
  17 -1.0       !SURGE MARGIN (DEFAULT=0.85)
  18 -1.0       !SPOOL SPEED (DEFAULT=1.0)
  19 4.9        !PRESSURE RATIO
  20 0.90       !ISENTROPIC EFFICIENCY
  21 0.0        !ERROR SELECTOR
  22 4.0        !COMPRESSOR MAP NUMBER
  23 0.0        !ANGLE
  !TURBINE COOLING 1
  24 0.90       !BLEED AIR
  25 0.0        !FLOW LOSS
  26 1.0        !PRESSURE RECOVERY
  27 0.0        !PRESSURE LOSS
  !TURBINE COOLING 2
  28 0.70      !BLEED AIR
  29 0.0       !FLOW LOSS
  30 1.0       !PRESSURE RECOVERY
```

```
 31 0.0      !PRESSURE LOSS
!COLD SIDE HEAT EXCHANGER
 32 0.1     !COLD SIDE PRESSURE LOSS
 33 0.73    !EFFECTIVENESS
 34 1.0     !TYPE:RECUPERATOR
 35 0.02    !MASS FLOW LEAKAGE
!DUCTER
 36 0.0     !NO INTERCOOLING
 37 0.0     !PRESSURE LOSS
 38 0.0     !EFFICIENCY
 39 0.0     !LIMITING VALUE OF FUEL FLOW
!BURNER
 40 0.065    !PRESSURE LOSS
 41 0.998    !EFFICIENCY
 42 -1.0     !FUEL FLOW
!HP TURBINE
 43 0.0      !AUXILIARY POWER REQUIRED
 44 0.8      !NON-DIMENSIONAL MASSFLOW (DEFAULT=0.8)
 45 0.6      !NON-DIMENSIONAL SPEED (DEFAULT=0.6)
 46 0.87     !ISENTROPIC EFFICIENCY
 47 -1.0     !COMPRESSOR TURBINE
 48 2.0      !COMPRESSOR NUMBER
 49 3.0      !TURBINE MAP NUMBER
 50 1000.    !POWER LAW INDEX
 51 0.0      !ANGLE
!DUCTER
 52 0.0     !NO INTERCOOLING
 53 0.0     !PRESSURE LOSS
 54 0.0     !EFFICIENCY
 55 0.0     !LIMITING VALUE OF FUEL FLOW
!IP TURBINE
 56 0.0      !AUXILIARY POWER REQUIRED
 57 0.81     !NON-DIMENSIONAL MASS FLOW (DEFAULT=0.8)
 58 0.6      !NON-DIMENSIONAL SPEED (DEFAULT=0.6)
 59 0.87     !ISENTROPIC EFFICIENCY
 60 -1.0     !COMPRESSOR TURBINE
 61 1.0      !COMPRESSOR NUMBER
 62 3.0      !TURBINE MAP NUMBER
 63 1000.0  !POWER LAW INDEX
 64 0.0      !ANGLE
!DUCTER
 65 0.0      !NO INTERCOOLING
 66 0.0      !PRESSURE LOSS
 67 0.0      !EFFICIENCY
 68 0.0      !LIMITING VALUE OF FUEL FLOW
!POWER TURBINE
 69 25000000.00 !POWER REQUIRED
 70 0.81          !NON-DIMENSIONAL MASS FLOW  (DEFAULT=0.8)
 71 0.583         !NON-DIMENSIONAL SPEED (DEFAULT=0.6)
 72 0.89          !ISENTROPIC EFFICIENCY
 73 1.0           !RELATIVE ROTATIONAL SPEED
 74 0.0           !COMPRESSOR NUMBER
 75 5.0           !TURBINE MAP NUMBER
 76 1000.0        !AUXILIARY WORK CONSTANT (GENERATOR)
 77 -1.0          !COMPRESSOR WORK
!HOT HEAT EXCHANGER
 78 0.1     !HOT SIDE PRESSURE LOSS
 79 0.73    !EFFECTIVENESS
 80 1.0     !TYPE:RECUPERATOR
 81 0.02    !MASS FLOW LEAKAGE
!DUCTER
 82 0.0     !NO INTERCOOLING
 83 0.02    !PRESSURE LOSS
 84 0.0     !EFFICIENCY
 85 0.0     !LIMITING VALUE OF FUEL FLOW
!CONVERGENT NOZZLE
 86 -1.0    !AIR FIXED
!PERFORMANCE
 87 1.0     !PROPELLER EFFICIENCY
 88 0.0     !SCALING INDEX
 89 0.0     !REQUIRED THRUST
-1
1 2  66.8        !INLET MASS FLOW
4 6  310.00     !INTERCOOLER OUTLET TEMPERATURE
10 6 1509.5     !COMBUSTION OUTLET TEMPERATURE
```

Appendix A.1

-1

Time Now 01:50:20

****

The Units for this Run are as follows:-

Temperature = K Pressure = Atmospheres Length = metres

Area = sq metres Mass Flow = kg/sec Velocity = metres/sec

Force = Newtons s.f.c.(Thrust) = mg/N sec s.f.c.(Power) = mug/J

Sp. Thrust = N/kg/sec Power = Watts

1

***** DESIGN POINT ENGINE CALCULATIONS *****

***** AMBIENT AND INLET PARAMETERS *****
Alt. = 0.0 I.S.A. Dev. = 0.000 Mach No. = 0.00
Etar = 0.9951 Momentum Drag = 0.00

***** COMPRESSOR 1 PARAMETERS *****
PRSF = 0.19706E+01 ETASF = 0.10843E+01 WASF = 0.37703E+00
Z = 0.85000 PR = 3.010 ETA = 0.90000
PCN = 1.0000 CN = 1.00000 COMWK = 0.79488E+07

***** DUCT/AFTER BURNING 1 PARAMETERS *****
ETA = 0.9000 DLP = 0.0899 WFB = 0.0000

DUCTER IS USED AS AN INTERCOOLER!
****INTERCOOLER****HEAT REMOVED: 7279.32 KWATTS

***** CONVERGENT NOZZLE 1 PARAMETERS *****
NCOSF = 0.10000E+01
Area = 0.0988 Exit Velocity = 322.26 Gross Thrust = 26345.66
Nozzle Coeff. = 0.97512E+00

***** COMPRESSOR 2 PARAMETERS *****
PRSF = 0.38235E+01 ETASF = 0.10843E+01 WASF = 0.13394E+00
Z = 0.85000 PR = 4.900 ETA = 0.90000
PCN = 1.0000 CN = 1.00000 COMWK = 0.13267E+08

HETYP = 1.0 HEUA = 70.613

HETYP = 1.0 HEUA = 75.063

HETYP = 1.0 HEUA = 74.902

***** HEAT EXCHANGER COLD SIDE PARAMETERS *****

ETAD = 0.73000E+00
ETA = 0.73000 DLP = 1.4236

***** COMBUSTION CHAMBER PARAMETERS *****
ETASF = 0.99800E+00
ETA = 0.99800 DLP = 0.8328 WFB = 1.3330

***** TURBINE 1 PARAMETERS *****
CNSF = 0.10455E+03 ETASF = 0.97041E+00 TFSF = 0.20436E+01
DHSF = 0.40913E+04
TF = 430.924 ETA = 0.87000 CN = 2.750
AUXWK = 0.00000E+00

***** TURBINE 2 PARAMETERS *****
CNSF = 0.97730E+02 ETASF = 0.97438E+00 TFSF = 0.11795E+01
DHSF = 0.26305E+04
TF = 433.096 ETA = 0.87000 CN = 2.750
AUXWK = 0.00000E+00

***** TURBINE 3 PARAMETERS *****
CNSF = 0.73999E-02 ETASF = 0.10496E+01 TFSF = 0.42829E+00
DHSF = 0.52430E+05
TF = 222.117 ETA = 0.89000 CN = 2.166
AUXWK = 0.25000E+08

Additional Free Turbine Parameters:-
Speed = 100.0% Power = 0.25000E+08

HETYP = 1.0 HEUA = 74.902

***** HEAT EXCHANGER HOT SIDE PARAMETERS *****

ETAD = 0.73000E+00 HEUA = 74.902 ETASF = 0.00000E+00
ETA = 0.7300 DLP = 0.1041 TOTHOT = 642.5325

***** CONVERGENT NOZZLE 2 PARAMETERS *****
NCOSF = 0.10000E+01
Area = 1.6652 Exit Velocity = 98.73 Gross Thrust = 6534.46
Nozzle Coeff. = 0.97136E+00

Scale Factor on above Mass Flows, Areas, Thrusts & Powers = 1.0000

Station	F.A.R.	Mass Flow	Pstatic	Ptotal	Tstatic	Ttotal	Vel	Area
1	0.00000	66.800	1.00000	1.00000	288.15	288.15	0.0	******
2	0.00000	66.800	******	0.99510	******	288.15	******	******
3	0.00000	66.800	******	2.99525	******	406.24	******	******
4	0.00000	66.800	******	2.90540	******	310.00	******	******
5	0.00000	66.800	1.53424	2.90540	258.24	310.00	322.3	0.0988
6	0.00000	66.800	******	14.23644	******	505.65	******	******
7	0.00000	60.120	******	14.23644	******	505.65	******	******
8	0.00000	60.120	******	12.81279	******	761.36	******	******
9	0.00000	60.120	******	12.81279	******	761.36	******	******
10	0.02217	61.453	******	11.97996	******	1509.50	******	******
11	0.02057	66.129	******	11.97996	******	1445.39	******	******
12	0.02057	66.129	******	6.60779	******	1283.77	******	******
13	0.01996	68.133	******	6.60779	******	1262.97	******	******
14	0.01996	68.133	******	6.60779	******	1262.97	******	******
15	0.01996	68.133	******	4.48713	******	1167.18	******	******
16	0.01996	68.133	******	4.48713	******	1167.18	******	******
17	0.01996	68.133	******	1.04118	******	856.22	******	******
18	0.01996	68.133	******	1.02036	******	856.22	******	******
19	0.01996	68.133	1.00000	1.02036	851.96	856.22	98.7	1.6652
20	0.00000	6.680	******	14.23644	******	505.65	******	******
21	0.00000	4.676	******	14.23644	******	505.65	******	******
22	0.00000	2.004	******	14.23644	******	505.65	******	******
23	0.01996	68.133	******	0.93706	******	642.53	******	******

Shaft Power = 25000000.00
Net Thrust = 32880.12
Equiv. Power = 27120010.00
Fuel Flow = 1.3330
S.F.C. = 53.3220
E.S.F.C. = 49.1537
Sp. Sh. Power = 374251.50
Sp. Eq. Power = 405988.19
Sh. Th. Effy. = 0.4349
Time Now 01:50:20

Appendix A.1

Table A.1: “Turbomatch” input file supplement sample of temperature calibration at ISA sea level standards

```
5 6 1425 !TET (K)
-1
1 -400 !ALTITUDE (M)
-1
-1
2 -47.6 !TEMPERATURE ( ºC)
-1
-1
2 -37.6
-1
-1
2 -27.6
-1
-1
2 -17.6
-1
-1
2 -7.6
-1
-1
2 2.4
-1
-1
2 12.4
-1
-1
2 22.4
-1
-1
2 32.4
-1
-1
1 -200
-1
-1
2 -46.3
-1
-1
2 -36.3
-1
-1
2 -26.3
-1
-1
2 -16.3
-1
-1
2 -6.3
-1
-1
2 3.7
-1
-1
2 13.7
-1
-1
2 23.7
-1
-1
2 33.7
-1
-1
```

Appendix A.2

Table A.2: Marine Vessel Design Parameters (* Ship power prediction input parameters)

Marine Vessel Design Parameter	**Destroyer**	**RoPax Fast Ferry**	**LNG Carrier (Q-max)**
L (m)*	147.0	191.0	335
B (m)*	18.0	25.3	54.0
T_f (m)*	5.1	6.5	12.0
T_a (m)*	5.1	6.5	12.0
Δ (tons)	7351.9	17722.9	169293.7
S_H (m^2)	2829.5	4985.0	20965.3
C_B*	0.50	0.55	0.75
C_P*	0.58	0.59	0.76
C_{WP}*	0.69	0.69	0.80
C_M*	0.78	0.93	0.98
LCB (%)*	-0.8	-2.0	-2.0
1+k	1.146	1.148	1.157
h_b (m)*	-1.2	3	6
A_{BT} (m^2)*	10	25	60
A_T (m^2)*	20	30	50
Stern Type*	V-stern	Normal-Stern	Pram & Gondola
Skeg type rudder twin screw (m^2)*	40	0	0
Shaft brackets(m^2)*	10	0	0
Bossings (m^2)*	10	0	0
Bilge Keels(m^2)*	50	100	200
Shatfs (m^2)	15	0	0
Stabilizer fins(m2)*	10	20	0
n_{BTO}*	1	2	1
d_{BTO}*	2	2	3.5
C_{BTO}*	0.005	0.005 & 0.006	0.005
A_F (m^2)*	250	350	600
A_L (m^2)*	1500	3000	3000
CD_t*	0.85	0.9	0.9
CD_l-AF*	0.6	0.45	0.55
δ_a*	0.65	0.6	0.5
K_h (μm)*	120	120	120
N_{prop}*	2	2	2
F_n	0.257 (Cruise) 0.413 (Boost) 0.379 (Design)	0.344	0.178
V_s (knots)*	19 (Cruise) 30.5 (Boost) 28 (Design)	29	20
λ	0.62	0.63	0.91

Table A.3: Propeller Design Parameters (* Ship power prediction input parameters)

Propeller Design Parameter	**Destroyer**	**RoPax Fast Ferry**	**LNG Carrier (Q-max)**
D_{prop}*	4.1	5.1	9.2
A_E/A_O*	0.751	0.763	0.844
P/D*	1.254	1.150	1.034
N_{blades}*	5	5	5
k_{sp} (μm)*	30	30	30
N_S (rpm)	128.5 (Cruise) 227.2 (Boost) 201.0 (Design)	174.4	70.9
η_{owe}	0.726 (Cruise) 0.698 (Boost) 0.711 (28knots)	0.711	0.69

APPENDIX B

Contains:

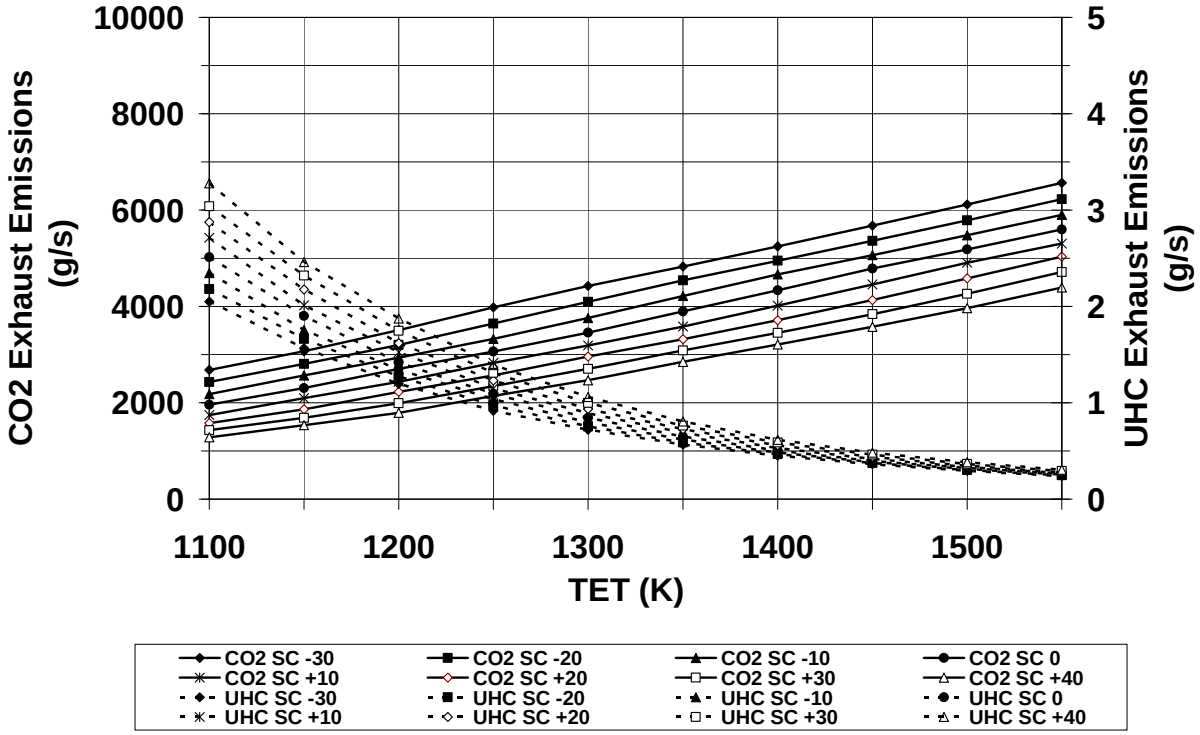

Figure B.1: Simple cycle (SC) – The effect of ambient (T_{amb}) & turbine entry temperature (TET) on carbon dioxide (CO2) and unburned hydrocarbons (UHC) exhaust emissions

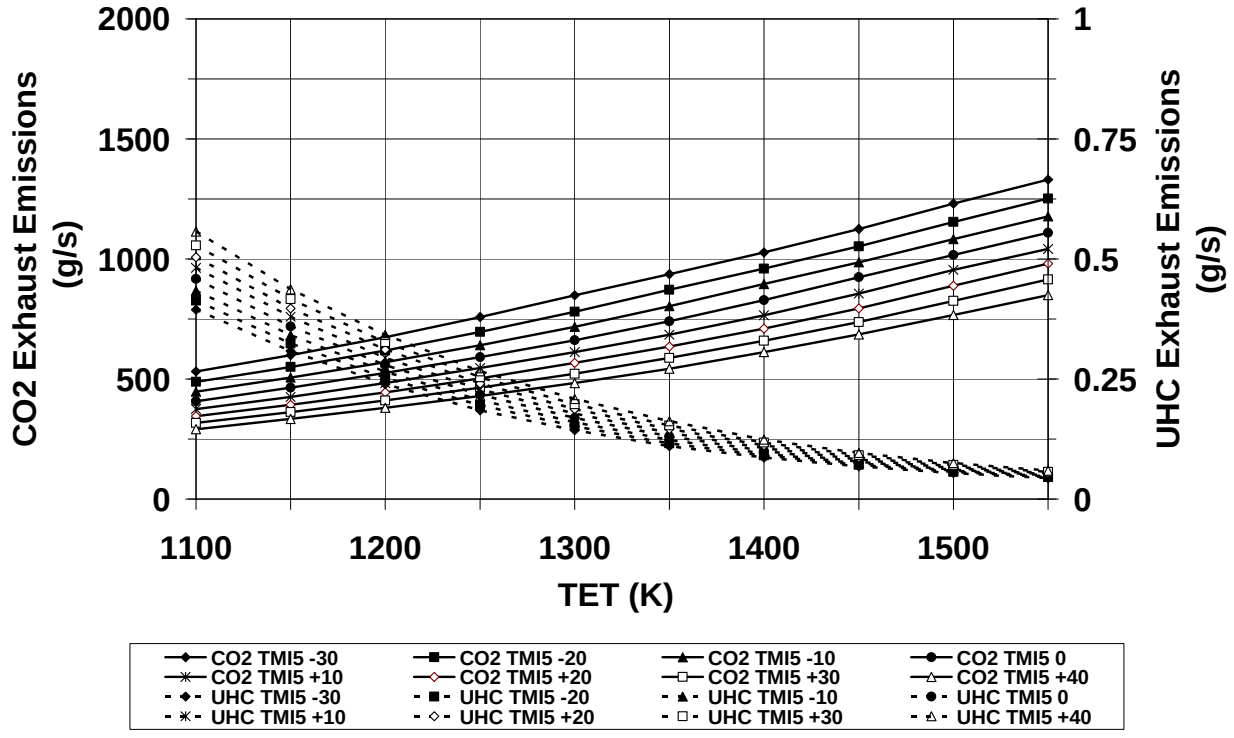

Figure B.2: Twin mode intercooled cycle (TMI) (Low power) – The effect of ambient (T_{amb}) & turbine entry temperature (TET) on carbon dioxide (CO2) and unburned hydrocarbons (UHC) exhaust emissions

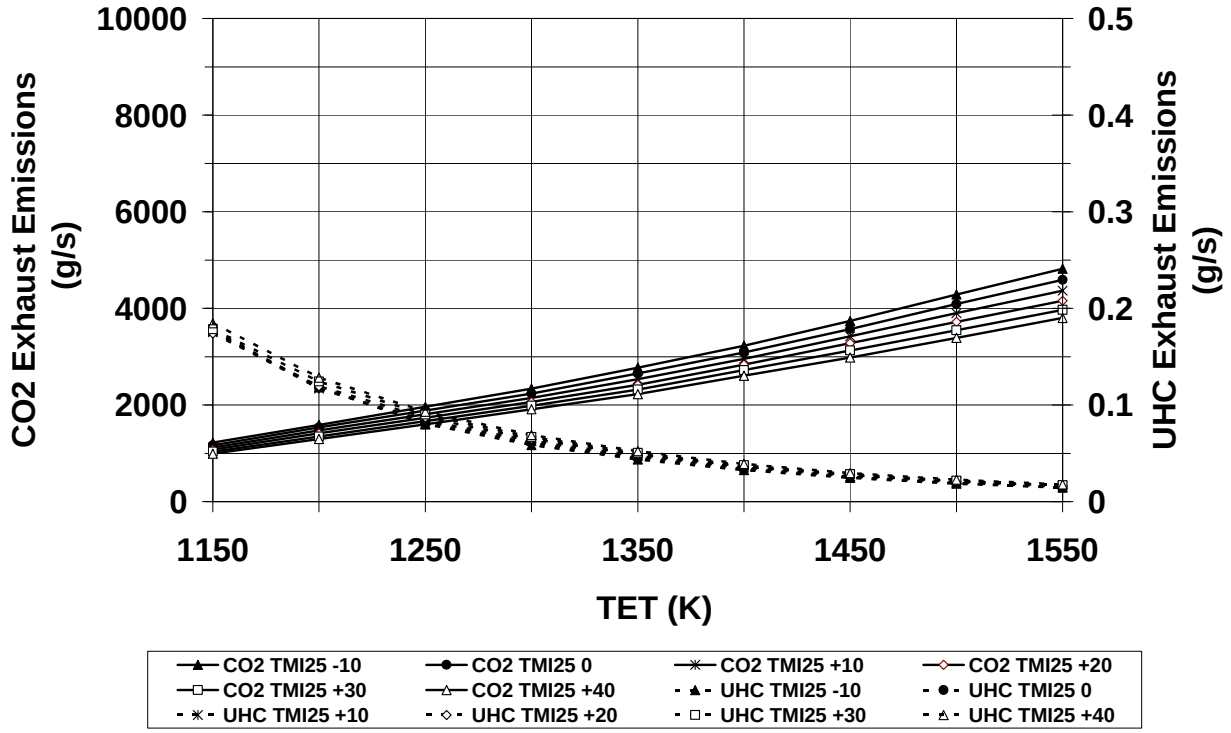

Figure B.3: Twin mode intercooled cycle (TMI) (High power) – The effect of ambient (T_{amb}) & turbine entry temperature (TET) on carbon dioxide (CO2) and unburned hydrocarbons (UHC) exhaust emissions

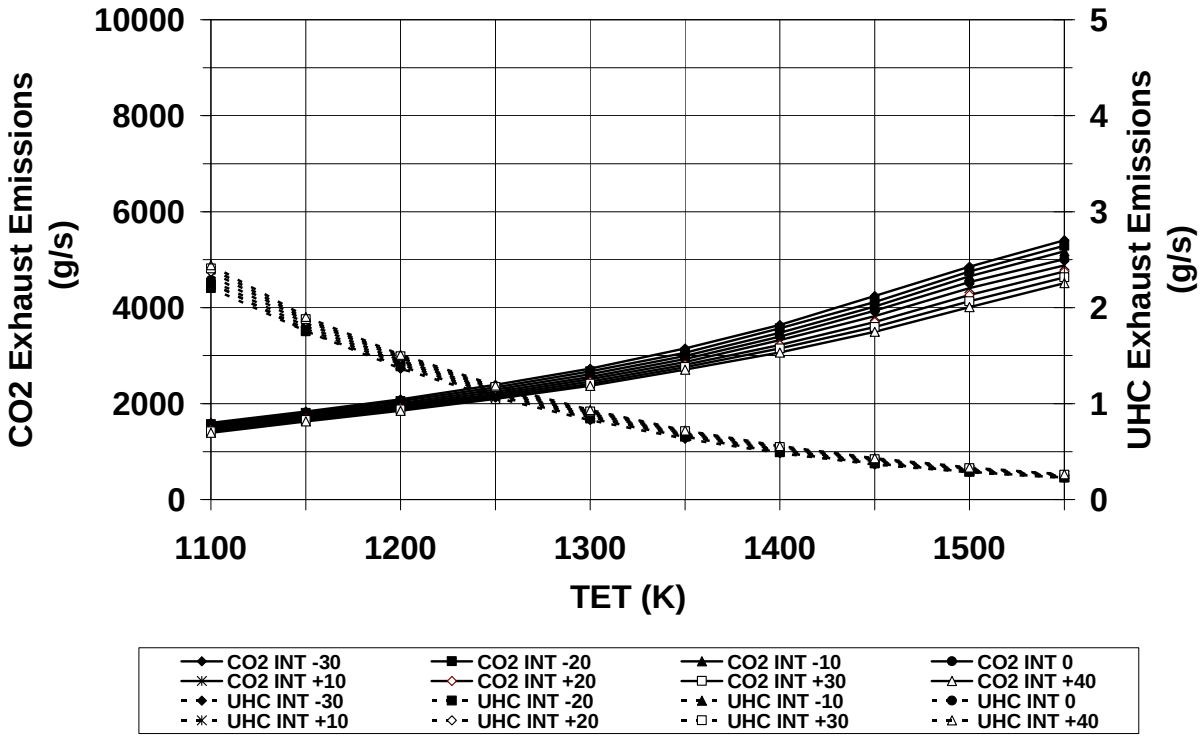

Figure B.4: Intercooled cycle (INT) – The effect of ambient (T_{amb}) & turbine entry temperature (TET) on carbon dioxide (CO2) and unburned hydrocarbons (UHC) exhaust emissions

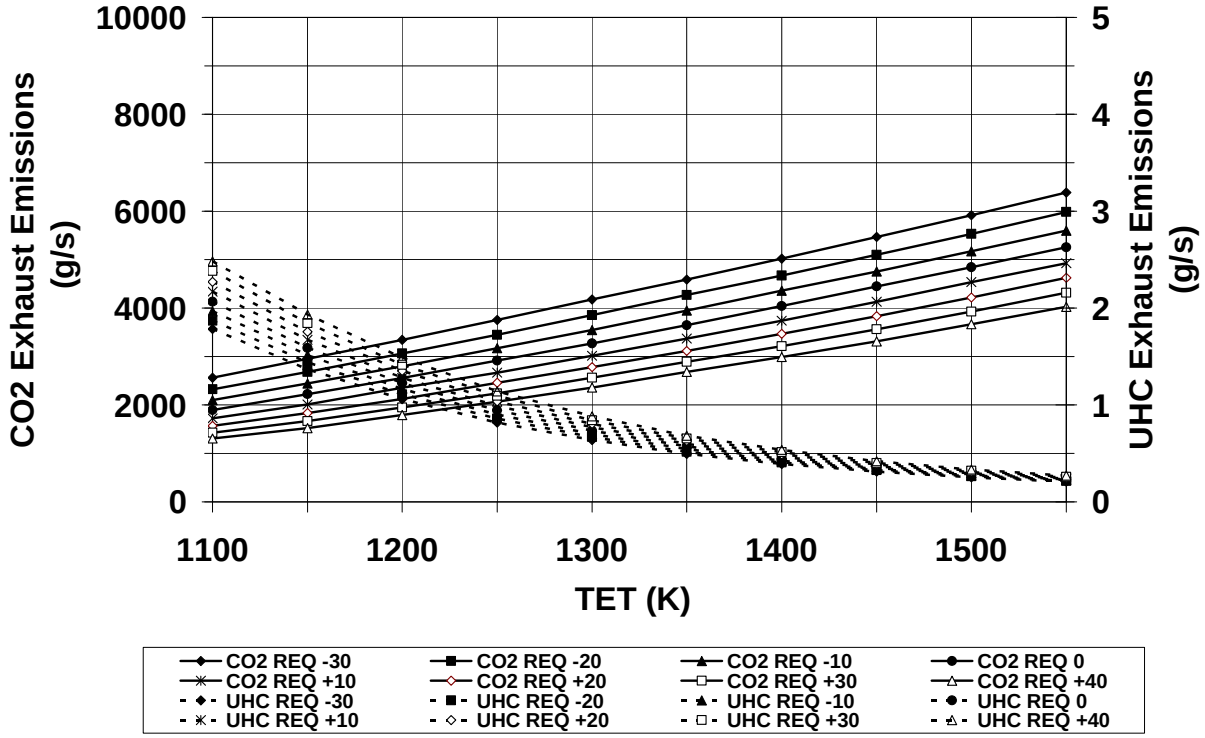

Figure B.5: Recuperated cycle (REQ) – The effect of ambient (T_{amb}) & turbine entry temperature (TET) on carbon dioxide (CO2) and unburned hydrocarbons (UHC) exhaust emissions

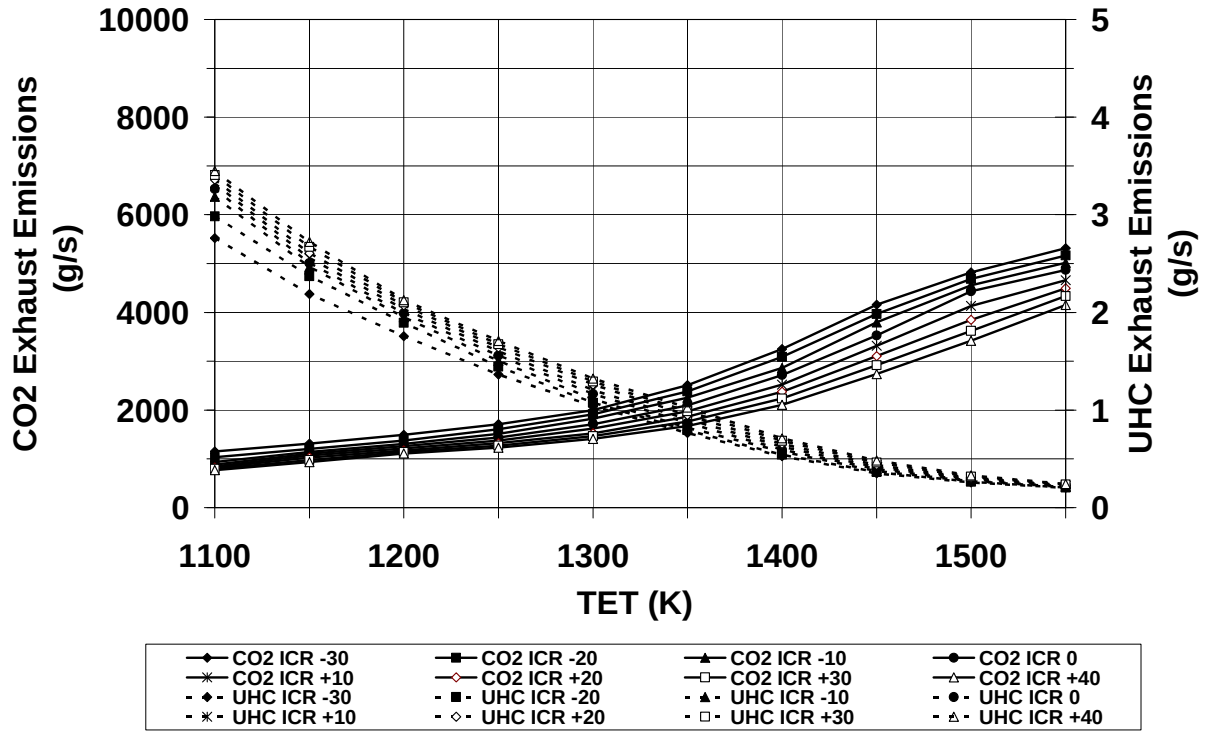

Figure B.6: Intercooled/recuperated cycle (ICR) – The effect of ambient (T_{amb}) & turbine entry temperature (TET) on carbon Dioxide (CO2) and unburned hydrocarbons (UHC) exhaust emissions

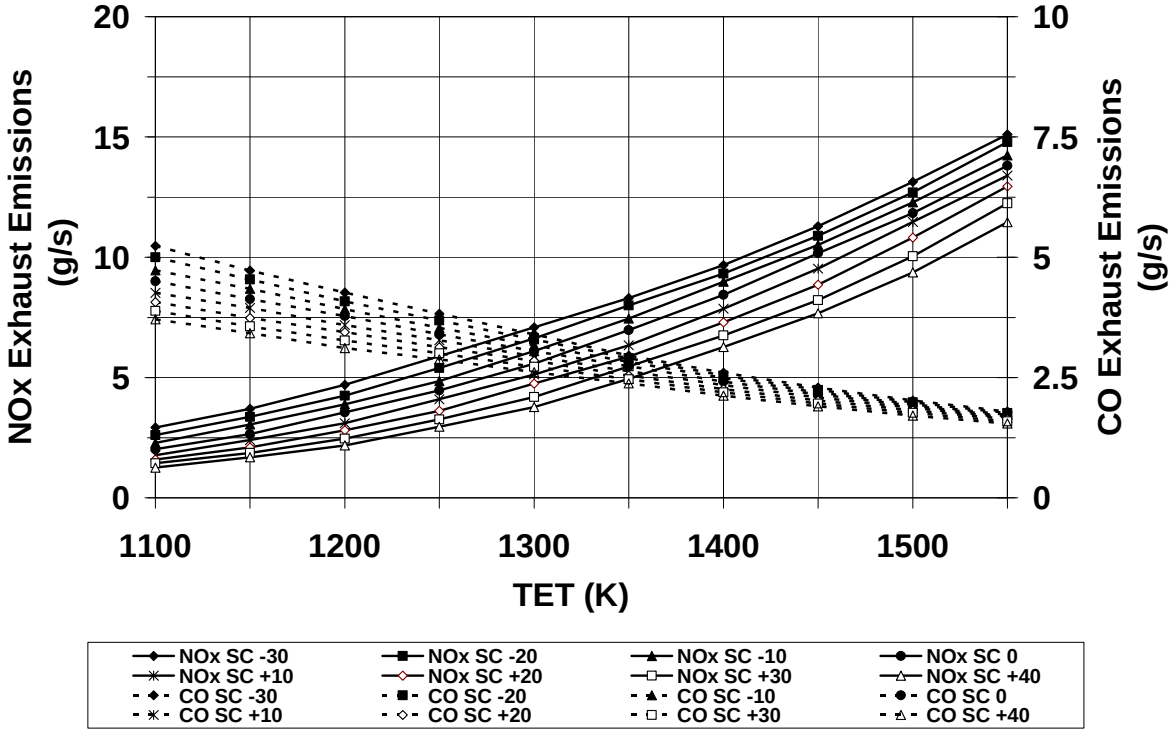

Figure B.7: Simple cycle (SC) – The effect of ambient (T_{amb}) & turbine entry temperature (TET) on nitric oxide (NOx) and carbon monoxide (CO) exhaust emissions

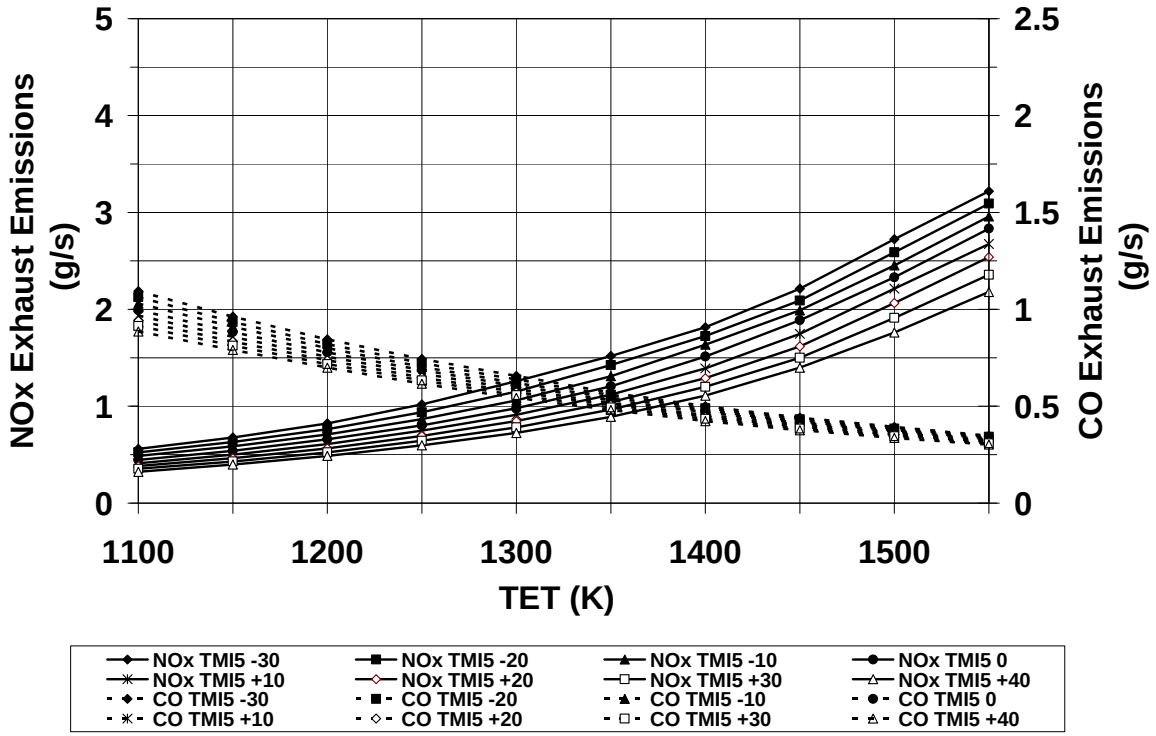

Figure B.8: Twin mode intercooled cycle (TMI) (Low power) – The effect of ambient (T_{amb}) & turbine entry temperature (TET) on nitric oxide (NOx) and carbon monoxide (CO) exhaust emissions

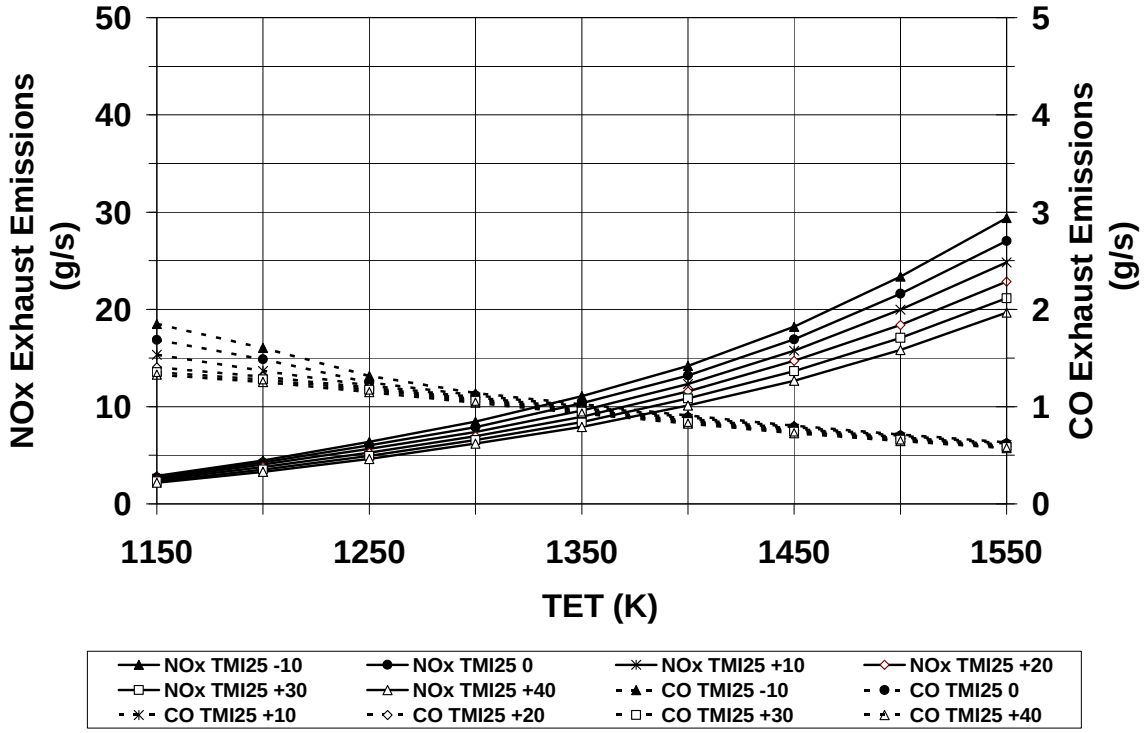

Figure B.9: Twin mode intercooled cycle (TMI) (High power) – The effect of ambient (T_{amb}) & turbine entry temperature (TET) on nitric oxide (NOx) and carbon monoxide (CO) exhaust emissions

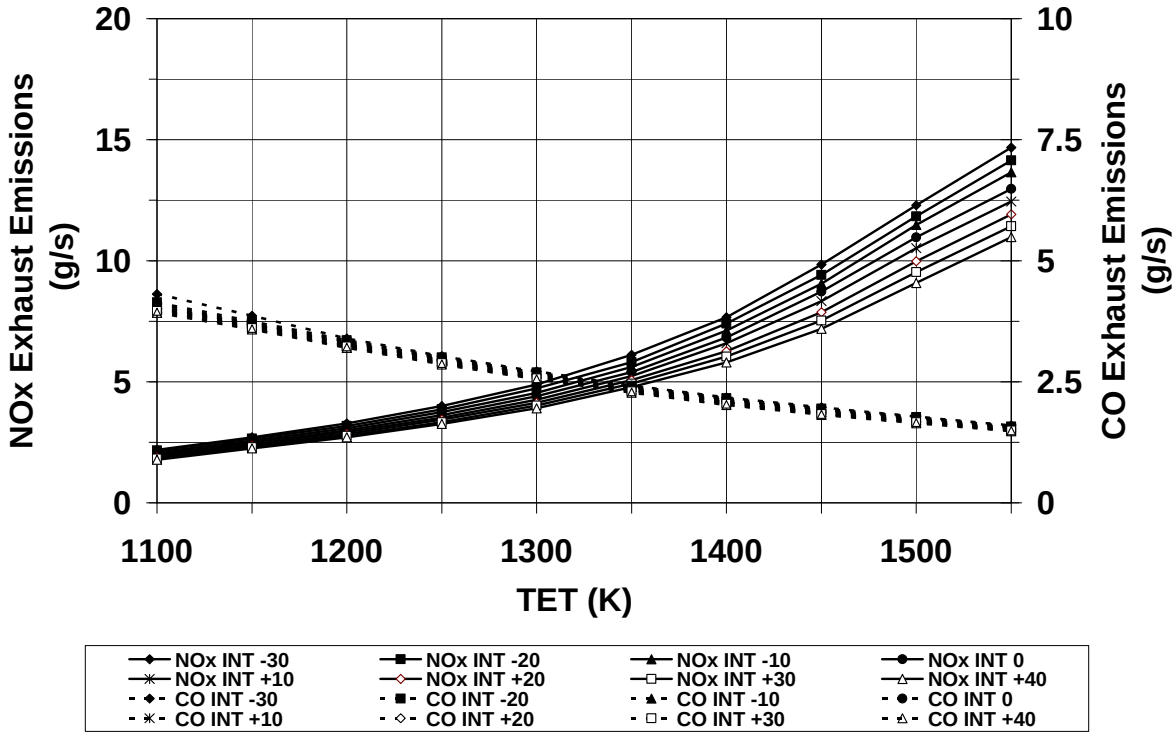

Figure B.10: Intercooled cycle (INT) – The effect of ambient (T_{amb}) & turbine entry temperature (TET) on nitric oxide (NOx) and carbon monoxide (CO) exhaust emissions

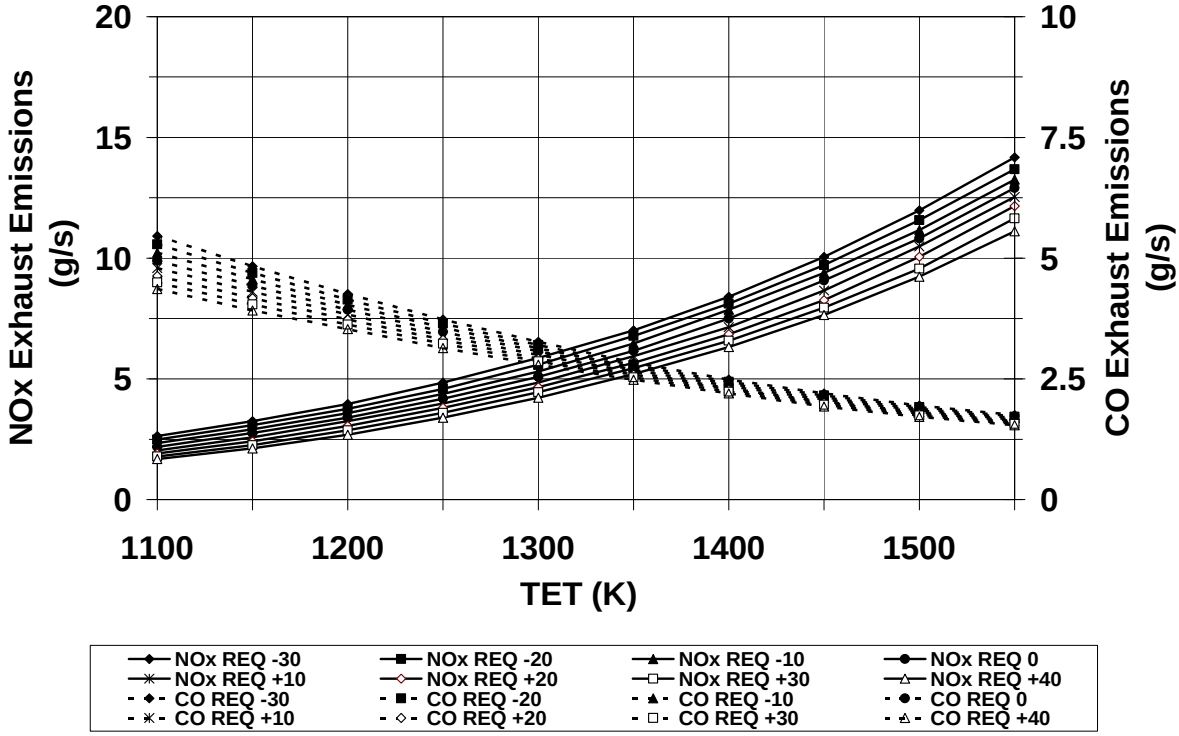

Figure B.11: Recuperated cycle (REQ) – The effect of ambient (T_{amb}) & turbine entry emperature (TET) on nitric oxide (NOx) and carbon monoxide (CO) exhaust emissions

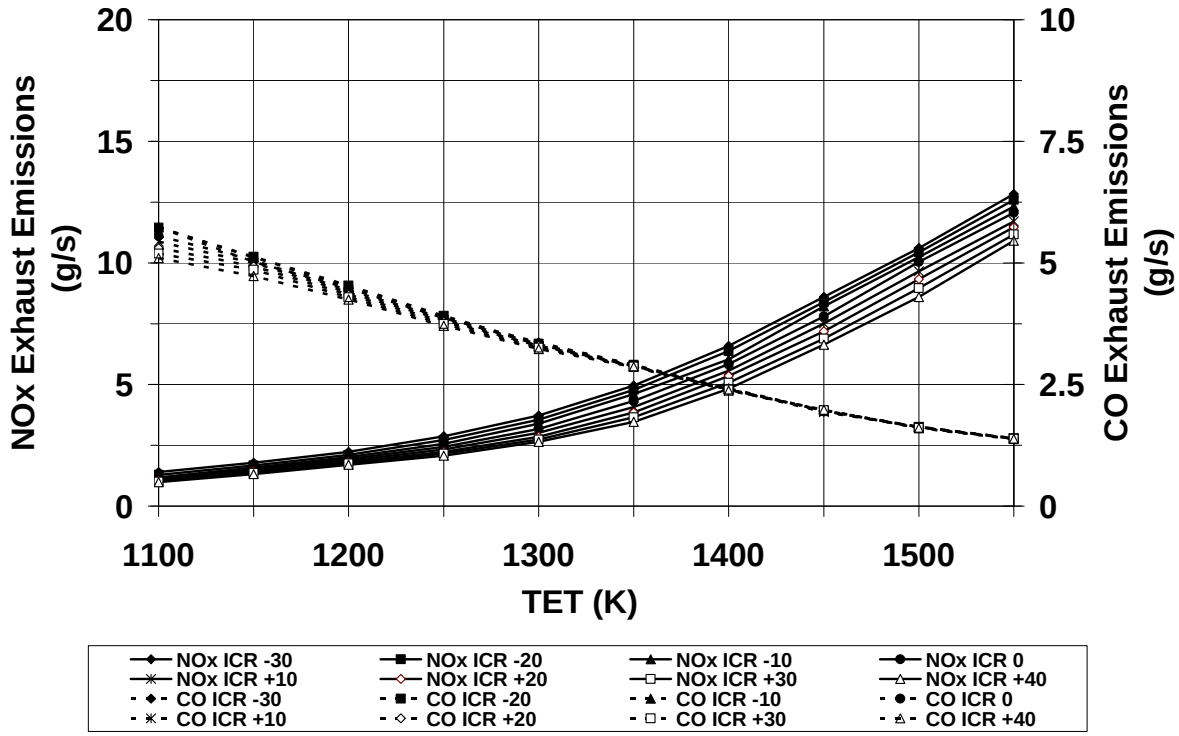

Figure B.12: Intercooled/Recuperated cycle (ICR) – The effect of ambient (T_{amb}) & turbine entry temperature (TET) on nitric oxide (NOx) and carbon monoxide (CO) exhaust emissions

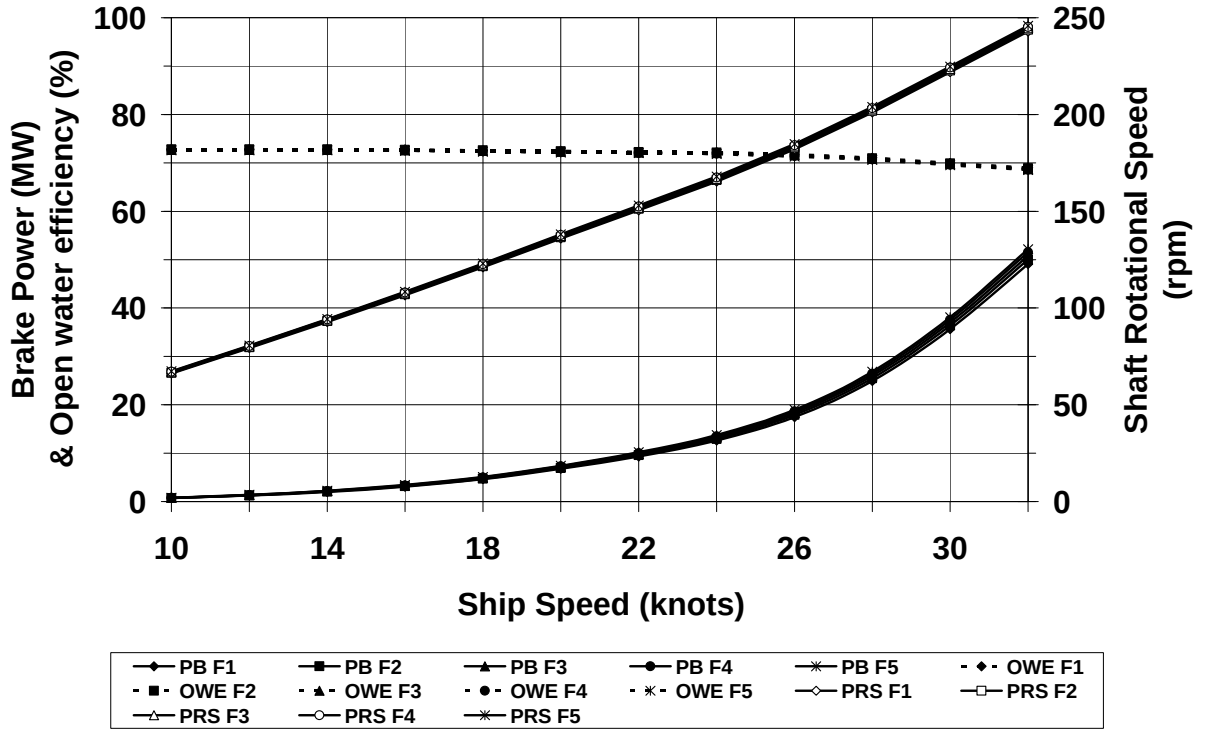

Figure B.13: Marine vessel type: Destroyer – The effect of ship speed (SS) and hull fouling (F#) progression on required power plant brake power (PB), propeller open water efficiency (OWE) & propeller shaft rotational speed (PRS)

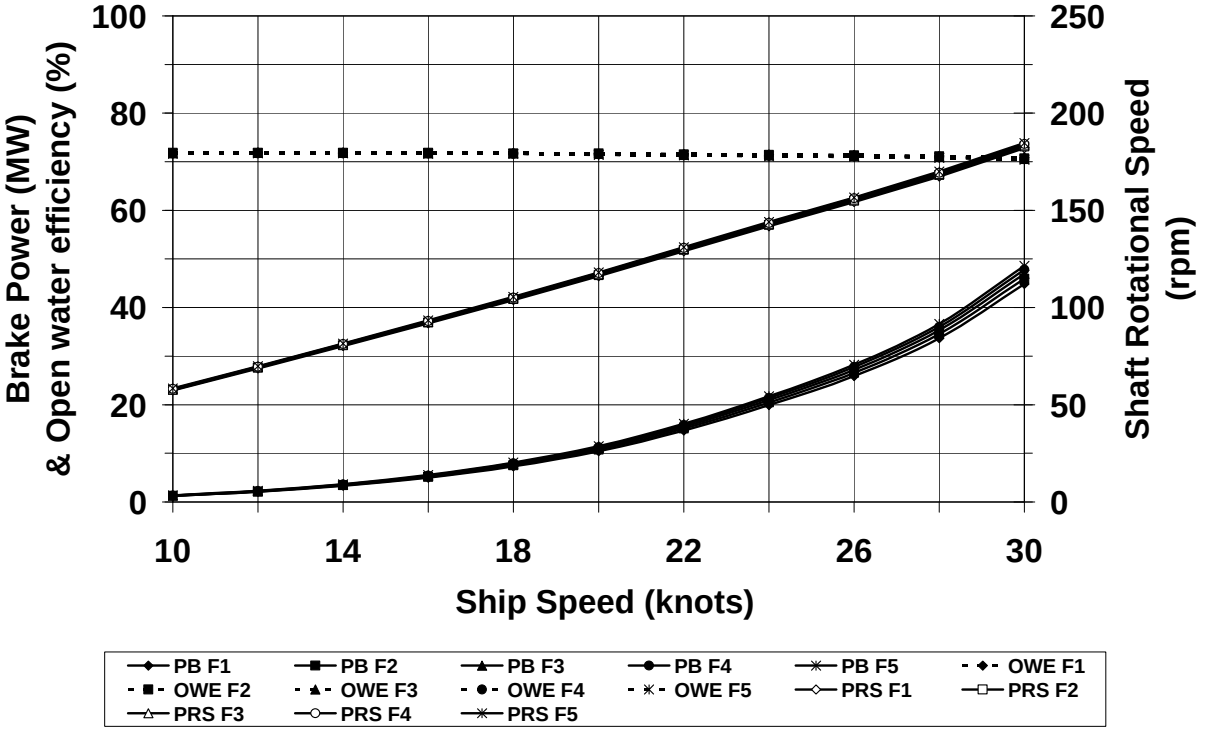

Figure B.14: Marine Vessel Type: RoPax fast ferry – The effect of ship speed (SS) and hull fouling (F#) progression on required power plant brake power (PB), propeller open water efficiency (OWE) & propeller shaft rotational speed (PRS)

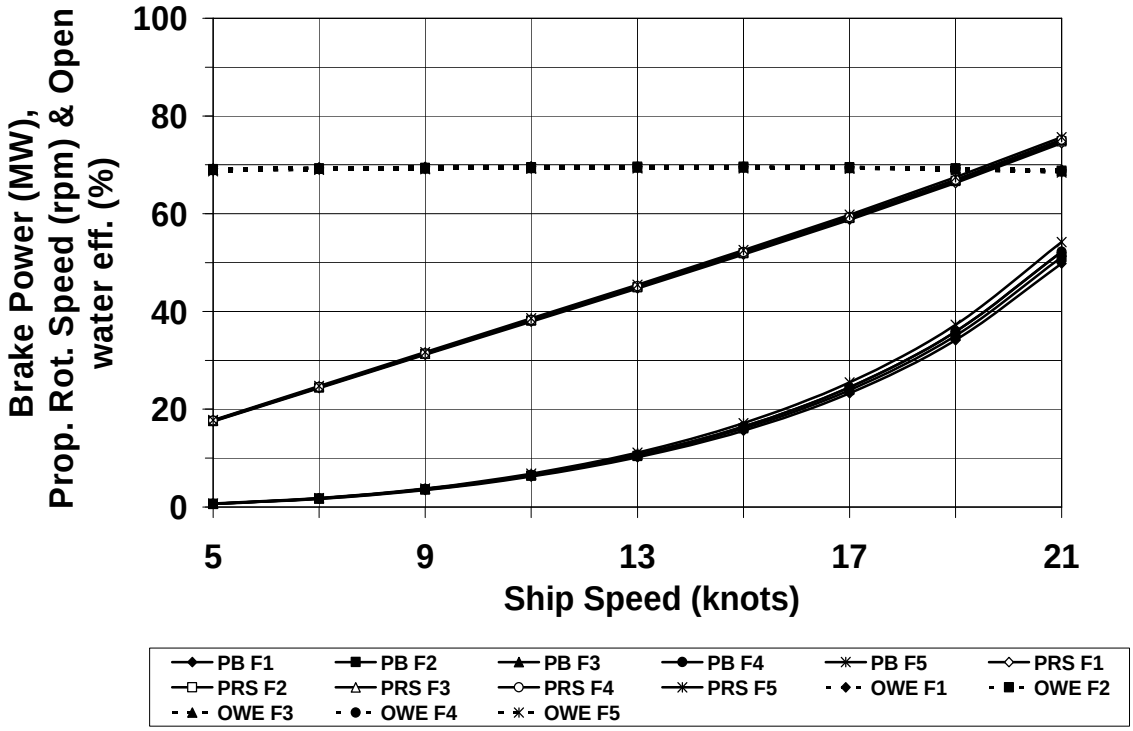

Figure B.15: Marine vessel type: LNG carrier – The effect of ship speed (SS) and hull fouling (F#) progression on required power plant brake power (PB), propeller open water efficiency (OWE) & propeller shaft rotational speed (PRS)

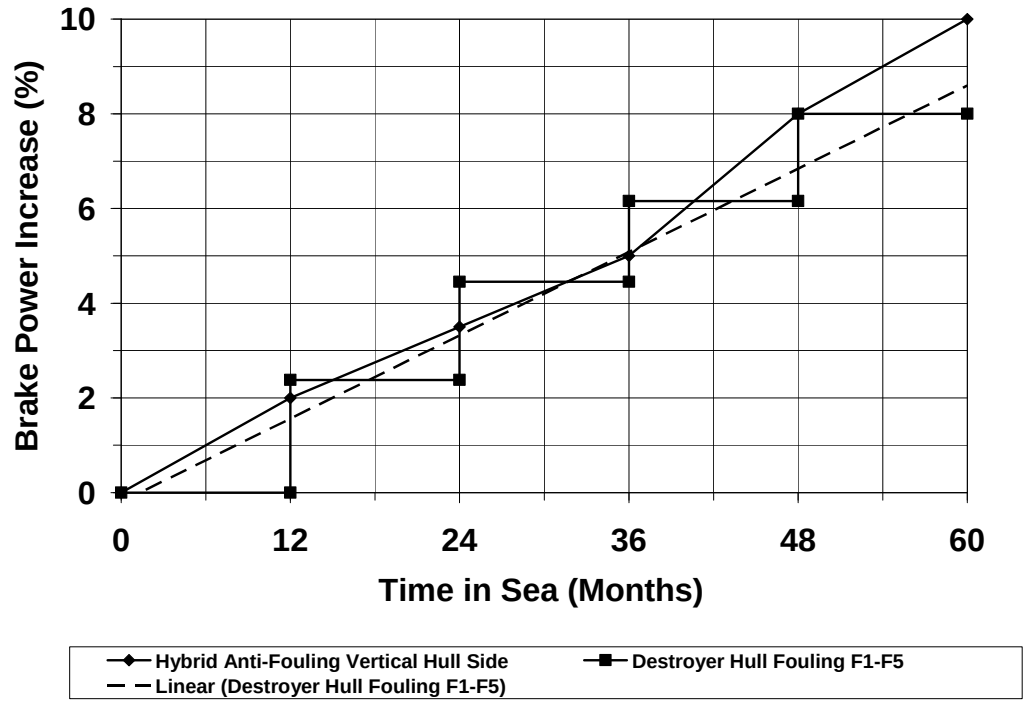

Figure B.16: Destroyer – Brake power increase due to resistance from hull fouling and comparison with hybrid anti-fouling system performance [Chapter 2, Ref. 6]. Values for destroyer are the average of cruise and boost speed

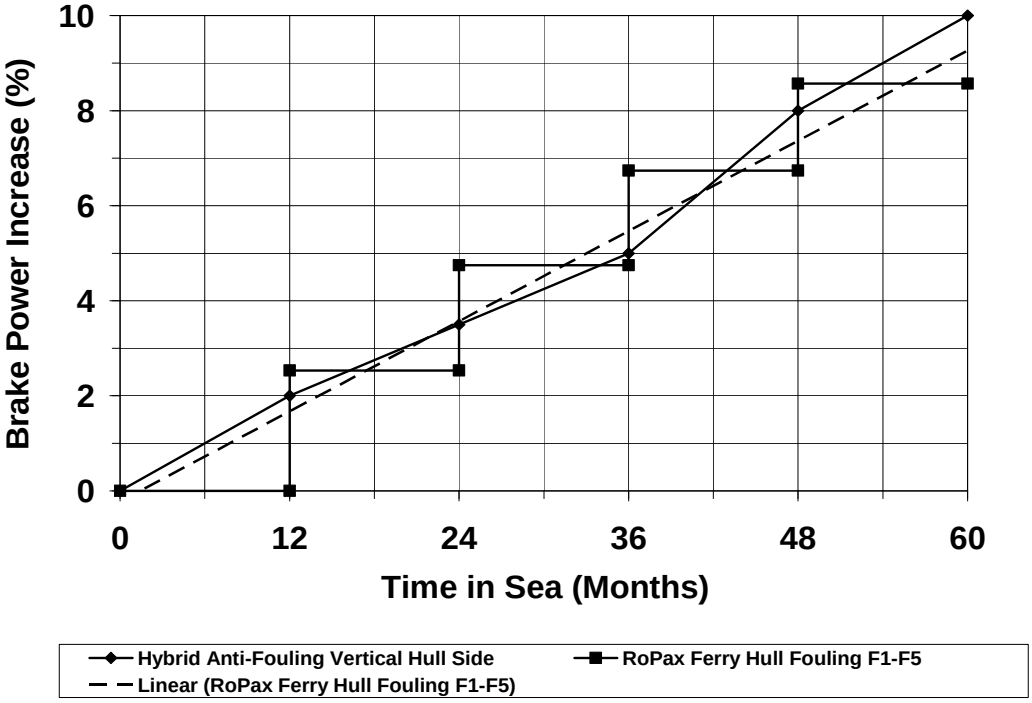

Figure B.17: RoPax fast ferry – Brake power increase due to resistance from hull fouling and comparison with hybrid anti-fouling system performance [Chapter 2, Ref. 6]

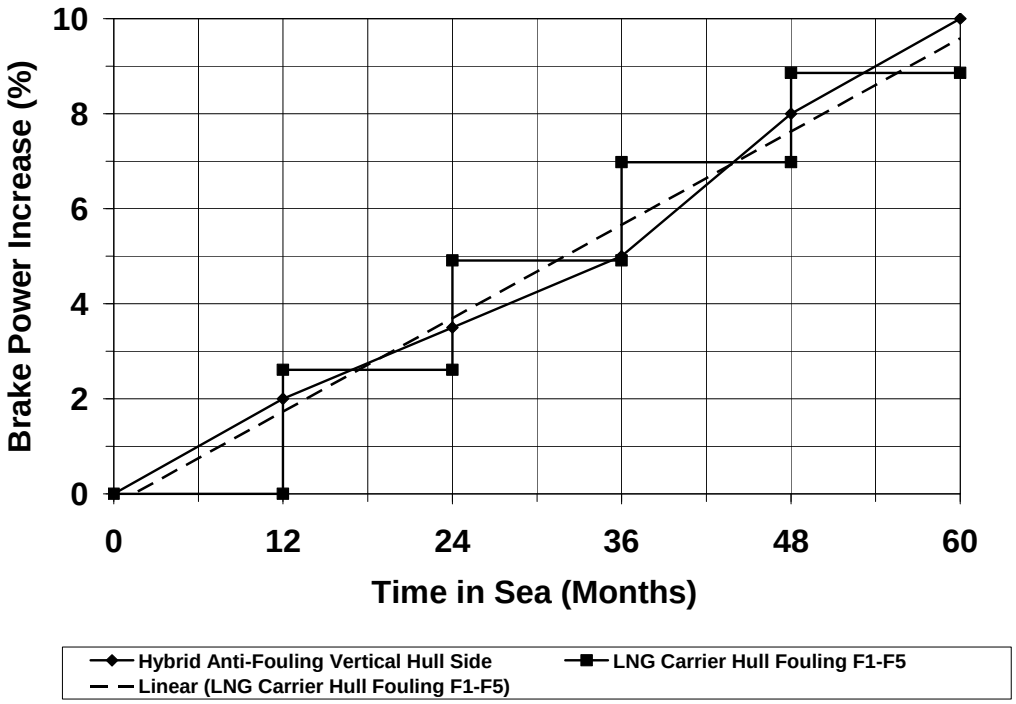

Figure B.18: LNG carrier – Brake power increase due to resistance from hull fouling and comparison with hybrid anti-fouling system performance [Chapter 2, Ref. 6]

APPENDIX C

Contains:

9. **[Table C.19]:** Cost of taxed UHC exhaust emissions of all power plants.

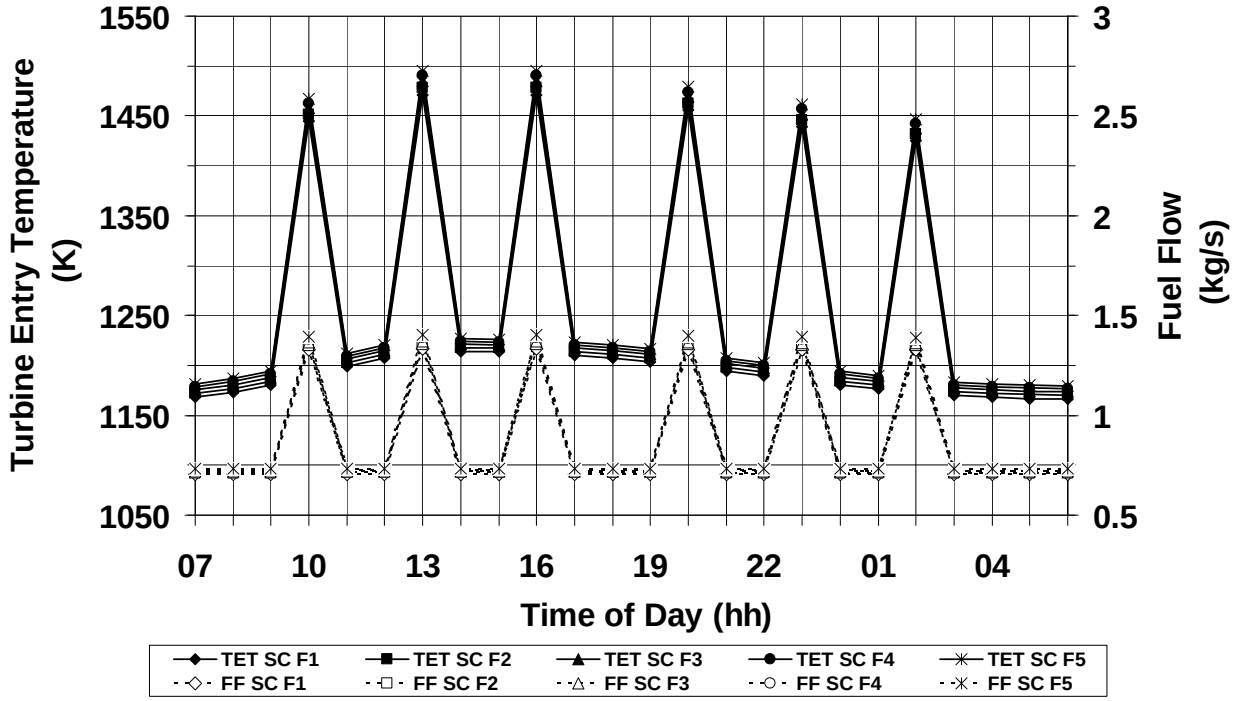

Figure C.1: Simple cycle (SC) - Turbine entry temperature (TET) and fuel flow (FF) variation against time of day, during journey with annual hull fouling progression (F#) and ideal weather conditions

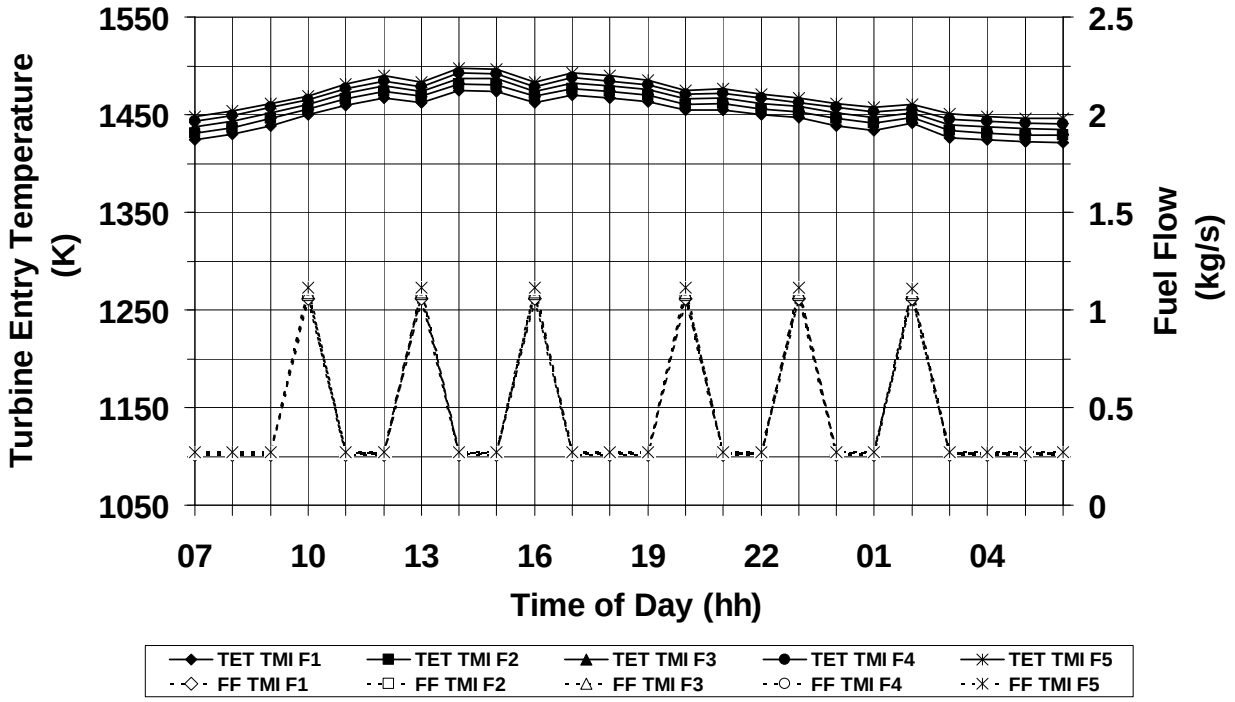

Figure C.2: Twin mode intercooled cycle (TMI) - Turbine entry temperature (TET) and fuel flow (FF) variation against time of day, during journey with annual hull fouling progression (F#) and ideal weather conditions

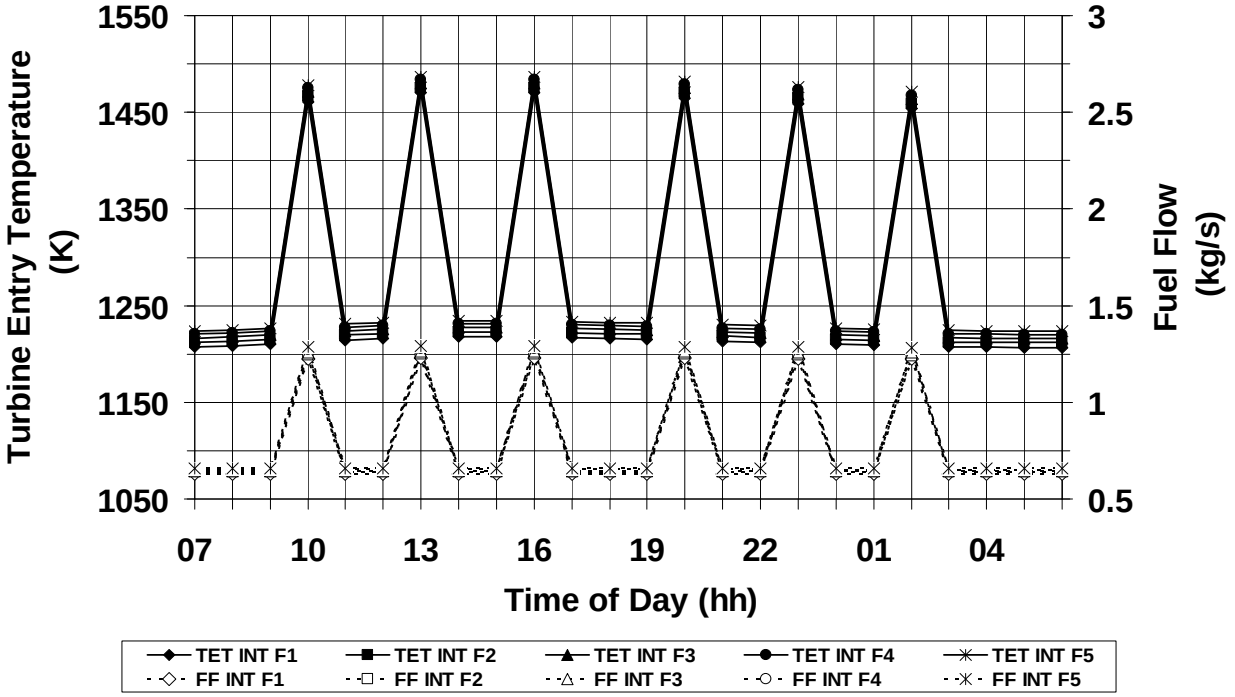

Figure C.3: Intercooled cycle (INT) - Turbine entry temperature (TET) and fuel flow (FF) variation against time of day, during journey with annual hull fouling progression (F#) and ideal weather conditions

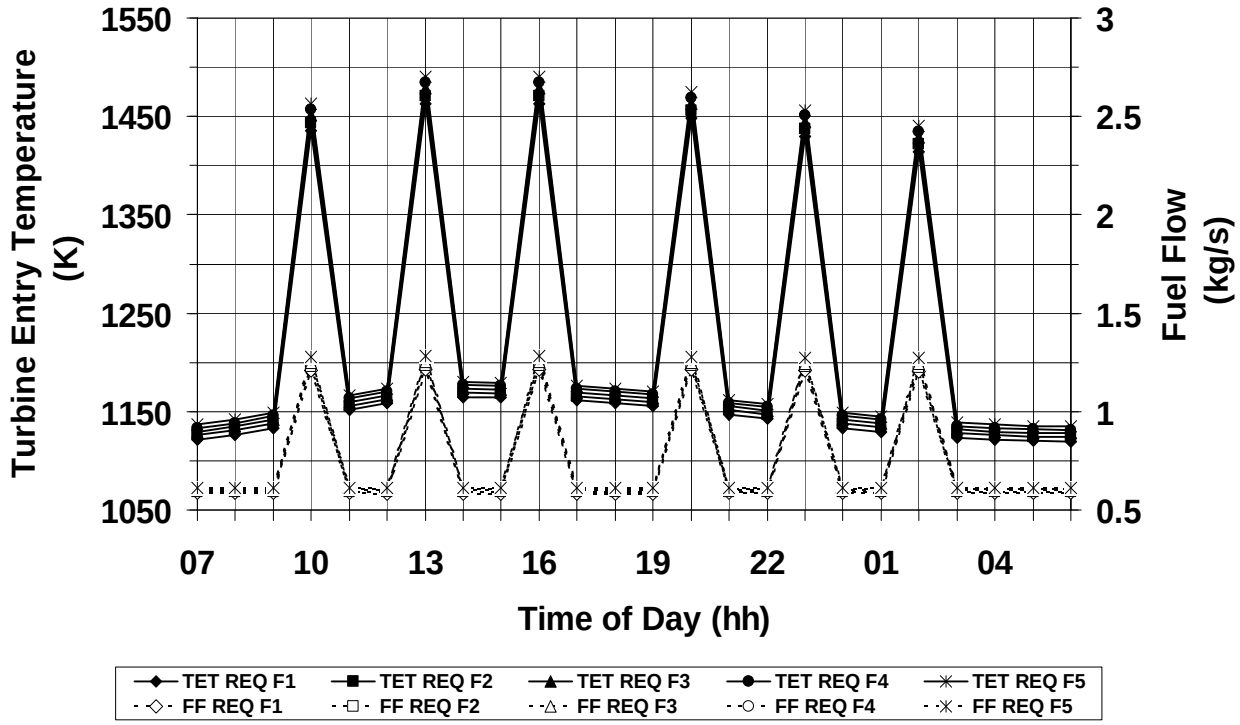

Figure C.4: Recuperated cycle (REQ) - Turbine entry temperature (TET) and fuel flow (FF) variation against time of day, during journey with annual hull fouling progression (F#) and ideal weather conditions

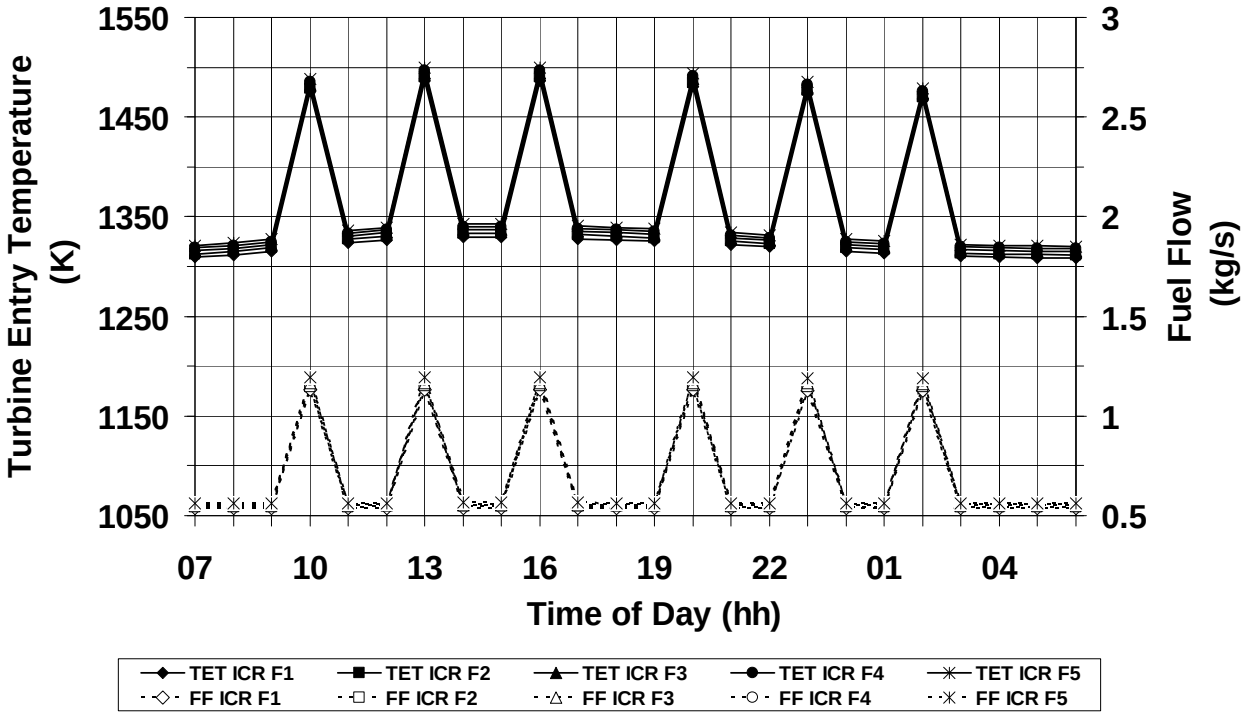

Figure C.5: Intercooled/recuperated cycle (ICR) - Turbine entry temperature (TET) and fuel flow (FF) variation against time of day, during journey with annual hull fouling progression (F#) and ideal weather conditions

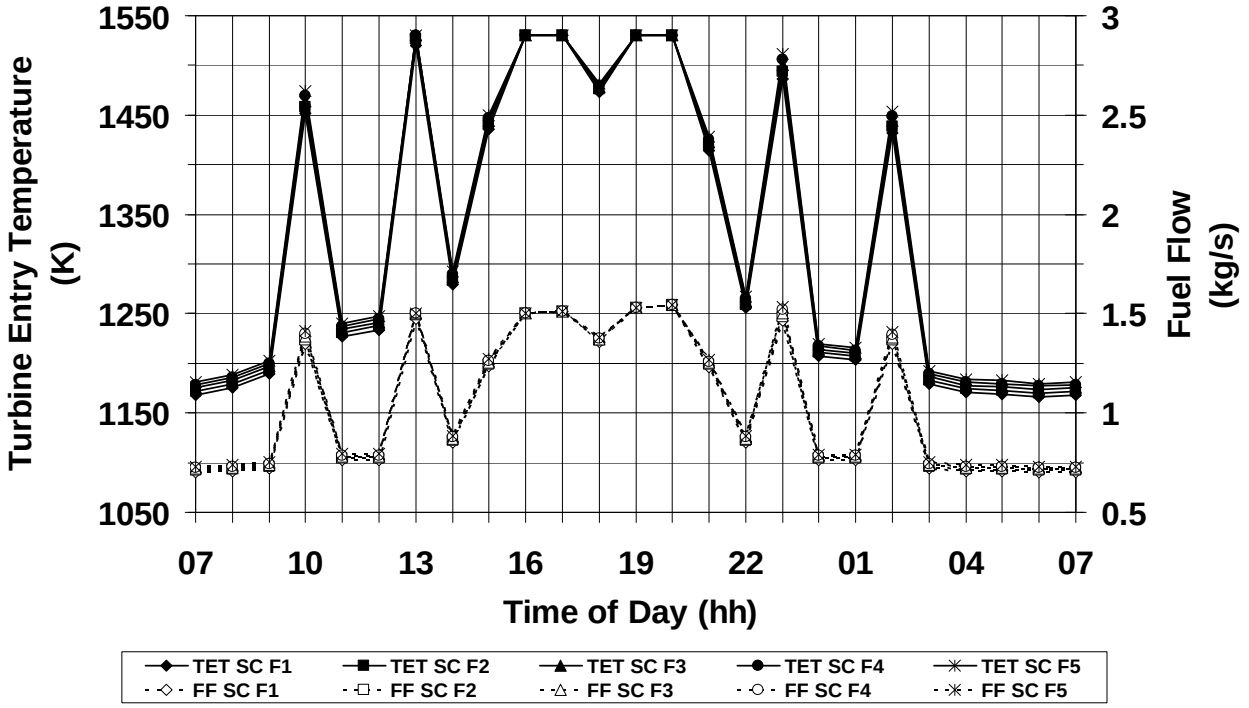

Figure C.6: Simple cycle (SC) - Turbine entry temperature (TET) and fuel flow (FF) variation against time of day, during journey with annual hull fouling progression (F#) and adverse weather conditions

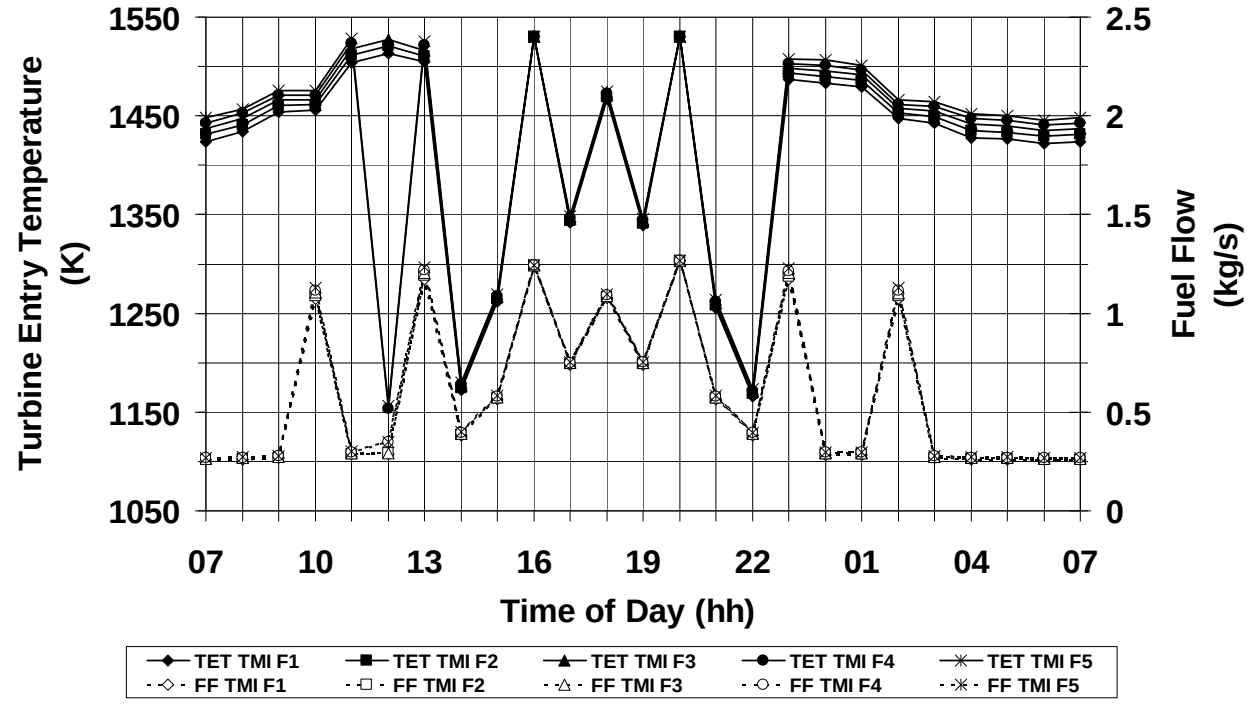

Figure C.7: Twin mode intercooled cycle (TMI) - Turbine entry temperature (TET) and fuel flow (FF) variation against time of day, during journey with annual hull fouling progression (F#) and adverse weather conditions

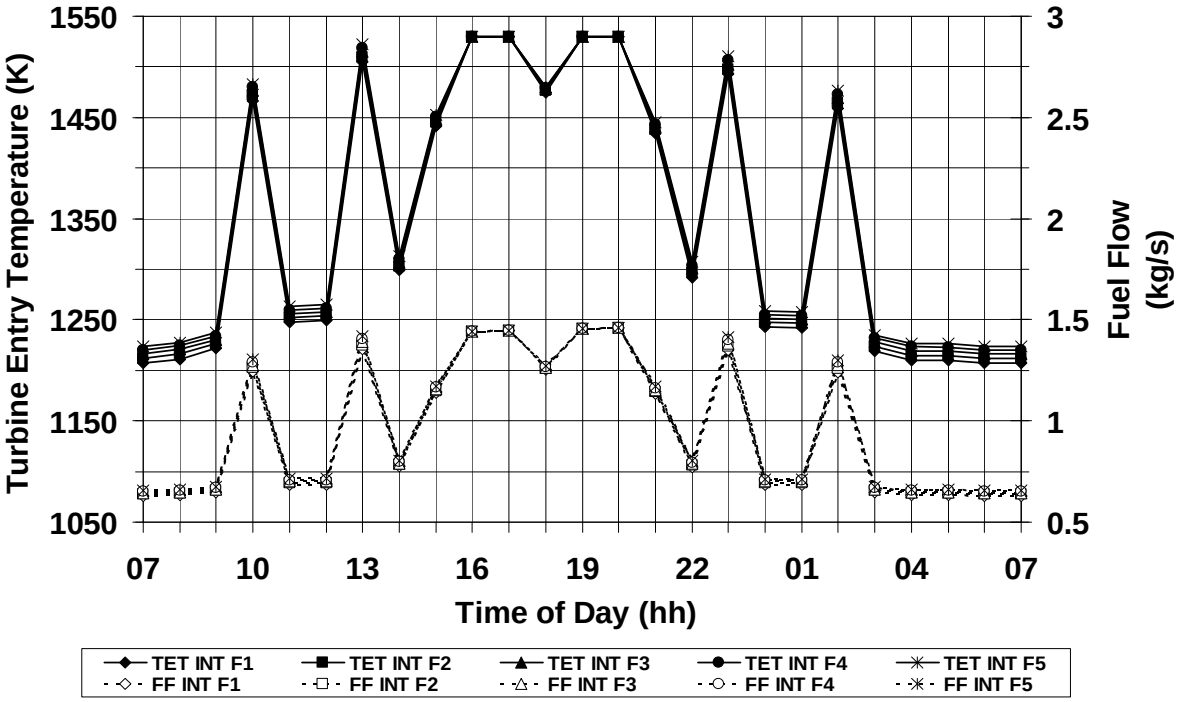

Figure C.8: Intercooled cycle (INT) - Turbine entry temperature (TET) and fuel flow (FF) variation against time of day, during journey with annual hull fouling progression (F#) and adverse weather conditions

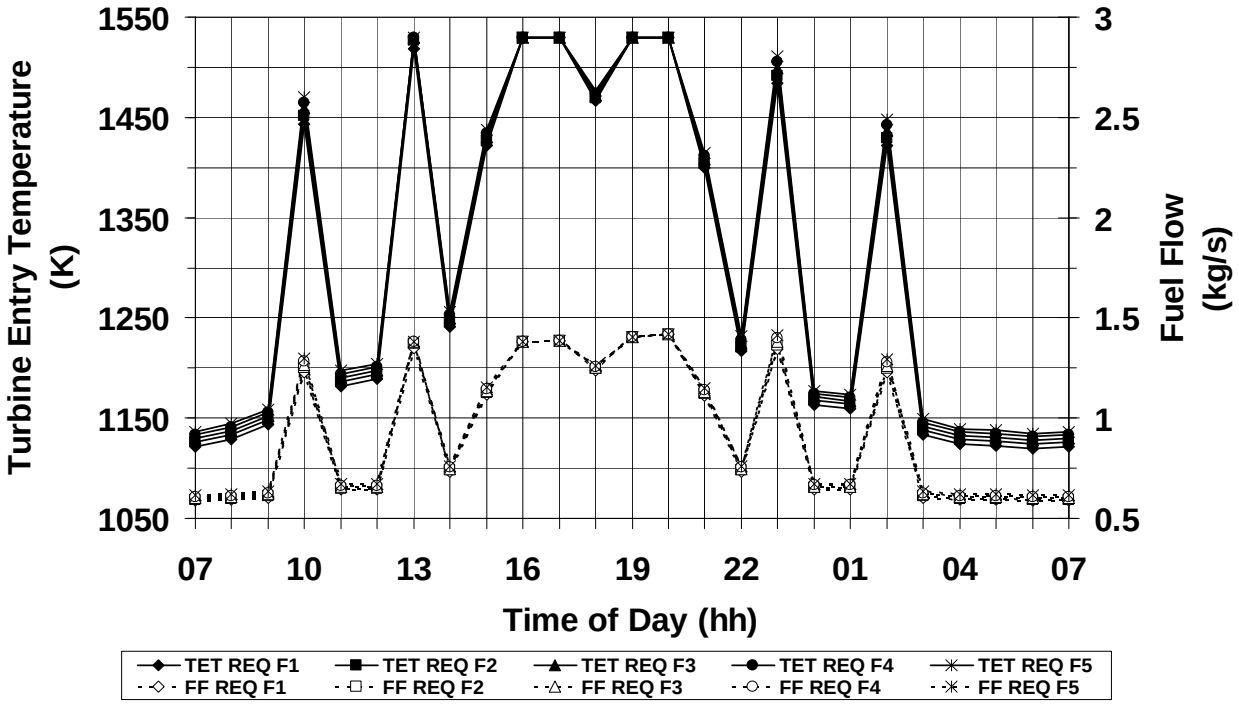

Figure C.9: Recuperated cycle (REQ) - Turbine entry temperature (TET) and fuel flow (FF) variation against time of day, during journey with annual hull fouling progression (F#) and adverse weather conditions

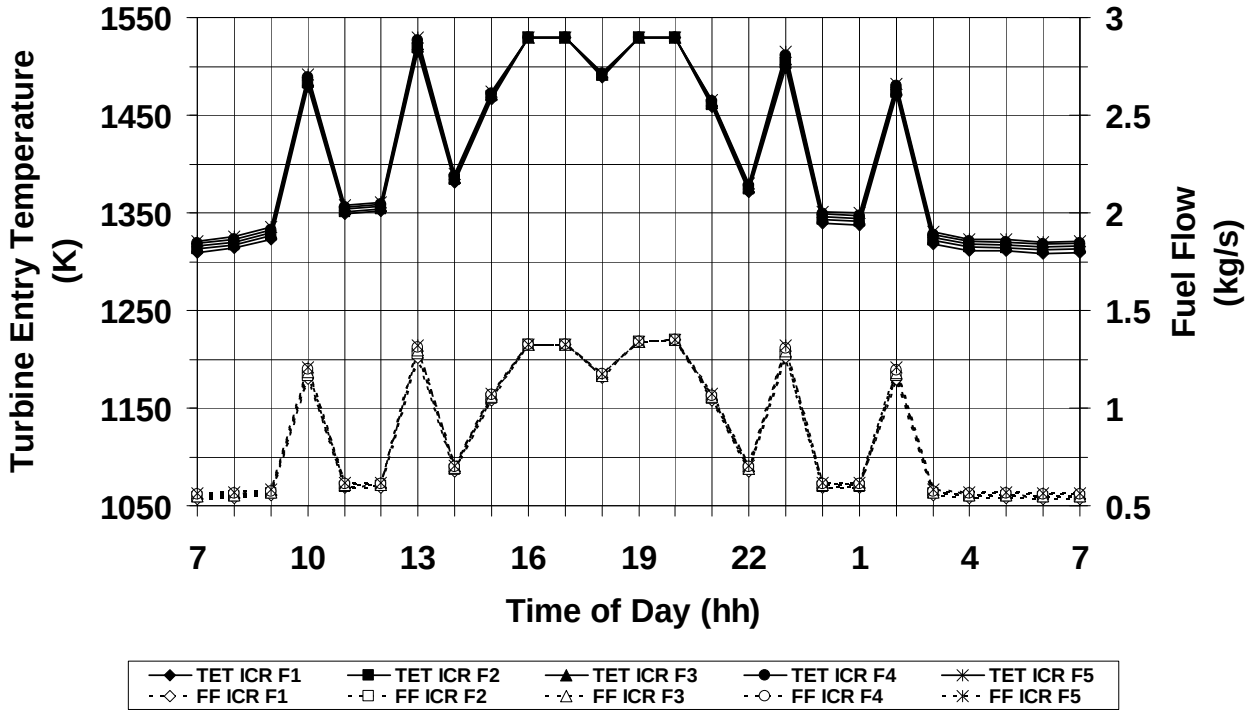

Figure C.10: Intercooled/recuperated cycle (ICR) - Turbine entry temperature (TET) and fuel flow (FF) variation against time of day, during journey with annual hull fouling progression (F#) and adverse weather conditions

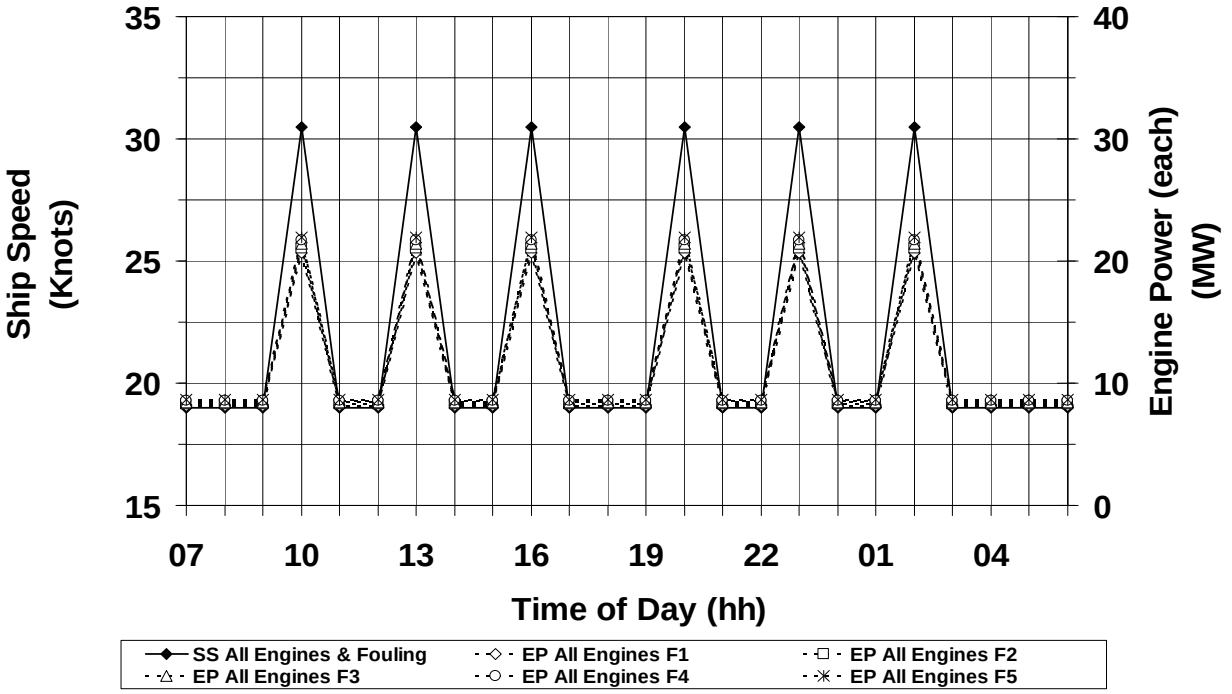

Figure.C.11: All Engines – Ship speed (SS) and Engine power (EP) (for each engine) variation against time of day, during journey with annual hull fouling progression (F#) and ideal weather conditions

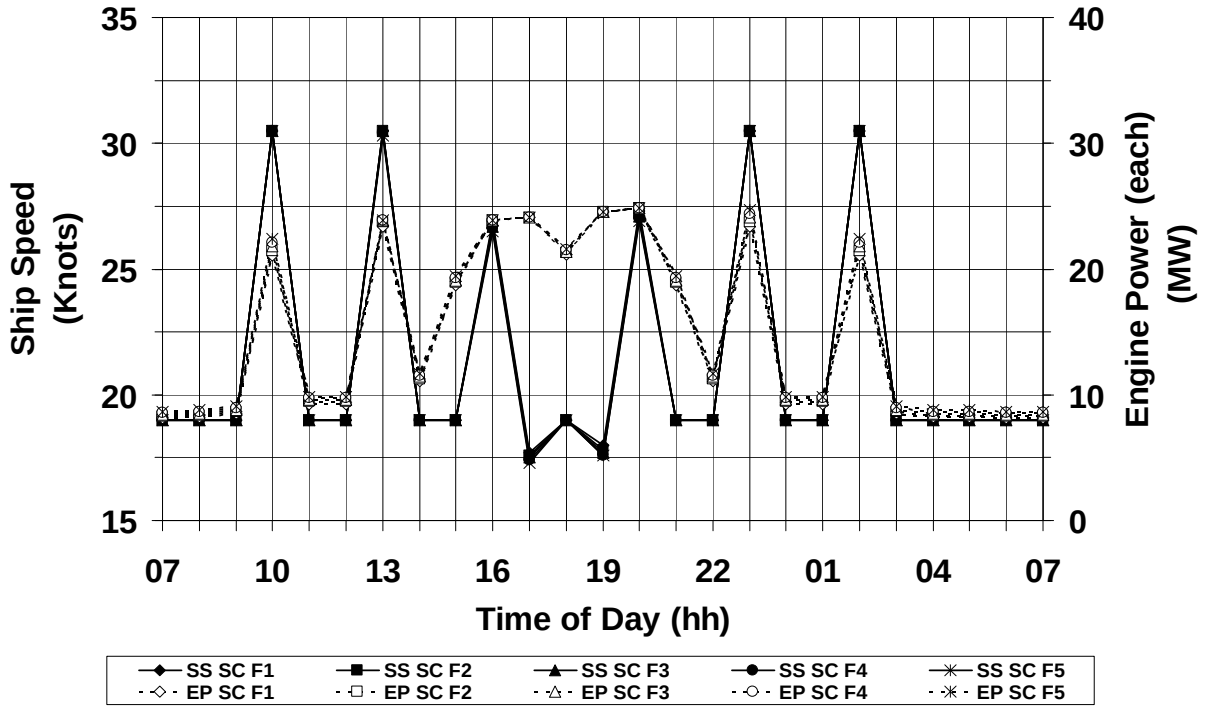

Figure C.12: Simple cycle (SC) – Ship speed (SS) and engine power (EP) (for each engine) variation against time of day, during journey with annual hull fouling progression (F#) and adverse weather conditions

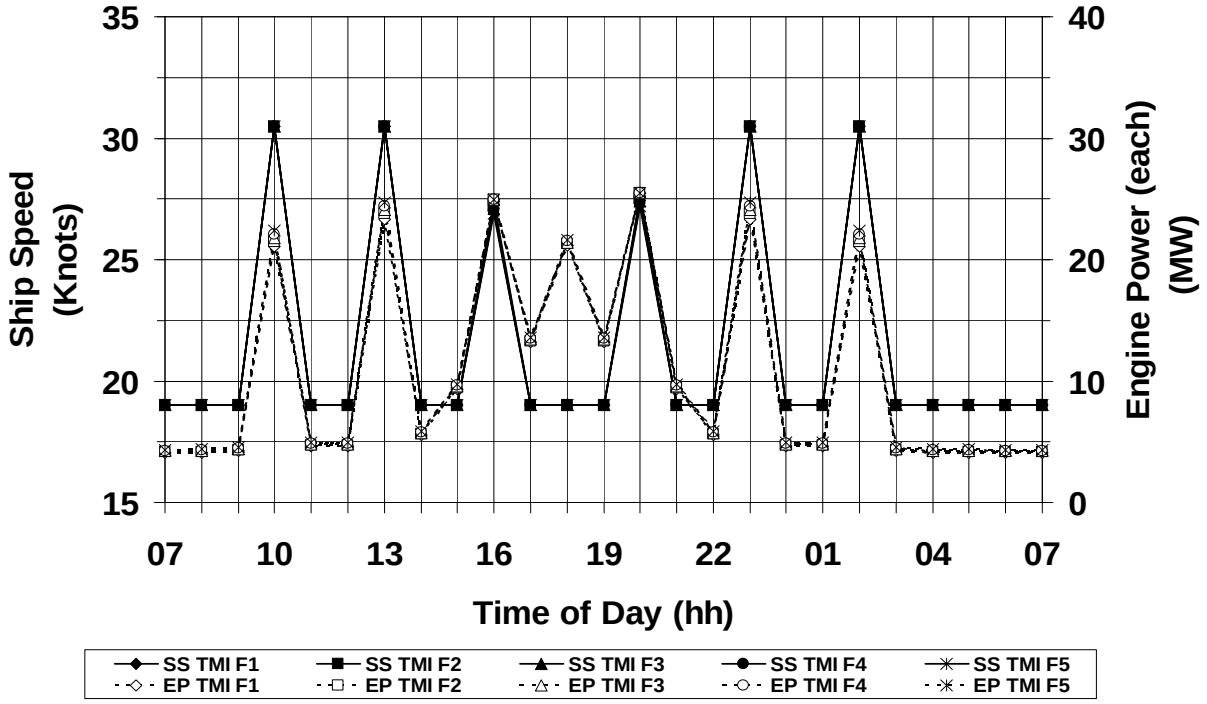

Figure C.13: Twin mode intercooled cycle (TMI) – Ship speed (SS) and engine power (EP) (for each engine) variation against Time of day, during journey with annual hull fouling progression (F#) and adverse weather conditions

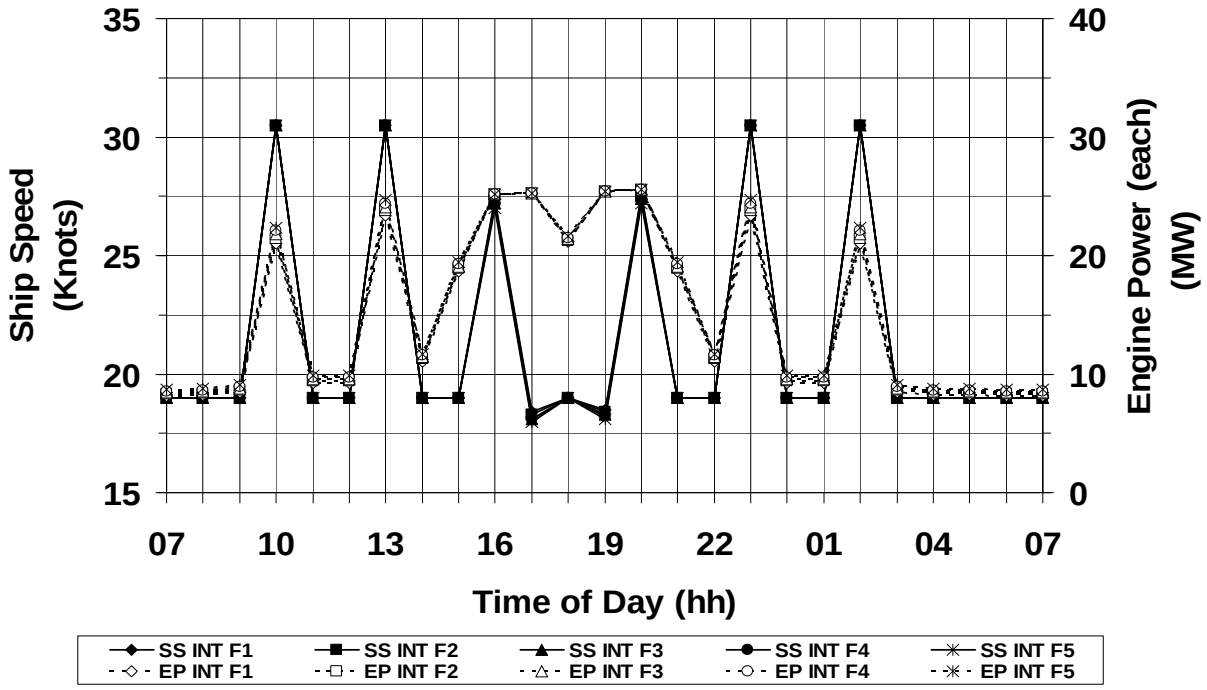

Figure C.14: Intercooled cycle (INT) – Ship speed (SS) and engine power (EP) (for each engine) variation against time of day, during journey with annual hull fouling progression (F#) and adverse weather conditions

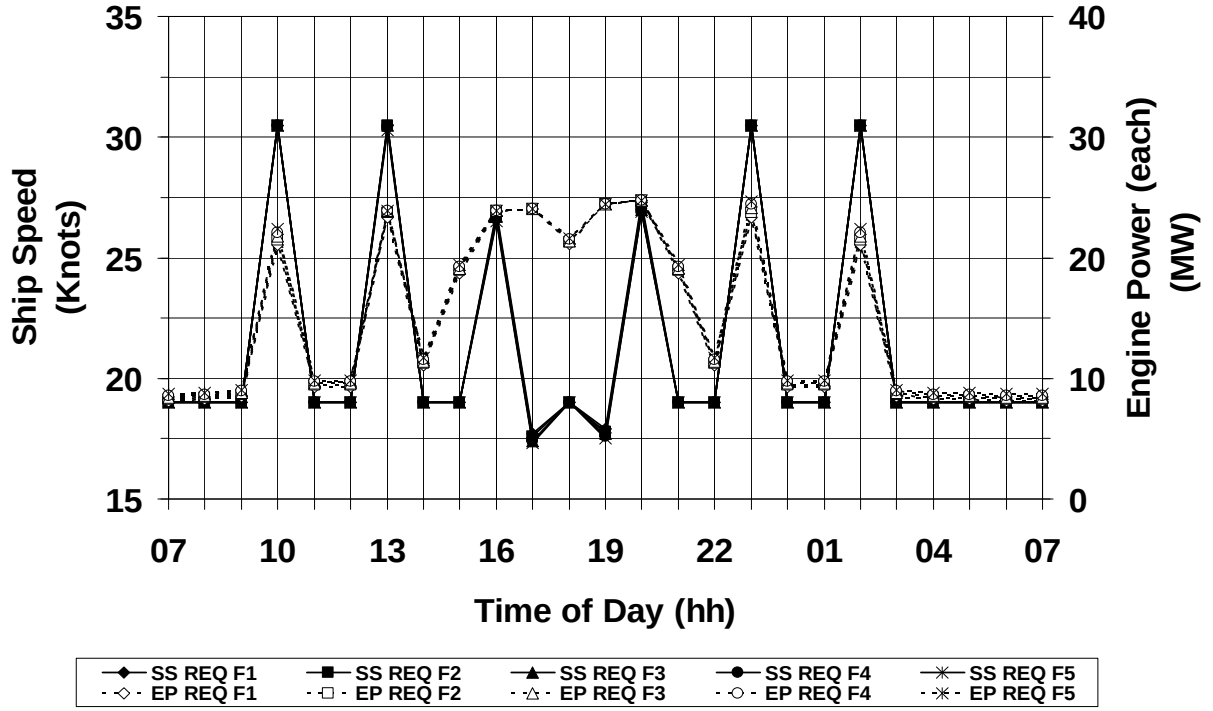

Figure C.15: Recuperated cycle (REQ) – Ship speed (SS) and engine power (EP) (for each engine) variation against time of day, during journey with annual hull fouling progression (F#) and adverse weather conditions

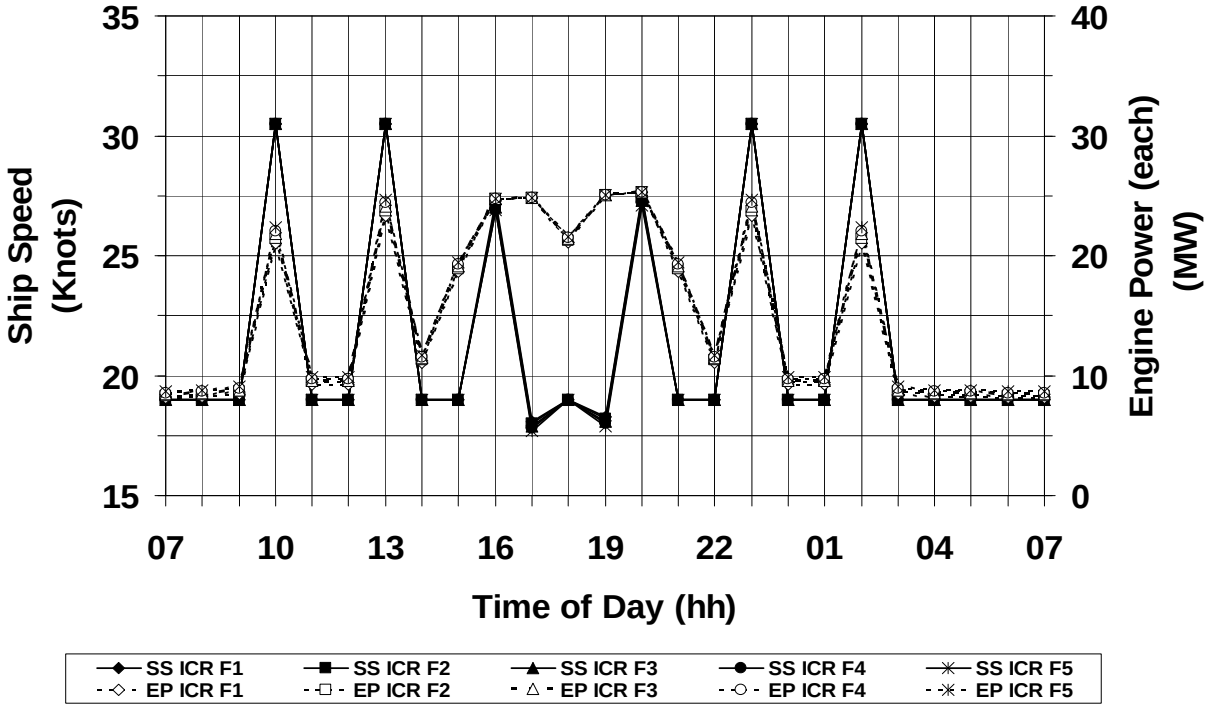

Figure C.16: Intercooled/recuperated cycle (ICR) – Ship speed (SS) and engine power (EP) (for each engine) variation against time of day, during journey with annual hull Fouling progression (F#) and adverse weather conditions

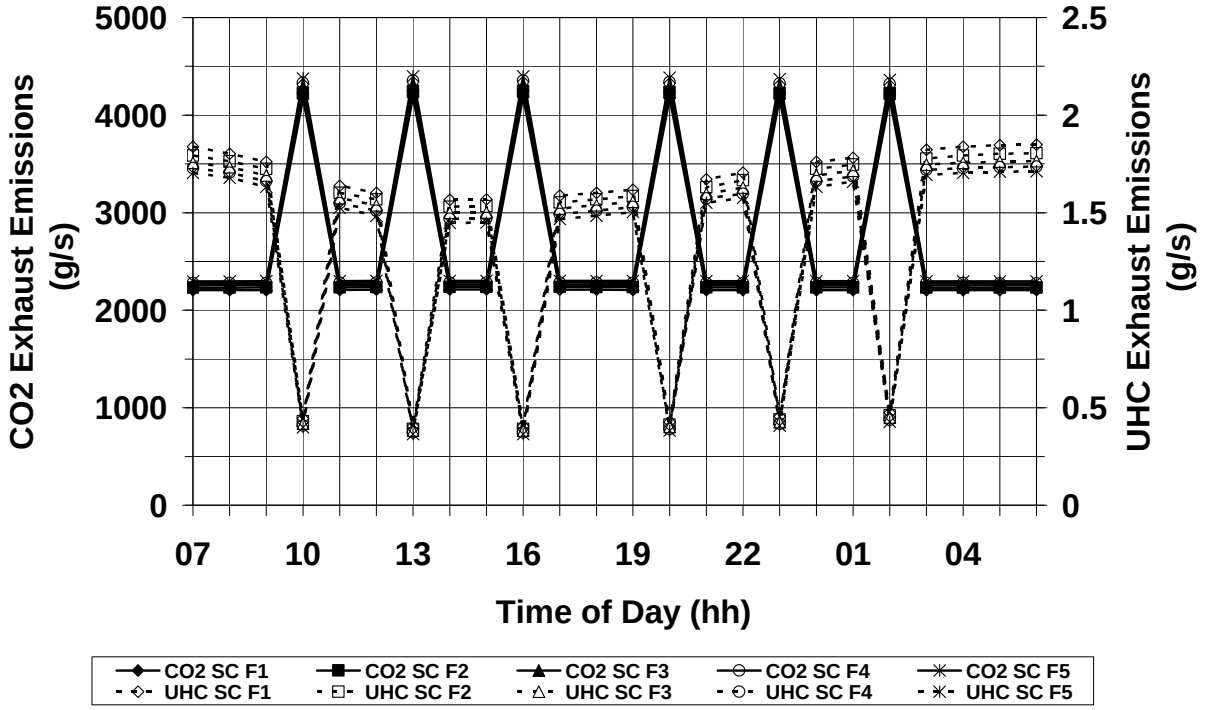

Figure C.17: Simple cycle (SC) – Carbon dioxide (CO2) and unburned hydrocarbons (UHC) exhaust emissions variation against time of day, during journey with annual hull fouling progression (F#) and ideal weather conditions

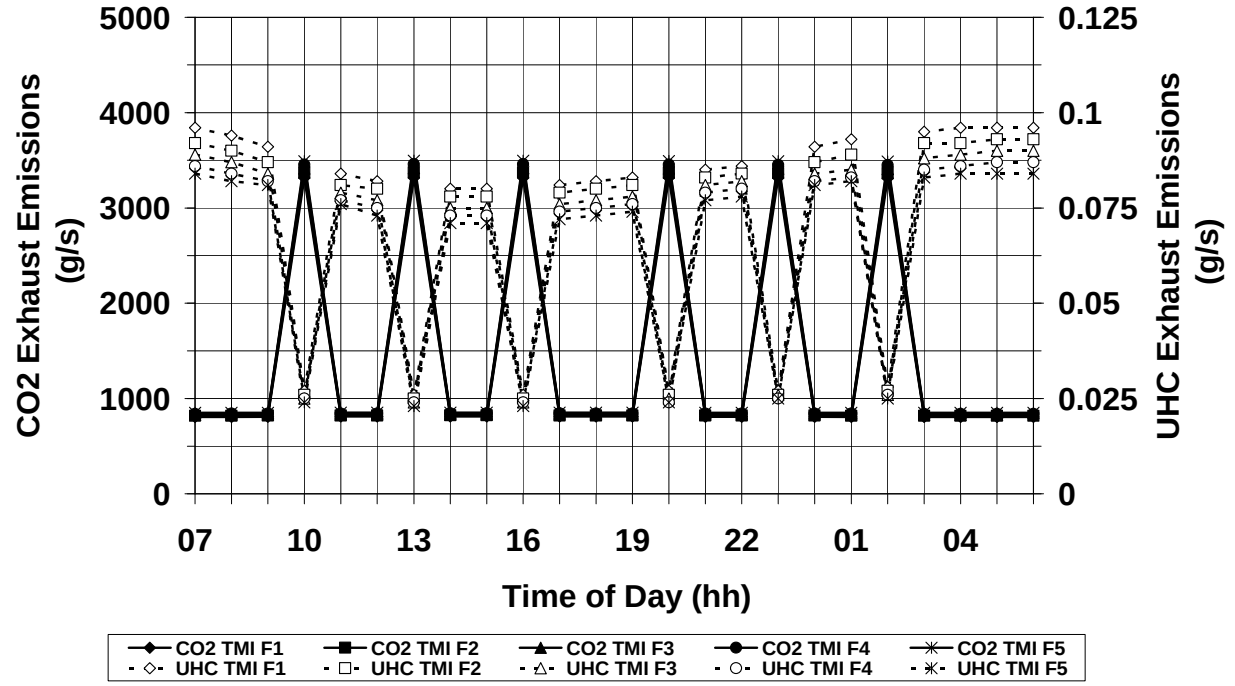

Figure C.18: Twin mode intercooled cycle (TMI) – Carbon dioxide (CO2) and unburned Hydrocarbons (UHC) exhaust emissions variation against time of day, during journey with annual hull fouling progression (F#) and ideal weather conditions

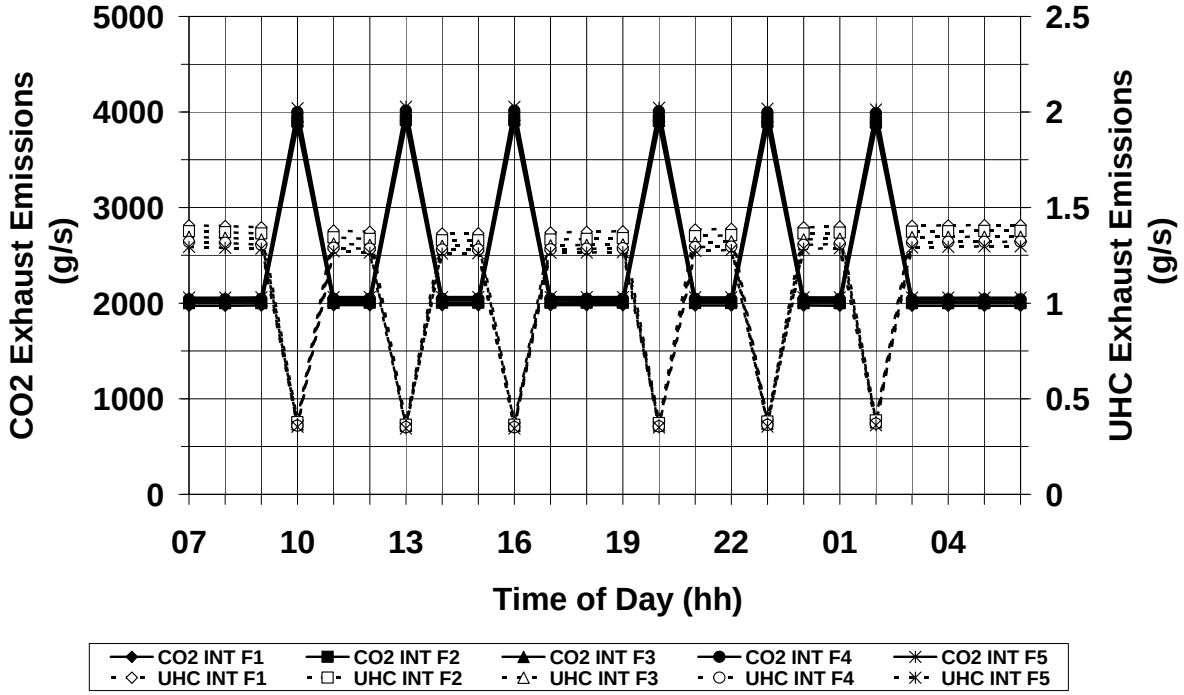

Figure C.19: Intercooled cycle (INT) – Carbon dioxide (CO2) and unburned hydrocarbons (UHC) exhaust emissions variation against time of day, during journey with annual hull fouling progression (F#) and ideal weather conditions

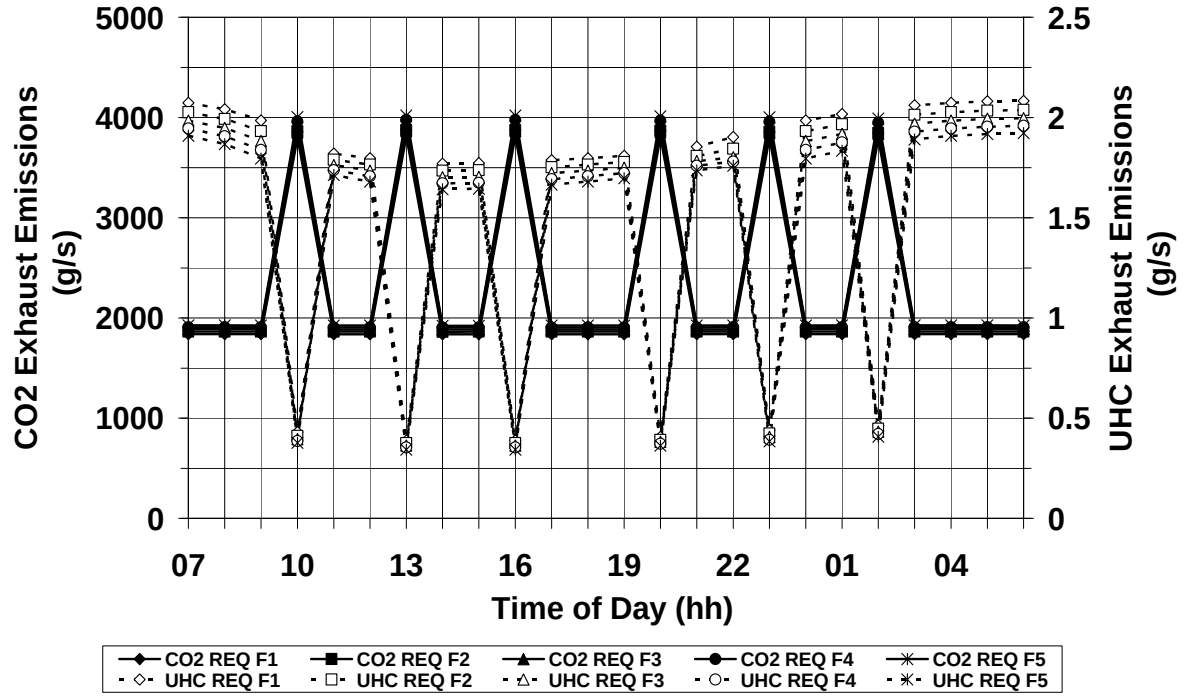

Figure C.20: Requperated cycle (REQ) – Carbon dioxide (CO2) and unburned hydrocarbons (UHC) exhaust emissions variation against time of day, during journey with annual hull fouling progression (F#) and ideal weather conditions

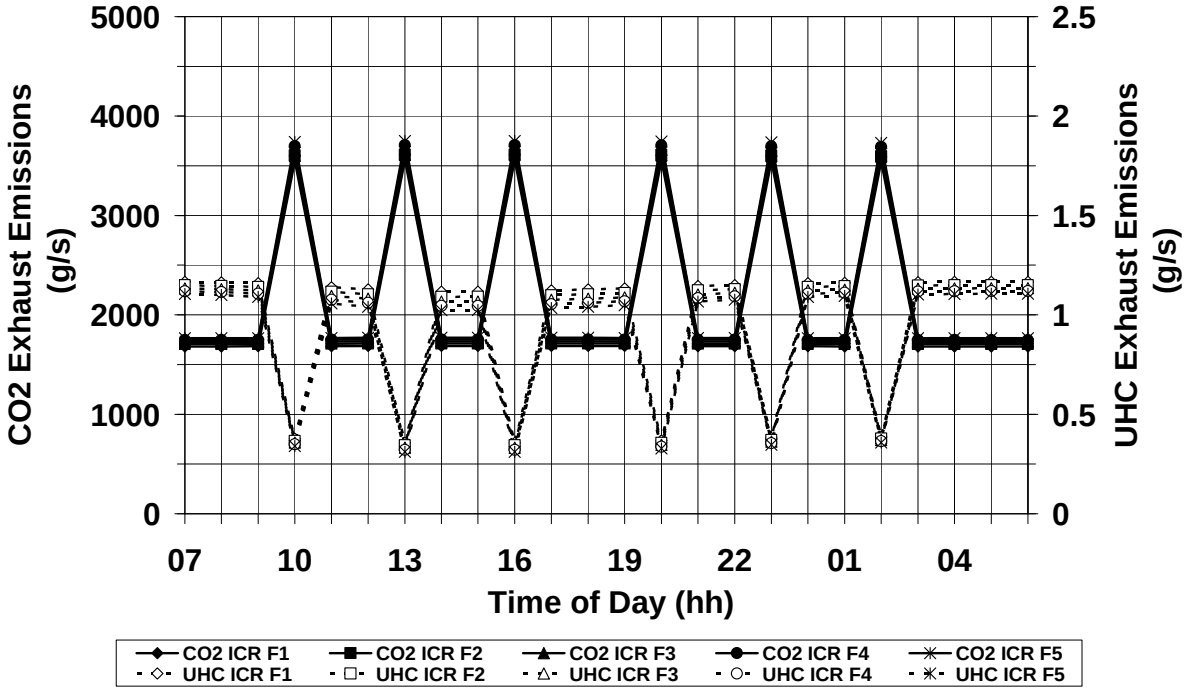

Figure C.21: Intercooled/recuperated cycle (ICR) – Carbon dioxide (CO2) and unburned hydrocarbons (UHC) exhaust emissions variation against time of day, during journey with annual hull fouling progression (F#) and ideal weather conditions

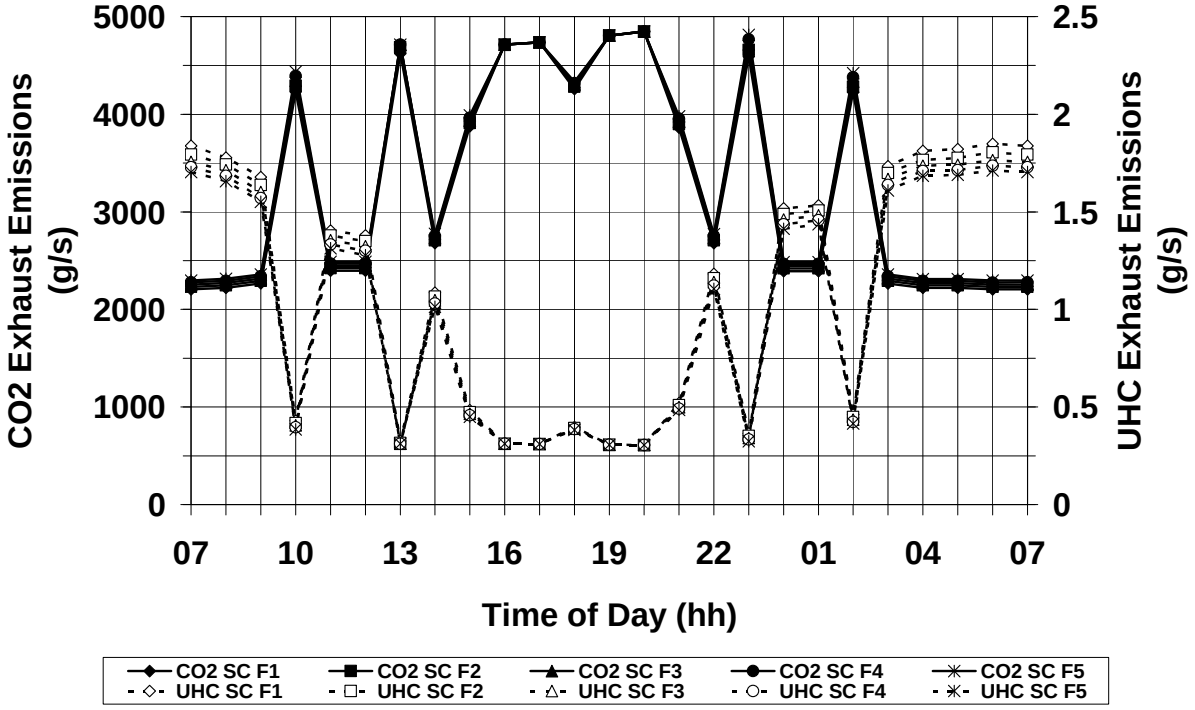

Figure C.22: Simple cycle (SC) – Carbon dioxide (CO2) and unburned hydrocarbons (UHC) exhaust emissions variation against time of day, during journey with annual hull fouling progression (F#) and adverse weather conditions

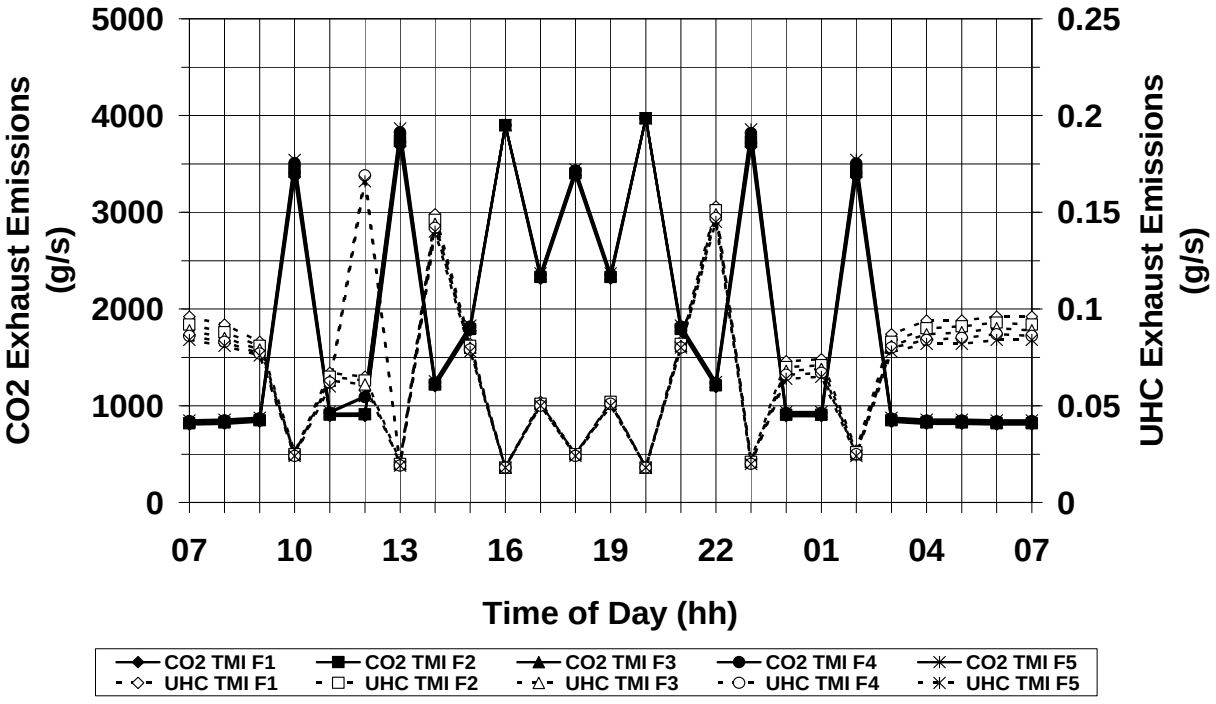

Figure C.23: Twin mode intercooled cycle (TMI) – Carbon dioxide (CO2) and unburned hydrocarbons (UHC) exhaust emissions variation against time of day, during journey with annual hull fouling progression (F#) and adverse weather conditions

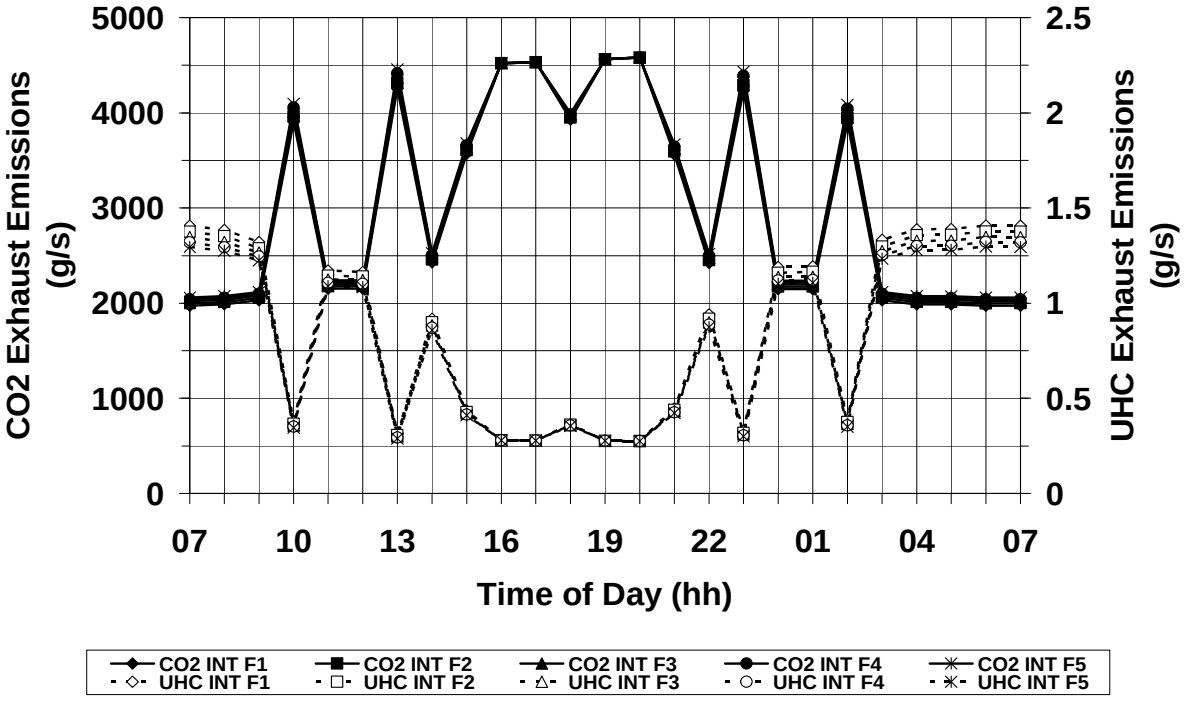

Figure C.24: Intercooled cycle (INT) – Carbon dioxide (CO2) and unburned hydrocarbons (UHC) exhaust emissions variation against time of day, during journey with annual hull fouling progression (F#) and adverse weather conditions

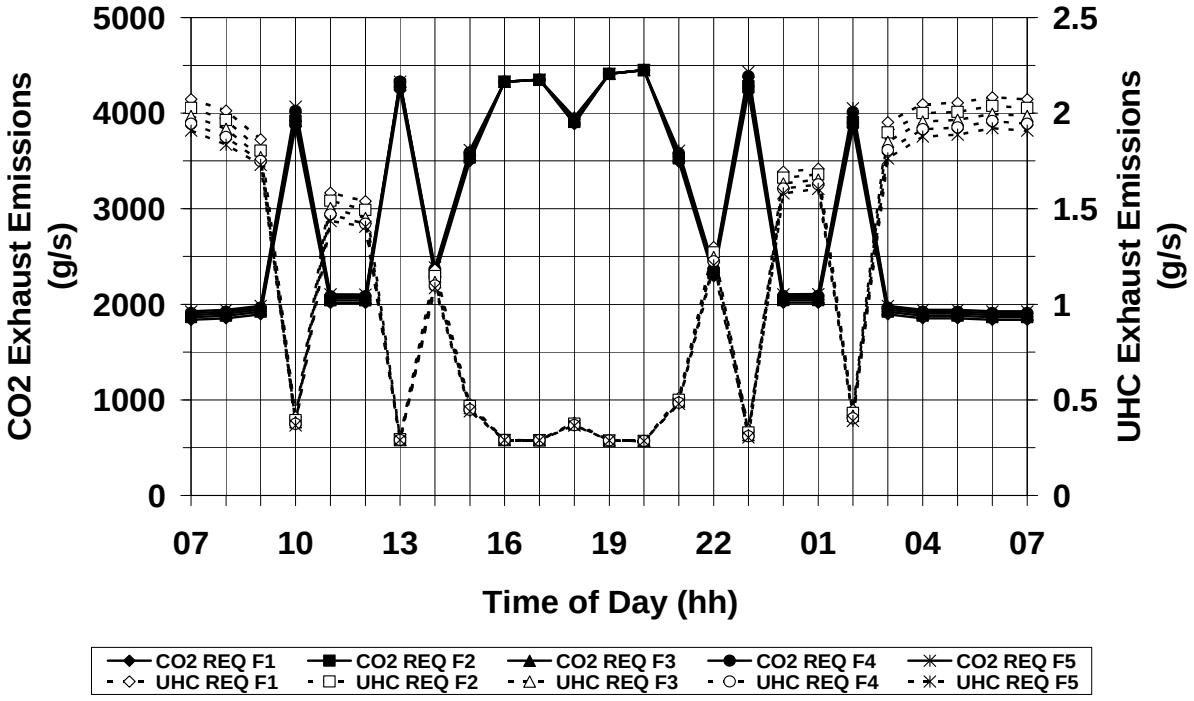

Figure C.25: Recuperated cycle (REQ) – Carbon dioxide (CO2) and unburned hydrocarbons (UHC) exhaust emissions variation against time of day, during journey with annual hull fouling progression (F#) and adverse weather conditions

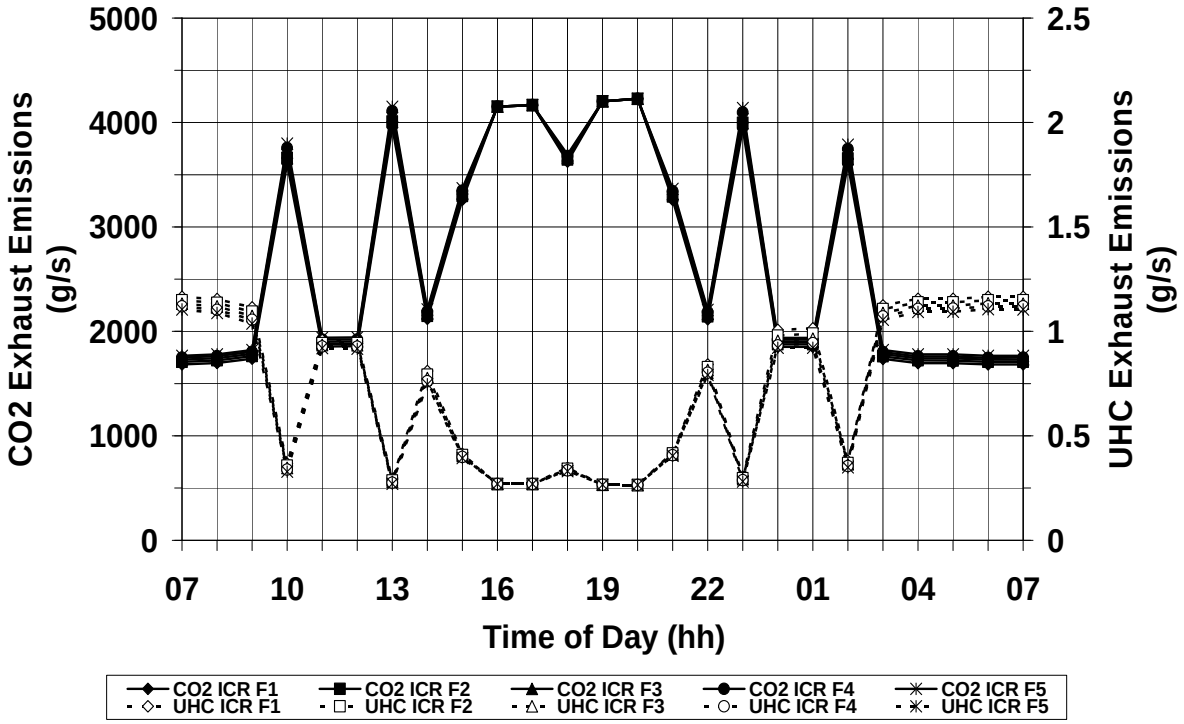

Figure C.26: Intercooled/recuperated cycle (ICR) – Carbon dioxide (CO2) and unburned hydrocarbons (UHC) exhaust emissions variation against time of day, during journey with annual hull fouling progression (F#) and adverse weather conditions

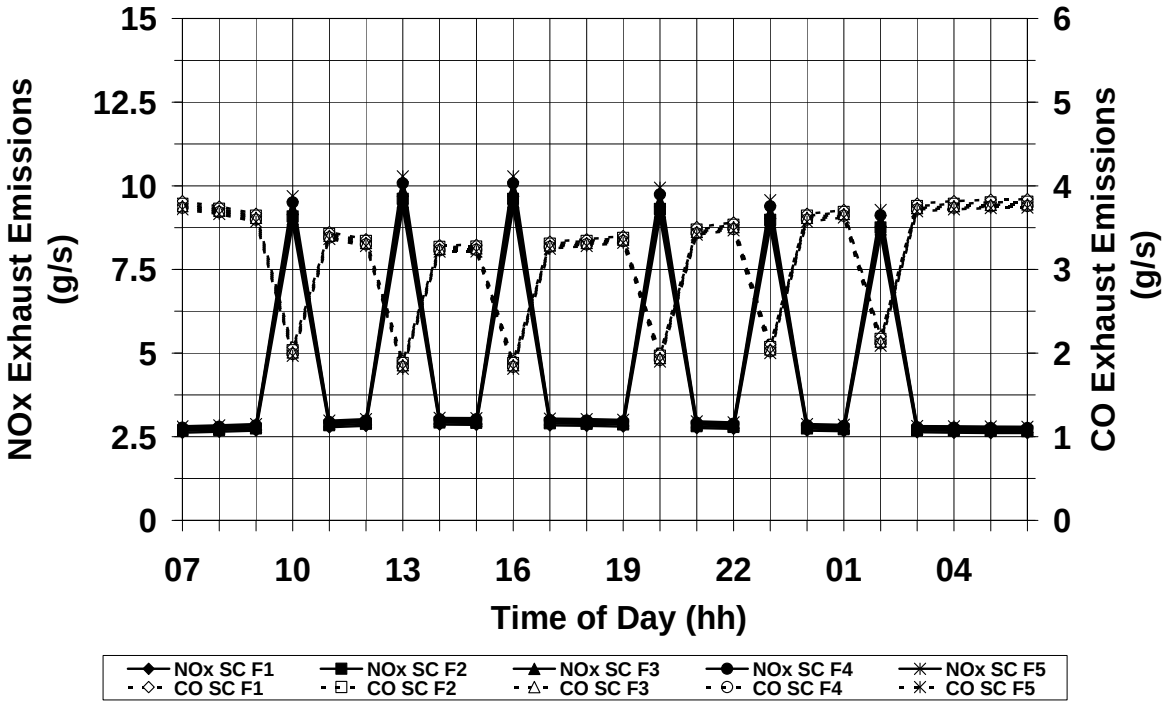

Figure C.27: Simple cycle (SC) – Nitric oxide (NOx) and carbon monoxide (CO) exhaust emissions variation against time of day, during journey with annual hull fouling progression (F#) and ideal weather conditions

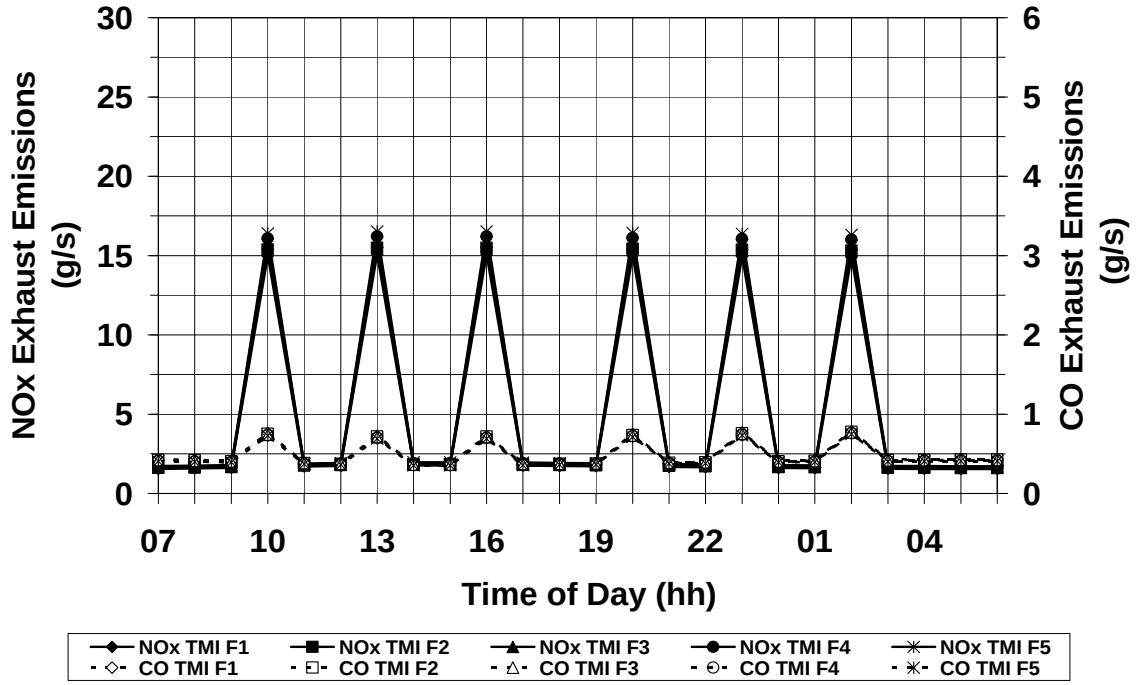

Figure C.28: Twin mode intercooled cycle (TMI) – Nitric oxide (NOx) and carbon monoxide (CO) exhaust emissions variation against time of day, during journey with annual hull fouling progression (F#) and ideal weather conditions

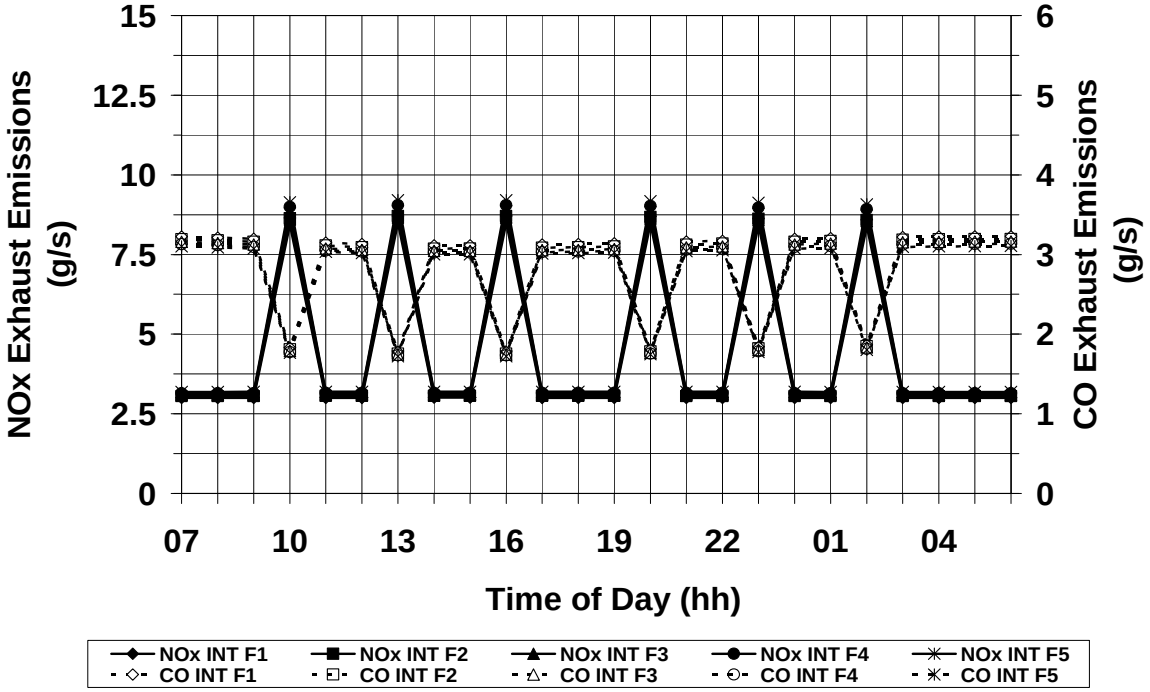

Figure C.29: Intercooled cycle (INT) – Nitric oxide (NOx) and carbon monoxide (CO) exhaust emissions variation against time of day, during journey with annual hull fouling progression (F#) and ideal weather conditions

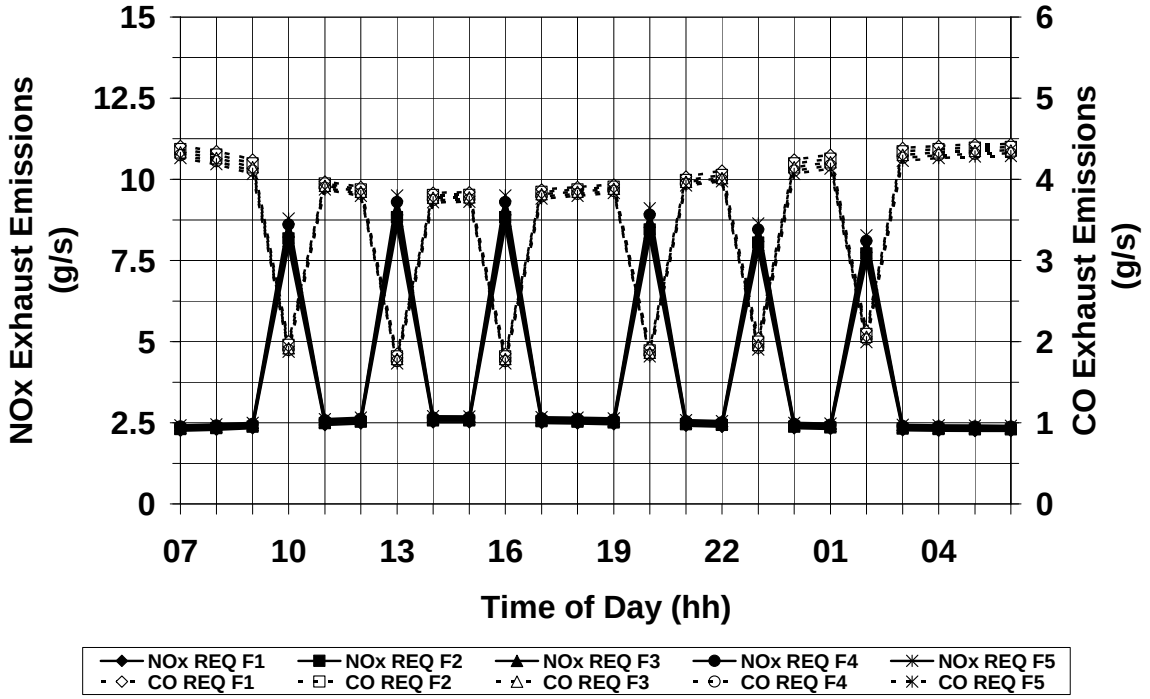

Figure C.30: Recuperated cycle (REQ) – Nitric Oxide (NOx) and carbon monoxide (CO) exhaust emissions variation against time of day, during journey with annual hull fouling progression (F#) and ideal weather conditions

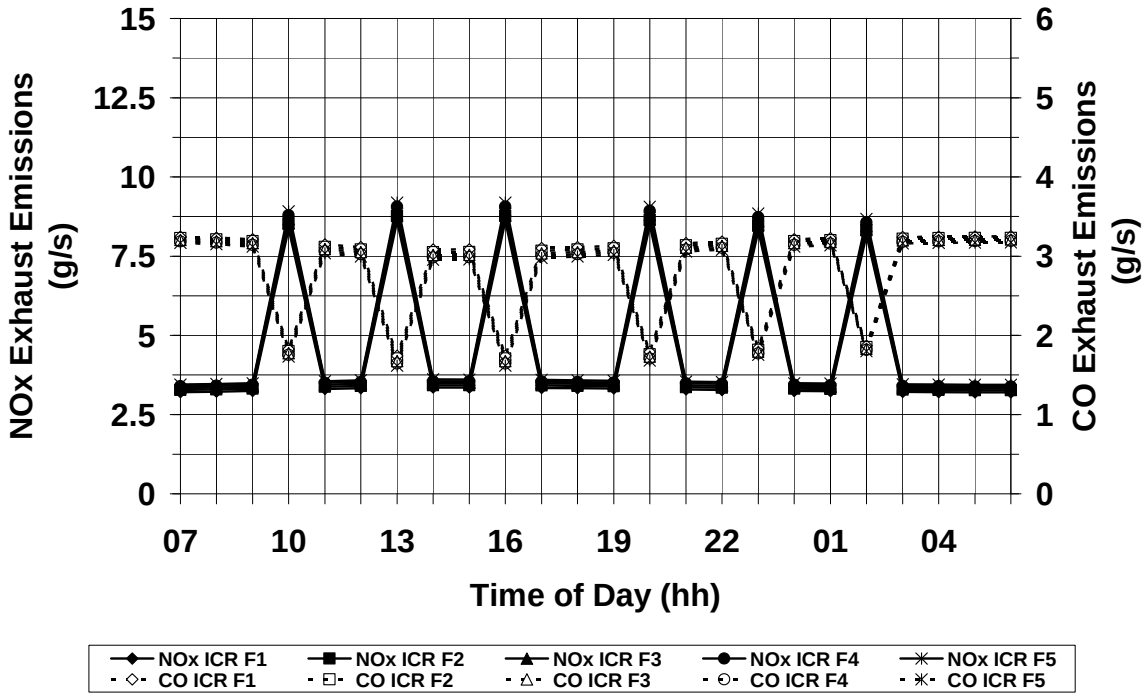

Figure C.31: Intercooled/recuperated cycle (ICR) – Nitric oxide (NOx) and carbon monoxide (CO) exhaust emissions variation against time of day, during journey with annual hull fouling progression (F#) and ideal weather conditions

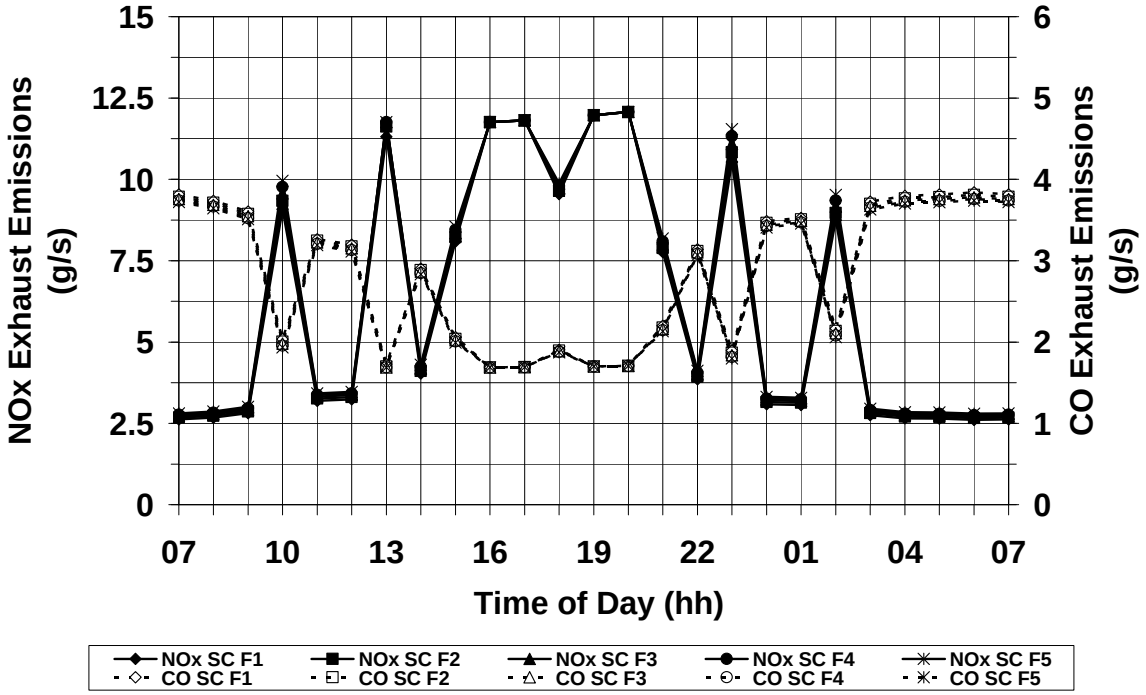

Figure C.32: Simple cycle (SC) – Nitric oxide (NOx) and carbon monoxide (CO) exhaust emissions variation against time of day, during journey with annual hull fouling progression (F#) and adverse weather conditions

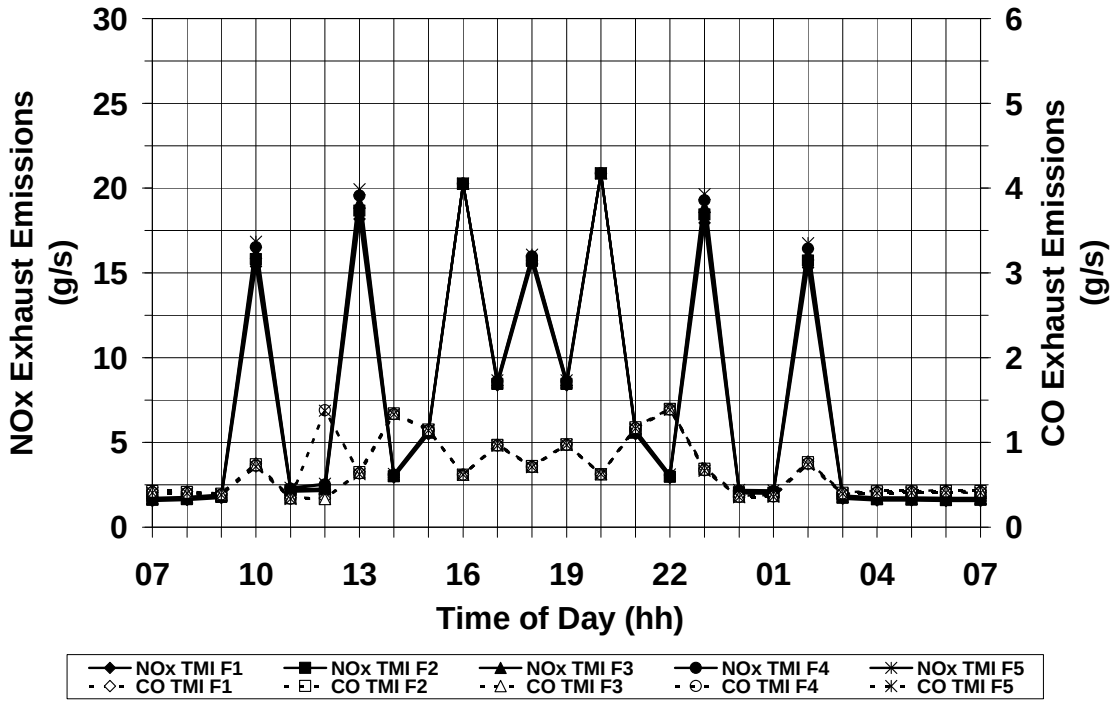

Figure C.33: Twin mode intercooled cycle (TMI) – Nitric oxide (NOx) and carbon monoxide (CO) exhaust emissions variation against time of day, during journey with annual hull fouling progression (F#) and adverse weather conditions

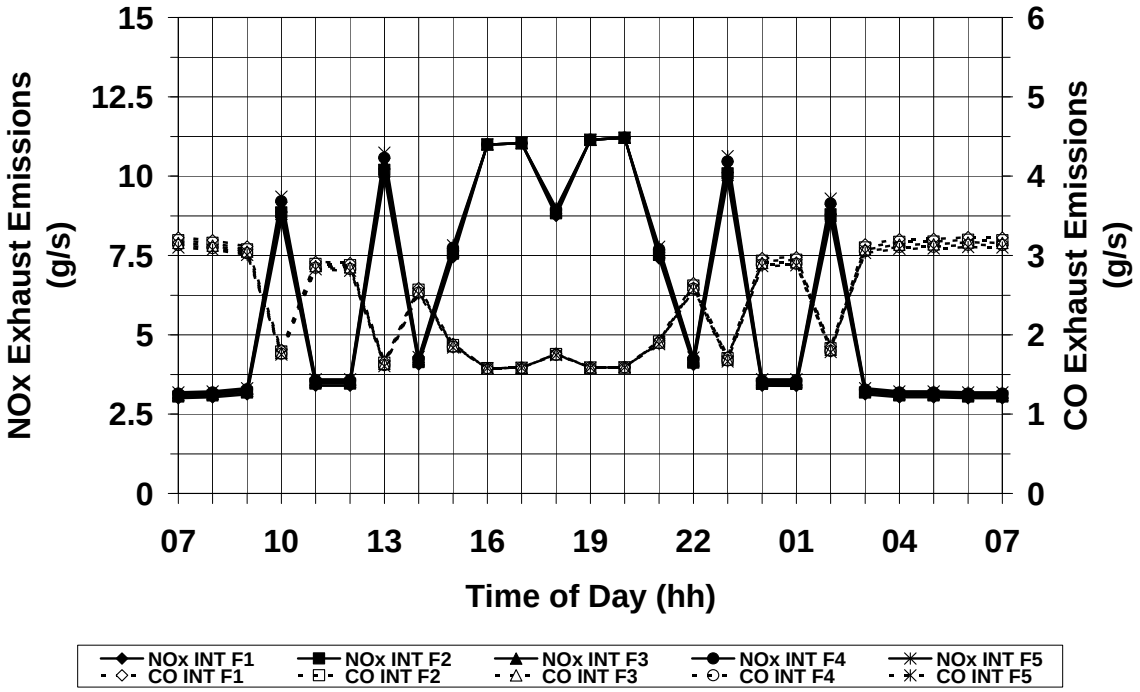

Figure C.34: Intercooled cycle (INT) – Nitric oxide (NOx) and carbon monoxide (CO) exhaust emissions variation against time of day, during journey with annual hull fouling progression (F#) and adverse weather conditions

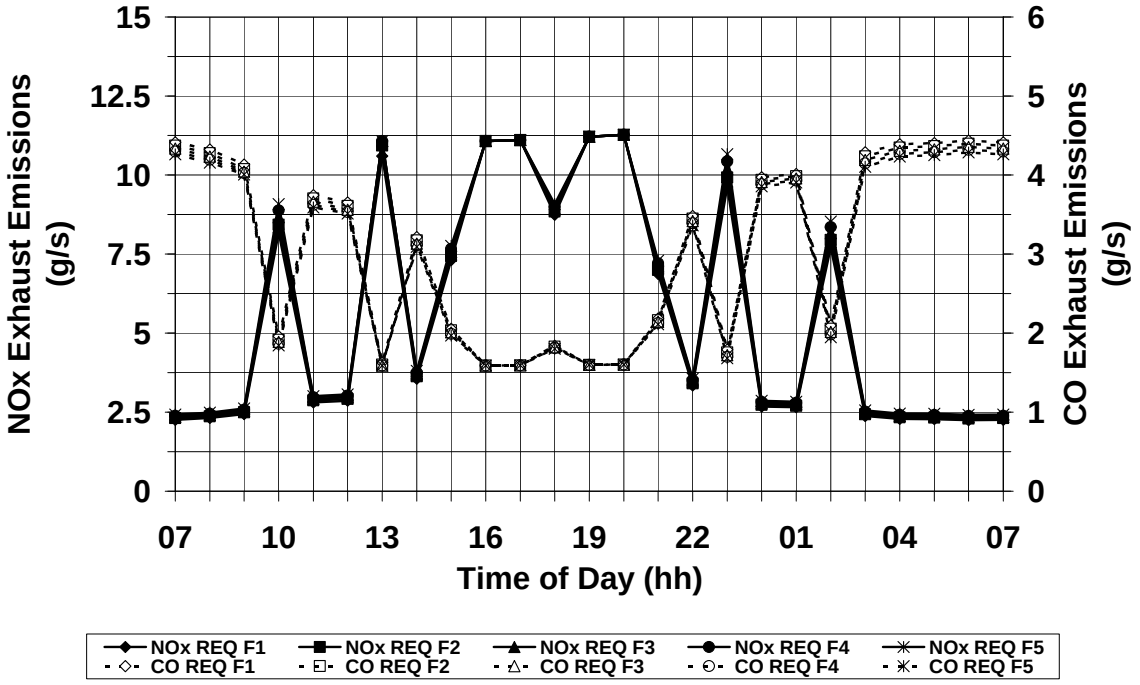

Figure C.35: Recuperated cycle (REQ) – Nitric oxide (NOx) and carbon monoxide (CO) exhaust emissions variation against time of day, during journey with annual hull fouling progression (F#) and adverse weather conditions

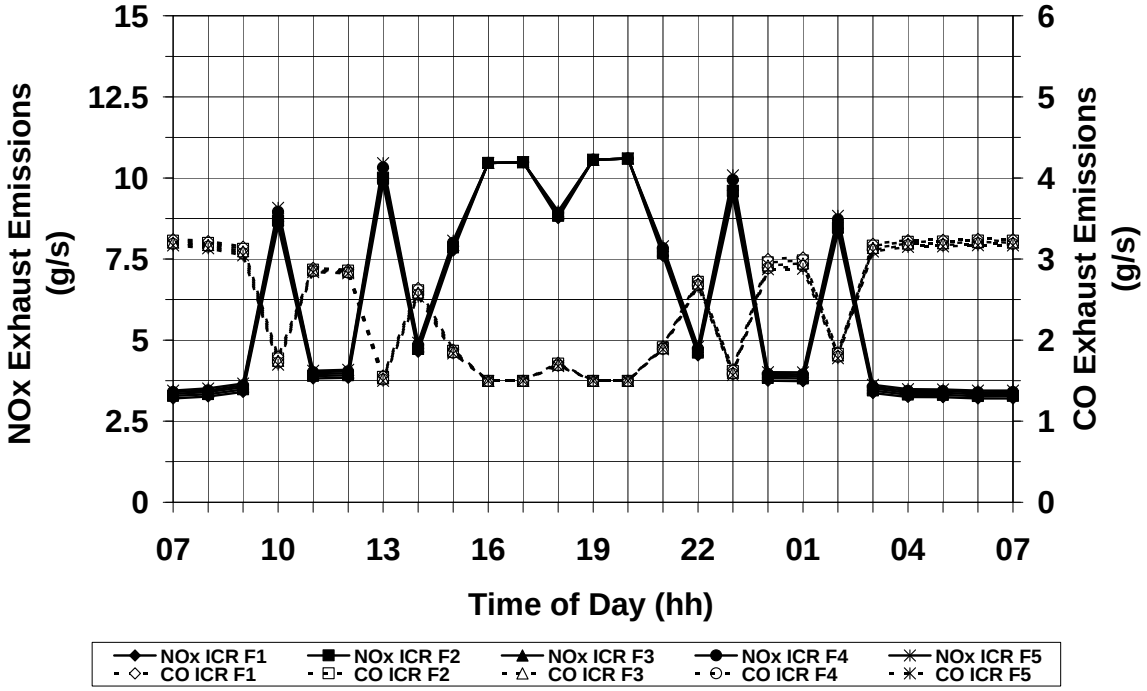

Figure C.36: Intercooled/recuperated cycle (ICR) – Nitric oxide (NOx) and carbon monoxide (CO) exhaust emissions variation against time of day, during journey with annual hull fouling progression (F#) and adverse weather conditions

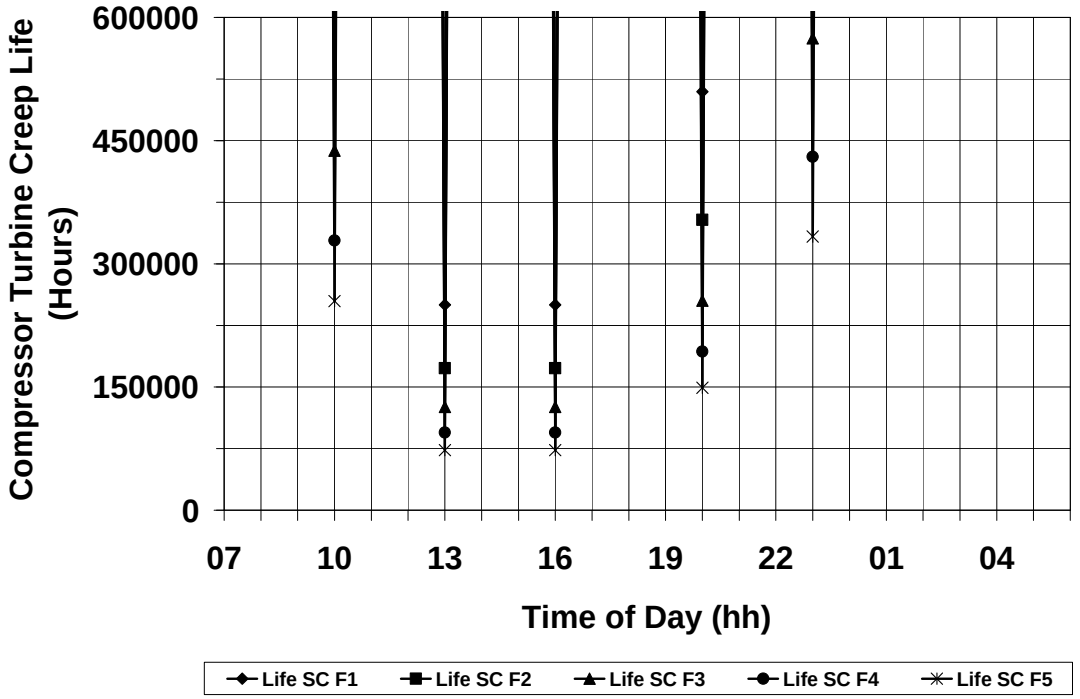

Figure C.37: Simple cycle (SC) – Compressor turbine creep life variation against time of day, during journey with annual hull fouling progression (F#) and ideal weather conditions

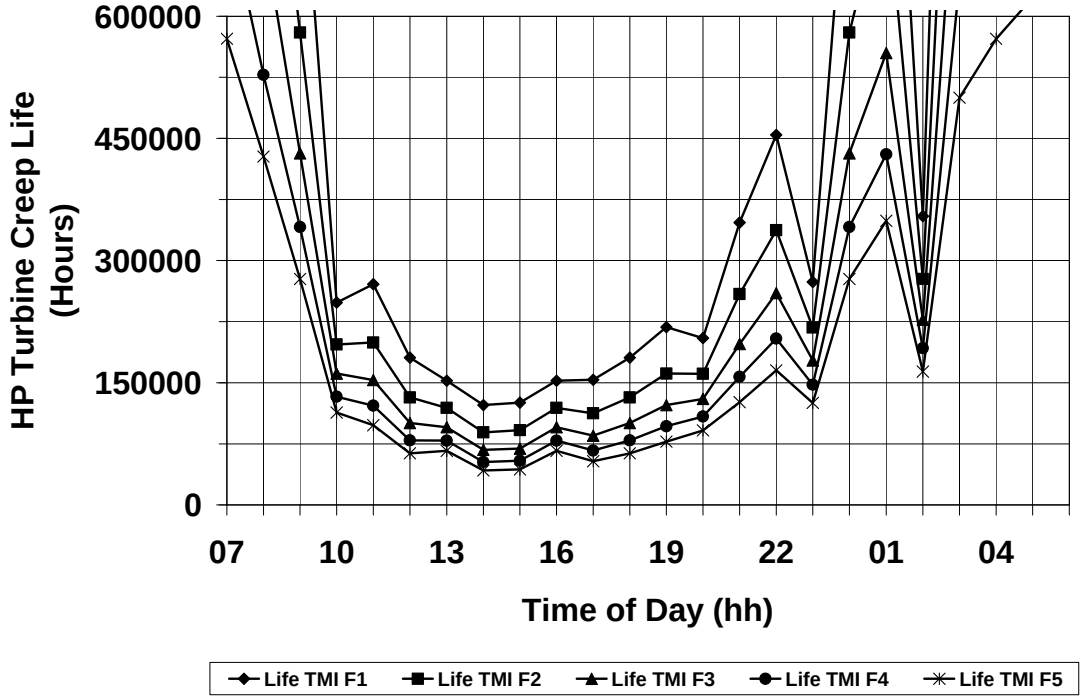

Figure C.38: Twin mode intercooled cycle (TMI) – HP turbine creep life variation against Time of day, during journey with annual hull fouling progression (F#) and ideal weather conditions

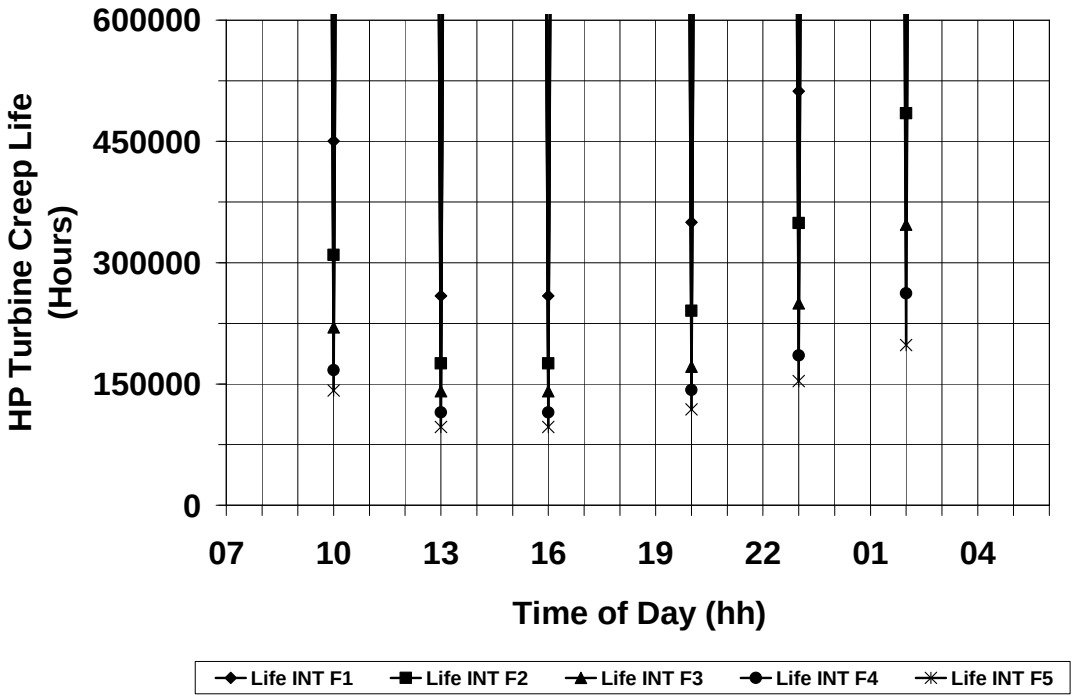

Figure C.39: Intercooled cycle (INT) – HP Turbine creep life variation against time of day, during journey with annual hull fouling progression (F#) and ideal weather conditions

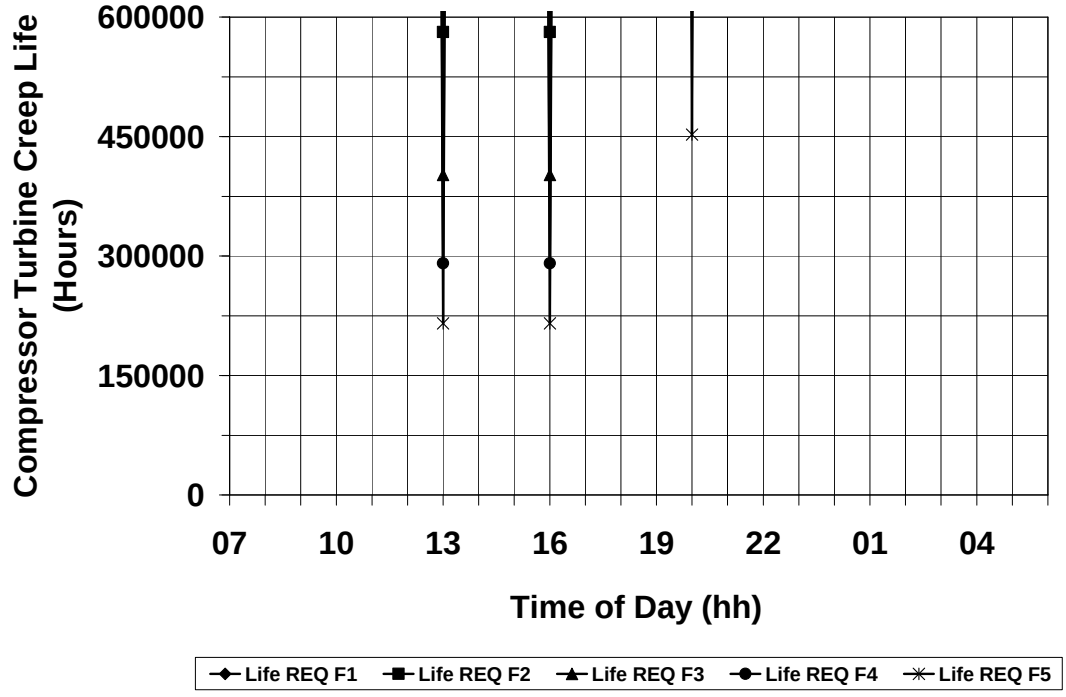

Figure C.40: Recuperated cycle (REQ) – Compressor turbine creep life variation against time of day, during journey with annual hull fouling progression (F#) and ideal weather conditions

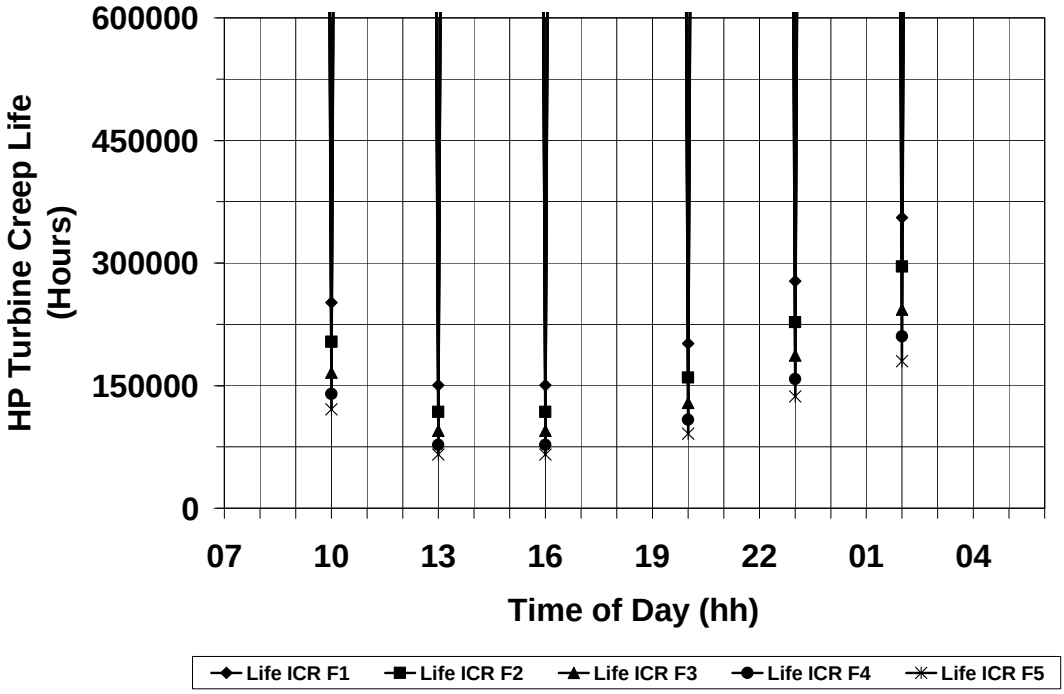

Figure C.41: Intercooled/recuperated cycle (ICR) – HP turbine creep life variation against time of day, during journey with annual hull fouling progression (F#) and ideal weather conditions

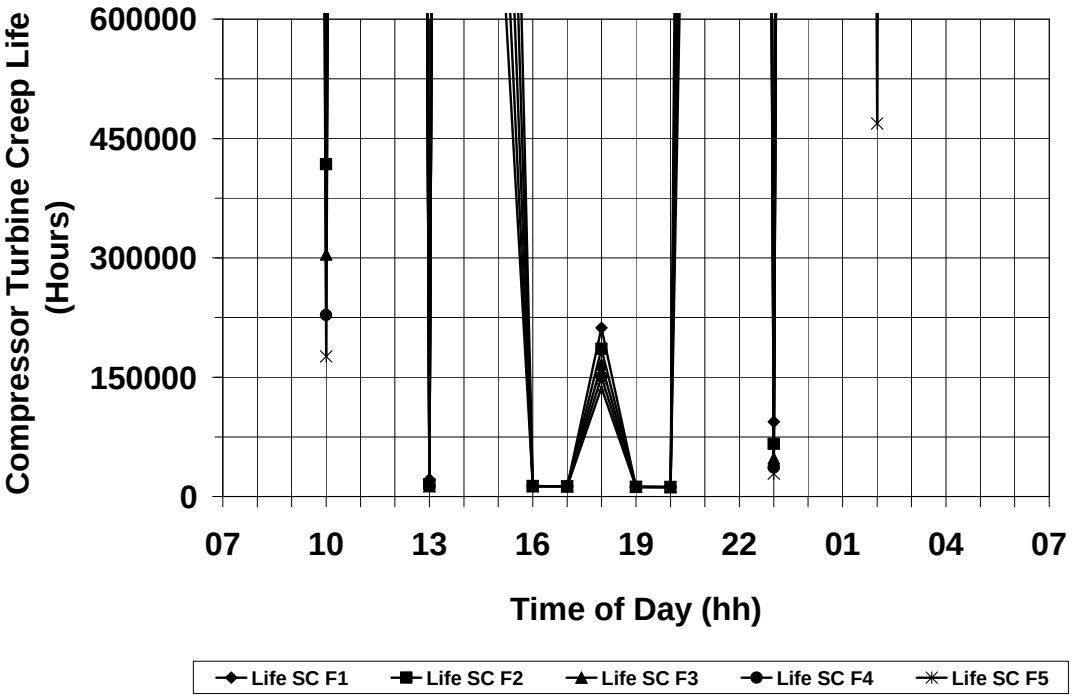

Figure C.42: Simple cycle (SC) – Compressor turbine creep life variation against time of day, during journey with annual hull fouling progression (F#) and weather conditions

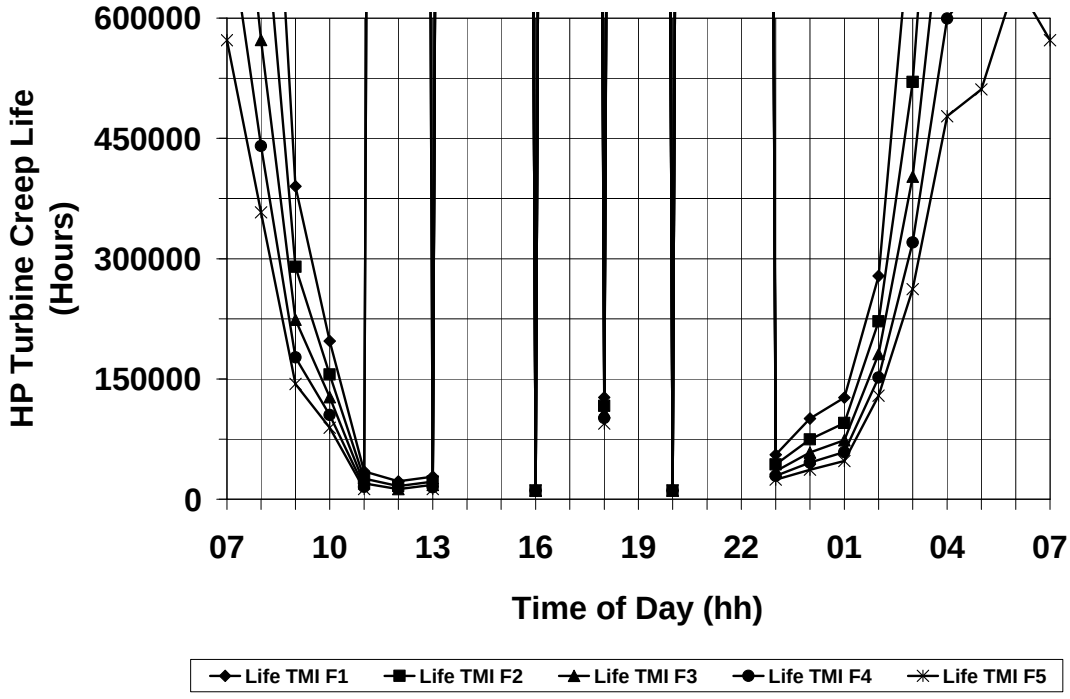

Figure C.43: Twin mode intercooled cycle (TMI) – HP Turbine creep life variation against time of day, during journey with annual hull fouling progression (F#) and adverse weather conditions

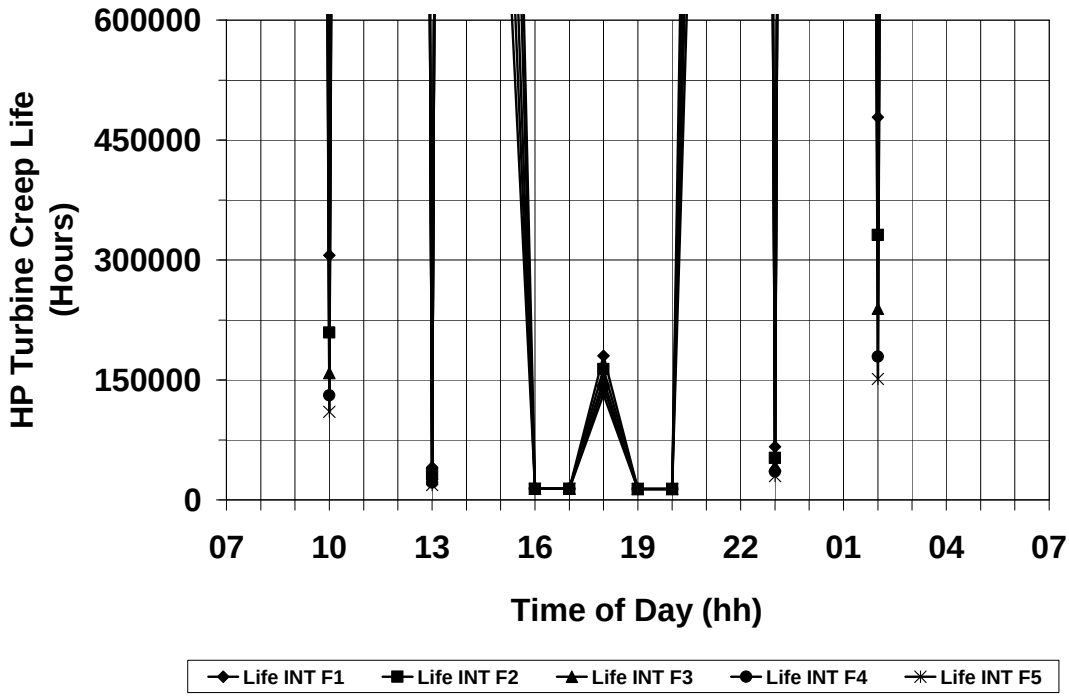

Figure C.44: Intercooled cycle (INT) – HP turbine creep life variation against time of day, during journey with annual hull fouling progression (F#) and adverse weather conditions

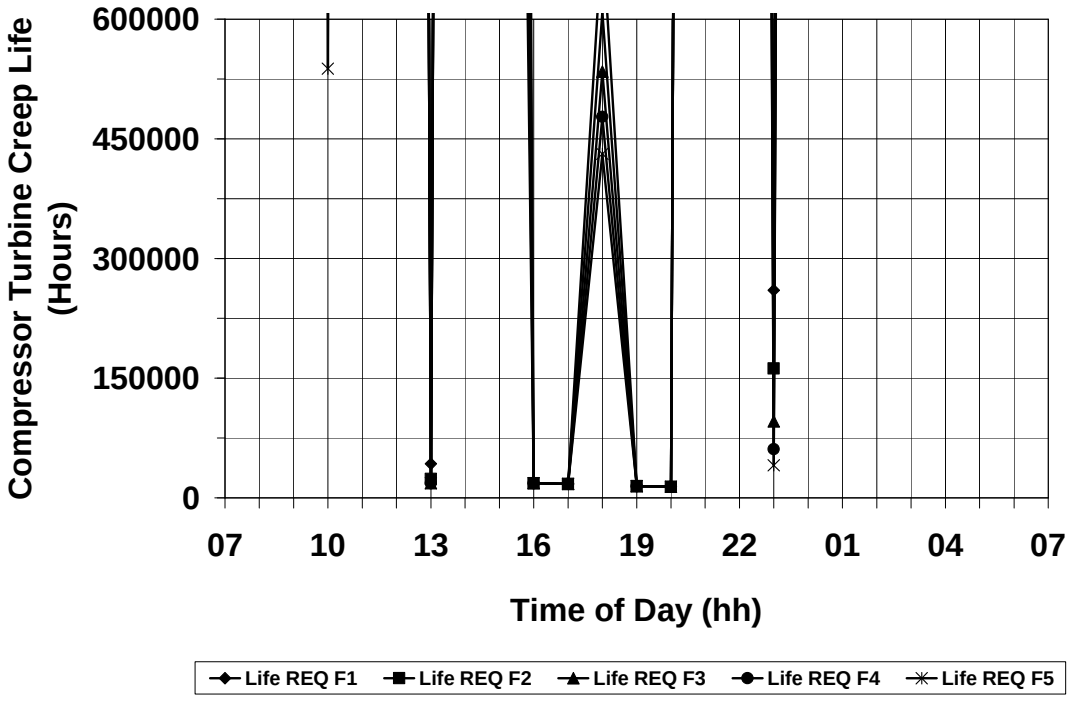

Figure C.45: Recuperated cycle (REQ) – Compressor turbine creep life variation against time of day, during journey with annual hull fouling progression (F#) and adverse weather conditions

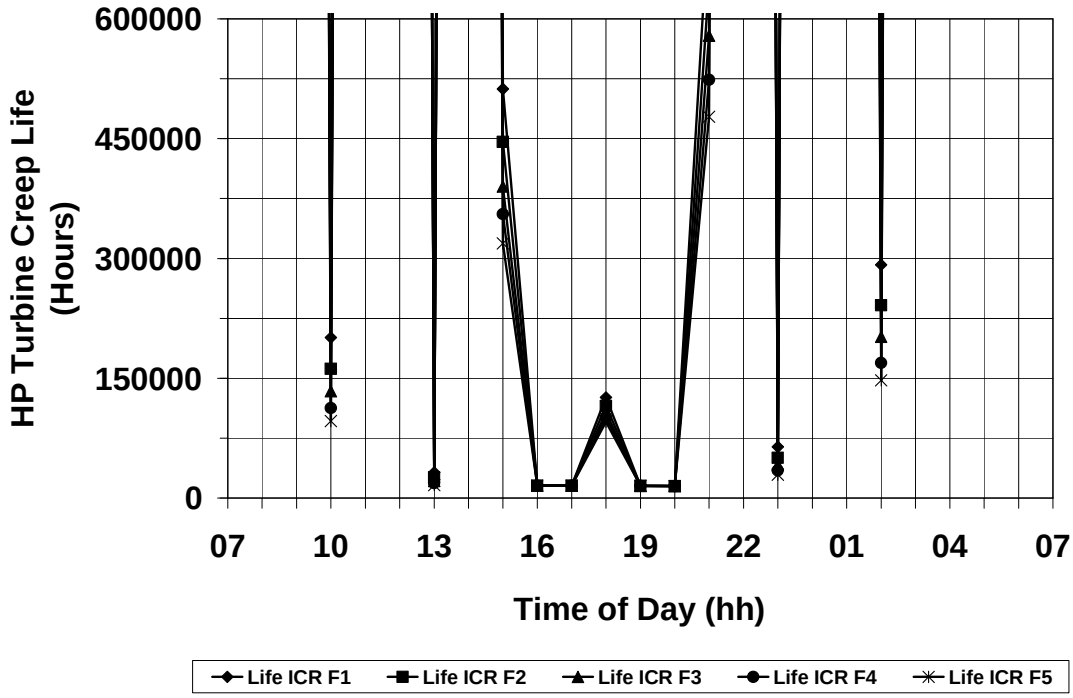

Figure C.46: Intercooled/recuperated cycle (ICR) – HP turbine creep life variation against time of day, during journey with annual hull fouling progression (F#) and adverse weather conditions

Appendix C.5

Table C.1: Hull fouling F1 – Quantified engine (Cruise & Boost) parameters per journey at ideal weather conditions

Engine Cruise --- Boost	Fuel Consumption (kg)	HP Turbine Life Consumption (%)	Total NOx Emissions (kg)	Total CO Emissions (kg)	Total CO2 Emissions (kg)	Total UHC Emissions (kg)	Operational Time per Journey (hours)
SC	74319.0	0.001248	370.5	275.8	233218	120.5	24.0
	28740.1	0.001248	193.9	43.8	90184.9	9.41	6.0
TMI x2	39510.4	0.008211	430.4	42.5	123973.5	6.30	24.0
INT	67307.21	0.001616	376.9	245.1	211213.5	98.3	24.0
	26513.2	0.001616	182.4	39.2	83199.0	8.31	6.0
REQ	64132.7	0.000341	328.3	311.2	201249.4	134.0	24.0
	26171.2	0.000341	174.7	42.5	82121.0	9.06	6.0
ICR	59226.6	0.002865	393.1	244.9	185863.7	82.4	24.0
	24428.5	0.002864	181.9	38.9	76658.7	8.02	6.0

Table C.2: Hull fouling F2 – Quantified engine (Cruise & Boost) parameters per journey at ideal weather conditions

Engine Cruise --- Boost	Fuel Consumption (kg)	HP Turbine Life Consumption (%)	Total NOx Emissions (kg)	Total CO Emissions (kg)	Total CO2 Emissions (kg)	Total UHC Emissions (kg)	Operational Time per Journey (hours)
SC	75286.3	0.001798	379.4	273.4	236252.9	117.7	24.0
	29154.6	0.001798	199.2	43.2	91485.3	9.10	6.0
TMI x2	40133.2	0.010993	442.8	41.8	125927.6	6.09	24.0
INT	68222.5	0.002372	385.0	242.3	214082.1	95.9	24.0
	26901.3	0.002372	186.9	38.8	84416.4	8.07	6.0
REQ	65079.3	0.000520	337.1	307.8	204221.7	130.9	24.0
	26591.1	0.000520	180.2	41.7	83443.3	8.73	6.0
ICR	60121.7	0.003592	402.1	242.6	188677.9	80.8	24.0
	24820.8	0.003592	185.5	38.3	77894.76	7.78	6.0

Table C.3: Hull fouling F3 – Quantified engine (Cruise & Boost) parameters per journey at ideal weather conditions

Engine Cruise --- Boost	Fuel Consumption (kg)	HP Turbine Life Consumption (%)	Total NOx Emissions (kg)	Total CO Emissions (kg)	Total CO2 Emissions (kg)	Total UHC Emissions (kg)	Operational Time per Journey (hours)
SC	76140.1	0.002475	387.5	271.4	238932.6	115.3	24.0
	29521.3	0.002475	204.0	42.6	92634.2	8.85	6.0
TMI x2	40677.6	0.014223	453.8	41.3	127635.8	5.90	24.0
INT	69023.6	0.003145	392.2	239.8	216597.4	93.7	24.0
	27240.7	0.003145	190.9	38.4	85483.5	7.88	6.0
REQ	65910.3	0.000753	344.9	304.8	206826.2	128.2	24.0
	26959.3	0.000753	185.1	40.9	84594.8	8.44	6.0
ICR	60908.1	0.004436	409.2	240.4	191135.0	79.4	24.0
	25165.1	0.004435	188.6	37.7	78967.6	7.57	6.0

Table C.4: Hull fouling F4 – Quantified engine (Cruise & Boost) parameters per journey at ideal weather conditions

Engine Cruise ---------- Boost	**Fuel Consumption (kg)**	**HP Turbine Life Consumption (%)**	**Total NOx Emissions (kg)**	**Total CO Emissions (kg)**	**Total CO2 Emissions (kg)**	**Total UHC Emissions (kg)**	**Operational Time per Journey (hours)**
SC	76912.14	0.003288	394.9	269.6	241354.9	113.3	24.0
	29853.0	0.003288	208.5	42.2	93676.2	8.64	6.0
TMI x2	41164.7	0.017835	463.9	40.7	129164.0	5.74	24.0
INT	69741.1	0.003963	398.6	237.7	218852.5	92.0	24.0
	27546.2	0.003963	194.5	38.1	86442.0	7.72	6.0
REQ	66658.6	0.001043	352.1	302.1	209174.2	125.7	24.0
	27291.1	0.001043	189.6	40.3	85637.6	8.19	6.0
ICR	61615.1	0.005327	415.8	238.3	193354.6	78.0	24.0
	25474.9	0.005326	191.3	37.2	79940.2	7.37	6.0

Table C.5: Hull fouling F5 – Quantified engine (Cruise & Boost) parameters per journey at ideal weather conditions

Engine Cruise ---------- Boost	**Fuel Consumption (kg)**	**HP Turbine Life Consumption (%)**	**Total NOx Emissions (kg)**	**Total CO Emissions (kg)**	**Total CO2 Emissions (kg)**	**Total UHC Emissions (kg)**	**Operational Time per Journey (hours)**
SC	77616.1	0.004248	401.8	267.9	243566.8	111.5	24.0
	30155.3	0.004248	212.6	41.7	94626.3	8.44	6.0
TMI x2	41606.3	0.021879	473.2	40.3	130549.7	5.59	24.0
INT	70392.7	0.004771	404.4	235.9	220897.5	90.5	24.0
	27823.1	0.004771	197.7	37.9	87310.9	7.59	6.0
REQ	67339.6	0.001405	358.8	299.6	211310.9	123.4	24.0
	27592.7	0.001405	193.8	39.8	86581.6	7.98	6.0
ICR	62258.7	0.006253	421.7	236.3	195373.5	76.7	24.0
	25756.1	0.006252	193.9	36.7	80824.8	7.18	6.0

Appendix C.5

Table C.6: Hull fouling F1 – Quantified engine (Cruise & Boost) parameters per journey at adverse weather conditions

Engine Cruise ---------- Boost	Fuel Consumption (kg)	HP Turbine Life Consumption (%)	Total NOx Emissions (kg)	Total CO Emissions (kg)	Total CO2 Emissions (kg)	Total UHC Emissions (kg)	Operational Time per Journey (hours)
SC	93068.2	0.040929	559.9	244.9	292046.7	90.7	24.30
	36124.9	0.022419	263.0	47.3	113356.4	9.34	7.0
TMI x2	52723.5	0.040603	648.3	58.6	165432.7	5.89	24.20
INT	85374.8	0.035488	544.3	212.4	267901.1	72.3	24.24
	33639.0	0.019556	244.9	43.1	105552.8	8.36	7.0
REQ	82471.0	0.030372	508.1	265.8	258785.4	99.0	24.30
	33078.2	0.015567	241.9	45.0	103792.3	8.86	7.0
ICR	76814.7	0.034229	550.4	212.45	241049.2	62.8	24.26
	31087.7	0.019379	237.27	41.6	97553.7	8.00	7.0

Table C.7: Hull fouling F2 – Quantified engine (Cruise & Boost) parameters per journey at adverse weather conditions

Engine Cruise ---------- Boost	Fuel Consumption (kg)	HP Turbine Life Consumption (%)	Total NOx Emissions (kg)	Total CO Emissions (kg)	Total CO2 Emissions (kg)	Total UHC Emissions (kg)	Operational Time per Journey (hours)
SC	92188.11	0.038369	551.6	246.5	289283.1	92.5	24.29
	36436.7	0.024958	267.3	46.8	114334.9	9.14	7.0
TMI x2	52171.3	0.035354	637.2	59.1	163699.9	6.04	24.19
INT	84568.5	0.034128	537.1	214.1	265368.7	73.8	24.23
	33925.1	0.020899	248.2	42.8	106455.0	8.22	7.0
REQ	81630.1	0.028184	499.9	268.3	256149.0	101.22	24.29
	33387.8	0.017751	246.3	44.4	104765.4	8.63	7.0
ICR	76018.5	0.032741	543.2	213.8	238551.2	63.7	24.25
	31375.7	0.020819	240.0	41.3	98455.6	7.86	7.0

Table C.8: Hull fouling F3 – Quantified engine (Cruise & Boost) parameters per journey at adverse weather conditions

Engine Cruise ---------- Boost	Fuel Consumption (kg)	HP Turbine Life Consumption (%)	Total NOx Emissions (kg)	Total CO Emissions (kg)	Total CO2 Emissions (kg)	Total UHC Emissions (kg)	Operational Time per Journey (hours)
SC	93804.8	0.042766	566.9	243.6	294353.5	89.2	24.32
	36677.1	0.02677	270.5	46.4	115088.2	8.99	7.0
TMI x2	53204.6	0.046540	658.2	58.2	166942.1	5.75	24.21
INT	86101.4	0.036984	550.8	211.0	270183.4	71.1	24.25
	34177.5	0.022373	251.2	42.6	107246.0	8.09	7.0
REQ	83206.0	0.032094	514.9	263.9	261095.5	97.2	24.32
	33627.3	0.019468	249.7	44.0	105517.7	8.46	7.0
ICR	77511.0	0.035747	556.8	211.2	243232.2	61.9	24.27
	31628.6	0.022286	242.4	40.9	99250.8	7.75	7.0

Appendix C.5

Table C.9: Hull fouling F4 – Quantified engine (Cruise & Boost) parameters per journey at adverse weather conditions

Engine Cruise --- Boost	Fuel Consumption (kg)	HP Turbine Life Consumption (%)	Total NOx Emissions (kg)	Total CO Emissions (kg)	Total CO2 Emissions (kg)	Total UHC Emissions (kg)	Operational Time per Journey (hours)
SC	94459.4	0.043657	572.9	242.7	296406.9	87.9	24.33
	36864.9	0.027635	273.0	46.2	115677.2	8.87	7.0
TMI x2	53817.8	0.043289	667.9	61.6	168866.2	6.03	24.21
INT	86737.5	0.038584	556.5	209.7	272178.3	69.9	24.26
	34404.6	0.023951	253.9	42.3	107956.5	7.99	7.0
REQ	83824.31	0.032772	520.5	262.2	263035.6	95.5	24.33
	33814.5	0.020139	252.3	43.7	106104.5	8.34	7.0
ICR	78141.07	0.037301	562.5	210.0	245214.4	61.1	24.29
	31855.4	0.023796	244.6	40.7	99962.7	7.64	7.0

Table C.10: Hull fouling F5 – Quantified engine (Cruise & Boost) parameters per journey at adverse weather conditions

Engine Cruise --- Boost	Fuel Consumption (kg)	HP Turbine Life Consumption (%)	Total NOx Emissions (kg)	Total CO Emissions (kg)	Total CO2 Emissions (kg)	Total UHC Emissions (kg)	Operational Time per Journey (hours)
SC	95049.6	0.044681	578.4	241.7	298264.0	86.8	24.34
	37038.3	0.028632	275.4	45.9	116220.3	8.76	7.0
TMI x2	54213.8	0.048374	676.2	61.3	170109.0	5.92	24.22
INT	87332.2	0.040238	561.9	208.7	274043.6	69.0	24.28
	34610.9	0.025577	256.4	42.1	108605.9	7.90	7.0
REQ	84393.17	0.033685	525.7	260.7	264819.8	94.1	24.35
	33985.0	0.021046	254.7	43.4	106640.7	8.24	7.0
ICR	78709.6	0.039035	567.8	208.9	246993.9	60.4	24.30
	32062.1	0.025480	246.6	40.4	100612.0	7.54	7.0

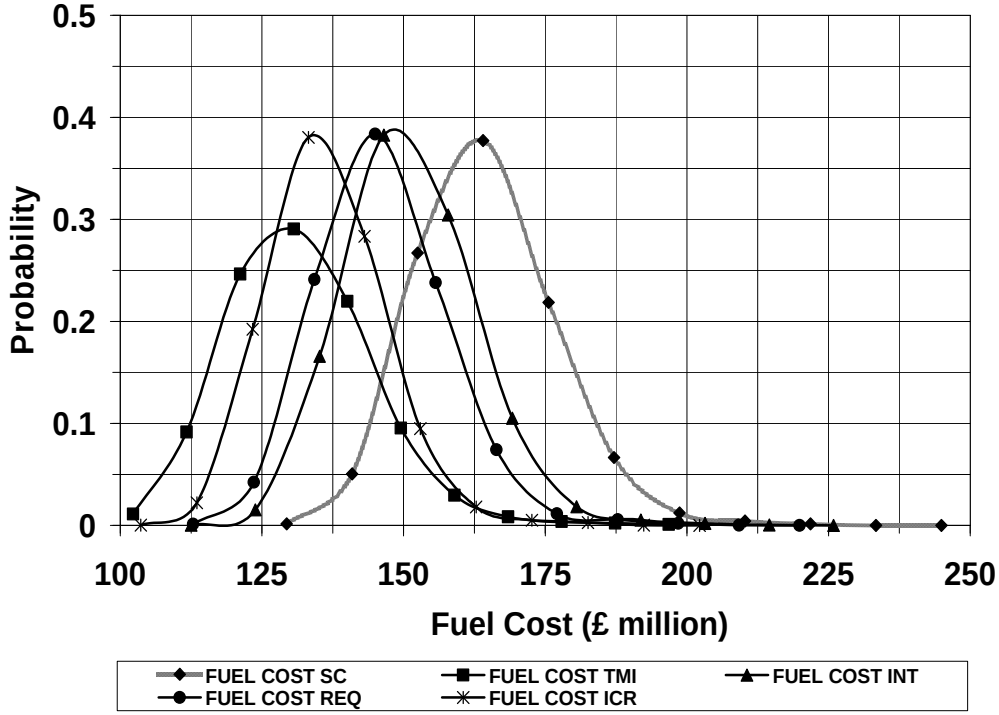

Figure C.47: Destroyer – Probability distribution of fuel cost of each power plant

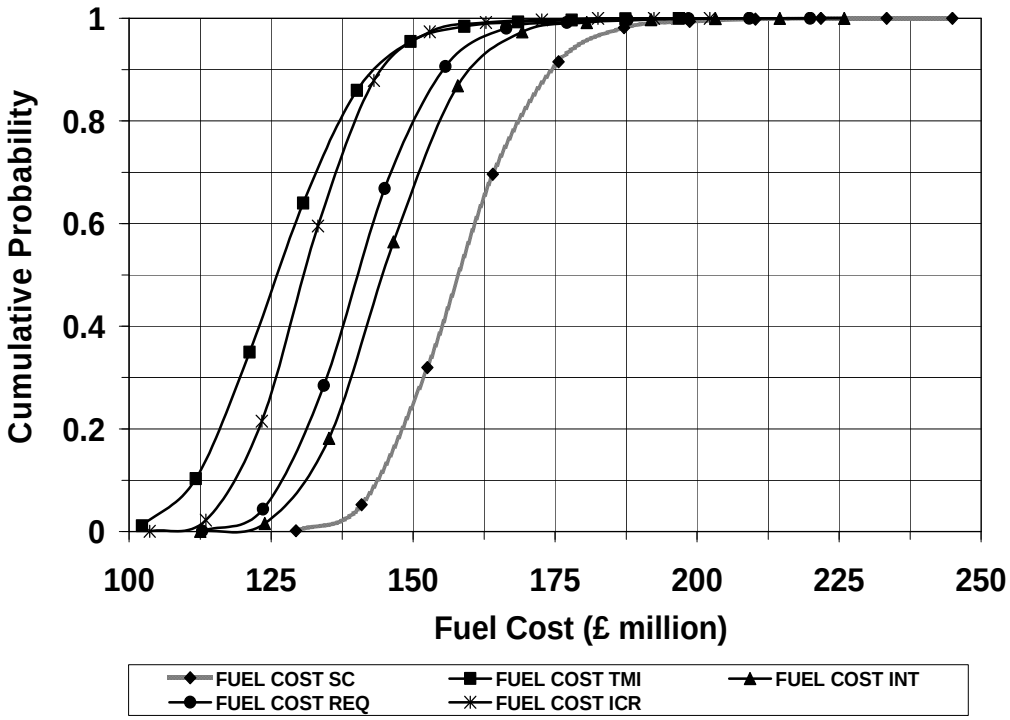

Figure C.48: Destroyer – Cumulative probability distribution of fuel cost of each power plant

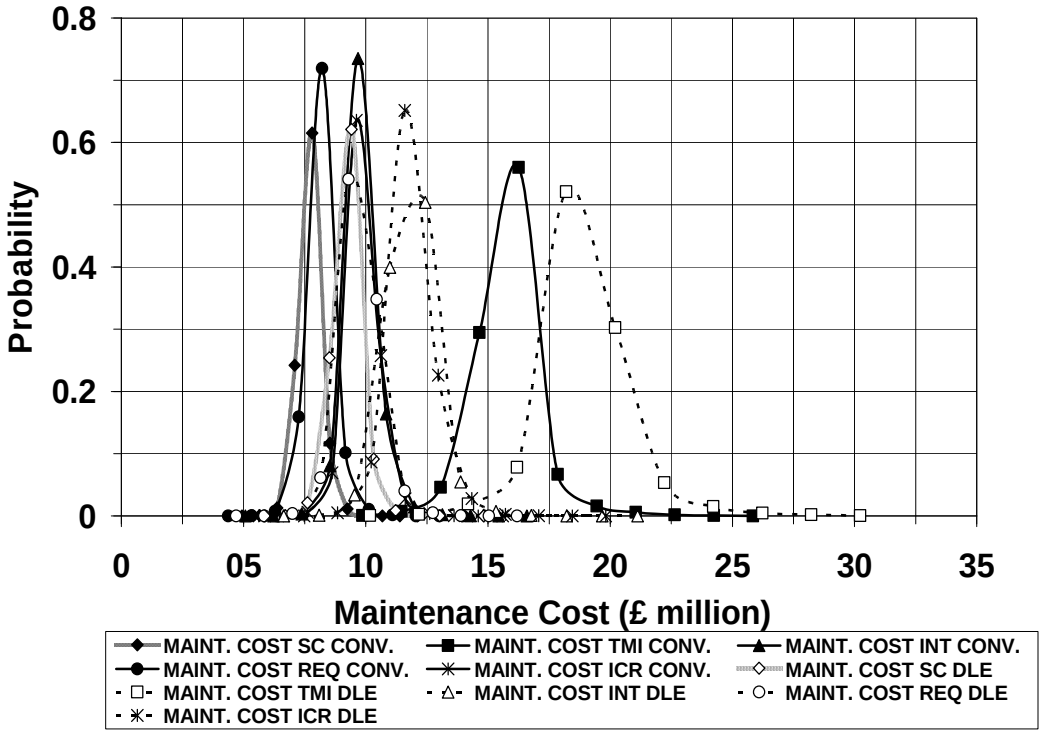

Figure C.49: Destroyer – Probability distribution of maintenance cost of each power plant (initial capital cost from 20% to 65% over the reference power plant)

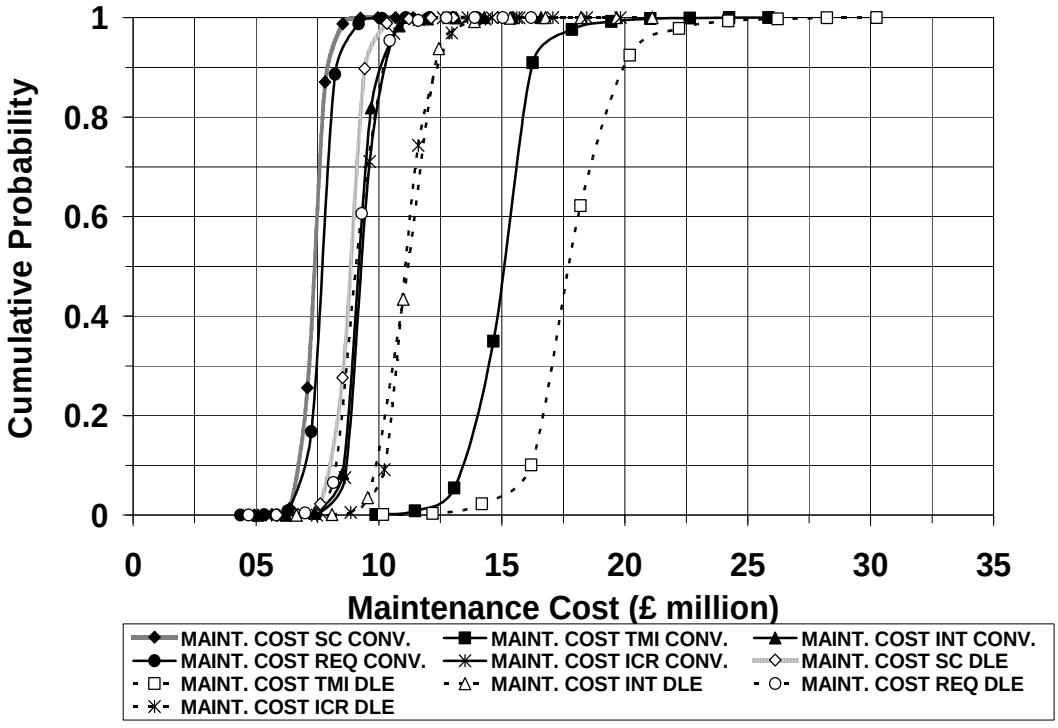

Figure C.50: Destroyer – Cumulative probability distribution of maintenance cost of each power plant (initial capital cost from 20% to 65% over the reference power plant)

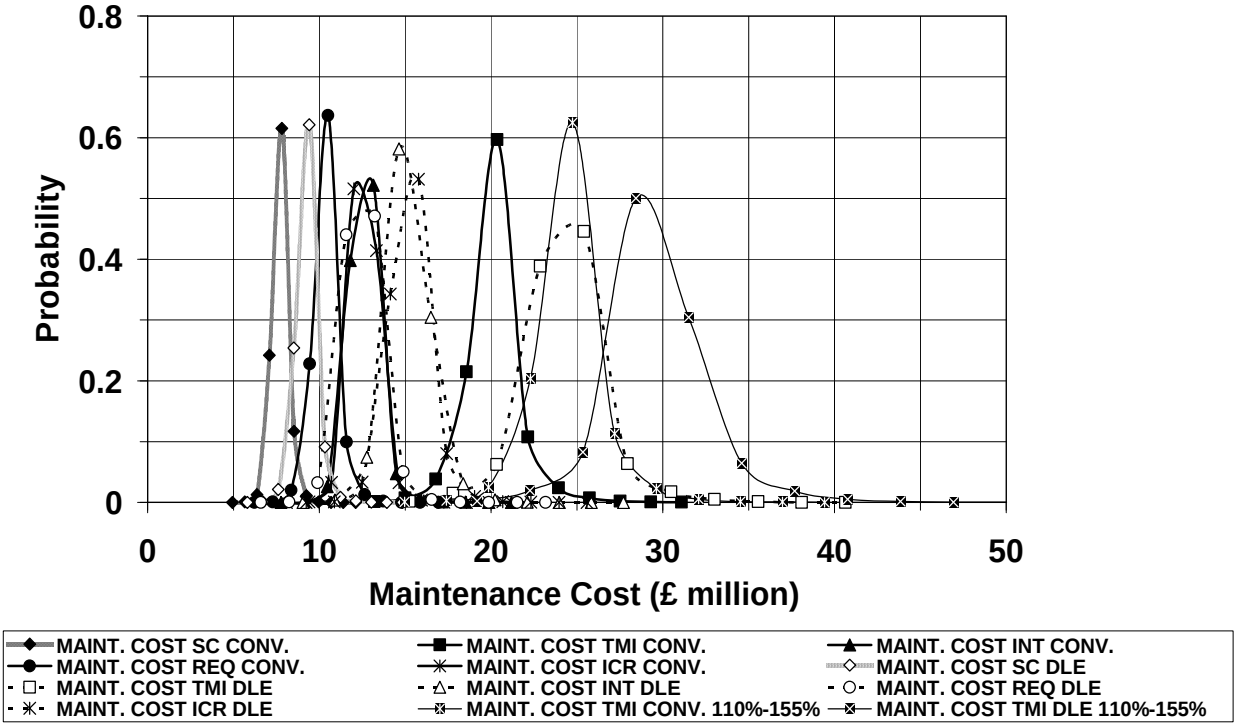

Figure C.51: Destroyer – Probability distribution of maintenance cost of each power plant (initial capital cost from 65% to 110% over the reference power plant). TMI power plant initial capital cost is extended to a range from 110% to 155%

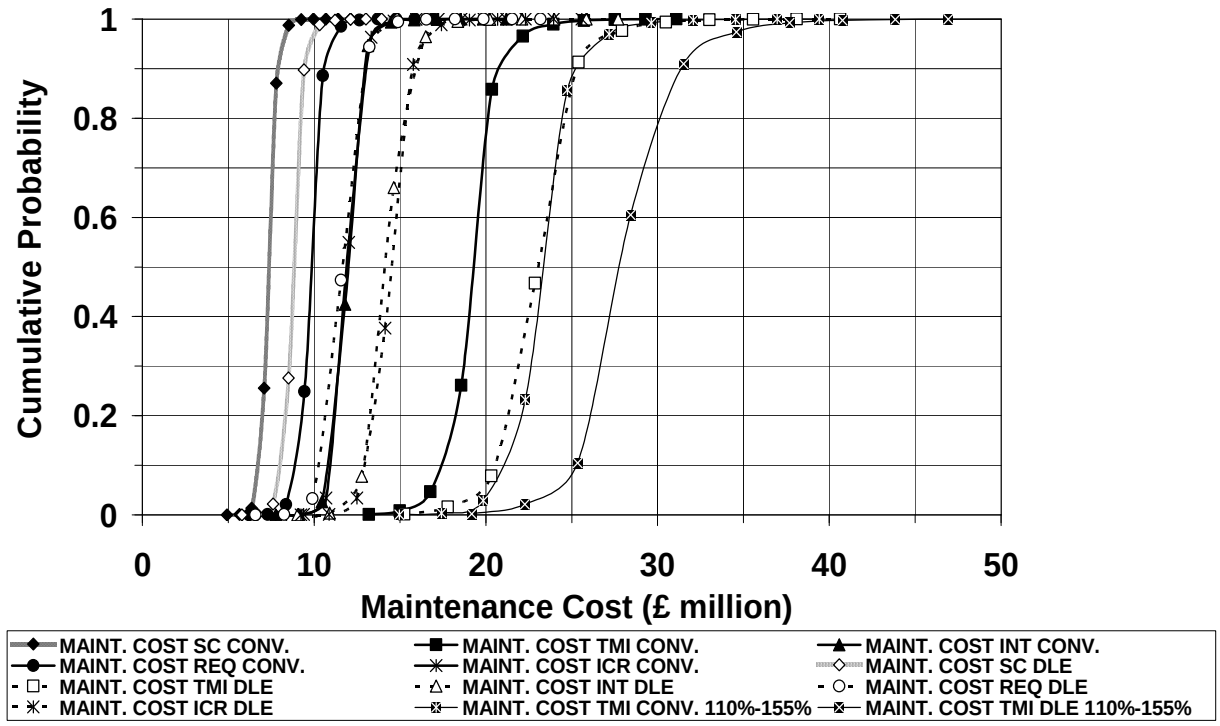

Figure C.52: Destroyer – Cumulative probability distribution of maintenance cost of each power plant (initial capital cost from 65% to 110% over the reference power plant). TMI power plant initial capital cost is extended to a range from 110% to 155%

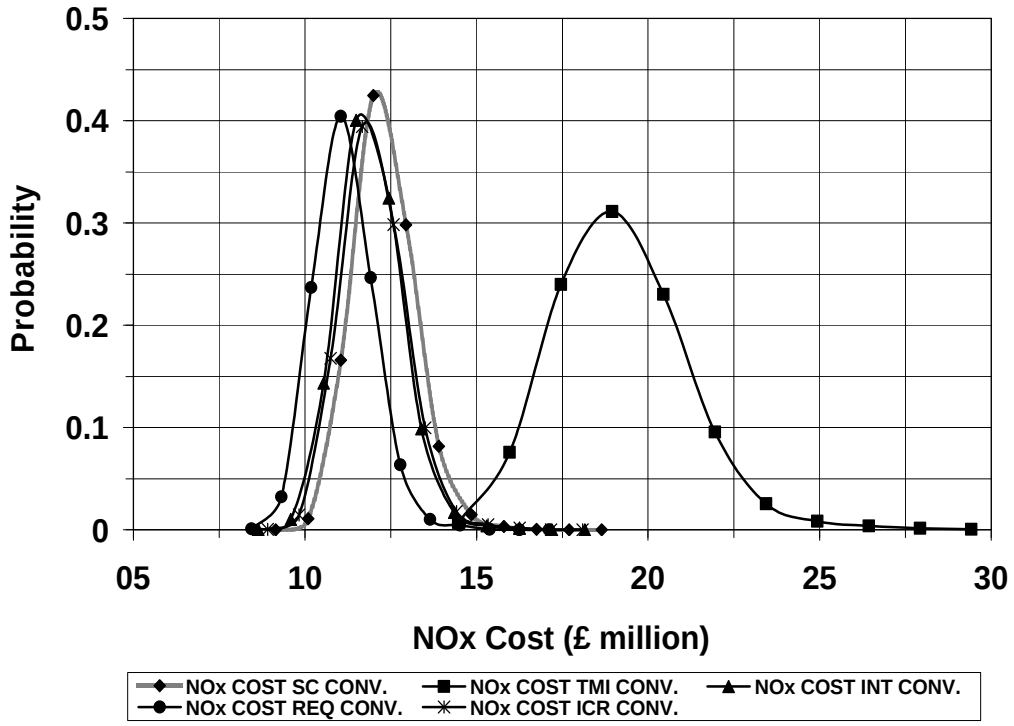

Figure C.53: Destroyer – Probability distribution of cost of taxed NOx exhaust emissions of each power plant with conventional combustors

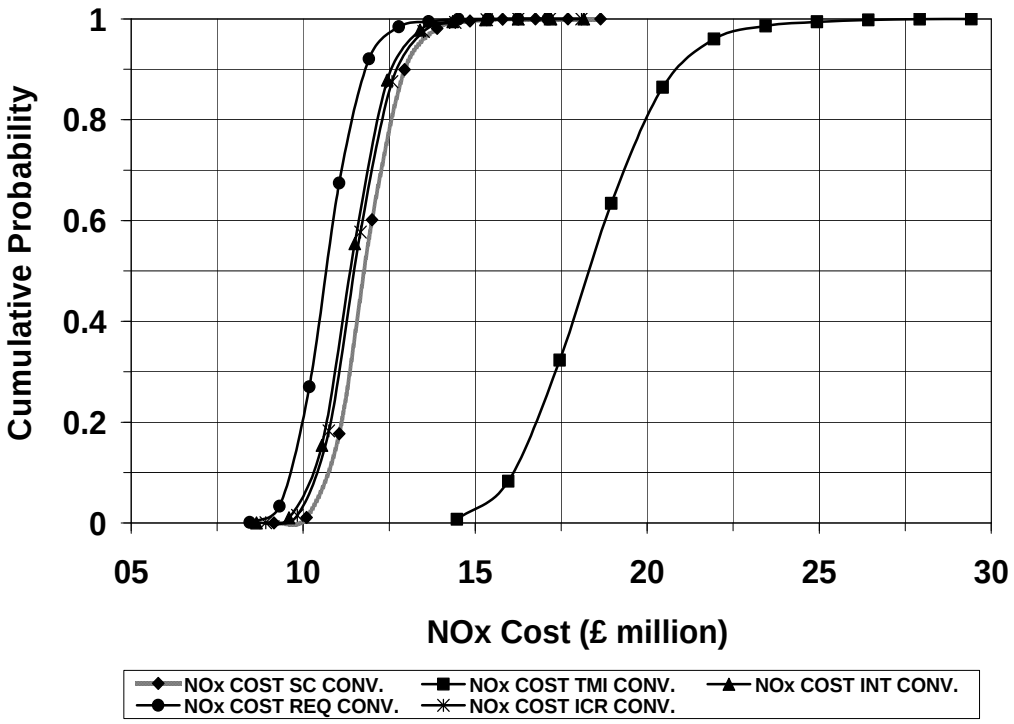

Figure C.54: Destroyer – Cumulative probability distribution of cost of taxed NOx exhaust emissions of each power plant with conventional combustors

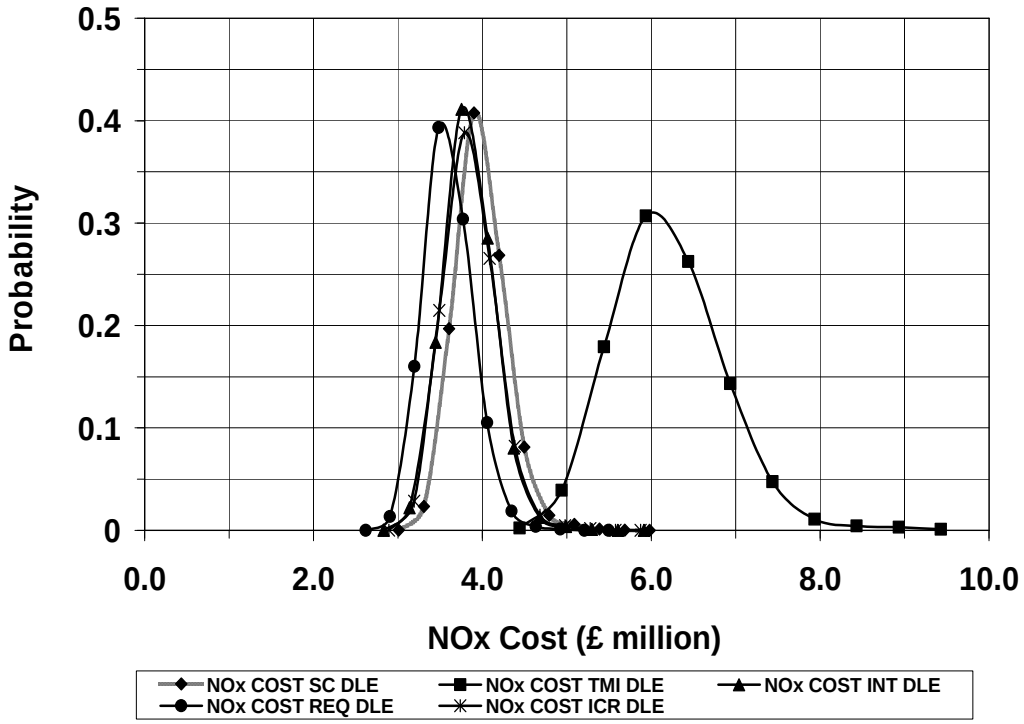

FigureC.55: Destroyer – Probability distribution of cost of taxed NOx exhaust emissions of each power plant with DLE combustors

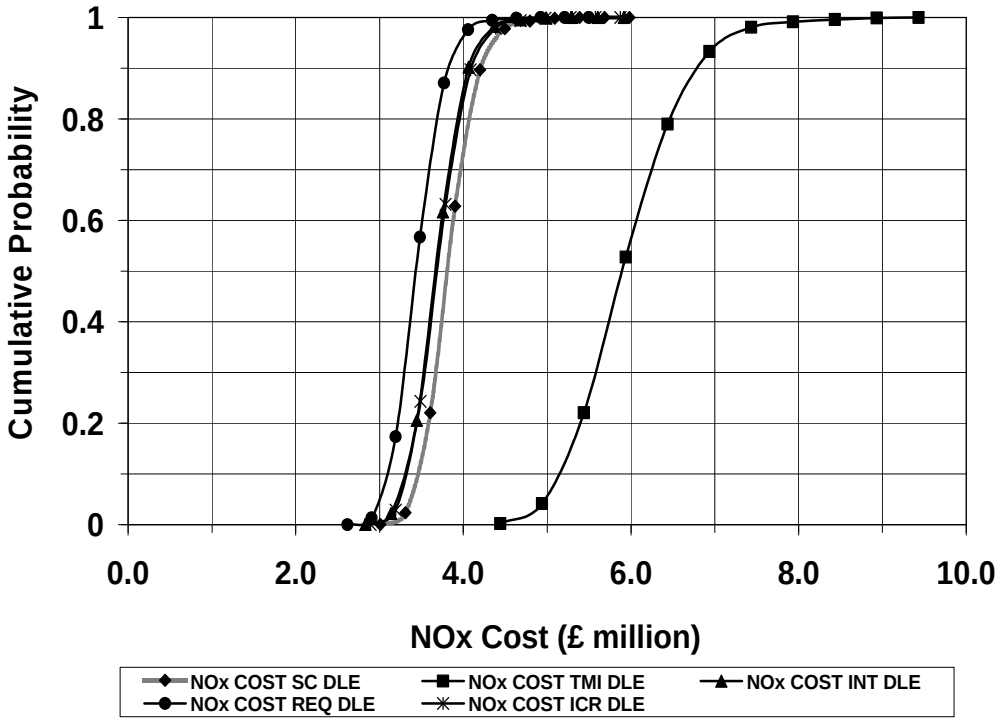

Figure C.56: Destroyer – Cumulative probability distribution of cost of taxed NOx exhaust emissions of each power plant with DLE combustors

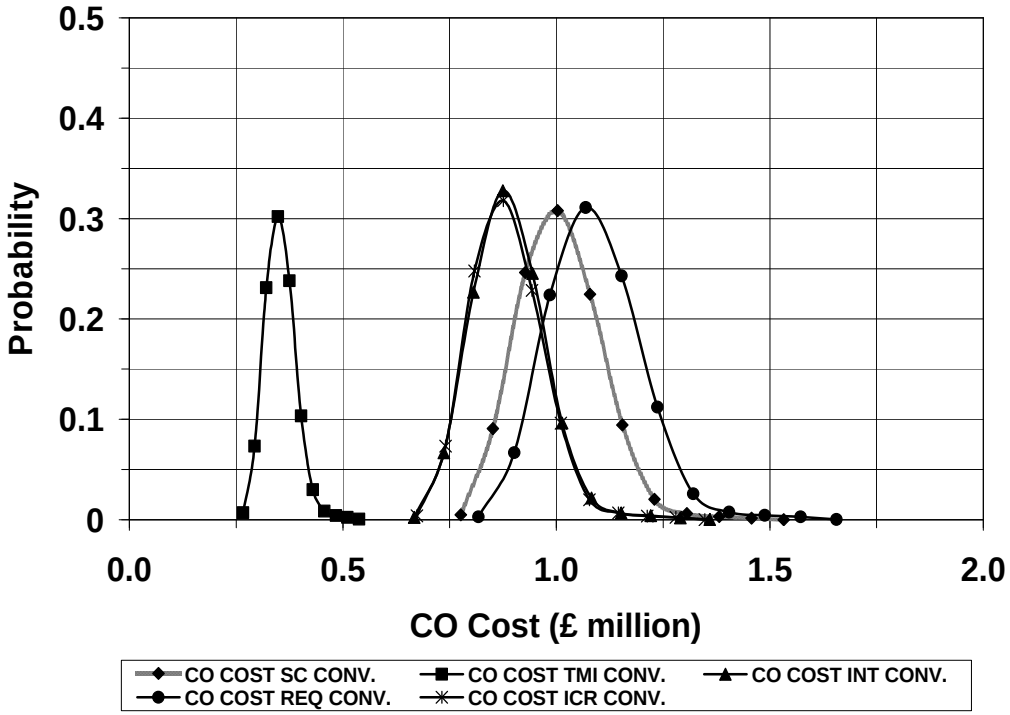

Figure C.57: Destroyer – Probability distribution of cost of taxed CO exhaust emissions of each power plant with conventional combustors

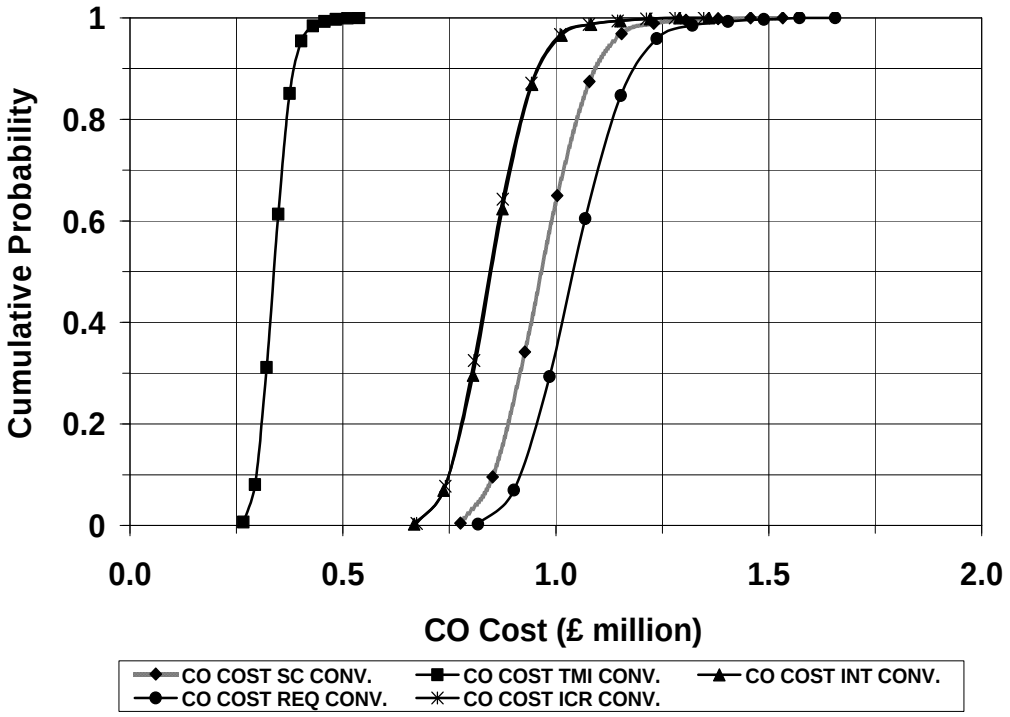

Figure C.58: Destroyer – Cumulative probability distribution of cost of taxed CO exhaust emissions of each power plant with conventional combustors

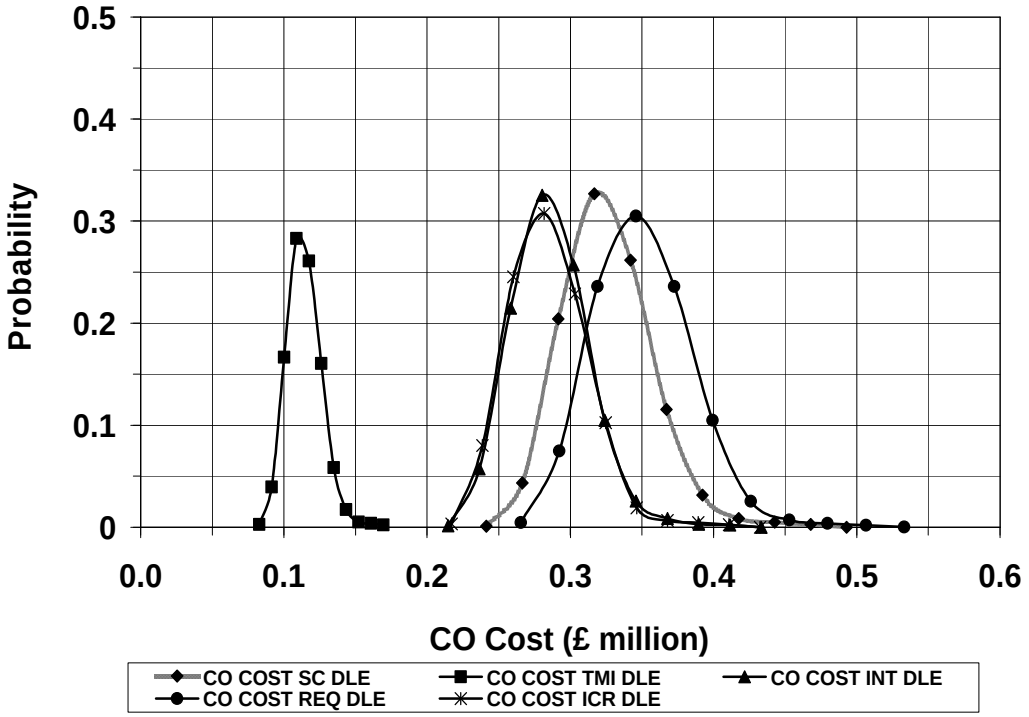

Figure C.59: Destroyer – Probability distribution of cost of taxed CO exhaust emissions of each power plant with DLE combustors

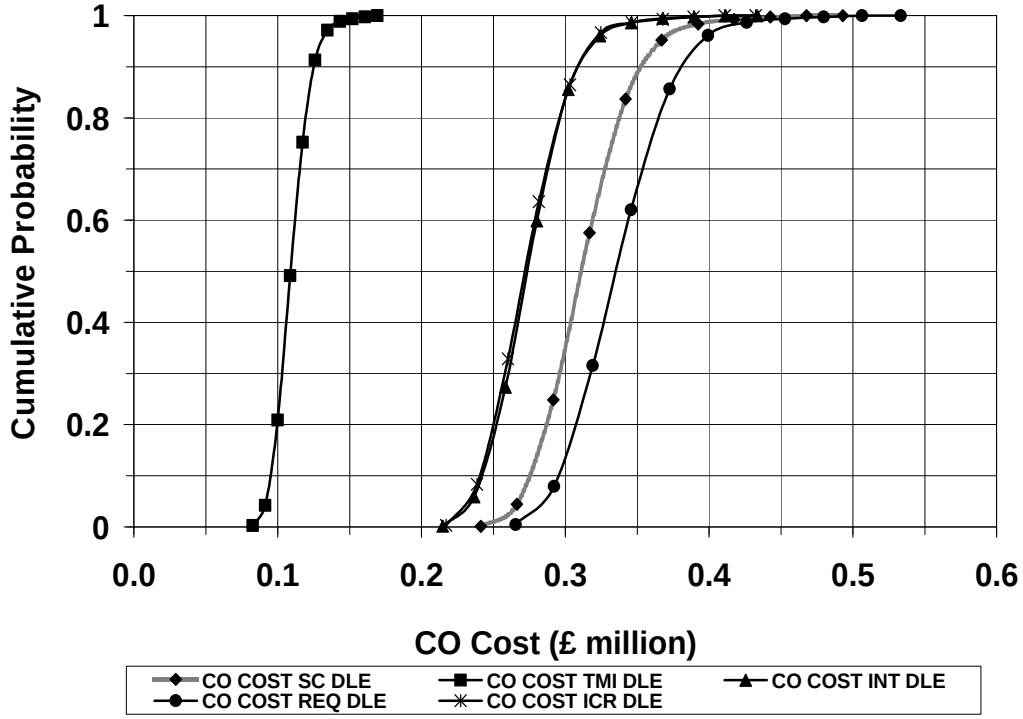

Figure C.60: Destroyer – Cumulative probability distribution of cost of taxed CO exhaust emissions of each power plant with DLE combustors

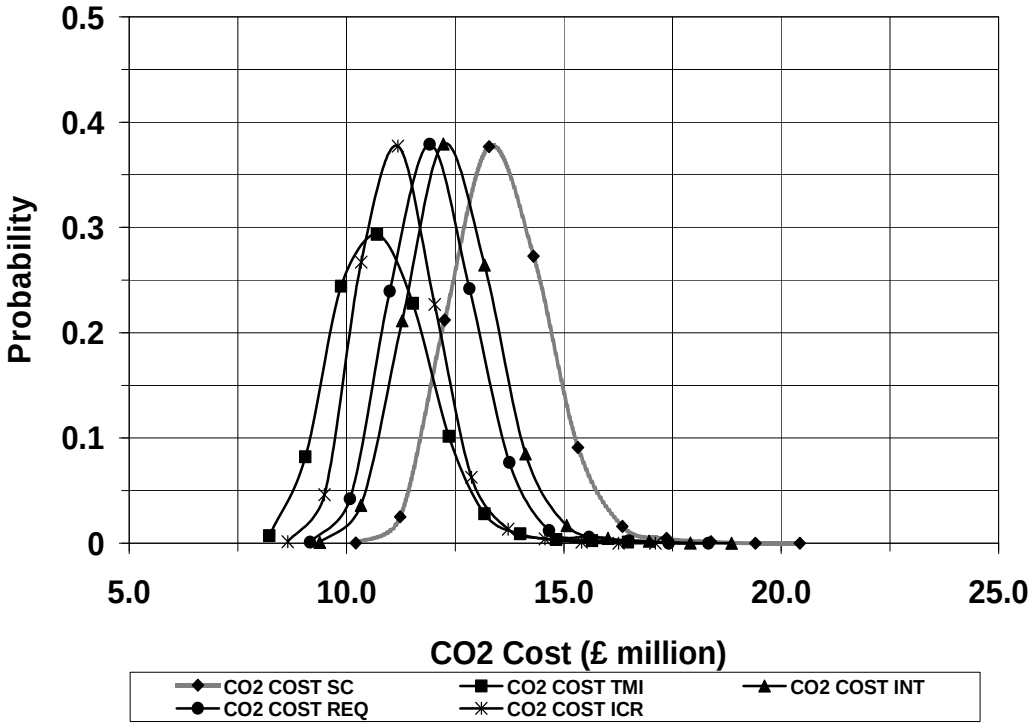

Figure C.61: Destroyer – Probability distribution of cost of taxed CO2 exhaust emissions of each power plant

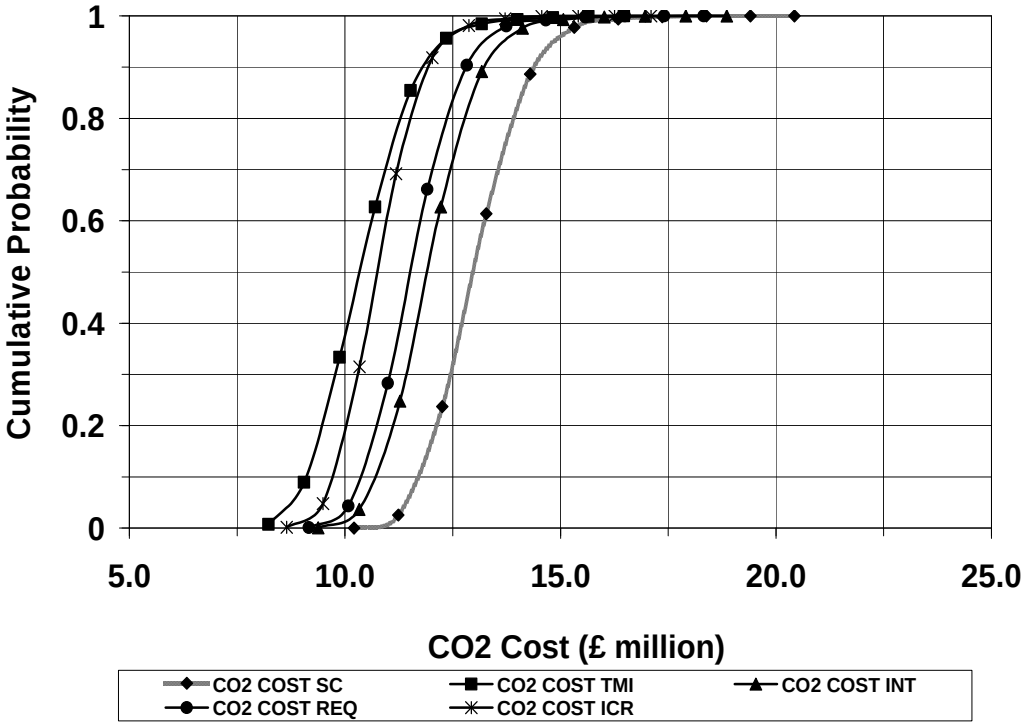

Figure C.62: Destroyer – Cumulative probability distribution of cost of taxed CO2 exhaust emissions of each power plant

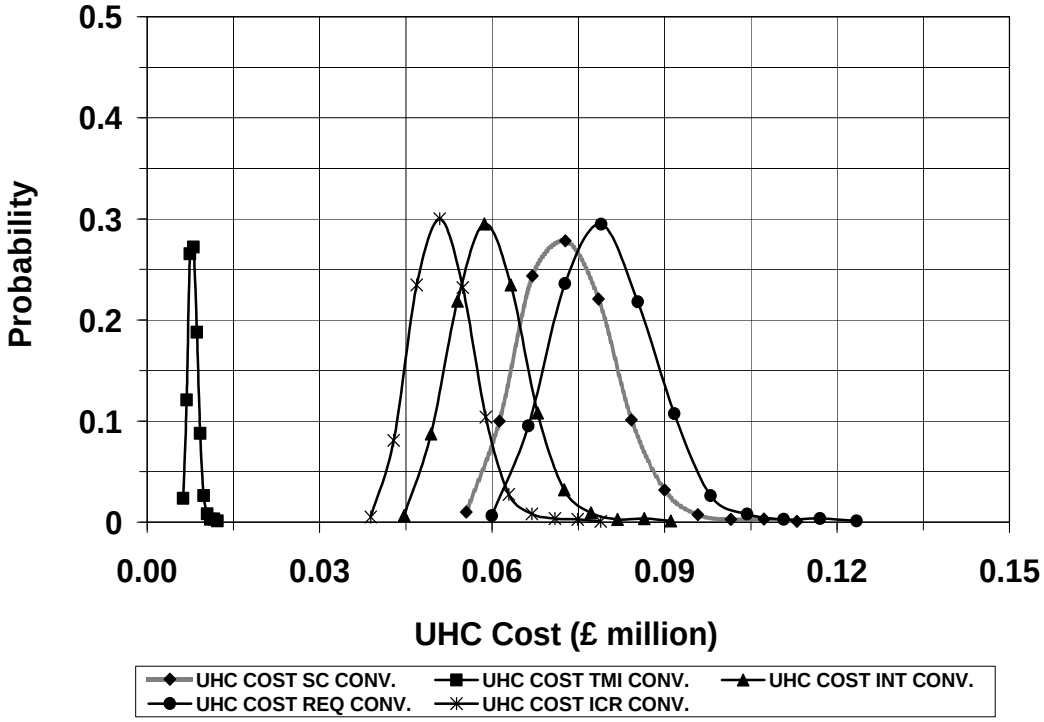

Figure C.63: Destroyer – Probability distribution of cost of taxed UHC exhaust emissions of each power plant with conventional combustors

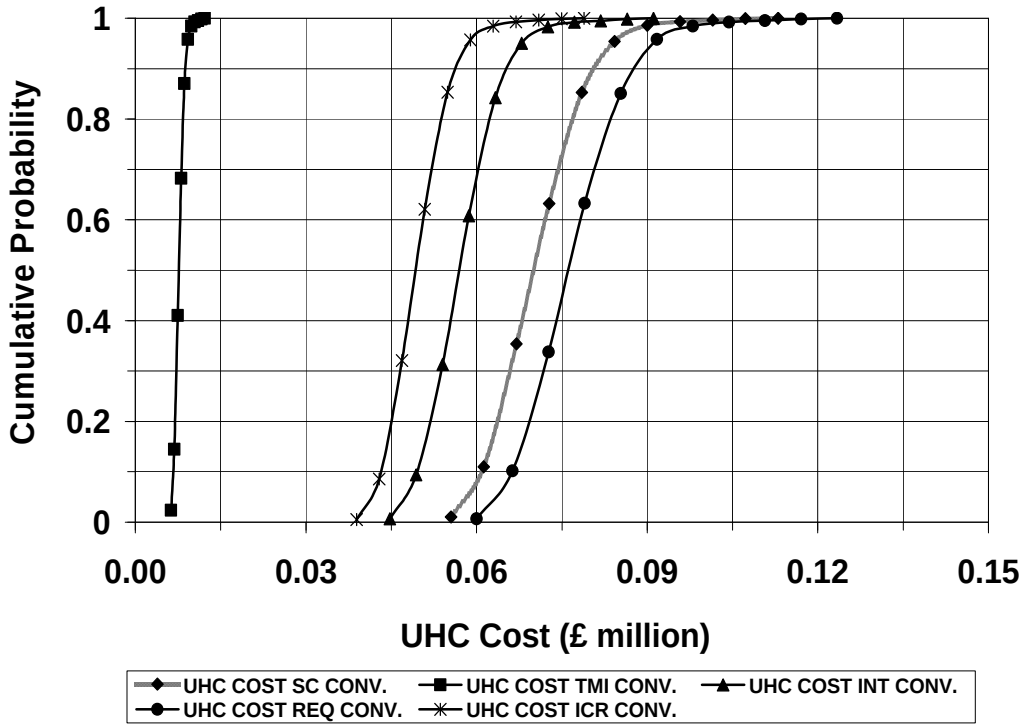

Figure C.64: Destroyer – Cumulative probability distribution of cost of taxed UHC exhaust emissions of each power plant with conventional combustors

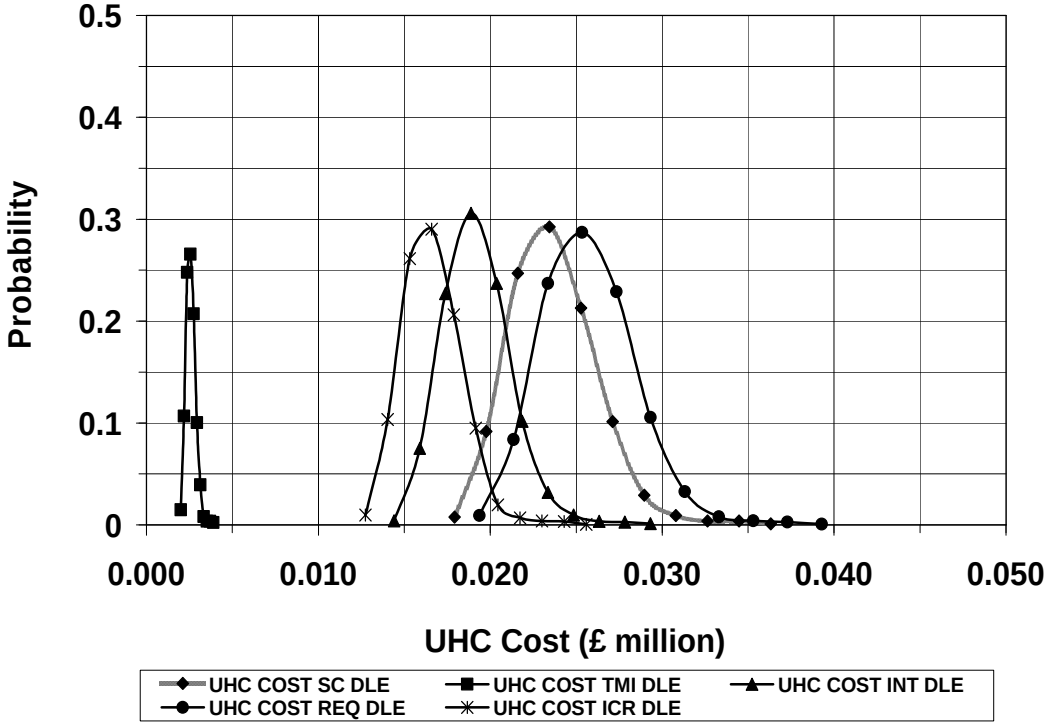

Figure C.65: Destroyer – Probability distribution of cost of taxed UHC exhaust emissions of each power plant with DLE combustors

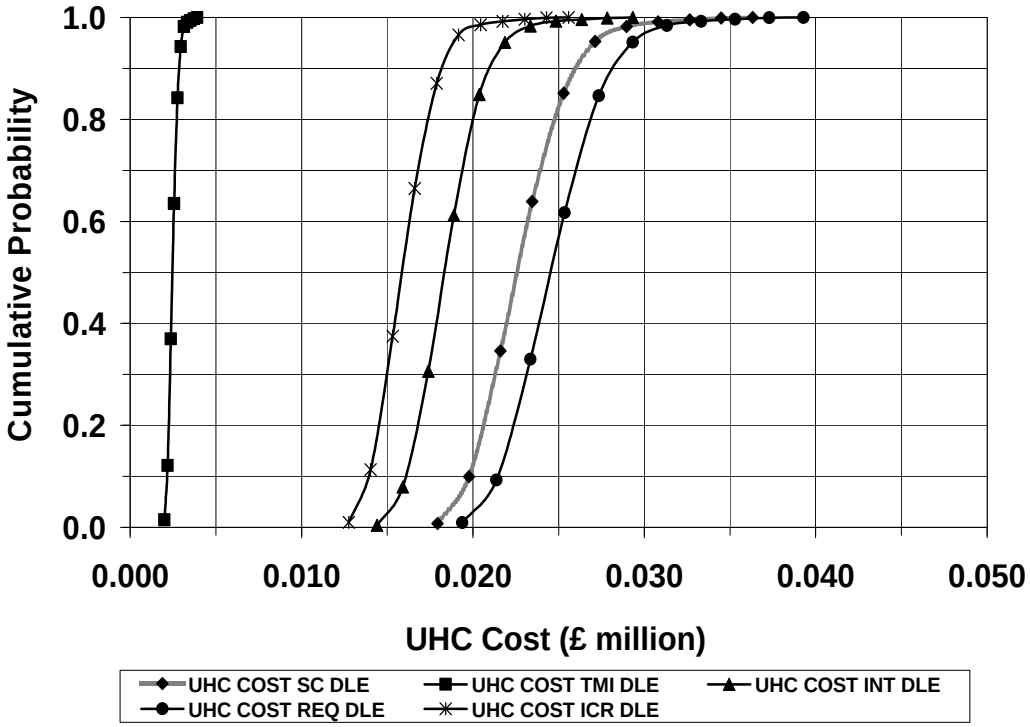

Figure C.66: Destroyer – Cumulative probability distribution of cost of taxed UHC exhaust emissions of each power plant with DLE combustors

Table C.11: Destroyer - Minimum-maximum and standard deviation of NPC of all power plants with PD_0 range from 20% to 65% from reference cycle

Engine (20%-65%) Conventional & DLE Combustor	Minimum NPC (£ million)		Maximum NPC (£ million)		Standard Deviation (£ million)	
SC-Reference cycle	168.7	167.1	322.4	316.7	13.97	13.58
TMI	159.5	147.3	300.0	286.7	12.76	12.66
INT	154.1	160.4	311.4	306.6	14.29	13.29
REQ	155.1	153.3	302.6	292.3	13.41	12.63
ICR	147.2	146.1	282.4	280.5	12.28	12.22

Table C.12: Destroyer - Minimum-maximum and standard deviation of NPC of all power plants with PD_0 range from 65% to 110% from reference cycle. TMI power plant is extended from 110% to 155%

Engine (65%-110%) Conventional & DLE Combustor	Minimum NPC (£ million)		Maximum NPC (£ million)		Standard Deviation (£ million)	
SC-Reference cycle	168.7	167.1	322.4	316.7	13.97	13.58
TMI	167.6	163.4	299.2	312.4	12.03	13.54
TMI (110%-155%)	169.1	177.8	326.6	330.5	14.31	13.88
INT	176.3	174.2	327.9	325.5	13.78	13.75
REQ	168.8	163.9	310.8	315.9	12.91	13.81
ICR	162.8	164.8	298.6	298.4	12.34	12.14

Table C.13: Destroyer - Minimum-maximum and standard deviation of maintenance cost of all power plants with PD_0 range from 20% to 65% from reference cycle

Engine (20%-65%) Conventional & DLE Combustor	Minimum Maint. Cost (£ million)		Maximum Maint. Cost (£ million)		Standard Deviation (£ million)	
SC-Reference cycle	4.57	5.35	12.47	15.28	0.71	0.90
TMI	9.06	9.16	26.62	31.22	1.58	2.00
INT	4.49	5.92	17.16	21.84	1.15	1.44
REQ	3.88	4.12	14.45	16.76	0.96	1.15
ICR	5.12	5.42	16.10	20.50	0.99	1.37

Table C.14: Destroyer - Minimum-maximum and standard deviation of maintenance cost of all power plants with PD_0 range from 65% to 110% from reference cycle. TMI power plant is extended from 110% to 155%

Engine (65%-110%) Conventional & DLE Combustor	Minimum Maint. Cost (£ million)		Maximum Maint. Cost (£ million)		Standard Deviation (£ million)	
SC-Reference Cycle	4.57	5.35	12.47	15.28	0.71	0.90
TMI	12.30	13.96	29.98	41.90	1.78	2.54
TMI (110%-155%)	13.72	17.64	40.64	51.40	2.44	3.08
INT	7.09	8.10	21.86	28.64	1.34	1.87
REQ	5.67	5.75	17.47	24.01	1.07	1.66
ICR	7.42	8.41	21.84	26.40	1.31	1.64

Table C.15: Destroyer - Minimum-maximum and standard deviation of fuel cost of all power plants

Engine	Minimum Fuel Cost (£ million)	Maximum Fuel Cost (£ million)	Standard Deviation (£ million)
SC-Reference Cycle	123.6	250.7	11.55
TMI	97.6	201.5	9.44
INT	106.9	231.6	11.33
REQ	106.1	224.9	10.80
ICR	98.7	207.2	9.86

Table C.16: Destroyer - Minimum-maximum and standard deviation of cost of taxed NOx exhaust emissions of all power plants

Engine Conventional & DLE Combustor	Minimum NOx Cost (£ million)		Maximum NOx Cost (£ million)		Standard Deviation (£ million)	
SC-Reference Cycle	8.67	2.86	19.12	6.13	0.95	0.29
TMI	13.72	4.18	30.18	9.68	1.48	0.49
INT	8.16	2.67	18.63	6.07	0.95	0.31
REQ	7.61	2.54	17.33	5.63	0.88	0.28
ICR	8.45	2.74	18.54	6.02	0.92	0.29

Table C.17: Destroyer - Minimum-maximum and standard deviation of cost of taxed CO exhaust emissions of all power plants

Engine Conventional & DLE Combustor	Minimum CO Cost (£ million)		Maximum CO Cost (£ million)		Standard Deviation (£ million)	
SC-Reference Cycle	0.738	0.228	1.570	0.505	0.075	0.025
TMI	0.252	0.078	0.550	0.174	0.028	0.009
INT	0.632	0.203	1.394	0.444	0.069	0.022
REQ	0.806	0.251	1.697	0.554	0.081	0.028
ICR	0.639	0.206	1.381	0.443	0.067	0.021

Table C.18: Destroyer - Minimum-maximum and standard deviation of dost of taxed CO2 exhaust emissions of all power plants

Engine	Minimum CO2 Cost (£ million)	Maximum CO2 Cost (£ million)	Standard Deviation (£ million)
SC-Reference Cycle	9.70	20.93	1.02
TMI	7.80	16.88	0.82
INT	8.91	19.33	0.95
REQ	8.57	18.72	0.92
ICR	8.22	17.52	0.85

Table C.19: Destroyer - Minimum-maximum and standard deviation of cost of taxed UHC exhaust emissions of all power plants

Engine Conventional & DLE Combustor	Minimum UHC Cost (£ million)		Maximum UHC Cost (£ million)		Standard Deviation (£ million)	
SC-Reference Cycle	0.052	0.017	0.115	0.037	0.0057	0.0018
TMI	0.006	0.0018	0.013	0.0039	0.0006	0.0002
INT	0.042	0.013	0.093	0.030	0.0046	0.0015
REQ	0.057	0.018	0.128	0.041	0.0065	0.0020
ICR	0.037	0.012	0.080	0.026	0.0040	0.0012

APPENDIX D

Contains:

8. **[Table D.18]:** Cost of taxed CO_2 exhaust emissions of all power plants.
9. **[Table D.19]:** Cost of taxed UHC exhaust emissions of all power plants.

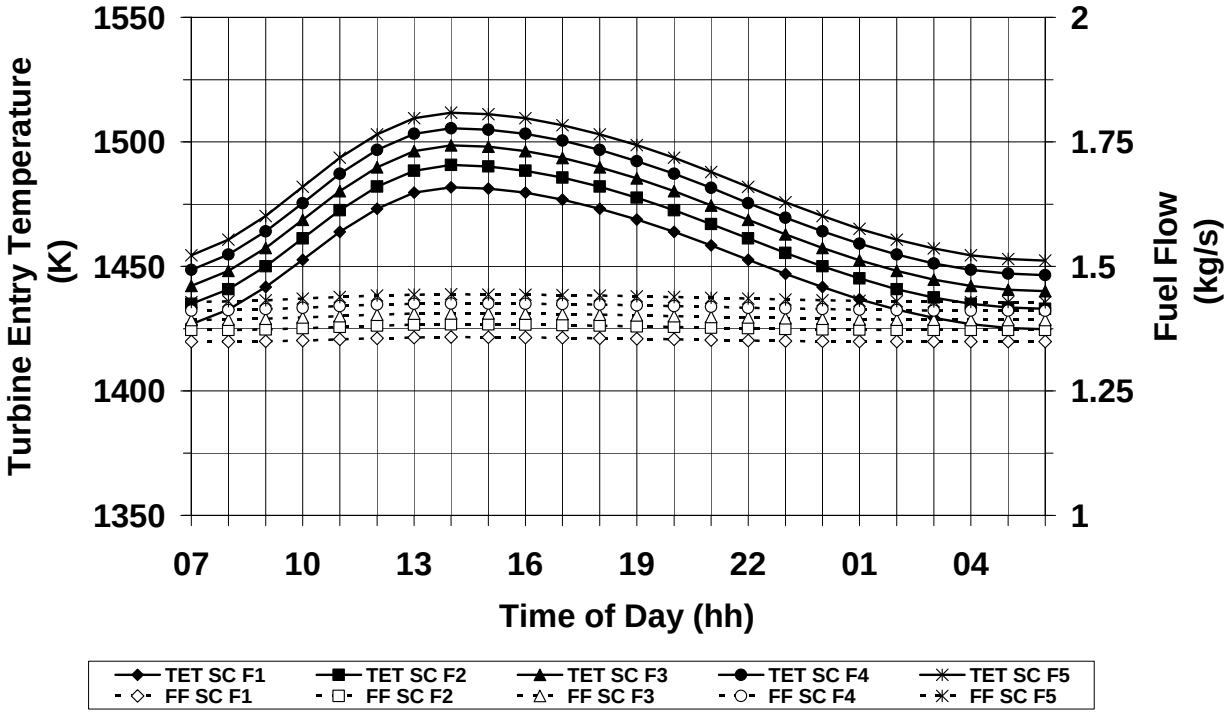

Figure D.1: Simple cycle (SC) - Turbine entry temperature (TET) and fuel flow (FF) variation against time of day, during journey with annual hull fouling progression (F#) and ideal weather conditions

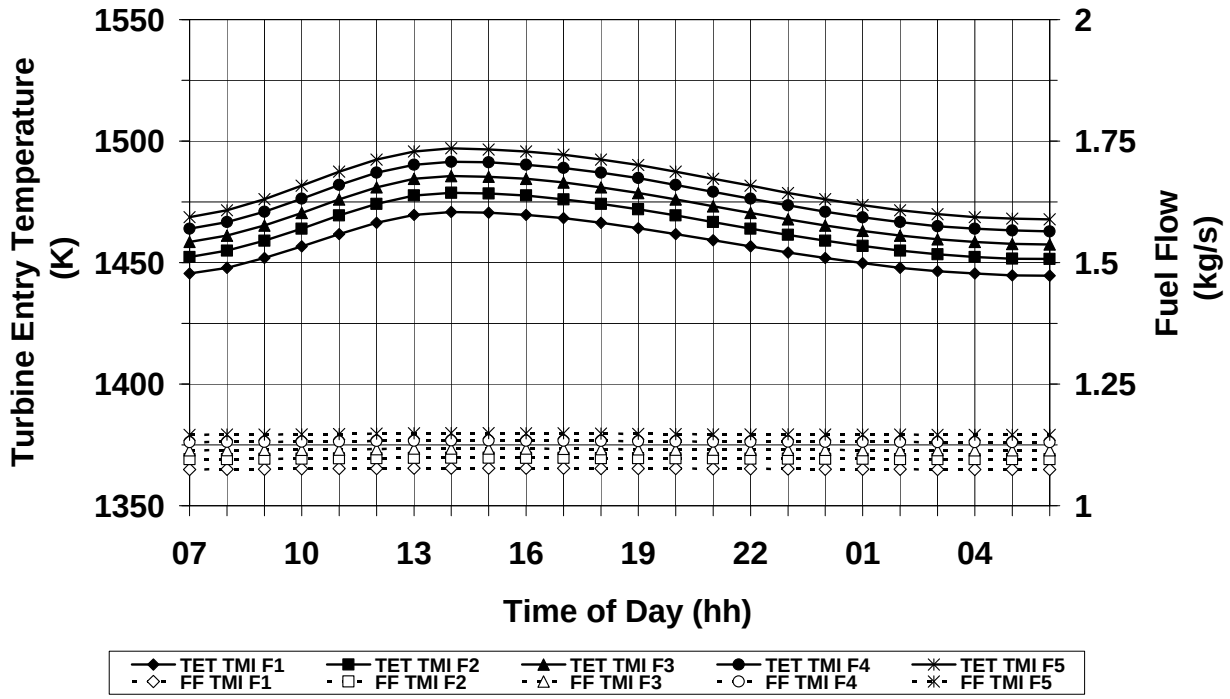

Figure D.2: Twin mode intercooled cycle (TMI) - Turbine entry temperature (TET) and fuel flow (FF) variation against time of day, during journey with annual hull fouling progression (F#) and ideal weather conditions

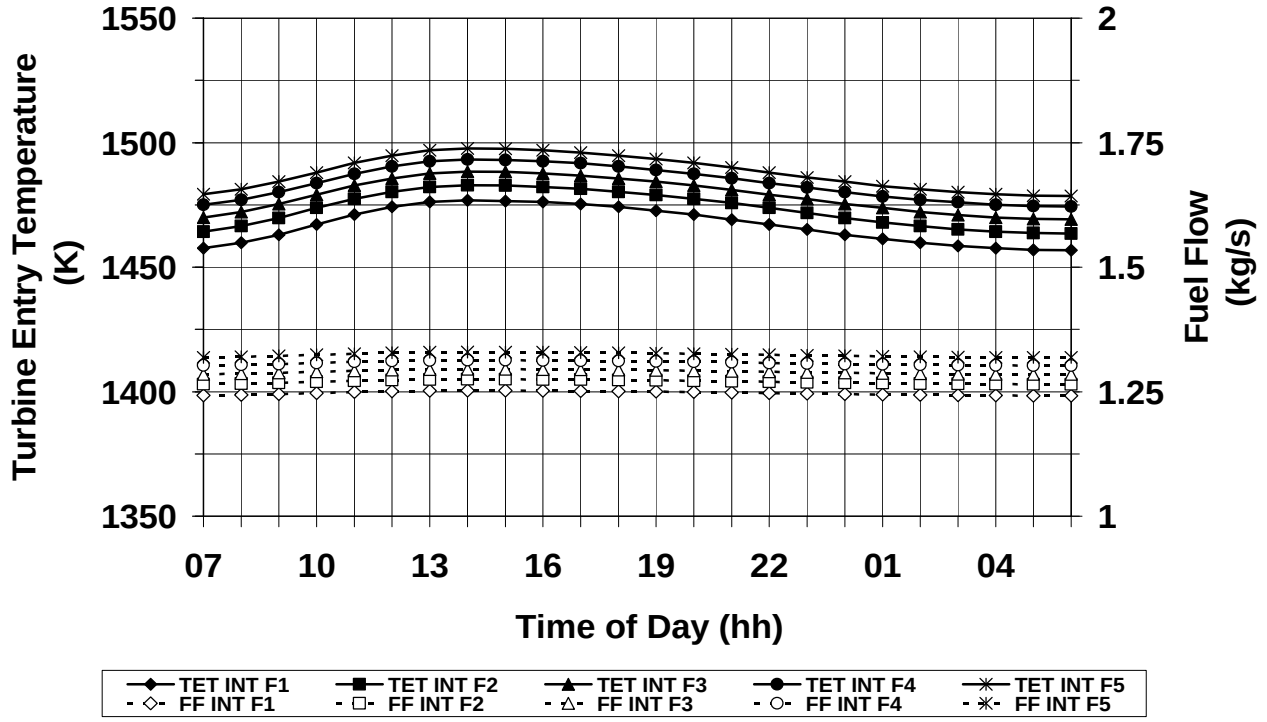

Figure D.3: Intercooled cycle (INT) - Turbine entry temperature (TET) and fuel flow (FF) variation against time of day, during journey with annual hull fouling progression (F#) and ideal weather conditions

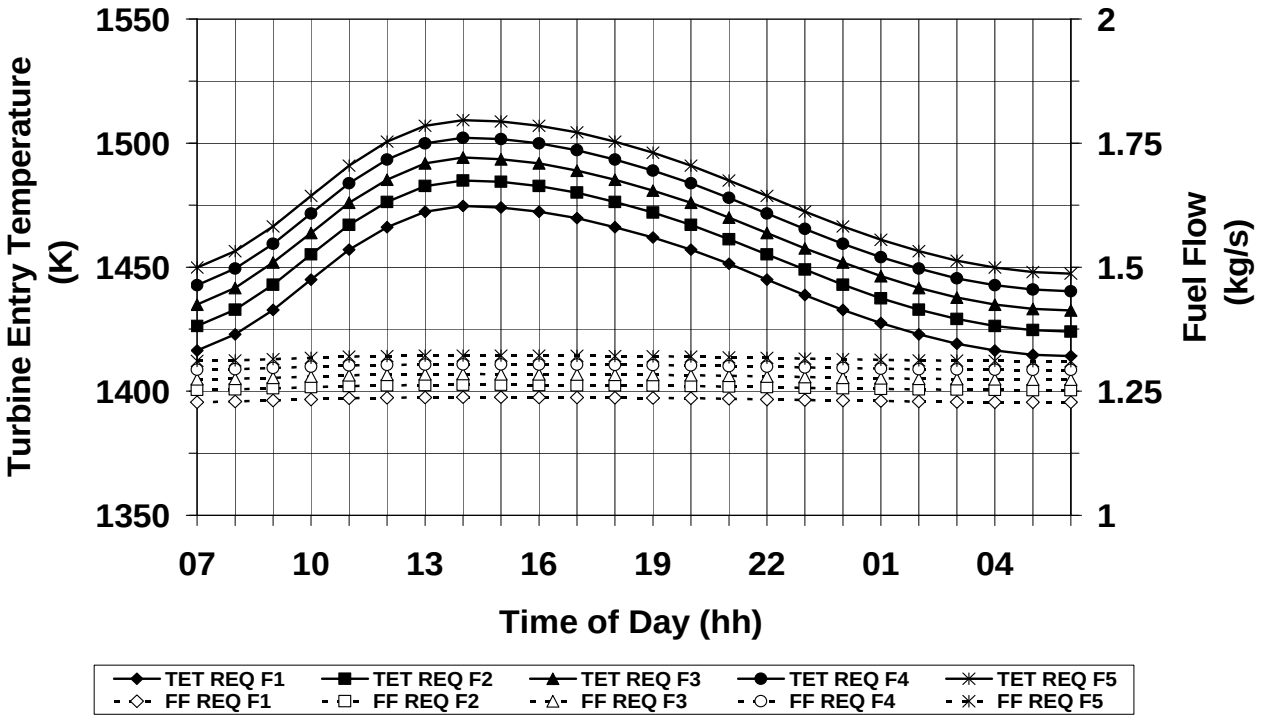

Figure D.4: Recuperated cycle (REQ) - Turbine entry temperature (TET) and fuel flow (FF) variation against time of day, during journey with annual hull fouling progression (F#) and ideal weather conditions

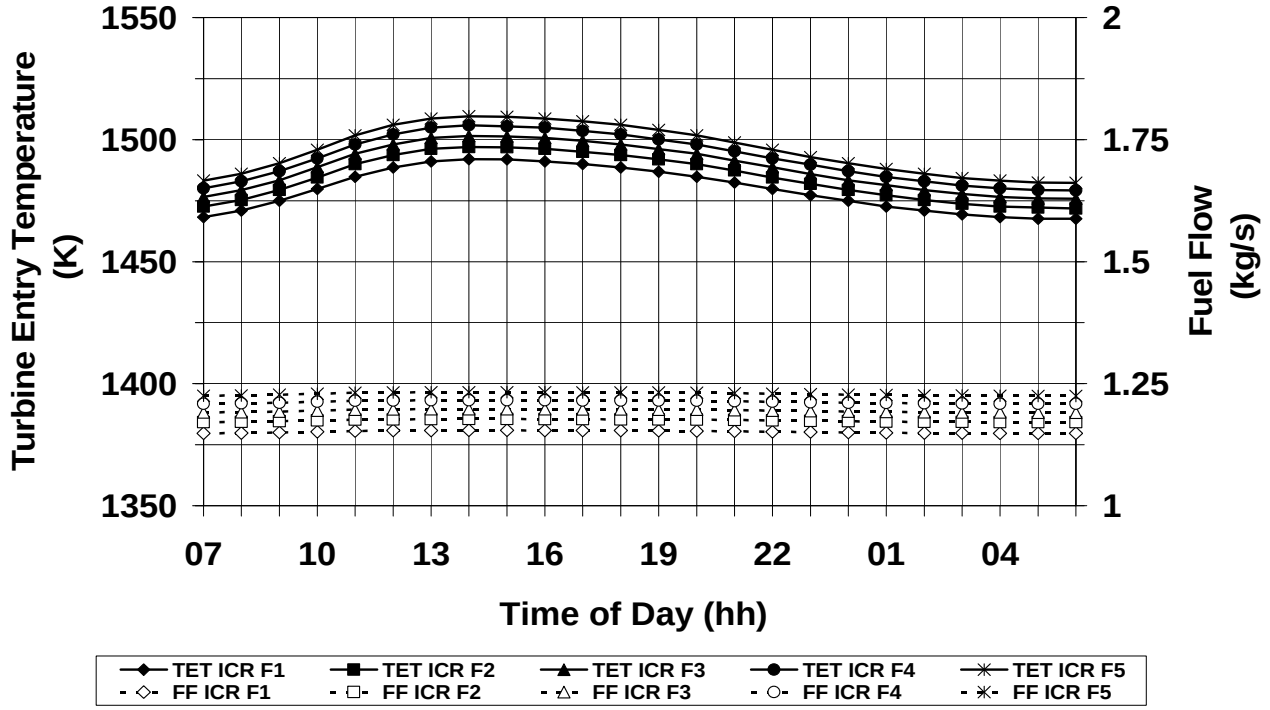

Figure D.5: Intercooled/recuperated cycle (ICR) - Turbine entry temperature (TET) and fuel flow (FF) variation against time of day, during journey with annual hull fouling progression (F#) and ideal weather conditions

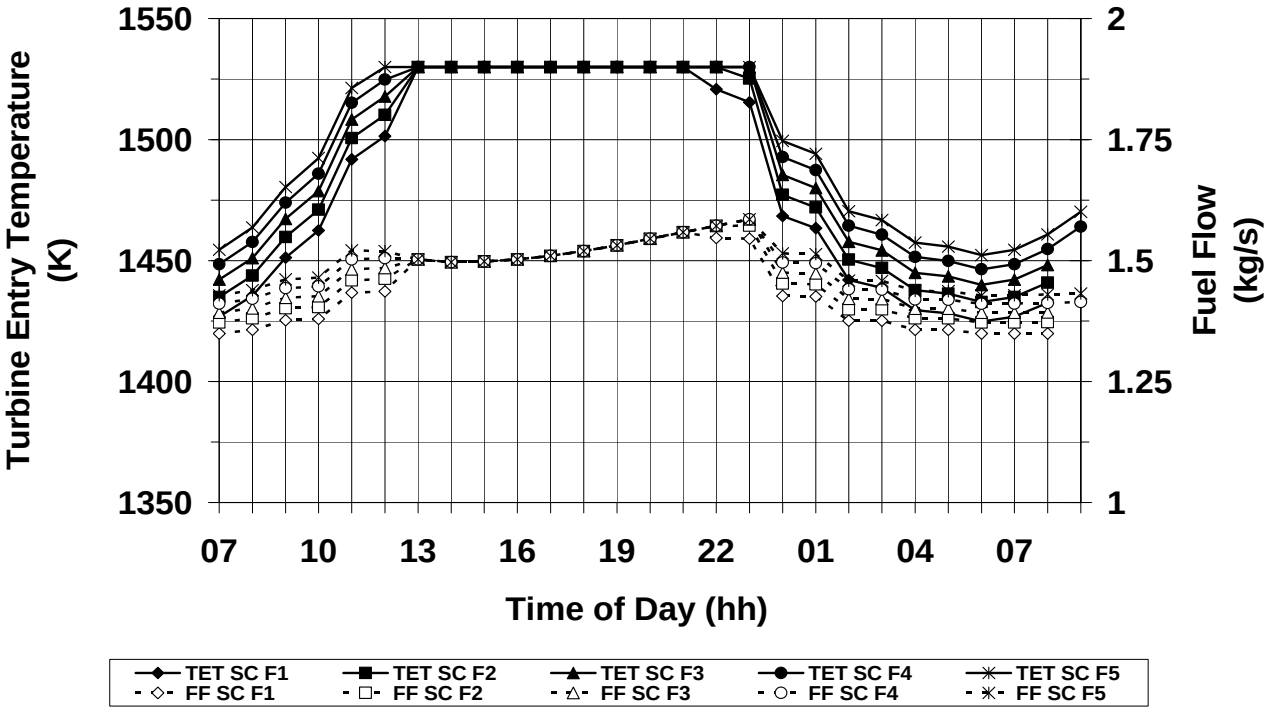

Figure D.6: Simple cycle (SC) - Turbine entry temperature (TET) and fuel flow (FF) variation against time of day, during journey with annual hull fouling progression (F#) and adverse weather conditions

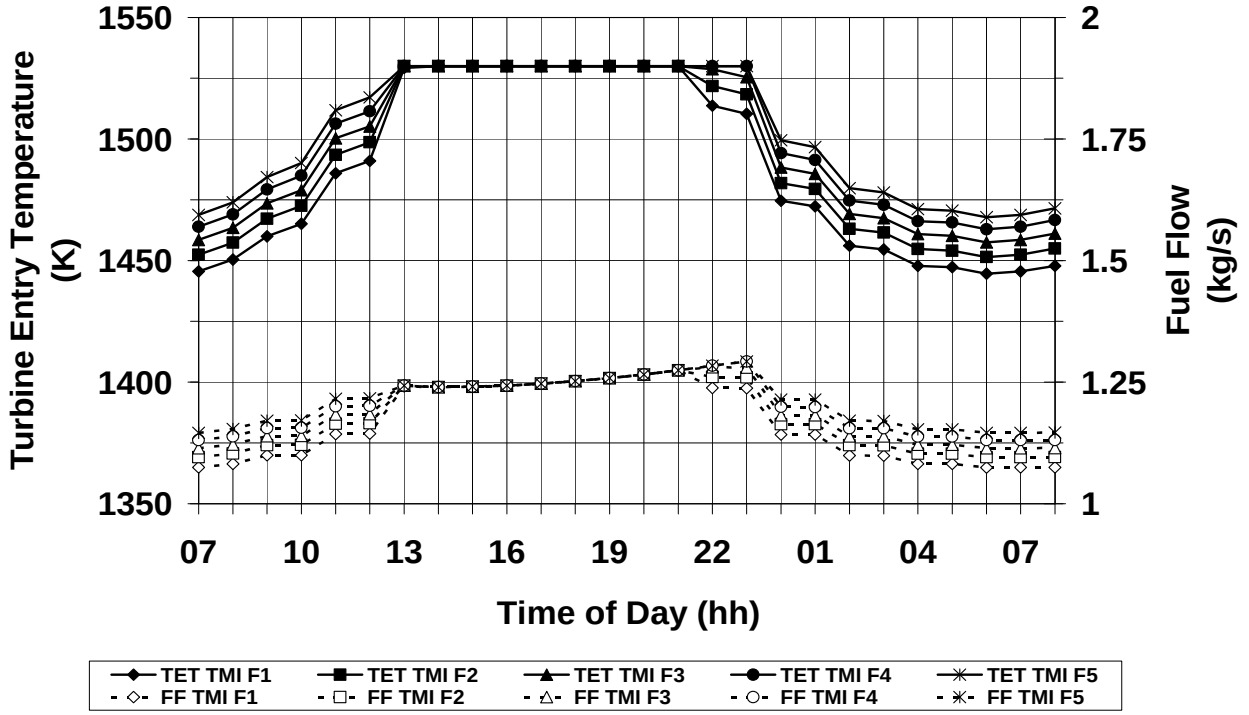

Figure D.7: Twin mode intercooled cycle (TMI) - Turbine entry temperature (TET) and fuel flow (FF) variation against time of day, during journey with annual hull fouling progression (F#) and adverse weather conditions

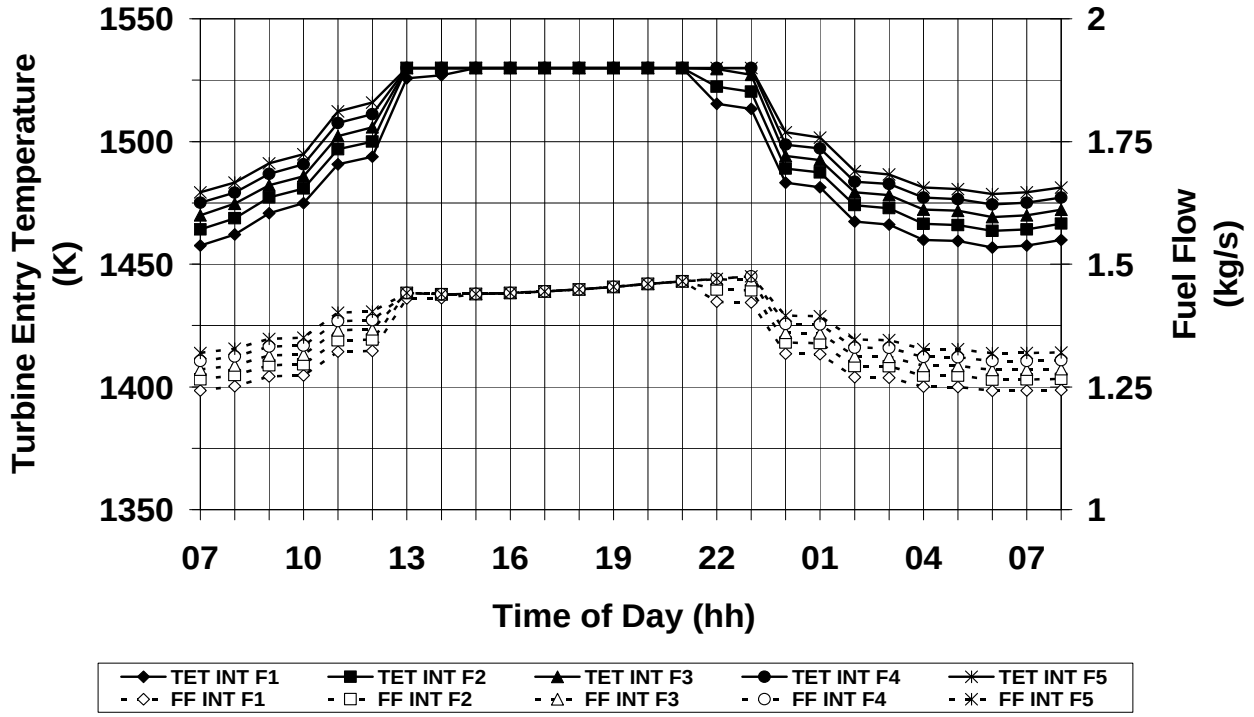

Figure D.8: Intercooled cycle (INT) - Turbine entry temperature (TET) and fuel flow (FF) variation against time of day, during journey with annual hull fouling progression (F#) and adverse weather conditions

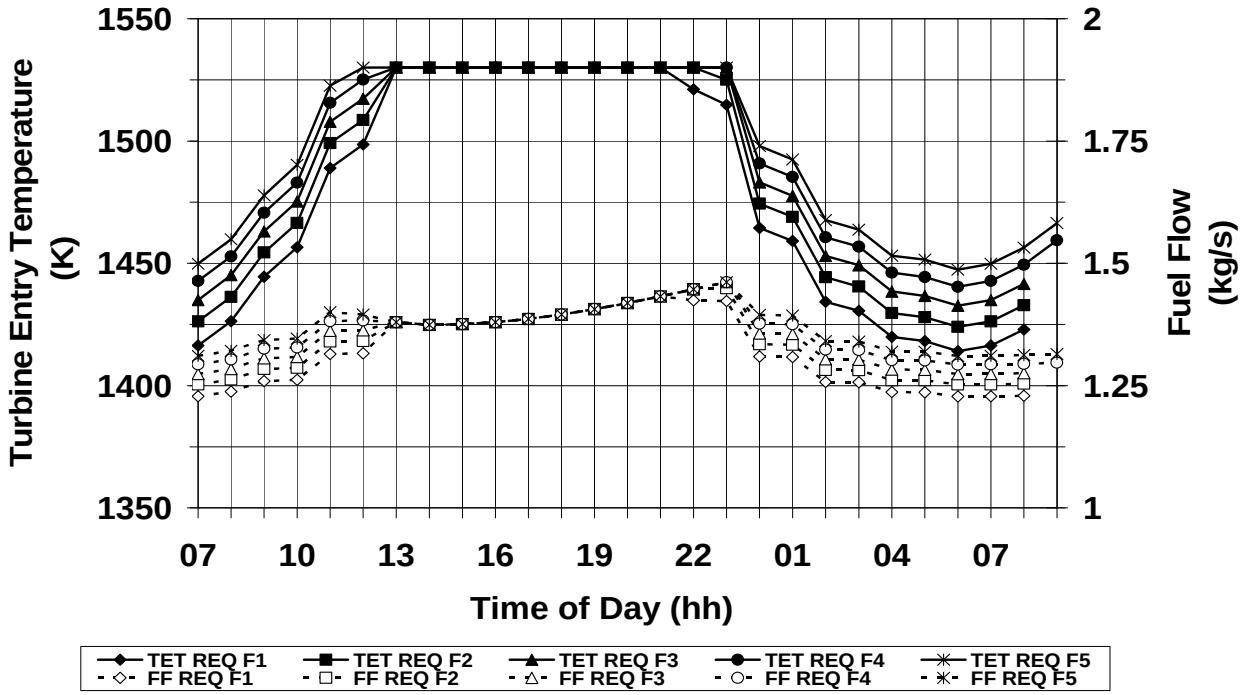

Figure D.9: Recuperated cycle (REQ) - Turbine entry temperature (TET) and fuel flow (FF) variation against time of day, during journey with annual hull fouling progression (F#) and adverse weather conditions

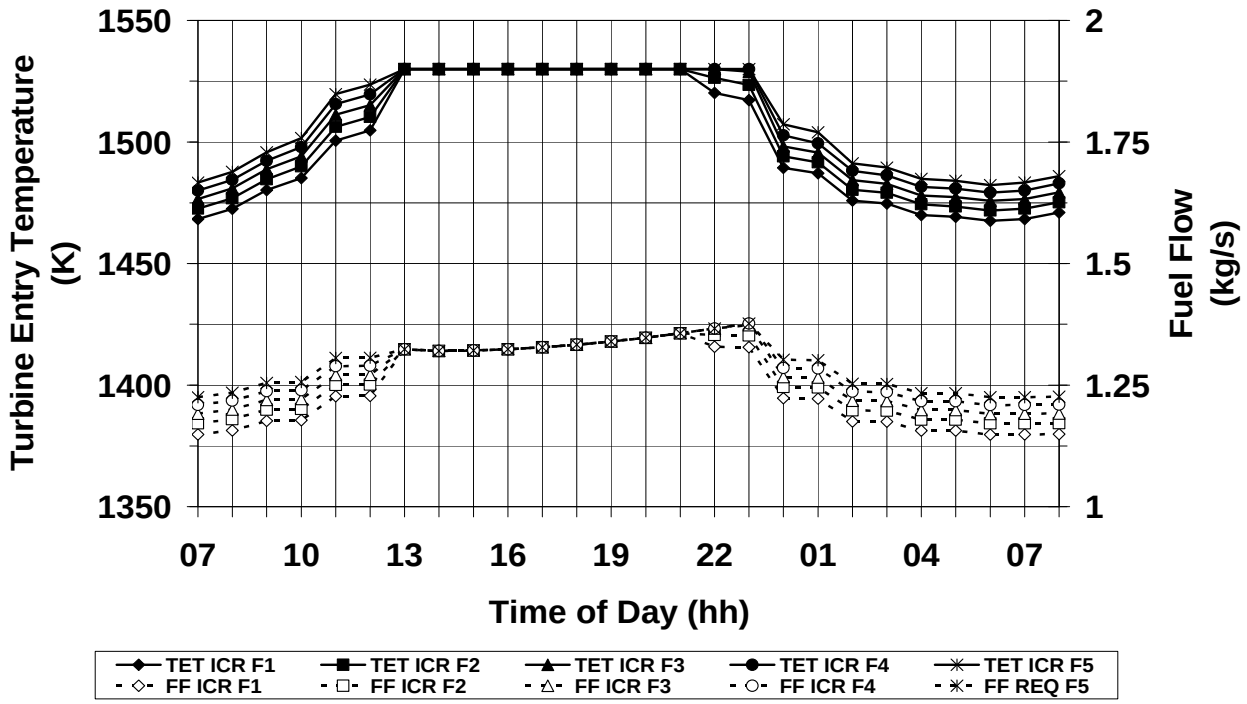

Figure D.10: Intercooled/recuperated cycle (ICR) - Turbine entry temperature (TET) and fuel flow (FF) variation against time of day, during journey with annual hull fouling progression (F#) and adverse weather conditions

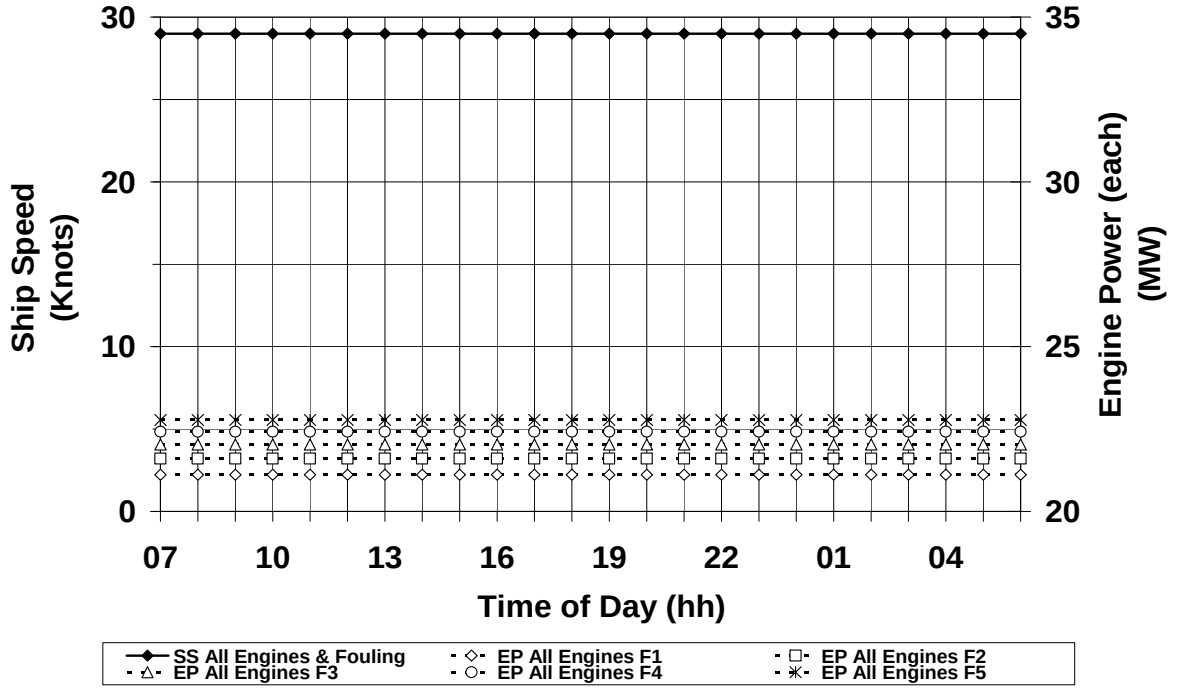

Figure D.11: All Engines – Ship speed (SS) and engine power (EP) (for each engine) variation against time of day, during journey with annual hull fouling progression (F#) and ideal weather conditions

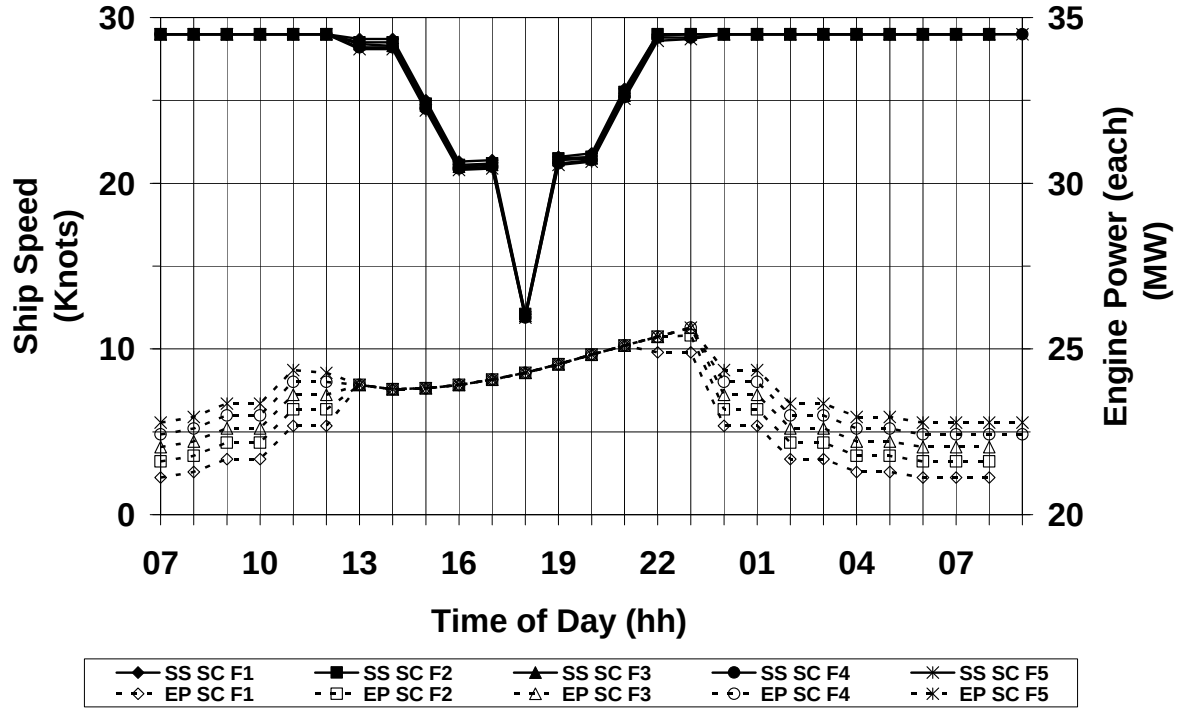

Figure D.12: Simple cycle (SC) – Ship speed (SS) and engine power (EP) (for each engine) variation against time of day, during journey with annual hull fouling progression (F#) and adverse weather conditions

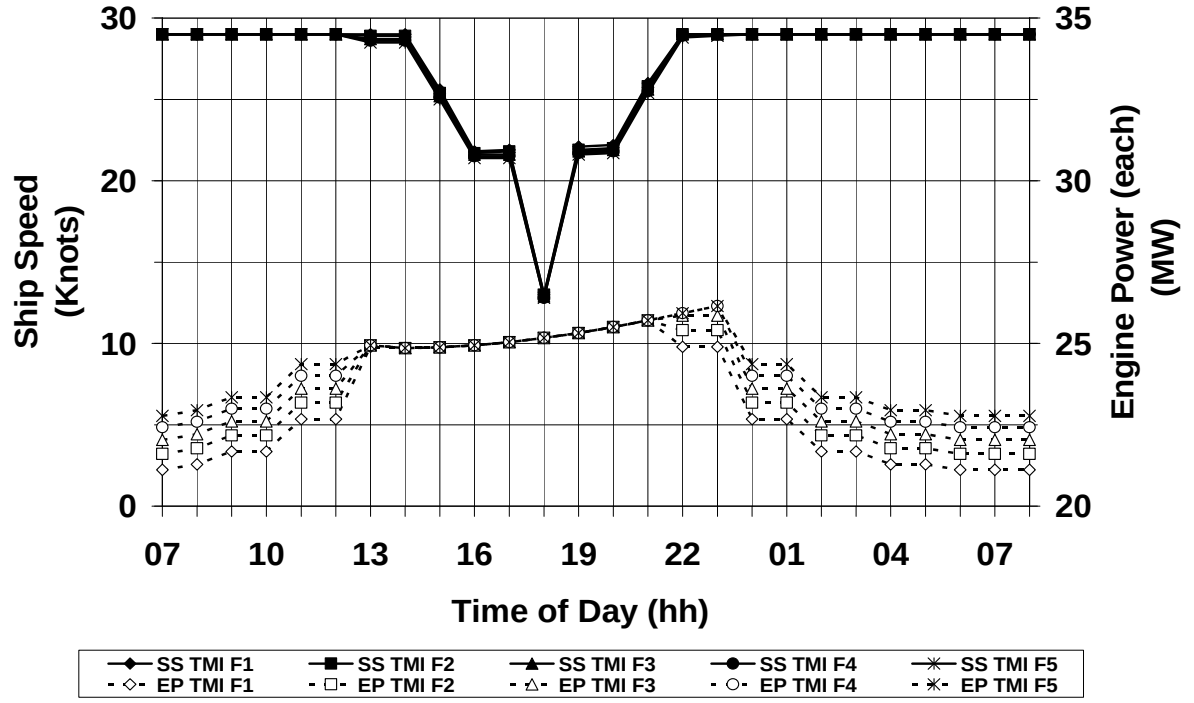

Figure D.13: Twin mode intercooled cycle (TMI) – Ship speed (SS) and engine power (EP) (for each engine) variation against time of day, during journey with annual hull fouling progression (F#) and adverse weather conditions

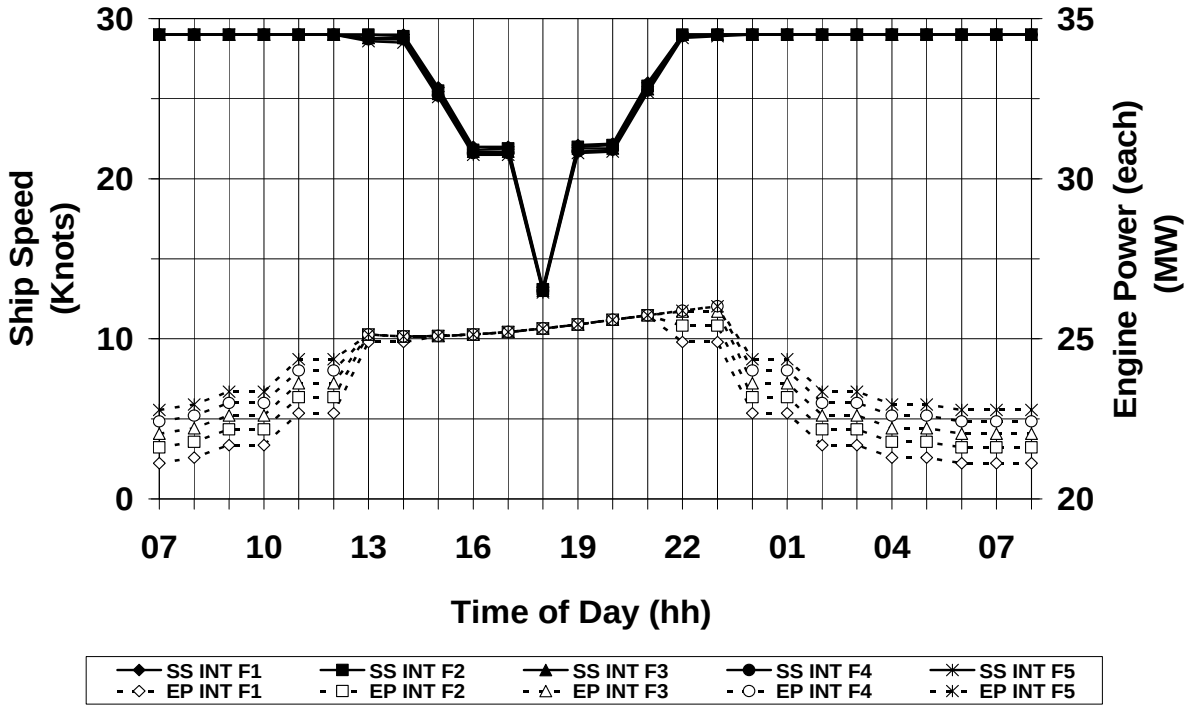

Figure D.14: Intercooled Cycle (INT) – Ship speed (SS) and engine power (EP) (for each engine) variation against time of day, during journey with annual hull fouling progression (F#) and adverse weather Conditions

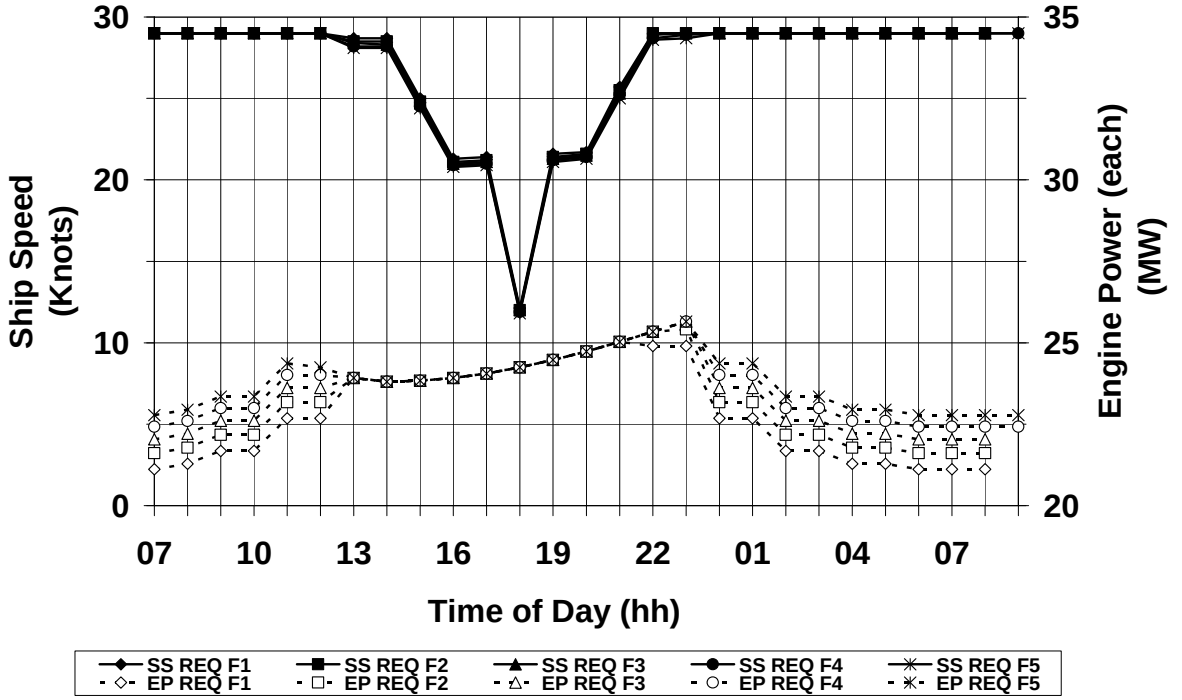

Figure D.15: Recuperated Cycle (REQ) – Ship speed (SS) and engine power (EP) (for each engine) variation against time of day, during journey with annual hull fouling progression (F#) and adverse weather conditions

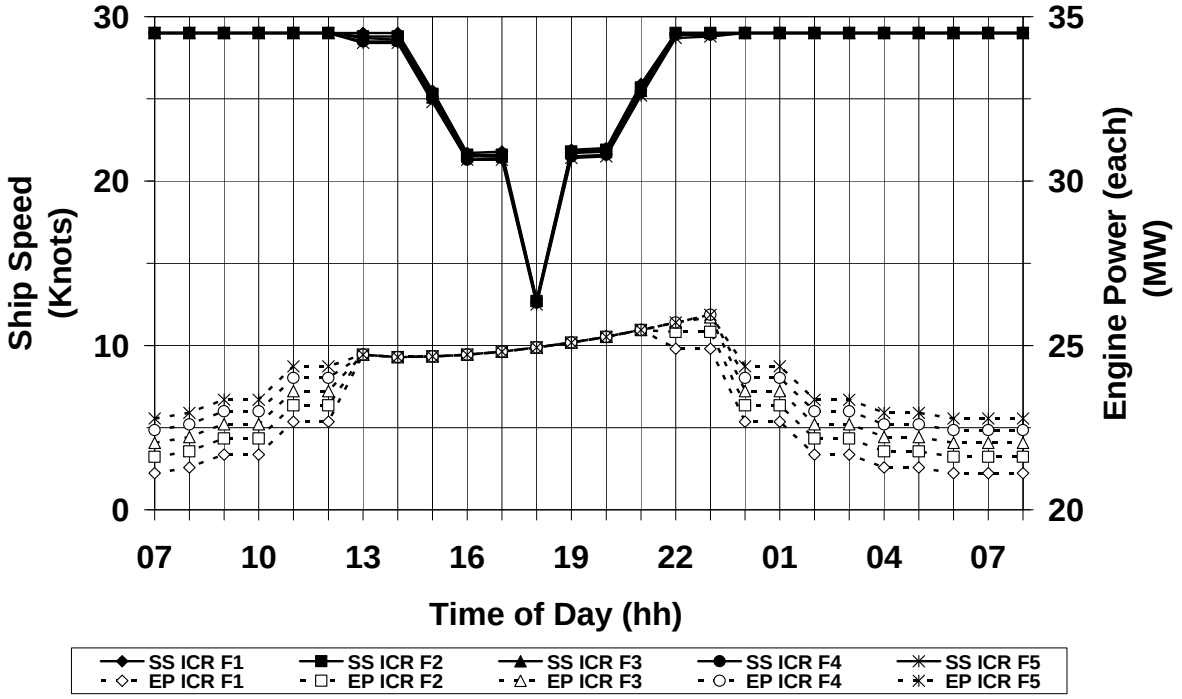

Figure D.16: Intercooled/recuperated cycle (ICR) – Ship speed (SS) and engine power (EP) (for each engine) variation against time of day, during journey with annual hull fouling progression (F#) and adverse weather conditions

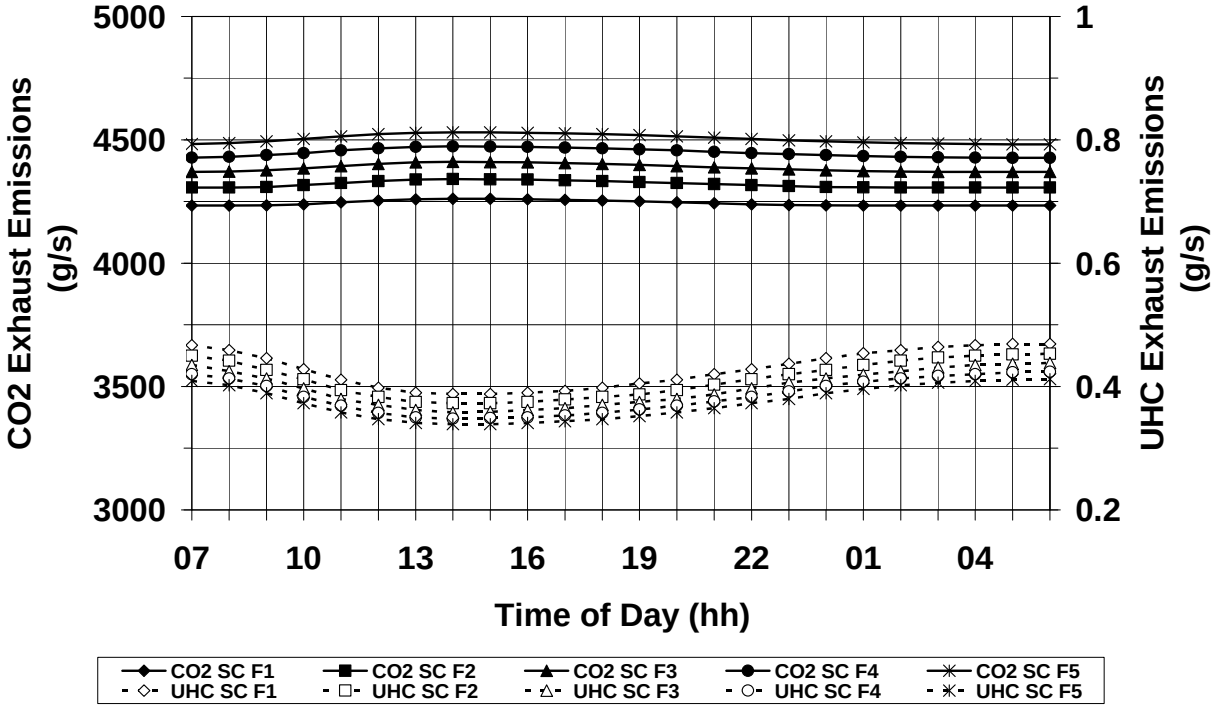

Figure D.17: Simple cycle (SC) – Carbon dioxide (CO2) and unburned hydrocarbons (UHC) exhaust emissions variation against time of day, during journey with annual hull fouling progression (F#) and ideal weather conditions

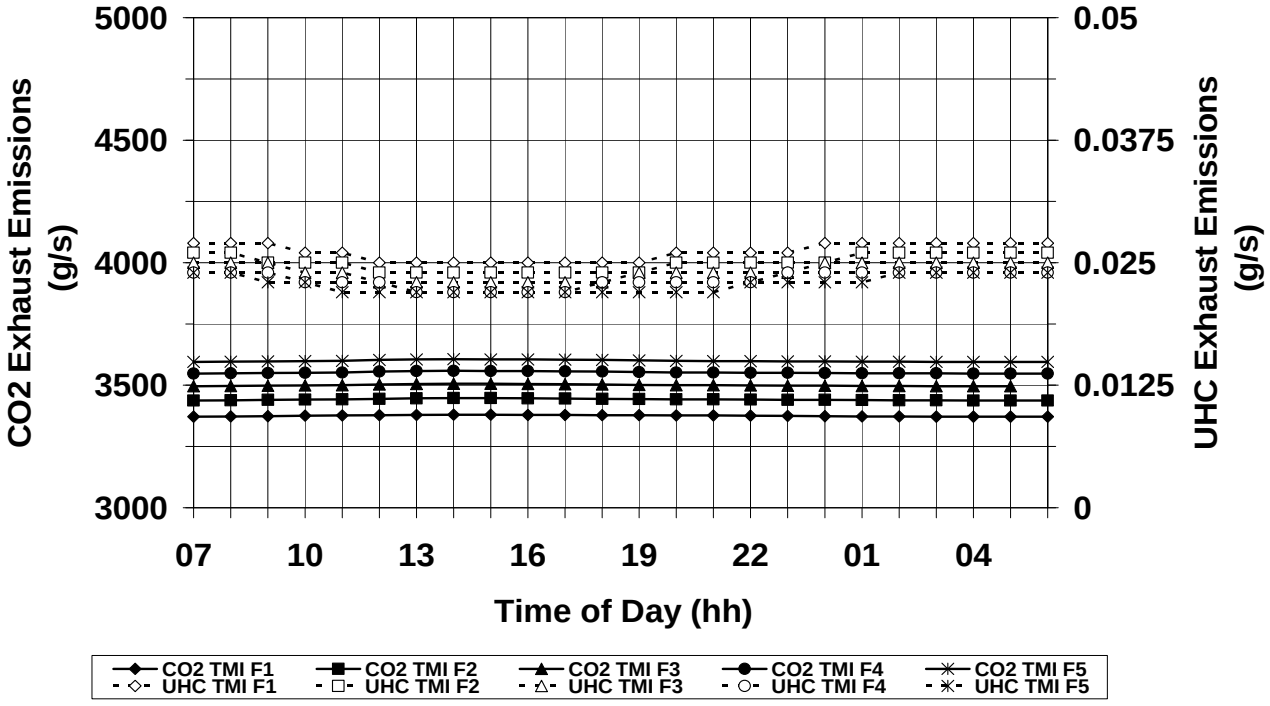

Figure D.18: Twin mode intercooled cycle (TMI) – Carbon dioxide (CO2) and unburned hydrocarbons (UHC) exhaust emissions variation against time of day, during journey with annual hull fouling progression (F#) and ideal weather conditions

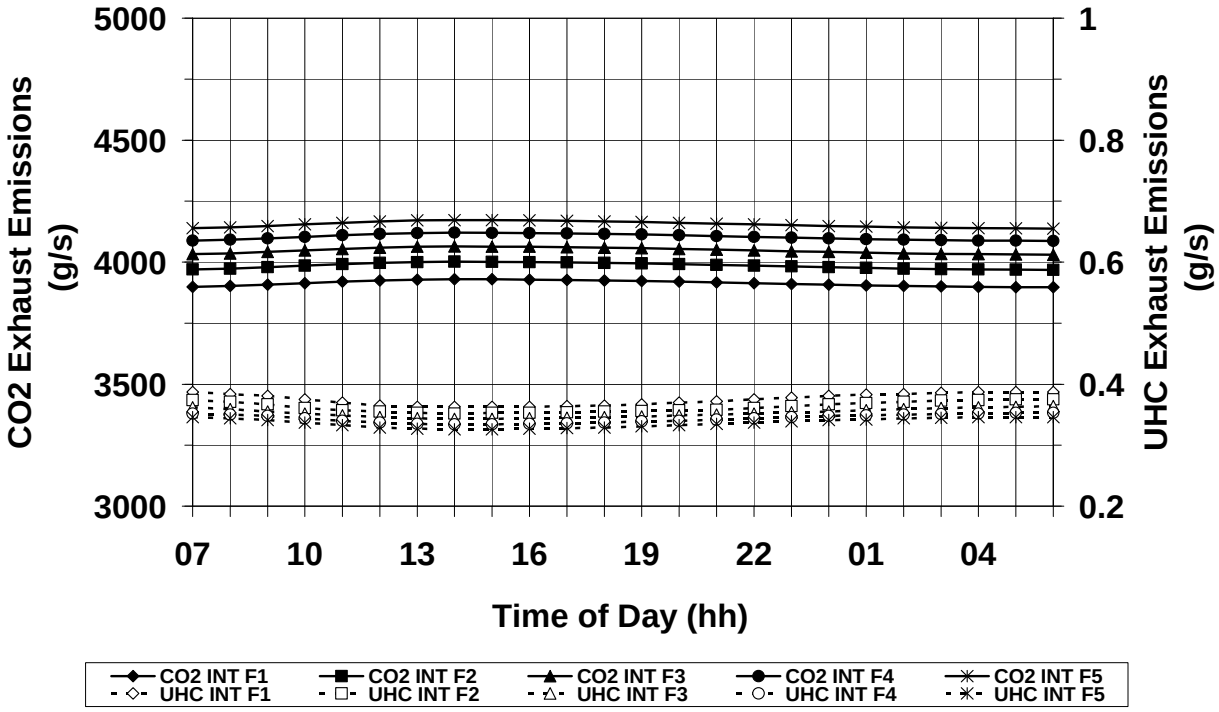

Figure D.19: Intercooled cycle (INT) – Carbon dioxide (CO2) and unburned hydrocarbons (UHC) exhaust emissions variation against time of day, during journey with annual hull fouling progression (F#) and ideal weather conditions

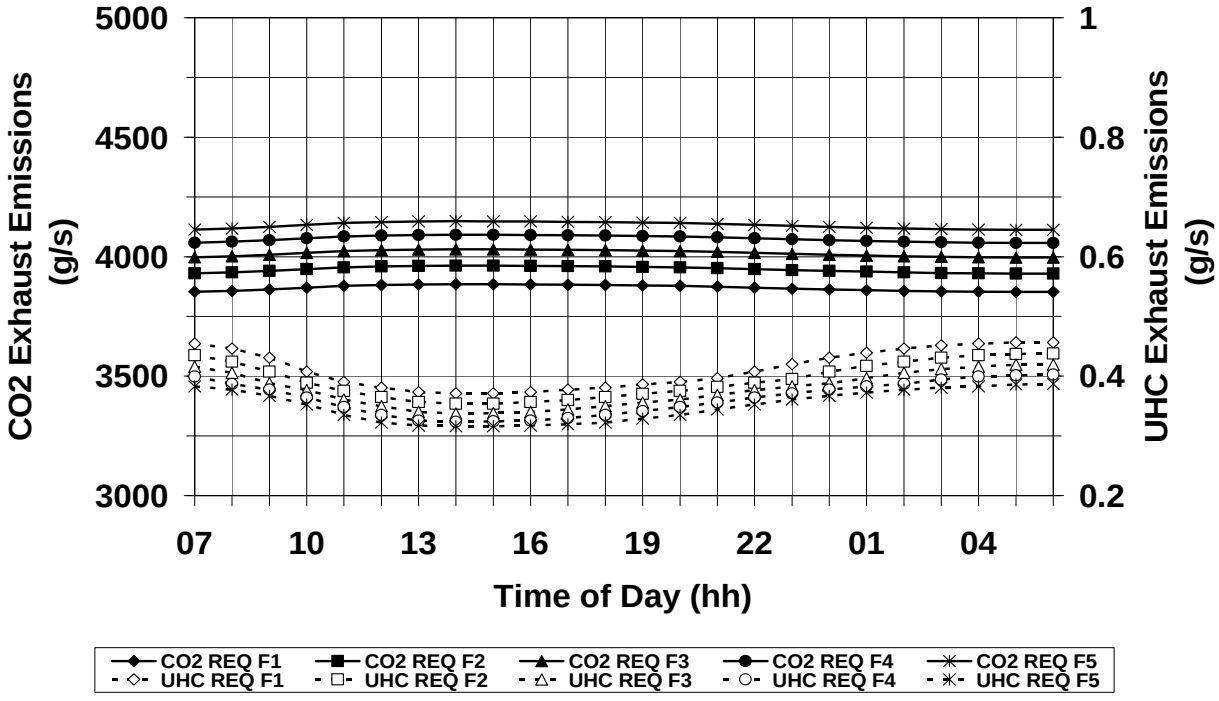

Figure D.20: Requperated cycle (REQ) – Carbon dioxide (CO2) and unburned hydrocarbons (UHC) exhaust emissions variation against time of day, during journey with annual hull fouling progression (F#) and ideal weather conditions

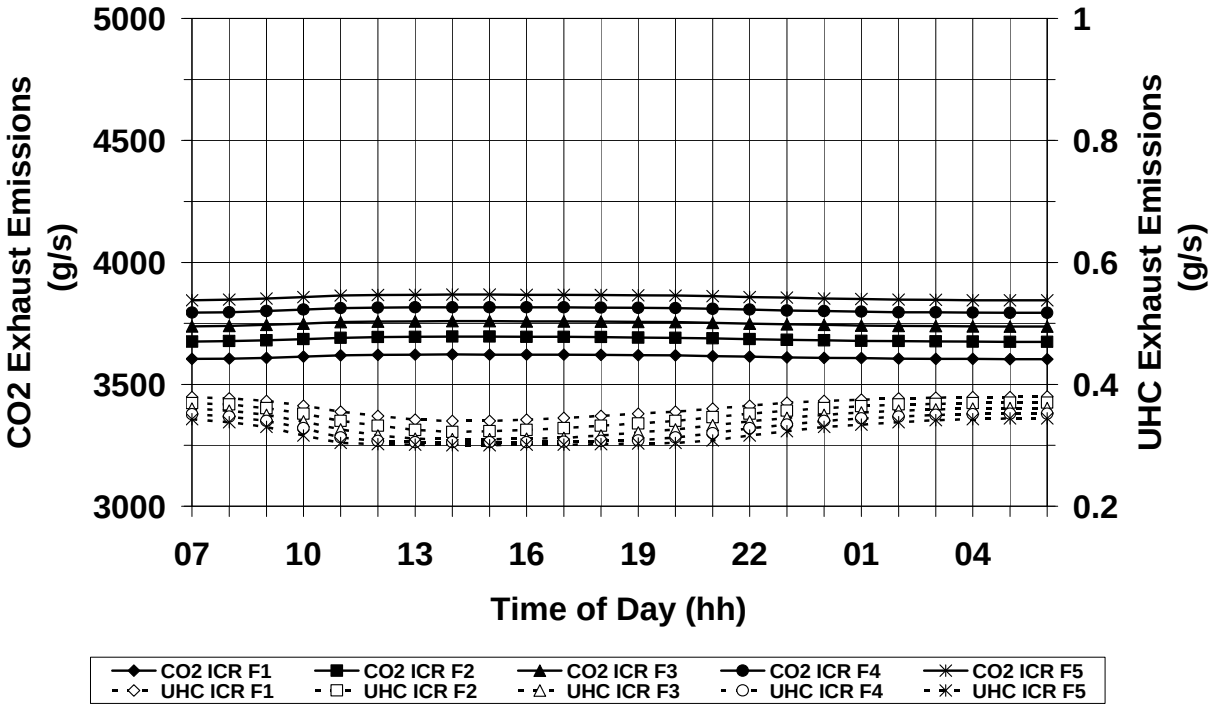

Figure D.21: Intercooled/recuperated cycle (ICR) – Carbon dioxide (CO2) and unburned hydrocarbons (UHC) exhaust emissions variation against time of day, during journey with annual hull fouling progression (F#) and ideal weather conditions

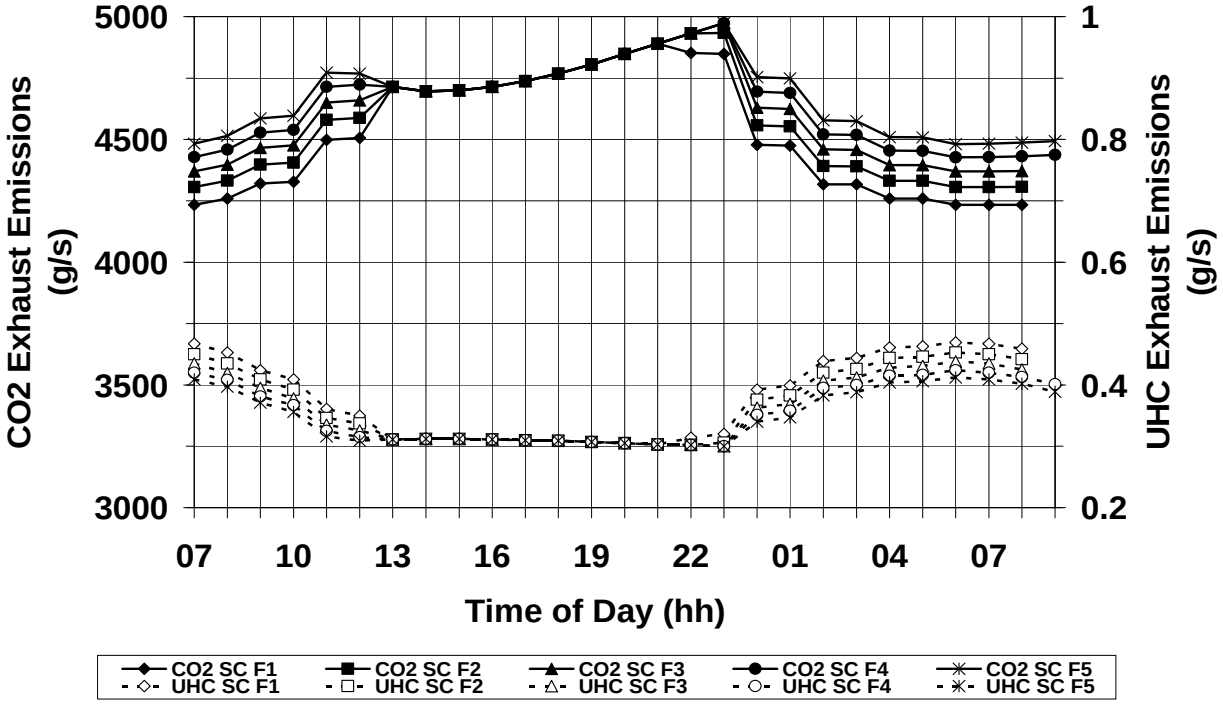

Figure D.22: Simple cycle (SC) – Carbon dioxide (CO2) and unburned hydrocarbons (UHC) exhaust emissions variation against time of day, during journey with annual hull fouling progression (F#) and adverse weather conditions

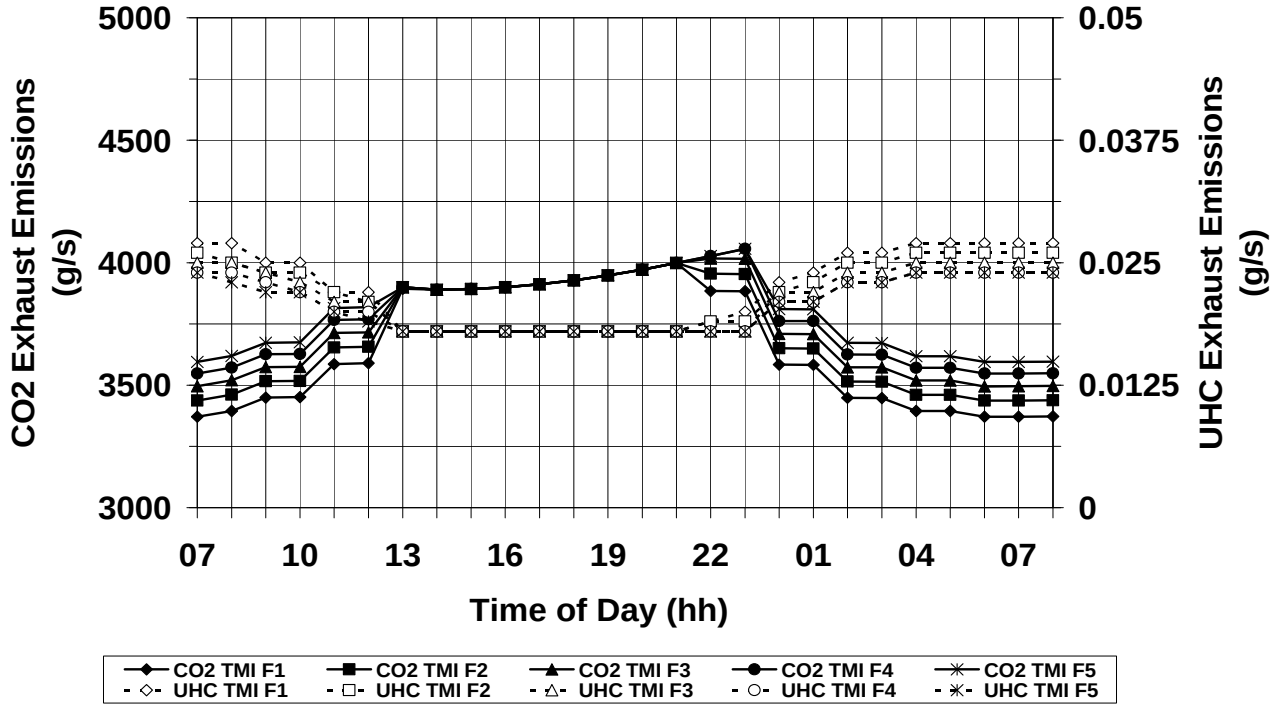

Figure D.23: Twin mode intercooled cycle (TMI) – Carbon dioxide (CO2) and unburned hydrocarbons (UHC) exhaust emissions variation against time of day, during journey with annual hull fouling progression (F#) and adverse weather conditions

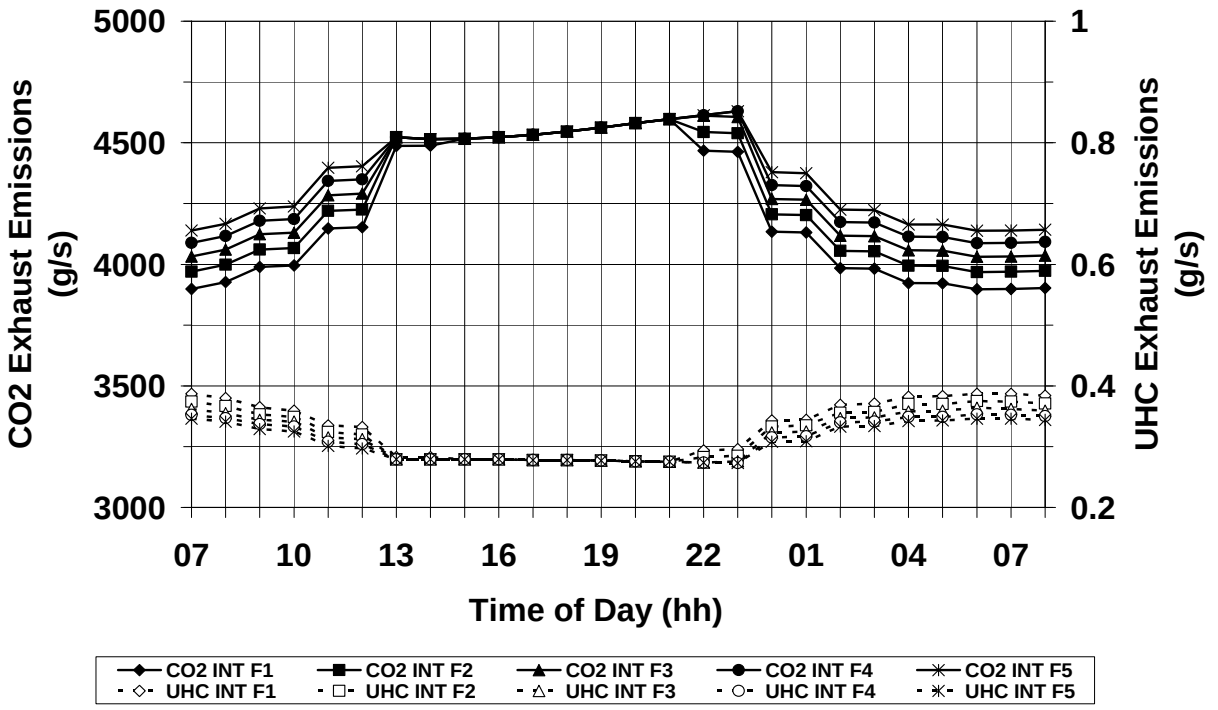

Figure D.24: Intercooled cycle (INT) – Carbon dioxide (CO2) and unburned hydrocarbons (UHC) exhaust emissions variation against time of day, during journey with annual hull fouling progression (F#) and adverse weather conditions

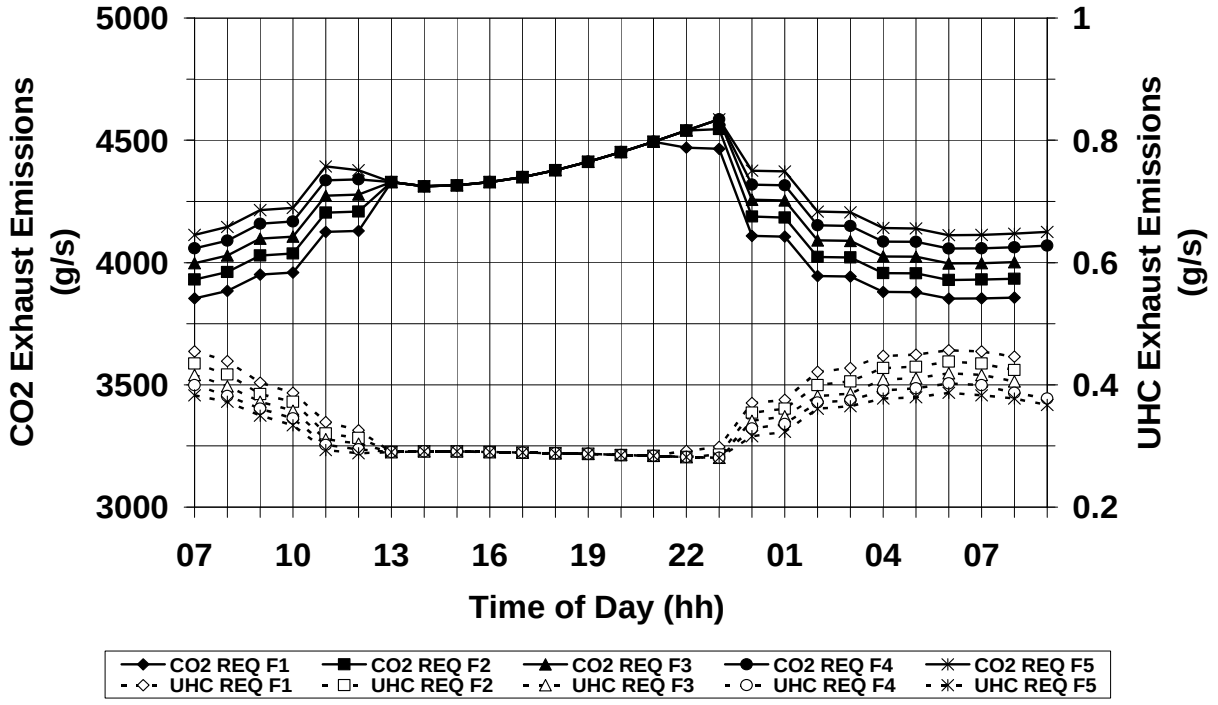

Figure D.25: Recuperated cycle (REQ) – Carbon dioxide (CO2) and unburned hydrocarbons (UHC) exhaust emissions variation against time of day, during journey with annual hull fouling progression (F#) and adverse weather conditions

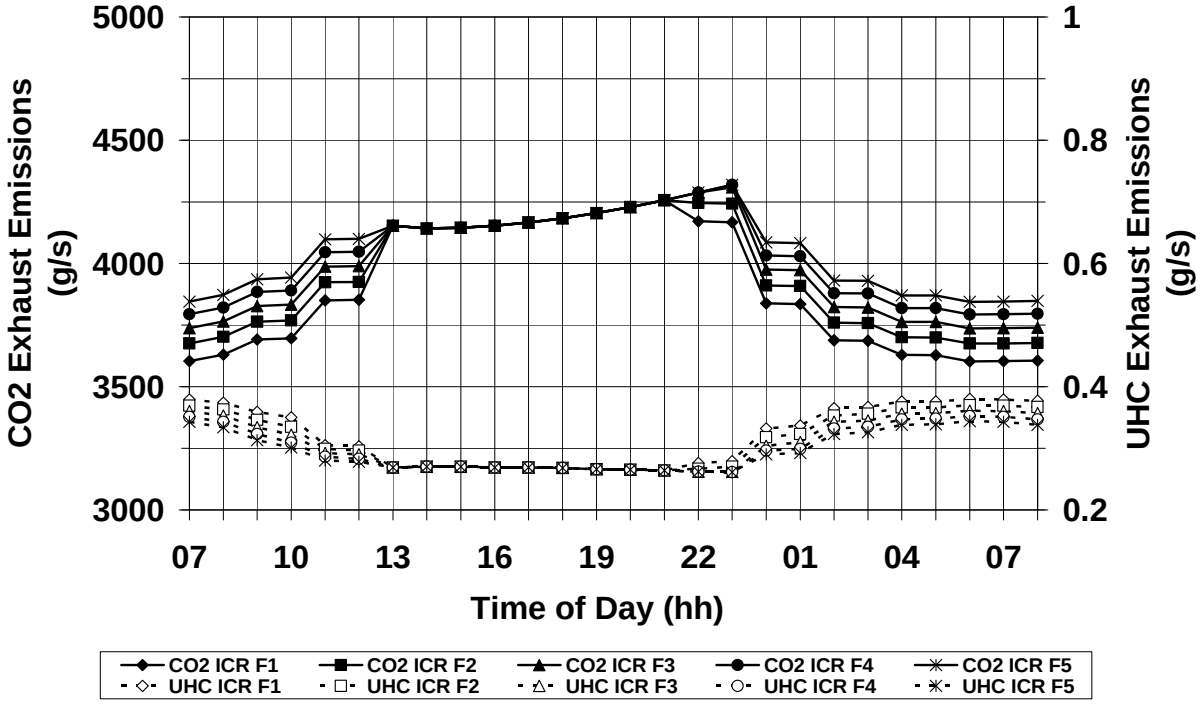

Figure D.26: Intercooled/recuperated cycle (ICR) – Carbon dioxide (CO2) and unburned hydrocarbons (UHC) exhaust emissions variation against time of day, during journey with annual hull fouling progression (F#) and adverse weather conditions

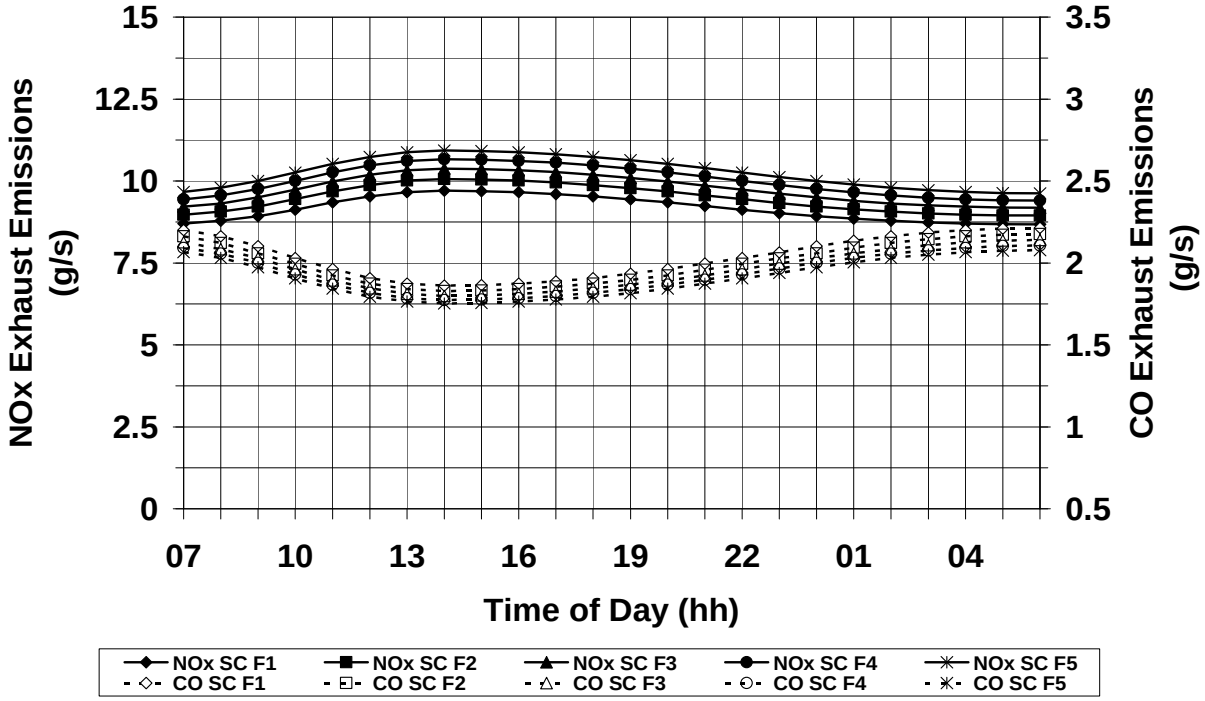

Figure D.27: Simple cycle (SC) – Nitric oxide (NOx) and carbon monoxide (CO) exhaust emissions variation against time of day, during journey with annual hull fouling progression (F#) and ideal weather conditions

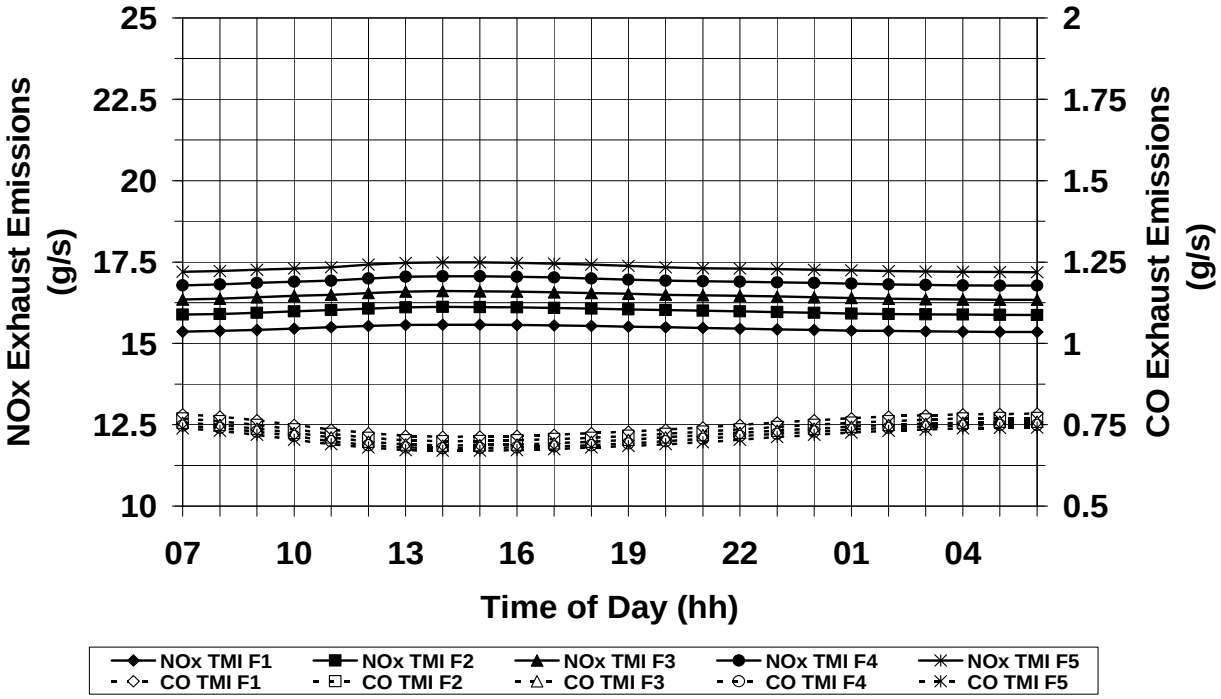

Figure D.28: Twin mode intercooled cycle (TMI) – Nitric oxide (NOx) and carbon monoxide (CO) exhaust emissions variation against time of day, during journey with annual hull fouling progression (F#) and ideal weather conditions

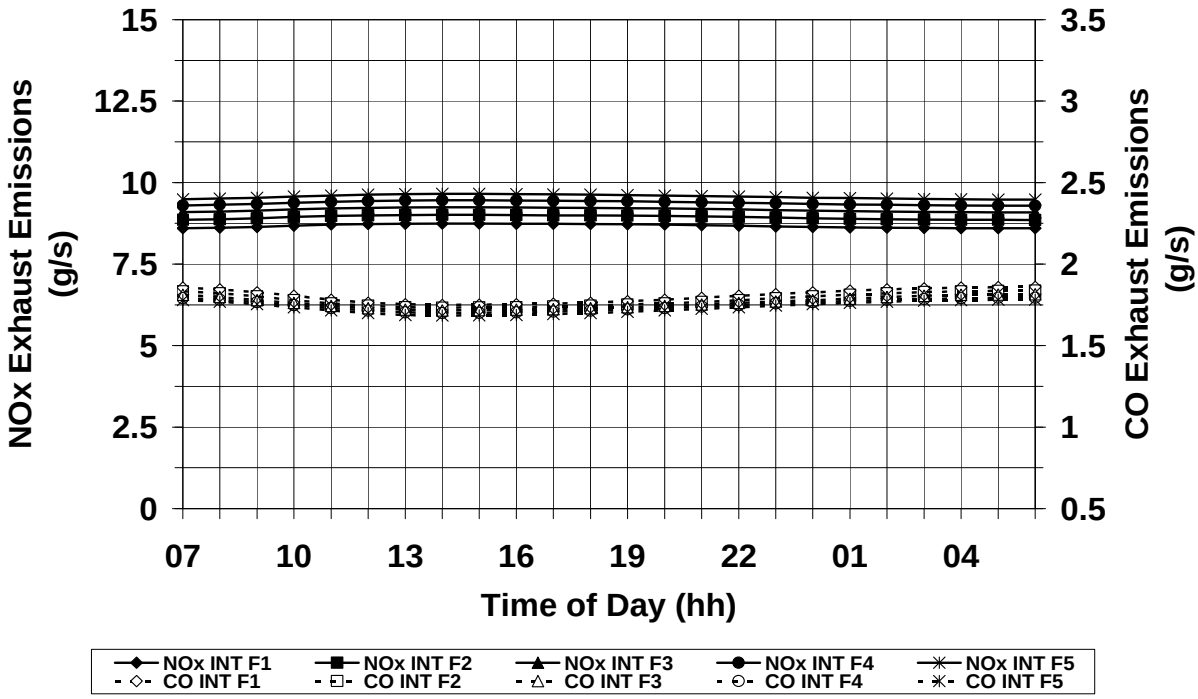

Figure D.29: Intercooled cycle (INT) – Nitric oxide (NOx) and carbon monoxide (CO) exhaust emissions variation against time of day, during journey with annual hull fouling progression (F#) and ideal weather conditions

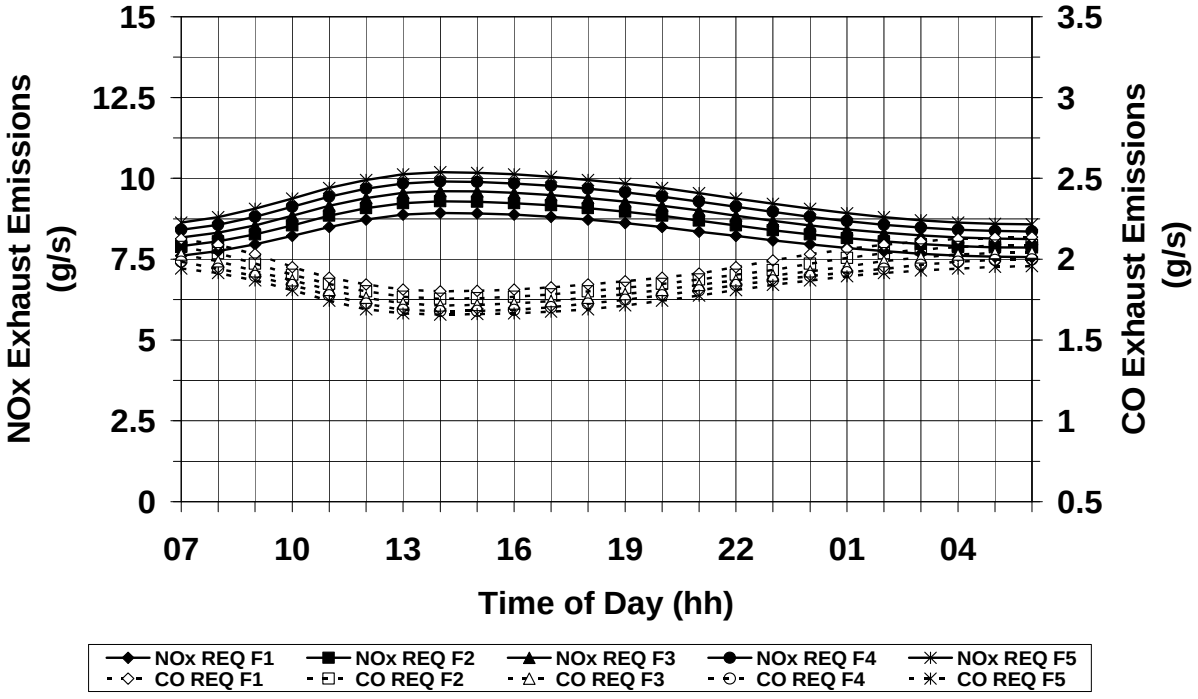

Figure D.30: Recuperated Cycle (REQ) – Nitric oxide (NOx) and carbon monoxide (CO) exhaust emissions variation against time of day, during journey with annual hull fouling progression (F#) and ideal weather conditions

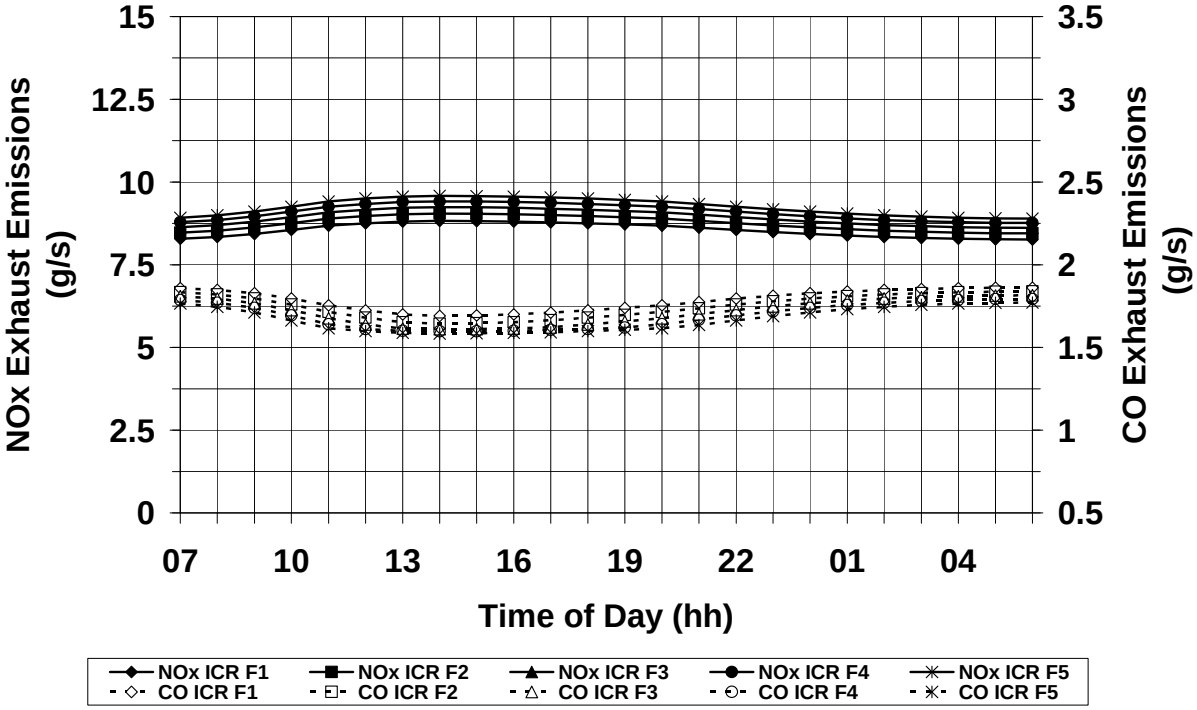

Figure D.31: Intercooled/recuperated cycle (ICR) – Nitric oxide (NOx) and carbon monoxide (CO) exhaust emissions variation against time of day, during journey with annual hull fouling progression (F#) and ideal weather conditions

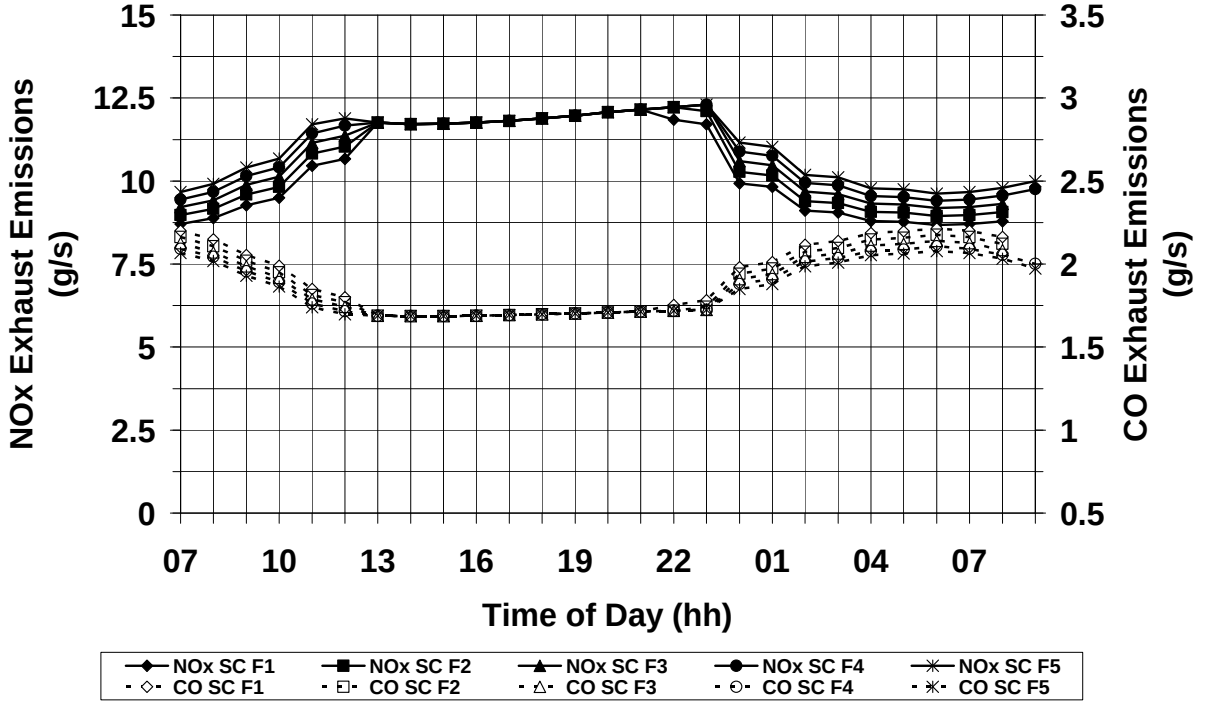

Figure D.32: Simple cycle (SC) – Nitric oxide (NOx) and carbon monoxide (CO) exhaust emissions variation against time of day, during journey with annual hull fouling progression (F#) and adverse weather conditions

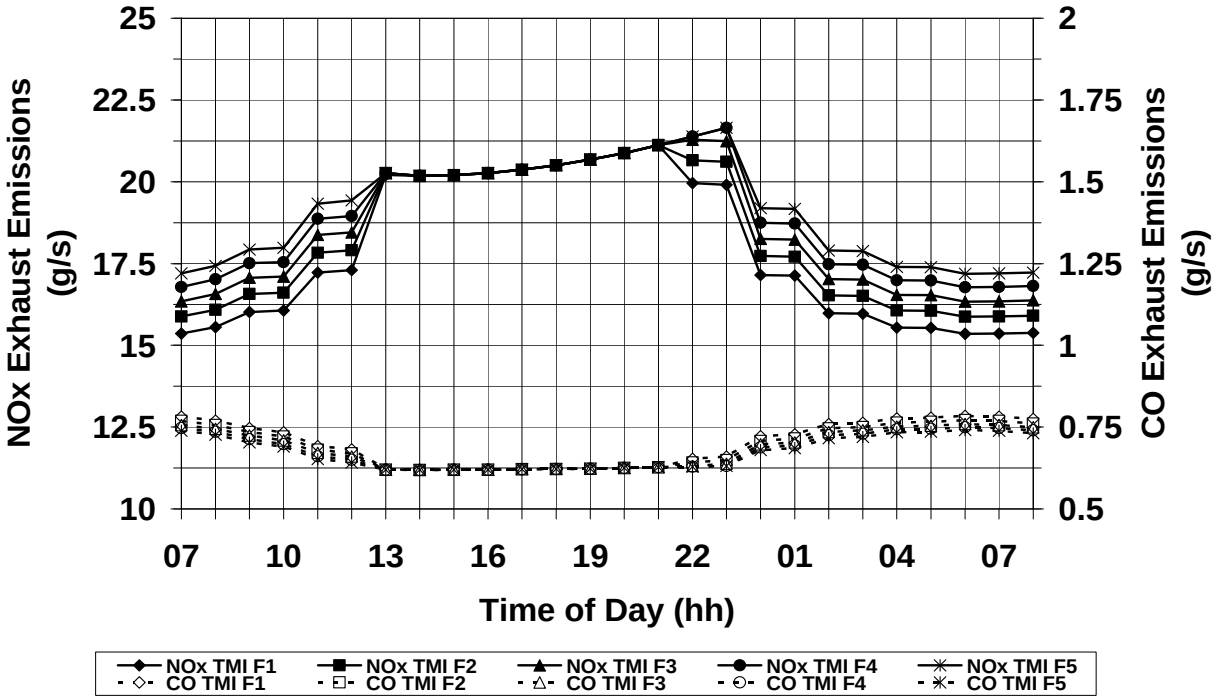

Figure D.33: Twin mode intercooled Cycle (TMI) – Nitric oxide (NOx) and carbon monoxide (CO) exhaust emissions variation against time of day, during journey with annual hull fouling progression (F#) and adverse weather conditions

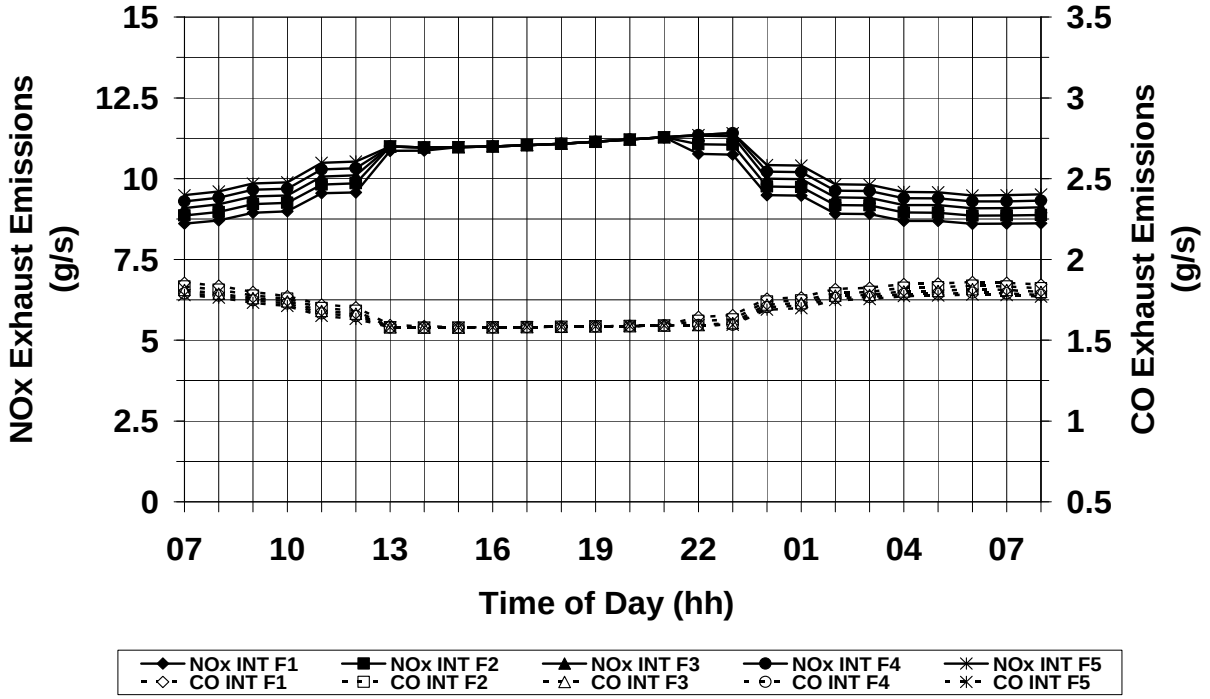

Figure D.34: Intercooled cycle (INT) – Nitric oxide (NOx) and carbon monoxide (CO) exhaust emissions variation against time of day, during journey with annual hull fouling progression (F#) and adverse weather conditions

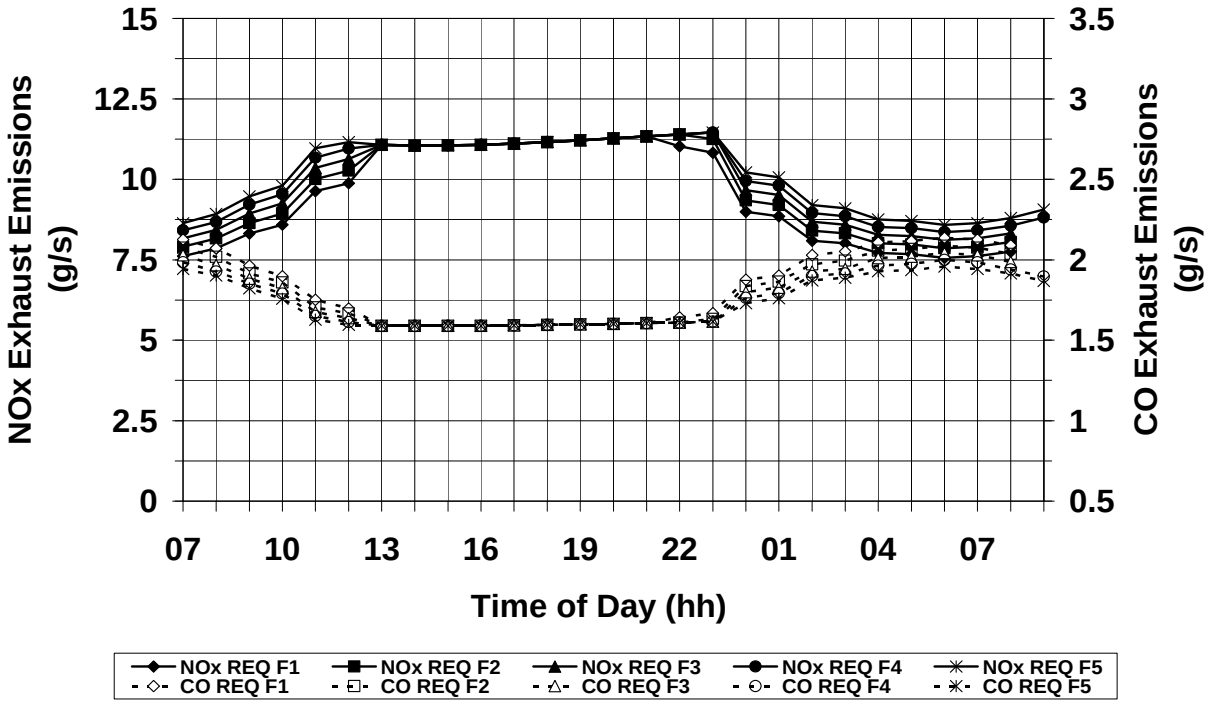

Figure D.35: Recuperated cycle (REQ) – Nitric oxide (NOx) and carbon monoxide (CO) exhaust emissions variation against time of day, during journey with annual hull fouling progression (F#) and adverse weather conditions

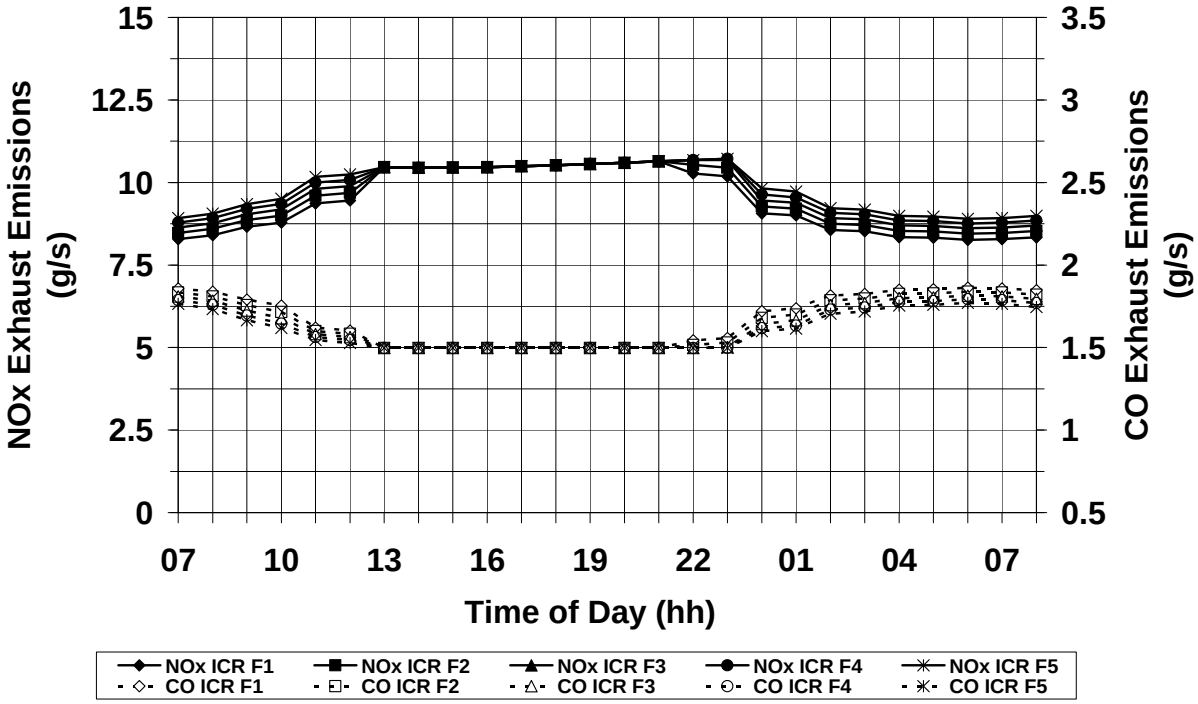

Figure D.36: Intercooled/recuperated cycle (ICR) – Nitric oxide (NOx) and carbon monoxide (CO) exhaust emissions variation against time of day, during journey with annual hull fouling progression (F#) and adverse weather conditions

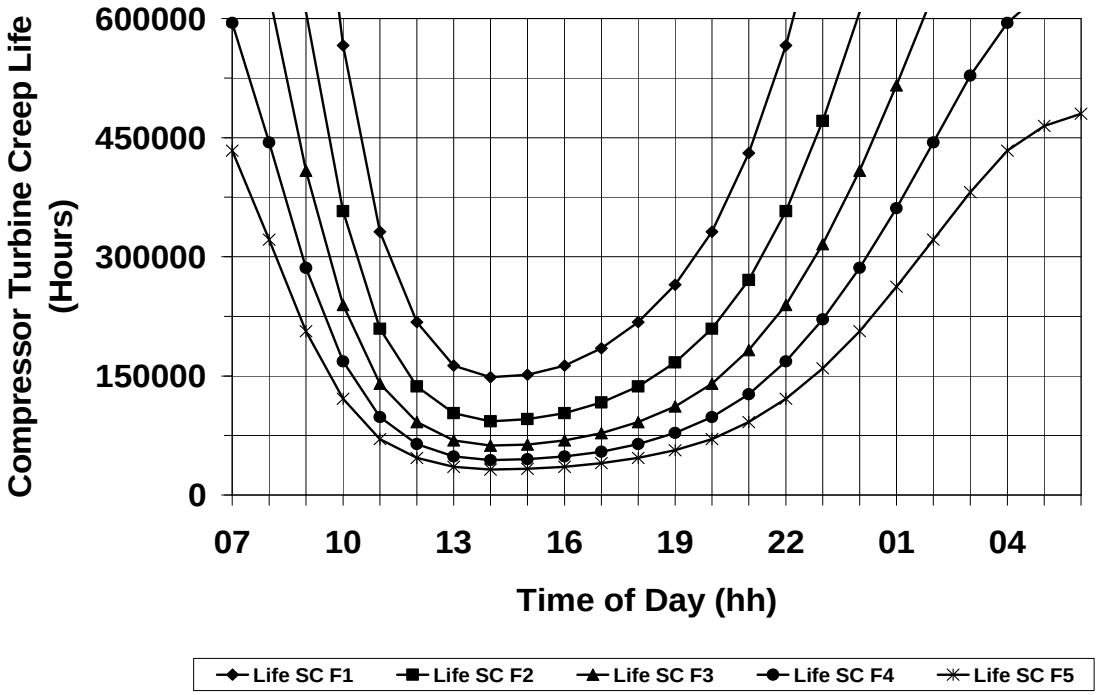

Figure D.37: Simple cycle (SC) – Compressor turbine creep life variation against time of day, during journey with annual hull fouling progression (F#) and ideal weather conditions

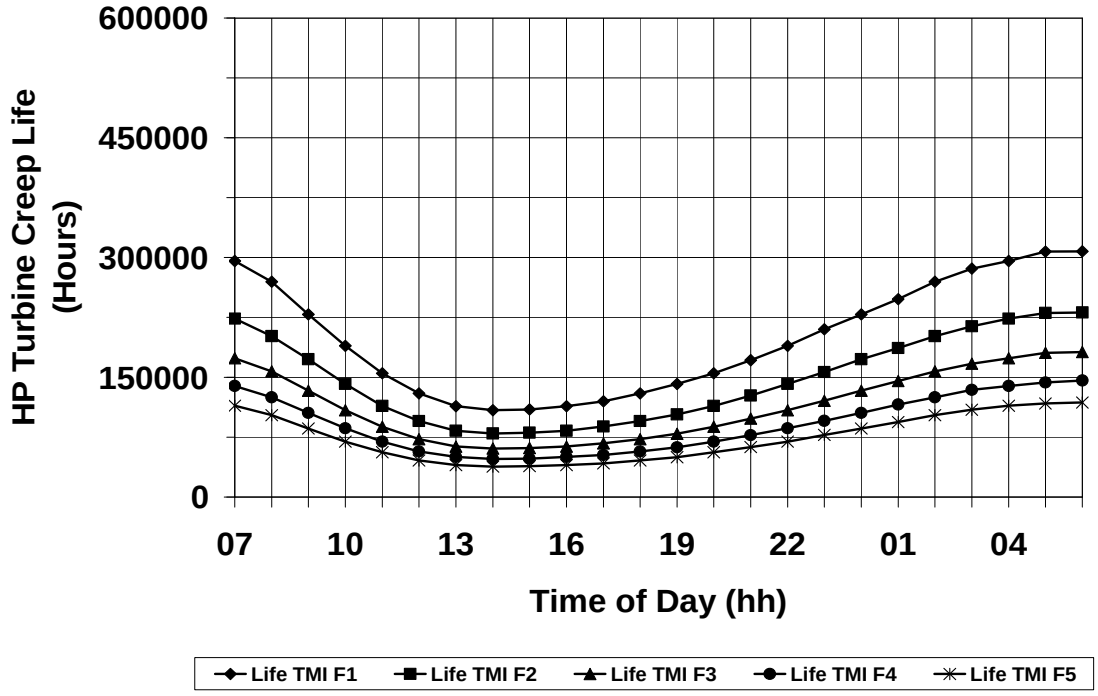

Figure D.38: Twin mode intercooled cycle (TMI) – HP turbine creep life variation against time of day, during journey with annual hull fouling progression (F#) and ideal weather conditions

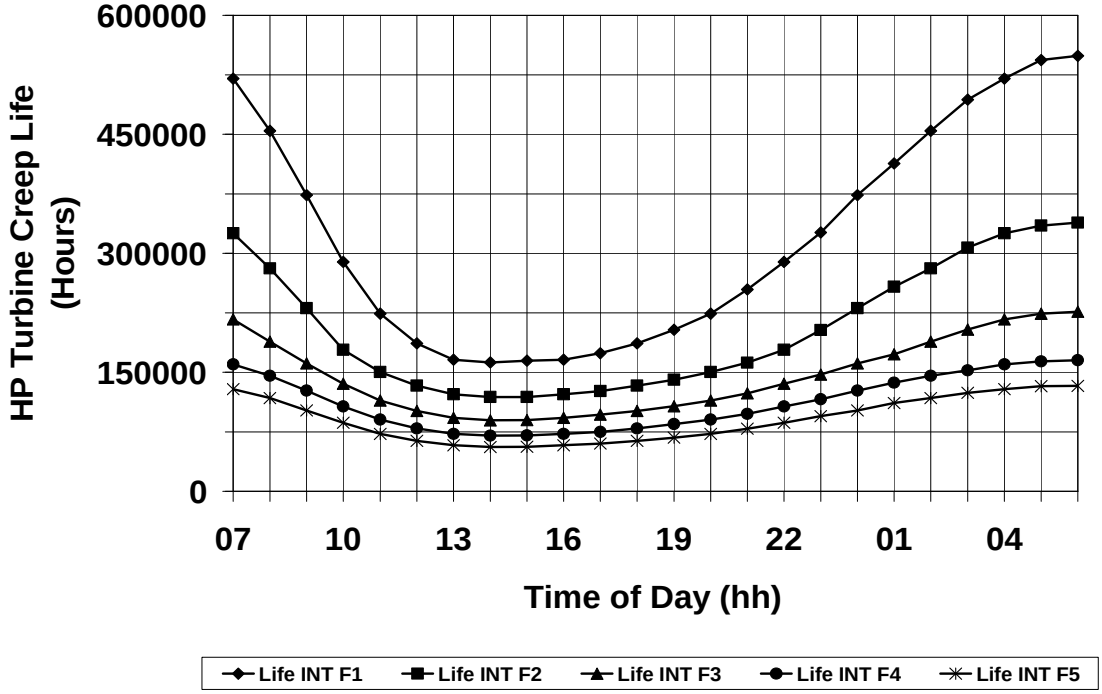

Figure D.39: Intercooled cycle (INT) – HP turbine creep life variation against time of day, during journey with annual hull fouling progression (F#) and ideal weather conditions

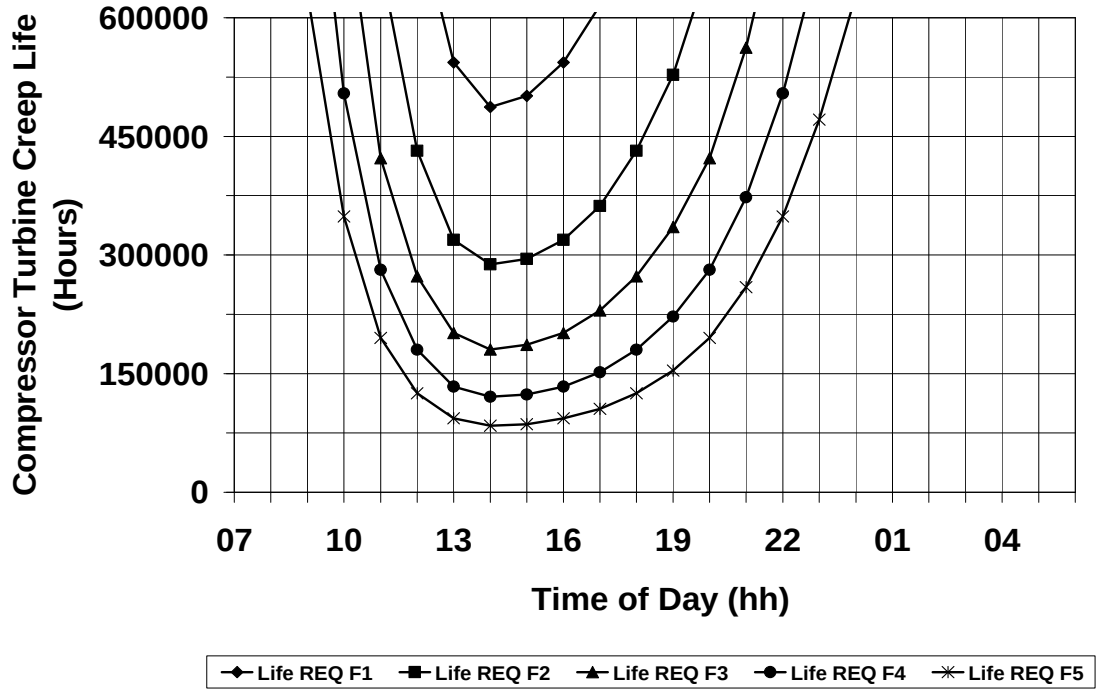

Figure D.40: Recuperated cycle (REQ) – Compressor turbine creep life variation against time of day, during journey with annual hull fouling progression (F#) and ideal weather conditions

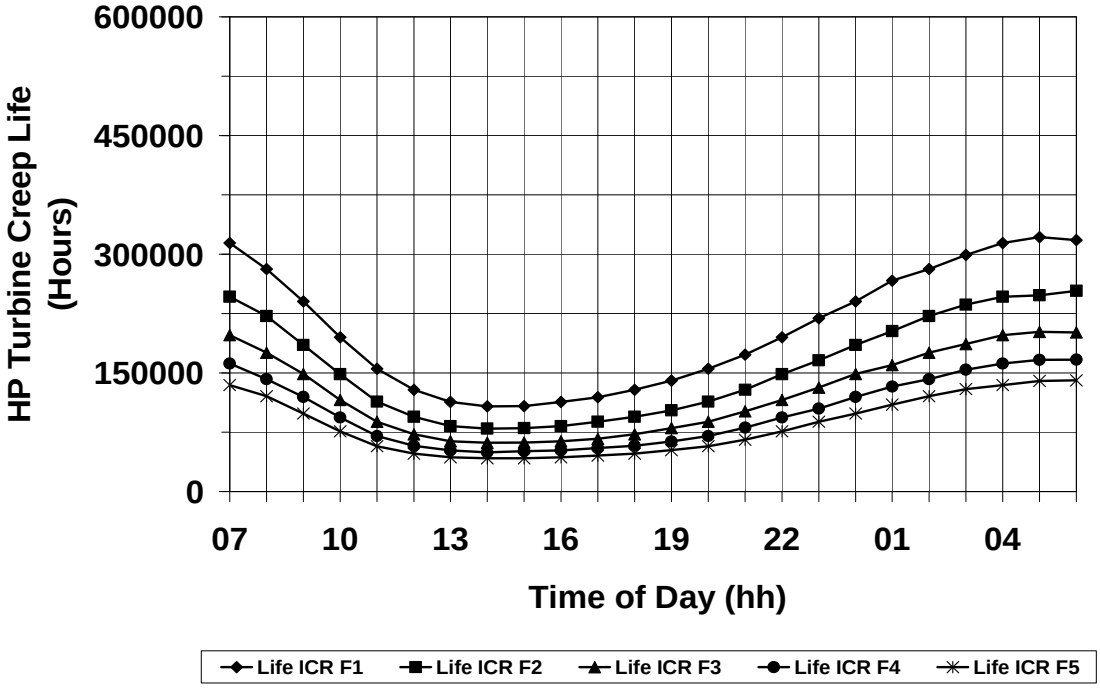

Figure D.41: Intercooled/recuperated Cycle (ICR) – HP Turbine creep life variation against time of day, during journey with annual hull fouling progression (F#) and ideal weather conditions

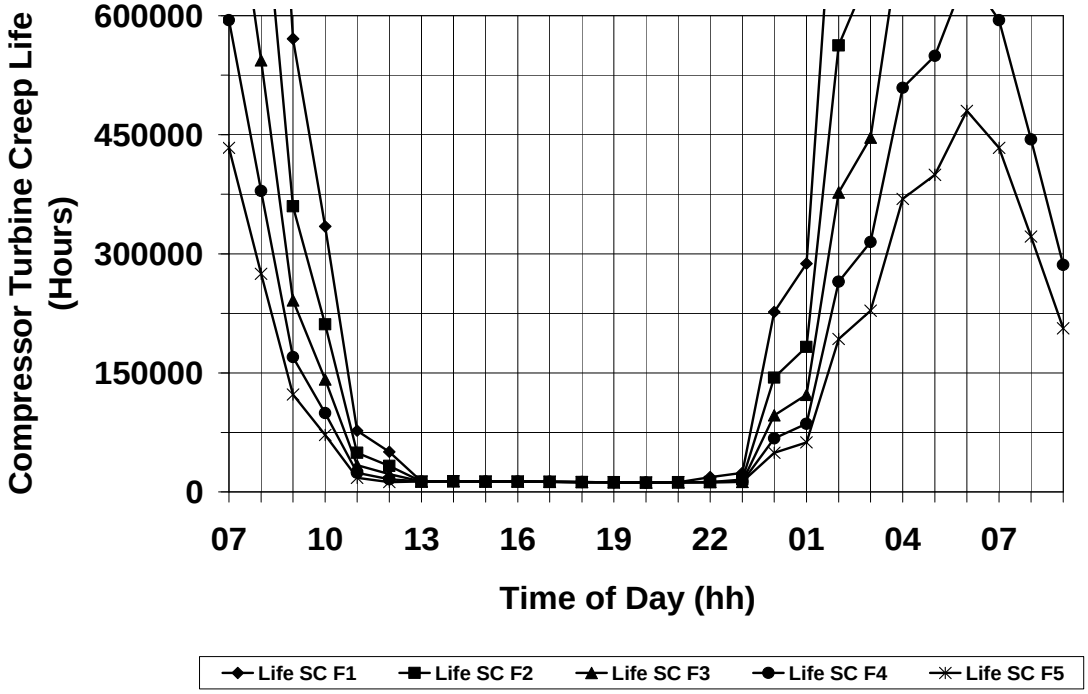

Figure D.42: Simple cycle (SC) – Compressor turbine creep life variation against time of day, during journey with annual hull fouling progression (F#) and weather Conditions

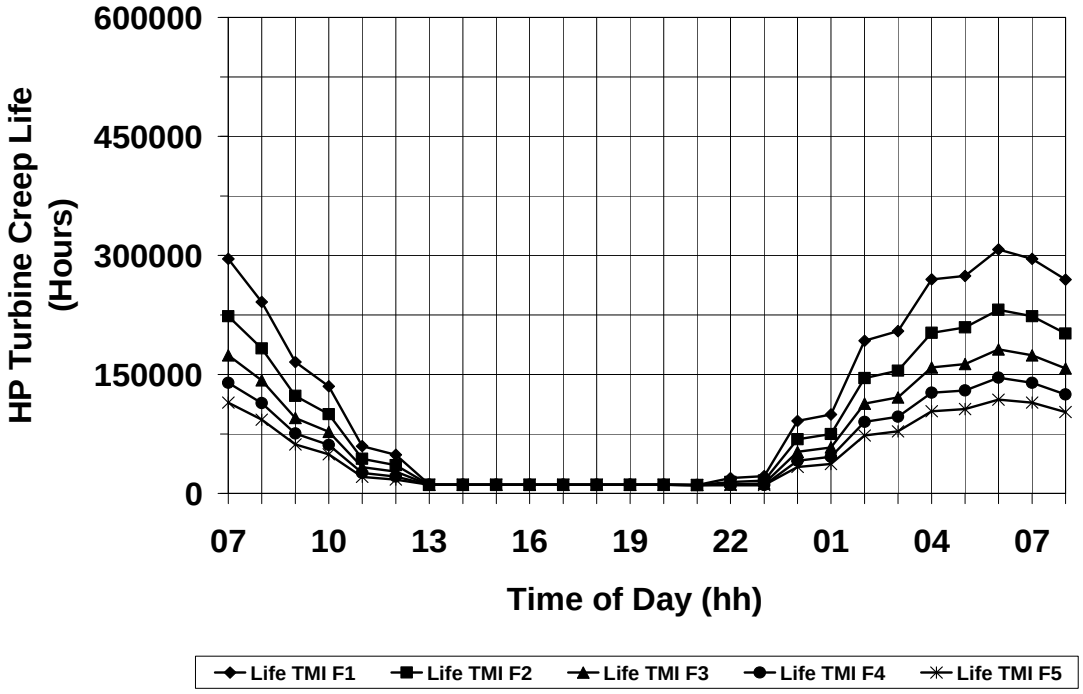

Figure D.43: Twin mode intercooled cycle (TMI) – HP turbine creep life variation against time of day, during journey with annual hull fouling progression (F#) and adverse weather conditions

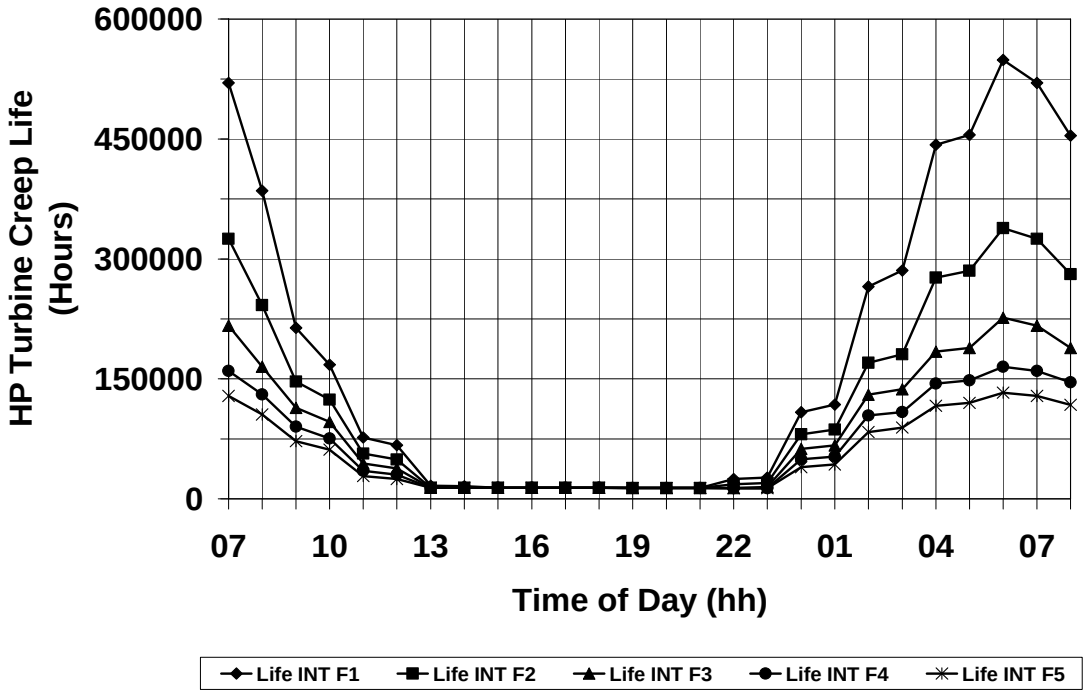

Figure D.44: Intercooled cycle (INT) – HP turbine creep life variation against time of day, during journey with annual hull fouling progression (F#) and adverse weather conditions

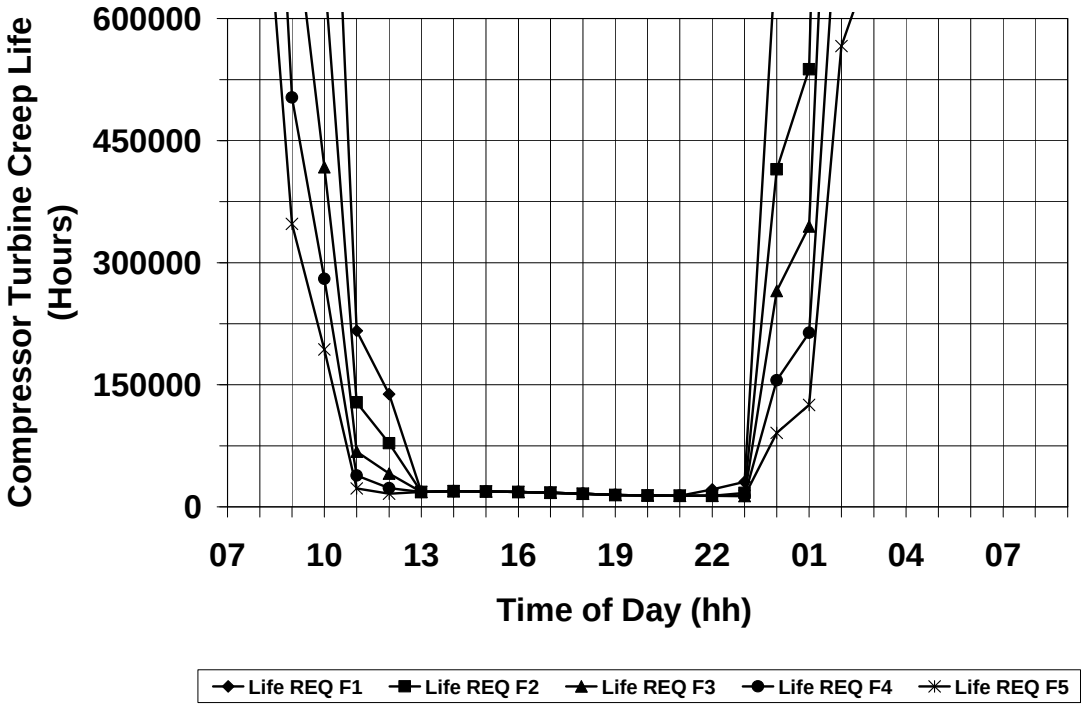

Figure D.45: Recuperated cycle (REQ) – Compressor turbine creep life variation against time of day, during journey with annual hull fouling progression (F#) and adverse weather conditions

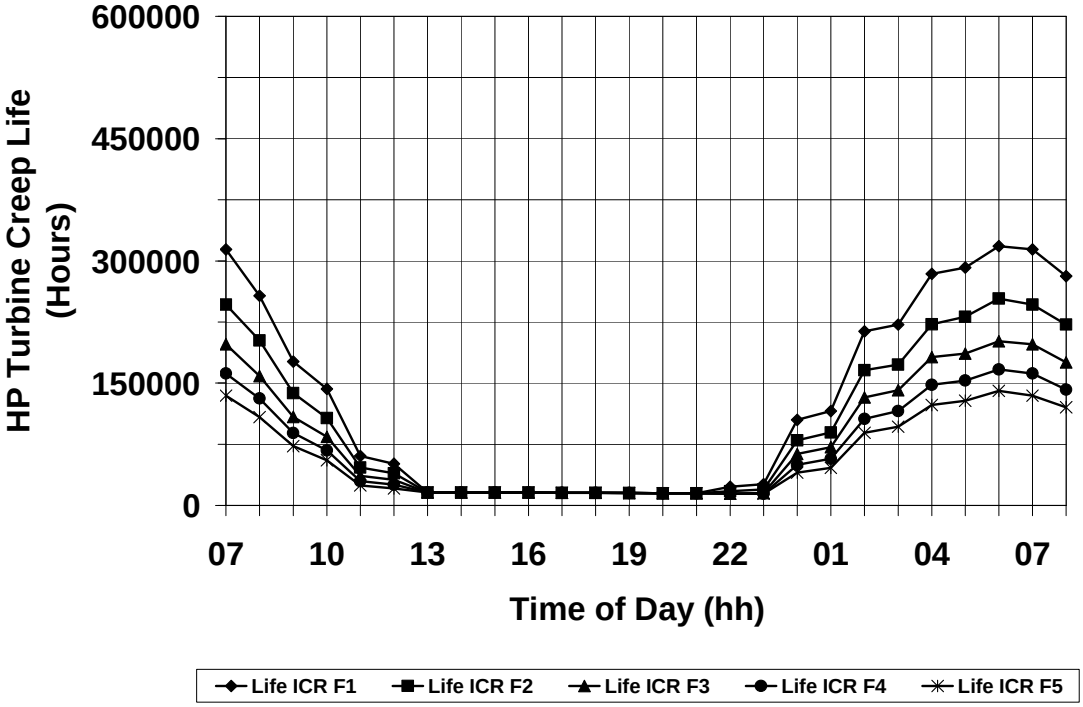

Figure D.46: Intercooled/recuperated cycle (ICR) – HP turbine creep life variation against time of day, during journey with annual hull fouling progression (F#) and adverse weather conditions

Appendix D.5

Table D.1: Hull Fouling F1 – Quantified engine (each) parameters per journey at ideal weather conditions

Engine	Fuel Consumption (kg)	HP Turbine Life Consumption (%)	Total NOx Emissions (kg)	Total CO Emissions (kg)	Total CO2 Emissions (kg)	Total UHC Emissions (kg)	Operational Time per Journey (hours)
SC	116833.7	0.00642	791.2	175.8	366619.3	37.0	24.0
TMI	92937.3	0.01375	1335.3	64.7	291613.3	2.25	24.0
INT	107759.7	0.00902	749.4	155.9	338152.7	32.4	24.0
REQ	106535.7	0.00185	711.5	169.6	334302.4	33.5	24.0
ICR	99480.93	0.01359	738.1	154.2	312187.4	31.3	24.0

Table D.2: Hull Fouling F2 – Quantified engine (each) parameters per journey at ideal weather conditions

Engine	Fuel Consumption (kg)	HP Turbine Life Consumption (%)	Total NOx Emissions (kg)	Total CO Emissions (kg)	Total CO2 Emissions (kg)	Total UHC Emissions (kg)	Operational Time per Journey (hours)
SC	118935.5	0.01016	818.4	172.6	373213.1	35.6	24.0
TMI	94768.5	0.01867	1381.3	63.5	297359.0	2.16	24.0
INT	109725.4	0.01334	772.2	153.9	344326.3	31.3	24.0
REQ	108667.0	0.00316	739.67	165.5	340989.3	34.0	24.0
ICR	101468.4	0.01816	756.3	151.2	318423.1	30.1	24.0

Table D.3: Hull Fouling F3 – Quantified engine (each) parameters per journey at ideal weather conditions

Engine	Fuel Consumption (kg)	HP Turbine Life Consumption (%)	Total NOx Emissions (kg)	Total CO Emissions (kg)	Total CO2 Emissions (kg)	Total UHC Emissions (kg)	Operational Time per Journey (hours)
SC	120793.3	0.01517	842.9	169.7	379039.4	34.3	24.0
TMI	96370.2	0.02421	1422.4	62.5	302384.7	2.09	24.0
INT	111447.5	0.01822	792.2	152.4	349731.4	30.4	24.0
REQ	110537.5	0.00501	765.1	165.8	346855.7	32.6	24.0
ICR	103211.0	0.02329	771.8	148.4	323888.7	29.1	24.0

Table D.4: Hull Fouling F4 – Quantified engine (each) parameters per journey at ideal weather conditions

Engine	Fuel Consumption (kg)	HP Turbine Life Consumption (%)	Total NOx Emissions (kg)	Total CO Emissions (kg)	Total CO2 Emissions (kg)	Total UHC Emissions (kg)	Operational Time per Journey (hours)
SC	122474.9	0.02156	865.7	167.3	384321.9	33.26	24.0
TMI	97801.7	0.03046	1460.6	61.7	306876.4	2.02	24.0
INT	112992.2	0.02361	810.3	150.9	354576.3	29.7	24.0
REQ	112219.7	0.00755	788.4	158.6	352131.5	31.3	24.0
ICR	104773.4	0.02880	786.1	146.2	328786.9	28.3	24.0

Table D.5: Hull Fouling F5 – Quantified engine (each) parameters per journey at ideal weather conditions

Engine	Fuel Consumption (kg)	HP Turbine Life Consumption (%)	Total NOx Emissions (kg)	Total CO Emissions (kg)	Total CO2 Emissions (kg)	Total UHC Emissions (kg)	Operational Time per Journey (hours)
SC	124030.5	0.02962	887.0	165.1	389197.1	32.3	24.0
TMI	99108.3	0.03843	1496.4	60.9	310976.1	1.97	24.0
INT	114398.2	0.02921	826.8	149.8	358984.4	29.1	24.0
REQ	113757.0	0.01087	810.4	155.9	356959.5	30.3	24.0
ICR	106197.8	0.03477	799.04	144.3	333259.1	27.6	24.0

Appendix D.5

Table D.6: Hull Fouling F1 – Quantified engine (each) parameters per journey at adverse weather conditions

Engine	Fuel Consumption (kg)	HP Turbine Life Consumption (%)	Total NOx Emissions (kg)	Total CO Emissions (kg)	Total CO2 Emissions (kg)	Total UHC Emissions (kg)	Operational Time per Journey (hours)
SC	134278.5	0.08551	966.6	179.3	421351.3	35.3	25.53
TMI	107882.8	0.10324	1660.1	64.7	338508.1	2.08	25.44
INT	124529.1	0.07842	910.3	158.9	390762.7	30.6	25.42
REQ	122995.3	0.06439	883.6	170.5	385942.3	33.6	25.53
ICR	115398.7	0.07661	874.4	154.7	362117.7	29.7	25.46

Table D.7: Hull Fouling F2 – Quantified engine (each) parameters per journey at adverse weather conditions

Engine	Fuel Consumption (kg)	HP Turbine Life Consumption (%)	Total NOx Emissions (kg)	Total CO Emissions (kg)	Total CO2 Emissions (kg)	Total UHC Emissions (kg)	Operational Time per Journey (hours)
SC	136014.8	0.09340	987.5	177.4	426796.3	34.4	25.56
TMI	109338.8	0.11083	1696.9	64.1	343076.8	2.03	25.47
INT	126157.6	0.08652	928.5	157.7	395867.6	29.9	25.45
REQ	124744.5	0.07099	905.3	168.1	391430.3	32.6	25.57
ICR	116993.9	0.08229	888.4	153.3	367134.0	29.1	25.49

Table D.8: Hull Fouling F3 – Quantified engine (each) parameters per journey at adverse weather conditions

Engine	Fuel Consumption (kg)	HP Turbine Life Consumption (%)	Total NOx Emissions (kg)	Total CO Emissions (kg)	Total CO2 Emissions (kg)	Total UHC Emissions (kg)	Operational Time per Journey (hours)
SC	137420.8	0.098617	1004.5	175.8	431205.2	33.7	25.58
TMI	110664.7	0.11842	1730.5	63.5	347237.1	1.98	25.50
INT	127600.8	0.09425	944.5	156.9	400402.8	29.4	25.48
REQ	126133.8	0.07504	922.8	166.1	395787.3	31.8	25.59
ICR	118357.4	0.08820	900.3	152	371410.4	28.5	25.51

Table D.9: Hull Fouling F4 – Quantified engine (each) parameters per journey at adverse weather conditions

Engine	Fuel Consumption (kg)	HP Turbine Life Consumption (%)	Total NOx Emissions (kg)	Total CO Emissions (kg)	Total CO2 Emissions (kg)	Total UHC Emissions (kg)	Operational Time per Journey (hours)
SC	138733.0	0.10350	1020.2	174.6	435319.5	33.1	26.01
TMI	111753.5	0.12546	1758.97	63.1	350653.6	1.95	25.52
INT	128752.6	0.09975	957.4	156.2	404015.3	28.9	25.50
REQ	127413.1	0.07894	938.8	164.4	399803.7	31.1	26.01
ICR	119564.1	0.09241	910.7	151	375186.2	28.1	25.54

Table D.10: Hull Fouling F5 – Quantified engine (each) parameters per journey at adverse weather conditions

Engine	Fuel Consumption (kg)	HP Turbine Life Consumption (%)	Total NOx Emissions (kg)	Total CO Emissions (kg)	Total CO2 Emissions (kg)	Total UHC Emissions (kg)	Operational Time per Journey (hours)
SC	139891.0	0.10903	1034.6	173.4	438957.9	32.6	26.04
TMI	112710.9	0.13168	1784.1	62.7	353657.4	1.92	25.54
INT	129824.5	0.10371	969.2	155.7	407373.4	28.6	25.52
REQ	128568.9	0.08394	953.4	163.2	403422.5	30.5	26.04
ICR	120649.5	0.09674	920.3	150.1	378588.9	27.7	25.57

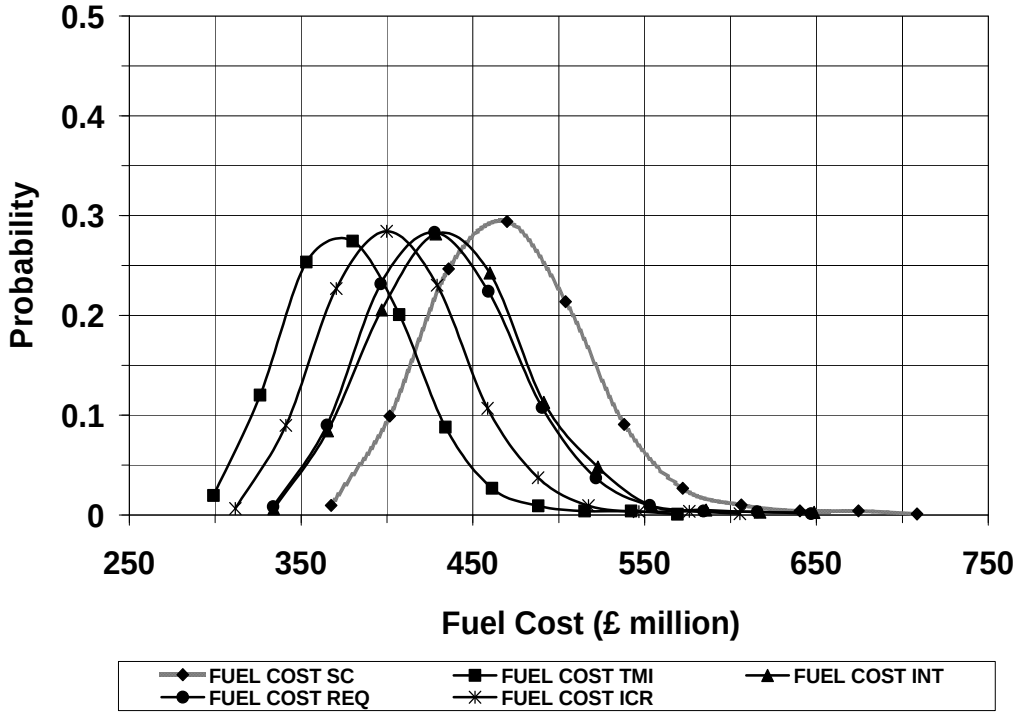

Figure D.47: RoPax fast ferry – Probability distribution of fuel cost of each power plant

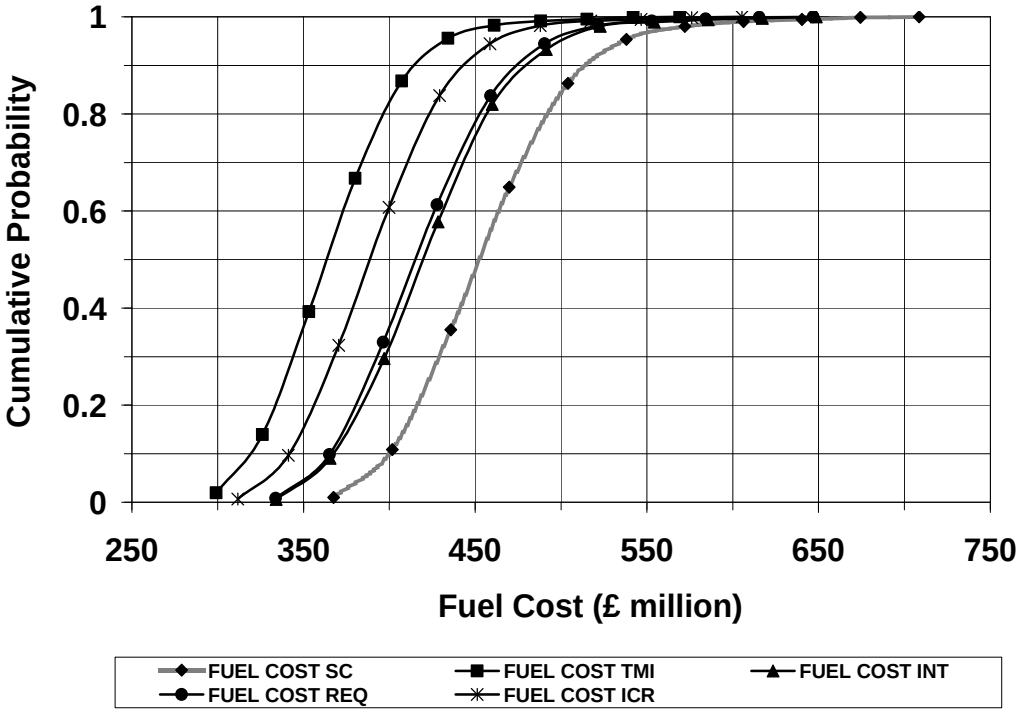

Figure D.48: RoPax fast ferry – Cumulative probability distribution of fuel cost of each power plant

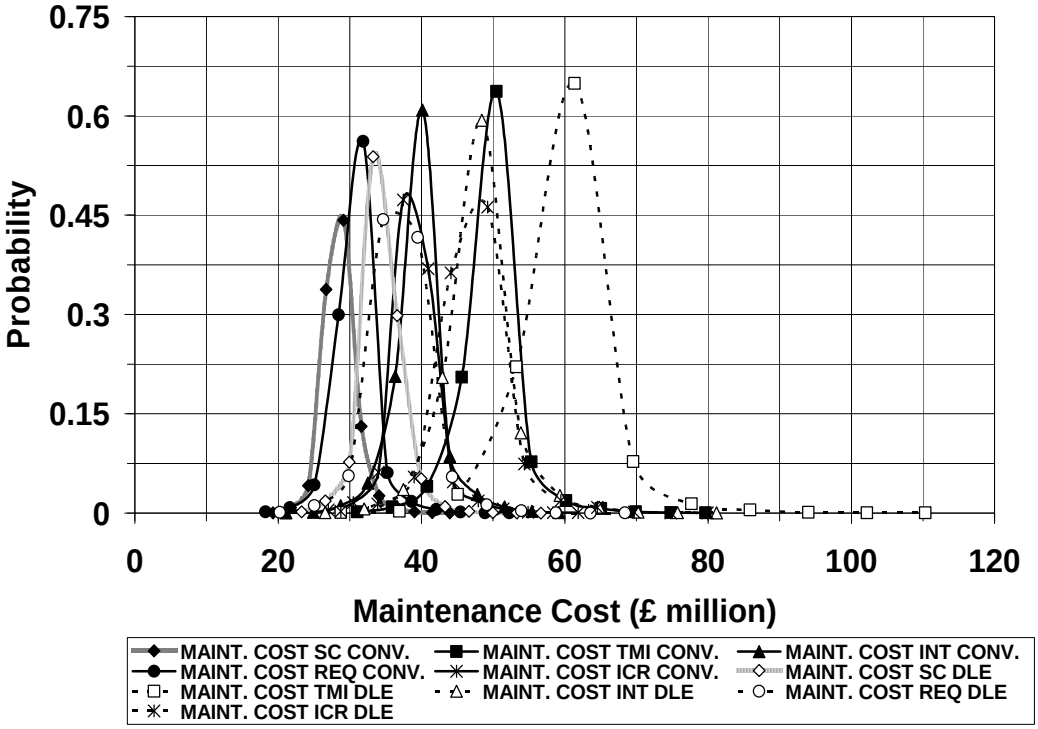

Figure D.49: RoPax fast ferry – Probability distribution of maintenance cost of each power plant (initial capital cost from 20% to 65% over the reference power plant)

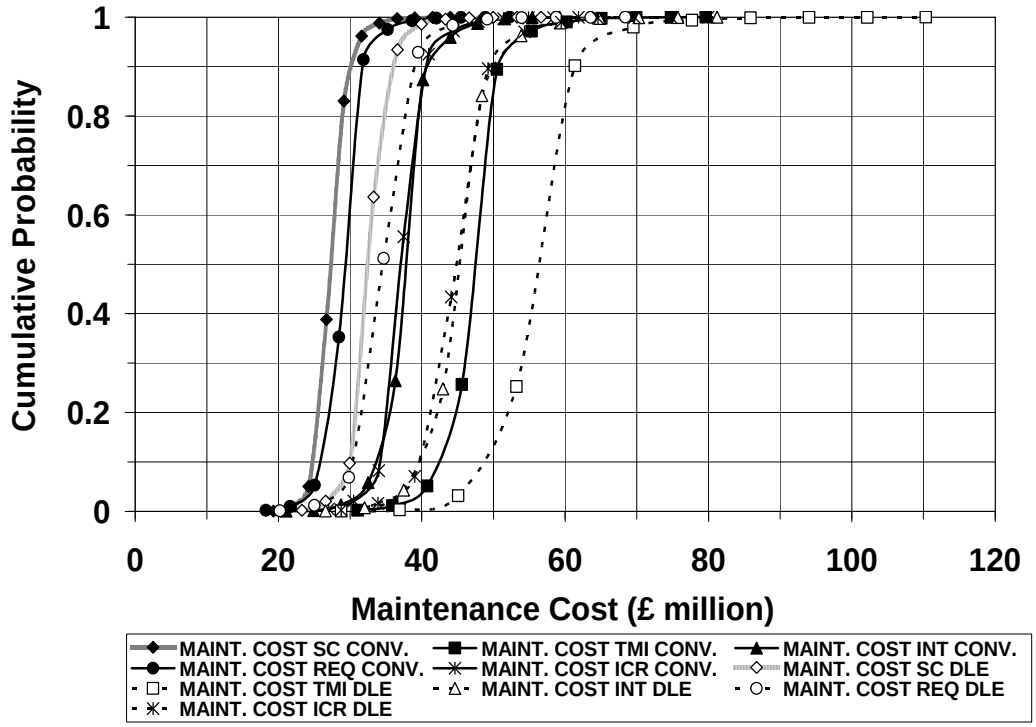

Figure D.50: RoPax fast ferry – Cumulative probability distribution of maintenance cost of each power plant (initial capital cost from 20% to 65% over the reference power plant)

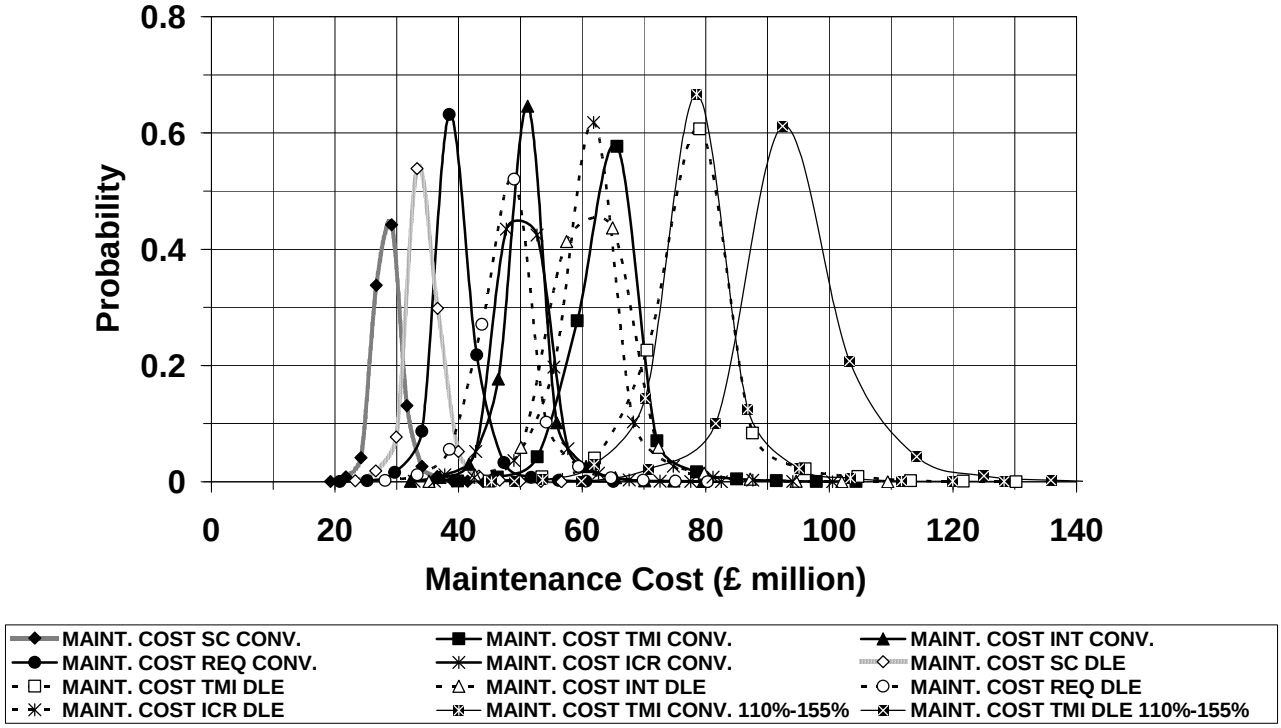

Figure D.51: RoPax fast ferry – Probability distribution of maintenance cost of each power plant (initial capital cost from 65% to 110% over the reference power plant). TMI power plant initial capital cost is extended to a range from 110% to 155%

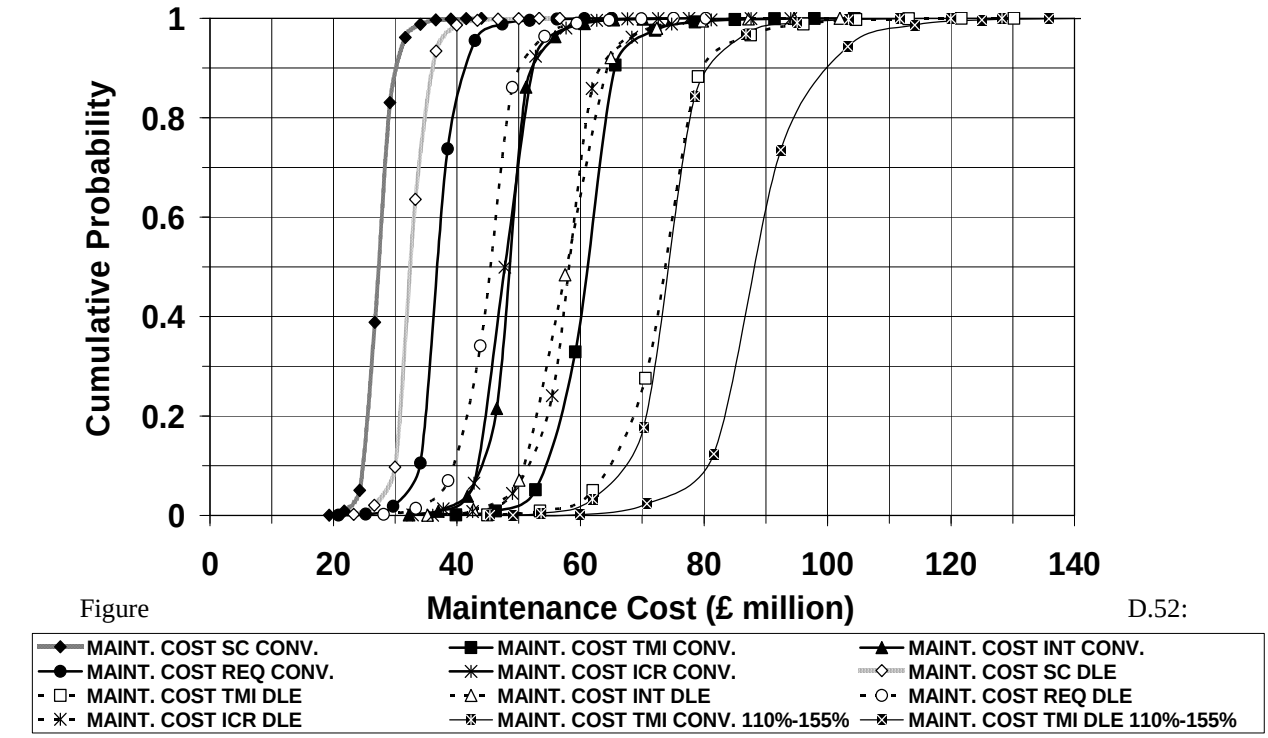

Figure D.52: RoPax fast ferry – Cumulative probability distribution of maintenance cost of each power plant (initial capital cost from 65% to 110% over the reference power plant). TMI Power plant initial capital cost is extended to a range from 110% to 155%

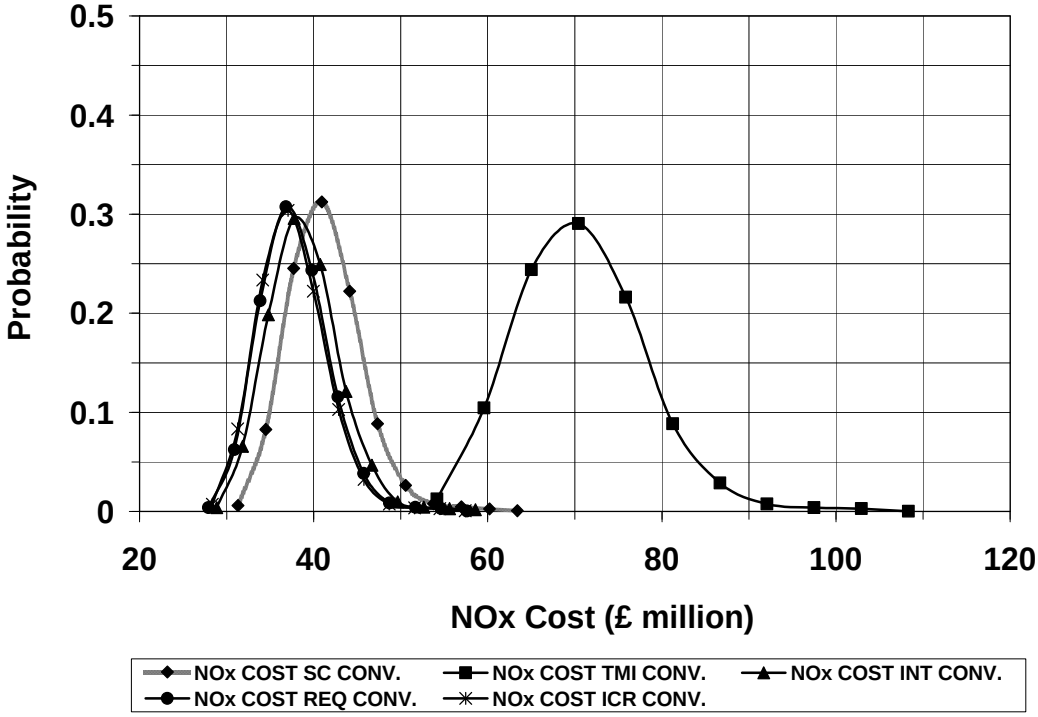

Figure D.53: RoPax fast ferry – Probability distribution of cost of taxed NOx exhaust emissions of each power plant with conventional combustors

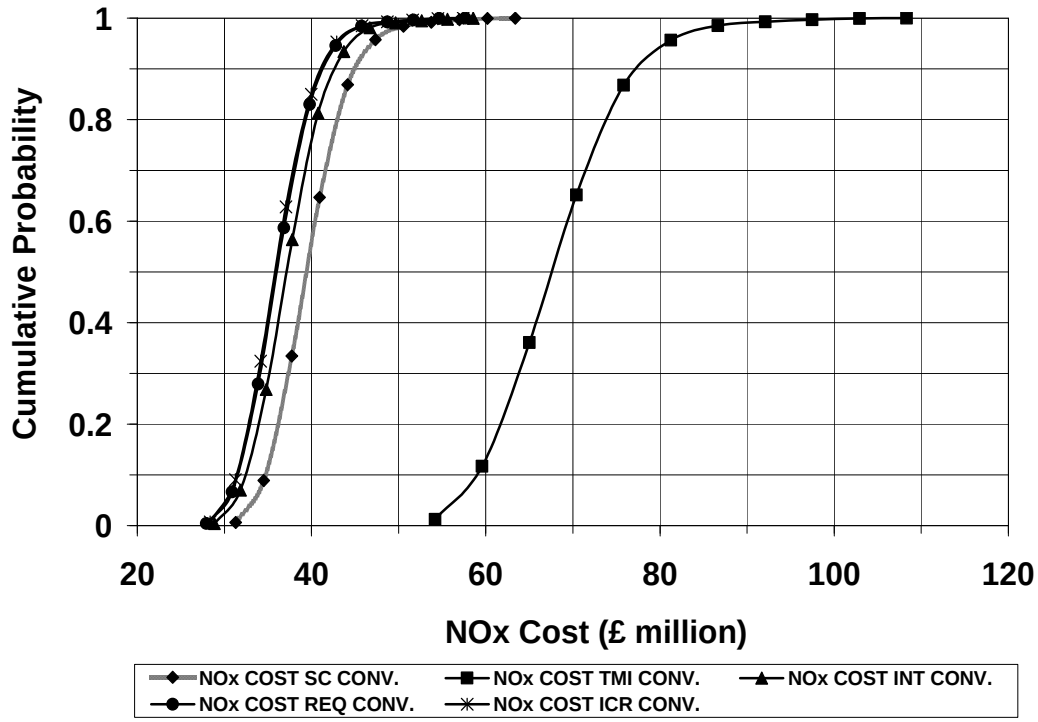

Figure D.54: RoPax fast ferry – Cumulative probability distribution of cost of taxed NOx exhaust emissions of each power plant with conventional combustors

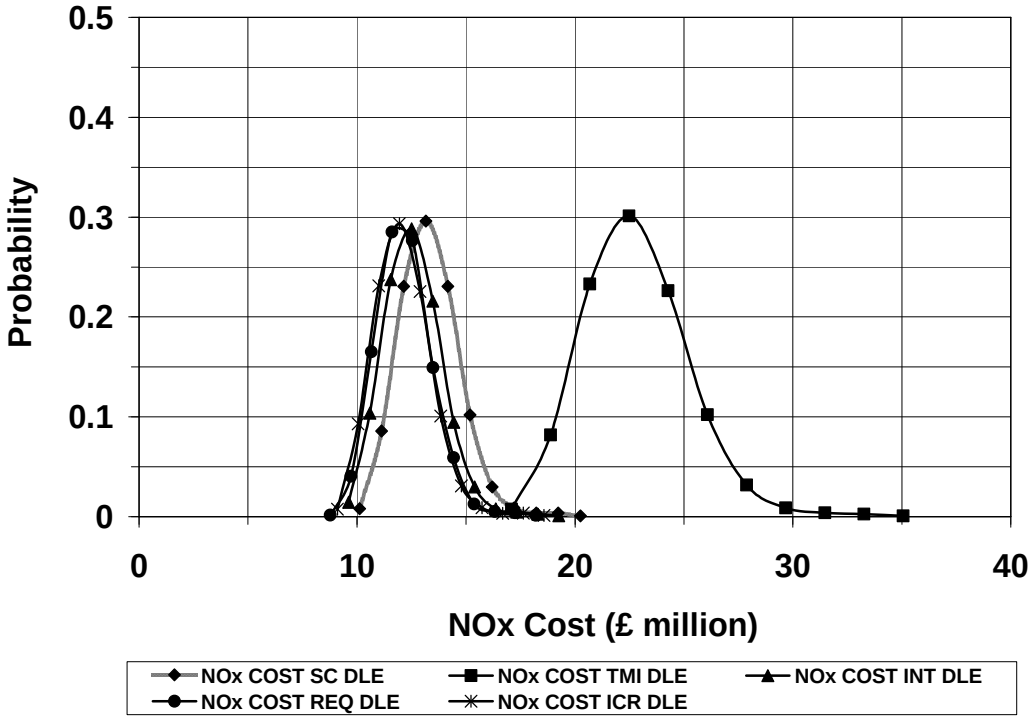

Figure D.55: RoPax fast ferry – Probability distribution of cost of taxed NOx exhaust emissions of each power plant with DLE combustors

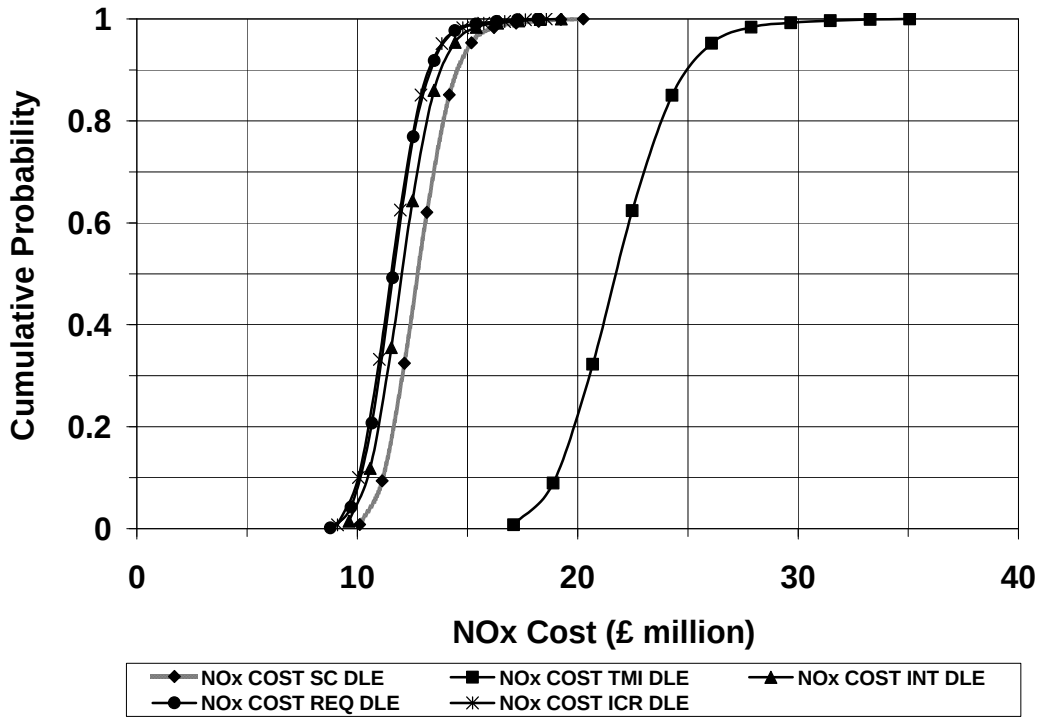

Figure D.56: RoPax fast ferry – Cumulative probability distribution of cost of taxed NOx exhaust emissions of each power plant with DLE combustors

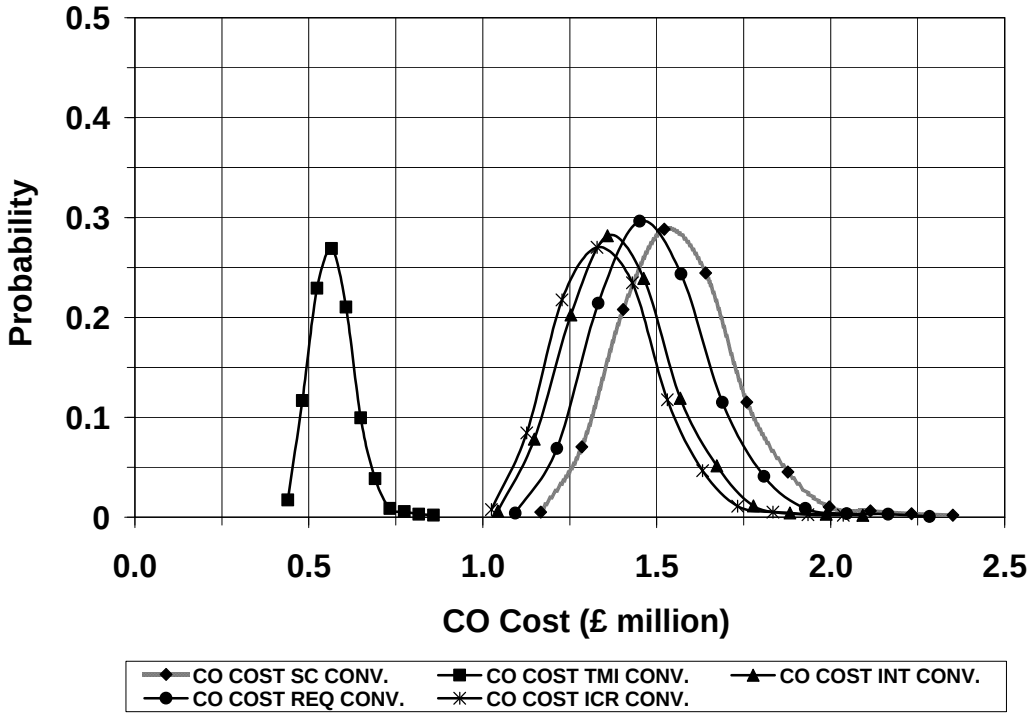

Figure D.57: RoPax fast ferry – Probability distribution of cost of taxed CO exhaust emissions of each power plant with conventional combustors

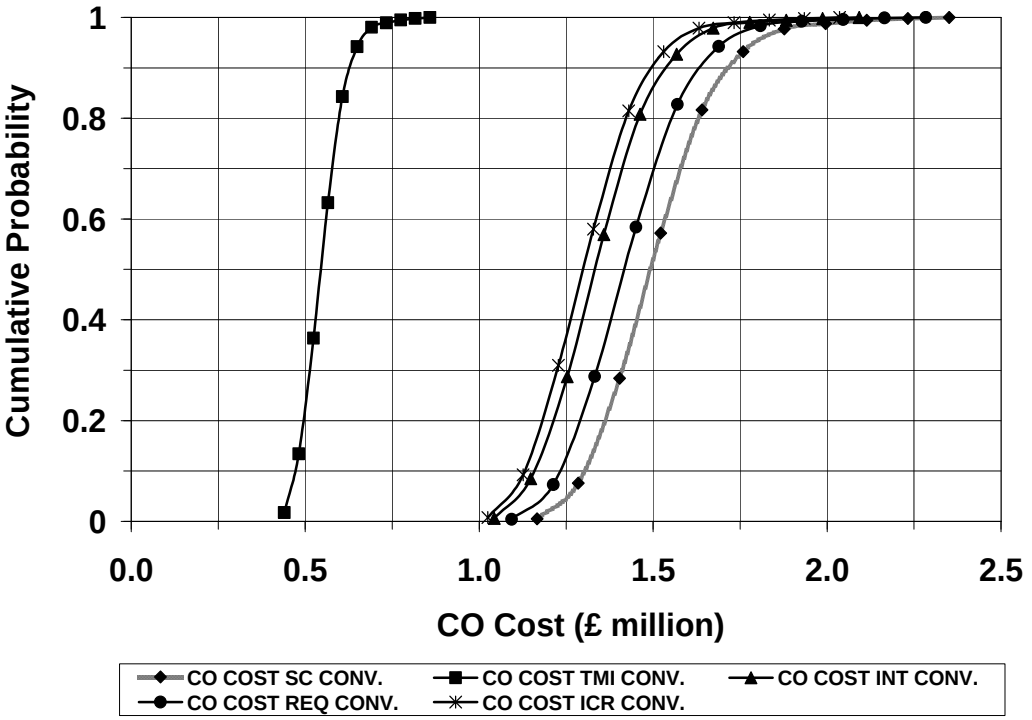

Figure D.58: RoPax fast ferry – Cumulative probability distribution of cost of taxed CO exhaust emissions of each power plant with conventional combustors

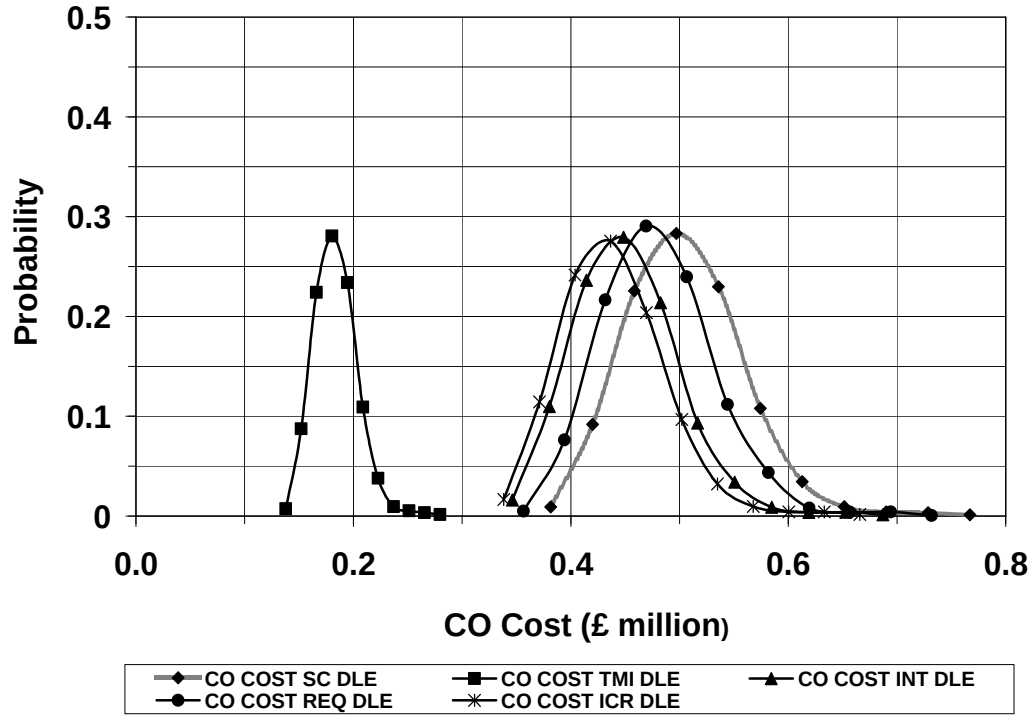

Figure D.59: RoPax fast ferry – Probability distribution of cost of taxed CO exhaust emissions of each power plant with DLE combustors

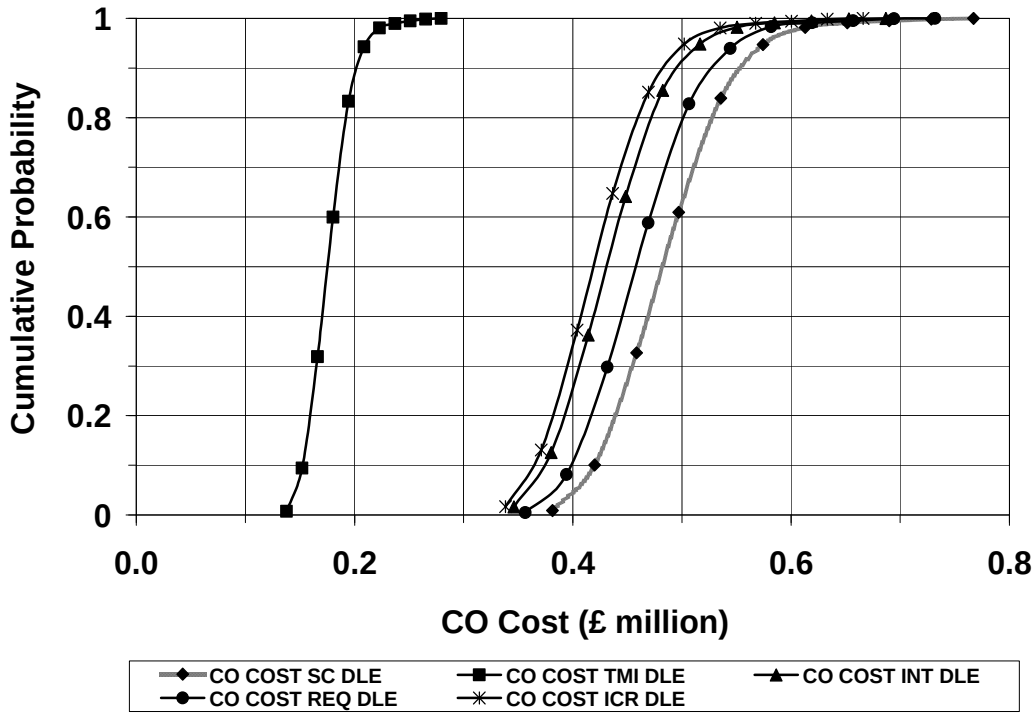

Figure D.60: RoPax fast ferry – Cumulative probability distribution of cost of taxed CO exhaust emissions of each power plant with DLE combustors

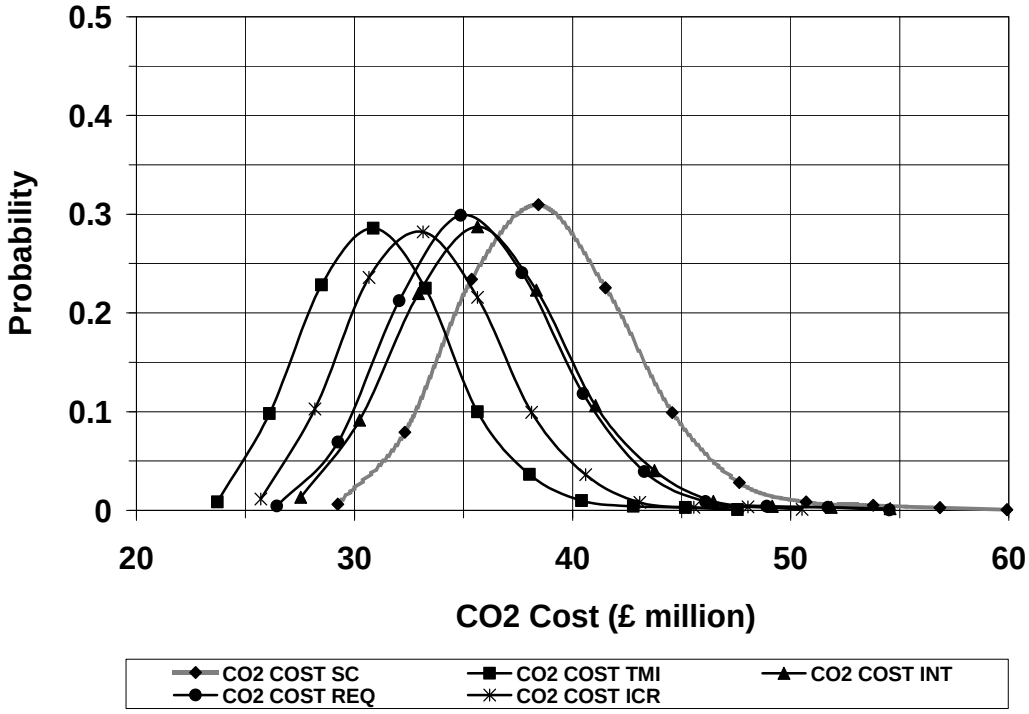

Figure D.61: RoPax fast ferry – Probability distribution of cost of taxed CO2 exhaust emissions of each power plant

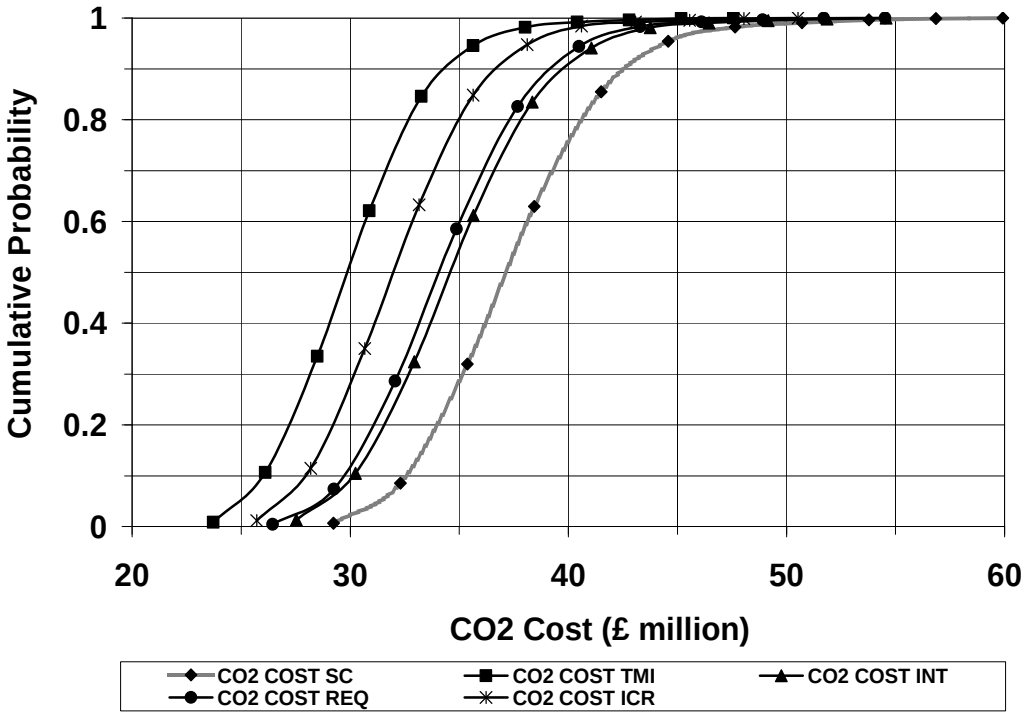

Figure D.62: RoPax fast ferry – Cumulative probability distribution of cost of taxed CO2 exhaust emissions of each power plant

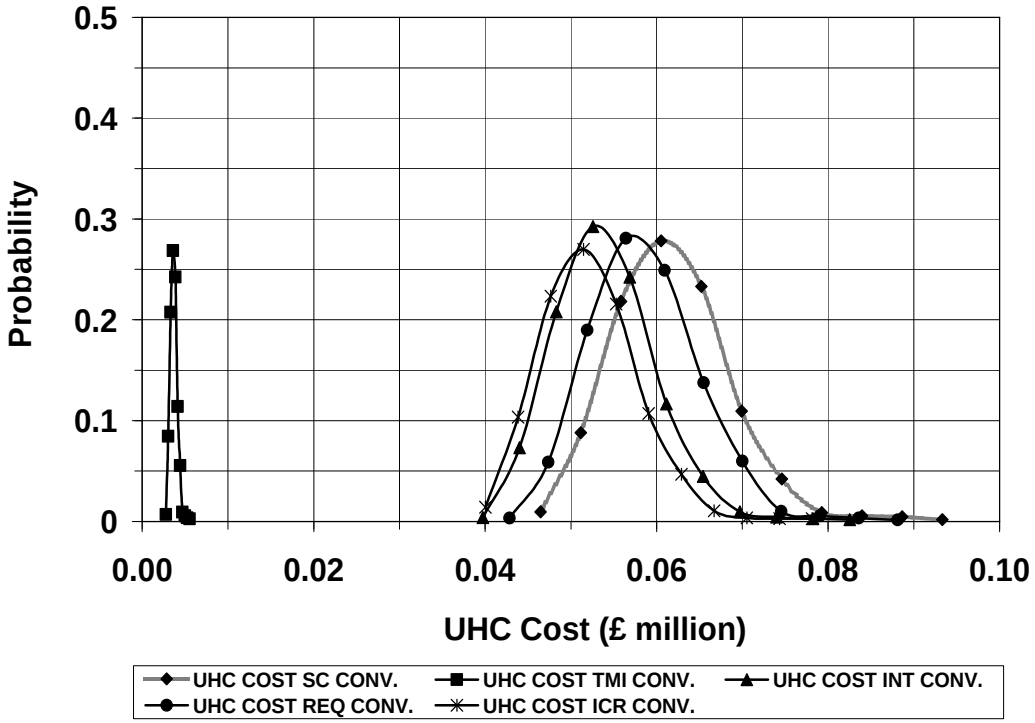

Figure D.63: RoPax fast ferry – Probability distribution of cost of taxed UHC exhaust emissions of each power plant with conventional combustors

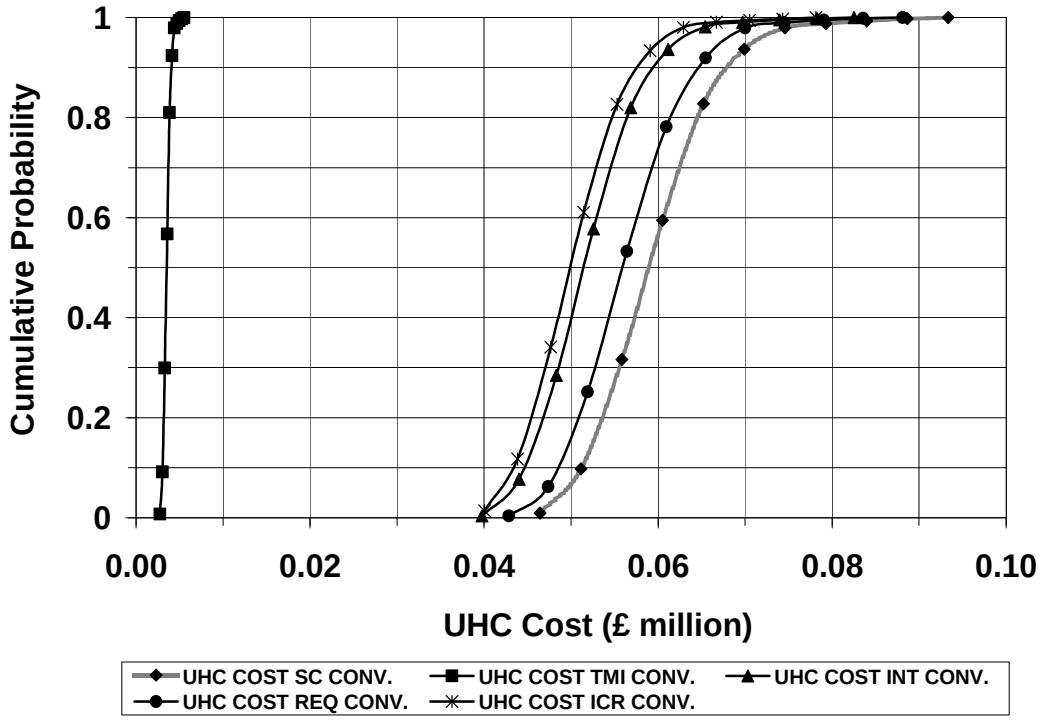

Figure D.64: RoPax fast ferry – Cumulative probability distribution of cost of taxed UHC exhaust emissions of each power plant with conventional combustors

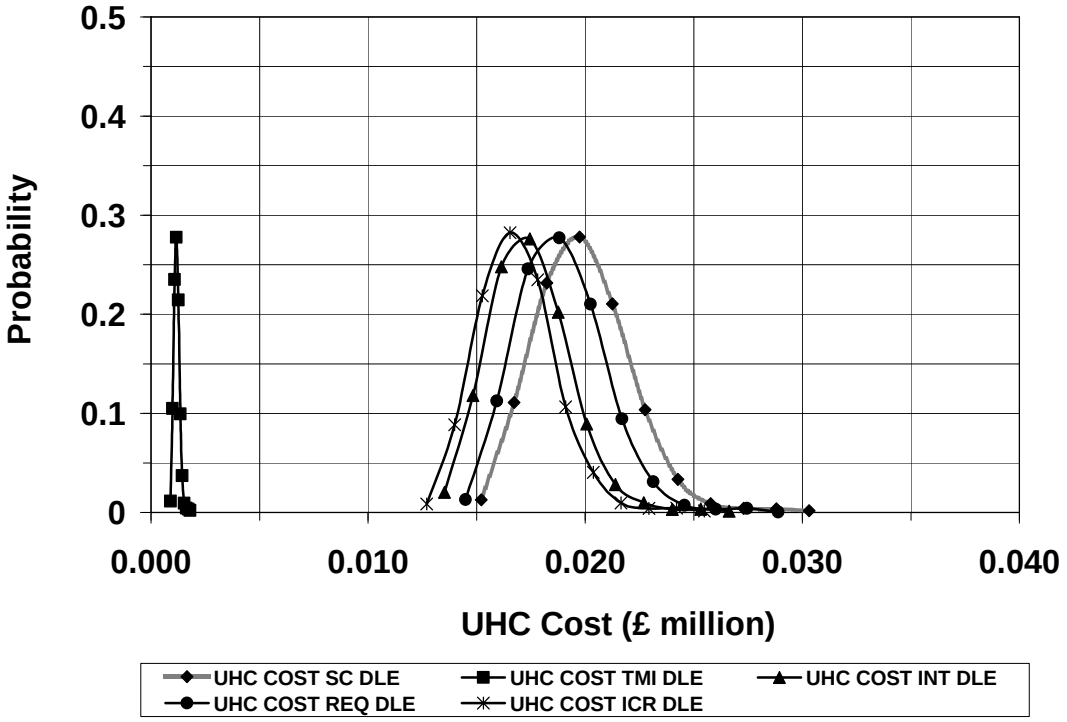

Figure D.65: RoPax fast ferry – Probability distribution of cost of taxed UHC exhaust emissions of each power plant with DLE combustors

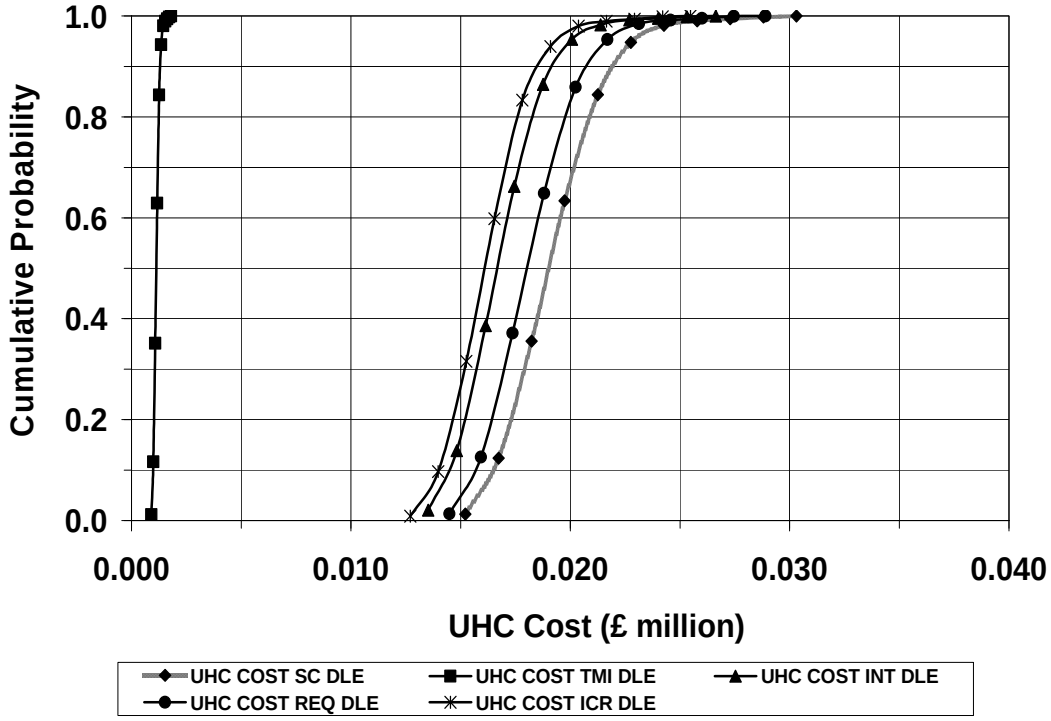

Figure D.66: RoPax fast ferry – Cumulative probability distribution of cost of taxed UHC exhaust emissions of each power plant with DLE combustors

Appendix D.7

Table D.11: RoPax Fast Ferry - Minimum-maximum and standard deviation of NPC of all power plants with PD_0 range from 20% to 65% from reference cycle

Engine (20%-65%) Conventional & DLE Combustor	**Minimum NPC (£ million)**		**Maximum NPC (£ million)**		**Standard Deviation (£ million)**	
SC-Reference Cycle	455.1	438.6	916.3	882.5	41.92	40.20
TMI	421.5	368.7	847.2	797.2	38.69	38.94
INT	419.5	432.2	853.3	848.1	39.42	37.81
REQ	421.8	406.6	857.6	828.3	39.60	38.38
ICR	409.8	402.0	813.8	805.8	36.81	36.70

Table D.12: RoPax fast ferry - Minimum-maximum and standard deviation of NPC of all power plants with PD_0 from 65% to 110% from reference cycle. TMI power plant is extended from 110% to 155%

Engine (65%-110%) Conventional & DLE Combustor	**Minimum NPC (£ million)**		**Maximum NPC (£ million)**		**Standard Deviation (£ million)**	
SC- Reference Cycle	455.1	438.6	916.3	882.5	41.92	40.20
TMI	426.8	437.6	877.1	841.0	40.92	38.47
TMI (110%-155%)	443.8	413.9	899.3	883.1	41.14	42.64
INT	435.1	452.7	890.2	880.9	41.42	38.92
REQ	410.5	419.3	873.5	839.2	42.08	38.16
ICR	422.5	426.8	836.8	836.9	37.66	37.26

Table D13: RoPax fast ferry - Minimum-maximum and standard deviation of maintenance cost of all power plants with PD_0 range from 20% to 65% from reference cycle

Engine (20%-65%) Conventional & DLE Combustor	**Minimum Maint. Cost (£ million)**		**Maximum Maint. Cost (£ million)**		**Standard Deviation (£ million)**	
SC-Reference Cycle	18.04	21.58	45.18	58.30	2.46	3.38
TMI	28.61	24.66	82.06	114.4	4.84	8.15
INT	19.18	23.82	61.11	83.92	3.81	5.73
REQ	16.58	17.84	53.96	70.78	3.40	4.82
ICR	25.26	26.20	63.63	82.48	3.48	5.10

Table D.14: RoPax fast ferry - Minimum-maximum and standard deviation of maintenance cost of all power plants with PD_0 range from 65% to 110% from reference cycle. TMI power plant is extended from 110% to 155%

Engine (65%-110%) Conventional & DLE Combustor	**Minimum Maint. Cost (£ million)**		**Maximum Maint. Cost (£ million)**		**Standard Deviation (£ million)**	
SC-Reference Cycle	18.04	21.58	45.18	58.30	2.46	3.38
TMI	36.60	40.68	107.54	134.46	6.44	8.52
TMI (110%-155%)	41.18	43.62	132.40	162.94	8.29	10.84
INT	29.84	31.50	81.94	113.14	4.72	7.42
REQ	18.58	25.48	67.24	82.92	4.42	5.21
ICR	30.32	32.86	85.00	103.72	4.97	6.44

Appendix D.7

Table D.15: RoPax fast ferry - Minimum-maximum and standard deviation of fuel cost of all power plants

Engine	Minimum Fuel Cost (£ million)	Maximum Fuel Cost (£ million)	Standard Deviation (£ million)
SC- Reference Cycle	350.5	725.5	34.09
TMI	285.6	582.6	26.98
INT	318.1	664.4	31.44
REQ	318.1	662.5	31.30
ICR	297.1	620.0	29.36

Table D.16: RoPax fast ferry - Minimum-maximum and standard deviation of cost of taxed NOx exhaust emissions for all power plants

Engine Conventional & DLE Combustor	Minimum NOx Cost (£ million)		Maximum NOx Cost (£ million)		Standard Deviation (£ million)	
SC – Reference Cycle	29.68	9.61	64.98	20.76	3.20	1.01
TMI	49.16	16.34	110.55	35.63	5.56	1.75
INT	27.36	9.12	60.06	19.72	2.96	0.96
REQ	26.42	8.30	59.10	18.66	2.97	0.95
ICR	26.9	8.62	58.86	19.04	2.90	0.95

Table D.17: RoPax fast ferry - Minimum-maximum and standard deviation of cost of taxed CO exhaust emissions for all power plants

Engine Conventional & DLE Combustor	Minimum CO Cost (£ million)		Maximum CO Cost (£ million)		Standard Deviation (£ million)	
SC – Reference Cycle	1.114	0.362	2.412	0.786	0.118	0.038
TMI	0.418	0.132	0.878	0.286	0.042	0.014
INT	0.990	0.328	2.145	0.704	0.105	0.034
REQ	1.031	0.336	2.342	0.750	0.118	0.037
ICR	0.974	0.325	2.086	0.682	0.101	0.032

Table D.18: RoPax fast ferry - Minimum-maximum and standard deviation of cost of taxed CO2 exhaust emissions for all power plants

Engine	Minimum CO2 Cost (£ million)	Maximum CO2 Cost (£ million)	Standard Deviation (£ million)
SC – Reference Cycle	27.70	61.44	3.06
TMI	22.52	48.76	2.38
INT	25.22	55.06	2.72
REQ	25.04	55.92	2.81
ICR	24.46	51.76	2.48

Table D.19: RoPax fast ferry - Minimum-maximum and standard deviation of cost of taxed UHC exhaust emissions for all power plants

Engine Conventional & DLE Combustor	Minimum UHC Cost (£ million)		Maximum UHC Cost (£ million)		Standard Deviation (£ million)	
SC – Reference Cycle	0.044	0.014	0.095	0.031	0.0046	0.0015
TMI	0.0026	0.0008	0.0056	0.0018	0.0003	0.00009
INT	0.036	0.013	0.084	0.027	0.0043	0.0013
REQ	0.042	0.014	0.090	0.028	0.0045	0.0014
ICR	0.038	0.012	0.080	0.026	0.0038	0.0013

APPENDIX E

Contains:

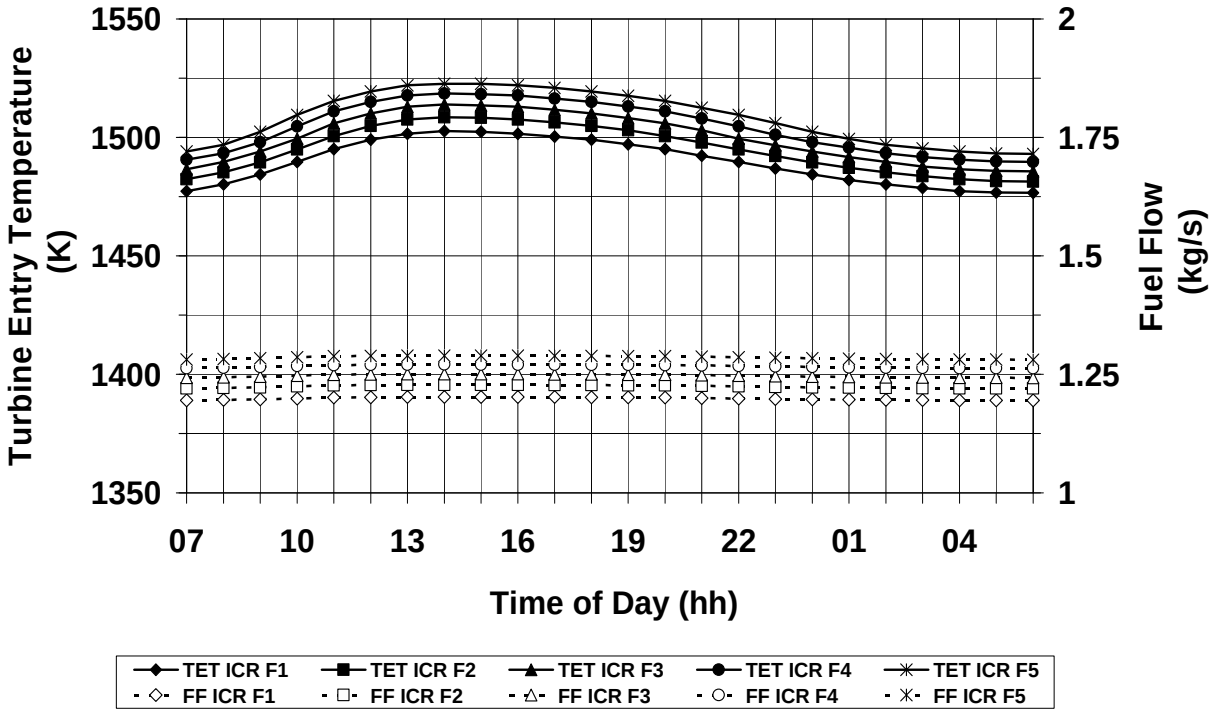

Figure E.1: Intercooled/recuperated cycle (ICR) - Turbine entry temperature (TET) and fuel flow (FF) variation against time of day, during journey with annual hull fouling progression (F#) and ideal weather conditions

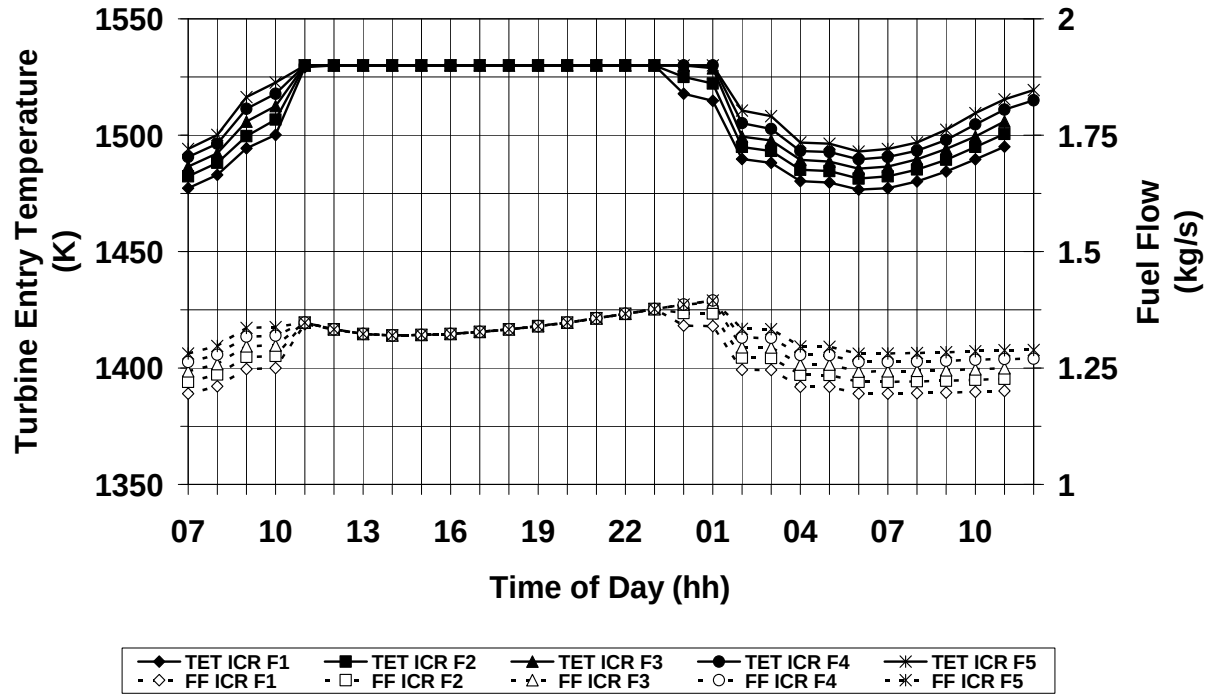

Figure E.2: Intercooled/recuperated cycle (ICR) - Turbine entry temperature (TET) and fuel flow (FF) variation against time of day, during journey with annual hull fouling progression (F#) and adverse weather conditions

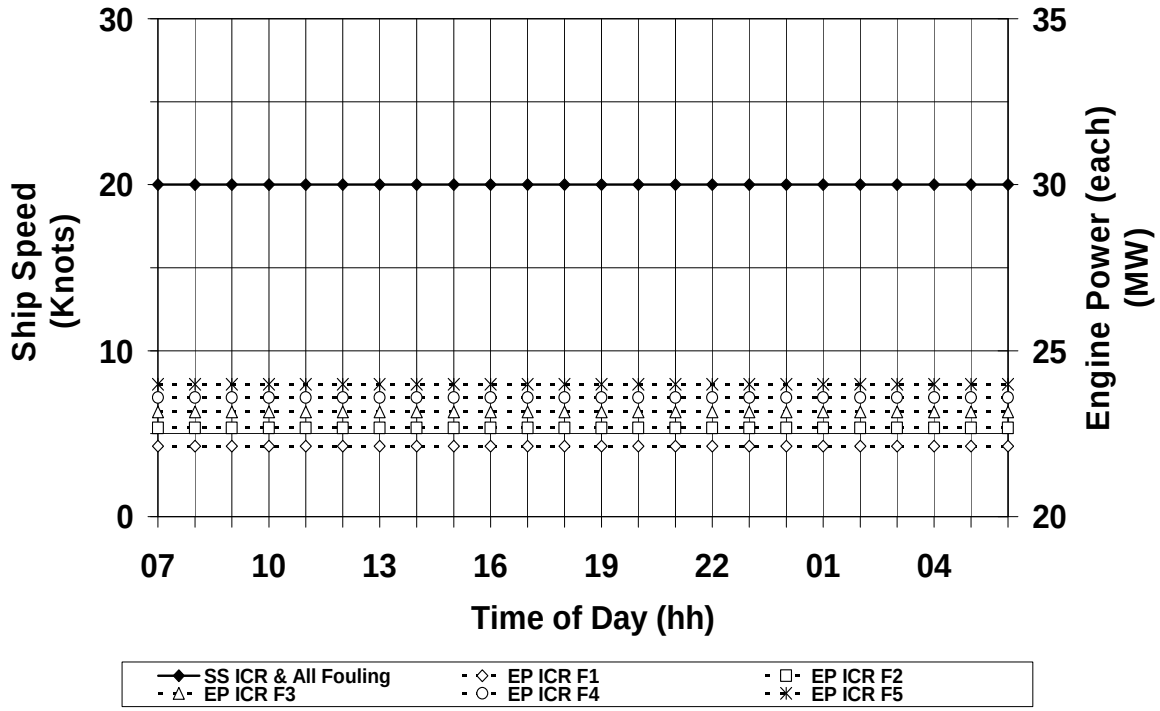

Figure E.3: Intercooled/recuperated cycle (ICR) – Ship speed (SS) and engine power (EP) (for each engine) variation against time of day, during journey with annual hull fouling progression (F#) and ideal weather conditions

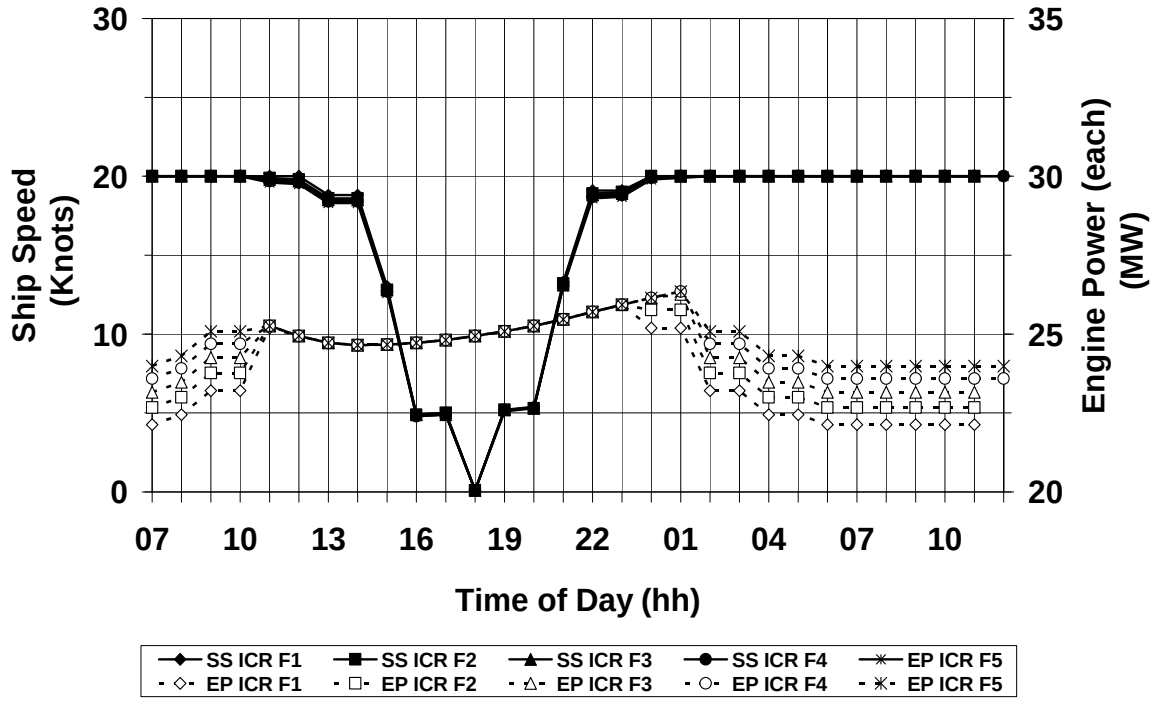

Figure E.4: Intercooled/recuperated cycle (ICR) – Ship speed (SS) and engine power (EP) (for each engine) variation against time of day, during journey with annual hull Fouling progression (F#) and adverse weather conditions

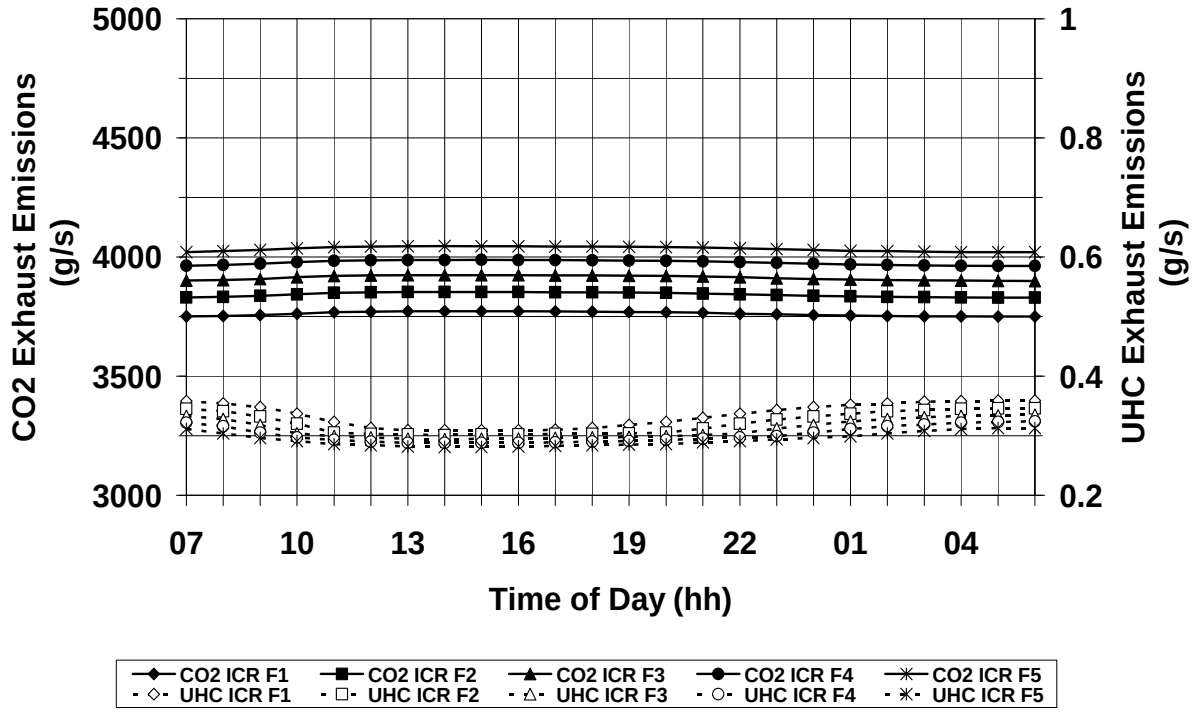

Figure E.5: Intercooled/recuperated cycle (ICR) – Carbon dioxide (CO2) and unburned hydrocarbons (UHC) exhaust emissions variation against time of day, during journey with annual hull fouling progression (F#) and ideal weather conditions

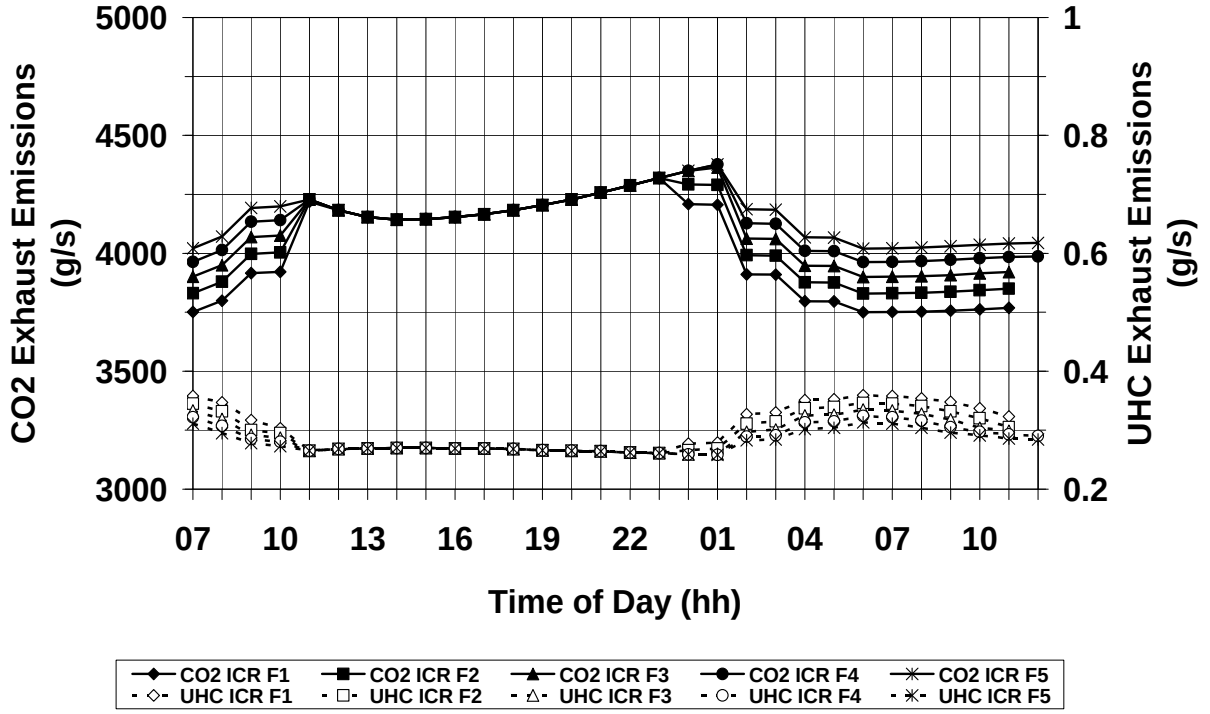

Figure E.6: Intercooled/recuperated cycle (ICR) – Carbon dioxide (CO2) and unburned hydrocarbons (UHC) exhaust emissions variation against time of day, during journey with annual hull fouling progression (F#) and adverse weather conditions

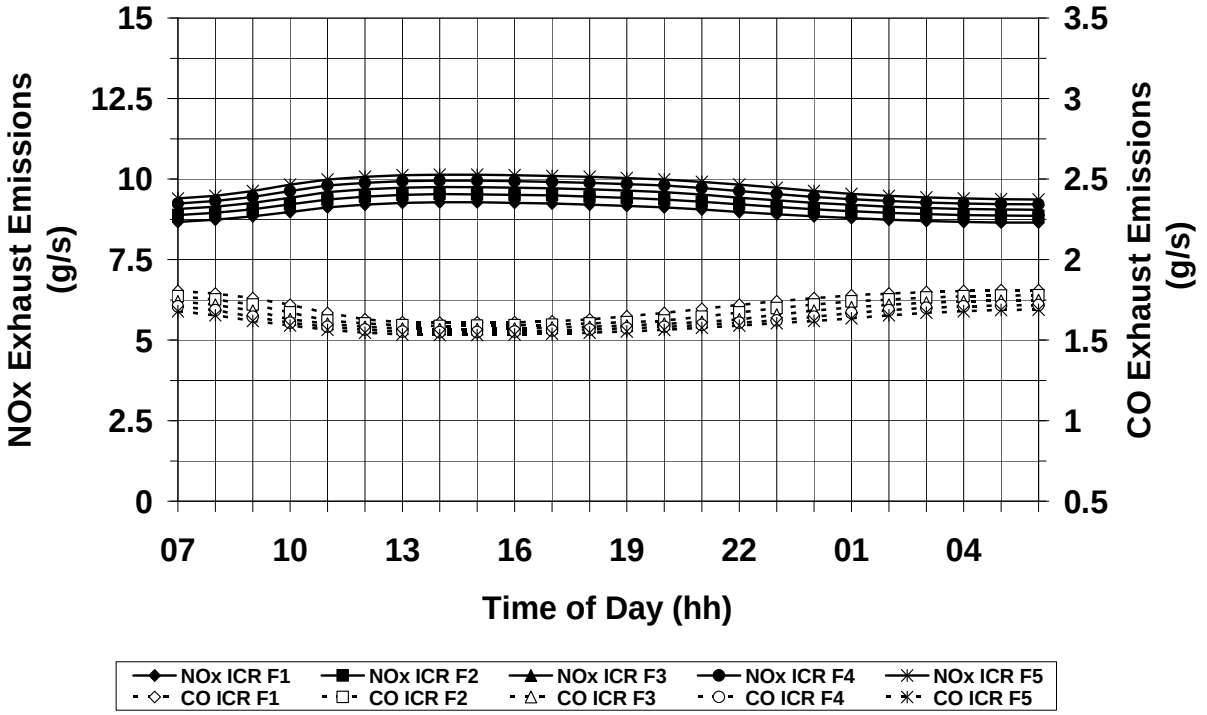

Figure E.7: Intercooled/recuperated cycle (ICR) – Nitric oxide (NOx) and carbon monoxide (CO) exhaust emissions variation against time of day, during journey with annual hull fouling progression (F#) and ideal weather conditions

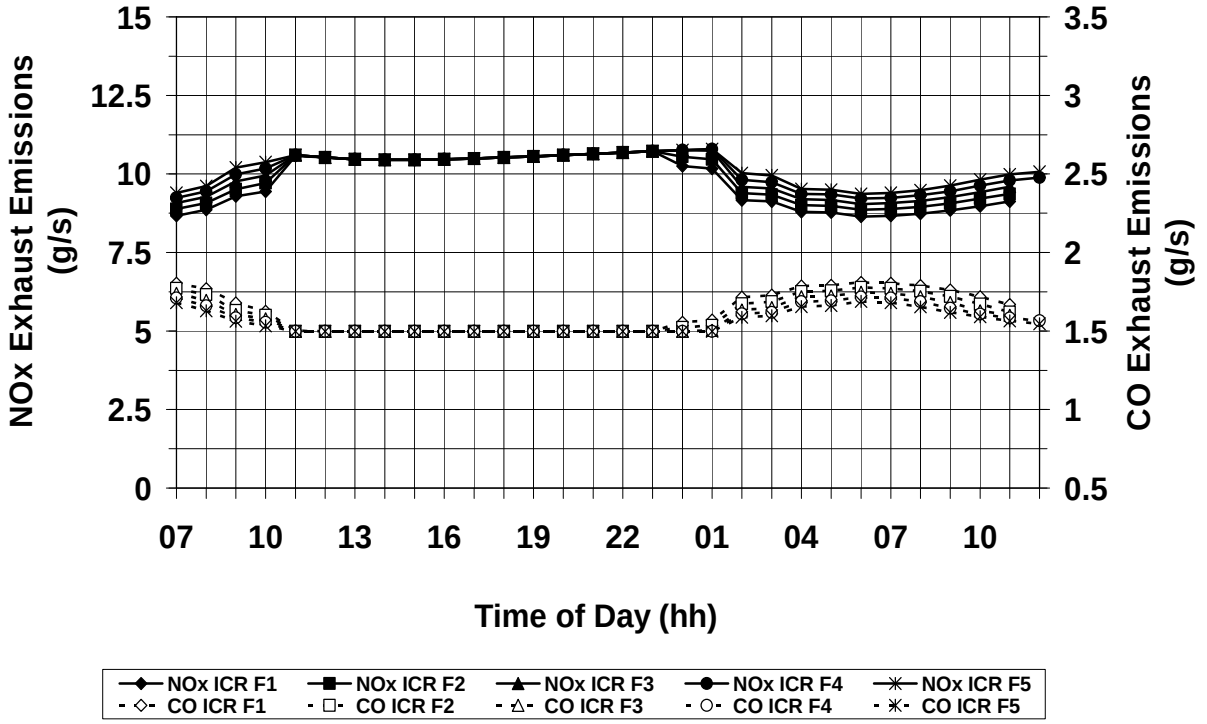

Figure E.8: Intercooled/recuperated Cycle (ICR) – Nitric oxide (NOx) and Carbon monoxide (CO) exhaust emissions variation against time of day, during journey with annual hull fouling progression (F#) and adverse weather conditions

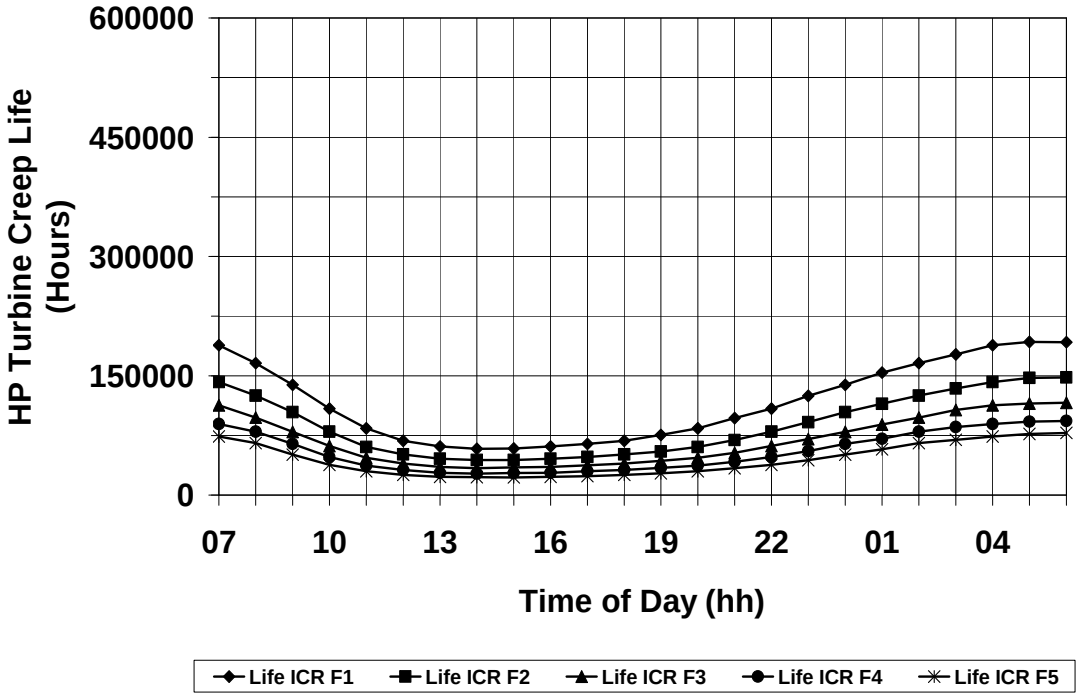

Figure E.9: Intercooled/recuperated cycle (ICR) – Compressor HP turbine creep life variation against time of day, during journey with annual hull fouling progression (F#) and ideal weather conditions

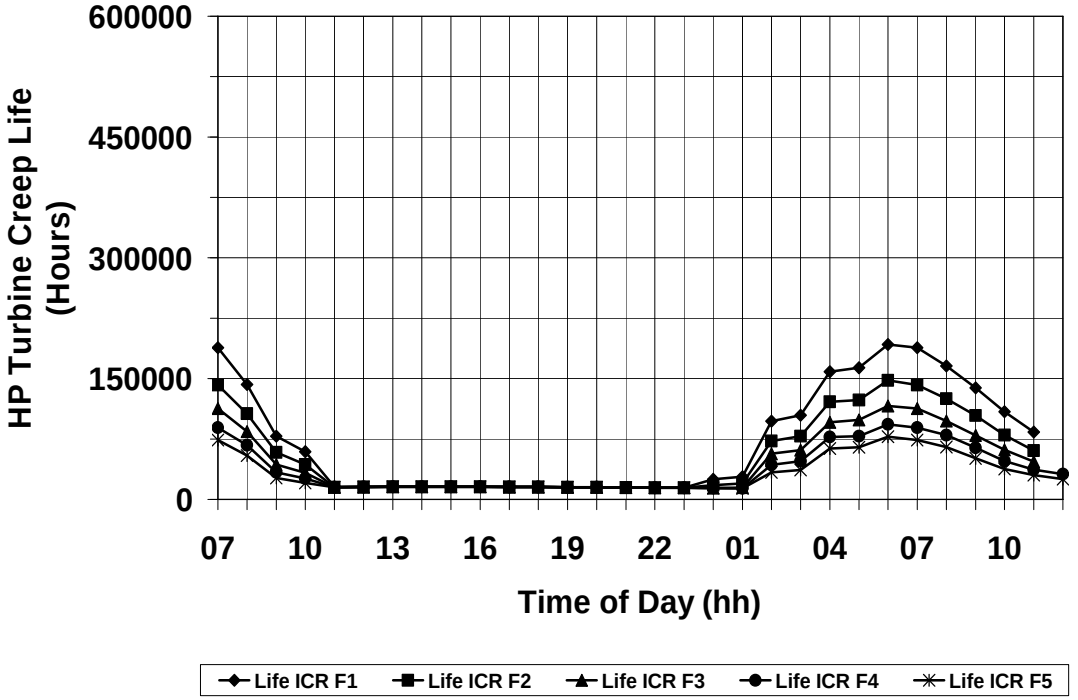

Figure E.10: Intercooled/recuperated cycle (ICR) – Compressor HP turbine creep life variation against time of day, during journey with annual hull fouling progression (F#) and adverse weather conditions

Appendix E.5

Table E.1: Hull fouling F1-F5 – Quantified engine (ICR) parameters per journey at ideal weather conditions

Hull Fouling	Fuel Consumption (kg)	HP Turbine Life Consumption (%)	Total NOx Emissions (kg)	Total CO Emissions (kg)	Total CO2 Emissions (kg)	Total UHC Emissions (kg)	Operational Time per Trip (hours)
F1	103575.1	0.024528	704.67	147.87	325021.9	28.90	24.0
F2	105789.5	0.032999	723.0	144.88	331969.3	27.79	24.0
F3	107737.0	0.042515	739.39	142.39	338089.3	26.87	24.0
F4	109484.6	0.053496	754.36	140.21	343572.2	26.09	24.0
F5	111077.4	0.066066	768.28	138.22	348566.2	25.40	24.0

Table E.2: Hull fouling F1-F5 – Quantified engine (ICR) parameters per journey at adverse weather conditions

Hull Fouling	Fuel Consumption (kg)	HP Turbine Life Consumption (%)	Total NOx Emissions (kg)	Total CO Emissions (kg)	Total CO2 Emissions (kg)	Total UHC Emissions (kg)	Operational Time per Trip (hours)
F1	132948.7	0.104584	921.06	168.54	417184.8	31.45	28.52
F2	134741.8	0.112085	935.46	166.80	422806.0	30.75	28.56
F3	136203.7	0.120004	947.53	165.19	427400.2	30.14	28.58
F4	137446.5	0.126105	957.85	164.0	431295.7	29.68	29.01
F5	138637.3	0.132894	967.86	163.01	435028.9	29.28	29.04

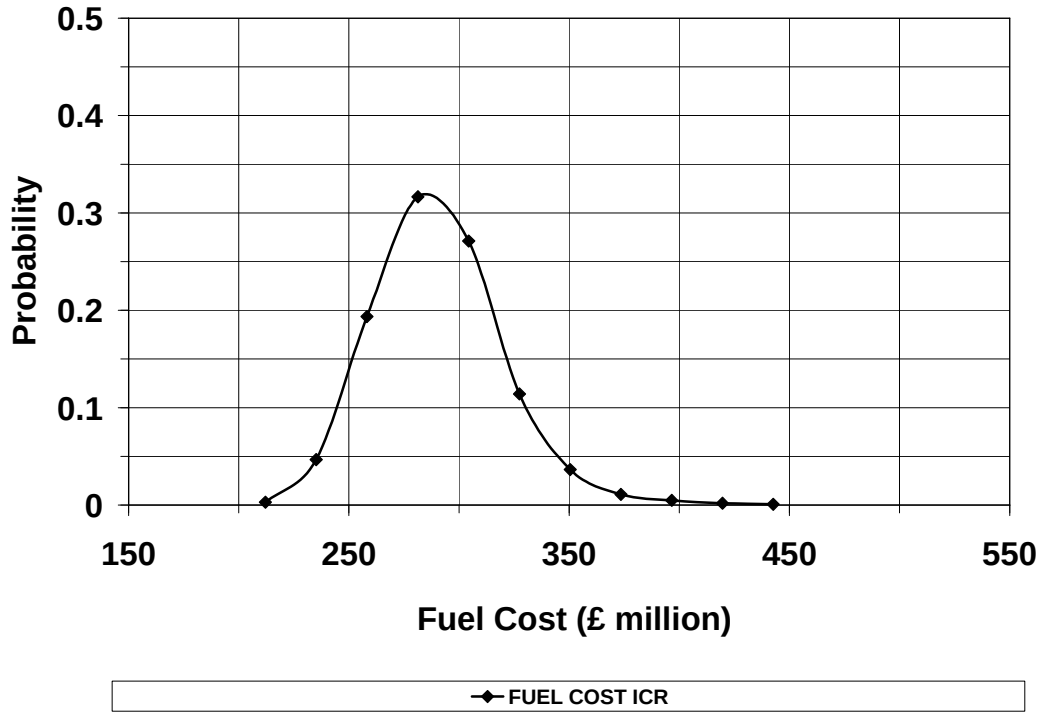

Figure E.11: LNG carrier – Probability distribution of fuel cost of ICR power plant

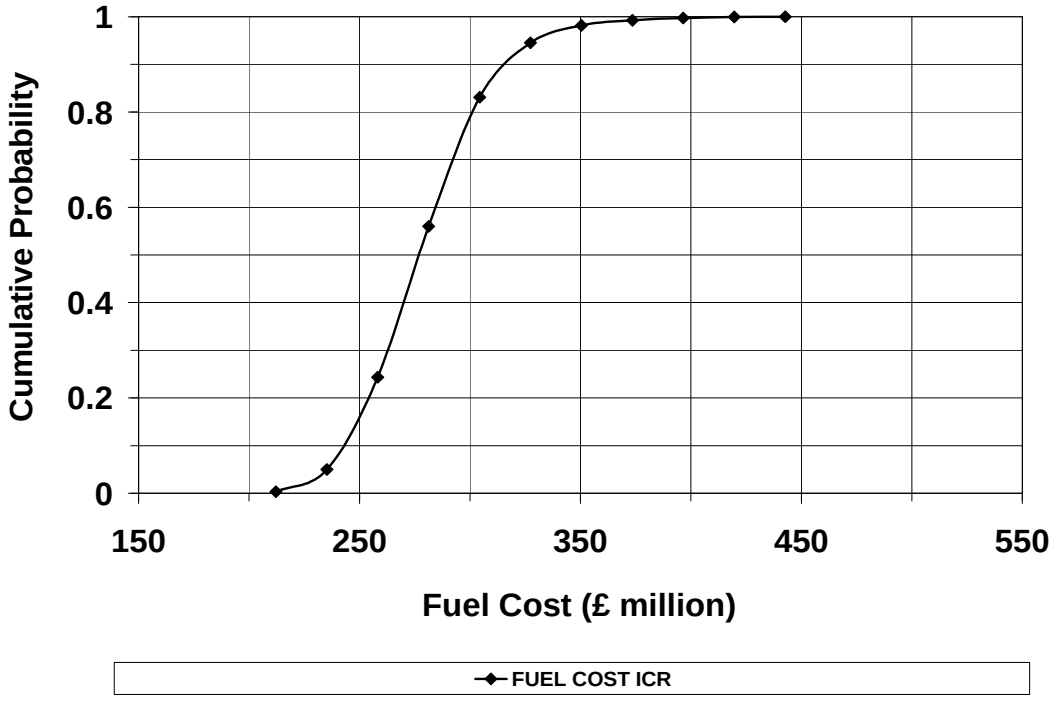

Figure E.12: LNG carrier – Cumulative probability distribution of fuel cost of ICR power plant

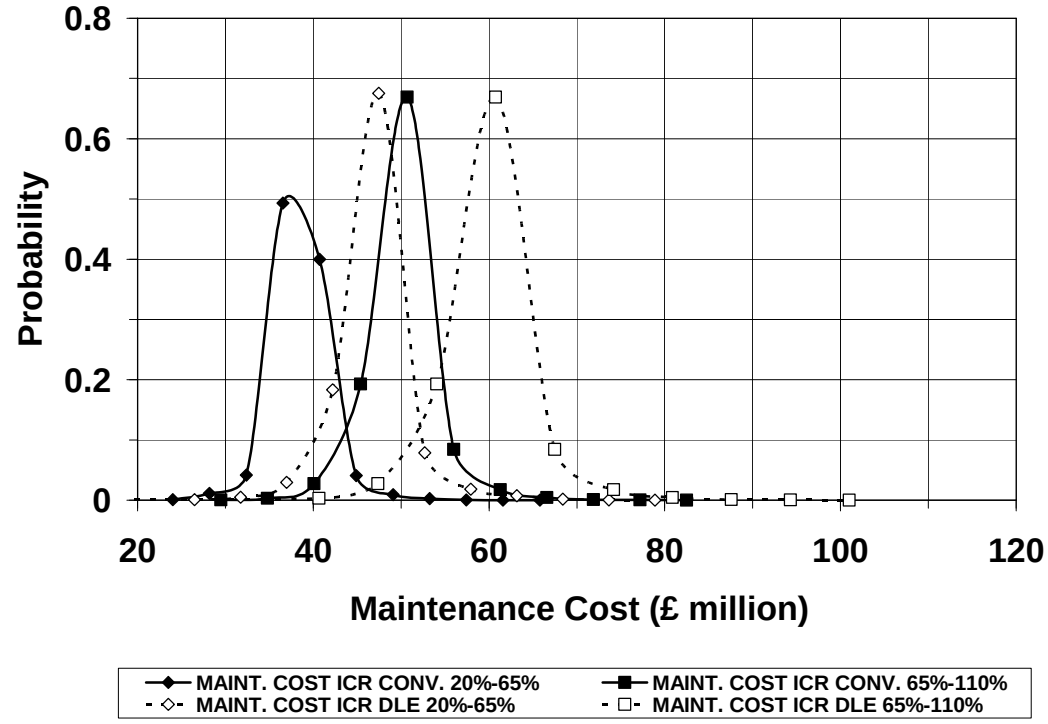

Figure E.13: LNG carrier – Probability distribution of maintenance cost of ICR power plant (initial capital cost from, 1: 20% to 65% and 2: from 65% to 110% over the reference power plant)

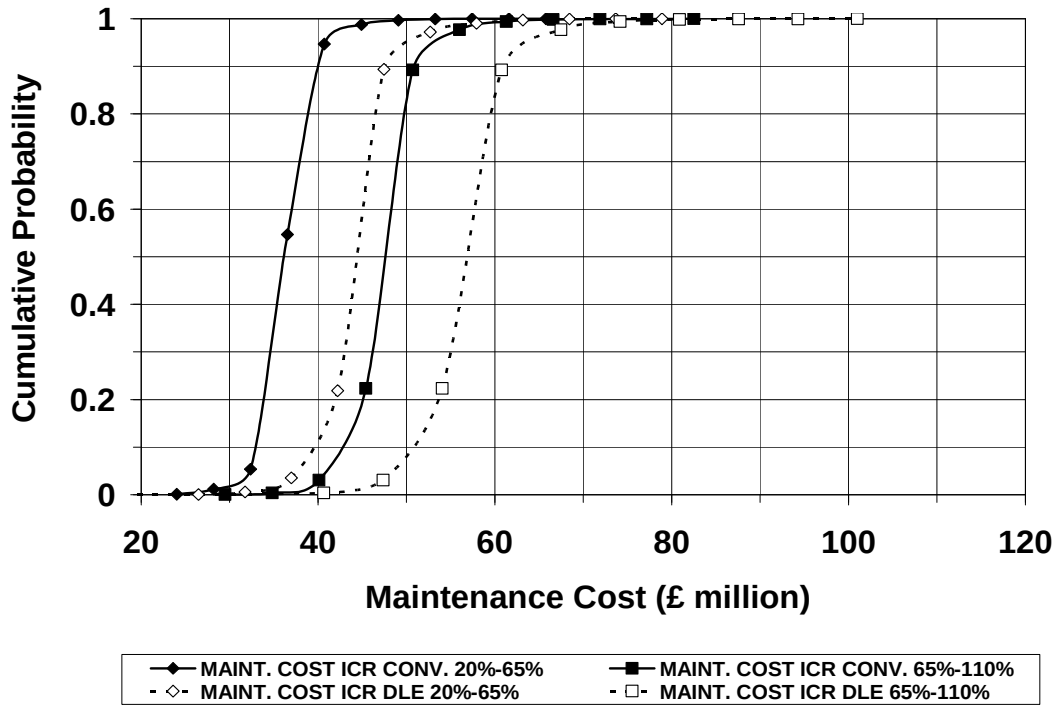

Figure E.14: LNG carrier –Cumulative probability distribution of maintenance cost of ICR power plant (initial capital cost from, 1: 20% to 65% and 2: from 65% to 110% over the reference power plant)

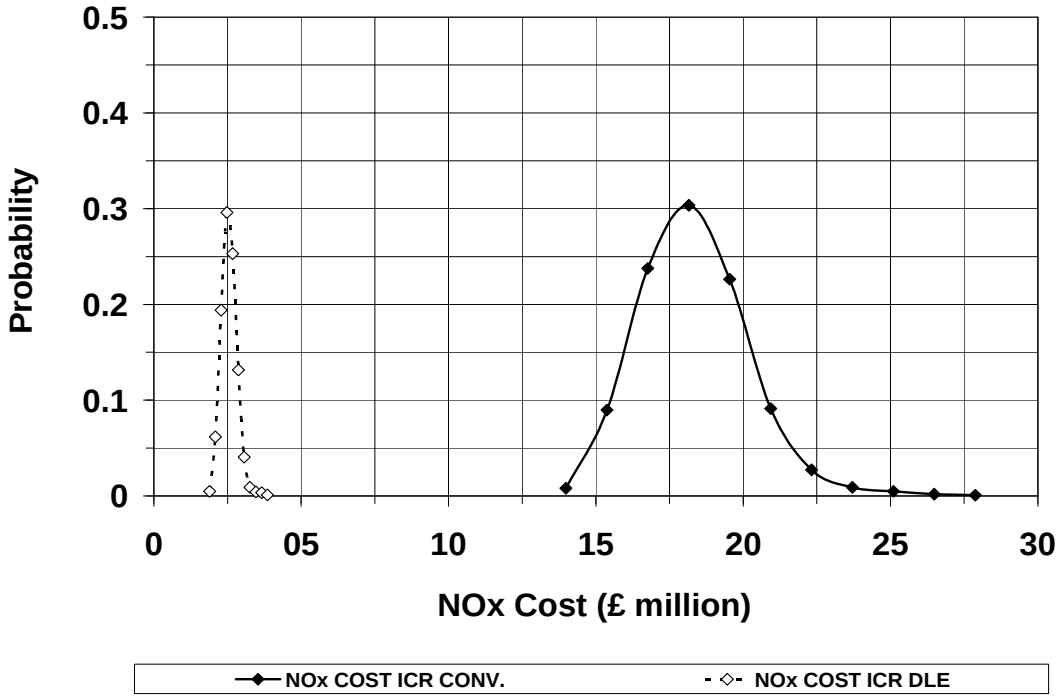

Figure E.15: LNG carrier – Probability distribution of cost of taxed NOx exhaust emissions of ICR power plant with conventional & DLE combustors

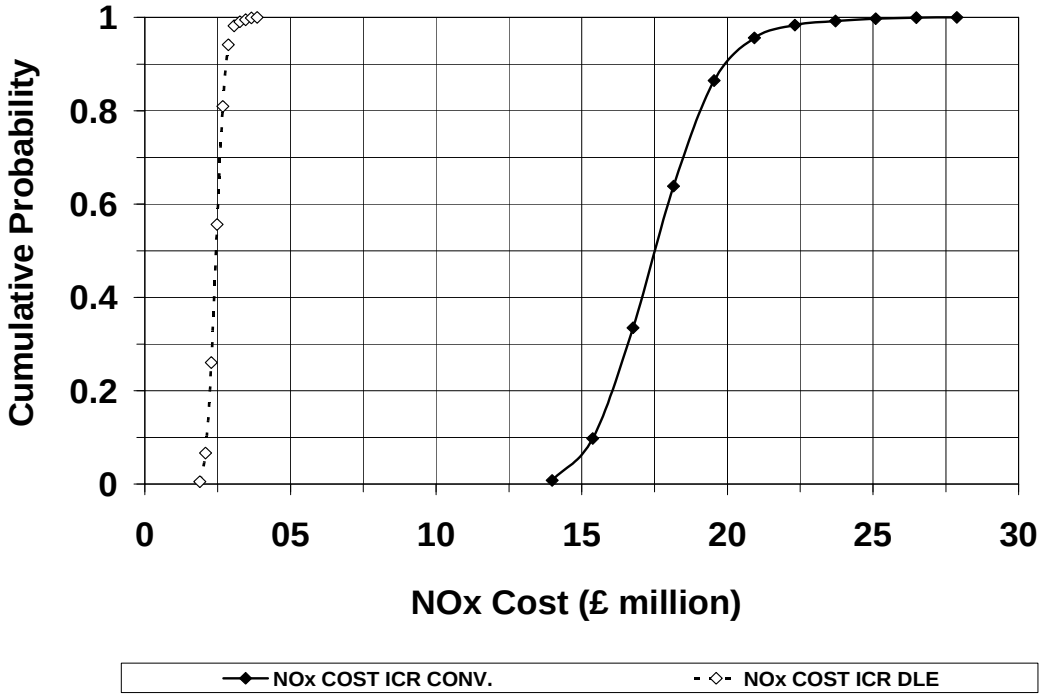

Figure E.16: LNG carrier – Cumulative probability distribution of cost of taxed NOx exhaust emissions of ICR power plant with conventional & DLE combustors

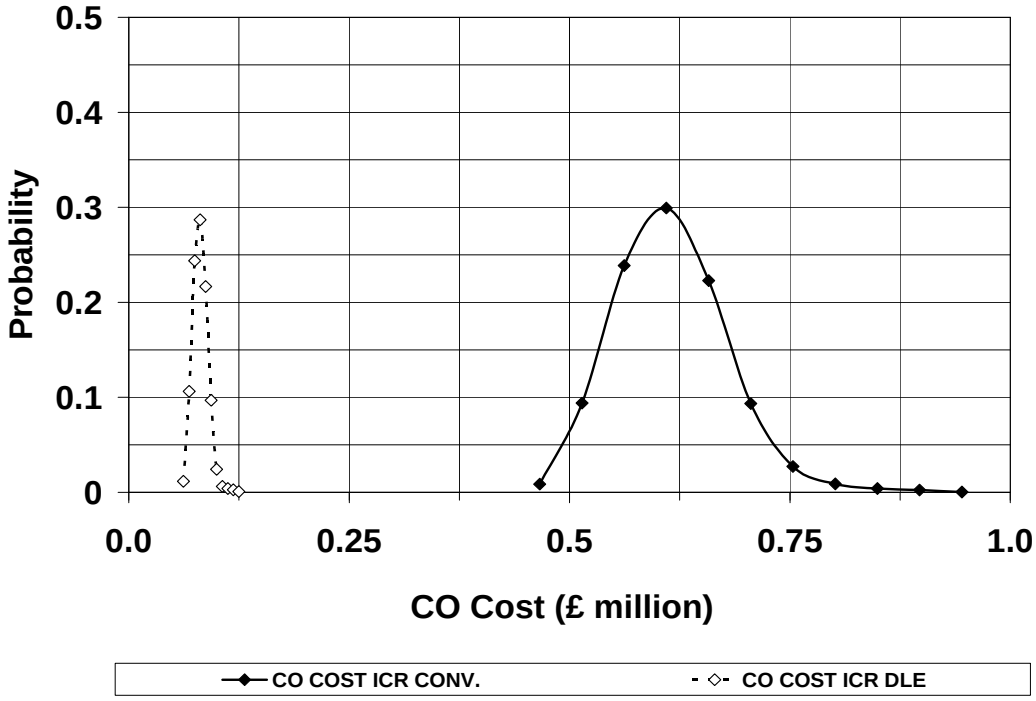

Figure E.17: LNG carrier – Probability distribution of cost of taxed CO exhaust emissions of ICR power plant with conventional & DLE combustors

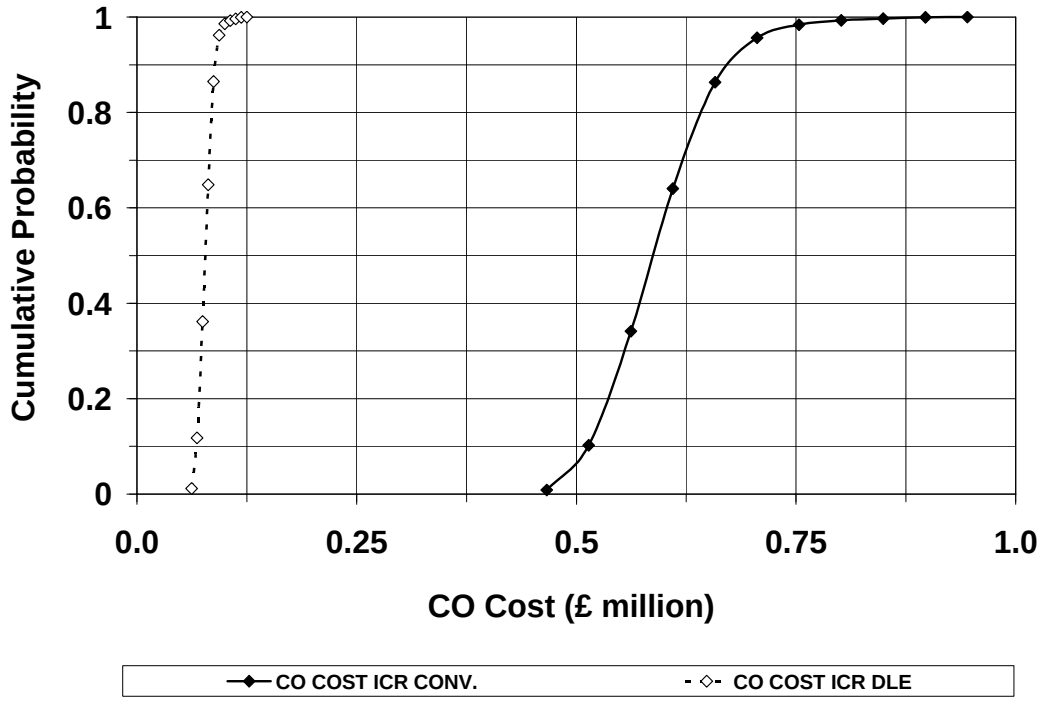

Figure E.18: LNG carrier – Cumulative probability distribution of cost of taxed CO exhaust emissions of ICR power plant with conventional & DLE combustors

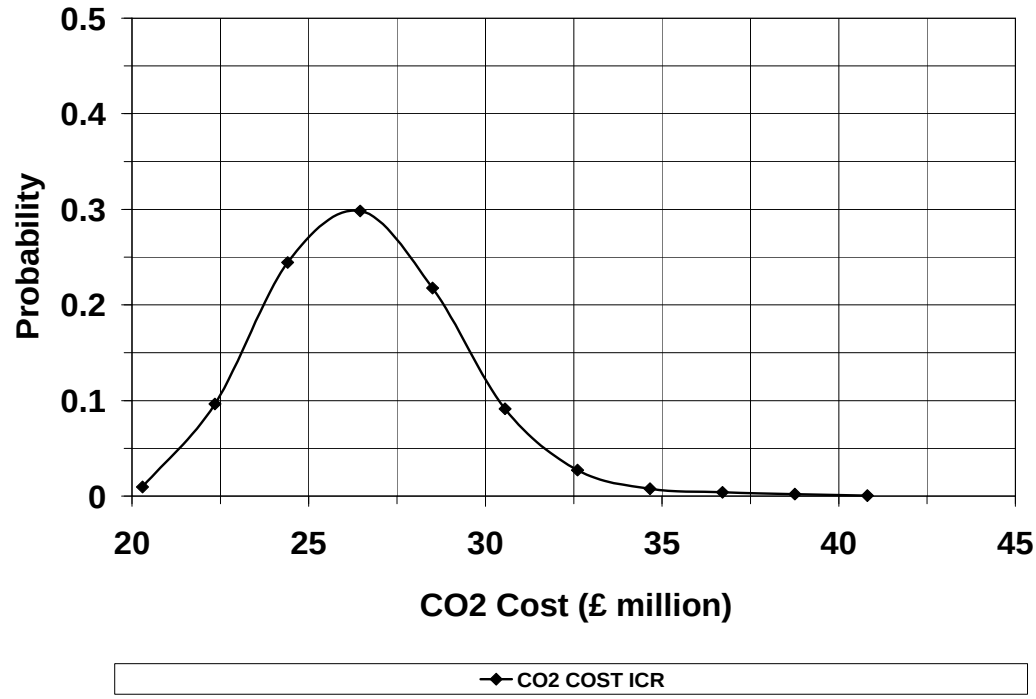

Figure E.19: LNG carrier – Probability distribution of cost of taxed CO2 exhaust emissions of ICR power plant

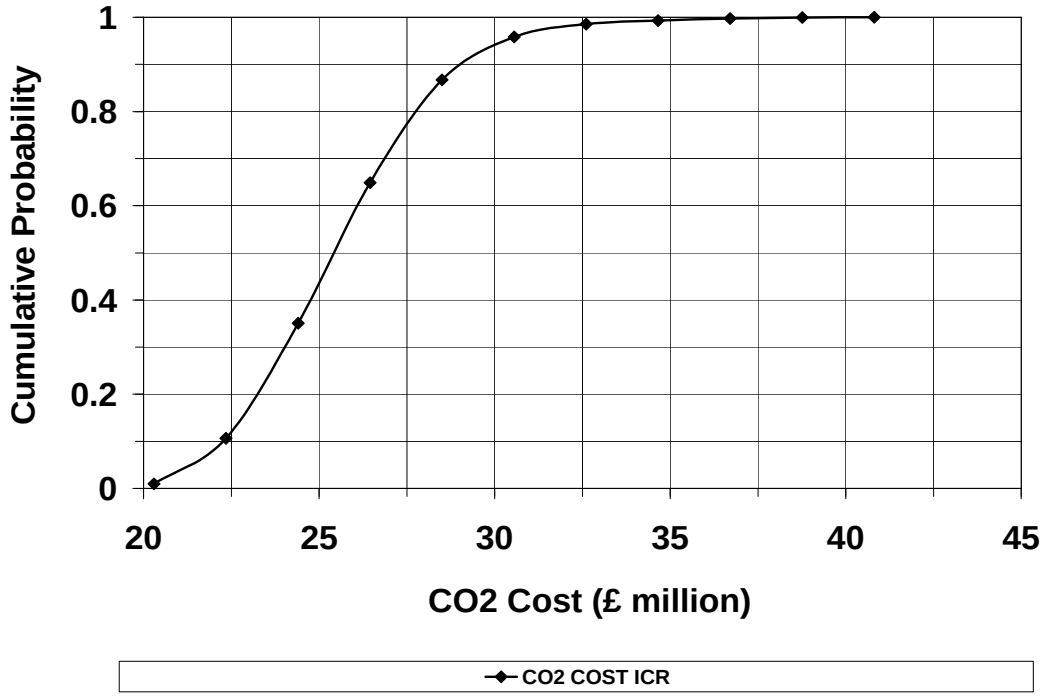

Figure E.20: LNG carrier – Cumulative probability distribution of cost of taxed CO2 exhaust emissions of ICR power plant

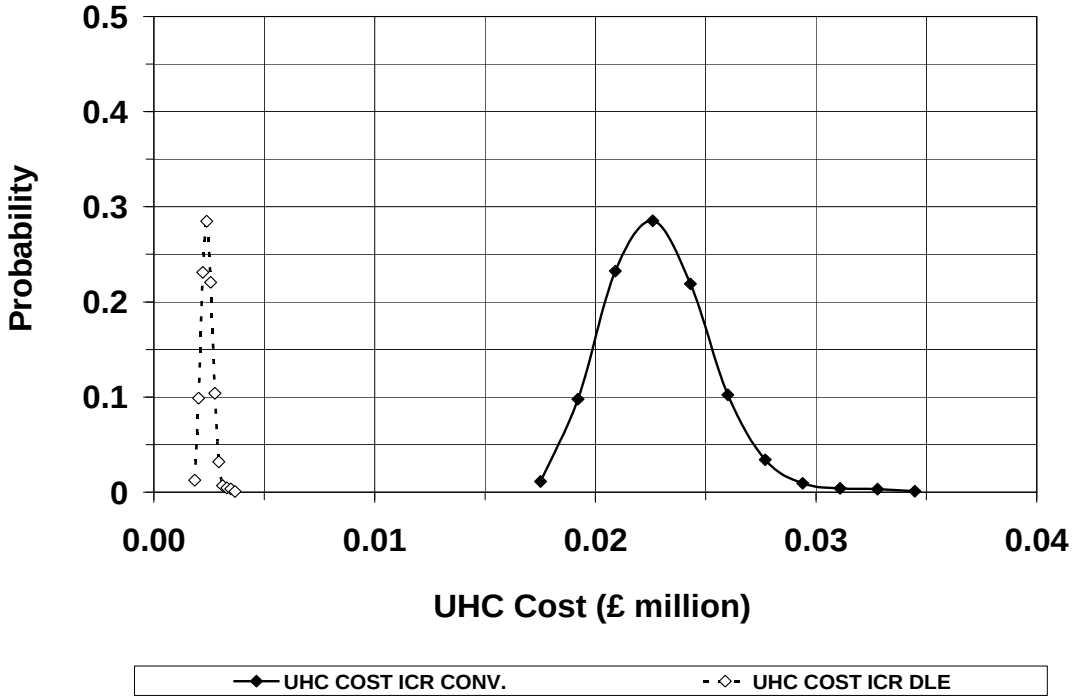

Figure E.21: LNG carrier – Probability distribution of cost of taxed UHC exhaust emissions of ICR power plant with conventional & DLE combustors

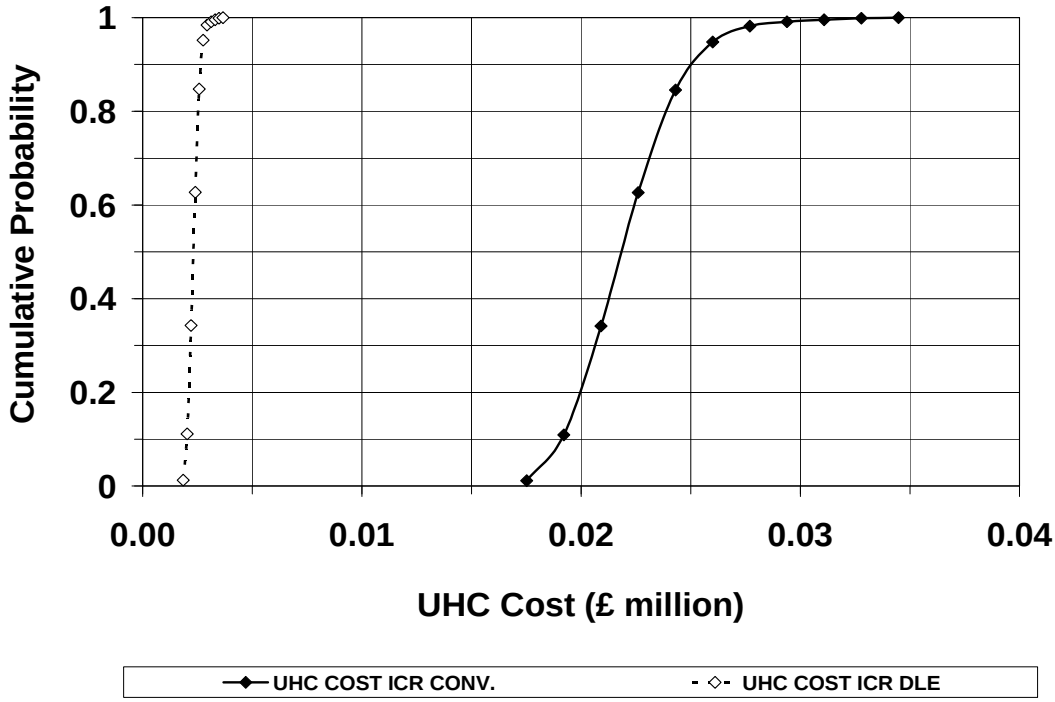

Figure E.22: LNG Carrier – Cumulative probability distribution of cost of taxed UHC exhaust emissions of ICR power plant with conventional & DLE combustors

Table E.3: LNG Carrier - Minimum-maximum and standard deviation of cost of quantified engine parameters

Engine Life Cycle Cost Parameter (£ million)	**Minimum Cost Conv. & DLE Combustor**		**Maximum Cost Conv. & DLE Combustor**		**Standard Deviation Conv. & DLE Combustor**	
NPC (20%-65%)	291.2	286.6	603.6	612.2	28.38	29.58
NPC (65%-110%)	291.0	305.1	608.8	639.6	28.9	30.4
Fuel	207.0		452.4		22.28	
Maintenance (20%-65%)	21.92	23.86	67.86	81.52	4.16	5.24
Maintenance (65%110%)	26.86	37.4	85.14	111.2	5.28	6.7
NOx	13.28	1.792	28.56	3.94	1.38	0.196
CO	0.442	0.058	0.968	0.128	0.048	0.0062
CO2	18.72		41.82		2.04	
UHC	0.016	0.0018	0.034	0.0036	0.0016	0.00018

APPENDIX F

Contains:

Appendix F.1

Table F.1: Variation of salt water density and kinematic viscosity with temperature (interpolate linearly for other salinities) [Chapter 2, Ref. 7]

Sea-water Temperature deg. ^{o}C	**Kinematic Viscosity of Salt Water ν (m^2/sec)10^6**	**Density of Salt Water, ρ_s (kg/m^3)**
0	1.82844	1028.0
1	1.76915	1027.9
2	1.71306	1027.8
3	1.65988	1027.8
4	1.60940	1027.7
5	1.56142	1027.6
6	1.51584	1027.4
7	1.47242	1027.3
8	1.43102	1027.1
9	1.39152	1027.0
10	1.35383	1026.9
11	1.31773	1026.7
12	1.28324	1026.6
13	1.25028	1026.3
14	1.21862	1026.1
15	1.18832	1025.9
16	1.15916	1025.7
17	1.13125	1025.4
18	1.10438	1025.2
19	1.07854	1025.0
20	1.05372	1024.7
21	1.02981	1024.4
22	1.00678	1024.1
23	0.98457	1023.8
24	0.96315	1023.5
25	0.94252	1023.2
26	0.92255	1022.9
27	0.90331	1022.6
28	0.88470	1022.3
29	0.86671	1022.0
30	0.84931	1021.7

Appendix F.2

Table F.2: Wageningen B-series polynomials [Chapter 2, Ref. 11]

C_T	s	t	u	v	C_Q	s	t	u	v
0.0088	0	0	0	0	0.00379	0	0	0	0
-0.2046	1	0	0	0	0.00887	2	0	0	0
0.16635	0	1	0	0	-0.0322	1	1	0	0
0.15811	0	2	0	0	0.00345	0	2	0	0
-0.1476	2	0	1	0	-0.0409	0	1	1	0
-0.4815	1	1	1	0	-0.108	1	1	1	0
0.41544	0	2	1	0	-0.0885	2	1	1	0
0.0144	0	0	0	1	0.18856	0	2	1	0
-0.053	2	0	0	1	-0.0037	1	0	0	1
0.01435	0	1	0	1	0.00514	0	1	0	1
0.06068	1	1	0	1	0.02094	1	1	0	1
-0.0126	0	0	1	1	0.00474	2	1	0	1
0.01097	1	0	1	1	-0.0072	2	0	1	1
-0.1337	0	3	0	0	0.00438	1	1	1	1
0.00638	0	6	0	0	-0.0269	0	2	1	1
-0.0013	2	6	0	0	0.05581	3	0	1	0
0.1685	3	0	1	0	0.01619	0	3	1	0
-0.0507	0	0	2	0	0.00318	1	3	1	0
0.08546	2	0	2	0	0.0159	0	0	2	0
-0.0504	3	0	2	0	0.04717	1	0	2	0
0.01047	1	6	2	0	0.01963	3	0	2	0
-0.0065	2	6	2	0	-0.0503	0	1	2	0
-0.0084	0	3	0	1	-0.0301	3	1	2	0
0.01684	1	3	0	1	0.04171	2	2	2	0
-0.001	3	3	0	1	-0.0398	0	3	2	0
-0.0318	0	3	1	1	-0.0035	0	6	2	0
0.0186	1	0	2	1	-0.0107	3	0	0	1
-0.0041	0	2	2	1	0.00111	3	3	0	1
-0.0006	0	0	0	2	-0.0003	0	6	0	1
-0.005	1	0	0	2	0.0036	3	0	1	1
0.0026	2	0	0	2	-0.0014	0	6	1	1
-0.0006	3	0	0	2	-0.0038	1	0	2	1
-0.0016	1	2	0	2	0.01268	0	2	2	1
-0.0003	1	6	0	2	-0.0032	2	3	2	1
0.00012	2	6	0	2	0.00334	0	6	2	1
0.00069	0	0	1	2	-0.0018	1	1	0	2
0.00422	0	3	1	2	0.00011	3	2	0	2
5.7E-05	3	6	1	2	-3E-05	3	6	0	2
-0.0015	0	3	2	2	0.00027	1	0	1	2
					0.00083	2	0	1	2
					0.00155	0	2	1	2
					0.0003	0	6	1	2
					-0.0002	0	0	2	2
					-0.0004	0	3	2	2
					8.7E-05	3	3	2	2
					-0.0005	0	6	2	2
					5.5E-05	1	6	2	2

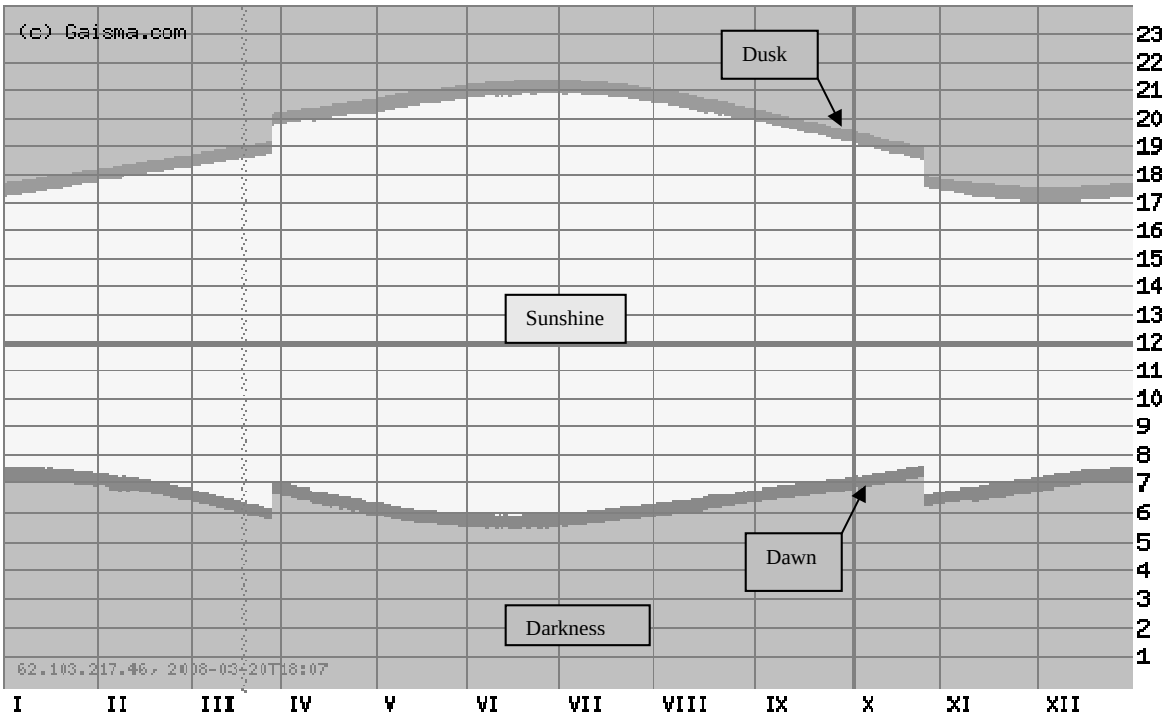

Figure F.1: Sunrise, sunset, dawn and dusk times in Greece (Athens) for each month of year [Chapter 5, Ref. 27]

Table F.3: Average monthly ambient air temperature in Greece (Athens) for each month of year [Chapter 5, Ref. 27]

Temperature °C	10.30	10.14	12.11	15.99	20.66	24.93	26.82	26.67	23.88	19.68	14.98	11.48
Month	Jan	Feb	Mar	Apr	May	Jun	Jul	Aug	Sep	Oct	Nov	Dec

Appendix F.4

Table F.4: Case studies dataset of RoPax fast ferry and Destroyer naval vessel

Case studies dataset of RoPax fast ferry and Destroyer naval vessel		
Gas turbine Power plant	**Hull fouling level**	**Sea-state profile**
Simple cycle SC	F1	No weather conditions (Ideal)
	F2	
	F3	
	F4	
	F5	
Twin mode intercooled cycle TMI	F1	
	F2	
	F3	
	F4	
	F5	
Intercooled Cycle INT	F1	
	F2	
	F3	
	F4	
	F5	
Recuperated cycle REQ	F1	
	F2	
	F3	
	F4	
	F5	
Intercooled/ Recuperated Cycle ICR	F1	
	F2	
	F3	
	F4	
	F5	
Simple cycle SC	F1	Adverse weather conditions
	F2	
	F3	
	F4	
	F5	
Twin mode intercooled cycle TMI	F1	
	F2	
	F3	
	F4	
	F5	
Intercooled Cycle INT	F1	
	F2	
	F3	
	F4	
	F5	
Recuperated cycle REQ	F1	
	F2	
	F3	
	F4	
	F5	
Intercooled/ Recuperated Cycle ICR	F1	
	F2	
	F3	
	F4	
	F5	

Table F.5: Case study dataset LNG carrier

Case study dataset of LNG carrier		
Gas turbine Power plant	**Hull fouling level**	**Sea-state profile**
Intercooled/ Recuperated Cycle ICR	F1	No weather conditions (Ideal)
	F2	
	F3	
	F4	
	F5	
Intercooled/ Recuperated Cycle ICR	F1	Adverse weather conditions
	F2	
	F3	
	F4	
	F5	

Table 17—Variation of Form Coefficients and Elements of Hull Shape, Based on Lindblad (1961) and Todd (1945)

Type of ship		Slow speed cargo ship	Medium speed cargo ship	Cargo liners	Passenger and cargo, fruit ships	High-speed passenger liners, ferries, etc.	Fast passenger liners, trawlers, tugs	Cross-channel ships	Destroyers
C_B		0.80	0.75	0.70	0.65	0.60	0.55	0.54 –0.52	0.46–0.54
C_M		0.99–0.995	0.985–0.99	0.98	0.98	0.97	0.93	0.915–0.905	0.76–0.85
C_P		0.809–0.805	0.762–0.758	0.715	0.664	0.62	0.59	0.59 –0.575	0.56–0.64
C_{WP}		0.88	0.84	0.81	0.78	0.71	0.69	0.69 –0.675	0.68–0.76
Fn		0.15–0.18	0.18–0.19	0.21	0.24	0.24–0.30	0.24 –0.36	0.36 –0.45	0.45 and above
L_P percent		35	25	12	5	0	0	0	0
L_R/L_B		0.7	0.8	0.9	1.0	1.0–1.1	1.1–1.2	1.2	0.55
LCB percent L_{PP} from PP ⊠		1.5–2.5 fwd	1.0–2.0 fwd	0–1.0 aft	1.0–2.0 aft	1.5–2.0 aft	2.0–2.8 aft	2.0–3.0 aft	0.5–2.0 aft
Sectional area curve shape	Fwd	Straight with U sections, slightly convex with V sections and raked stem	Straight with slight hollow at extreme fore end	Straight with some hollow forward giving S-shape	S-Shape—fine entrance essential with pronounced hollow forward	S-Shape for Fn = 0.24, becoming straight above this value, with addition of bulb	S-Shape at Fn = 0.24 straight above Fn = 0.27	S-Shape with hollow forward at Fn = 0.36 becoming straighter for 0.45	Maximum area aft of midships. Straight or slightly convex area curve forward
	Aft	Straight or slightly convex with easy shoulder	Straight or slightly convex	Straight except at extreme aft end	Straight except at extreme aft end	Straight except at extreme aft end	S-Shape	Straight with hollow at extreme aft end	Good buttock lines aft and transom stern
LWL shape	Fwd	Slightly convex throughout	Slightly convex or straight	Slightly hollow forward, or straight with longer entrance	S-Shaped, hollow forward	Fine *WL*, almost straight with slight hollow	Fine *WL*, S-shaped below Fn = 0.30 straight above this value	Up to Fn = 0.30 fine *WL* with hollow, above Fn = 0.3, *WL* endings fuller and straight, or hollow with bulb	Maximum beam aft of midships. Waterline forward quite straight or even a little convex
	Aft	Slightly convex. If possible the slope should not exceed 20 deg	Slightly convex	Slightly convex	Slightly convex	Full *WL*, nearly straight	Full, straight or convex	Full *WL*, convex	*WL* aft very full to suit transom stern and cover screws
Half-angle of entrance on LWL (i_E)		35 deg	27 deg	12 deg with hollow *LWL*, 16 deg if *LWL* is straight	10 deg	6 deg	8½-10 deg	6–7 deg below Fn = 0.30. Above this speed, 9 deg with straight *WL*, 6 deg with hollow and bulb	4–11 deg

Figure F.2: A guide of main form coefficients and elements of the hull shape [Chapter 5, Ref. 4]